506
C 215p
no. 621

C

CONTRIBUTIONS TO EMBRYOLOGY

VOLUME XXXVII
NOS. 252 TO 258

1902

CARNEGIE INSTITUTION OF WASHINGTON PUBLICATION 621
WASHINGTON, D. C.
1962

CONNECTICUT
STATE LIBRARY

APR 3 1962

HARTFORD
CONNECTICUT

4/3

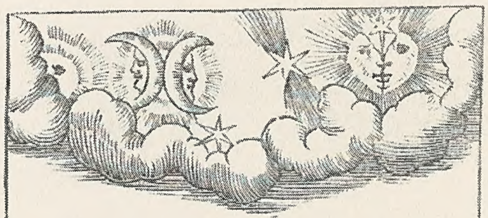

The Beckwith-Browning-Peterson
Teratology Collection

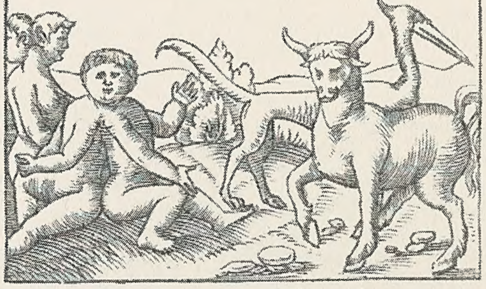

Smithsonian Libraries
2017

CONTRIBUTIONS TO EMBRYOLOGY

VOLUME XXXVII
NOS. 252 TO 258

CARNEGIE INSTITUTION OF WASHINGTON PUBLICATION 621
WASHINGTON, D. C.
1962

This book issued March 1962

Library of Congress Catalog Card Numbers
Contribution 252: 62–12214
253: 62–12215
254: 62–12216
255: 62–12217
256: 62–12218
257: 62–12219
258: 62–12220

PORT CITY PRESS, INC., BALTIMORE, MARYLAND

QM
601
.C66
1915
v.37
SCDIRB

CONTENTS

PAGES

252. The Proliferation of Neural Crest from Forebrain Levels in the Rat (eight plates and seven text figures) 1–12

George W. Bartelmez

253. The Early Development of the Human Brain (thirty plates) 13–32

George W. Bartelmez and A. S. Dekaban

254. Anatomical Analysis of Rabbit Trophoblast Invasion (fifteen plates and one text figure) 33–55

Bent G. Böving

255. On the Chick Spleen: Origin; Patterns of Normal Development and Their Experimental Modification (fourteen plates and one text figure) 57–85

L. E. DeLanney and J. D. Ebert in collaboration with C. M. Coffman and A. M. Mun

256. Development of the Ventricles and Spiral Outflow Tract in the Human Heart (nine plates and nine text figures) 87–114

Pieter A. de Vries and John B. de C. M. Saunders

257. The Primordial Germ Cells in the Male Human Embryo (five plates) 115–119

Roberto Narbaitz

258. The Development of the Sternomastoid and Trapezius Muscles (thirteen plates and two text figures). 121–129

J. McKenzie

CONTRIBUTIONS TO EMBRYOLOGY, NO. 252

THE PROLIFERATION OF NEURAL CREST FROM FOREBRAIN LEVELS IN THE RAT

George W. Bartelmez

Department of Embryology, Carnegie Institution of Washington, Baltimore, and
Department of Anatomy, Johns Hopkins Medical School, Baltimore

With eight plates and seven text figures

CONTENTS

PAGE

Introduction 3

History 3

Methods and Material 4

The Optic Primordium and the Boundary between Forebrain and Midbrain 6

Transitional Zone and Neural Crest of the Forebrain 8
  Lateral Lip 9

Neural Crest from the Primary Optic Vesicle 9

Discussion 10
  Speculations on the Fate of the Crest of the Forebrain 11

Summary 11

Addendum 11

Literature Cited 12

THE PROLIFERATION OF NEURAL CREST FROM FOREBRAIN LEVELS IN THE RAT

INTRODUCTION

Neural crest arising from the lateral edges of the neural folds of the forebrain has been described in species from all classes of vertebrates from fish to mammals. The proliferation of crest from the primary optic vesicle has been reported in man (Bartelmez and Blount, 1954) and in some other mammals (Bartelmez, 1960). In view of the many detailed studies that have been made on other classes and the small number of mammals investigated, it seemed wise to begin a comparative study of the migration of neural crest from the optic vesicle in mammals, as it may be confined to this class; perhaps in some species all the forebrain crest comes from the optic vesicles.

HISTORY

The history of research on the neural crest has been presented admirably by Raven (1931), Starck (1937), and Hörstadius (1950). A few details on the crest of the head may be added with a somewhat different emphasis. His (1868) was the first to present evidence that ganglia arise from cells derived from the neural folds. He described a gradual tapering of the neural epithelium to the ectoderm of the head in a chick which was probably in the 6-somite stage. He termed the transitional zone "Zwischenstrang," and derived from it a strand of deeply staining mesenchymal cells extending from the hindbrain to the rostral end of the optic vesicles. He showed that certain cranial ganglia arise from these cells. When Balfour (1878) was hailed as the discoverer of the "neural ridge" (in selachians) His (1879) called attention to his previous paper and added further details. His reconstruction of the cranial neural crest in the chick is still used in current textbooks of avian embryology. Proliferations of neural crest were promptly reported by various investigators in embryos from all classes of vertebrates. The origin of ganglia from the neural tube was in accord with current theory.

In 1878, Marshall noted that not all neural crest cells enter cranial ganglia, and Van Wijhe (1883) stated that the crest rostral to the trigeminal level does not produce any ganglion cells. Kastschenko (1888) described degenerated cells among the proliferating crest cells, and it was subsequently assumed that all crest cells that do not produce ganglia undergo degeneration. This "coagulation necrosis," however, has been encountered in various very rapidly growing areas of young embryos of many species.

A new chapter in this field of research was opened by Platt (1893 ss.) when she announced that she had followed "mesectoderm" into the branchial arches in *Necturus* and found it developing into cartilage. The dogmatists were outraged at this attack on the Doctrine of the Germ Layers, but her findings were promptly confirmed by Kupffer in cyclostomes (1895 ss.), Dohrn in selachians (1902), and Brauer (1904) in *Gymnophiona*. Although little attention was paid to his work, Grynfeltt (1898) also made a significant attack on the Dogma when he found that cells migrate from the edge of the secondary optic vesicle ("optic cup") in the rabbit to produce the sphincter iridis and the myoepithelial cells of the dilator iridis. The pluripotentiality of epithelium derived from the optic vesicle was later demonstrated experimentally by many investigators, in Amphibia at least.

The role of neural crest and ectodermal placodes in the development of cranial ganglia was first clarified by Landacre (1910) when he applied to the development of the head of *Ameiurus* the analysis of the adult cranial ganglia of anamniotes developed by Strong (1895), Johnston (1898), Herrick (1899), and others. Subsequently, in the urodele *Plethodon,* Landacre (1921) was able to follow the crest cells by means of their characteristic pigment and yolk granules into the branchial arches and demonstrate their differentiation into cartilage as Platt had described the process in *Necturus.* At the same time Stone (1922) was analyzing the development of the head in *Amblystoma* both morphologically and experimentally. After removal of part of the crest at the level of the fifth nerve, easily recognizable in early stages by the deep pigmentation of the cells, he found Meckel's and the quadrate cartilages reduced in size. The extirpation of crest cells from more caudal branchial arches resulted in defects in the corresponding cartilages and in the external gills. In 1929 he reported the differentiation of cartilage in transplants of neural crest. Raven (1931, 1933*a*, *b*), also working with urodeles, traced the crest primordium back to early neurulae and studied its differentiation in normal and experimental material. He was highly critical in the interpretation of his homoplastic and heteroplastic transplantations and isolations so that his conclusions as to the differentiation of crest into cartilage as well as connective tissue and ganglia are the more convincing.

The most detailed study of neural crest and epiblast proliferation in birds is that of Ortmann (1943). His interpretations are based on a wide knowledge of the literature of comparative embryology, and his observations are admirably documented and correlated with findings in other species.

From 1920 to 1931 Celestino da Costa studied the development of the neural crest in the guinea pig, the species in which the first description of neural crest in a mammal had been given by Chiarugi (1894). Celestino da Costa's first paper reported a proliferation of crest from the epiblast in forebrain levels, beginning in embryos of 5 to 6 somites (in which the neural folds are still open). The optic primordia are confined to the forebrain. Since the optic foveolae had already appeared at 6 somites and neural crest was formed at optic levels it was obvious that in the guinea pig, as in other species, the forebrain produces neural crest. He found that the strand of forebrain crest became continuous with that from the midbrain. At 10 somites the process was over for the most part, but in 12- to 16-somite stages there was still some evidence of proliferation from the margins of the anterior neuropore. He could follow the crest cells into the connective-tissue capsule of the optic vesicle. His definitive monograph of 1931 was based on 87 embryos between a 1-somite stage and an embryo 7.5 mm. long. His evidence for the proliferation of crest was based primarily on the continuity of neural epithelium with loosely arranged crest cells which were well differentiated from the paraxial mesenchyme.

In his study of more than 200 young rat embryos, Adelmann (1925) devoted his attention primarily to the development of the sensory ganglia and their relation to the subdivisions of the neural folds. He found no convincing evidence of crest proliferation from forebrain levels.

Holmdahl (1928) had so few stages from any one of the species he studied that his failure to find crest proliferating from the forebrain carries but little weight.

METHODS AND MATERIAL

Massive proliferations of neural crest which involve the disaggregation of the lateral edge of the neural folds into "mesenchyme" and which persist for some time can be readily recognized in thick sections of indifferently preserved material, even with low powers of the microscope. These conditions obtain in trigeminal and other hindbrain levels where the origin of the neural crest has been described in every vertebrate that has been studied. The recognition of the migration of single cells or small groups calls for cytologic methods even when the absence of a sharp boundary between epithelium and mesenchyme suggests proliferation. When the period of migration is brief a close series of stages is essential. In early somite stages the various systems of the embryo develop at different rates even in littermates; consequently a close series of somite stages may be wholly inadequate for deciphering the more rapid changes in the neural crest. As Landacre (1914) and Celestino da Costa (1931) pointed out, the seriation must be based on progressive changes in the proliferation of crest at the particular level under investigation. The findings reported below confirm this conclusion.

The study of the proliferation of neural crest cells from the human optic vesicle (Bartelmez and Blount, 1954) showed that a relatively short delay in fixation, especially one involving a cessation of the circulation, resulted in a shrinkage or retraction of the pseudopods of migrating cells as well as in form changes in the epithelial cells which made it impossible to follow cell boundaries. Furthermore, it is necessary to have a favorable plane of section of the region studied, even if the sections are thin, so that unambiguous evidences of migration can be obtained. Accurate orientation for sectioning, based on portraits of the intact embryos, is therefore essential. Portraits are required also for reconstructions; uncontrolled stacking of plates can produce weird distortions and usually results in incorrect profiles.

The most satisfactory method for processing the embryos was found after much experimentation to be as follows:

Fix in aqueous chrome-sublimate-formol (Bensley) with or without subsequent mordanting in 1 per cent osmic acid, or put embryos directly into the strong Flemming mixture using only 0.1 per cent acetic acid (Benda). The implantation site should be opened to expose the embryo. Fix for about 12 hours.

The use of fixatives with high acid content tends to result in the shriveling of the pseudopods of the neuroepithelial cells. Cell boundaries are difficult to follow in material fixed in Bouin's picro-formol-5 per cent acetic mixture or acetic Zenker, although both preserve the general form relations admirably if the dehydration is sufficiently gradual.

Wash in several changes of distilled water for 3 to 6 hours.

Dehydration after any fixative containing chrome salts should be done in the dark. It must be very gradual. The most satisfactory method is that of C. H. Heuser as described by O. O. Heard (1957). The embryo is put into a plastic tube (insoluble in alcohol and in clearing agents), where it remains until it is transferred to paraffin. Such "traps" are filled and immersed in bottles, ten times their volume, filled with an appropriate solution of alcohol or the like. The number and size of the holes in one or both caps of the trap regulate the rate of transfer. The bottle with trap should be filled and slowly rotated on a vertical wheel so that the trap slips slowly back and forth within it. Young embryos must be stained *in toto*

DSI

so that they can be oriented. A crystal of eosin added to the absolute alcohol is sufficient.

Double embedding is greatly to be preferred for young mammalian embryos and is essential after fixatives like osmic acid, chrome-sublimate, or formol. The parloidin of Mallinckrodt is satisfactory for this purpose; it may be dissolved in either alcohol-ether or, according to the method of Peterfi, in methyl benzoate. A 2 per cent solution is sufficient to prevent distortion. Dry celloidin is added gradually to the solvent to make 1 per cent and 2 per cent solutions. The increase in concentration of celloidin is very gradual when the process is carried out with the embryo in a trap on a vertical revolving wheel. After 24 hours or more in 2 per cent celloidin the embryo with surrounding celloidin can be dropped into chloroform briefly and then cleared in cedar or pine oil, or it can be transferred directly to a chloroform-paraffin mixture. This method leaves the embryo clearly visible within the celloidin so that it can be photographed if necessary and oriented under a binocular dissector during embedding. If a slip of paper marked thus ↑‾ with a soft lead pencil is placed in the bottom of the embedding dish the embryo can be oriented with reference to it. After the block has been mounted for cutting, the paper is stripped off, leaving the orienting lines on the paraffin.

For the study of individual cells the sections should not exceed 6 microns; a satisfactory stain is the Azan modification of Mallory's triple stain. Masson's triple stain is equally good. Any of the iron hematoxylin methods may be used, although they are less satisfactory for photomicrographs of cells.

The forebrain and part of the midbrain of seven embryos were reconstructed; projection reconstructions of four of them are presented in figures 1 to 7. They were prepared from tracings made with the Edinger apparatus at a magnification of 200 diameters. A reconstruction projected on the horizontal plane requires the determination of the angle between the midsagittal plane of the embryo and the plane in which the embryo was sectioned. Transverse sections are most satisfactory. They are seldom at an angle of exactly 90° to the median plane. A line to indicate the mid-line is accordingly drawn on millimeter paper at the appropriate angle to the lines that are to represent the individual sections. Measurements from the mid-line of the section to the lateral edge of the structure being reconstructed can then be plotted. The distance between the plots of successive sections is determined by the thickness of the sections and the magnification used.

For a reconstruction of the midsagittal plane it is essential to have a guide if the profile of the embryo is to be correctly reproduced. The most satisfactory guide is an accurately posed profile portrait of the intact embryo enlarged to the proper size. Sharp profiles cannot be obtained photographically unless the amnion has been removed. If removal of the amnion is not feasible it is necessary to plot the profile of the embryo by measurements from the contours of yolk sac and allantois. Unless adequately controlled, a reconstruction is not likely to give a correct representation of the external form of the embryo or of the relations of its component parts.

Since a fairly complete series of rat embryos was available, the study was begun on this species. The material was collected in 1925 in the Department of Anatomy of the University of California; Dr. H. M. Evans observed and confirmed insemination in 100 young rats; 97 of them provided normal embryos. Stages between 3 and 12 somites were preserved and sectioned for a study of the cytoplasm of neural crest cells. None of the methods used made it possible to follow crest cells satisfactorily after they had dispersed and divided several times. The sections were laid aside until they were needed for the present study. Some of the older stages studied are from material prepared by F. L. Landacre. These specimens were also collected from the Evans Rat Colony and were presented by Dr. R. A. Knouff to the Carnegie Collection of Embryos after Landacre's death. I am also indebted to the Department of Zoology, Montana State University, for laboratory facilities. Dr. L. G. Browman provided the embryo shown in figures 9 and 10, plate 1. It is also a pleasure to acknowledge Dr. M. E. Rawles' suggestions as to the description of the method of reconstruction.

The present study is based on serial sections of 83 embryos, which are divided into four groups on the basis of the differentiation of the optic primordium. (See plates 2 and 3.)

1. Stages preceding the appearance of the optic foveola —10 embryos ranging from 3–4 to 5 somites.
2. Seventeen embryos with flattened forebrain folds and optic foveolae ranging from 4–5 to 7 somites.
3. Stages in the elevation of the forebrain folds and the ballooning of the optic vesicles—41 embryos with 8 to 15 somites.
4. Stages similar to group 3 in which the anterior neuropore had closed—15 embryos ranging from 13 to 16 somites. The neuropore is closed in most 15- and all 16-somite embryos of the series.

In determining the number of somites the dispersion of the first somite must be taken into account. Rostrally it merges gradually into the looser mesenchyme of the head, and the myocoel, when it appears at all, is poorly defined. No dermatome is differentiated. In 7- to 8-somite stages the first somite has become so diffuse that it is readily overlooked. In these stages there is a large dorsal aortic ramus in the interspace between it and somite II, which is clearly delimited and well differentiated. By 10 somites the first recognizable somite is the original somite II, and it is so regarded in the enumeration above.

THE OPTIC PRIMORDIUM AND THE BOUNDARY BETWEEN FOREBRAIN AND MIDBRAIN

Ten of the embryos studied show no optic foveolae. In most of them the neural folds are domed. In all but 2, however, there are indications of an optic primordium. Thus, at the rostral end the neural folds have thickened laterally, ranging from 37 to 44 microns as compared with 25 to 34 microns medially. In 4 of the group the transition is abrupt so that a limiting sulcus can be recognized (see arrows in figs. 14, 15, and 17, pl. 2). In 3 embryos the thickened area has a wider marginal velum (see arrows, fig. 14, pl. 2; fig. 23, pl. 3), and in 2 specimens the area has flattened where the neural folds are widest (compare fig. 14 with fig. 15, pl. 2). When traced back from later stages the thickened area is seen to be the primordium of the optic vesicle (see text figs. 1–7). The evidence for this statement is the following:

Three embryos (5- to 6-somite littermates) present

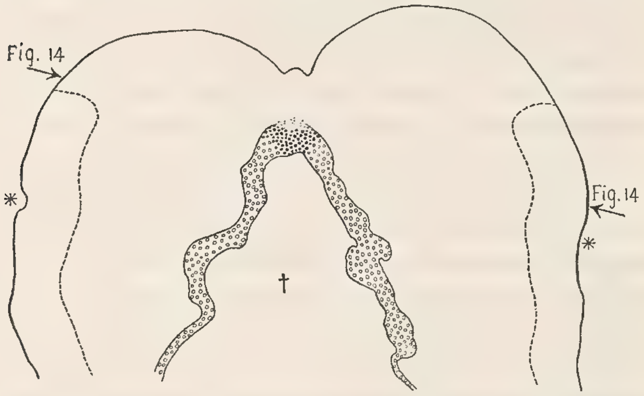

Fig. 1. Projection reconstruction on horizontal plane of fore- and midbrain of a 4-somite embryo (see p. 5). Form relations of yolk sac, embryo, and amnion well preserved by fixing in formol-chrome-sublimate, double embedding, and sectioning at 7 microns. Plane of section shown by arrows which indicate location of figure 14, plate 2. Forebrain-midbrain sulcus indicated by * (see p. 10). Broken lines mark extent of lateral crest primordium which extends through fore-, mid-, and hindbrain. Coarse stipple shows chorda with prechordal plate at its end (fine stipple). Entoderm indicated by circles. † marks location of anterior intestinal portal. W47L5.[1] × 200.

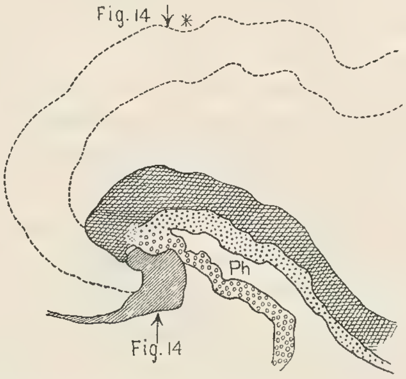

Fig. 2. Midsagittal projection reconstruction of same embryo as in figure 1. Profile based on contours of yolk sac and allantois (see p. 5). Notch marked by * corresponds to constriction of neural folds indicated in figure 1 and is interpreted as pros-mesencephalic sulcus. Longitudinal axis of forebrain is at an angle of about 120° to that of midbrain, indicating region of cranial flexure. Profile of right neural fold indicated by broken lines. Floor of neural groove, cross-hatched; head entoderm hatched. *Ph,* lumen of pharynx. Other conventions as in figure 1. × 200.

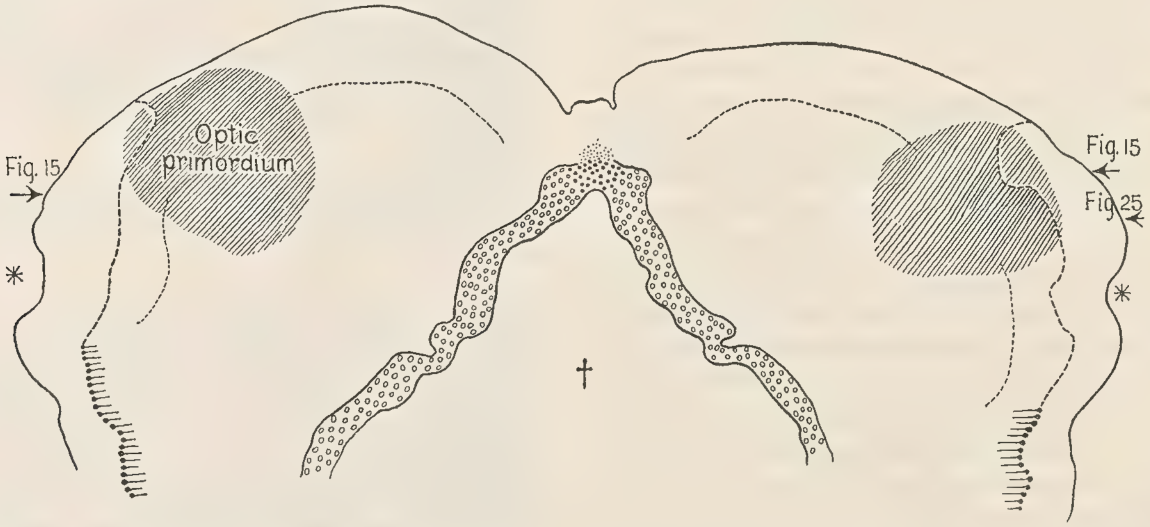

Fig. 3. Reconstruction of a 5-somite embryo fixed in formol, mordanted in Os_2O_4, and double embedded. Forebrain foreshortened in this projection in horizontal plane of head (see fig. 4). Pros-mesencephalic sulcus marked by *. Hatched area of forebrain corresponds to the optic primordium identified by thickening of neural epithelium (compare fig. 5). Location of figures 15, pl. 2, and 25, pl. 4, marked by arrows. Fine broken line marks boundary between neural crest and paraxial mesenchyme. Heavy broken line indicates position of lateral crest primordium; area of midbrain proliferating neural crest indicated by hatching. † marks location of anterior intestinal portal. Chorda and entoderm as in figure 1. GH60L4. × 200.

[1] The embryos are designated as follows: W47 indicates the color and number of the rat; L5 marks the embryo as the fifth implantation site from the tubal junction on the left.

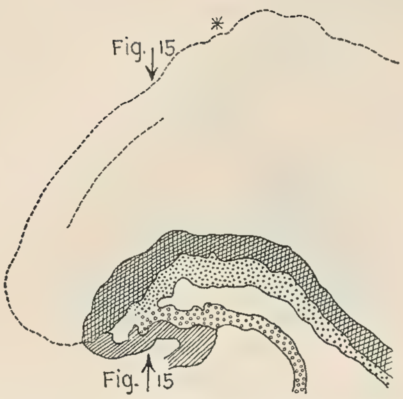

Fig. 4. Midsagittal reconstruction of same embryo as in figure 3. Profile of embryo controlled by contour of yolk sac in photograph of intact specimen (fig. 8, pl. 1). Arrows indicate plane of section and locus of figure 15, plate 2. Depression at * corresponds to pros-mesencephalic sulcus. Other conventions as in figure 2. × 200.

stages from the flattened thickening to well developed optic foveolae. Figure 3 is a reconstruction of the earliest stage in which the optic primordium could be plotted accurately. Here only the thickened forebrain areas are present. In the second embryo of this group there is an adumbration of a foveola on one side beginning 24 microns from the tip of the neural fold and extending for 66 microns; on the other side the corresponding area is only flattened. In the third specimen, figure 5, both foveolae reach a depth of 10 microns (compare fig. 17, pl. 2). The optic primordium serves to indicate the region of the forebrain. In 5 embryos with well developed foveolae, and also in 2 of earlier stages, all of which have been reconstructed graphically, there is a short but definite constriction of the neural folds immediately caudal to the optic primordium (* in figs. 1 to 7). It can be interpreted as the sulcus between forebrain and midbrain and can be traced back to a 4-somite stage (fig. 1). The thickened area of the neural folds in

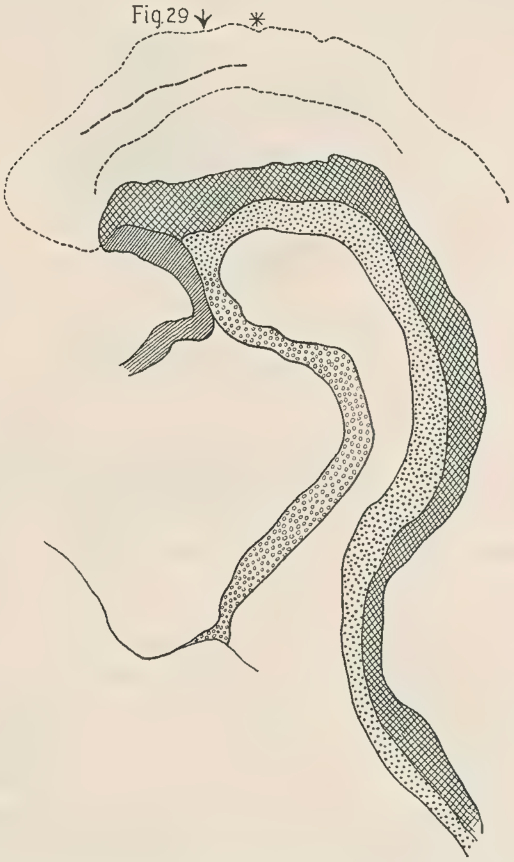

Fig. 6. Midsagittal projection of same embryo as in figure 5. Profile of neural fold based on contours of embryo and yolk sac of 6- to 7-somite embryo shown in figure 11, plate 1. Fine broken lines indicate thickness of neural epithelium. Coarse broken line marks center of optic sulcus. × 200.

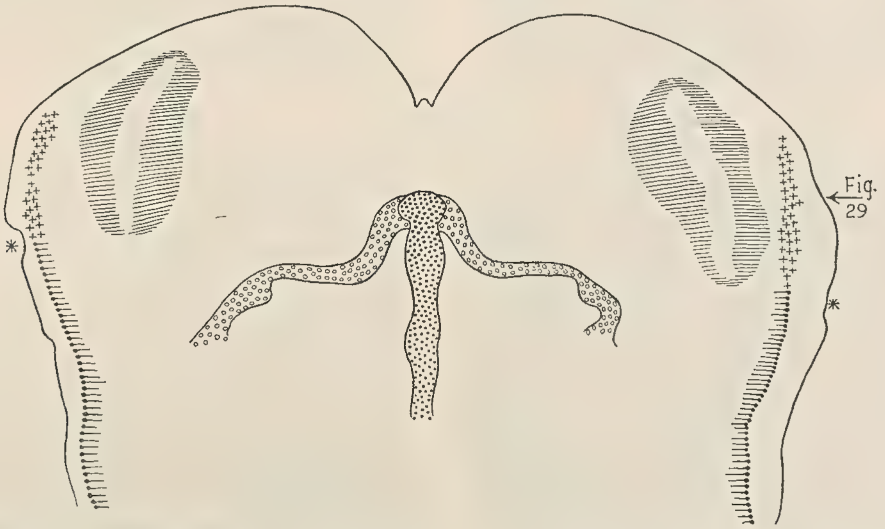

Fig. 5. Horizontal projection reconstruction of a 6-somite embryo with well developed optic foveolae. Optic primordium hatched except for middle of optic sulcus. Junction of fore- and midbrain marked by caudal ends of optic primordia and pros-mesencephalic sulcus (*). Primordium lateral to optic area is proliferating crest (+ + +, see fig. 29, pl. 5). It is continuous with midbrain crest (hatching) (see p. 9). Figure 33, plate 6, shows appearance of midbrain proliferation (compare with fig. 32). Other conventions as in figure 1. GH60R4. Fixed in modified Flemming, embedded in celloidin-paraffin, and cut at 5 microns. × 200.

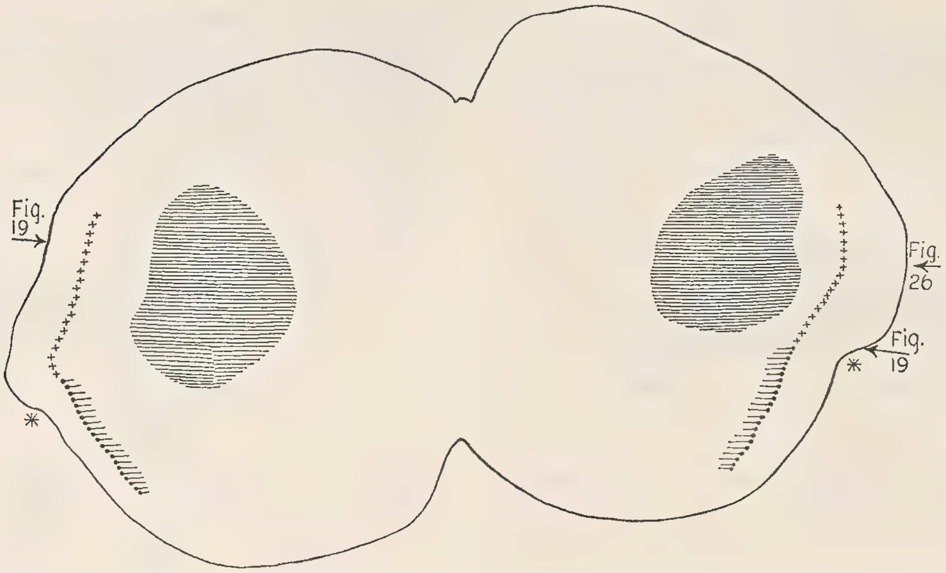

Fig. 7. Horizontal projection of forebrain and part of midbrain of a 6- to 7-somite embryo similar to embryos of figures 9, 10, and 11, plate 1. Cut perpendicular to forebrain. Plane of section marked by arrows showing location of figures 19, plate 2, and 26, plate 4. Optic primordia outlined by hatching. Extent of forebrain crest proliferation indicated by + + +; midbrain proliferation hatched. W67R2. × 200.

the 4-somite embryo is rostral to the sulcus. In the later stages the forebrain folds are growing wider as the foveola deepens. (Compare figs. 17 and 19, pl. 2.) In the embryo of figure 19 the plane of section was transverse to the forebrain, which is widest at this level (see fig. 7, based on a similar embryo). The appearance of the surface view of the intact embryo at this stage is shown in figures 9 and 10, plate 1. The constriction between forebrain and midbrain is indicated by arrows in figures 9 and 10. Figure 11 (pl. 1) shows a profile of a similar embryo. The cranial flexure in this specimen obviously is not as acute as in the models figured by Adelmann (1925, figs. 12 and 13). The broad saucer-like forebrain of rat embryos characteristic of this period resembles that of the human embryo H87 (Bartelmez, 1922, fig. 3) and the rhesus embryo of figure 216C, plate 29, in Heuser and Streeter (1941). The widening of the neural folds before their elevation is also found in other mammalian embryos and cannot be regarded as abnormal.

As the neural folds arise the foveolae deepen rapidly (fig. 20, pl. 3) and soon become directed laterally so that in sections the typical form of the primary optic vesicle appears (figs. 21, 22, pl. 3). This regularly occurs some time before the closure of the anterior neuropore.

The process of closure progresses at various rates in different embryos, for it cannot be correlated with either the differentiation of the neural folds, the number of somites, or any other feature. As figures 20 to 23, plate 3, show, the primary optic vesicle is enveloped by a sheath of crest cells from the outset. These cells are derived from the lateral edges of the forebrain folds. (See below.)

TRANSITIONAL ZONE AND NEURAL CREST OF THE FOREBRAIN

The early neural folds are domed, and the neural epithelium appears to continue as such onto the rounded lateral edge. Here it is definitely thicker than the adjoining epiblast. The epithelium gradually thins out toward the lateral head fold (fig. 14, pl. 2). In some embryos of the 3- to 4-somite period the lateral extremity of the neural fold and the adjacent epiblast differ from the definitive neural epithelium in that they lack the basement membrane (fig. 24, pl. 4). Sometimes this region can be distinguished under low magnification by its vacuolated appearance, which results from the shrinkage of many cells during the technical procedure and probably indicates an especially high water content of the cytoplasm. This differentiated zone extends throughout the rostral end of the embryo and can be termed "transitional zone." It clearly corresponds to the "Zwischenstrang" of His (1868). Mitoses are especially abundant at the lateral extremity; the region soon becomes differentiated from the adjacent neural epithelium by the irregularly arranged nuclei. The radial arrangement, typical of the neural folds, is lost, owing to several factors. Cell divisions in rapid succession result in groups of nuclei smaller than their neighbors. Sometimes mitoses are completed in the midst of the epithelium, the nuclei not being shifted to the future ependymal surface during early prophase as is usual in the neural folds and neural tube. The thickening and overgrowth of the neural epithelium produce a "lateral lip" which reaches a thickness of 98 microns by the time the optic primordium is well differentiated (see fig. 15, pl. 2; fig. 25, pl. 4). Until the neuropore becomes a mere slit, the lateral lip is a prominent feature of the embryo (fig. 12, pl. 1; figs. 17, 19, pl. 2; figs. 20, 21, pl. 3).

Lateral lip. With the continued widening of the forebrain folds, the lateral lip becomes bilaminar as the neural epithelium spreads laterally beyond the transitional zone. The dorsal lamina of the lip is accordingly neural epithelium which will contribute to the thalamus; the ventral lamina is the thickened dorsal part of the transitional zone (figs. 17, 19, pl. 2). Since the bilaminar lip is confined to the region of the optic primordium, it too is a characteristic feature of the forebrain. The ventral lamina may thicken and have three to five ranks of nuclei so that it comes almost into contact with the overlying dorsal lamina (fig. 17, pl. 2, left). Rostrally a sprout of the primary carotid artery enters between the two laminae, neither of which has a basement membrane. The inner ranks of the ventral lamina promptly disaggregate, and then the core of the lip consists of typical neural crest cells (fig. 26. pl. 4). This process begins at the middle of the forebrain and spreads to its caudal end, paralleling the optic primordium (figs. 5, 7, pp. 7, 8). After this massive delamination, single cells continue to migrate into the core of the lip (figs. 30, 31, pl. 5). Sometimes the ventral lamina remains thin and only individual cells or small groups appear to be separating from it (figs. 28, 29, pl. 5). As the crest cells accumulate they spread medially. They are clearly differentiated from the flattened paraxial mesenchyme cells, which have smaller nuclei and delicate processes that fade out into invisibility (figs. 32, 33, pl. 6). The migrating crest cells with their deeply staining spheroidal nuclei, coarse irregular nucleoli, and dense blunt cytoplasmic processes appear under low magnification as a dark cloud so long as they remain close together (fig. 19, pl. 2; fig. 32, pl. 6). These evidences of crest formation at optic levels effectually dispose of the suggestion that the neural crest in the forebrain is simply midbrain crest that has spread forward.

As the neural folds of the forebrain rise up and the optic vesicle balloons out, the lateral lip becomes thinner and narrower (figs. 20, 21, pl. 3). The 9-somite embryo from which figure 21 was taken still shows evidences of migration from the crest primordium (fig. 27, pl. 4). Such migration was found in 7 other embryos along the lips of the narrowing anterior neuropore. In one of these embryos, which had 13 somites, no migration from the optic vesicle was observed. After crest formation from the vesicle begins, the lateral crest primordium disappears as such.

In 6- to 7-somite stages the proliferation from the forebrain establishes continuity with the crest from the midbrain and becomes closely applied to the surface epithelium of the developing mandibular arch (fig. 19, pl. 2, left). This surface epithelium is, in part at least, derived from the transitional zone of 3- to 4-somite stages. It likewise contributes cells to the forebrain crest. Although evidences for this statement are not abundant in the present material, they are unmistakable (figs. 34, 35, pl. 6). In one embryo a group of seven cells appears as an excrescence on the epiblast, projecting into the strand of crest cells (fig. 33, pl. 6). It may be that the cells leave the epithelium very rapidly so that stages in migration are rarely encountered.

The extent and relations of the crest which spreads into the maxillomandibular region and which arises in part from the mandibular epiblast will require the study of more embryos from the 6- to 9-somite period than are available at present. Detailed models will have to be prepared to show the relations clearly. It is at least worth noting that, shortly after the crest spreads into this region, the mandibular arch becomes a prominent feature of the head (compare fig. 11 with fig. 13, pl. 1).

NEURAL CREST FROM THE PRIMARY OPTIC VESICLE

In the rat most of the crest cells in the forebrain arise from the lateral crest primordium. There are, however, cells that migrate from the walls of the optic vesicle which also contribute to its sheath. This migration is not so prominent a feature of the early vesicle as in *Homo,* but it is readily demonstrated. The course of events is similar in the two species as far as the appearances in histologic preparations are concerned. The stages in the rat can be seriated as follows:

In 8-somite embryos the marginal velum of the optic vesicle is obscured by the shifting of many nuclei toward the mesenchymal surface. (Compare the lateral with the superior and inferior surfaces of the vesicles in fig. 23, pl. 3.) As some cells become actively amoeboid, pseudopods extend out among the adjacent crest cells and the basement membrane disappears (figs. 40, 41, pl. 8). Under low magnification no boundary can be drawn between the neural epithelium and the crest because of this interdigitation (fig. 22, pl. 3). These conditions can be seen more clearly in figure 42, plate 8. This figure and the other figures on plates 7 and 8 show transitions between cells that extend through the entire wall of the vesicle and have small pseudopods (* in fig. 38, pl. 7) and cells that have only a slender tongue of cytoplasm still within the epithelium (arrows in figs. 40, 41, 42, pl. 8). The arrow at the left in figure 38 (pl. 7) presents a transition between an emerging cell and the cells in mitosis at the middle of figure 40 (pl. 8) which are free. Such rounded cells occupying dimples in the surface of the vesicle are rather common; frequently they are in mitosis. They may well be cells that have just separated from the epithelium. They have not been included in the enumerations cited below, however.

Among 43 embryos with primary optic vesicles 120 cells had pseudopods or the cell bodies projecting well beyond their neighbors. Of these embryos 80 per cent belong to the 11- to 14-somite period. Stages in migration were observed on all surfaces of the vesicle; the majority (66 per cent) were on the lateral surface. In 7 additional embryos groups of two or more cells protruded from the surface, apparently on the way out. (See arrows in fig. 41, pl. 8.)

Mitotic figures occasionally found at the mesenchymal surfaces of the neural epithelium (figs. 36 arrow, 37, pl. 7) occur in all regions of the embryo where crest cells are arising, and in early stages of proliferation they are more common in the midbrain and hindbrain than in the forebrain. Among 60 embryos between 8 and 14 somites, 7 of these mitoses were found on the outer surface of the optic vesicle.

The dividing cell indicated by the arrow in figure 36 (pl. 7) is still within the neural epithelium. It can be interpreted as a cell that shifted to the mesenchymal rather than to the ependymal surface before or during the early prophase and was in the process of liberating a daughter cell to the crest[1] (fig. 39, pl. 7; fig. 40, pl. 8). It is also possible that the cells in figures 36 and 37 had migrated to the mesenchymal surface and had begun to divide before separating from the epithelium. Dividing cells are frequently found closely applied to the surface of sites of crest formation, and it may be that, as in tissue cultures, isolation serves as a stimulus to cell division.

Toward the end of crest proliferation, collagenic fibers begin to appear in the paraxial mesenchyme but are rare in the sheath of the optic vesicle. Such fibers as are present are closely associated with cells which have smaller nuclei than the majority of sheath cells, indicating that there are few paraxial mesenchyme cells in the sheath aside from occasional perivascular cells.

DISCUSSION

The question of proliferation of crest cells from the forebrain resolves itself into the demonstration of the boundary between forebrain and midbrain. Any adequate series of stages shows that the early optic primordium extends as far as the sulcus between forebrain and midbrain. When the vesicle is followed back to 5- to 6-somite stages, in which the evagination has begun with the appearance of the foveola, the optic primordium can be delimited. Its caudal end defines the caudal end of the forebrain. There is abundant evidence of proliferation from this level of the transitional zone between neural fold and head epiblast. This part of the primordium is coextensive with the optic primordium. Forebrain crest cannot therefore be denied in the rat. Additional evidence is provided by the presence of a short constriction of the neural folds immediately caudal to the optic primordium in these early stages. This constriction can be seen as a notch caudal to the left foveola in the portrait of an intact embryo taken in 80 per cent alcohol before any obvious shrinkage had occurred (figs. 9, 10, pl. 1). It is present also in the reconstructions at * in text figures 1 to 7 (pp. 6–8). It can be followed accordingly to a 4-somite stage. It could easily be overlooked or dismissed as an artifact in a Born wax plate model, especially one based on an embryo embedded in paraffin alone. Since it appears in different sections on the two sides in my reconstructions of double-embedded embryos, it can hardly be dismissed as due to artificially distorted sections.

A third piece of evidence on the origin of crest cells from the forebrain is the distinctive form of the crest primordium from which they arise. Where the crest primordium is coextensive with the optic primordium it comes to lie ventral to the neural epithelium as the neural folds expand (figs. 15, 17, 19, pl. 2; figs. 25, 26, pl. 4), producing the "bilaminar lateral lip" (see p. 9). Crest arises only from the ventral lamina of the lip. In the midbrain, on the other hand, the crest primordium constitutes the entire lateral extremity of the neural fold (fig. 16, pl. 2), which disaggregates *in toto* during proliferation (fig. 33, pl. 6). Transitions between the two types of crest formation are seen in the region of the sulcus between fore- and midbrain (fig. 33, pl. 6). Cytologically, however, the evidences of migration are the same in all regions of the head that produce neural crest.

It may be added that pseudopods which extend from the mesenchymal surface of the crest primordium and of the optic vesicle are not secretion blebs such as appear on the ependymal surfaces. In appropriately fixed material they are protoplasmic extensions with mitochondria and other granules such as characterize the cytoplasm.

This evidence of the formation of crest at forebrain levels fully confirms the observations of Celestino da Costa (1920 to 1931) in the guinea pig, adding cytologic data to his histologic findings. The subsequent migration of cells and small cell groups from the primary optic vesicle in the rat (pls. 7, 8) is essentially similar to that in man (Bartelmez, 1954). It differs only in being less extensive in the rat, as might be expected in view of the extensive proliferation from the lateral crest primordium of the forebrain of which no clear evidence has been found in *Homo*. It is worth noting that the lateral surface of the primary optic vesicle which in the rat is most active in proliferating crest cells is the surface that gives rise to the nervous layer of the retina.

---

[1] A striking example of this type of crest-cell formation is presented in figure 11 of Bartelmez (1960).

Speculations on the fate of the crest of the forebrain. The admirably controlled experiments of Rawles (1940, 1947) demonstrated the origin of pigment cells from the spinal neural crest in the mouse. Since this origin has been established in all other classes of vertebrates (see reviews by DuShane, 1943, 1944, and Rawles, 1952) it would seem probable that it holds for mammals in general. The investigation of the forebrain crest by Rawles' methods can be expected to show that the pigment cells of the uvea, and the meninges as well, have the same origin. It may be that only pigment cells arise from the crest which Harvey and Burr (1926) and Flexner (1929) found contributing to the leptomeninges in Amphibia. The proof in anamniotes that crest cells, indistinguishable from other mesenchyme cells, eventually give rise to the various types of pigment cells, to branchial cartilages, and to connective tissue makes it obvious that the potentialities of the crest can be established only experimentally in species which have no cytologic characters that identify them throughout the entire period of differentiation.

The forebrain crest is so extensive in the rat that it may well be expected to produce more than pigment cells. There are few degenerating cells. It does not give rise to ganglion cells but presumably produces neurilemma cells. Its spread into the prospective maxillomandibular area suggests specific contributions to this region as is certainly true in Amphibia. The close association of the mandibular ramus of nerve V with Meckel's cartilage is of interest in this connection.

There is no basis for interpreting the cells that migrate from the epiblast of the head in the rat. In the embryos studied there is nothing resembling a discrete ophthalmicus profundus placode, nor is there evidence of a discrete epibranchial placode associated with the Gasserian ganglion such as Landacre (1932) found contributing to the geniculate ganglion in the rat.

SUMMARY

The optic primordium can be identified in 4-somite stages as a thickening of the neural folds (pl. 2) and can be followed to stages with optic vesicles. Its caudal end serves to identify the boundary between forebrain and midbrain, which is indicated also by a constriction of the neural folds (figs. 1 to 7, pp. 6–8).

In embryos of 4 to 5 somites the primordium of the neural crest is differentiated in forebrain, midbrain, and hindbrain levels as a transitional zone adjoining the neural epithelium (p. 8; figs. 14 to 16, pl. 2; fig. 24, pl. 4).

In the forebrain the lateral expansion of the neural folds at the level of the optic primordium brings the crest primordium ventral to it, producing a prominent bilaminar "lateral lip" in 5-somite stages (figs. 17, 19, pl. 2). As a result, only the ventral moiety of the lip and the adjacent epiblast produce neural crest (pl. 5; fig. 32, pl. 6). In the midbrain, on the other hand, the crest primordium comprises the lateral extremity of the neural fold (fig. 16, pl. 2), and subsequently the entire edge of the neural fold appears to be dissociating into crest (fig. 33, pl. 6). The mode of origin of the crest, as well as the optic primordium, serves to differentiate forebrain from midbrain.

The migration of neural crest cells in the forebrain begins in some 5-somite embryos. Individual cells may leave the crest primordium (figs. 28, 29, pl. 5), or the inner strata of the thickened primordium may disaggregate into free crest cells (fig. 26, pl. 4; figs. 30, 31, pl. 5; fig. 32, pl. 6). This proliferation reaches its height in 6- to 7-somite stages and then disappears in caudal forebrain levels as the neural folds arise and the optic vesicle takes form. Subsequently the crest primordium is confined to the lips of the anterior neuropore (fig. 27, pl. 4), where it persists and proliferates until the migration from the primary optic vesicle begins.

The proliferation from the primary optic vesicle is largely a migration of individual cells; most of them come from the lateral surface of the vesicle (pls. 7, 8). It is not so extensive as in man, but the evidences of migration are the same. In the rat it reaches its height in 11- to 14-somite stages.

The bulk of the connective tissue sheath of the optic vesicle consists of crest cells. They do not produce collagenous fibers as early as the smaller paraxial mesenchyme cells, which seem to be few and far between except as perivascular cells.

The epiblast of the prospective mandibular arch region gives rise to crest cells (figs. 34, 35, pl. 6).

As the changes in neural crest formation are more rapid than the formation of somites, a close series based on somite number is wholly inadequate for following the development of the neural crest.

ADDENDUM

After this paper was submitted for publication a reprint of an address by the late J. P. Hill came to hand. It had been delivered to the Anatomical Society of Great Britain and Ireland in 1920 but had not been published. Professor Hill and Dr. Katharine M. Watson observed the contributions of neural crest and epibranchial placodes to the various cranial ganglia and also concluded that crest "furnishes the bulk of the mesenchyme of the mandibular arches."

Dr. T. Thomas Flynn, who is working over the manuscripts left by Professor Hill, has published this abstract:

The early development of the brain in marsupials. By J. P. Hill and K. M. Watson, 1958, Jour. Anat., vol. 92, pp. 493–497.

LITERATURE CITED

Adelmann, H. B. 1925. The development of the neural folds and cranial ganglia of the rat. *J. Comp. Neurol., 39,* 19–171.

Balfour, F. M. 1878. *A Monograph on the Development of Elasmobranch Fishes.* London, 295 pp.

Bartelmez, G. W. 1922. The origin of the otic and optic primordia in man. *J. Comp. Neurol., 34,* 201–232.

Bartelmez, G. W., and M. P. Blount. 1954. The formation of neural crest from the primary optic vesicle in man. *Carnegie Inst. Wash. Publ.* 603, *Contribs. Embryol., 35,* 55–71.

Bartelmez, G. W. 1960. Neural crest from the forebrain in mammals. In memoriam amici Normand Hoerr. *Anat. Record, 138,* 269–281.

Brauer, A. 1904. Beiträge zur Kenntnis der Entwicklung und Anatomie der Gymnophionen, IV. *Zool. Jahrb. Suppl. 7,* 409–428.

Celestino da Costa, A. 1920. Note sur la créte ganglionnaire cranienne chez le Cobaye. *Compt. rend. soc. biol.* (*Paris*), *83,* 1651.

Celestino da Costa, A. 1931. Sur la constitution et le développement des ébauches ganglionnaires craniens chez les mammifères. *Arch. biol.* (*Liége*), *42,* 71–105.

Chiarugi, G. 1894. *Contribuzioni allo studio dello sviluppo dei nervi encefalici nei mammiferi.* Firenze, 71 pp., 3 tavole.

Dohrn, A. 1902. Weitere Beiträge zur Beurteilung der Occipitalregion und der Ganglienleiste der Selachier. *Mitt. Zool. Sta. Neapel., 15,* 555–654.

DuShane, G. P. 1943. The embryology of vertebrate pigment cells. 1. Amphibia. *Quart. Rev. Biol., 18,* 109–127.

DuShane, G. P. 1944. The embryology of vertebrate pigment cells. 2. Birds. *Quart. Rev. Biol., 19,* 228–262.

Flexner, L. B. 1929. The development of the meninges in Amphibia: a study of normal and experimental animals. *Carnegie Inst. Wash. Publ.* 394, *Contribs. Embryol., 20,* 31–50.

Goronowitsch. 1893. Untersuchungen über die Entwicklung der sogenannten Ganglienleisten im Kopfe der Vogelembryonen. *Morphol. Jahrb., 20,* 187–259.

Grynfeltt, E. 1898. Sur le développement du muscle dilatateur de la pupille chez le lapin. *Compt. rend. acad. sci.* (*Paris*), *127,* 966–968.

Harvey, S., and H. Burr. 1926. The development of the meninges. *Arch. Neurol. Psychiat., 15,* 545–565.

Heard, O. O. 1957. Methods used by C. H. Heuser in preparing and sectioning early embryos. *Carnegie Inst. Wash. Publ.* 611, *Contribs. Embryol., 36,* 1–18.

Herrick, C. J. 1899. The cranial and first spinal nerves of *Menidia. J. Comp. Neurol., 9,* 153–455.

Heuser, C. H., and G. L. Streeter. 1941. Development of the macaque embryo. *Carnegie Inst. Wash. Publ.* 525, *Contribs. Embryol., 29,* 15–55.

His, W. 1868. *Untersuchungen über die erste Anlage des Wirbeltierleibes. Die erste Entwickelung des Hühnchens im Ei.* Leipzig, 237 pp.

His, W. 1879. Ueber die Anfänge des peripherischen Nervensystemes. *Arch. Anat. u. Physiol., Anat. Abt.,* pp. 455–482.

Holmdahl, D. E. 1928. Die Entstehung und weitere Entwicklung der Neuralleiste (Ganglienleiste) bei Vögeln und Säugetieren. *Z. mikrosk.-anat. Forsch., 14,* 99–289.

Hörstadius, S. 1950. *The Neural Crest.* Oxford University Press, London, 111 pp.

Johnston, J. B. 1898. The hind brain and cranial nerves of *Acipenser. Anat. Anz., 14,* 580–602.

Kastschenko, N. 1888. Zur Entwicklungsgeschichte des Selachierembryos. *Anat. Anz., 3,* 445–467.

Kupffer, C. v. 1895. *Studien zur vergleichenden Entwicklungsgeschichte des Kopfes der Cranioten. Heft III: Die Entwicklung der Kopfnerven von Ammocoetes planeri.* Munich, 80 pp.

Landacre, F. L. 1910. The origin of the cranial ganglia in *Ameiurus. J. Comp. Neurol., 20,* 389–411.

Landacre, F. L. 1914. Embryonic cerebral ganglia and the doctrine of nerve components. *Folia Neurobiol., 8,* 601–615.

Landacre, F. L. 1921. The fate of the neural crest in the head of urodeles. *J. Comp. Neurol., 33,* 1–43.

Landacre, F. L. 1932. The epibranchial placode of the facial nerve of the rat. *J. Comp. Neurol., 56,* 215–256.

Ortmann, R. 1943. Ueber Placoden und Neuralleiste beim Entenembryo, ein Beitrag zum Kopfproblem. *Z. Anat. Entwicklungsgeschichte, 112,* 537–587.

Platt, J. B. 1893. Ectodermic origin of the cartilages of the head. *Anat. Anz., 8,* 506–509.

Raven, Chr. P. 1931. Zur Entwicklung der Ganglienleiste. I. *Arch. Entwicklungsmech., 125,* 210–292.

Raven, Chr. P. 1933*a*. II. *Ibid., 129,* 179–198.

Raven, Chr. P. 1933*b*. III. *Ibid., 130,* 517–561.

Rawles, M. E. 1940. The development of melanophores from embryonic mouse tissues grown in the coelom of chick embryos. *Proc. Natl. Acad. Sci. U. S., 26,* 673–680.

Rawles, M. E. 1947. Origin of pigment cells from the neural crest in the mouse embryo. *Physiol. Zoöl., 20,* 248–266.

Rawles, M. E. 1952. Transplantation of normal embryonic tissues. *Ann. N. Y. Acad. Sci., 55,* 302–312.

Starck, D. 1937. Ueber einige Entwicklungsvorgänge am Kopf der Urodelen. *Morphol. Jahrb., 79,* 358–435.

Stone, L. C. 1922. Experiments on the development of the cranial ganglia and the lateral line sense organs in *Amblystoma punctatum. J. Exptl. Zool., 35,* 421–496.

Stone, L. C. 1929. Experiments showing the role of migrating neural crest (mesectoderm) in the formation of head skeleton and loose connective tissue in *Rana palustris. Arch. Entwicklungsmech., 118,* 40–77.

Strong, O. S. 1895. The cranial nerves of Amphibia; a contribution to the morphology of the vertebrate nervous system. *J. Morphol., 10,* 101–230.

Van Wijhe, J. W. 1883. Ueber die Mesodermasegmente und die Entwicklung der Nerven des Selachierkopfes. *Verhandel. Koninkl. Ned. Akad. Wetenschap. Amsterdam.*

Wen, I. Chuan. 1928. The anatomy of human embryos with seventeen to twenty-three pairs of somites. *J. Comp. Neurol., 45,* 301–376.

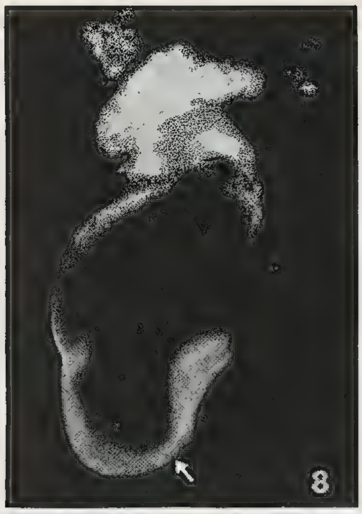

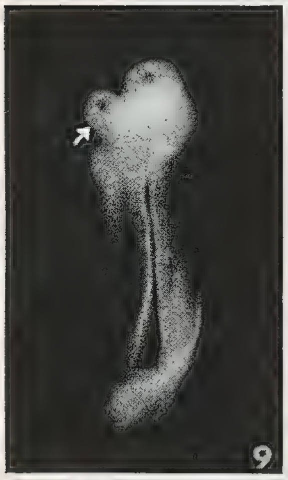

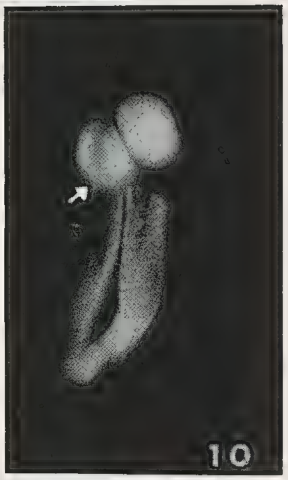

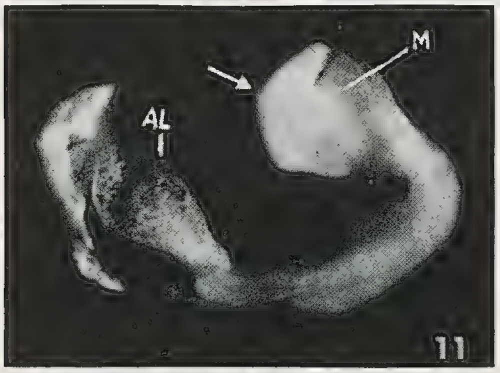

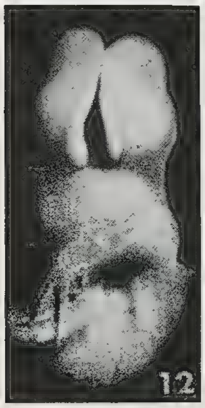

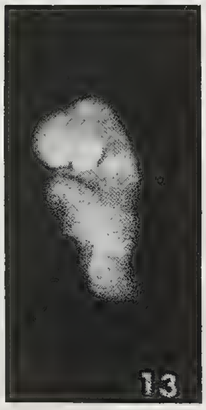

Plate 1. Rat embryos photographed in 80 per cent alcohol (except for fig. 8).

Fig. 8. Profile of a 5-somite embryo with amnion and yolk sac intact. Photographed in formol. × 20. Obtained 9 days 21 hours after insemination. Arrow indicates somite 2. Reconstructions of head are shown in figures 3 and 4, sections in figures 15, plate 2, and 25, plate 4.

Fig. 9. Dorsal view of forebrain of a 6-somite embryo showing optic foveolae in the broad forebrain plate (compare transverse section in fig. 19, pl. 2). Arrow indicates sulcus (notch) between fore- and midbrain. × 22. Obtained 10 days 12 hours after insemination (courtesy of Dr. L. G. Browman).

Fig. 10. Oblique view of same embryo to show the prominent "lateral lip" in the forebrain lateral to left foveola. Constriction (notch indicated by arrow) between forebrain and midbrain at left is adjacent to caudal end of foveola.

Fig. 11. Profile of a 6- to 7-somite embryo in which cranial flexure (indicated by arrow) is still greater than a right angle, and forebrain folds have not yet begun to rise; at left, allantois (*AL*) and part of yolk sac. *M,* mandibular arch. Obtained 10 days 6 hours after insemination.

Fig. 12. Frontal view of a 9-somite embryo, showing lateral lip at margin of anterior neuropore (see fig. 27, pl. 4). × 22.

Fig. 13. Profile of head of 10-somite embryo before impending change from U form to C form. Mandibular arch has become prominent (see p. 9). Obtained 10 days 13 hours after insemination. × 17.8.

Plate 2. Photomicrographs by R. Grill of transverse sections taken at 200 diameters.

Fig. 14. From 4-somite embryo taken at level of forebrain indicated in reconstruction (figs. 1 and 2, p. 6). Lateral thickening of left neural fold can be followed in succeeding stages and identified as optic primordium. It is also distinguished by a wide marginal velum. Arrow indicates its medial boundary. Brace includes epithelial area where basement membrane is lacking. This "transitional zone" subsequently produces neural crest (see p. 8). W47L5, section 14, taken 91 microns from rostral end of embryo.

Fig. 15. From a 5-somite embryo at forebrain level indicated in figures 3 and 4. Arrows point to limiting sulcus of optic primordium, which has grown wider and flatter. As this process continues, neural folds spread laterally and extend beyond transitional zone so that margin becomes bilaminar. Both laminae continue to thicken, and a "lateral lip" becomes prominent (see fig. 10, pl. 1). Its inferior lamina is the crest primordium. GH60L4, section 18, taken 90 microns from rostral end.

Fig. 16. Section from 4-somite embryo through *midbrain* showing characteristic form of lateral lip at this level where it consists entirely of crest primordium (compare fig. 17). W41L3. Section 28, 140 microns from rostral end.

Fig. 17. Section of 5-somite embryo passing at right through early optic foveola (inverted arrow). A more caudal level appears on left where primordium has flattened prior to appearance of optic sulcus. Continued lateral expansion of neural folds has produced a bilaminar lateral lip. Its dorsal lamina is prospective thalamic wall; its ventral lamina is the thickened part of transitional zone from which most of neural crest of forebrain arises. Arrow at right indicates medial boundary of optic primordium. BH99R1. Section 26, 104 microns from rostral end near end of head fold.

Fig. 18. From a more advanced 5-somite embryo through optic foveolae taken 68 microns from rostral end. At arrow, sprout from primary carotid has entered between laminae of lateral lip. Formation of neural crest from its ventral lamina at more caudal levels of this embryo is shown in figures 30 and 31, plate 5, and figure 32, plate 6. BH64R1. Section 17.

Fig. 19. From a 6- to 7-somite embryo cut perpendicular to surface of forebrain. It shows maximal expansion of forebrain folds before their elevation (see fig. 7, p. 8; figs. 9, 10, pl. 1). At right ramus of primitive carotid between laminae of lateral lip. Caudal (lower) end of section passes through rostral hindbrain (see fig. 11, pl. 1). Trigeminal ("cristal") sulcus indicated by †. Strand of crest cells closely applied to epiblast at left (compare fig. 33, pl. 6). *mand.,* mandibular arch. W67R2. Section 29, 145 microns from rostral end.

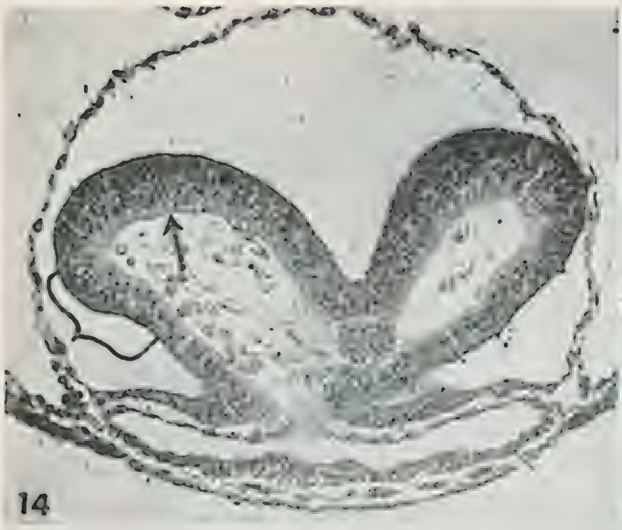
14

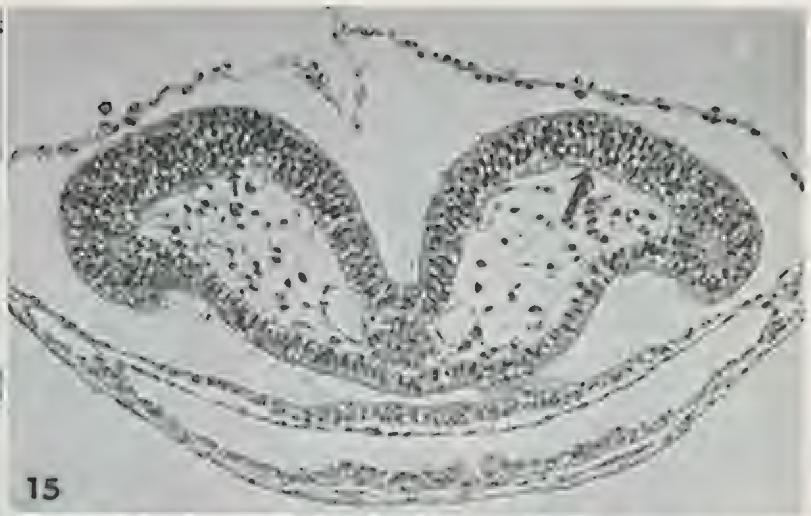
15

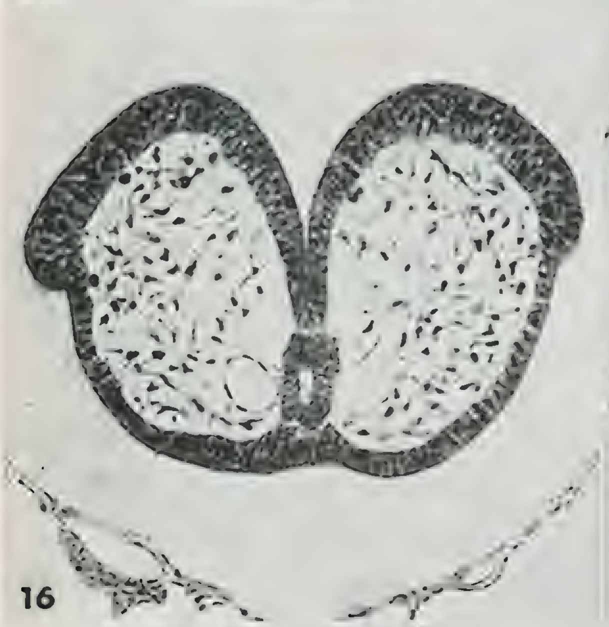
16

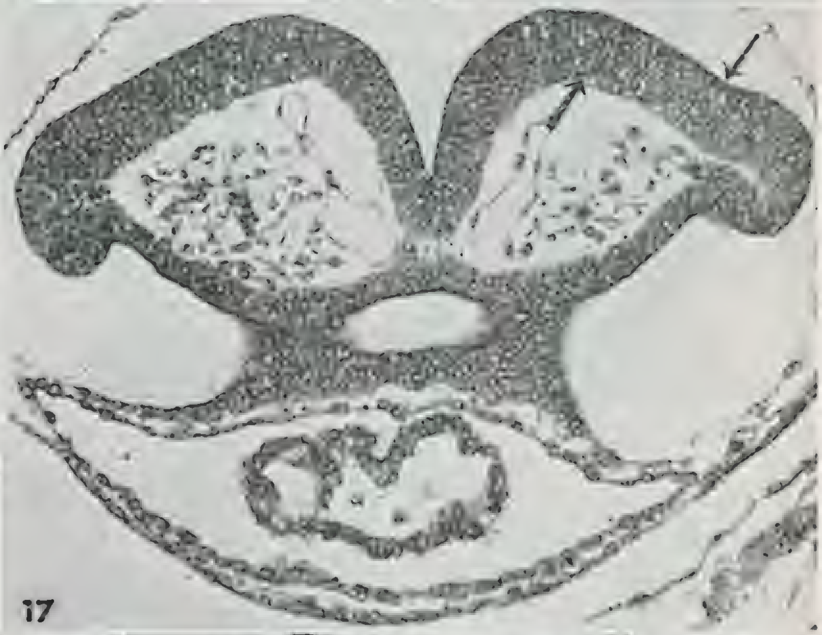
17

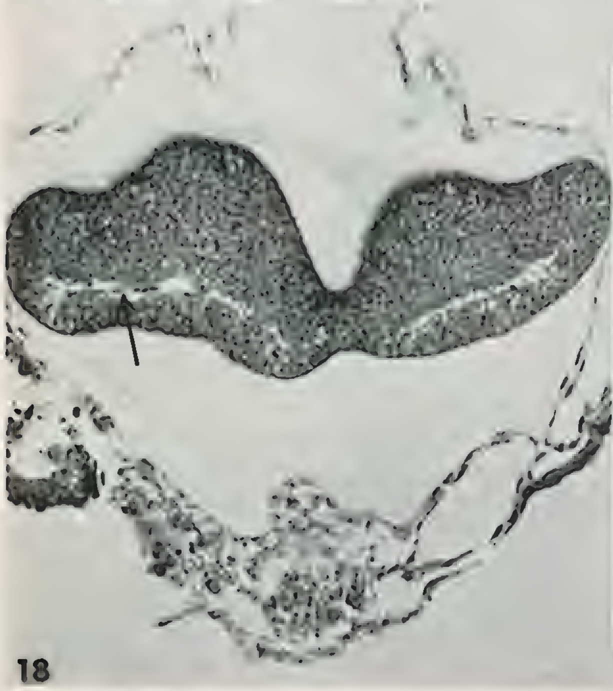
18

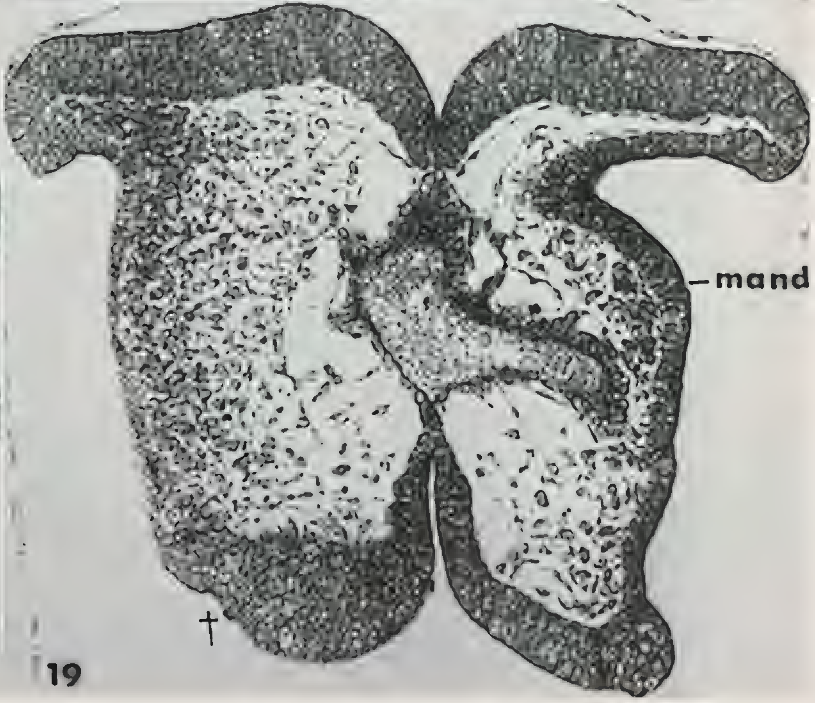
19

Plate 3. Photomicrographs from forebrain showing elevation of neural folds and formation of early optic vesicle. × 200.

Fig. 20. Early stage in elevation of forebrain folds in 8- to 9-somite embryo. On right, section passes through middle of foveola. Optic invaginations are becoming directed laterally, and lateral lip has been shifted dorsally. W22L2. Section 33, 231 microns from rostral end.

Fig. 21. From a 9-somite embryo with wide-open anterior neuropore (see fig. 12, pl. 1). Optic vesicle enveloped by sheath of crest cells derived from lateral crest primordium, which, on right, is in intimate contact with neural crest, to which it is still contributing cells (see fig. 27, pl. 4, taken from same embryo). Midbrain in this embryo is still a flat plate. W67L1.

Fig. 22. Transverse section of forebrain of 9-somite embryo in which neuropore has become slitlike. Neural folds are rising in midbrain. A "proliferating mitosis" was found on one optic vesicle (compare fig. 36, pl. 7), and two cells were migrating from its superior wall as in figure 41, plate 8. W28R3. Section 38.

Fig. 23. Longitudinal section of optic vesicle of a 15-somite embryo. Narrowing of optic lumen may be associated with rapid growth of future dorsal thalamic wall. Arrows indicate marginal velum of superior and inferior walls. Velum and basement membrane are absent on thin lateral wall from which cells are migrating. W34R6. Section 45.

20

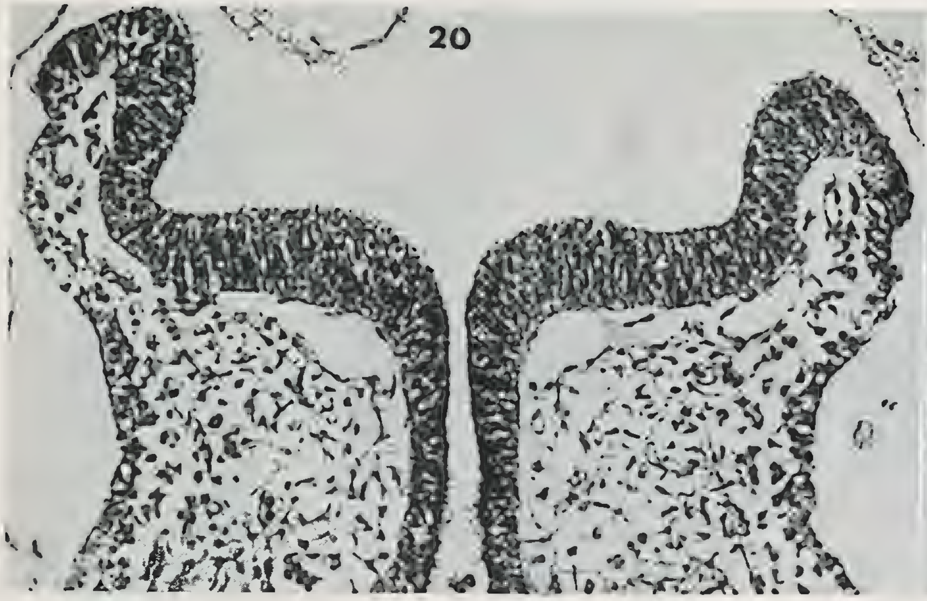

21

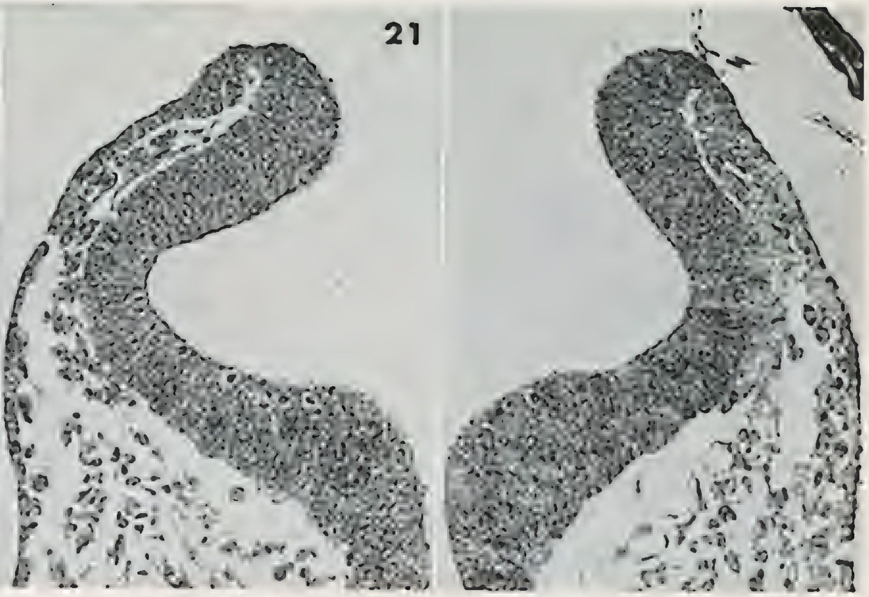

22

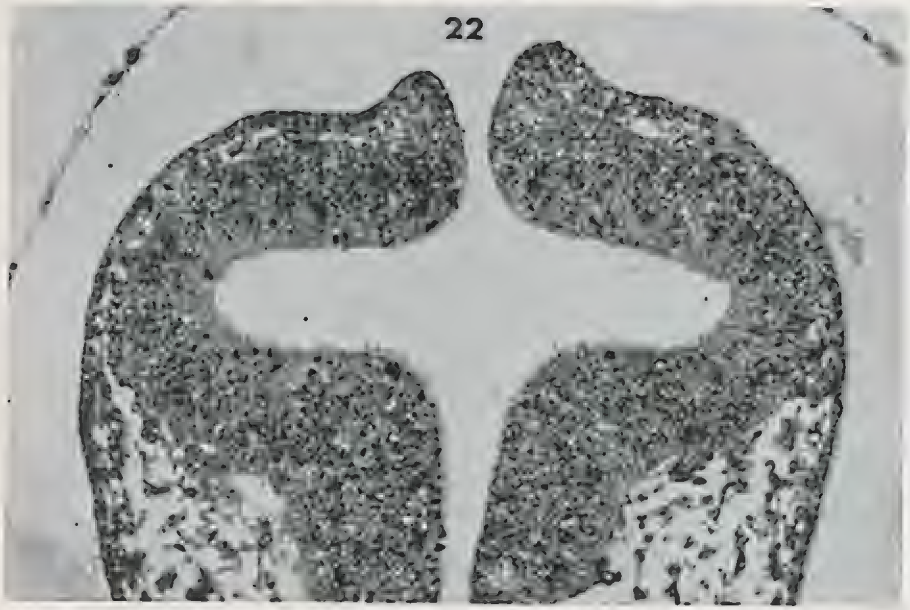

23

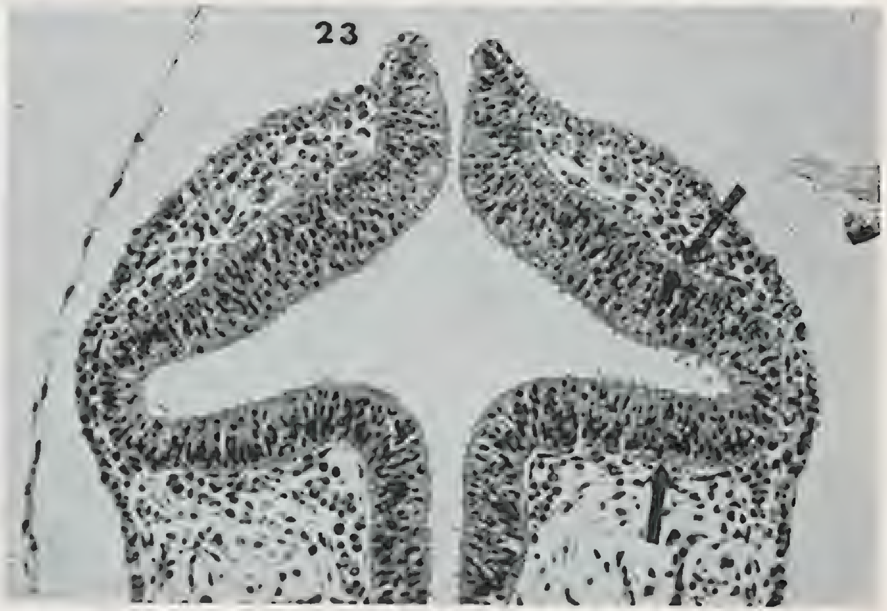

Plate 4. Development of neural crest primordium in forebrain. Dorsal side is up. Photomicrographs × 1000 Zeiss 3.0 mm. apochromatic immersion lens, aperture 1.40, ocular × 10.

Fig. 24. Crest primordium (indicated by brace) in a 4-somite embryo taken through forebrain, 96 microns from rostral end. Arrow marks end of basement membrane of neural epithelium; it is absent in primordium, which is also distinguished by numerous large vacuoles (see p. 8). Rostrocaudal extent of primordium is indicated in reconstruction of similar embryo (figs. 1, 2, p. 6). W41L1, fixed in modified Flemming, double-embedded in celloidin-paraffin, cut at 4 microns, and stained with iron hematoxylin.

Fig. 25. From the 5-somite embryo of figure 8, plate 1, taken 95 microns from rostral end. See projection reconstruction figures 3, 4, pages 6, 7. Crest primordium has thickened and shifted ventromedially as optic primordium expanded. Lateral lip is developing bilaminar form characteristic of forebrain. GH60L4, fixed in formol-saline, mordanted in osmic acid, double-embedded in celloidin-paraffin, cut at 5 microns, and stained with iron hematoxylin.

Fig. 26. Lateral extremity of neural fold from same 6- to 7-somite embryo as figure 19, plate 2. Lateral lip has two laminae: dorsal is neural epithelium, ventral is crest primordium, inner strata of which have disaggregated into typical neural crest cells. Arrow indicates center of optic foveola. Level of section indicated in figure 7. W67R2, fixed in acetic Zenker, double-embedded in celloidin-paraffin, cut at 5 microns, and stained with toluidine blue and erythrosin.

Fig. 27. Edge of neuropore of 9-somite littermate of the preceding. Cells are still migrating from crest primordium and contributing to sheath of optic vesicle. Borders of migrating cells accentuated with ink (compare fig. 34, pl. 6). Figure 21, plate 3, shows caudal level of forebrain. W67L1, fixed in Bouin, embedded in paraffin, cut at 5 microns, and stained with toluidine blue and erythrosin.

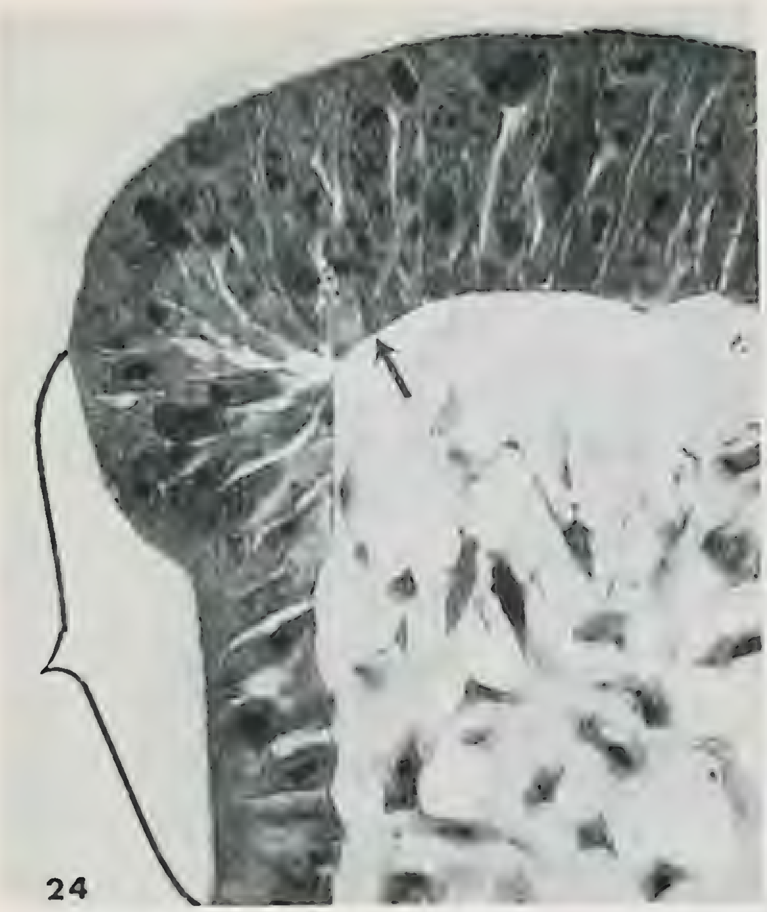

24

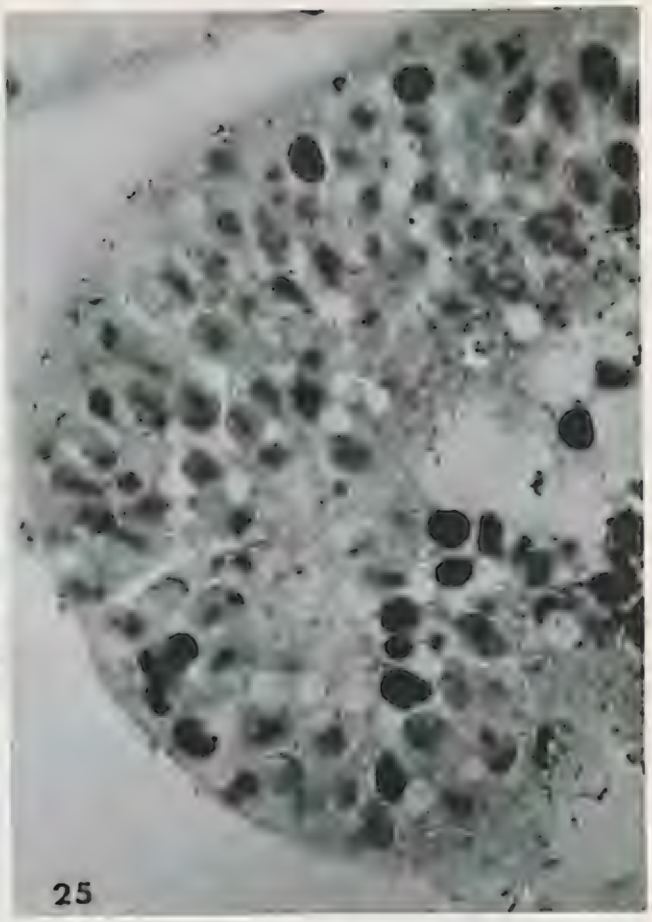

25

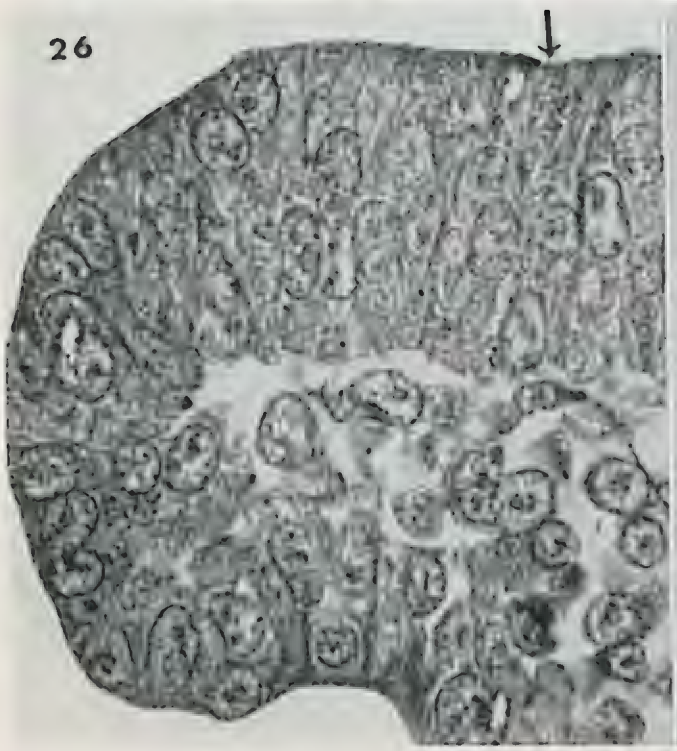

26

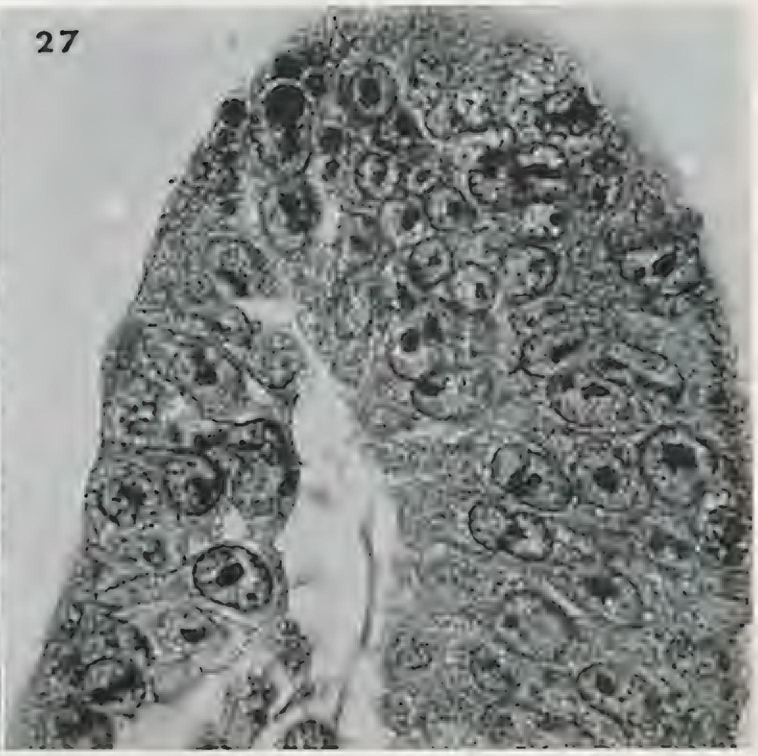

27

Plate 5. Neural crest proliferation in forebrain from ventral lamina of lateral lip. Borders of migrating cells accentuated with ink. Photomicrographs × 1000. Optical system as in plate 4.

Fig. 28. From a 5-somite embryo with early optic foveolae taken near the caudal end of forebrain. Cell migration from ventral lamina of lateral lip. Lower arrow indicates cell with peripheral pseudopod and slim peripheral end. Cell at right-hand arrow has progressed so that nucleus and most of cytoplasm are outside of epithelium. On either side of it are typical free neural crest cells. Arrow with ⁎ indicates end of basement membrane of neural epithelium. W60L2, fixed in acetic Zenker, embedded in paraffin, cut at 7 microns, and stained with Mallory-Azan.

Fig. 29. From a 6-somite embryo with early optic foveolae. Active proliferation from lateral lip. Taken from caudal forebrain, 108 microns from rostral end of embryo. Pseudopods of 6 cells extend between free crest cells of lateral lip. Two cells (⁎ ⁎) show stages in reduction of intraepithelial processes. Cell at left of group is almost free. Arrow marks end of basement membrane of neural epithelium. Level of section indicated in figures 5 and 6. GH60R4, fixed in modified Flemming, double-embedded in celloidin-paraffin, cut at 5 microns, and stained with iron hematoxylin.

Fig. 30. From a 5-somite embryo. In core of lateral lip 12 free crest cells. Two cells indicated by lower left-hand arrow have only slim cytoplasmic processes still within ventral lamina. Arrow at lower right marks cell with large pseudopod. At lateral extremity of lip (arrow), two cells are partly out of epithelium. BH64R1, fixed in formol-chrome-sublimate, mordanted with osmic acid, embedded in celloidin-paraffin, cut at 4 microns, and stained with iron hematoxylin.

Fig. 31. From same embryo as figure 30 taken 12 microns farther caudally. Two cells (lower arrows) are slipping out from ventral lamina. A recently liberated crest cell in prophase is indicated by arrow at right.

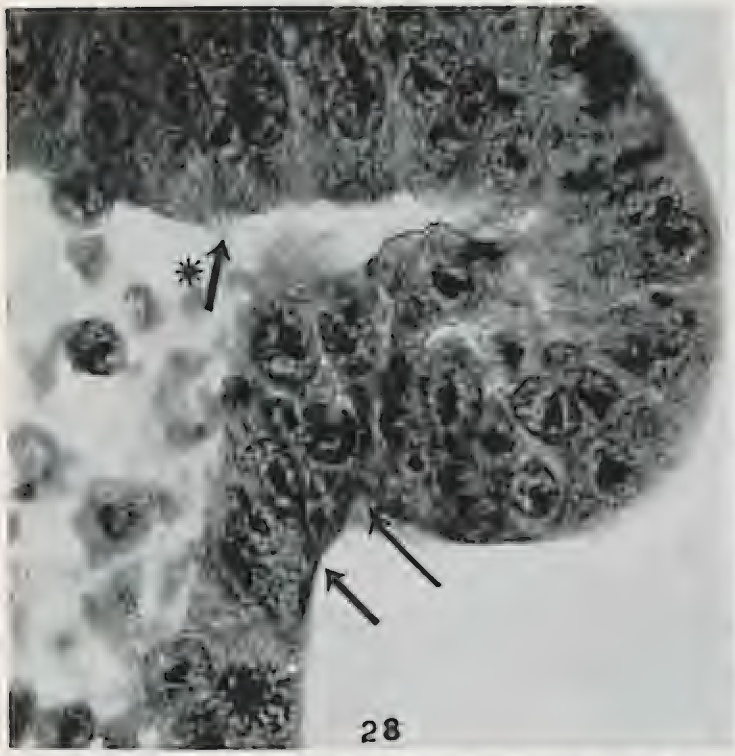

28

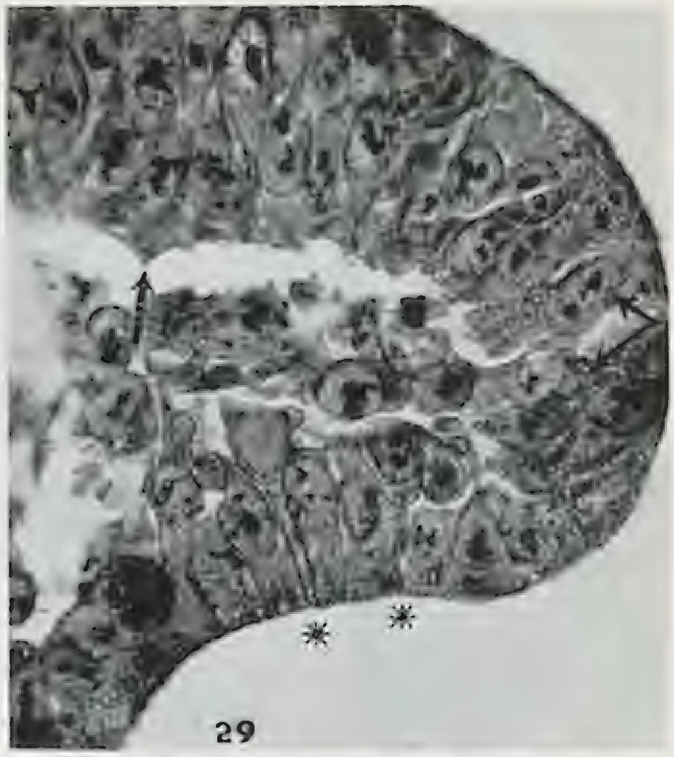

29

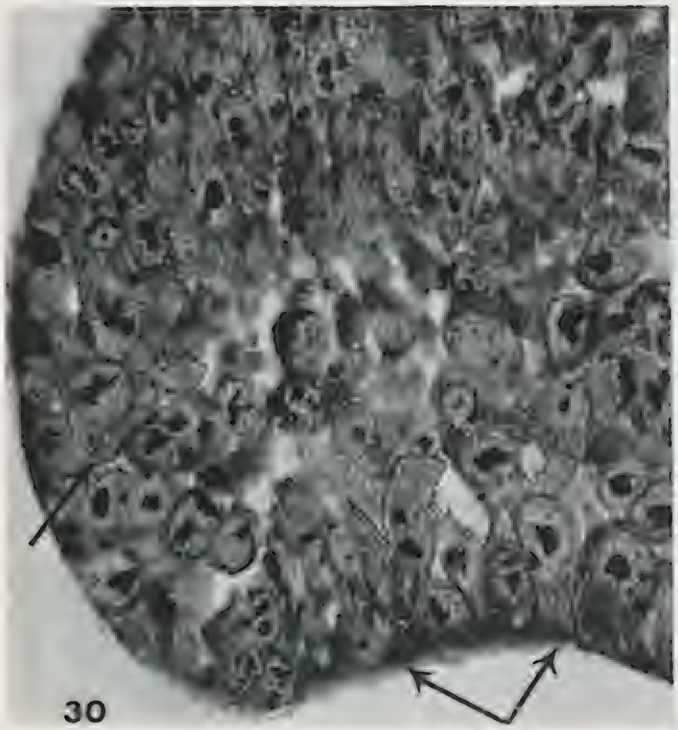

30

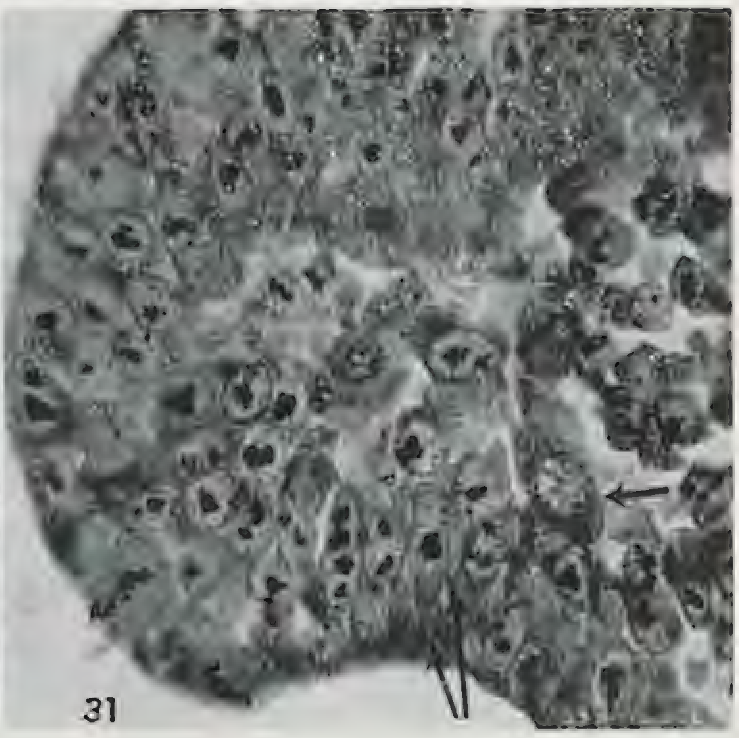

31

Plate 6. Photomicrographs showing proliferation of neural crest at various levels. Migrating cells outlined with ink. Optical system as in plate 4.

Fig. 32. Section of lateral lip of forebrain magnified 750 diameters to show crest cells welling out medially from lateral lip. They are larger, they have larger nucleoli, and cytoplasm stains more intensely than in paraxial mesenchyme cells at right. Note nucleoli of crest cells are of the neuroepithelial type. From same field as figures 30 and 31, plate 5. See page 9. BH64R1.

Fig. 33. From same 5-somite embryo as figure 32, taken through *midbrain* near its junction with forebrain. Unlike forebrain levels, lateral lip consists only of crest primordium. Farther caudally, lateral extremity of neural fold is disaggregating into crest. At lower left-hand edge of figure a group of seven cells from the epiblast appears to be joining the neural crest (compare with figs. 34 and 35). × 750.

Fig. 34. From a 6-somite embryo taken near rostral end of optic primordium, showing migration (arrows) from adjacent epiblast of mandibular area (cell borders strengthened with ink). Basement membrane is continuous except where pseudopods protrude. Similar evidences of migration from surface epithelium of this embryo were noted at four additional points. Mesenchymal surface of neural epithelium appears at lower border of figure. From same embryo as figures 5 and 6, page 7, and figure 29, plate 5. GH60R4. × 1000.

Fig. 35. At arrow an epiblastic cell has only part of its cytoplasm within the epithelium. The nucleus (solid black) protrudes beyond it, and a long slim pseudopod reaches a crest cell. W60R2, fixed in modified Flemming, embedded in celloidin-paraffin, cut at 5 microns, and stained with iron hematoxylin. Untouched photomicrograph. × 1000.

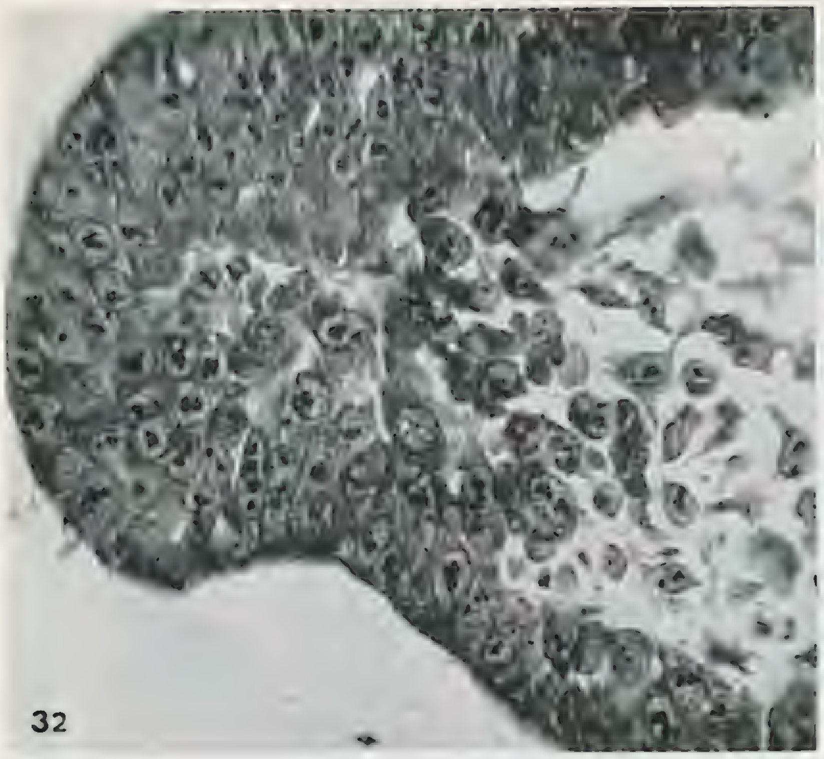
32

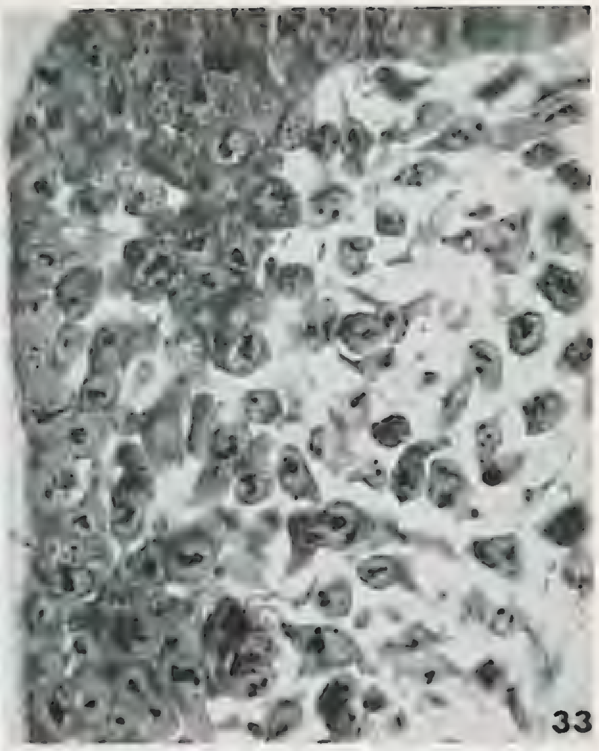
33

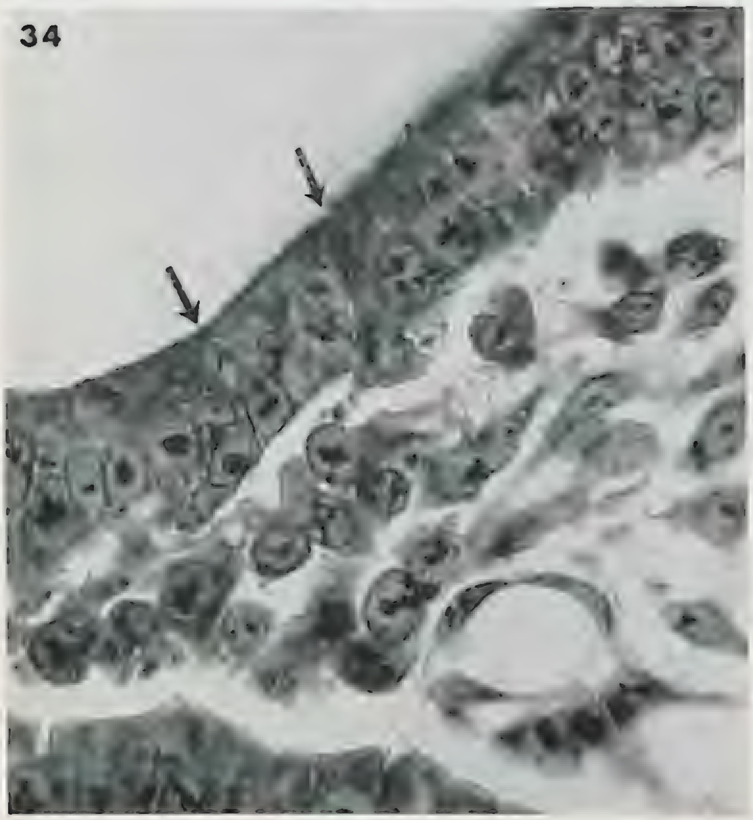
34

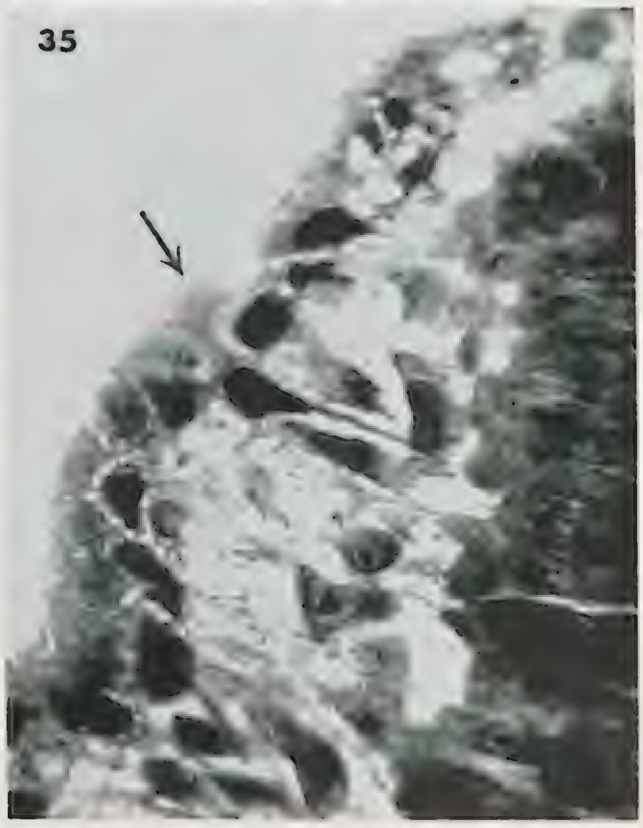
35

Plate 7. Proliferation of crest cells from primary optic vesicle. Cells described are outlined with ink. Photomicrographs × 1000. Optical system as in plate 4. Ependymal surface is up.

Fig. 36. From lateral surface of vesicle of a 12-somite embryo, showing a dividing cell (arrow) which has rounded up at mesenchymal surface. It may be about to contribute a daughter to neural crest, or it may be about to leave epithelium, as it appears to have been doing in figure 37. Usually migrants do not divide until they are completely free from epithelium. Boundary of dividing cell can be readily followed because texture of cytoplasm in late prophase ("bubbly stage") differentiates it from neighbors. Interkinetic epithelial cell boundaries can rarely be followed after Bouin fixation. Surface epithelium at left. BH89L6, fixed in Bouin, embedded in paraffin, cut at 7 microns, and stained with Mallory-Azan.

Fig. 37. Lateral surface of vesicle from 15-somite embryo. Cell at arrow is half of an anaphase. Other half in adjoining section is free from epithelium. It appears to be on verge of being liberated. Only one rank of sheath cells at this level. Cells below surface epithelium are amniotic epithelium. GH26L2, fixed in hot Bouin, embedded in paraffin, cut at 7 microns, and stained with iron hematoxylin. This type of fixation is excellent for counting mitoses but results in great shrinkage.

Fig. 38. From an 11-somite embryo cut perpendicular to lateral surface of optic vesicle. Emerging cell (∗) at center extends through entire thickness of epithelium; cell at arrow has emerged except for small pseudopod beside which basement membrane of neural epithelium ends. Rounding up of crest cells after separation from epithelium is characteristic. W28R6, fixed in acetic Zenker, embedded in paraffin, cut at 7 microns, and stained with Mallory-Azan.

Fig. 39. From a neighboring section of same optic vesicle. Cell with pseudopod extending among crest cells (arrow) has separated from ependymal surface. Cells at either side of it also appear to be migrating. Cell at surface (upper right) has emerged and rounded up (see Bartelmez, 1960, fig. 6).

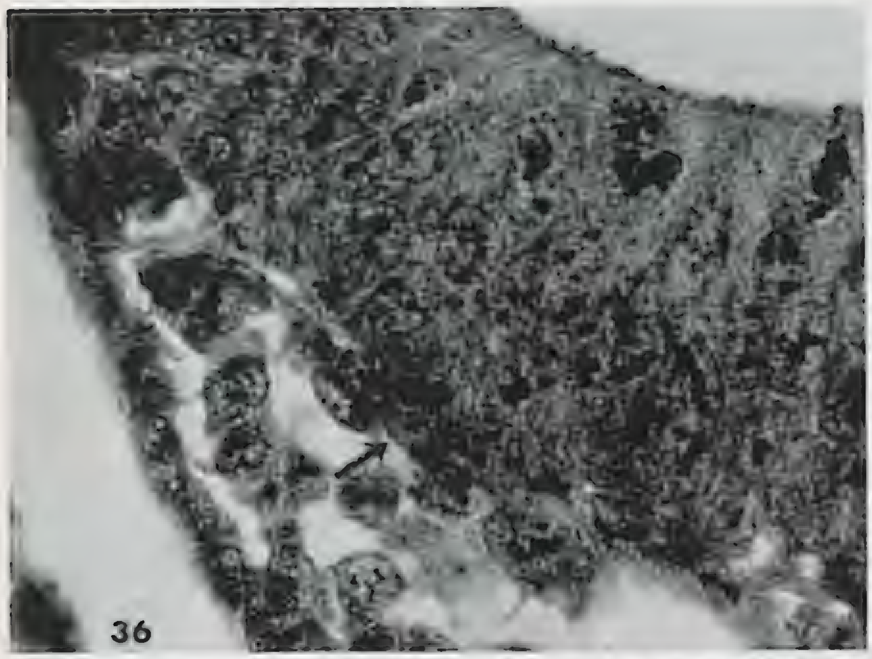

36

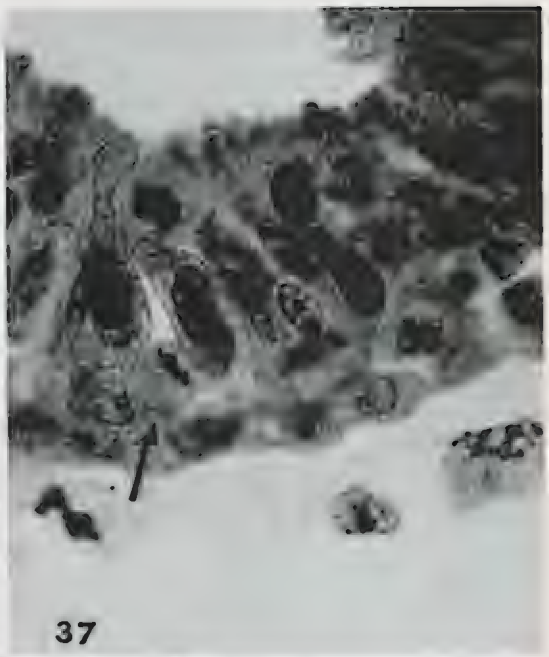

37

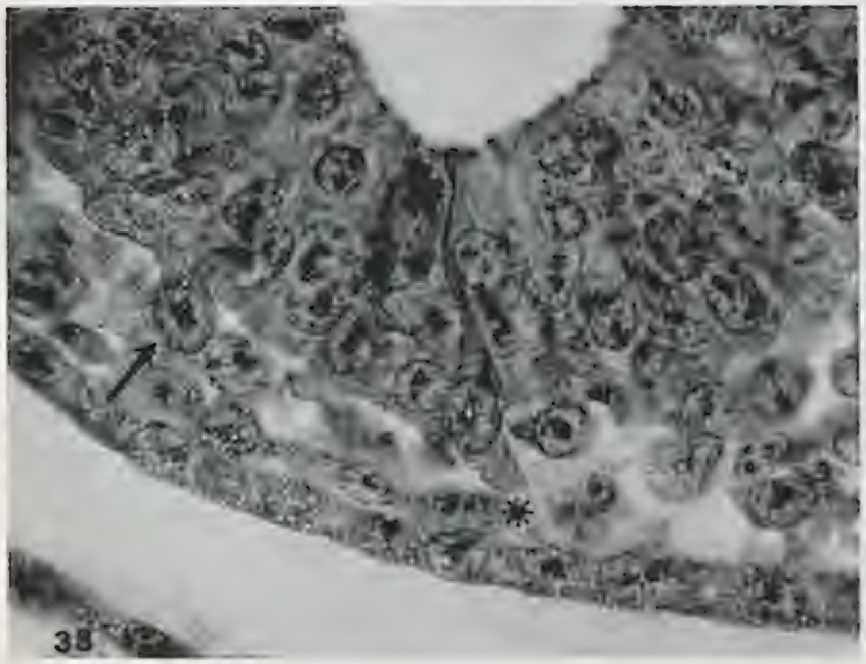

38

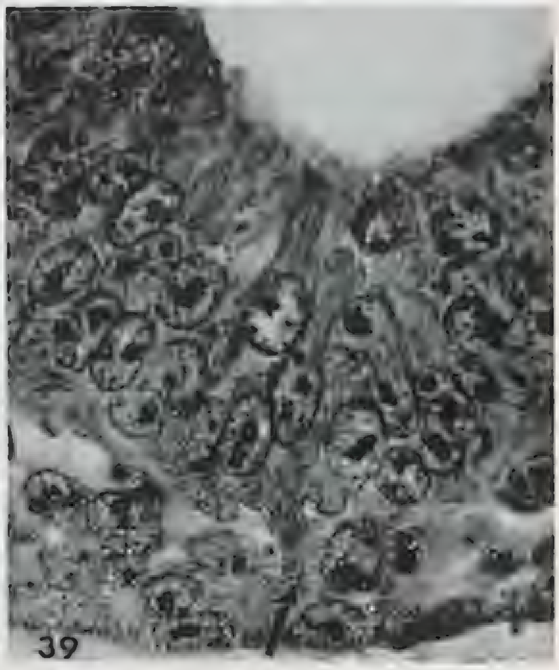

39

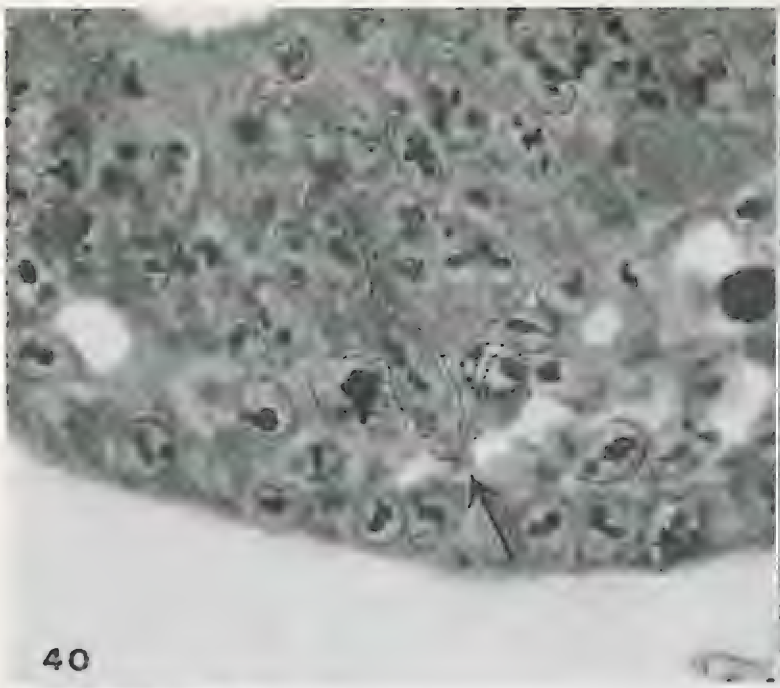
40

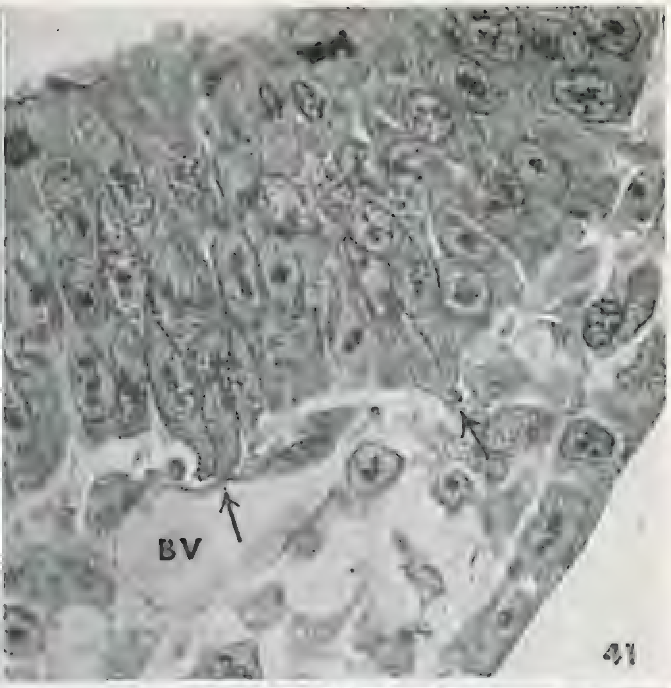

41

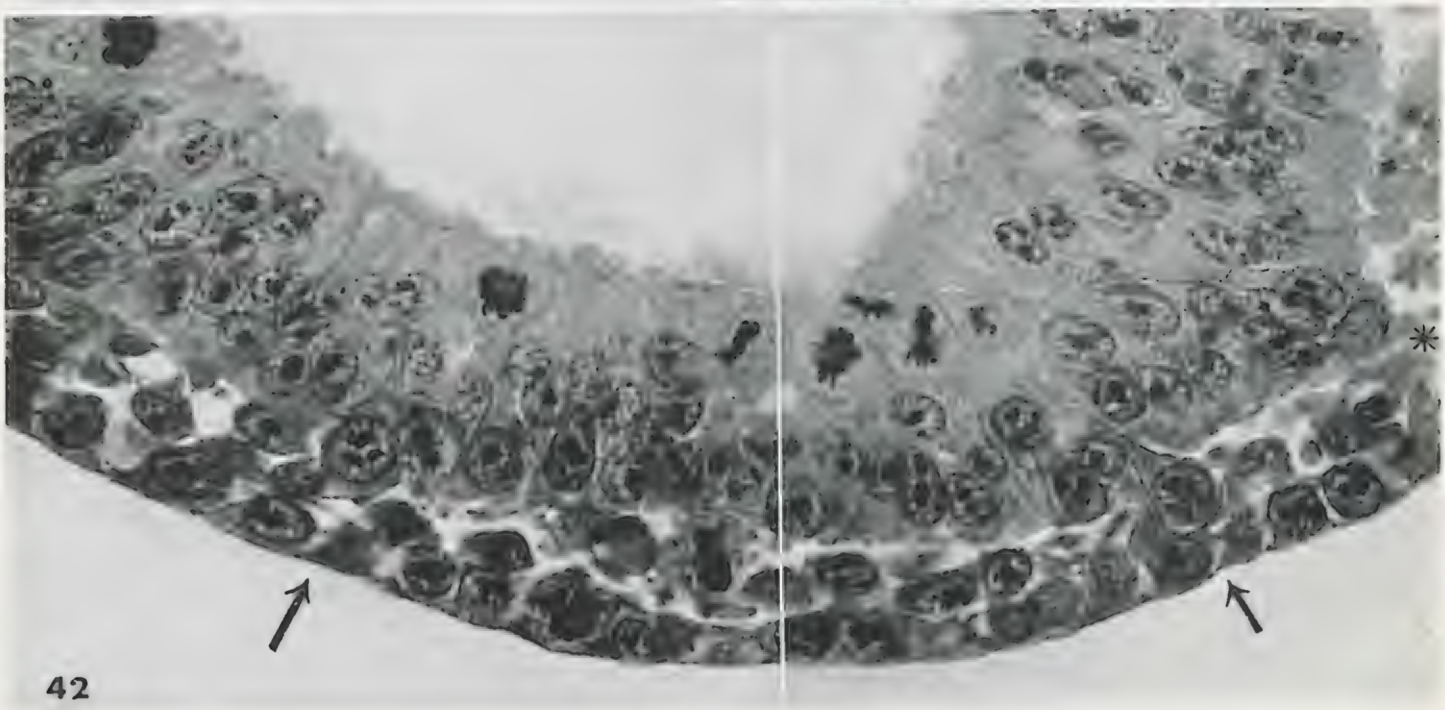

42

Plate 8. Stages in migration of cells from primary optic vesicle. Borders of migrants strengthened with ink. Photomicrographs × 1000. Same optical system as in plate 4.

Fig. 40. Section of lateral surface of vesicle from 13-somite embryo. At middle of figure epithelial cell with pseudopod (arrow), its nucleus two-thirds outside of epithelium. It is flanked by crest cells in mitosis. Its pseudopod touches a surface epithelial cell. Basement membrane entirely absent on this surface. B77R6, fixed in Bouin, embedded in paraffin, cut at 7 microns, and stained with iron hematoxylin. From a preparation by F. L. Landacre.

Fig. 41. From superior surface of optic vesicle of an 11-somite embryo. Arrow at left indicates group of three cells which have separated from ependymal surface and have developed pseudopods projecting beyond surface of epithelium. Two cells at right have short pseudopods. Elsewhere on this surface there is a marginal velum. *BV* indicates element of vascular plexus of vesicle. G36R2, fixed in modified Flemming, embedded in celloidin-paraffin, cut at 5 microns, and stained with aniline acid fuchsin.

Fig. 42. Lateral wall (at left) and part of superior wall (at right) of optic vesicle cut perpendicular to both surfaces. Two emerging cells (arrows) on lateral wall, where many nuclei are close to surface. At right (∗) a group of four cells appears to be leaving superior wall. Elsewhere this wall has well defined marginal velum and basement membrane. Eleven-somite G36L5, fixed in formol-chrome-sublimate, embedded in celloidin-paraffin, cut at 4 microns, and stained with Masson's trichrome.

CONTRIBUTIONS TO EMBRYOLOGY, NO. 253

THE EARLY DEVELOPMENT OF THE HUMAN BRAIN

G. W. Bartelmez and A. S. Dekaban

Department of Embryology, Carnegie Institution of Washington, Baltimore, and
Section on Developmental Neurology, Branch of Surgical Neurology
National Institute of Neurological Diseases and Blindness
National Institutes of Health, Bethesda, Maryland

With 30 Plates

CONTENTS

PAGE

Introduction 15

Material 15

Methods 17

Landmarks 17

Anatomy of Embryonic Brains 18
- Horizon xxii, Embryos Ranging from 24 to 27 mm. (Crown-Rump Length) 18
- Horizon xx, Embryos Ranging from 18 to 23 mm. (C. R. L.) 19
- Horizon xix, Embryos Ranging from 16.3 to 19.1 mm. (C. R. L.) 20
- Horizon xvii, Embryos Ranging from 10.9 to 14.2 mm. (Greatest Length) 20
- Horizon xvi, Embryos Ranging from 7 to 11 mm. (G. L.) 21
- Horizon xv, Embryos Ranging from 7.1 to 9 mm. (G. L.) 22
- Horizon xiv, Embryos Ranging from 5.5 to 7.3 mm. (G. L.) 22
- Horizon xiii, Embryos with More than 29 Somites Ranging from 4 to 6 mm. (G. L.) 23
- Horizon xii, Embryos with 21 to 29 Somites, Ranging in Length from 3.8 to 4.9 mm. 24
- Horizon xi, Embryos of 13 to 20 Somites, Ranging in Length from 3 to 5 mm. 24
- Horizon x, Embryos from 4 to 12 Somites 24

Sequence of Events in Early Development of the Brain 25
- Horizon xi 25
- Horizon xiii 25
- Horizon xiv 25
- Horizon xv 26
- Horizon xvi 26
- Horizon xvii 26
- Horizon xix 27
- Horizon xx 27
- Horizon xxii 27

Discussion 27
- Relation of the Cranial Flexure to the Midbrain 27
- Segmentation of the Neural Tube 28
- Optic Primordia 28
- The Primary Subdivisions of the Brain 29
- Differential Growth of Various Components of the Developing Brain 29

Conclusions 30

Literature Cited 31

THE EARLY DEVELOPMENT OF THE HUMAN BRAIN

INTRODUCTION

The primary subdivisions of the brain (telencephalon, diencephalon, mesencephalon, metencephalon, and myelencephalon) have similar relations and comparable functions in all vertebrates. Accordingly, the landmarks that define their boundaries can be regarded as reliable for following their development. On the basis of a more complete series of well preserved embryos than has been available hitherto, we present evidence that the subdivisions of the adult brain can be traced back to neural-fold stages in which a series of growth centers can be recognized, differing from one another in form, size, and relations. The possibility of following the constrictions between the various subdivisions throughout development has been doubted by some, notably Hochstetter (1919). At present we are convinced that they can be distinguished if certain criteria are followed. These are: (*a*) constrictions involve the neural tube as a whole; (*b*) constrictions do not give rise primarily to any neural centers; (*c*) constrictions change in relative length and width, and in certain stages they become inconspicuous in models.

The anatomical descriptions of progressive stages of development have important practical implications. It is known, for example, that congenital malformations of the central nervous system in man are common and that they are responsible for a substantial portion of fetal wastage as well as infant mortality and morbidity. In certain patients comprehensive clinical studies may indicate the underlying abnormality, such as dysraphism, arhinencephaly, hypoplasia of the cerebellum, or absence of the corpus callosum. In addition, anatomical examination of the affected brains may reveal in detail such abnormalities as lyssencephaly, polymicrogyria, or other cortical dysgeneses. These very complex cerebral malformations can only be understood and unraveled in the light of normal development.

An investigation of early development of the brain must necessarily begin with a stage in which the major landmarks of the adult brain can be readily identified. As progressively younger stages are analyzed certain landmarks can no longer be recognized, although others persist at least to the third week of gestation. We believe that the evidence on which this study is based can be followed more satisfactorily in this inverted sequence, and the detailed description is so presented. It is followed by a summary of the sequence of events written in the conventional manner, as far as the eighth week of gestation.

MATERIAL

The study is based on human embryos in the Collection of the Department of Embryology of the Carnegie Institution of Washington. There is probably no more complete series of stages of the embryonic development of any species than this, and it is also unique in its detailed documentation. Our classification of the material is based on Streeter's (1942 et seq.) grouping of the embryos in the Collection that have been serially sectioned. The wealth of normal, well preserved specimens enabled him to make the following contributions: (1) to establish criteria of external form and internal structure that characterize each group ("horizon"); (2) to determine the variability within each group; (3) to indicate rates of growth and differentiation in particular organs by noting the most rapid changes within each horizon. He also made estimates of ovulation age by comparisons with embryos from timed pregnancies in rhesus monkeys, since the rate of development appears to be similar in the two species during the first 7 weeks of gestation.

The procedure introduced by Streeter, together with his splendid illustrations, proved to be more satisfactory for the classification and determination of the stage of embryonic development than the method employed by Keibel (1897ss.) and others who have prepared "Normentafeln." In such tables the anatomy of individual embryos is summarized, each one serving as the type of a particular stage of development. Seriation based on size alone is highly unsatisfactory. Individuals more or less similar in other respects vary in size before, as well as after, birth. It must be remembered also that the high water content of embryonic tissue results in considerable shrinkage during dehydration and embedding. Under the most favorable conditions this amounts to from 7 to 10 per cent of the length in 80 per cent alcohol. (See footnote to table 1.) Delay in fixation or too rapid dehydration may result in a shrinkage of 20 per cent or more. An additional uncertainty is introduced when the investigator neglects to state the particular axis that he measured. During the early period of somite formation the extent of the cranial and dorsal flexures is so variable that measurements of length have no value whatsoever as indices of differentiation. During this period there is little evidence of integration of the organism as a whole, the various systems developing at different rates; embryos with the same number of somites may differ appreciably as to the form and differentiation of other organ systems.

TABLE 1. Embryos Studied in Detail

Carnegie No.	Horizon	Greatest Length in 80% Alcohol	Plane of Section	Histological Condition
		"Sitting Height," mm.		
8394	xxii	25	Transverse	Excellent
840	xxii	25−	Transverse	Good
6202	xx	21	Sagittal	Excellent
8965	xix	19	Transverse	Good
5609	xix	18	Frontal	Good
9325	xix	17	Transverse	Excellent
6524	xviii	ca. 12+	Transverse	Excellent
6520	xvii	ca. 14	Transverse	Excellent
9282	xvii	12	Transverse	Good
8789	xvii	12	Sagittal	Excellent
9100	xvii	12	Sagittal	Excellent
6510	xvi	ca. 10	Frontal	Excellent
6514	xvi	ca. 9	Sagittal	Good
8773	xvi	11 *	Frontal	Excellent
6517	xvi	ca. 10+	Transverse	Excellent
6516	xvi	ca. 10+	Sagittal	Good
8098	xvi	10	Frontal	Good
6512	xvi	ca. 7	Transverse	Excellent
6506	xv	ca. 7	Frontal	Excellent
8966	xv	7+	Sagittal	Excellent
6502	xiv	7−	Transverse	Excellent
8314	xiv	ca. 8	Transverse	Excellent
8552	xiv	7−	Transverse	Excellent
8999	xiv	6	Sagittal	Excellent
2841	xiv	5+	Transverse	Good
836	xiii	4	Transverse	Excellent
8119	xiii	5+	Transverse	Excellent
8239	xiii	4+	Sagittal	Good
		Number of Somites		
8944	xii	25	Sagittal	Excellent
8943	xii	22 to 23	Transverse	Excellent
7665	xi	19	Transverse	Excellent
7611	xi	15 to 16	Transverse	Excellent
5074	x	10	Transverse	Excellent
1201	x	8	Transverse	Good

* This embryo was 13 mm. long when measured fresh by A. Hertig. It was fixed promptly in Bouin and had already been reduced by 15 per cent in 80 per cent alcohol.

METHODS

The procedures used in the histologic preparation of the embryos have been described in detail by Heard (1957). The most significant feature for our purposes is the accurate control of the reconstructions and models by means of photographs of the intact specimens in alcohol. Such control is admirably provided by the Born-Lewis method (W. H. Lewis, 1915). All the sections of each series were photographed without distortion by projection at exactly the same magnification. The wax plates were piled using a tempe prepared from an accurately posed profile of the embryo, and the model was checked with reference to photographs of dorsal, ventral, and lateral views of the embryo. A pair of guide lines perpendicular to each other was drawn on each wax plate, which was then laid on the corresponding photomicrograph so that the guide lines could be transferred to it. Since the guide lines are perpendicular to the plane of section and to each other the serial sections are provided with three axes perpendicular to one another, and any organ can be modeled with the control of the external form. Measurements from the guide lines similiarly serve for preparing projection reconstructions (see fig. 1, pl. 1; fig. 13, pl. 6, etc.). Especially in regard to the brain it is essential that the extent and relations of the cranial and dorsal flexures be controlled with reference to the external form of the head.

The magnification used in making wax or plaster models must be low enough to keep them reasonable in size. Descriptions of the brain based primarily on plastic reconstructions are apt to omit significant details which are not clearly visible at the magnification used. But projection reconstructions can be made at any magnification, and details observed under high magnification in the original sections can be located and utilized for analysis. In order to emphasize the changes in relative size of the parts of the brain most reconstructions have been reproduced at approximately the same size.

LANDMARKS

Certain landmarks can be followed through the entire course of development from the adult brain to neural fold stages.

1. The cranial flexure presents an abrupt change in the neural axis at the level of the midbrain. In adult brains *hardened in situ* the axis shifts at the midbrain through an arc approximating 90° (see p. 27).

2. A *constriction* of the neural tube divides the forebrain from the midbrain (sulcus pros-mesencephalicus). A similar constriction (isthmus) separates the midbrain from the hindbrain. No gray centers develop primarily in these constrictions, although secondary invasions occur.

3. The *primordia* of the *optic vesicles* characterize the entire forebrain in early stages of development. They join one another rostrally in the mid-line at the future site of the chiasma.

4. The *primordium* of the *mammillary body* is located ventrally at the caudal end of the forebrain.

5. The differentiated epithelium of the *oral hypophysis* identifies the infundibular region.

6. *Rhombomeres 1–2 and 4,* which are distinctive in form, facilitate the identification of the regions of the hindbrain.

From about the fifth week of gestation, additional landmarks can be recognized:

7. The evagination of the cerebral vesicle brings into being the sulcus di-telencephalicus which crosses the mid-line at the *velum transversum,* indicating the site of the interventricular foramen of Monro. The telencephalic limb of the velum transversum is thin whereas the diencephalic limb remains thicker.

8. Localized thickenings of the embryonic lamina terminalis are the *primordia* of the *optic chiasma* and of the *commissure bed* in which the cerebral commissures develop.

9. The *corpus striatum* first appears as a thickening of the ventrolateral wall of the cerebral vesicle.

10. The *epithalamus* is distinguished by the *epiphysis* and later by the *habenular complex* from which the *fasciculus retroflexus* arises.

11. The *zona limitans intrathalamica* divides the dorsal from the ventral thalamus.

12. The *sulcus hypothalamicus* (sulcus limitans Monroi) marks the dorsal border of the hypothalamus.

13. The *mesencephalic tegmentum* is distinguished at first by its thickness in the mid-line; often it is separated from the mammillary area by an external sulcus.

14. The di-mesencephalic sulcus comes to be distinguished dorsally by the *posterior commissure.*

15. The mes-metencephalic sulcus (isthmus) is marked dorsally by the decussation of NN. IV. The *fovea* (recessus) *isthmi* is a feature of this sulcus ventrally.

16. The *pontine flexure* is associated with the rapid growth of the cerebellar lamina.

17. The *primordium hippocampi* and *area epithelialis* serve to indicate localized growth in the cerebral vesicle.

18. The lateral choroid plexuses which arise from the area epithelialis unite in the mid-line at the *paraphysis* which adjoins the velum transversum.

ANATOMY OF EMBRYONIC BRAINS

Our description begins with the brains of embryos from the eighth week which belong to Streeter's horizon xxii. This represents the transitional period between the embryonic and the fetal periods. From this stage the development of the major subdivisions of the brain is traced to embryos with open neural folds (horizon x). The analysis of development in each group begins with an outline of characteristic features of the landmarks that delimit subdivisions and is followed by a description of the main neural structures that can be recognized.

Horizon xxii, Embryos Ranging from 24 to 27 mm. (Crown-Rump Length)[1]

Figure 1 (pl. 1) shows the reconstruction of the brain of embryo 840, which was sectioned in the plane indicated by arrows marked 2 (this is the level shown in fig. 2, pl. 2); arrows marked 5 indicate the plane of section in which the brain of embryo 8394 was cut (see figs. 5–8, pl. 3). The cerebral vesicles, unlike the massive cerebral hemispheres of the mature brain, are simply thin-walled outpouchings of the lateral walls of the neural tube. At this stage, the cerebral vesicles are united in the mid-line only by the lamina terminalis, which stretches from the optic chiasma to the velum transversum. The deep fissure between the telencephalon and the diencephalon extends laterally from the velum transversum along the junction of the cerebral vesicle and thalamus (adult sulcus terminalis) to the optic chiasma (see fig. 8, pl. 3; fig. 9, pl. 4). On the ventricular surface this fissure passes along the caudal border of the corpus striatum toward the mid-line to join the optic sulcus. Thus the medial walls of the corpus striatum and the lamina terminalis enclose the lumen of the telencephalon medium ("cavum Monroi" of Hochstetter, 1919) which is in broad communication with the lateral ventricles (fig. 8, pl. 3) and with the diencephalic ventricle, which eventually constitutes the greater part of the third ventricle.

The constriction between mid- and 'tweenbrain is occupied dorsally by the posterior commissure (fig. 1, pl. 1, figs. 3 and 4, pl. 2, S.DM.). On the ventral surface it terminates at the external postmammillary sulcus, which is conspicuous at this stage. An abrupt change in the axis of the neural tube occurs at the midbrain, marking the cranial flexure which has given rise to the deep cleft between hypothalamus and midbrain. It marks the site of the adult interpeduncular fossa. The isthmus (sulcus mes-rhombencephalicus) is the constriction marked by the recessus isthmi which has a corresponding elevation on the ventral surface (tuberculum interpedunculare of Hochstetter, 1919).

Adjoining the dorsal edge of the isthmus is the massive cerebellar plate of the rhombencephalon (fig. 8, pl. 3). It does not yet reach the mid-line, but the roof plate at this level is thicker than the membranous roof of the fourth ventricle. The hindbrain is histologically the most highly differentiated division, and the largest if we include the fourth ventricle; this is also true in all earlier stages.

Telencephalon (*endbrain*). The lamina terminalis (fig. 1, pl. 1) consists of four distinct parts: (1) the primordium of the chiasma, which has decussating retinal fibers rostrally and fine fibers caudally, the latter appearing to arise largely from the hypothalamus and constituting the postoptic commissure; (2) a short membranous segment dorsal to the chiasma; (3) the commissure bed which later is greatly expanded by the development of the anterior and hippocampal commissures as well as the corpus callosum (see Streeter, 1912, figs. 66 to 68 and 70; Hochstetter, 1919, text figures 7 to 11, 15); (4) dorsal to the commissure bed the lamina terminalis again becomes a delicate membrane. At the paraphyseal arch (Bailey, 1916) the two lateral choroid plexuses are united in the mid-line (fig. 8, pl. 3). The thin rostral limb of the velum transversum is telencephalic; the thicker, caudal limb is diencephalic.

The rhinencephalic region is well differentiated. The hippocampal formation extends from the olfactory area along the medial wall and then turns ventrally, indicating the growth center for the temporal lobe (fig. 1, pl. 1). The development of the hippocampus has been described and illustrated in detail by Hines (1922), whose terminology we follow. Its relations in this horizon are shown in figures 7 (pl. 3); 9 and 10 (pl. 4). The adjoining area epithelialis (fig. 5, pl. 3), where the wall of the cerebral vesicle remains a simple epithelium, has invaginated to form the lateral choroid plexus and more caudally has begun to fuse with the lateral thalamic wall, thus giving rise to the lamina affixa.

The corpus striatum is large relatively, with medial and lateral lobes (figs. 6 to 8, pl. 3, and 9, pl. 4). It is well differentiated histologically, and there are several fiber systems in its broad mantle layer extending to or from the thalamus. These fibers occupy the thickened wall of the di-telencephalic sulcus as the beginning of the internal capsule. This was noted by His in 1887. (See figs. 8, pl. 3, and 9, pl. 4.)

The earliest differentiation in the neopallium has appeared in the flattened wall overlying the corpus striatum (fig. 6, pl. 3). A slender strand of fibers extends from the striatal mantle layer toward the surface (arrow in fig. 9, pl. 4). Here cells have migrated superficially and produced the beginning of the "cortical plate" which will eventually develop into cerebral cortex (figs. 2, pl. 2, and 5, pl. 3).

---

[1] The range of lengths given in each horizon is confined to the embryos graded "excellent" by Streeter. Poorly preserved specimens exhibit greater variability, owing to post-mortem changes.

Diencephalon. The 'tweenbrain is divisible into four parts: epithalamus, dorsal thalamus, ventral thalamus, and hypothalamus. The sulcus dorsalis externus separates the epithalamus from the dorsal thalamus. The roof plate is smooth in some embryos of the group, although vascularization has begun (fig. 1, pl. 1); in others it has begun to fold (figs. 6 and 7, pl. 3). Its epithelial cells are taller near the epiphysis, the morphogenesis and histogenesis of which have been described in detail by Hochstetter (1923) (see Streeter, 1951, figs. 8 and 9). Adjoining the taenia is the stria medullaris thalami, to which structure Gilbert (1935) traced fibers from neuroblasts of the olfactory area. The stria medullaris reaches the habenula, the differentiated mantle layer of which gives rise to the fasciculus retroflexus (tractus habenulo-peduncularis); this fiber bundle is indicated in figure 1 (pl. 1) and appears clearly in figure 4 (pl. 2). A group of cells forming primordia of the paratenial nuclei as well as the fibers of the stria medullaris are visible in the rostral part of the epithalamus (figs. 5, 6, pl. 3). Caudally it is distinguished by the habenular complex (figs. 1, pl. 1; 4, pl. 2) and by the epiphysis.

The dorsal thalamus is separated from the ventral thalamus by the zona limitans intrathalamica (fig. 2, pl. 2), which runs into an inconspicuous sulcus medius. The ventral thalamus in turn is delimited from the hypothalamus by a clearly defined hypothalamic sulcus. At this stage the dorsal thalamus is the least differentiated part of the diencephalon, showing a prominent germinal layer and a poorly differentiated mantle layer without evidence of cell grouping. In contrast, the ventral thalamus shows a loose arrangement of the cells in the mantle layer with clear grouping as well as a conspicuous marginal layer (compare Dekaban, 1954). The dorsal thalamus increases in volume as we pass caudally, whereas the ventral thalamus is larger rostrally. The hypothalamus shows the most advanced differentiation of the subdivisions of the 'tweenbrain, since medial and lateral nuclear groups as well as infundibular and mammillary nuclei can be distinguished (figs. 6 to 8, pl. 3; figs. 9 and 10, pl. 4).

A long column of neuroblasts extends from the chiasma along the lateral wall toward the mammillary region (fig. 9, pl. 4), giving rise to a descending tract (tractus hypothalamicus of His). At this level the floor is thin in the mid-line, whereas in the mammillary region it is characteristically thick. The mammillary complex is defined by sulci fore and aft, and it gives rise to a sheet of fibers which constitute the mammillo-tegmental tract. The relations of oral and neural hypophysis to the infundibulum are manifest in figures 1 (pl. 1) and 12 (pl. 5).

Mesencephalon (midbrain). The posterior commissure occupies the dorsal surface of the di-mesencephalic sulcus (figs. 1, pl. 1; 3 and 4, pl. 2). Ballooning of the tectum rostrally and caudally indicates the colliculi in which lamination is present (fig. 4, pl. 2). The differentiation of the mesencephalic tegmentum has reached the stage in which it forms the substratum of a functioning reflex mechanism. Ventrolateral eminences foreshadow the cerebral peduncles (fig. 6, pl. 3).

Rhombencephalon (hindbrain). In the course of development the first histological differentiation begins in this subdivision, and the reflex neural circuits are physiologically active in the hindbrain prior to this stage (see p. 27). On the other hand, the two lateral laminae which will give rise to the cerebellum and pontine nuclei (His, 1891) lag behind all other centers of the brain in development; indeed, differentiation of the cerebellar cortex continues throughout the first year after birth (Dekaban, 1959).

Horizon xx, Embryos Ranging from 18 to 23 mm.
(C. R. L.)

Figure 12 (pl. 5) presents a reconstruction in the mid-sagittal plane based on six successive sections of a 22-mm. embryo (no. 6202) cut sagittally. It serves as a control for the relations shown in the projection reconstructions such as figure 1. Because the lamina terminalis was cut somewhat obliquely, the velum transversum and paraphysis do not show their usual form. The location of the paraphysis is indicated by the abrupt change in the thickness of the roof plate at the site of transition from the telencephalon medium to the thalamic roof. The membranous lamina terminalis is long, and the commissure bed is short and thick, resembling that shown in figure 1. The few optic fibers in the mid-line are grouped on the surface of the primordium of the chiasma and are separated from the postoptic commissure which occupies much of the primordium of the chiasma. The oral hypophysis adjoins the chiasma, and its relations to the neural lobe and the oral epithelium can be seen in figure 12 (pl. 5). The elongated hypothalamus is characteristic of this period. Just rostral to the epiphysis, at the caudal end of the habenula, the beginning of the habenular commissure can be identified. The plane of section is favorable for following the stria medullaris thalami and the fasciculus retroflexus. The midbrain is, as usual, associated with the cranial flexure. Only the superior end of the cerebellar plate was included in the reconstruction. This region will eventually fuse with its mate in the mid-line and produce the cerebellar vermis. The pontine flexure is less acute than in the brain represented in figure 1 (pl. 1). Attention is called to the median area of the roof of the fourth ventricle indicated by the asterisk in figure 12 (pl. 5). Here the epithelium is very thin and has not been vascularized like the rest of the roof plate. It is the area which Weed (1917) found to be highly permeable in pig embryos; it may, in fact, be a physiological foramen at this time.

Horizon xix, Embryos Ranging from 16.3 to 19.1 mm. (C. R. L.)

The reconstruction shown in figure 13 (pl. 6) is based on an embryo of 18 mm. (no. 5609) cut in the plane indicated by the arrows. Both the brain as a whole and the cerebral vesicles are smaller in absolute size than those of the preceding horizon. In addition, there are other features that indicate an earlier stage. The optic stalk (conus opticus) forms a prominent evagination of the lateral thalamic wall (fig. 17, pl. 7). No optic fibers have as yet reached the chiasma, but many nerve fibers are present in the postoptic component. The primordium of the epiphysis is in the form of a simple elevation of the thalamic roof (fig. 13, pl. 6). In some embryos of this group, however, a superior epiphyseal lobe can be distinguished. The constriction between thalamus and midbrain (sulcus di-mesencephalicus), although obvious in sections (figs. 14 to 16, pl. 7), is so broad and shallow that it is inconspicuous in the model of the brain. This constriction is marked dorsally by the posterior commissure and ventrally by the postmammillary sulcus. The relations of mes- and rhombencephalon are as in the more advanced stages.

Figures 20 (pl. 9) and 21 (pl. 10) are based on another embryo of this horizon. It is introduced here in order to supplement the projection reconstructions (fig. 13, pl. 6) with an illustration of a plastic model. This model was made and described by Bailey (1916, fig. 16), who clarified the development and the relations of the choroid plexuses of the forebrain. The embryo was subsequently studied by Hines (1922). Figure 21 (pl. 10) is a copy of her figure 15, and figure 20 (pl. 9) presents in part her analysis of the forebrain. Sulcus di-telencephalicus internus extends from the well defined velum transversum along the caudal border of the corpus striatum toward the chiasma. The medial eminence of the corpus striatum has extended into the telencephalon medium. At the paraphyseal arch the lateral choroid plexuses join each other (figs. 8, pl. 3, and 21, pl. 10). The compact bundle of olfactory fibers extends from the olfactory epithelium to the olfactory bulb (fig. 18, pl. 8).

Diencephalon. This subdivision is definitely less advanced in differentiation than in horizon xx. Its four parts can be readily identified (fig. 19, pl. 8). The epithalamus includes roof plate, stria medullaris, epiphysis, and habenular complex. A well defined sulcus medialis externus and the zona limitans intrathalamica separate dorsal from ventral thalamus. The latter is delimited from the hypothalamus by the sulcus hypothalamicus. In the dorsal thalamus the germinal layer is thicker than the mantle layer; the reverse is true in the ventral thalamus, where the mantle layer is as well differentiated as in the habenular region.

The following fiber tracts can be distinguished in the 'tweenbrain: stria medullaris, fasciculus retroflexus, tractus hypothalamo-tegmentalis, mamillo-peduncularis, and, above all, the components of the internal capsule. These have not yet been satisfactorily analyzed. The chiasma and infundibulum are relatively farther apart from each other than in the more advanced stages. A comparison of figures 13 (pl. 6) and 1 (pl. 1) indicates the difference in the extent to which the cerebral vesicle has expanded caudally. In horizon xx the di-telencephalic sulcus is narrow but completely lined by primitive meninx (figs. 14 and 15, pl. 7); the two subdivisions have not yet begun to fuse. The thickening of the wall of the sulcus between these two subdivisions contains fibers of the internal capsule as in the brains described above.

Horizon xvii, Embryos Ranging from 10.8 to 14.2 mm. (Greatest Length)

This group presents a distinctly earlier stage of development. This is more apparent in the external form, especially in the development of the face and certain internal organs, than in the brain, which is sufficiently similiar to that of group xx so that the same landmarks can be used in delimiting the major subdivisions. At this stage the sulcus di-telencephalicus is simply a fold of the wall of the forebrain (fig. 24, pl. 12). The di-mesencephalic sulcus is less conspicuous than it is later in development. Nonetheless, measurements of the transverse sections at this level demonstrate the constriction. The posterior commissure marking the sulcus dorsally is separated from the epiphysis by a short segment of the roof. The isthmus is short dorsally widening ventrally toward the recessus isthmi which is long and shallow (fig. 22, pl. 11).

Telencephalon. In the embryo shown in figure 22 (pl. 11) the cerebral vesicle had expanded somewhat beyond the lamina terminalis; caudally it had not yet reached the middle of the thalamus. The growth center that will form the temporal lobe is indicated by the inferior end of the primordium hippocampi. Hines (1922, figs. 13 and 14) shows a somewhat more advanced stage from this horizon. The site of origin of the lateral choroid plexus is marked by increased vascularity (fig. 29, pl. 13). Later stages are illustrated in figures 30 (pl. 13) and 19 (pl. 8). The corpus striatum shows evidence of rapid growth; its mantle zone is broad and like the marginal zone has many fibers (fig. 24, pl. 12).

In an embryo that appears to belong to this horizon Gilbert (1935) describes fibers that pass between the corpus striatum and the pars ventralis thalami; some continue to the mesencephalic tegmentum. We can confirm these findings in a 12-mm. embryo stained with silver (no. 9282). In this specimen fibers were followed along the lateral surface of the cerebral vesicle caudally from the lateral olfactory area. A strand of fibers is also present extending from the mantle zone of the striatum dorsally to the lateral wall of the cerebral vesicle as in our 25-mm. embryo (no. 8394); see figure 9 (pl. 4).

The conical optic stalk (fig. 25, pl. 12) is relatively larger than in more advanced stages. No retinal fibers have as yet reached the chiasma. The commissure bed (fig. 22, pl. 11) is long and tapering as in the embryos of horizon xix. Rostral to the velum transversum the telencephalic roof is elevated in a narrow median "keel" (Hochstetter, 1919) which has reached the height of its development (fig. 23, pl. 12). Its extent is indicated by the broken line in this region in figure 22 (pl. 11). Paraphyseal arch (fig. 29, pl. 13) and velum transversum are typical in form.

Diencephalon. The epiphysis is a simple evagination of the roof (fig. 22, pl. 11). Although the sulcus dorsalis is inconspicuous the habenular complex can be recognized by the differentiated mantle zone and the emerging fibers of the fasciculus retroflexus, which have united into a single trunk (fig. 26, pl. 12). The dorsal thalamus is separated from the ventral thalamus by the sulcus medius, which parallels the zona limitans intrathalamica (figs. 25 and 26, pl. 12). The dorsal thalamus is undifferentiated except for a narrow mantle layer. In the ventral thalamus there are broad strands of neuroblasts and many fibers. The hypothalamic sulcus is prominent. The lateral hypothalamic cell column is clearly differentiated (fig. 25, pl. 12). The mammillary region is characteristically thick, and the postmammillary sulcus is present.

Mesencephalon. The cranial flexure is more acute and the tectum longer and thinner than in the specimens described above. The tectum is undifferentiated except for a narrow marginal velum. The tegmentum, on the other hand, shows advanced structural organization and is thicker than any other region of the midbrain floor.

Rhombencephalon. This region does not differ significantly from that of more advanced stages (see fig. 28, pl. 12).

Horizon xvi, Embryos Ranging from 7 to 11 mm.
(G. L.)

The brain at this stage is manifestly simpler in form than in horizon xvii (compare fig. 33, pl. 15, with fig. 22, pl. 11). The cerebral vesicles appear as globular outpouchings of the dorsolateral wall of the forebrain. The ventricle of the telencephalon medium is larger than the lateral ventricles (figs. 35 and 36, pl. 16). The di-telencephalic sulcus forms a low ridge on the ventricular surface. In the mid-line the sulcus is emphasized by the abrupt change in the thickness of the limbs of the velum transversum (fig. 32, pl. 14, and fig. 33, pl. 15). The domed epiphysis borders on the broad, shallow di-mesencephalic sulcus. The broken line in figure 33 (pl. 15) is at the middle of the constriction as determined by measurements of the sections, which are transverse at this level. A shallow sulcus separates mammillary body from tegmentum. The posterior commissure has not yet appeared in this embryo but is present in others of this horizon. The isthmus is an obvious constriction of the tube. The five grooves on the ventricular surface of the alar and basal plates of the hindbrain (fig. 32, pl. 14) mark the rhombomeres, which are manifest transverse segments of the neural tube in earlier stages. Figure 39 (pl. 16) shows the root of the fifth cranial nerve which serves to identify the second rhombomere. The first rhombomere is relatively long, as can be judged by the distance between the isthmus and the root of cranial nerve V (fig. 33, pl. 15); its dorsolateral edge is greatly thickened and constitutes the cerebellar lamina.

Telencephalon. The cerebral vesicle has expanded only slightly beyond the dorsal membranous segment of the lamina terminalis. Its dorsal wall, has, however, already begun to differentiate. This is the earliest stage of the primordium hippocampi recognized by Hines (1922, figs. 7 to 9 and 22 to 25). Our figure 31 (pl. 13), from a similar embryo, shows the broad marginal velum and the ventricular sulcus (sulcus ventralis of Hines) which is the boundary between hippocampal formation and area epithelialis. This section was taken at the level of the hippocampal primordium where it is slightly thicker than any other part of the cerebral vesicle except the inferior wall, which has thickened laterally as the primordium of the corpus striatum (figs. 35, 36, pl. 16). The lamina terminalis of this embryo has the beginning of the "keel" (figs. 34 and 35, pl. 16) which was described in horizon xvii (fig. 23, pl. 12). The commissure bed and chiasma are similar though relatively smaller than in the preceding stage. From the olfactory pit strands of deeply staining cells extend to the neighboring wall of the cerebral vesicle indicating the site of the olfactory bulb (fig. 34, pl. 16; see Van Campenhout, 1933).

Diencephalon. The relation of the optic cups to their stalks (conus opticus) is shown in figures 36 and 37 (pl. 16). The hypothalamus is the most advanced region of the diencephalon; figures 37 and 38 (pl. 16) show the lateral hypothalamic cell group. These cells probably give rise to the tractus hypothalamicus which is present in embryos of this horizon (see Gilbert, 1935). The thickened epithelium of the oral hypophysis is in close apposition to the infundibular region in the mid-line (fig. 37, pl. 16). The relative distance between infundibulum and chiasma ridge has increased as compared with more advanced stages.

There is never any evidence of a floor plate rostral to the midbrain (Kingsbury, 1930). The mammillary recess is thick in the mid-line (fig. 33, pl. 15), and neuroblasts arise from it. Their processes extend caudally as the relatively large mammillo-tegmental tract. Compared with the hypothalamus the epithalamus is shorter and less differentiated. Rostral to the epiphysis the broader mantle zone of the lateral wall presages the habenular complex. The dorsal thalamus is separated from the ventral by the sulcus medialis externally and by the corresponding ventricular intrathalamic ridge (figs. 38 and 39, pl. 16).

Mesencephalon. The tectum does not differ materially from that in horizon xvii. The third and fourth cranial nerves are well developed, and their nuclei are situated in the caudal third of the tegmentum, which is in the process of structural differentiation.

Rhombencephalon. The rhombomeres (figs. 38 and 39, pl. 16) are related to the afferent roots of cranial nerves V, VII, IX, and X. The ganglia, fibers, and nuclei of cranial nerves V to XII were described and figured by Streeter (1905 and 1912) in embryos of this group. These observations were subsequently confirmed and extended by the study of human and other mammalian embryos stained by silver methods (Windle, 1935).

Horizon xv, Embryos Ranging from 7.1 to 9 mm. (G. L.)

Since figure 40 (pl. 17) is magnified so as to be as large as figure 33 (pl. 15), the brains appear similar in respect to the proportions of the subdivisions, although the earlier stage is less differentiated. The cerebral vesicles are of smaller relative size in comparison with the rest of the brain. The differences in the elements of the face in the two groups of embryos are reflected in the different relations of optic vesicles and nasal pits to the lamina terminalis. The form of the lamina terminalis in both is practically the same, and the roof plate thickens characteristically at the thalamic limb of the velum transversum. The di-telencephalic sulcus extends on the lateral surface rostrally to the optic stalk and produces a prominent ridge on the ventricular surface (figs. 42, 44, pl. 18). There is no evidence, as yet, of the thickening that could be interpreted as corpus striatum. The diencephalic roof is short; a slight elevation near its caudal end suggests an early stage of the epiphyseal evagination (fig. 40, pl. 17). Since both the dorsal thalamus and the alar plate of the midbrain are undifferentiated, the sulcus between them is so shallow that in a model it is more readily felt than seen. The measurements of the neural tube of the specimen shown in figure 40 (pl. 17) clearly demonstrate this constriction, the middle of which is indicated by the broken line. Ventrally the di-mesencephalic sulcus is marked by the groove between the mammillary body and the mesencephalic tegmentum. The isthmic constriction is accentuated by the expanded first rhombomere with its cerebellar lamina (fig. 42, pl. 18) and by the lateral recess of the fourth ventricle.

Telencephalon. The walls of the cerebral vesicles are uniform in thickness: they are merely domings of the forebrain wall dorsally (figs. 42 and 43, pl. 18). The telencephalon medium is relatively large, and the keel of horizons xvi and xvii can already be recognized. Both primordium chiasmatis and commissure bed are relatively large, and are separated by a notch. Close to the velum transversum the membranous segment of the lamina terminalis becomes very thin (fig. 43, pl. 18).

Diencephalon. The roof and floor are relatively shorter and thicker than in the embryos of horizon xvi. The epiphyseal evagination is indicated in the embryo of figure 40 (pl. 17). The more advanced embryos of horizon xv present transitions between it and that of figure 33 (pl. 15) (horizon xvi). In the hypothalamus, the lateral walls show evidence of differentiation, especially rostrally (figs. 41, 43, pl. 18). In the 6.9-mm. embryo "Br. 3," His (1904) saw fibers descending from this region; this finding has been confirmed by Gilbert (1935) in a similar specimen. Caudally, the medial thickening of the floor distinguishes the region of the mammillary recess. The oral hypophysis provides the evidence for marking the site of the infundibular region; the oral and neural epithelia are separated by a thin strand of mesenchyme except in the mid-line, where they are in intimate contact. In the epi- and hypothalamus there is some evidence of differentiation, but the dorsal and ventral thalamus cannot be clearly separated.

Mesencephalon. The tectum is almost as thick in the mid-line as it is laterally where a thin marginal velum has appeared. The tegmentum is relatively thinner than in later stages but has a mantle layer in which the nuclei of cranial nerves III and IV can be identified. In a 6-mm. embryo which appears to belong to this horizon, stained in toto with silver, Rhines and Windle (1941) also recognized the median longitudinal fasciculus.

Rhombencephalon. As far as the primary centers of the cranial nerves of this subdivision are concerned, the organization is almost as far advanced as in the preceding group.

Horizon xiv, Embryos Ranging from 5.5 to 7.3 mm. (G. L.)

The embryo shown in figure 45 (pl. 19) is one of the more advanced of the group. The fore- and midbrain appear as mere appendages of the large hindbrain (fig.

45, pl. 19). The doming of the dorsolateral forebrain wall has begun, although it is hardly possible to speak as yet of a cerebral vesicle (fig. 46, pl. 20). Similarly the transition of the thin telencephalic to the diencephalic roof is gradual. The di-mesencephalic sulcus is well marked externally (figs. 48, 49, pl. 20), as is also the post-mammillary sulcus (fig. 45, pl. 19). The asterisk in this figure indicates the sulcus between the two segments of the midbrain which are also present in other embryos of this and other stages. The roof at this point is thin; it may be the precursor of the minute transient evaginations of the midbrain roof described by Elze (1907) and Hochstetter (1919) in more advanced embryos. The tectum of the midbrain ends abruptly where a few fibers of cranial nerve IV have reached the mid-line. The membranous roof of the fourth ventricle begins at the isthmus, differing in this respect from the more advanced embryos. The elongated isthmus is the outstanding feature of this brain. Rhombomeres 2 to 6 are also manifestly transverse segments of the neural tube (fig. 50, pl. 21).

Prosencephalon. The primordium chiasmatis can be identified at the inferior end of the lamina terminalis by the confluence of the optic stalks. A thin segment of the lamina terminalis separates the primordium chiasmatis from the commissure bed (fig. 45, pl. 19). Rostral to the velum transversum the membranous lamina terminalis shows the beginning of the keel of the telencephalon medium. Figure 49 (pl. 20) shows the oral hypophysis which appears as a median plate consisting of tall epithelial cells. Its relation to the brain floor is unique, as there is some evidence of cell migration from the adjacent surfaces of both epithelia.

Diencephalon. The wall of the neural tube at the site of the future thalamus is uniformly thin and consists almost exclusively of a germinal layer (figs. 47, 48, pl. 20). The lateral walls of the hypothalamus are more conspicuous, and the mammillary region is thickened in the mid-line (fig. 45, pl. 19).

Mesencephalon. The specimen seen in figure 45 presents two enlargements of the neural tube at this level. In this embryo the naked early "pathfinder" axones arising from the neuroblasts of cranial nerves III have grown out into the mesenchyme and a few fibers of nerve IV can be followed in the marginal layer of the lateral wall to the site of their decussation.

Rhombencephalon. An outstanding feature of the hindbrain in this horizon is the evidence of rapid growth in the region of the isthmus and rhombomere 1, as can be judged from their relatively greater length compared with less advanced embryos. The large cerebellar lamina is another manifestation of this growth. The afferent root fibers of cranial nerves V, VII, IX, and X enter in rhombomeres 2, 4, 5, 6, and 7, respectively (fig. 50, pl. 21). In silver-stained sections of a "6-mm.+" human embryo, Wilson et al. (1941) found both afferent and efferent fibers of cranial nerves V, VII, VIII, IX, and X.

Horizon xiii, Embryos with More than 29 Somites Ranging from 4 to 6 mm. (G. L.)

At this stage the brain consists of a series of enlargements of the neural tube separated by relatively broad constrictions. The embryo shown in figure 53 (pl. 23) is one of the earliest of the group. The optic vesicles constitute the dominant feature of the forebrain. There is nothing to indicate the site of a future cerebral vesicle: no lateral evagination or thickening of the forebrain wall can be seen, nor is there an area with more numerous mitoses that could indicate the site of the future cerebral vesicle.

A well defined constriction separates forebrain and midbrain. Figure 52 (pl. 22) confirms the projection reconstructions of figure 53 (pl. 23) in regard to the relation of the cranial flexure to the midbrain. The midbrain is identified by its characteristically thick floor, by its relation to the forebrain as delimited by the optic vesicle, and by its relation to the isthmus (see pp. 27–28).

Prosencephalon. The rostral end of the neural tube represents both the future lamina terminalis and the thalamic roof plate. At this stage the wall of the entire segment is uniform in thickness. The primordium of the olfactory epithelium has appeared (fig. 54, pl. 24). The outer wall of the optic vesicle is flattened, indicating the area that will subsequently invaginate to form the secondary optic vesicle (compare fig. 55, pl. 24, and fig. 48, pl. 20). The optic stalks unite at the site of the future chiasma. Adjoining the persisting dorsal edge of the oral membrane is the differentiated epithelium of the oral hypophysis, which is applied to the infundibular area (fig. 55, pl. 24). Caudal to this area the floor of the neural tube is depressed, marking the site of the mammillary recess (fig. 56, pl. 24). The mammillary body which arises from this recess adjoins the pros-mesencephalic sulcus at all stages in which it can be recognized.

Mesencephalon. The roof of the midbrain in the specimen shown in figure 53 (pl. 23) has a thin spot (*) in the mid-line (compare fig. 56 and fig. 57, pl. 24). This corresponds to that in figures 51 and 52 (pl. 22). A similar spot was found in an embryo of horizon xvii. The floor plate is thicker at this level than elsewhere, foreshadowing the differentiation of the mesencephalic tegmentum (figs. 51 and 52, pl. 22). The floor thins out at the isthmus where there is a minute depression which can be identified as the recessus isthmi of more advanced embryos.

Rhombencephalon. Adjoining the isthmus, the roof plate gradually thins out into the membranous tela choroidea ventriculi IV. Dorsally at this level the ventricle is dilated, indicating the beginning of the separation of rhombomere 1 from rhombomere 2. This region is beginning to expand rapidly, as may be seen by comparison with embryos of horizon xiv. There is no evidence in the embryo shown in figure 53 (pl. 23) that any cranial nerve roots have developed. The neural crest which will produce ganglion and neurolemma cells is broadly attached to the dorsal edge of the hindbrain. The neural crest at the level of rhombomere 2 will contribute ganglionic neuroblasts and sheath cells to cranial nerve V, whereas the cells of the crest associated with the large rhombomere 4 contribute to NN. VII and at least sheath cells to N. VIII. Rhombomere 5 is similarly related to the crest for N. IX, and rhombomeres 6 and 7 to N. X (fig. 59, pl. 24). In a 4-mm. human embryo, Windle and Fitzgerald (1942) found a few neuroblasts differentiated in the primordium of the semilunar ganglion.

Horizon xii, Embryos with 21 to 29 Somites Ranging in Length from 3.8 to 4.9 mm.

The extent of the dorsal flexure in this horizon is the chief factor in this relatively great variability in length.

Figure 60 (pl. 25) is based on an embryo of 22 to 23 somites. The site of closure of the anterior neuropore is marked by a median ridge where the nuclei of the cells are irregularly arranged and the surface ectoderm is not differentiated (fig. 62, pl. 26). A deep, narrow constriction separates the forebrain and midbrain (fig. 65, pl. 28). The cranial flexure is at the level of the two midbrain neuromeres. The sulcus between midbrain and hindbrain (isthmus) is slightly broader than those between the rhombomeres. The neural tube in the model of 8943 shown in figure 65 (pl. 28) resembles that of the preceding embryo in the appearance of the optic vesicles and the mammillary recess (see also fig. 62, pl. 26).

The first neuromere of the midbrain (fig. 65, pl. 28) has a wide lumen, and its thickened floor plate foreshadows the mesencephalic tegmentum (fig. 60, pl. 26). The "cranial neural crest" arising from the second midbrain segment is continuous with the crest of rhombomere 2 (fig. 63, pl. 26), and probably contributes sheath cells to the ophthalmic trunk of cranial nerve V. The crest of NN. VII and VIII originates from rhombomere 4 and extends into the hyoid arch. The roof plate of the neural tube is thinner at this level than elsewhere (compare fig. 64, pl. 27, with fig. 63, pl. 26), presaging the rapid enlargement of the ventricle in more advanced embryos of horizon xii.

Horizon xi, Embryos of 13 to 20 Somites, Ranging in Length from 3 to 5 mm.

The 19-somite embryo on which the model and reconstruction (figs. 64, pl. 27, and 66, pl. 28) are based has a long, narrow anterior neuropore. The closure of the neural folds has proceeded dorsally from the chiasma as far as the middle of the optic vesicle, independently of the closure that is proceeding forward from the midbrain. The site of final closure of the neuropore varies (Davis, 1923, p. 14, and Streeter, 1942, fig. 6, xi). Most of the lateral wall of the forebrain has evaginated to form the optic vesicle (see p. 28). The pros-mesencephalic sulcus is well defined; it turns caudally toward the mammillary recess (fig. 66, pl. 28). The angle of the cranial flexure is about 100°. Rhombomeres 1-2, 3, 4, 5, and 6 constitute distinct enlargements of the neural tube.

Prosencephalon. In the region of the neuropore the folds are high and the optic evaginations are directed laterally. Their tapering form and low peripheral wall are characteristic of this stage. The migration of crest cells from the optic vesicle has begun (Bartelmez and Blount, 1954). The union of the optic stalks rostrally marks the primordium chiasmatis. The differentiation of the oral hypophysis is evidenced (1) by the pale staining of the cytoplasm of the epithelial cells (as in fig. 61, pl. 26), (2) by the contact with the neural epithelium, and (3) by the fact that the thickened epithelium adjoins the intact oral membrane (fig. 64, pl. 27).

Mesencephalon. The first midbrain neuromere is large, as may be seen in figure 66 (pl. 28); the second neuromere is less distinct.

Rhombencephalon. Rhombomeres 1–2 and 4 are of similar relative size as in the preceding embryo. Rhombomere 4 of this stage, however, differs from more advanced embryos by having a narrow lumen ventrally. In the embryo shown in figure 66 (pl. 28), a cord of crest cells extends from the hindbrain to the epibranchial placode of N. VII. The proliferation of crest from rhombomere 5 is inconspicuous at this stage, and small numbers of crest cells are also arising from rhombomere 6.

Horizon x, Embryos from 4 to 12 Somites

The only perfectly preserved embryo in this group is the 10-somite embryo (no. 5074) described and illustrated in detail by Corner (1929). The neural folds had closed as far as rhombomere 4, but the surface epithelium covers the edges of the folds as far forward as the forebrain (figs. 69 and 70, pl. 30). This is indicated by the double broken line in figure 67 (pl. 29). The figure shows a cellular tag at the tip of the primordium chiasmatis which may be the beginning of the rostrocaudal closure of the neuropore. Thickenings of the neural epithelium extend diagonally across each forebrain fold so that they meet rostrally in the "torus opticus," which can readily be identified as the primordium chiasmatis of later stages (Corner, 1929, figs. 1 and 2). There is a sulcus in each optic thickening caudally (fig. 69, pl. 30), which is the beginning of the evagination that produces the optic vesicle. The neural folds become narrower abruptly just caudal to the optic primordium indicating the pros-mesencephalic sulcus. The neural groove widens into the midbrain, which is narrower dorsally than the forebrain. There is only a single midbrain segment. At this level the axis of the neural folds turns gradually through an angle of about 110°, thus marking the cranial flexure. There is a further narrowing of the folds in the hindbrain, where shallow lateral sulci separate the rhombomeres, which are prominent as ventral depressions (fig. 67, pl. 29). As in the embryos of horizon xi, the first hindbrain segment is long. From it and from the midbrain a continuous strand of the neural crest is being proliferated. Rhombomere 4 is characterized by its thick lateral walls and narrow lumen as well as by the juxtaposition of the seventh and eighth neural crests and the otic disc. Rhombomeres 5 and 6 are faintly indicated; the end of the basal depression corresponding to rhombomere 6 is 40 microns rostral to the level of the first somite.

For the 8-somite embryo shown in figure 68 (pl. 29), the plane of section was perpendicular to the surface of the forebrain folds so that they could be readily plotted (Bartelmez and Evans, 1926, fig. 19, pl. 9). The optic primordia (fig. 71, pl. 30) extend diagonally across the forebrain folds and meet in the mid-line rostrally as in the embryo described by Corner. Near the caudal end of the optic primordia there is the merest adumbration of a sulcus corresponding to the optic sulcus of the 10-somite embryo. This is the earliest stage in which morphologic evidence of the optic primordium has been recognized.

Immediately rostral to the oral membrane, the ectoderm is thicker in the mid-line and better differentiated as shown by a lightly staining cytoplasmic zone (fig. 71, pl. 30). Caudal to the optic primordium the pros-mesencephalic sulcus is well defined since the midbrain folds are narrower than the flaring folds of the forebrain. At the midbrain there is the usual shift of the neural axis. The cranial neural crest originates from the dorsal edge of the midbrain and the large first hindbrain segment. Rhombomere 4 is recognized by its narrow lumen dorsally and its relations as described for the preceding embryo, whereas rhombomeres 5 and 6 can be identified only by slight, although definite, enlargements of the neural tube.

SEQUENCE OF EVENTS IN EARLY DEVELOPMENT OF THE BRAIN

Before the neural folds have begun to close they present a linear series of growth centers which appear as enlargements separated by constrictions. In a 4-somite embryo (no. 3709) modeled on the basis of photographs and sketches of the intact specimen (Bartelmez, 1923, fig. 2), the neural folds are widest in the first segment. This becomes the forebrain. At the level of the second segment the neural axis shifts through an angle of about 110°. This change in axis constitutes the cranial flexure. It occurs at the midbrain in every subsequent stage (see p. 27). In the 4-somite embryo there are three segments between the midbrain and the level of the first somite. The development of all the definitive structures of the hindbrain can be traced by identifying these segments. In the 8-somite embryo (fig. 68, pl. 29) the folds are wide and flaring in the forebrain, higher and narrower in the midbrain and in the hindbrain, which presents four segments. The second of these is distinguished by its form and relations (see p. 28). Thickened areas of the folds of the forebrain of this embryo can be followed through later stages. They become the optic vesicles and their stalks (figs. 67 and 68, pl. 29; 69 and 71, pl. 30). Their junction at the rostral end of the neural folds in the mid-line becomes the primordium chiasmatis. The oral hypophysis can be recognized as a median area of differentiated and thickened surface epithelium immediately rostral to the oral membrane (figs. 68, pl. 29, and 71, pl. 30). Since this oral epithelium remains in intimate contact with the neural epithelium the infundibular region is defined. Cells of the neural crest are proliferating from the midbrain and first hindbrain segment ("trigeminal crest") and from the fourth rhombomere ("acustico-facial crest").

Horizon xi. As the neural folds rise and approach one another the rapidly expanding optic primordium assumes the characteristic form of the optic vesicle (Streeter, 1942, fig. 6, xi). In the more advanced embryos, typical neural crest cells migrate from the optic vesicle (Bartelmez and Blount, 1954). A depression in the brain floor caudal to the infundibular region appears which marks the site of the mammillary body (fig. 64, pl. 27). In some embryos of this horizon two segments appear in the midbrain. Thickening of the floor and basal plates foreshadows the tegmentum of the mesencephalon. Local growth in the hindbrain brings into prominence rhombomere 5, and the neural crest of N. X proliferates from rhombomeres 6 and 7.

Horizon xiii. The thickening of the outer wall of the optic vesicle presages the neural layer of the retina that will invaginate to form the optic cup (fig. 55, pl. 24). The floor of the forebrain has become thinner as the mammillary recess deepened. There is nothing to indicate the site of the cerebral vesicle. The olfactory placode makes its appearance (fig. 54, pl. 24). Accelerated growth at the rostral end of the hindbrain results in the separation of rhombomeres 1 and 2.

Horizon xiv. The first evidence of the cerebral vesicle appears in a form of doming of the lateral forebrain wall dorsally (fig. 46, pl. 20). The enlargement of the telencephalic ventricle is uniform, and its roof thins out in the mid-line. As a result the lamina terminalis is differentiated from the roof of the diencephalon, which remains thicker (fig. 45, pl. 19). At this point of transition the di-telencephalic sulcus reaches the mid-line, defining the velum transversum. In all the subsequent stages we are considering, the telencephalic limb of the velum transversum is thinner than the diencephalic.

Two localized thickenings appear in the lamina terminalis, namely the primordia of chiasma and commissure bed. The increased separation of the infundibular and mammillary regions gives evidence of the growth of the hypothalamus (compare fig. 53, pl. 23, and fig. 45, pl. 19). The oral hypophysis is in intimate relation with the neural epithelium, and in one specimen (no. 6502) cells appear to be migrating from the adjacent surfaces of both. The hypothalamus, bounded dorsally by the sulcus hypothalamicus, is the only diencephalic region showing signs of differentiation. In the caudal one-third of the mesencephalic tegmentum neuroblasts have given rise to the "pathfinder" axones of nerves III and IV. The elongation of the isthmus and rhombomere 1 is an outstanding event; the dorsolateral thickening of rhombomere 1 has produced the cerebellar lamina; the beginning of the pontine flexure and lateral recess of the fourth ventricle can be recognized. The afferent and efferent root fibers of cranial nerves V to X appear in embryos of this group. The relation of cranial nerves to rhombomeres is shown in figure 45 (pl. 19) (see also fig. 50, pl. 21).

Horizon xv. The cerebral vesicle is now more clearly outlined, and the di-telencephalic sulcus appears as a prominent ridge on the ventricular surface. There is, as yet, no evidence of the striatal eminence. The telencephalon medium is relatively large. The separation of the optic vesicle from the brain wall has brought the optic stalk into prominence (fig. 41, pl. 18). The elongated primordia of chiasma and commissure bed are separated by a short membranous segment of the lamina terminalis (fig. 40, pl. 17). This segment becomes the lamina terminalis of the adult brain. The diencephalon is divided into two parts by the sulcus hypothalamicus (figs. 43, 44, pl. 18). The epiphysis can be recognized; rostral to it the development of a mantle zone indicates the site of the habenular complex in more advanced embryos. In the rostral hypothalamus neuroblasts of the thickened lateral wall (figs. 41 and 43, pl. 18) have given rise to the "tractus hypothalamicus" of His, which appears to be the beginning of the medial forebrain bundle. This is the earliest neuronal differentiation rostral to the midbrain. In the caudal part of the hypothalamus the developing mantle zone and thickened floor distinguish the mammillary region. A marginal velum has appeared in the mesencephalic tectum. Association bundles (medial and lateral fasciculi longitudinales) are present in the tegmentum of mid- and hindbrain.

Horizon xvi. The bubble-like cerebral vesicle extends somewhat beyond the lamina terminalis (fig. 33, pl. 15), and in the more advanced embryos of this group the earliest cortical differentiation has made its appearance. It is the thickening of its dorsal wall together with a widening of the marginal velum which defines the hippocampal primordium (Hines, 1922) (see fig. 31, pl. 13). The thickening of the ventrolateral wall of the cerebral vesicle marks the beginning of the corpus striatum (fig. 35, pl. 16). Typical neural crest cells between the olfactory epithelium and the brain mark the region of the olfactory bulb (fig. 34, pl. 16). The telencephalon medium has become larger, both relatively and absolutely. The four characteristic diencephalic regions are well defined. Dorsal and ventral thalamus are separated by a ridge on the ventricular surface which is associated with the zona limitans intrathalamica (figs. 38, 39, pl. 16). In the hypothalamus the infundibular recess has appeared. Its separation from the chiasma has increased with the development of the lateral hypothalamic cell column. To the fiber tract arising from this column the mammillotegmental system has been added. As the organization of the mesencephalic tegmentum progresses, the posterior commissure develops. The growth and differentiation of the hindbrain have eliminated the external sulci between the rhombomeres, but the dilatations of the ventricle in basal and alar plates still mark their locations (figs. 38 and 39, pl. 16).

Horizon xvii. The cerebral vesicle has expanded and differentiated. The hippocampal primordium and adjoining area epithelialis comprise most of the medial wall of the vesicle (figs. 22, pl. 11, and 31, pl. 13). A highly vascularized part of the area epithelialis adjoining the paraphysis begins to invaginate and soon produces the lateral choroid plexus (figs. 29 and 30, pl. 13). The olfactory bulb and septal nuclei have appeared. The corpus striatum has enlarged, and its mantle zone is rich in neuroblasts and fibers. The earliest of the internal capsule fibers have thickened the wall of the di-telencephalic sulcus. Certain of these fibers can be followed to the ventral thalamus. Others remain in its mantle layer or on the surface of the hypothalamus and reach the tegmentum. They join fibers which appear to come from the olfactory area. The first indication of neopallial differentiation is a slim bundle of fibers which extends from the mantle zone of the striatum to the adjacent wall of the cerebral vesicle. The chiasma and commissure bed are simply thickenings of the lamina terminalis. The epiphysis appears as a minute evagination of the roof of the epithalamus. Rostral to it habenular neuroblasts have given rise to the fasciculus retroflexus (figs. 22, pl. 11, and 26, pl. 12). The mantle zone is broad in the ventral thalamus but only indicated in the dorsal thalamus; they are sharply separated from one another by the zona limitans intrathalamica and the adjacent ventricular ridge (figs. 25 and 26, pl. 12). The hypothalamus continues to be the largest and most highly differentiated division of the 'tweenbrain. Differences in growth rates have brought the infundibular region relatively closer to the chiasma than in earlier horizons.

Horizon xix. The cerebral vesicle has extended forward beyond the olfactory bulb, and it also overlaps half of the thalamus caudally. Its expansion dorsally is indicated by the fact that neopallium now comprises a substantial part of the medial wall (figs. 20, pl. 9; 19, pl. 8). The primordium hippocampi is well defined by its thickness, marginal velum, and ventral limiting sulcus (fig. 19, pl. 8). The inferior extremity of the hippocampal formation extending into the developing temporal lobe has reached the level of the infundibulum. The expansion of the cerebral vesicle, combined with the enlargement of the corpus striatum, and the thickening of the di-telencephalic sulcus with its accumulating fibers (internal capsule) have resulted in the close approximation to the ventral thalamus (fig. 16, pl. 7). The relatively large choroid plexus of the lateral ventricle and area epithelialis are, however, still separated from the thalamus by primitive meninx (figs. 15, pl. 7, and 19, pl. 8). Subsequently the dorsal thalamus enlarges and expands into the lateral ventricle so that the area epithelialis becomes fused to the free surface of the thalamus. The telencephalon medium ("cavum Monroi" of Hochstetter) is still large; its lateral extent is marked by the medial eminence of the corpus striatum (fig. 16, pl. 7). Many fine fibers of the postoptic system are present on the caudal surface of the primordium chiasmatis; in the more advanced embryos of the group a few coarser retinal fibers have reached its rostral surface.

Figures 14 to 16 (pl. 7) show the divisions of the diencephalon at this stage. The epithalamus has increased in length with the dorsal thalamus; the rapid growth of this region can be appreciated by comparing figure 22 (pl. 11) and figure 1 (pl. 1). The stria medullaris adjoining the taenia thalami passes into the habenular complex, and this in turn gives rise to the fasciculus retroflexus. The epiphysis has developed a large superior lobe in some embryos of the group (Bailey, 1916). The ventral thalamus is still well in advance of the dorsal thalamus in differentiation. The relations of infundibulum to chiasma shown in figure 20 (pl. 9) are similar to those of earlier stages; in figure 13 (pl. 6), on the other hand, they are close together as in more advanced embryos. The cell groupings characteristic of the mammillary bodies are shown in figure 16 (pl. 7). In the dorsal wall of the di-mesencephalic sulcus the posterior commissure has become long and narrow and the sulcus itself has deepened, largely as a result of the growth of the thalamus. In the midbrain the outstanding event is the lateral outpouching at its caudal end, which foreshadows the inferior colliculus.

The earliest reflex response that has been obtained in human embryos was observed in specimens whose maturation would correspond to embryos of this horizon (Fitzgerald and Windle, 1941, and Hooker, 1942), although the neural mechanisms involved in this reaction had already been established in horizon xvi.

Horizon xx. The outstanding feature of embryos belonging to this group is the increase in size of all parts of the brain. The cerebral vesicles have expanded greatly, and they are relatively larger in comparison with the other subdivisions of the brain. The dorsal extremities of the cerebellar laminae have thickened materially (fig. 12, pl. 5); in older embryos they will eventually fuse in the mid-line, giving rise to the vermis cerebelli. In the roof of ventricle IV the site of the foramen of Magendie can be recognized (see pp. 19–20).

Horizon xxii. The growth of the neopallium has been largely responsible for the expansion of the cerebral vesicle (fig. 1, pl. 1). The earliest evidence of neopallial cortex has appeared in the wall overlying the corpus striatum where the lateral fissure will subsequently develop. It is manifested by the narrow superficial "cortical plate" which marks the beginning of cortical differentiation (fig. 5, pl. 3). There has been a corresponding development of the corpus striatum and the internal capsule. The relations of the cerebral vesicle and thalamus at successive levels are shown in figures 5 to 8 (pl. 3). No fibers have appeared as yet in the commissure bed. In advanced embryos of this group the optic tract has extended to the thalamus indicating the site of the lateral geniculate body (His, 1904; Hochstetter, 1919). In a 29-mm. embryo Dekaban (1954) identified the primordia of both geniculate bodies in this region. This and the cluster of habenular neuroblasts are the earliest cytoarchitectonic developments of the diencephalon dorsal to the hypothalamus. In the midbrain the outstanding events are the appearance of the superior colliculus and the differentiation of the tectum.

DISCUSSION

Certain of our interpretations require further elaboration.

Relation of cranial flexure to the midbrain. It has long been recognized that the adult forebrain, midbrain, and hindbrain differ fundamentally in their organization and they may well be expected to be distinct morphologically in early neural fold stages. In his profound discussion of the morphological plan of the brain, Kingsbury (1922 and 1930) pointed out that in its development the forebrain presents no segmental features and lacks anything resembling the floor plate or basal plate which appear in the midbrain and hindbrain. The midbrain differs from the hindbrain in that the ventral suture (septum medullae cranialis) is absent. He presented evidence that in Amphibia the hindbrain and spinal cord arise by the concrescence of the lateral moieties of the primordium of the nervous system; this occurs during the formation of the neural plate.

In the earliest embryos we are considering, the forebrain is characterized by the primordium of the optic vesicle; the first segment of the hindbrain can be followed from later stages by its form and relation to the cranial neural crest. Between them is the midbrain, separated fore and aft by sulci. When the reconstructions are controlled by profiles of the intact embryos, the shift in the neural axis is at the level of the midbrain (Bartelmez, 1923, and Corner, 1929). This flexure can be followed through all subsequent stages of development as the cranial flexure. In various embryos, prior to the appearance of the optic primordium, the midbrain has been identified by its relation to the cranial flexure and to the first hindbrain segment.

The midbrain and its relation to the cranial flexure have been demonstrated in 22 embryos in the Carnegie Collection with 8 to 30 somites. In most of them accurate profile photographs of the intact specimens served as controls for the reconstructions. Three of the embryos were sectioned in the sagittal plane (see fig. 52, pl. 22). Serious doubts can consequently be raised as to the accuracy of Thompson's (1907) reconstruction from sections of a 22–23 somite embryo in which the cranial flexure appears at the level of the isthmus and first hindbrain segment. There is no record of a study, photograph, or drawing of the intact specimen which might have served him as a control. Hochstetter's earliest stage (1919, fig. 1, pl. 1) shows the cranial flexure at the isthmus. Hochstetter states that Thompson's figure 2 served as a guide for the piling of the wax plates of the model. Photographs of the embryo before embedding, such as were routinely made of his specimens, could not be made in this instance because of a coagulum on the surface which also interfered with the sectioning. Our figures 53, plate 23, and 60, plate 25, are based on perfectly preserved embryos (see pls. 24 and 26) which correspond in their stage of development to the cited embryos of Hochstetter and Thompson, respectively.

Adelmann (1925, figs. 1 and 2) presents graphic reconstructions of a 5- and an 8-somite rat embryo in which the sharp flexure of the neural folds is rostral to the segment identified as midbrain. In his figures of models of 5-, 6-, and 8-somite embryos this flexure appears immediately caudal to the optic foveolae. In his reconstruction of a 9-somite specimen (fig. 3) the flexure we would term "cranial" is at the level of what he terms "mesencephalic segments," agreeing in this respect with all his later stages. Reconstructions of 4- to 7-somite rat embryos figured by Bartelmez (1962, figs. 2, 4, and 6) show the "cranial" flexure at the segment identified as midbrain. This interpretation is based on three considerations: (1) The segment in question adjoins the optic primordium (or optic foveola) which characterizes the forebrain. (2) Between the prosencephalon and mesencephalon a constriction of the neural folds can be recognized in intact embryos as well as in sections. It represents an early stage of the pros-mesencephalic sulcus. (3) The mode of formation of the neural crest in the rat changes at this sulcus to that characteristic of mid- and hindbrain.

Segmentation of the neural tube. The rostral end of the neuraxis of early vertebrate embryos presents a series of growth centers which usually appear as enlargements separated by constrictions (see Berquist, 1952, and our fig. 50, pl. 21). Kingsbury (1922 and 1930) and Kingsbury and Adelmann (1924) have pointed out the fundamentally distinct character of the forebrain and midbrain enlargements. No one familiar with Ray Lancaster's discussion of metamerism is likely to indulge in speculation concerning segments which might have contributed to the formation of the vertebrate head. However, the relations of certain cranial nerves to rhombomeres and pharyngeal pouches seem to suggest that these segmental structures have persisted in vertebrate development because of the importance of the associated nerves. Rhombomeres 1, 2, and 3 contribute crest cells to the ganglion and sheaths of NN. maxillaris and mandibularis; rhombomere 4 similarly contributes to N. VII, rh. 5 to N. IX, rh. 6 and 7 to N. X, a composite nerve like N. V. The two trunks of N. V fork about the mouth as N. VII forks about the hyomandibular pouch; N. IX has the same relation to the second pharyngeal pouch; N. X, to the third and fourth pouches. In each instance the motor component of the trunk is in the "posttrematic" ramus.

Optic primordia. Our histologic evidence indicates that the primordia of the optic vesicles arise laterally throughout the length of the forebrain as far as the pros-mesencephalic sulcus and meet at its rostral extremity in the mid-line. This would mean that the forebrain contributes the optic vesicles and their stalks, that is the retinae and the substrates for the optic nerve fibers. This does not necessarily conflict with the results of mechanical injuries and generalized chemical insults to the rapidly growing rostral end of the neural folds. Even a minute injury may seriously interfere with the differentiation of the forebrain as a whole, producing cyclopia or anophthalmia (see Kingsbury and Adelmann, 1924). Less ambiguous evidence as to the location of the optic primordia might perhaps be obtained by staining areas of the early neural folds with vital dyes and following their development.

The primordium of the optic chiasma can be recognized in all stages of development up to the appearance of decussating fibers of hypothalamic and telencephalic as well as of retinal origin. It occupies the rostral end of the di-telencephalic junction, which in neural fold stages is the rostral end of the neuraxis in the mid-line.

The primary subdivisions of the brain. The five subdivisions of the embryonic brain already recognized by v. Baer were adopted by His (1893). He named them as follows: telencephalon, diencephalon, mesencephalon, metencephalon, and rhombencephalon. In his recommendations for the B. N. A. he justified the inclusion of "metencephalon" as a major subdivision of the brain on the basis of the form and relations of the cerebellum and pons in the adult brain. He had shown, however, that they arise from a rostral thickening at the dorsolateral edge of the hindbrain. From the first appearance in horizon xiv it is obvious that the thickening which constitutes the "cerebellar lamina" arises from the alar plate of rhombomere 1. Neuroblasts migrating from it eventually encircle the rostral hindbrain and spread caudally as well. Since the hindbrain tegmentum (with the major nuclei of N.V) extends as far as the isthmus, and the motor nucleus of N. VII is included in the pontine levels, it appears that the adult "metencephalon" includes derivatives of rhombomeres 1 to 4.

We agree with His (1893) that the isthmus is a segment of the neural tube of considerable length, and this fact should not be overlooked. It is not a major subdivision, since in early stages it is simply a constriction between midbrain and hindbrain. It elongates after the somite period when the rhombomeres are still obvious segments of the neural tube (compare figs. 60, pl. 25; 53, pl. 23; 50, pl. 21; and 45, pl. 19). Its enlargement is subsequently brought about by the invasion of fiber tracts and adjacent neuroblasts.

Differential growth of various components of the developing brain. The distinctive form of the combined first two hindbrain segments (rhombomeres 1 and 2) and of rhombomere 4 in horizon x makes it possible to recognize the gradual increase in the distance between them. In horizon xi, rhombomere 3 has emerged in this location as a distinct segment of the neural tube (fig. 64, pl. 27). During the same period the neural tube between rhombomere 4 and the level of somite 1 increases in length. Since the original first somite can be recognized throughout horizon xi it can serve as a reliable landmark. In the older embryos of this group rhombomeres 5, 6, and 7 begin to be formed. In horizons xii and xiii the first hindbrain segment grows rapidly, and at the beginning of horizon xiv rhombomere 1 has become distinct from rhombomere 2 (fig. 50, pl. 21).

In horizons xi and xii the mammillary recess is practically in contact with the infundibular region which is marked by the oral hypophysis (figs. 64, pl. 27; 60, pl. 25). In horizon xiii (fig. 53, pl. 23) they are distinctly separated; the distance between them increases rapidly in subsequent stages (fig. 45, pl. 19; fig. 40, pl. 17) as the lateral hypothalamic cell column and the tractus hypothalamicus develop (fig. 43, pl. 18). With the differentiation of the habenula (fig. 33, pl. 15) the epithalamus also elongates, as is indicated by the relative increase in the distance between the rostral end of the thalamus and the epiphysis.

A considerable degree of confusion still exists regarding the differentiation of the rostral part of the midbrain. Streeter (1945 et seq.) came to the conclusion that the rostral area of what has always been called mesencephalic tectum does not contribute to the superior colliculus. He recognized the two segments between the forebrain and hindbrain in the 19- to 20-somite embryo 2053 and termed them pretectal and collicular areas, respectively. We have termed them first and second neuromeres of the midbrain. Both are recognizable in some but not all embryos of horizons xi, xii, xiii, and xiv. In all instances they correspond to the level of the characteristically thick mesencephalic tegmentum and the cranial flexure. Unfortunately, Streeter did not state the criteria by which he recognized the pretectal area. In horizon xv the region bordering on the constriction which we have followed through the series as the di-mesencephalic sulcus is labeled by him "pretectum" (1948, fig. 6, xv). In his figure 10, xvii, the area termed "pretectal" is located at the level of the posterior commissure. This interpretation led him to localize the region between the posterior commissure and the epiphysis as the "habenular nucleus." This is obviously an error; in this horizon the unmistakable fasciculus retroflexus can readily be seen (see fig. 22, pl. 11) emerging from the habenular nucleus. As in all vertebrates this nucleus is entirely rostral to the epiphysis.

Up to the end of the period we are describing (horizon xxii) the nucleus of the third nerve is in the caudal one-third of the mesencephalic tegmentum. Rostral to it are the cells associated with the posterior commissure and the median longitudinal fasciculus. Aside from the well known ability of primary neuroblasts to migrate, it may also be that in later stages the growth rate of the rostral tegmentum lags behind that of the caudal region so that the Edinger-Westphal nucleus eventually comes to lie at the di-mesencephalic boundary. This calls for further study. In the stages we are considering the constriction between midbrain and 'tweenbrain can be readily recognized, and there is no reason to doubt that the optic tectum differentiates as far rostrally as the di-mesencephalic sulcus.

During the fetal period the outstanding example of localized growth and progressive differentiation is the rapid enlargement of the cerebral hemispheres and their commissures.

CONCLUSIONS

The stage of development of any human embryo is most satisfactorily estimated by referring it to an age group (horizon) as defined by Streeter (see p. 15).

By identifying fundamental landmarks the major subdivisions of the brain can be followed from embryos of horizon xxii through successively earlier stages to neural fold stages in which only a series of simple growth centers is present. The identification of landmarks facilitates the recognition of regions with accelerated or slower growth rates. The potentialities of differential increases in size of various regions of the brain can be appreciated if it is borne in mind that the volume of the brain in horizon xix (embryos of 16 to 19 mm.) is about that of the adult epiphysis.

In the early stages the boundaries between forebrain, midbrain, and hindbrain can be recognized by identifying (1) the primordia of the optic vesicles, (2) the cranial flexure, and (3) the two segments of the hindbrain which are distinguished by their form and their relations to the neural crest. The "metencephalon" of His derives from the first four rhombomeres, the cerebellum and pons receiving most of their elements from the rostral rhombomeres.

In horizon x the primordia of optic vesicles and chiasma can be recognized. The subdivisions of the hindbrain can be identified by following this region from more advanced stages of development to the embryos belonging to this horizon. The midbrain is characterized by the cranial flexure in reconstructions controlled by profiles of intact embryos (see p. 27). The oral hypophysis is differentiated, and its intimate contact with the brain floor indicates the region of the infundibulum. Proliferations of neural crest mark the future sites of the afferent roots of cranial nerves V and VII. The otic plate appears.

In horizon xi, proliferation of cells derived from the optic vesicle and from rhombomeres 5 and 6 begins. The mammillary recess can be identified.

In horizons xi to xii the anterior neuropore is closing. As the fusion of the neural folds proceeds dorsally from the chiasma it meets its counterpart that is proceeding rostrally from the midbrain. The tegmentum of the midbrain can readily be recognized in horizon xii. The thinning of the hindbrain roof indicates the site of the fourth ventricle.

Horizon xiii brings the appearance of the olfactory placode and the fovea isthmi. The fourth ventricle has enlarged greatly, and the first rhombomere has become distinct from the second rhombomere.

Horizon xiv is a period of great activity. The endbrain is characterized by the appearance of the cerebral vesicle laterally and by the enlargement of the telencephalon medium. The roof of the telencephalon medium thins out, marking the site of the velum transversum. From this, the embryonic lamina terminalis extends toward the chiasma; near the chiasma it thickens and becomes the primordium of the commissure bed. The neuroblasts of NN. III and IV differentiate. The cerebellar lamina begins its rapid growth. The roots of cranial nerves V to XII are formed. The rhombomeres reach the height of their development (fig. 50, pl. 21).

In horizon xv the epiphysis can be recognized. The earliest differentiation of neuroblasts in the forebrain appears in the hypothalamus. The structural organization of the basal plate in midbrain and hindbrain is progressing rapidly.

Horizon xvi is distinguished by the development of fiber tracts in the hypothalamus and the differentiation of the first cortical region—primordium hippocampi and adjoining area epithelialis. The corpus striatum begins its rapid growth and differentiation. In the 'tweenbrain the habenular region is indicated by a distinct mantle zone. The sulcus medius separates dorsal and ventral thalamus, and the sulcus hypothalamicus marks the boundary between ventral thalamus and hypothalamus. A few fibers of the posterior commissure have appeared in some embryos of the group.

In horizon xvii, the differentiation of the hippocampal formation in the emerging temporal lobe takes place. The first fiber systems of the internal capsule are present in the wall of the di-telencephalic sulcus. In the most advanced embryos a thin bundle extends from the corpus striatum to the adjoining wall of the cerebral vesicle. The fasciculus retroflexus is arising from the well differentiated habenular region. The posterior commissure is well developed. In the early stages of horizon xviii the evagination of the area epithelialis begins to form the lateral choroid plexus at the level of the paraphysis.

The neopallium is growing rapidly in horizon xix, and the internal capsule enlarges. There are many fibers of the postoptic commissure in the primordium chiasmatis, and in some embryos a few retinal fibers can also be traced.

In horizon xx the cerebral vesicle has enlarged greatly, overlapping most of the diencephalon. Primitive meninx still lines the di-telencephalic sulcus. The inferior colliculus appears. The lateral moieties of the corpus cerebelli have become prominent. The region of the foramen of Magendie has differentiated and may be highly permeable at this time. The earliest reflex responses have been obtained from human embryos of this stage.

Horizon xxii is marked by the first appearance of a "cortical plate." Like the other early differentiations of the neopallium, this is in the region adjoining the corpus striatum. The area epithelialis has fused with the lateral thalamic wall, producing the lamina affixa.

LITERATURE CITED

Adelmann, H. B. 1925. The development of the neural folds and cranial ganglia of the rat. *J. Comp. Neurol., 39,* 19–123.

Bailey, P. 1916. Morphology of the roof plate of the forebrain and the lateral chorioid plexuses in the human embryo. *J. Comp. Neurol., 26,* 79–120.

Bartelmez, G. W. 1923. The subdivisions of the neural folds in man. *J. Comp. Neurol., 35,* 231–247.

Bartelmez, G. W. 1962. The proliferation of neural crest from the forebrain in the rat. *Carnegie Inst. Wash. Publ.* 621, *Contribs. Embryol., 37,* 1–12.

Bartelmez, G. W., and M. P. Blount. 1954. The formation of neural crest from the primary optic vesicle in man. *Carnegie Inst. Wash. Publ.* 603, *Contribs. Embryol., 35,* 55–71.

Bartelmez, G. W., and H. M. Evans. 1926. Development of the human embryo during the period of somite formation; including embryos with two to sixteen pairs of somites. *Carnegie Inst. Wash. Publ.* 362, *Contribs. Embryol., 17,* 1–67.

Berquist, H. 1952. Studies on the cerebral tube in vertebrates. The neuromeres. *Acta Zool., 33,* 117–191.

Corner, G. W. 1929. A well-preserved human embryo of ten somites. *Carnegie Inst. Wash. Publ.* 394, *Contribs. Embryol., 20,* 81–102.

Davis, C. L. 1923. Description of a human embryo having twenty paired somites. *Carnegie Inst. Wash. Publ.* 332, *Contribs. Embryol., 15,* 3–51.

Dekaban, A. S. 1954. Human thalamus, an anatomical, developmental and pathological study. II. Development of the human thalamic nuclei. *J. Comp. Neurol., 100,* 63–97.

Dekaban, A. S. 1959. *Neurology of Infancy.* Williams and Wilkins Co., Baltimore.

Elze, C. 1907. Beschreibung eines menschlichen Embryos von 7 mm. grösster Länge. *Anat. Hefte, 35,* 409–492.

Fitzgerald, J. E., and W. F. Windle. 1941. Some observations on early human fetal movements. *J. Comp. Neurol., 76,* 159–167.

Gilbert, M. S. 1935. Early development of human diencephalon. *J. Comp. Neurol., 62,* 81–115.

Heard, O. O. 1957. Methods used by C. H. Heuser in preparing and sectioning early embryos. *Carnegie Inst. Wash. Publ.* 611, *Contribs. Embryol., 36,* 1–18.

Heuser, C. H., and G. W. Corner. 1957. Developmental horizons in human embryos. Description of age group x, 4 to 12 somites. *Carnegie Inst. Wash. Publ.* 611, *Contribs. Embryol., 36,* 29–39.

Hines, M. 1922. Studies in the growth and differentiation of the telencephalon in man. The fissura hippocampi. *J. Comp. Neurol., 34,* 73–171.

His, W. 1887. Die Entwickelung der ersten Nervenbahnen beim menschlichen Embryo. Uebersichtliche Darstellung. *Arch. Anat. u. Entwicklungsges.,* pp. 368–378. Leipzig.

His, W. 1888. Zur Geschichte des Gehirns, sowie der centralen und peripherischen Nervenbahnen beim menschlichen Embryo. *Abhandl. math.-phys. Kl. königl. sächs. Ges. Wiss., 14,* 341–392.

His, W. 1891. Die Entwickelung des menschlichen Rautenhirns von Ende des ersten bis zum Beginn des dritten Monats. I. Verlängertes Mark. *Abhandl. math.-physik. Kl. königl. sächs. Ges. Wiss., 17,* 1–74.

His, W. 1893. Ueber das frontale Ende des Gehirnrohres. *Arch. Anat. u. Entwicklungsges.,* pp. 157–171. Leipzig.

His, W. 1893. Vorschläge zur Einteilung des Gehirns. *Arch. Anat. u. Entwicklungsges.,* pp. 172–179. Leipzig.

His, W. 1904. Die Entwickelung des menschlichen Gehirns während der ersten Monate. *Untersuchungsergebnisse.* 176 pp. Leipzig.

Hochstetter, F. 1919. Beiträge zur Entwicklungsgeschichte des menschlichen Gehirns, *1,* 1–170. Franz Deuticke, Vienna and Leipzig.

Hochstetter, F. 1923. Beiträge zur Entwicklungsgeschichte des menschlichen Gehirns, 2, part 1. Die Entwicklung der Zirbeldrüse, pp. 1–46. Franz Deuticke, Vienna and Leipzig.

Hochstetter, F. 1924. Beiträge zur Entwicklungsgeschichte des Hirnanhanges, pp. 47–78. Franz Deuticke, Vienna and Leipzig.

Hooker, D. 1942. Fetal reflexes and instinctual processes. *Psychosomat. Med., 4,* 199–205.

Keibel, F. 1897. *Normentafeln zur Entwicklungsgeschichte der Wirbelthiere.* I. Normentafel zur Entwicklungsgeschichte des Schweines *Sus scrofa domesticus,* 114 pp. Verlag von Gustav Fischer, Jena.

Kingsbury, B. F. 1922. The fundamental plan of the vertebrate brain. *J. Comp. Neurol., 34,* 461–491.

Kingsbury, B. F. 1930. The developmental significance of the floor plate of the brain and spinal cord. *J. Comp. Neurol., 50,* 177–207.

Kingsbury, B. F., and H. B. Adelmann. 1924. The morphological plan of the head. *Quart. J. Microscop. Sci., 68,* 239–285.

Lewis, W. H. 1915. The use of guide planes and plaster of Paris for reconstructions from serial sections: some points on reconstruction. *Anat. Record, 9,* 719–729.

Rhines, R., and W. F. Windle. 1941. Early development of fasciculus longitudinalis medialis and associated secondary neurons in rat, cat, and man. *J. Comp. Neurol., 75,* 165–189.

Streeter, G. L. 1905. The development of the cranial and spinal nerves in the occipital region of the human embryo. *Am. J. Anat., 4,* 83–116.

Streeter, G. L. 1908. The nuclei of origin of the cranial nerves in the 10 mm. human embryo. *Anat. Record, 2,* 111–115.

Streeter, G. L. 1912. The development of the nervous system. Chapter 14 in Keibel and Mall, *Human Embryology, 2,* 1–156. Philadelphia and London.

Streeter, G. L. 1942. Developmental horizons in human embryos. Description of age group xi, 13 to 20 somites, and age group xii, 21 to 29 somites. *Carnegie Inst. Wash. Publ.* 541, *Contribs. Embryol., 30,* 211–245.

Streeter, G. L. 1945. Developmental horizons in human embryos. Description of age group xiii, embryos about 4 or 5 millimeters long, and age group xiv, period of indentation of the lens vesicle. *Carnegie Inst. Wash. Publ.* 557, *Contribs. Embryol., 31,* 27–63.

Streeter, G. L. 1948. Developmental horizons in human embryos. Description of age groups xv, xvi, xvii, and xviii, being the third issue of a survey of the Carnegie Collection. *Carnegie Inst. Wash. Publ.* 575, *Contribs. Embryol., 32,* 133–203.

Streeter, G. L. 1951. Developmental horizons in human embryos. Description of age groups xix, xx, xxi, xxii, and xxiii, being the fifth issue of a survey of the Carnegie Collection. *Carnegie Inst. Wash. Publ.* 592, *Contribs. Embryol., 34,* 165–196.

Thompson, P. 1907. Description of a human embryo of twenty-three paired somites. *J. Anat. and Physiol., 41,* 159–171.

Van Campenhout, E. 1933. Contribution à l'étude de la formation des nerfs olfactifs. *Trans. Roy. Soc. Canada,* Sect. V, pp. 101–102.

Van Campenhout, E. 1948. La contribution des placodes épiblastique au développement des nerfs crâniens chez l'embryon humain. *Arch. Biol., 59,* 254–266.

Weed, L. H. 1917. The development of the cerebro-spinal spaces in pig and man. *Carnegie Inst. Wash. Publ.* 225, *Contribs. Embryol., 5,* 1–116.

Wen, I. C. 1928. Anatomy of human embryos with seventeen to twenty-three pairs of somites. *J. Comp. Neurol., 45,* 301–376.

Wilson, E. E., W. F. Windle, and J. E. Fitzgerald. 1941. Development of tractus solitarius. *J. Comp. Neurol., 74,* 287–307.

Windle, W. F. 1935. Neurofibrillar development of cat embryos: extent of development in telencephalon and diencephalon up to 15 mm. *J. Comp. Neurol., 63,* 139–171.

Windle, W. F., and J. E. Fitzgerald. 1942. Development of the human mesencephalic trigeminal root and related neurons. *J. Comp. Neurol., 77,* 597–608.

PLATES

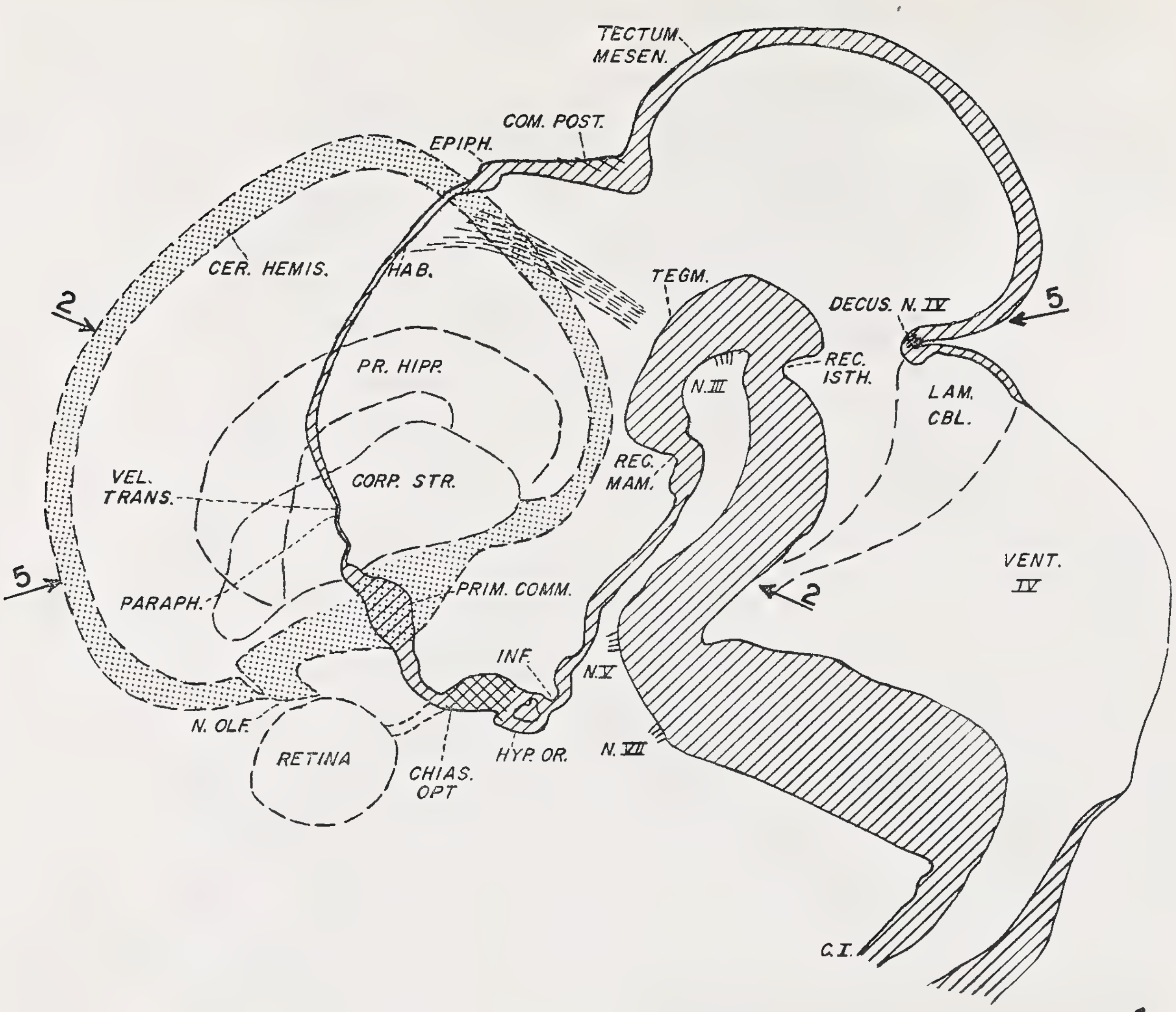

1

Fig. 1. Midsagittal projection reconstruction of brain of embryo 840 (24.5 mm. crown-rump length, horizon xxii). × 16. Cut surfaces are hatched, decussating fibers cross-hatched; profiles of lateral structures such as cerebral vesicles outlined with broken lines or stippled and arrows indicate level of sections. In the lists of abbreviations those on photomicrographs are indicated in parentheses and follow the abbreviations used in the reconstructions.

Abbreviations

CER. HEMIS., Vesicula cerebralis
CHIAS. OPT., Chiasma opticum
C. I., Nervus cervicalis I
CL. S., Colliculus superior
COM. POST. (CM. P.), Commissura posterior
CORP. STR., Corpus striatum
DECUS. N. IV, Decussatio N. IV
EPIPH., Epiphysis
ETH., Epithalamus
F. R., Fasciculus retroflexus
HAB. (HB.), Habenula
HYP. OR., Hypophysis oralis
INF., Infundibulum
LAM. CBL., Lamina cerebellaris
MS., Mesencephalon
N. OLF., Nervus olfactorius
N. III, V, VII, Nervi craniales III, V, VII
PARAPH., Paraphysis
PRIM. COMM., Primordium commissurale ("commissure bed")
PR. HIPP., Primordium hippocampi
REC. ISTH., Recessus isthmi
REC. MAM., Recessus mamillaris
S. DM., Sulcus di-mesencephalicus
ST. M., Stria medullaris thalami
STR., Striatum
TECTUM MESEN., Tectum mesencephali
TEGM., Tegmentum mesencephali
TH. D., Thalamus dorsalis
TH. V., Thalamus ventralis
V. C., Vesicula cerebralis
VEL. TRANS., Velum transversum
VENT. IV, Ventriculus IV
Z. C., Zona corticalis
Z. L. TH., Zona limitans intrathalamica

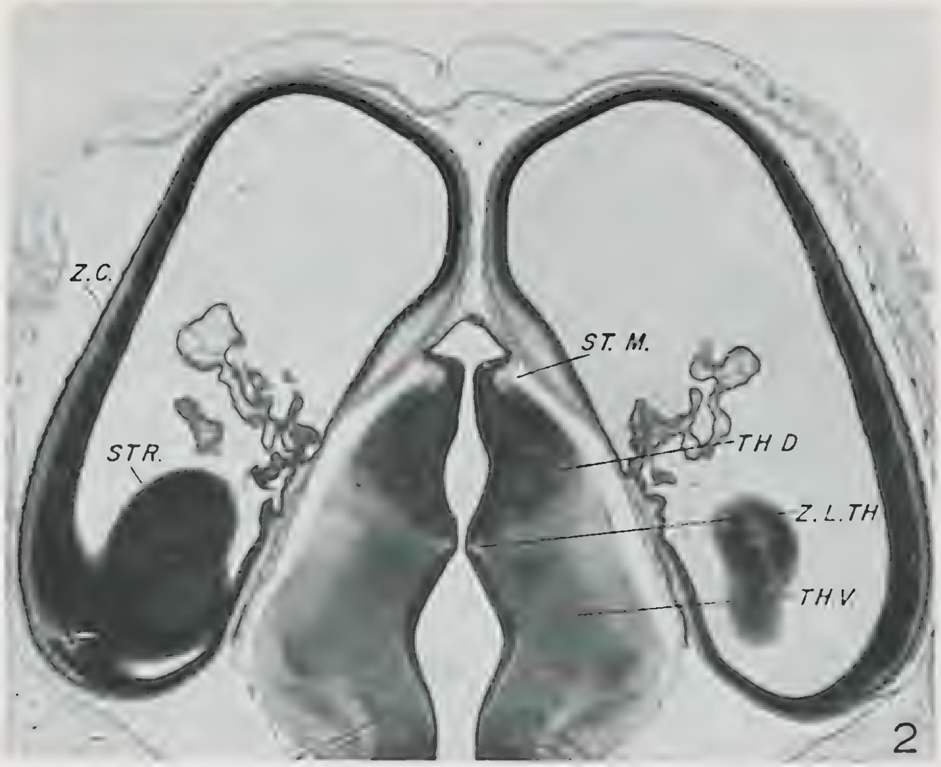

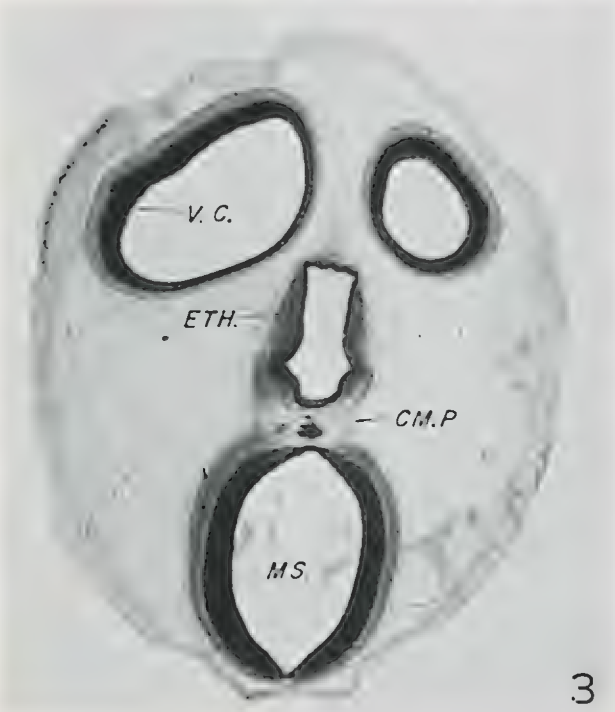

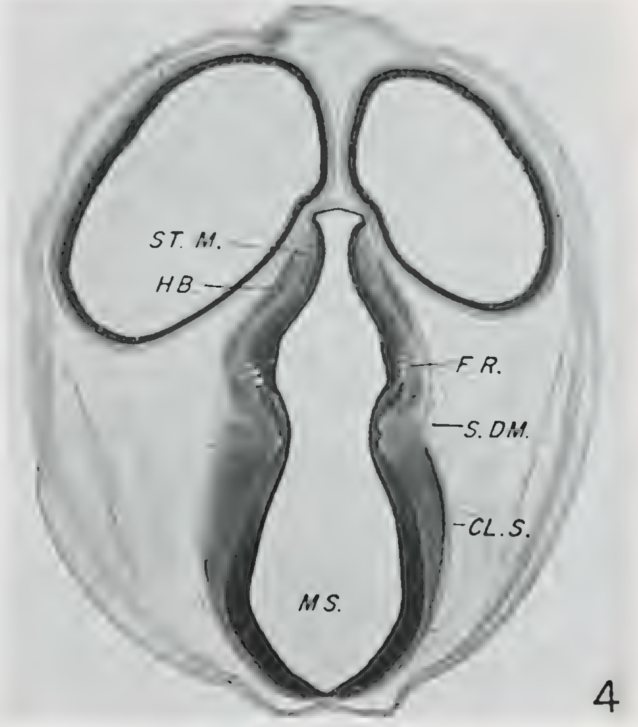

Fig. 2. Photomicrograph of brain of embryo 840, section 13-1-1, taken at level indicated in figure 1 by arrows 2. × 20.

Fig. 3. Photomicrograph of brain of embryo 8394 (25 mm. C. R. L., horizon xxii, section 3-3-5). Plane in which this embryo was cut is indicated in figure 1 by arrows 5. × 10.

Fig. 4. Photomicrograph from the same embryo as in figure 3, section 6-1-2. × 10.

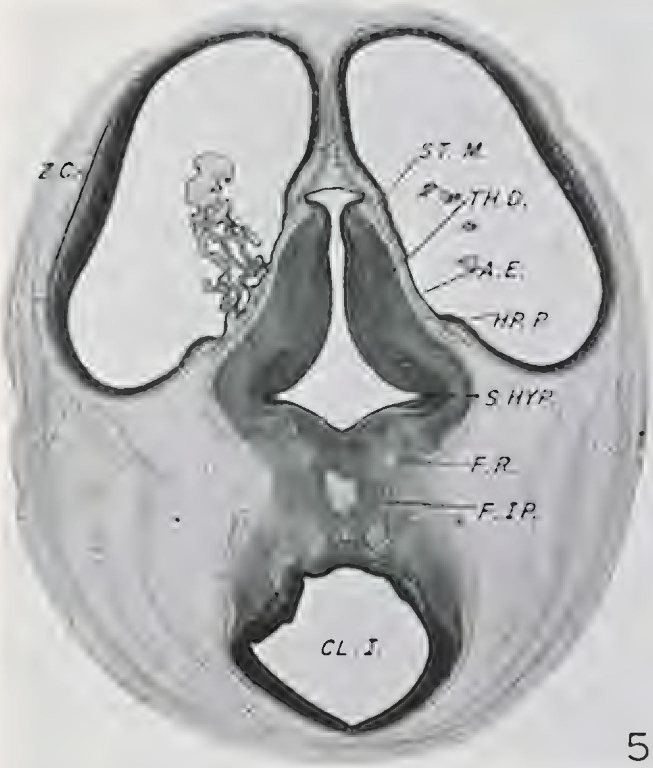

5

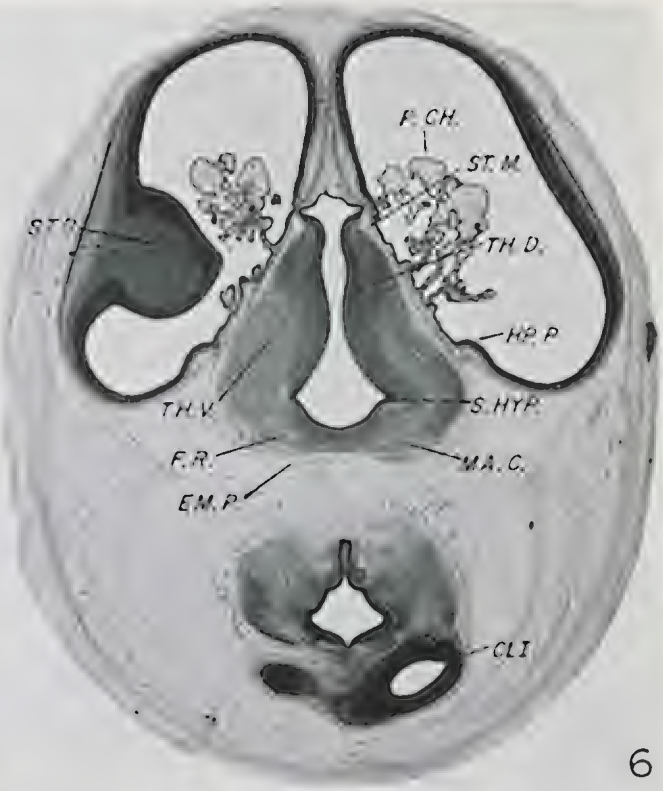

6

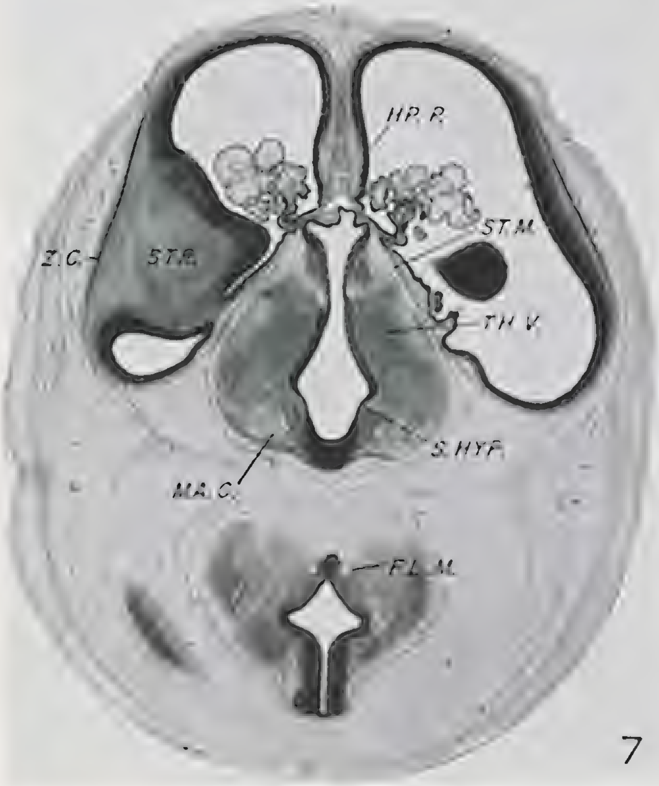

7

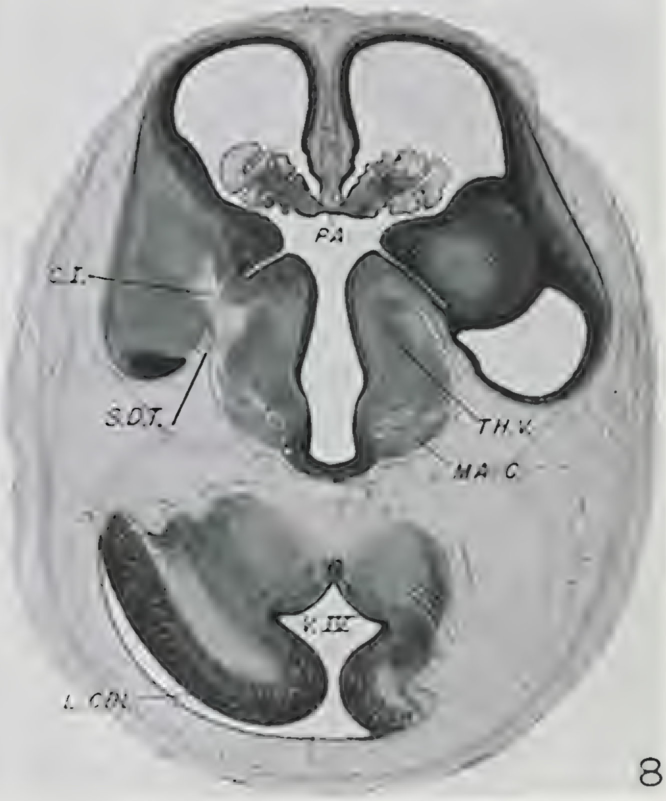

8

Plates 3 and 4. Photomicrographs from sections of embryo 8394 cut in plane indicated by arrows 5 in figure 1 (pl. 1). × 10.

Fig. 5. Section 11-1-3.
Fig. 6. Section 14-1-2. Level indicated by arrows 5.
Fig. 7. Section 16-2-2.
Fig. 8. Section 19-1-2.

Fig. 9. Section 22-1-1.
Fig. 10. Section 24-2-3.
Fig. 11. Section 33-2-2.

Abbreviations are on plate 4.

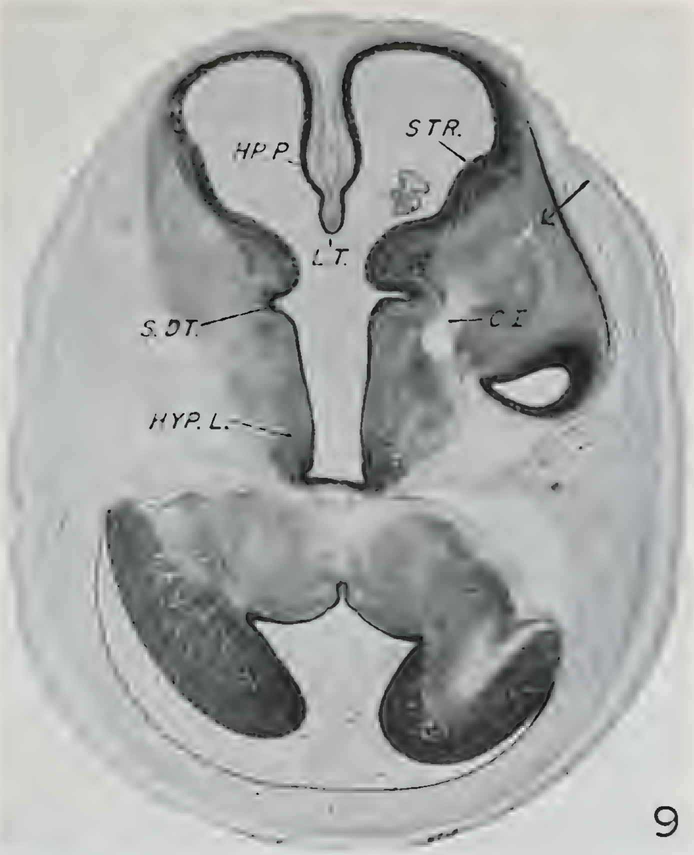

9

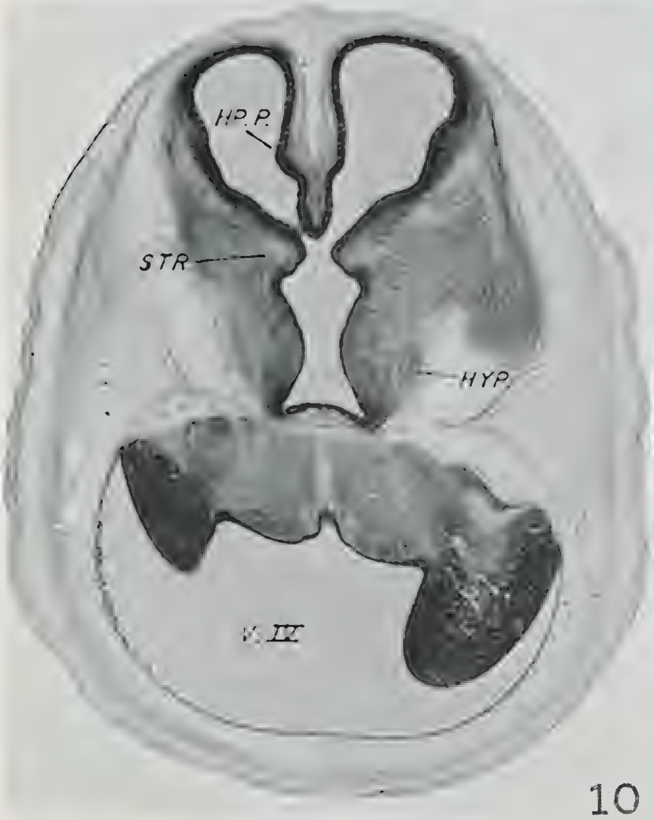

10

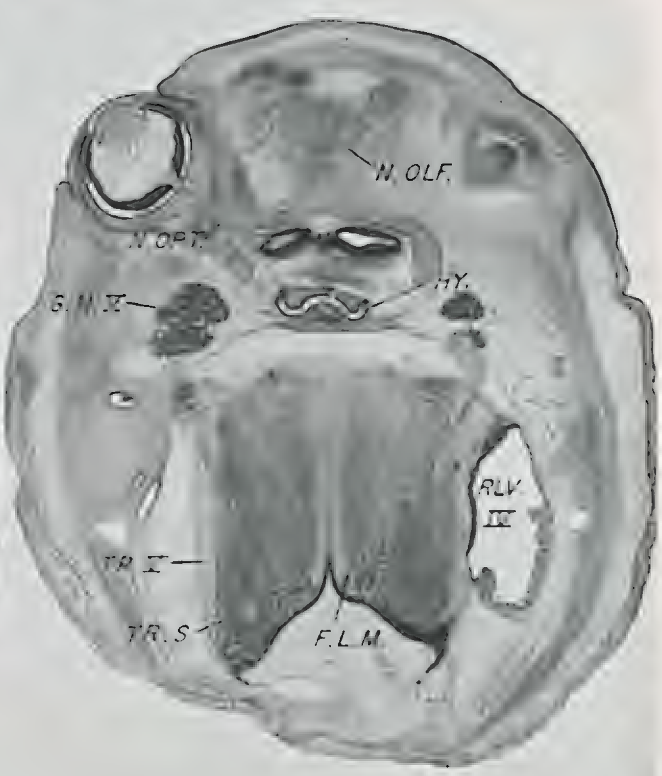

11

A. E., Area epithelialis
C. I., Capsula interna
CL. I., Colliculus inferior
EM. P., Eminentia pedunculi
F. IP., Fossa interpeduncularis
F. L. M., Fasciculus longitudinalis medialis
F. R., Fasciculus retroflexus
G. N. V, Ganglion nervi V
HP. P., Primordium hippocampi
HY., Hypophysis
HYP., Hypothalamus
HYP. L., Nucleus lateralis hypothalami
L. CBL., Lamina cerebellaris
L. T., Lamina terminalis
MA. C., Complexus mamillaris
N. OLF., Nervus olfactorius
N. OPT., Nervus opticus
PA., Paraphysis
P. CH., Plexus chorioideus lateralis
RLV. IV, Recessus lateralis ventriculi IV
S. D.T., Sulcus di-telencephalicus
S. HYP., Sulcus hypothalamicus
ST. M., Stria medullaris thalami
STR., Striatum
TH. D., Thalamus dorsalis
TH. V., Thalamus ventralis
TR. S., Tractus solitarius
TR. V, Tractus spinalis nervi V
V. IV, Ventriculus IV
Z. C., Zona corticalis
↑, Radiatio ad corticem

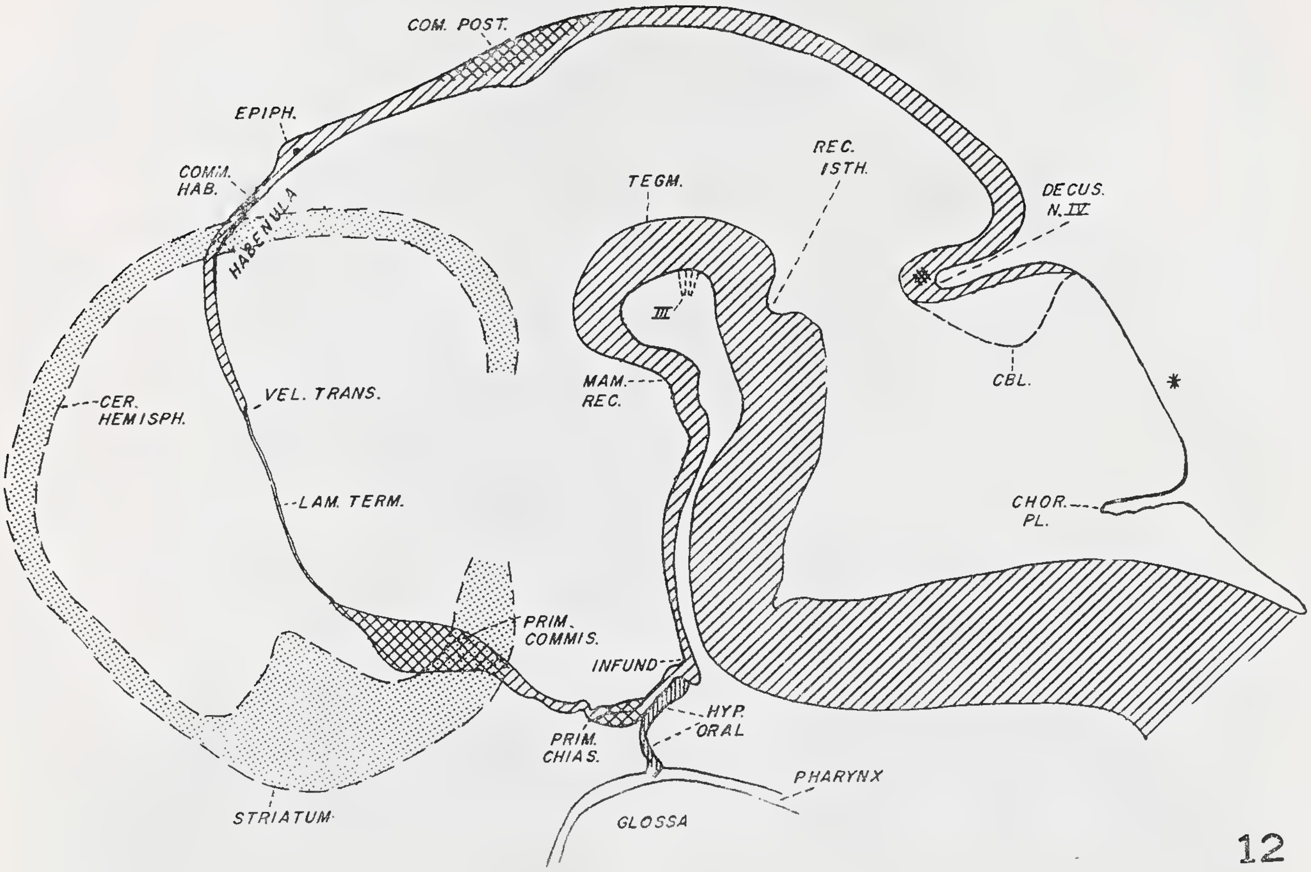

12

Fig. 12. Plotting from a combination of six successive sections of embryo 6202 (22 mm. C. R. L., horizon xx) cut in sagittal plane at 20 microns. Only paramedian portions of cerebral vesicle, corpus striatum, and cerebellum are included. × 15.7.

Abbreviations

CBL., Cerebellum
CER. HEMISPH., Vesicula cerebralis
CHOR. PL., Plexus chorioideus ventriculi IV
COMM. HAB., Commissura habenulae
COM. POST., Commissura posterior
DECUS. N. IV, Decussatio N. IV
EPIPH., Epiphysis
HYP. ORAL, Hypophysis oralis
INFUND., Infundibulum
LAM. TERM., Primordium laminae terminalis
MAM. REC., Recessus mamillaris
PRIM. CHIAS., Primordium chiasmatis
PRIM. COMMIS., Primordium commissurale
REC. ISTH. Recessus isthmi
TEGM., Tegmentum mesencephali
VEL. TRANS., Velum transversum
III, Radix N. III
*, Locus aperturae medialis ventriculi IV

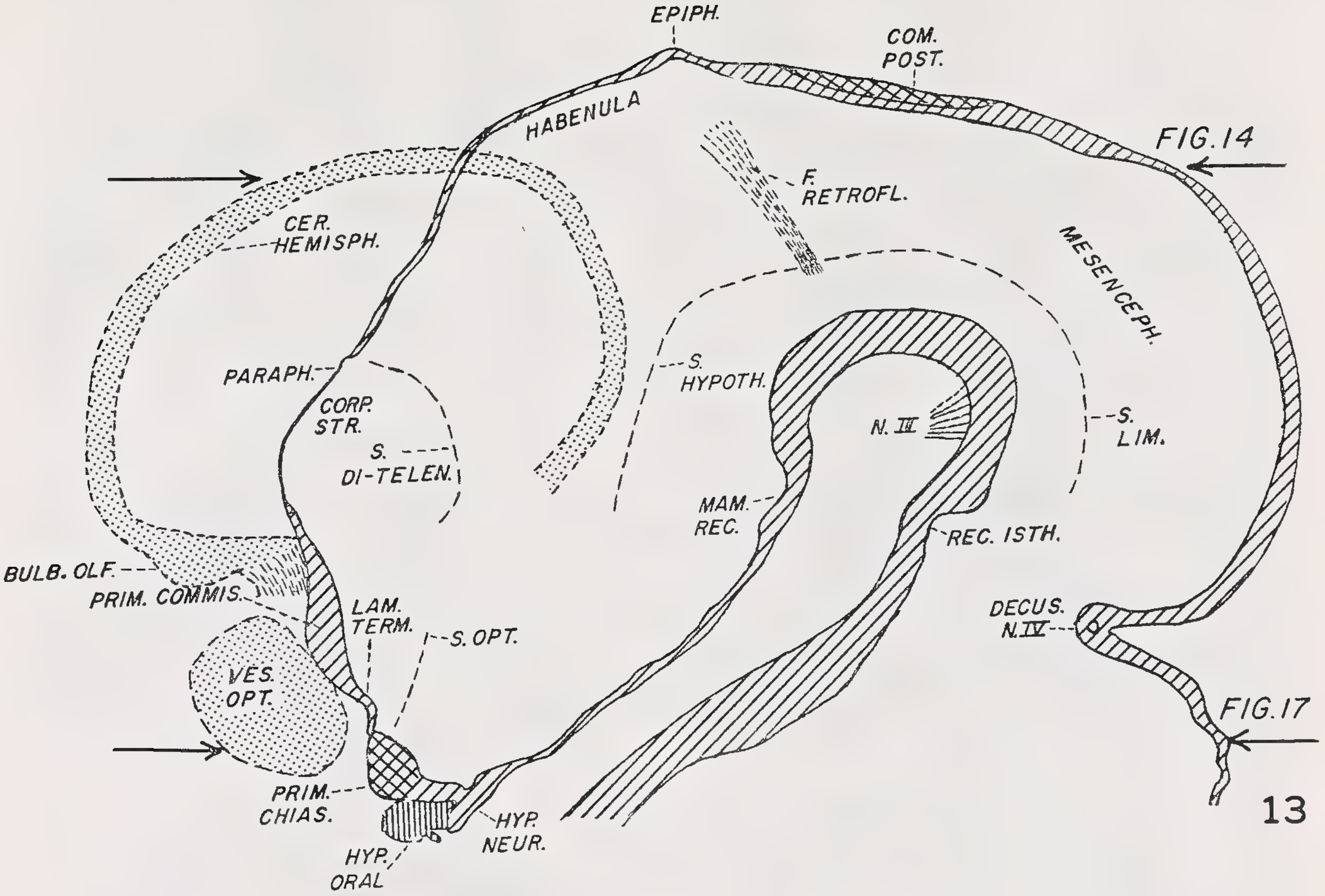

13

Fig. 13. Midsagittal projection reconstruction of brain of embryo 5609 (18 mm. C. R. L., horizon xix). × 24. Arrows indicate plane of section and levels of figures 14 and 17.

Abbreviations

BULB. OLF., Bulbus olfactorius
CER. HEMISPH., Vesicula cerebralis
COM. POST., Commissura posterior
CORP. STR., Corpus striatum
DECUS. N. IV, Decussatio N. IV
EPIPH., Epiphysis
F. RETROFL., Fasciculus retroflexus
HYP. NEUR., Hypophysis neuralis
HYP. ORAL, Hypophysis oralis
LAM. TERM., Primordium laminae terminalis
MAM. REC., Recessus mamillaris
MESENCEPH., Mesencephalon
N. III, Nervus III
PARAPH., Paraphysis
PRIM. CHIAS., Primordium chiasmatis
PRIM. COMMIS., Primordium commissurale
REC. ISTH., Recessus isthmi
S. DI-TELEN., Sulcus di-telencephalicus
S. HYPOTH., Sulcus hypothalamicus
S. LIM., Sulcus limitans
S. OPT., Sulcus opticus
VES. OPT., Vesicula optica

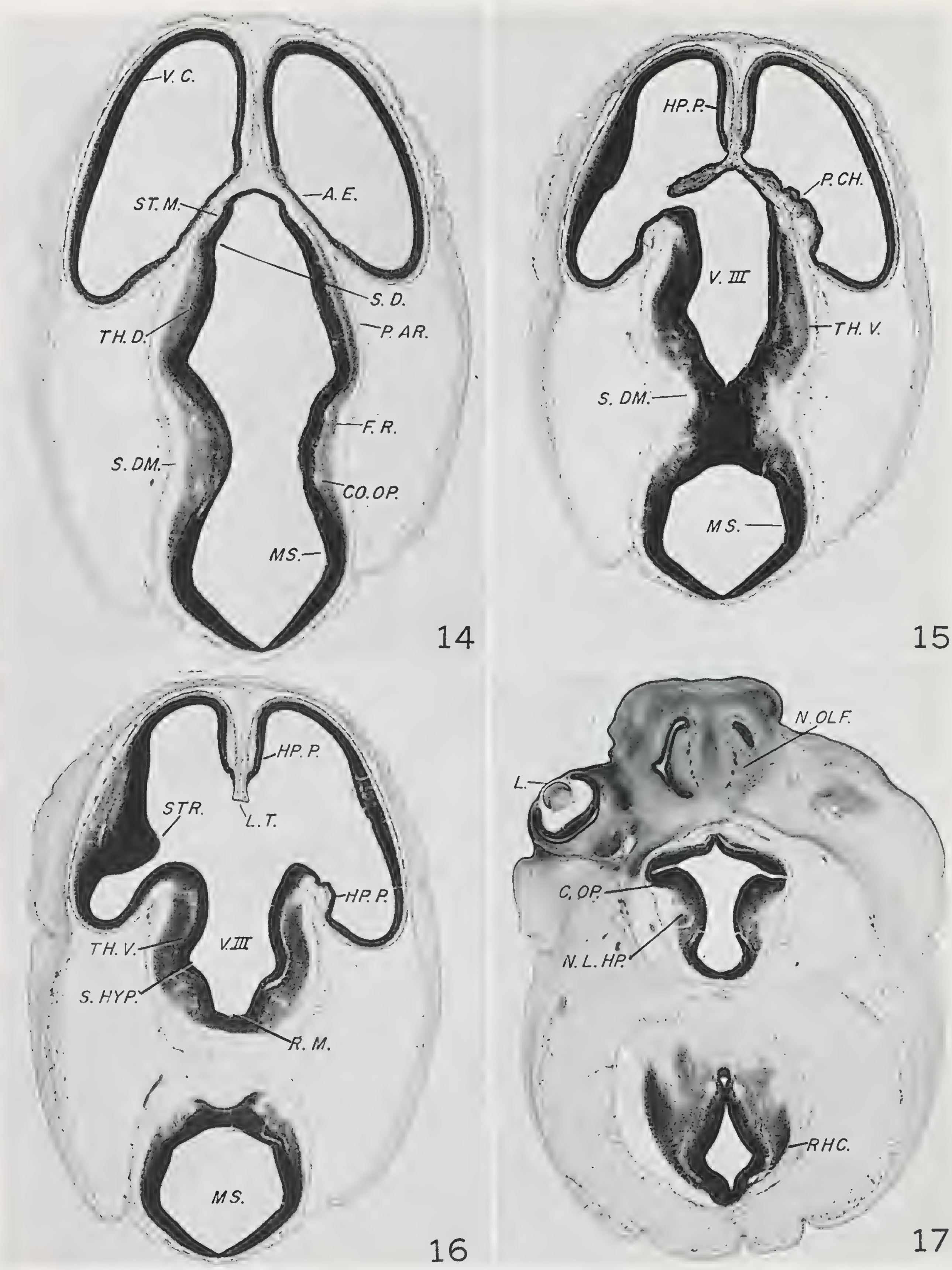

Photomicrographs from sections of embryo 5609. × 15. Plane of section indicated by arrows in figure 13 (pl. 6). Figure 14 represents section 19-3-5; figure 15, section 18-3-6; figure 16, section 18-2-3; figure 17, section 15-1-1.

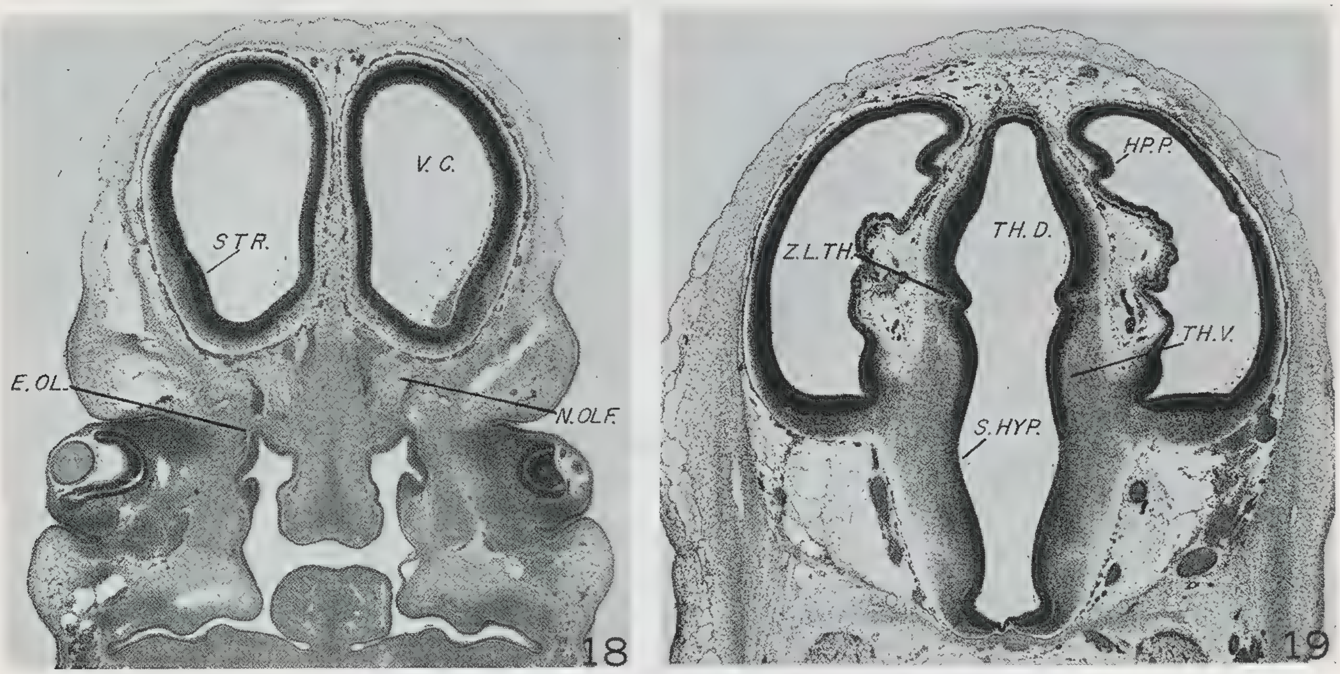

Photomicrographs from sections of embryo 8965 (horizon xix). × 18. Plane of section indicated in figure 20 (pl. 9). Figure 18 represents section 28-2-5; figure 19, section 19-2-3.

Abbreviations

A. E., Area epithelialis
CM. P. (C. OPR.), Commissura posterior
C. OP., Conus opticus
CO. OP., Commissura posterior
E. OL., Epithelium olfactorium
F. R., Fasciculus retroflexus
HP. P., Primordium hippocampi
L., Lens
L. T., Lamina terminalis
MS., Mesencephalon
N. L. HP., Nucleus lateralis hypothalami
N. OLF., Nervus olfactorius
P. AR., Pia-arachnoidea
P. CH., Plexus chorioideus lateralis
RHC., Rhombencephalon
R. M., Recessus mamillaris
S. D., Sulcus dorsalis thalami
S. DM., Sulcus di-mesencephalicus
S. HYP., Sulcus hypothalamicus
ST. M., Stria medullaris thalami
STR., Striatum
TH. D., Thalamus dorsalis
TH. V., Thalamus ventralis
V. C., Vesicula cerebralis
V. III, Ventriculus III
Z. L. TH., Zona limitans intrathalamica

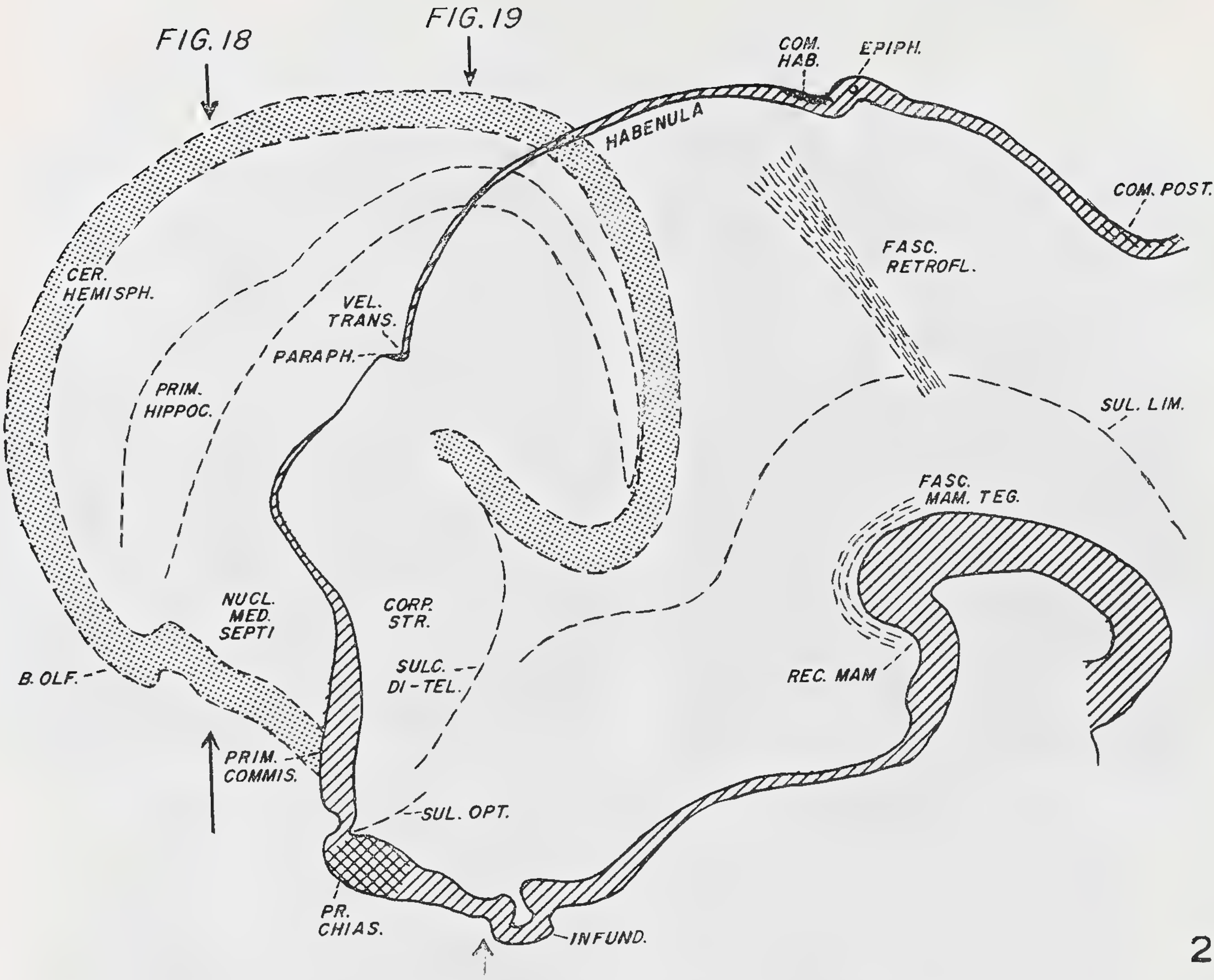

20

Fig. 20. Brain of embryo 8965, 19 mm. C. R. L., horizon xix, modified from Hines (1922, fig. 16). × 19. Analysis of figure 21 (pl. 10). Arrows indicate the level of figures 18 and 19 (pl. 8).

Abbreviations

B. OLF., Bulbus olfactorius
CER. HEMISPH., Vesicula cerebralis
COM. HAB., Commissura habenulae
COM. POST., Commissura posterior
CORP. STR., Corpus striatum
EPIPH., Epiphysis
FASC. RETROFL., Fasciculus retroflexus
FASC. MAM. TEG., Fasciculus mamillotegmentalis
INFUND., Infundibulum
LAM. TERM., Primordium laminae terminalis

NUCL. MED. SEPTI, Nucleus medianus septi
PARAPH., Paraphysis
PR. CHIAS., Primordium chiasmatis
PRIM. COMMIS., Primordium commissurale
PRIM. HIPPOC., Primordium hippocampi
REC. MAM., Recessus mamillaris
SULC. DI-TEL., Sulcus di-telencephalicus
SUL. LIM., Sulcus limitans
SUL. OPT., Sulcus opticus
VEL. TRANS., Velum transversum

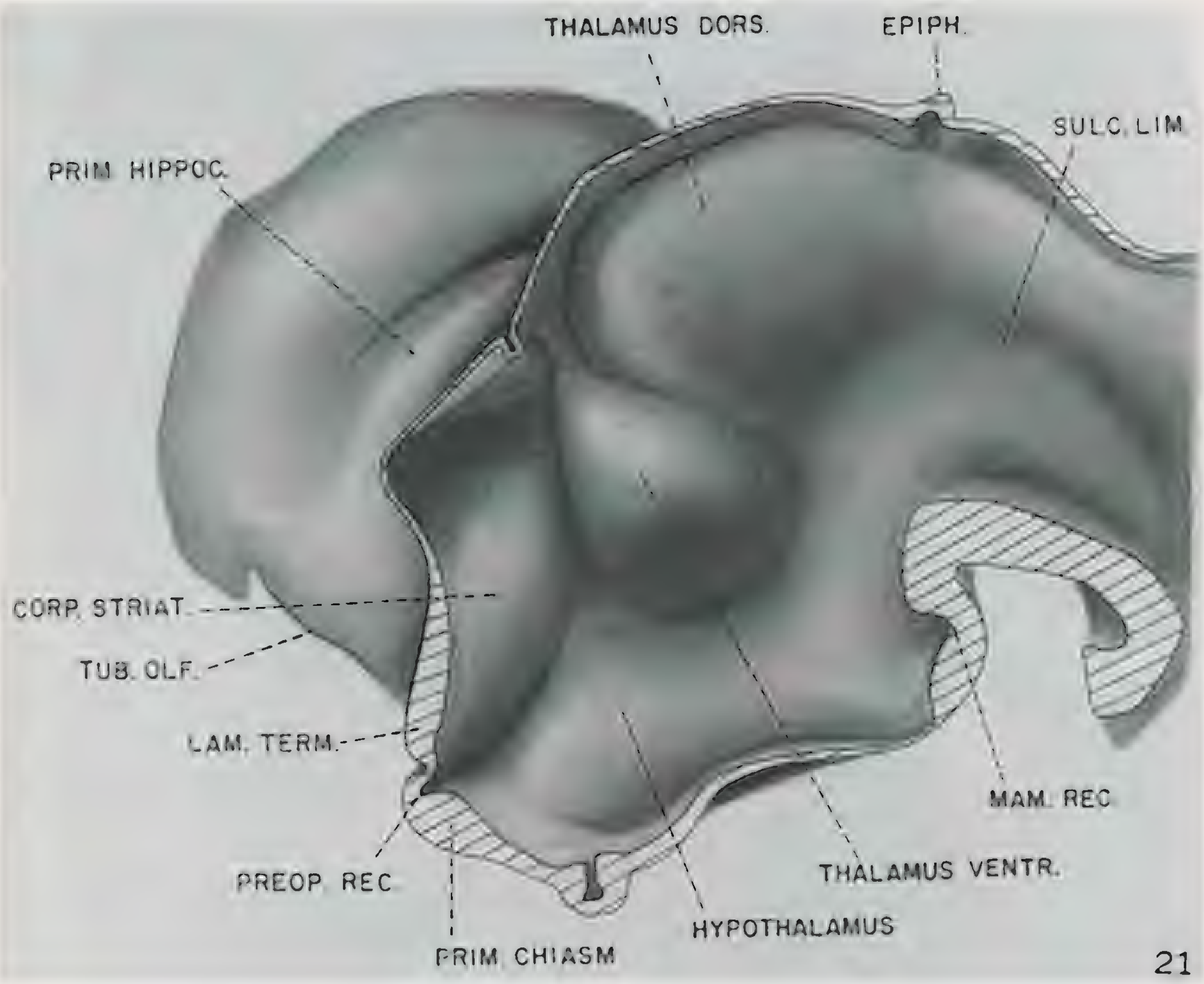

Fig. 21. Midsagittal section of model prepared by P. Bailey (1916) modified from Hines (1922, fig. 15). Sulcus di-telencephalicus extends from velum transversum along caudal border of corpus striatum to chiasma. Sulcus limitans (His) becomes sulcus hypothalamicus marking dorsal border of hypothalamus. Floor of brain in mid-line is membranous in region of lateral hypothalamic nucleus, massive in mammillary region. "Lam. term." indicates commissure bed of embryonic lamina terminalis.

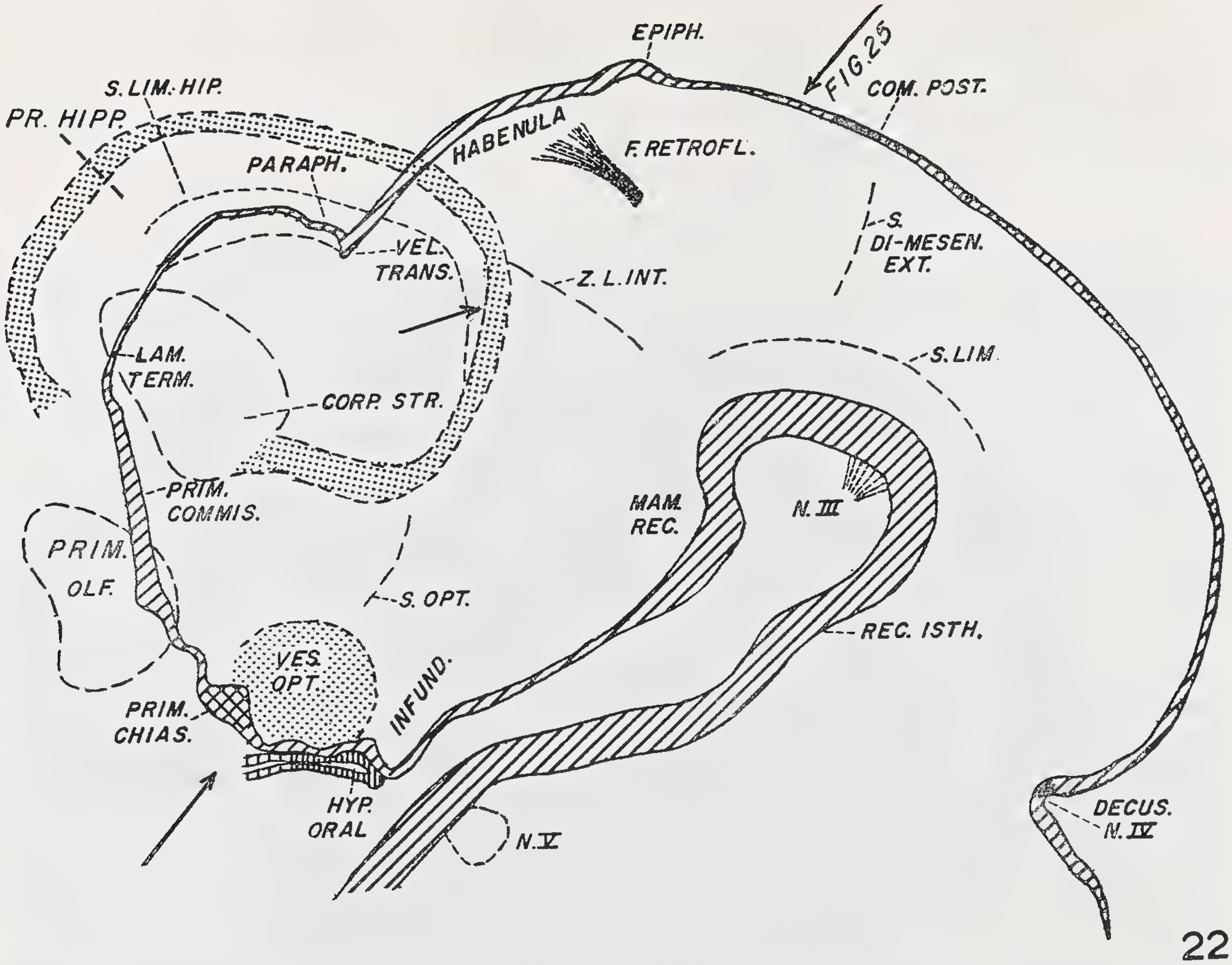

22

Fig. 22. Midsagittal projection reconstruction of brain of embryo 6520, 14 mm. greatest length, horizon xvii. Arrows indicate plane of section. Elevation of roof of telencephalon medium ("keel") is marked by broken line (see fig. 23, pl. 12). The broken line above lamina terminalis indicates "sulcus ventralis" between hippocampal formation and area epithelialis. × 33.

Abbreviations

COM. POST., Commissura posterior
C. OP., Conus opticus
CORP. STR., Corpus striatum
DECUS. N. IV, Decussatio N. IV
EPIPH., Epiphysis
F. R. (F. RETROFL.), Fasciculus retroflexus
G. N. V, Ganglion N. V
HP. P., Primordium hippocampi
HY., Hypophysis
HYP., Hypothalamus
HYP. ORAL, Hypophysis oralis
INF. (INFUND.), Infundibulum
IST., Isthmus
K., "Keel"
LAM. TERM., Primordium laminae terminalis
MAM. REC., Recessus mamillaris
MS., Mesencephalon
N. III, Nervus III
N. L. HP., Nucleus lateralis hypothalami
N. V, Radix N. V
PARAPH. Paraphysis
P. OL. (PRIM. OLF.), Primordium olfactorium
PR. HIPP., Primordium hippocampi
PRIM. CHIAS., Primordium chiasmatis
PRIM. COMMIS., Primordium commissurale
REC. ISTH., Recessus isthmi
RL. V. IV, Recessus lat. vent. IV
S. DT., Sulcus di-telencephalicus
(S. DI-MESEN. EXT.), Sulcus di-mesencephalicus
S. HYP., Sulcus hypothalamicus
S. L. (S. LIM.), Sulcus limitans
S. LIM. HIP., Sulcus limitans hippocampi
S. M., Sulcus medialis
S. OPT., Sulcus opticus
STR., Striatum
TH. D., Thalamus dorsalis
TH. V., Thalamus ventralis
TL. M., Telencephalon medium
V. C., Vesicula cerebralis
VEL. TRANS., Velum transversum
VES. OPT., Vesicula optica
V. III, Ventriculus III
Z. L. INT. (Z. L. TH.), Zona limitans intrathalamica

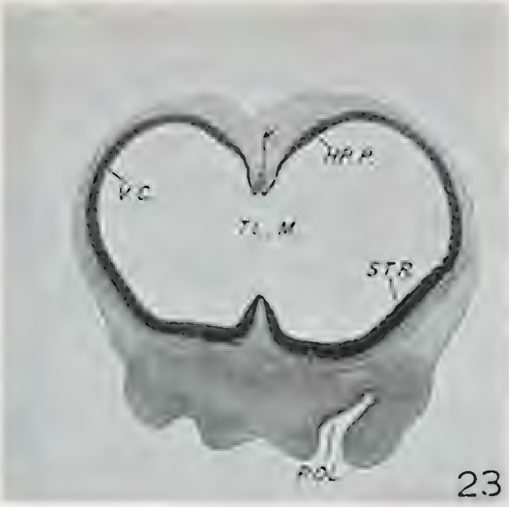

23

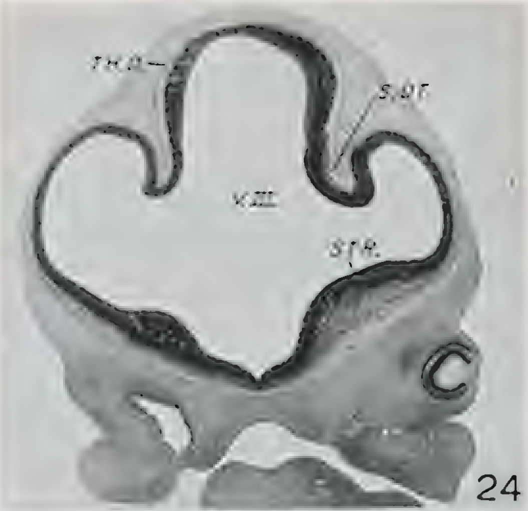

24

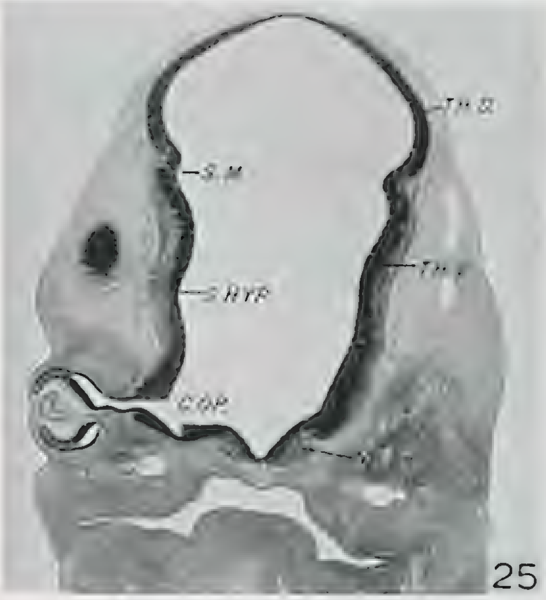

25

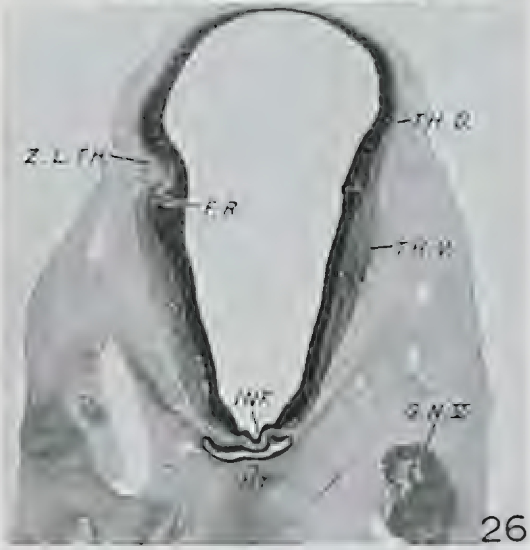

26

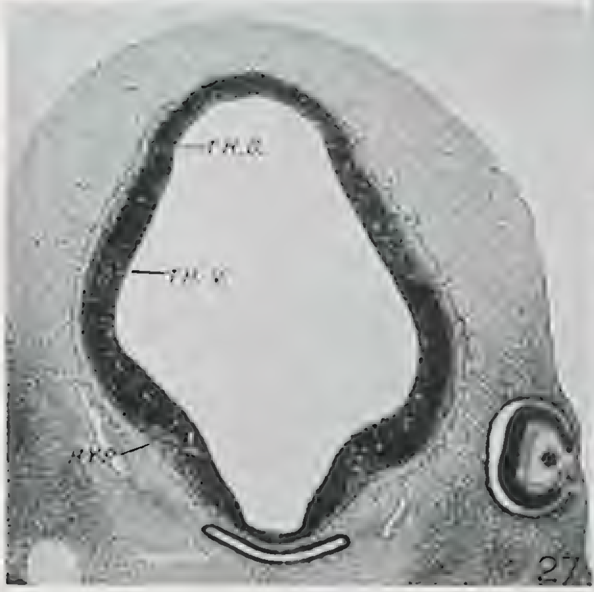

27

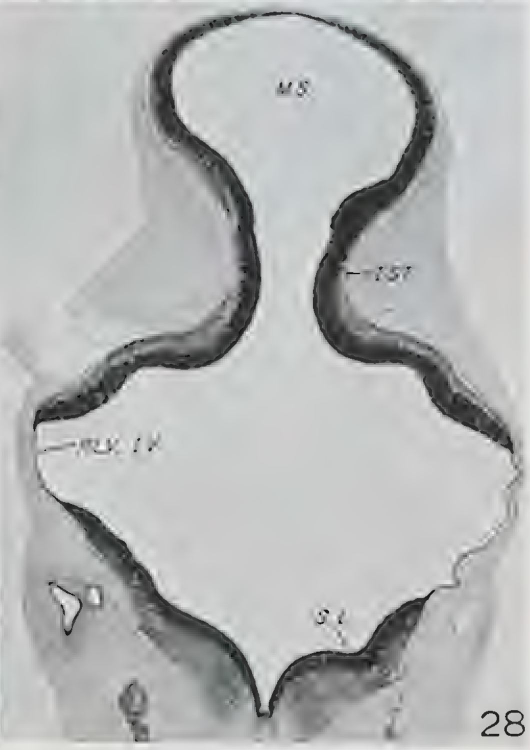

28

Photomicrographs from sections of embryo 6520, except for figure 27, all magnified × 17. Planes of section for 6520 shown by arrows in figure 22. Figure 23 represents section 32-3-2; figure 24, section 28-1-4; figure 25, section 23-3-4; figure 26, section 20-3-1; figure 27 (embryo 6510), section 15-3-2 (× 30); figure 28, section 11-2-2.

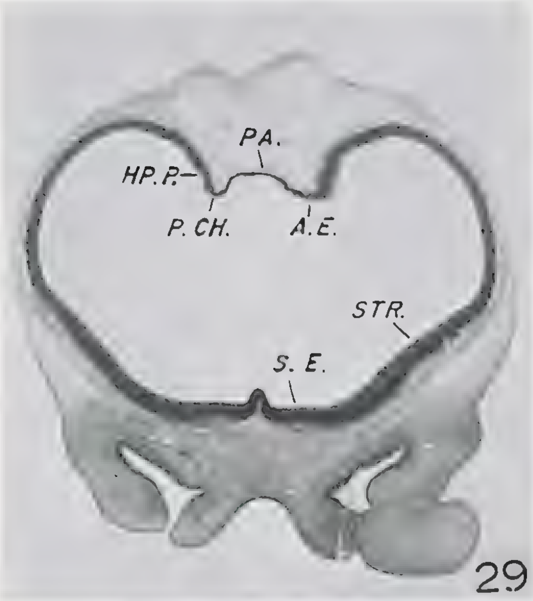

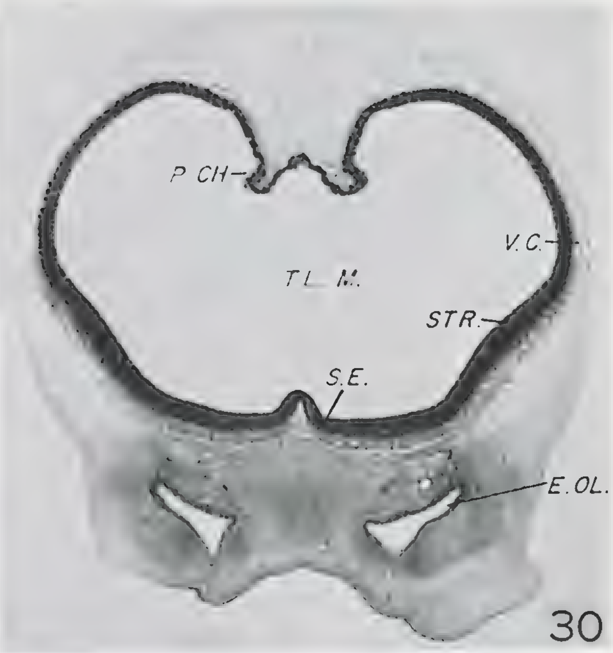

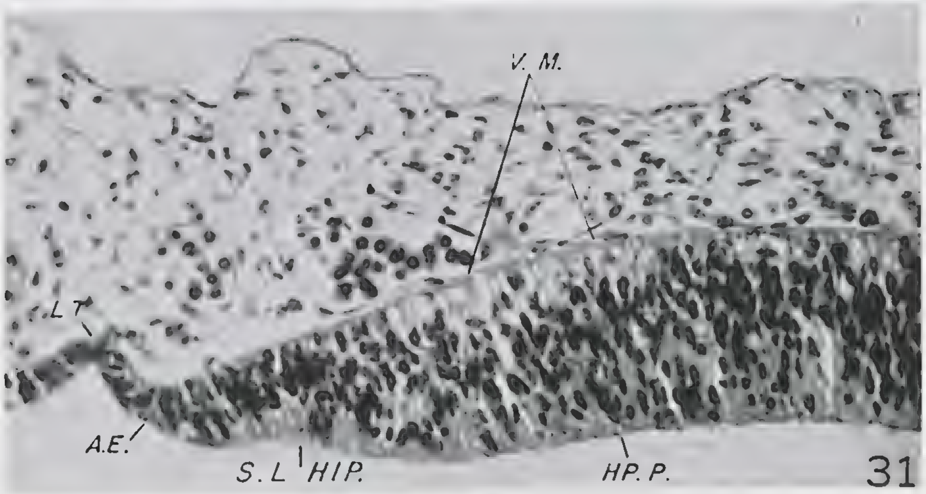

Fig. 29. Embryo 6520, section 30-2-3, horizon xvii, × 20.
Fig. 30. Embryo 6524, section 30-3-2, horizon xviii, × 25.
Fig. 31. Embryo 8098, section 5-5-5, horizon xvi, × 300.

Abbreviations

A. E., Area epithelialis
E. OL., Epithelium olfactorium
HP. P., Primordium hippocampi
L. T., Lamina terminalis
PA., Paraphysis
P. CH., Plexus chorioideus
S. E., Area septi
S. L. HIP., Sulcus limitans hippocampi
STR., Striatum
TL. M., Telencephalon medium
V. C., Vesicula cerebralis
V. M., Velum marginale

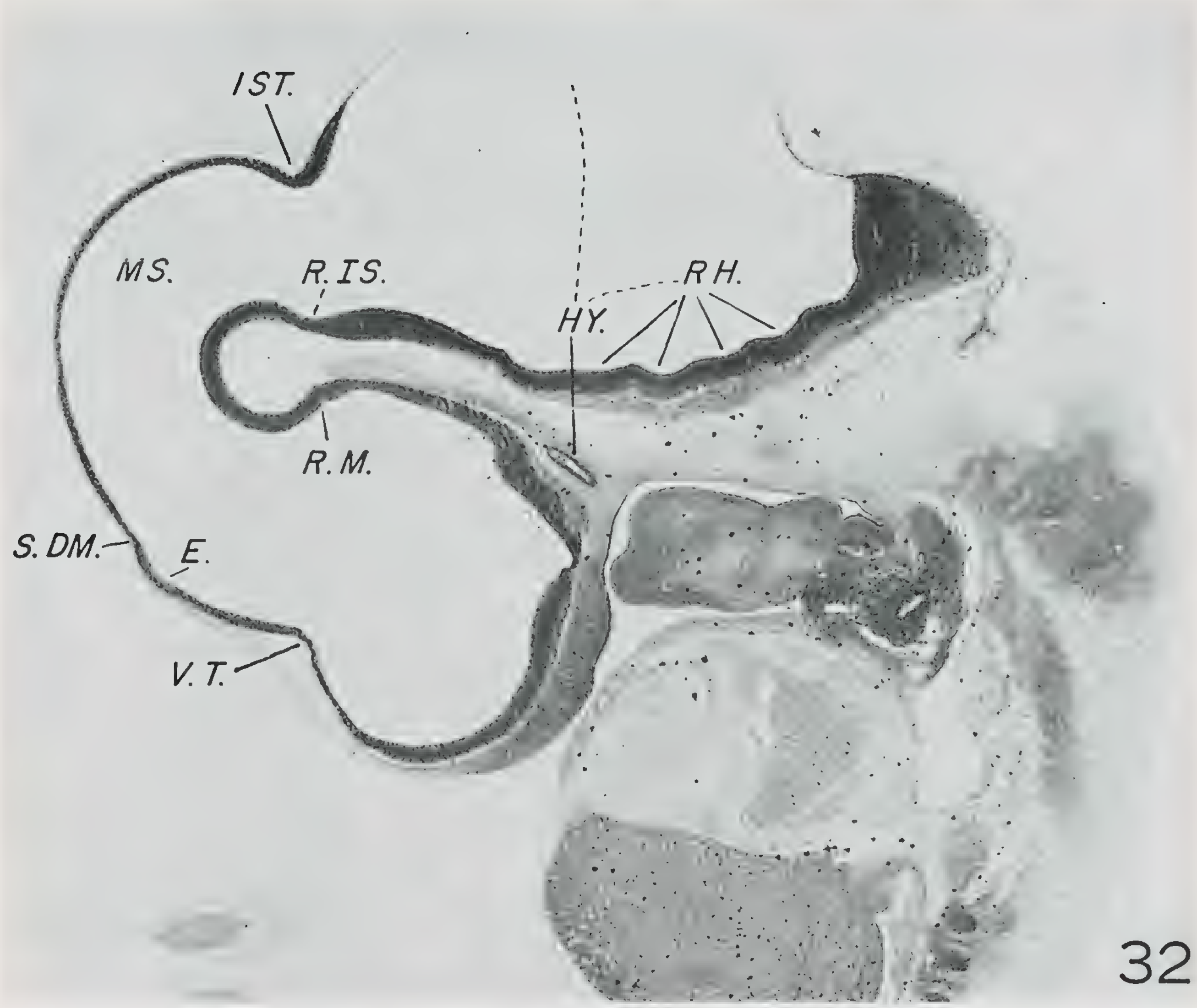

32

Fig. 32. Photomicrograph from median section 17-1-5 of embryo 6514, horizon xvi (ca. 9 mm. greatest length). × 30.

Abbreviations

E., Epiphysis
HY., Hypophysis
IST., Isthmus
MS., Mesencephalon
RH., Rhombomeres

R. IS., Recessus isthmi
R. M., Recessus mamillaris
S. DM., Sulcus di-mesencephalicus
V. T., Velum transversum

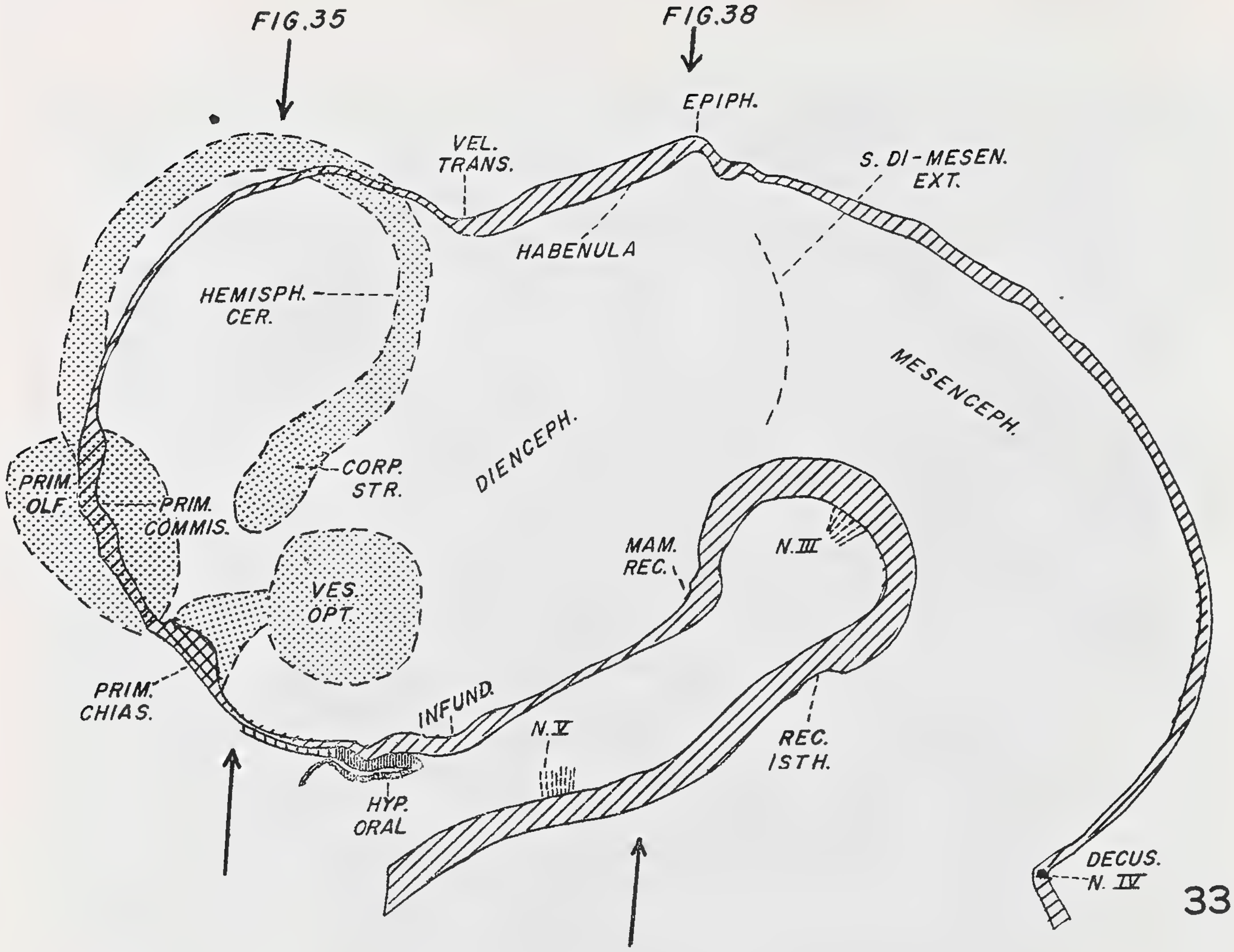

33

Fig. 33. Midsagittal projection reconstruction of brain of embryo 6510, horizon xvi (ca. 10 mm. G. L.). Arrows indicate plane of section. × 40.

Abbreviations

C. OP., Conus opticus
CORP. STR., Corpus striatum
DECUS. N. IV, Decussatio N. IV
DEN (DIENCEPH.), Diencephalon
EPIPH. (E.), Epiphysis
G. N. V, VII, X, Ganglion N. V, VII, X
HEMISPH. CER., Vesicula cerebralis
HP. P., Primordium hippocampi
HYP. L., Hypothalamus lateralis
HYP. ORAL, Hypophysis oralis
INFUND., Infundibulum
L. T., Lamina terminalis
MAM. REC., Recessus mamillaris
MESENCEPH., Mesencephalon
N. III, V, Nervus III, V
N. L. HP., Nucleus lateralis hypothalami
OT., Vesicula otica
PRIM. CHIAS., Primordium chiasmatis
PRIM. COMMIS., Primordium commissurale
PRIM. OLF. (P. OL.), Primordium olfactorium
REC. ISTH., Recessus isthmi
RH. 4, Rhombomere 4
S. DI-MESEN. EXT., Sulc. di-mesencephalicus
S. HYP., Sulcus hypothalamicus
STR., Striatum
V. C., Vesicula cerebralis
VEL. TRANS., Velum transversum
VES. OPT. (V. OP.), Vesicula optica
V. IV, Ventriculus IV
Z. L. TH., Zona limitans intrathalamica

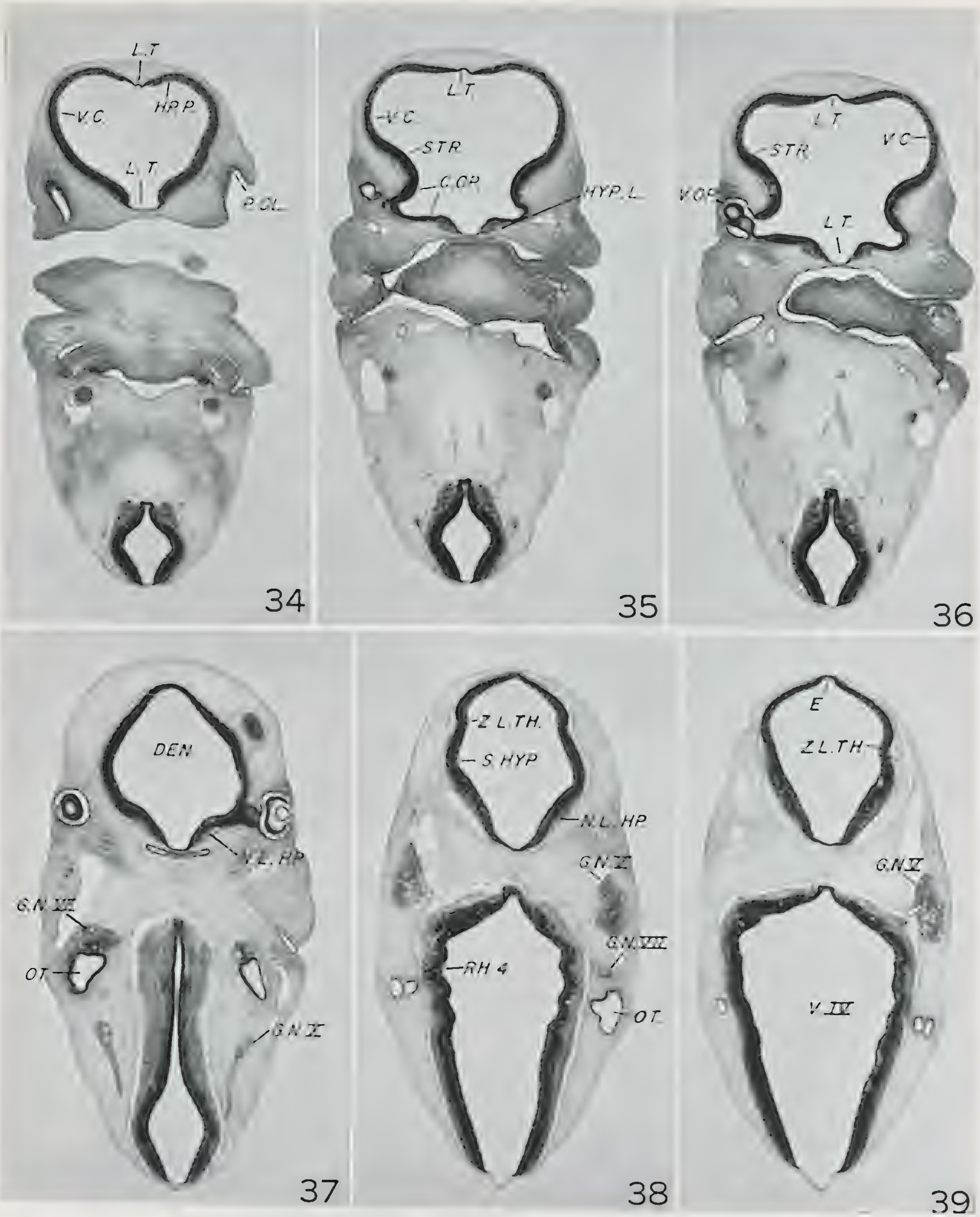

Photomicrographs from sections of 6510. × 15. Figure 34 represents section 22-2-3; figure 35, section 19-2-4; figure 36, section 18-3-4; figure 37, section 16-3-1; figure 38, section 13-3-3; figure 39, section 12-2-1.

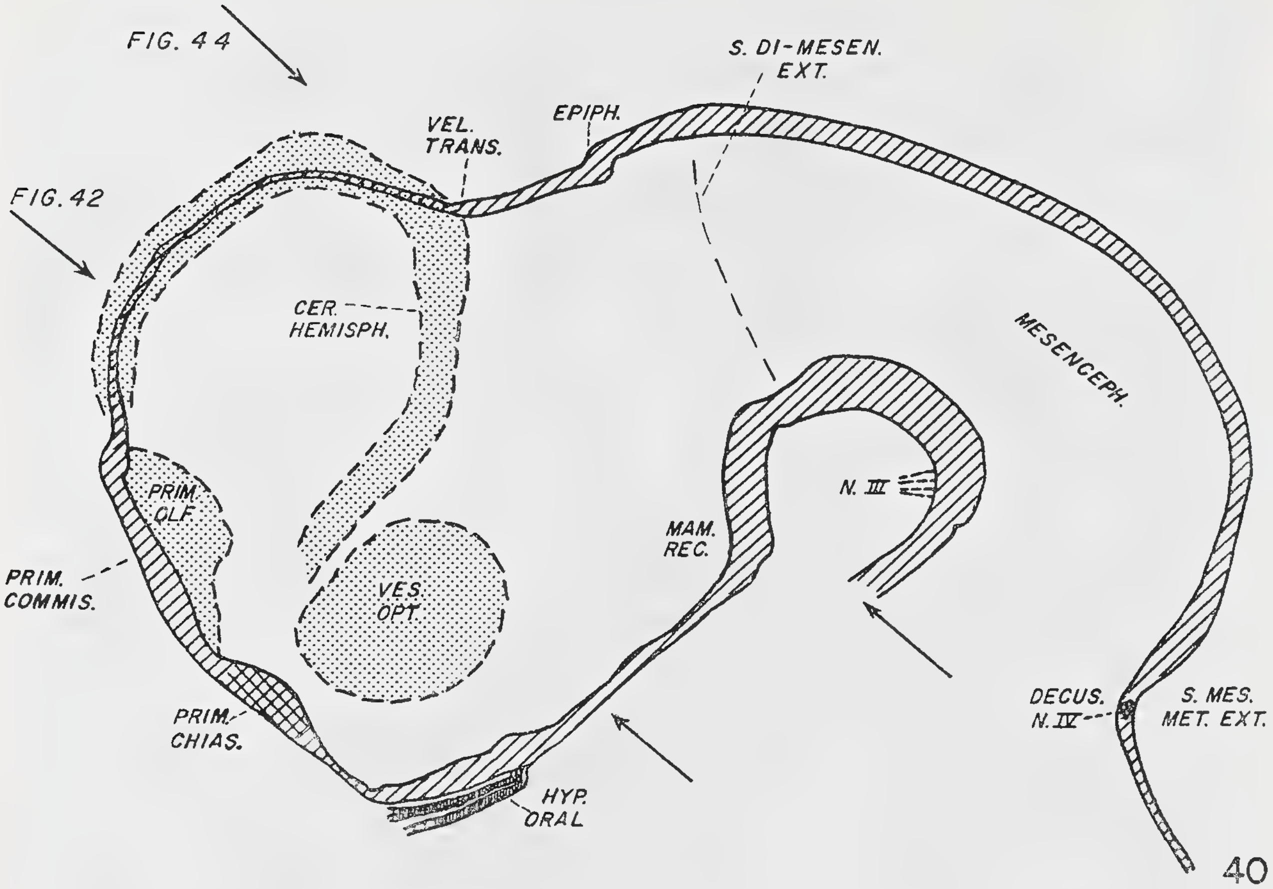

40

Fig. 40. Midsagittal projection reconstruction of brain of embryo 6506, horizon xv (ca. 7.5 mm. G. L.). × 52. Arrows indicate plane of section.

Abbreviations

CER. HEMISPH., Vesicula cerebralis
C. OP., Conus opticus
DECUS. N. IV, Decussatio N. IV
EPIPH., Epiphysis
G. N. V, Ganglion N. V
HYP. ORAL (HYP.), Hypophysis oralis
L. CBL., Lamina cerebellaris
L. T., Lamina terminalis
MAM. REC. (R. M.), Recessus mamillaris
MESENCEPH., Mesencephalon
N. L. HP., Nucleus lateralis hypothalami
N. III, Nervus III
P. C., Commissura posterior
PRIM. CHIAS., Primordium chiasmatis
PRIM. COMMIS., Primordium commissurale
PRIM. OLF. (P. OL.), Primordium olfactorium
RH. 2, Rhombomere 2
S. DI-MESEN. EXT., Sulcus di-mesencephalicus
S. MES. MET. EXT., Sulcus mes-metencephalicus externus
S. DT., Sulcus di-telencephalicus
S. HYP., Sulcus hypothalamicus
S. L., Sulcus limitans
V. C., Vesicula cerebralis
VEL. TRANS., Velum transversum
VES. OPT., Vesicula optica
V. IV, Ventriculus IV

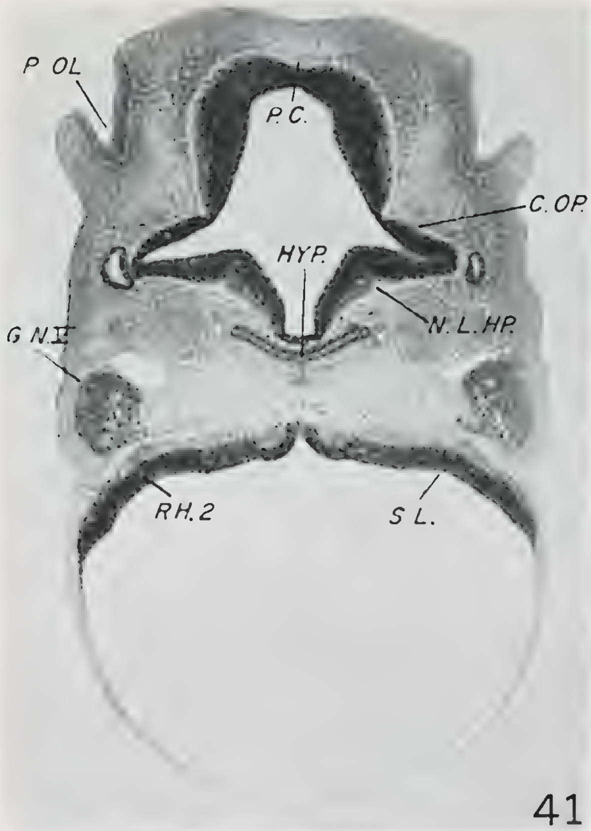

41

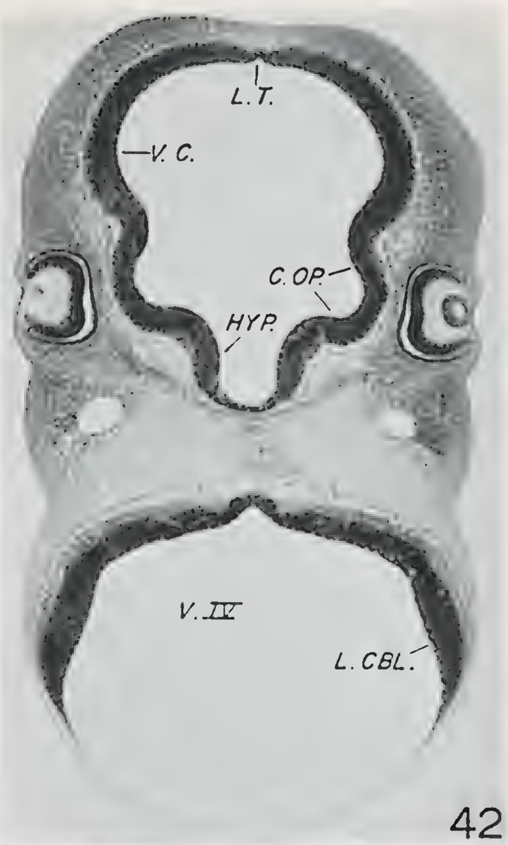

42

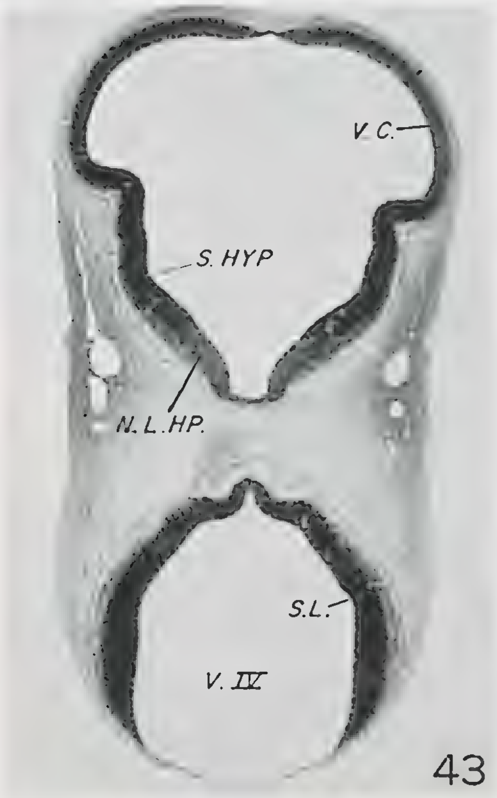

43

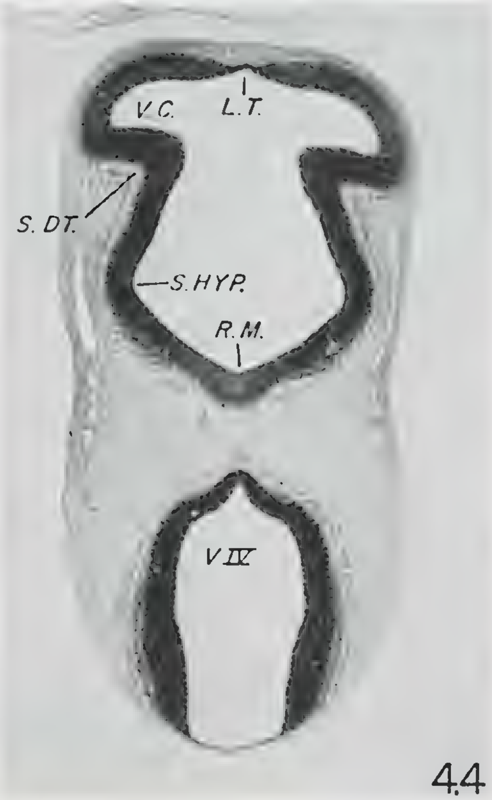

44

Photomicrographs from brain of embryo 6506. × 30. Figure 41 represents section 9-1-4; figure 42, section 7-4-3; figure 43, section 6-2-2; figure 44, section 5-2-2.

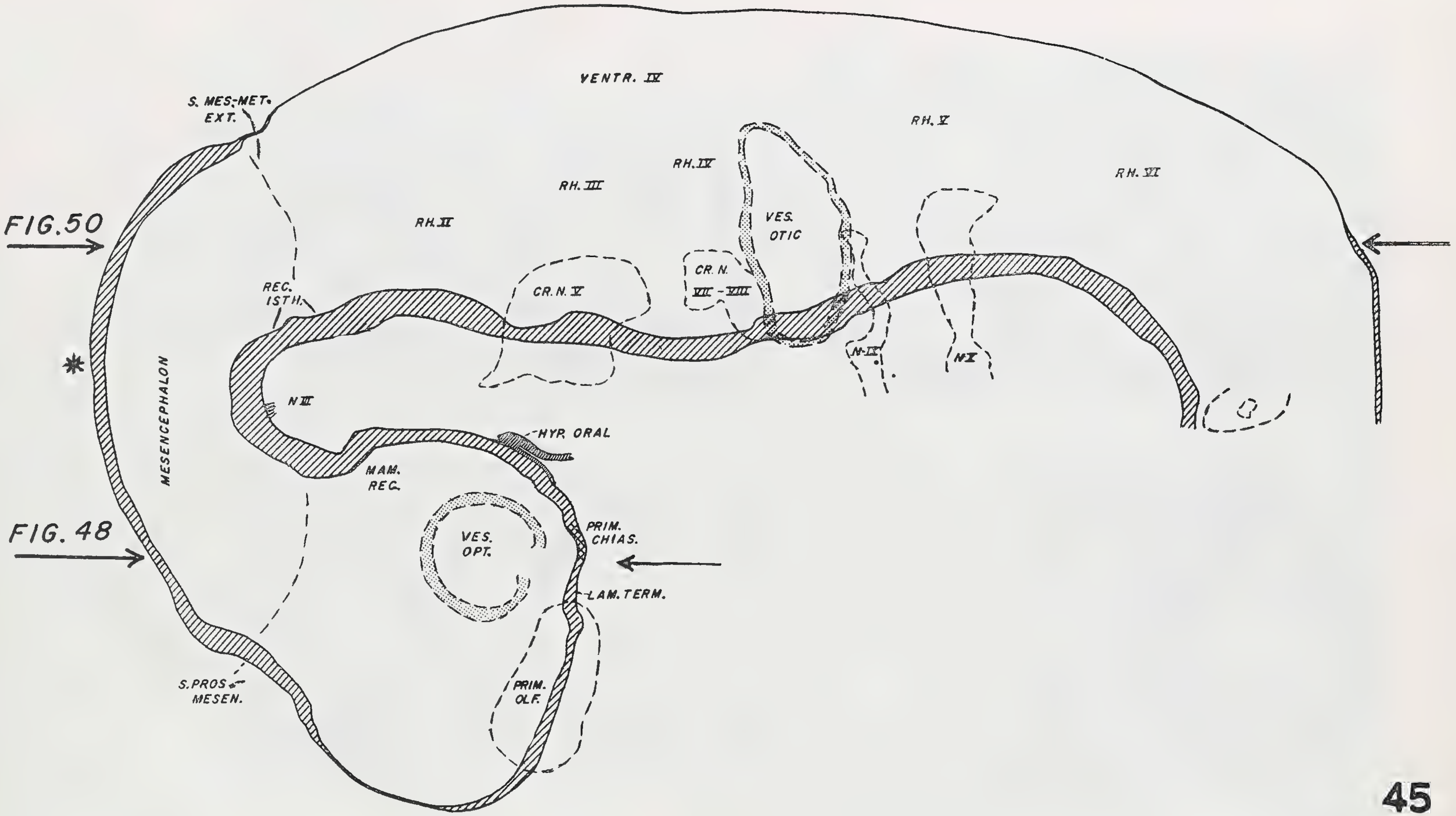

45

Fig. 45. Midsagittal projection reconstruction of brain of embryo 6502, horizon xiv (6.7 mm. G. L.). × 54.5. Arrows indicate plane of section. Note gradual thinning out of roof at junction of di- and tel-encephalon.

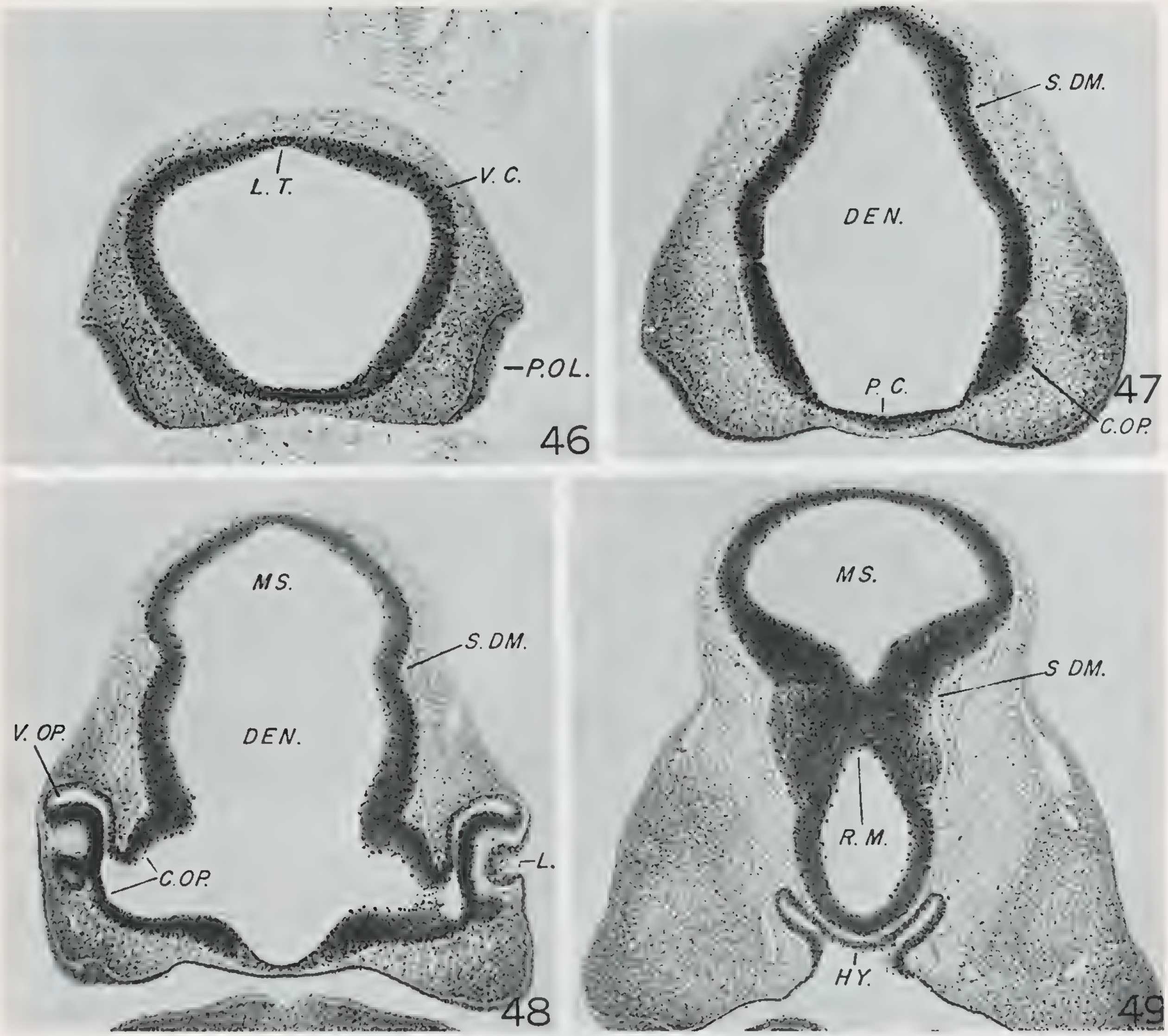

Photomicrographs from brain of embryo 6502. × 45. Figure 46 represents section 19-2-2; figure 47, section 16-4-3; figure 48, section 15-1-3; figure 49, section 12-5-2.

Abbreviations

CR. N. V, VII, VIII, Crista neuralis V, VII, VIII
C. OP., Conus opticus
DEN., Diencephalon
HY., Hypophysis
HYP. ORAL, Hypophysis oralis
L., Lens
LAM. TERM. (L. T.), Primordium laminae terminalis
MAM. REC. (R.M.), Recessus mamillaris
MS., Mesencephalon
N. III, IX, X, Nervi III, IX, X
PRIM. CHIAS. (P.C.), Primordium chiasmatis
PRIM. OLF. (P. OL.), Primordium olfactorium
REC. ISTH., Recessus isthmi
RH. II, III, IV, V, VI, Rhombomeres 2–6
S. DM., Sulcus di-mesencephalicus
S. MES-MET. EXT., Sulcus mes-metencephalicus externus
S. PROS. MESEN., Sulcus pros-mesencephalicus
V. C., Vesicula cerebralis
VENTR. IV, Ventriculus IV
VES. OPT. (V. OP.), Vesicula optica
VES. OTIC, Vesicula otica

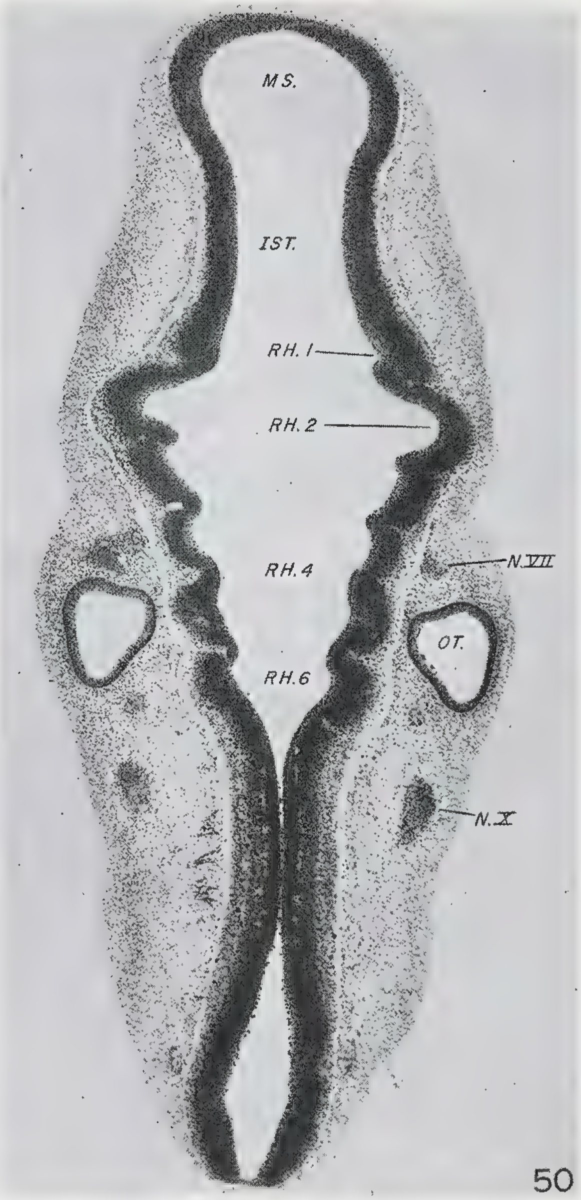

50

Fig. 50. Photomicrograph from a horizontal section (7-3-1) of hindbrain of embryo 6502. × 38. For plane of section see figure 45 (pl. 19).

Abbreviations

COR., Heart
HY., Hypophysis
IST., Isthmus
MS., Mesencephalon
MS. I, II, Mesencephalon 1, 2
N. VII, X, Nervi VII, X
OT., Vesicula otica
PEN., Prosencephalon
PH., Pharynx embryonalis
RH. 1, 2, 4, 6, Rhombomeres 1, 2, 4, 6

R. IS., Recessus isthmi
R. M., Recessus mamillaris
S. DT., Sulcus di-telencephalicus
S. MRH., Sulcus mes-rhombencephalicus
S. PM., Sulcus pros-mesencephalicus
S. PMA., Sulcus postmamillaris
TM., Tegmentum mesencephali
V. IV, Ventriculus IV
*, See page 23.

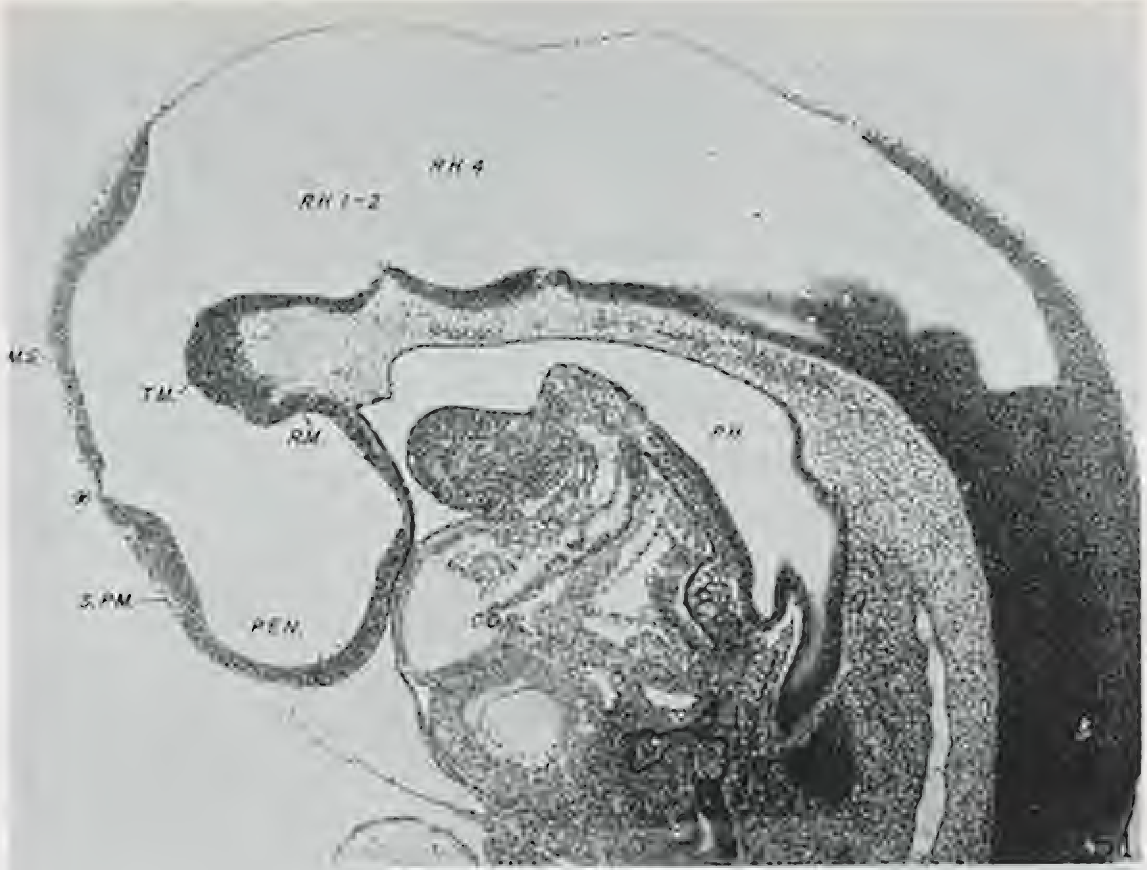

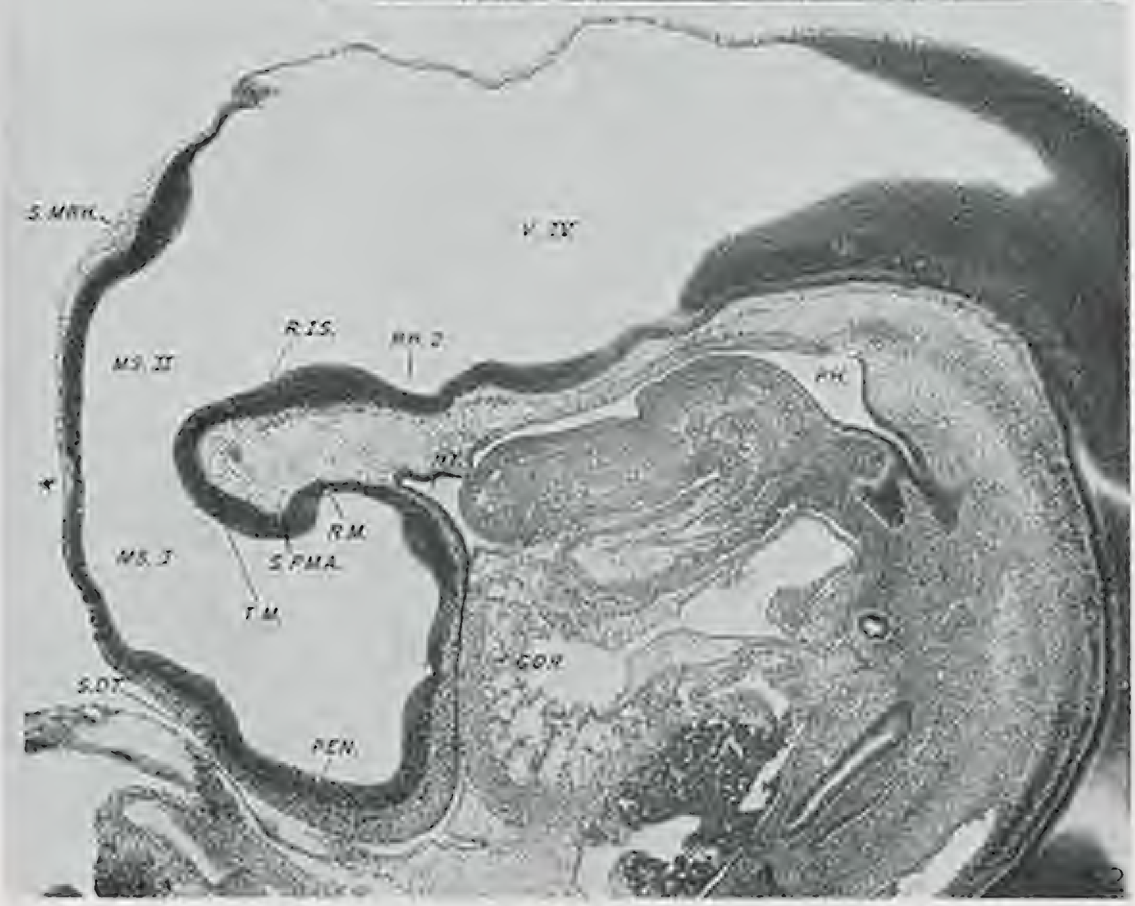

Fig. 51. Photomicrograph from sagittal section 2-6-9 of embryo 8239, horizon xiii (ca. 4 mm.). × 43.

Fig. 52. Photomicrograph from sagittal section 4-3-6 of embryo 8999, horizon xiv (6 mm. G. L.). × 36.5.

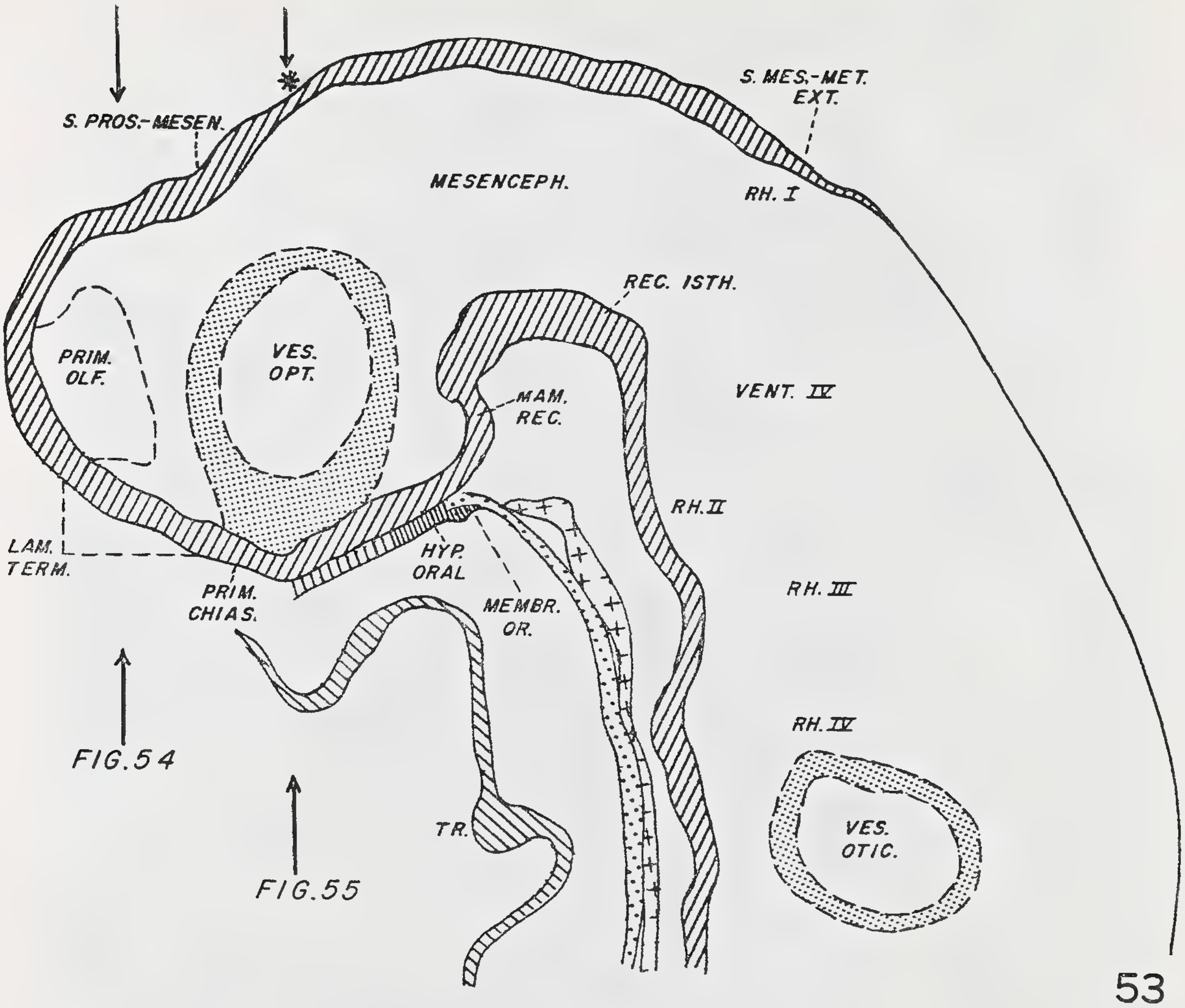

53

Fig. 53. Midsagittal projection reconstruction of brain of embryo 836, horizon xiii (4 mm. G. L., 30 somites). ×72. Arrows indicate plane of section. Chorda indicated by crosses; entoderm of pharynx dorsally by coarse stipple, ventrally by hatching.

Abbreviations

C. CR. V, VII-VIII, IX, X, Crista neuralis V, VII-VIII, IX, X
HYP. ORAL (HY.), Hypophysis oralis
IST., Isthmus
L., Lens
LAM. TERM. (LT.), Primordium laminae terminalis
MA., Processus maxillaris
MAM. REC. (RM.), Recessus mamillaris
MD., Arcus mandibularis
MEMBR. OR., Membrana oralis
MS. (MESENCEPH.), Mesencephalon
OT., Vesicula otica
PEN., Prosencephalon
PH., Pharynx embryonalis
PRIM. CHIAS., Primordium chiasmatis
PRIM. OLF. (P. OL.), Primordium olfactorium
REC. ISTH., Recessus isthmi
RH. I, II, III, IV, VII, Rhombomeres 1–4, 7
RH., Rhombencephalon
S. MES.-MET. EXT., Sulcus mes-metencephalicus
S. PROS.-MESEN., Sulcus pros-mesencephalicus
TR., Glandula thyroidea
VENT. IV, Ventriculus IV
VES. OPT. (V. OP.), Vesicula optica
VES. OTIC., Vesicula otica
*, See p. 23.

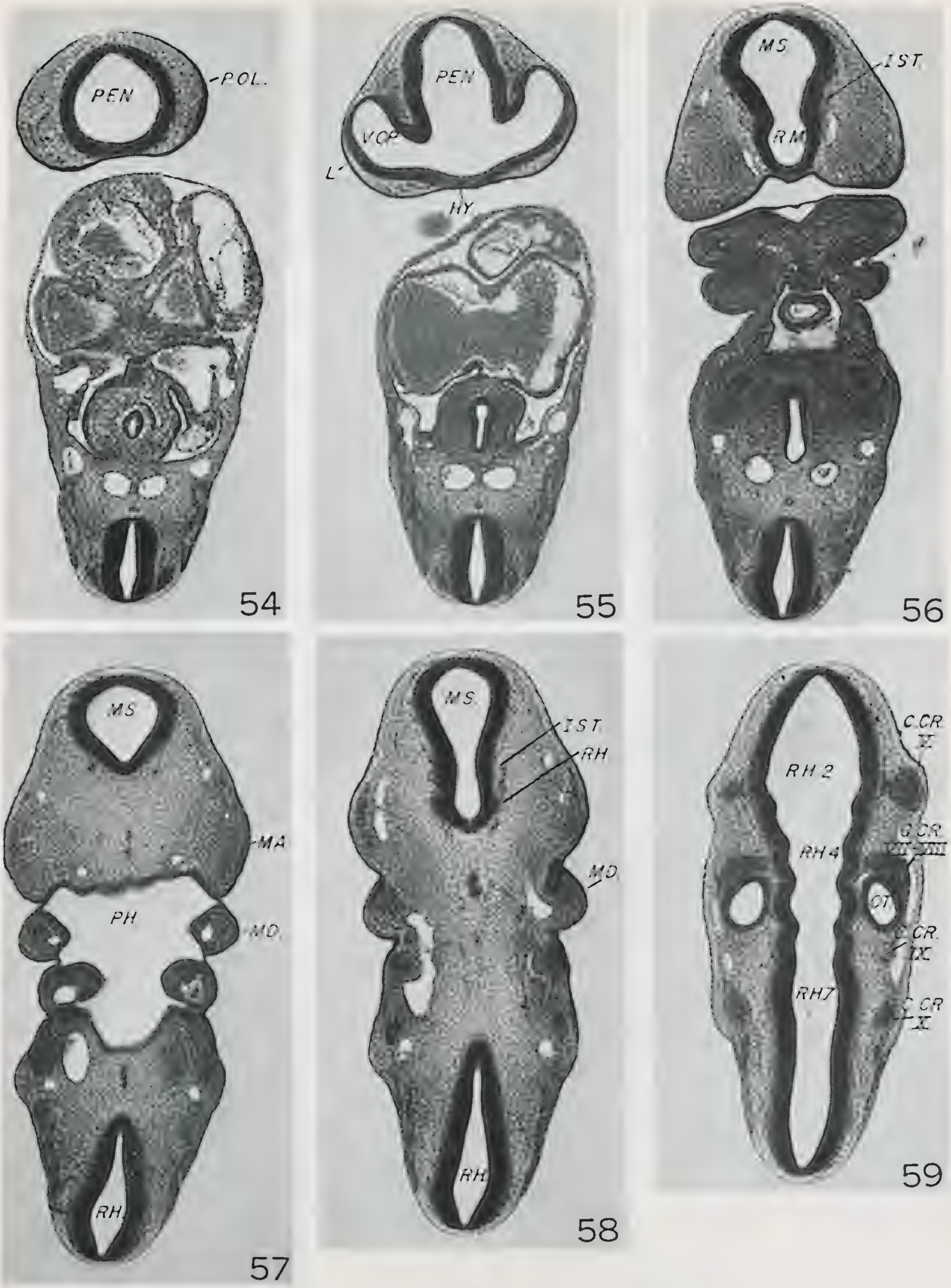

Photomicrographs from brain of embryo 836. × 35. Figure 54 represents section 7-2-2; figure 55, section 6-2-3; figure 56, section 5-2-5; figure 57, section 4-2-6; figure 58, section 4-1-5; figure 59, section 3-1-6.

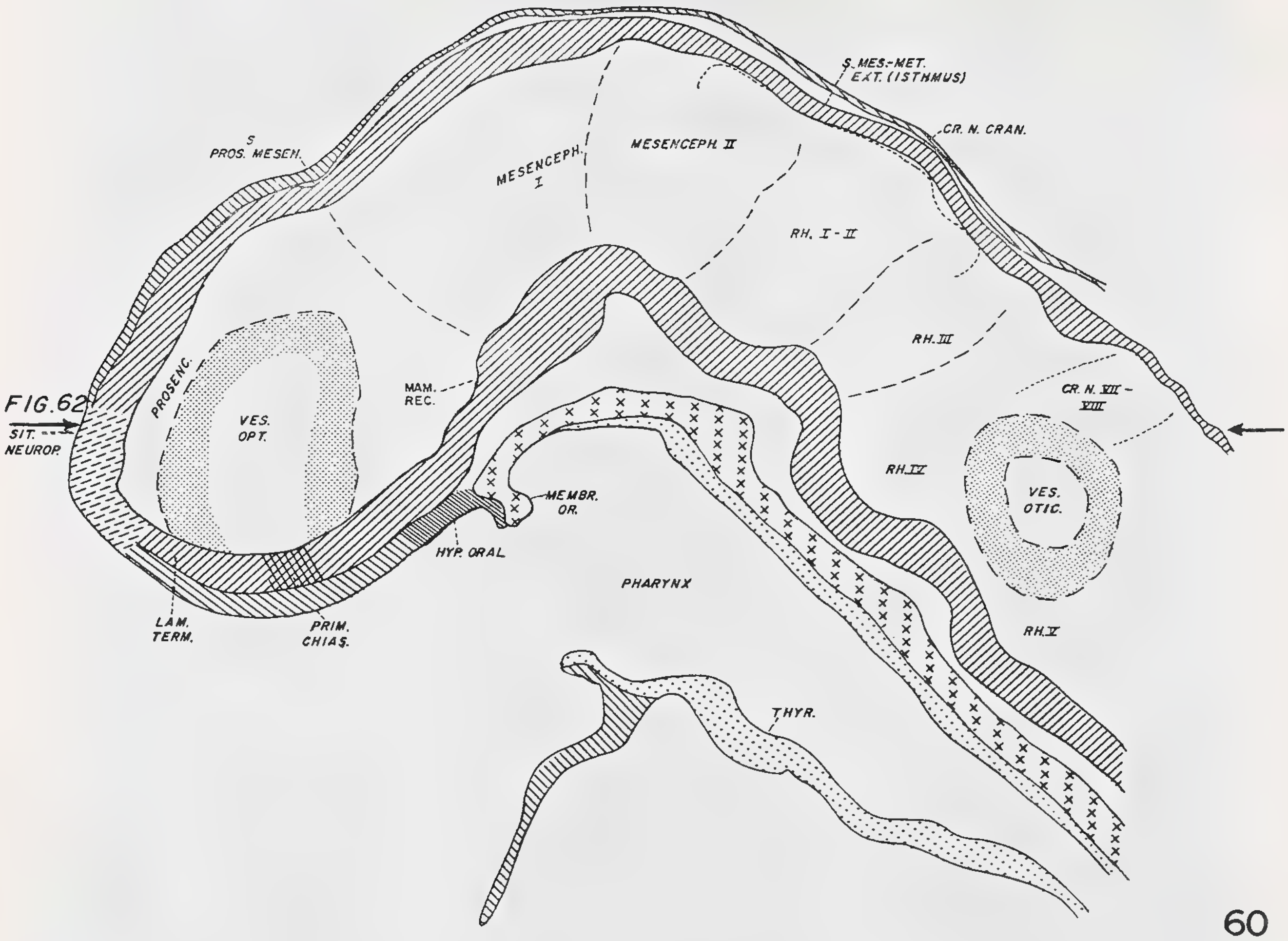

60

Fig. 60. Midsagittal projection reconstruction of brain of embryo 8943, horizon xii (3.9 mm. G. L., 22-23 somites). × 110. Chorda indicated by crosses; pharyngeal ectoderm, by coarse stipple. Arrows indicate plane of section.

Abbreviations

A. IN., Area infundibularis
C. CR. V, VII, VIII, Crista neuralis V, VII, VIII
CR. N. CRAN., Crista neuralis cranialis
HYP. ORAL (HY.), Hypophysis oralis
IST., Isthmus
LAM. TERM., Primordium laminae terminalis
MAM. REC., Recessus mamillaris
MD., Arcus mandibularis
MEMBR. OR., Membrana oralis
MESENCEPH. I, II, Mesencephalon I, II
MS., Mesencephalon
PRIM. CHIAS., Primordium chiasmatis
PROSENC., Prosencephalon
RH. I, II, III, IV, V, Rhombomeres 1–5
S. MES.-MET. EXT., Sulcus mes-metencephalicus
S. PROS. MESEN., Sulcus pros-mesencephalicus
SIT. NEUROP. (N. P.), Situs neuroporicus
THYR., Glandula thyroidea
VES. OPT. (V. OP.), Vesicula optica
VES. OTIC. (OT.), Vesicula otica
V. IV, Ventriculus IV

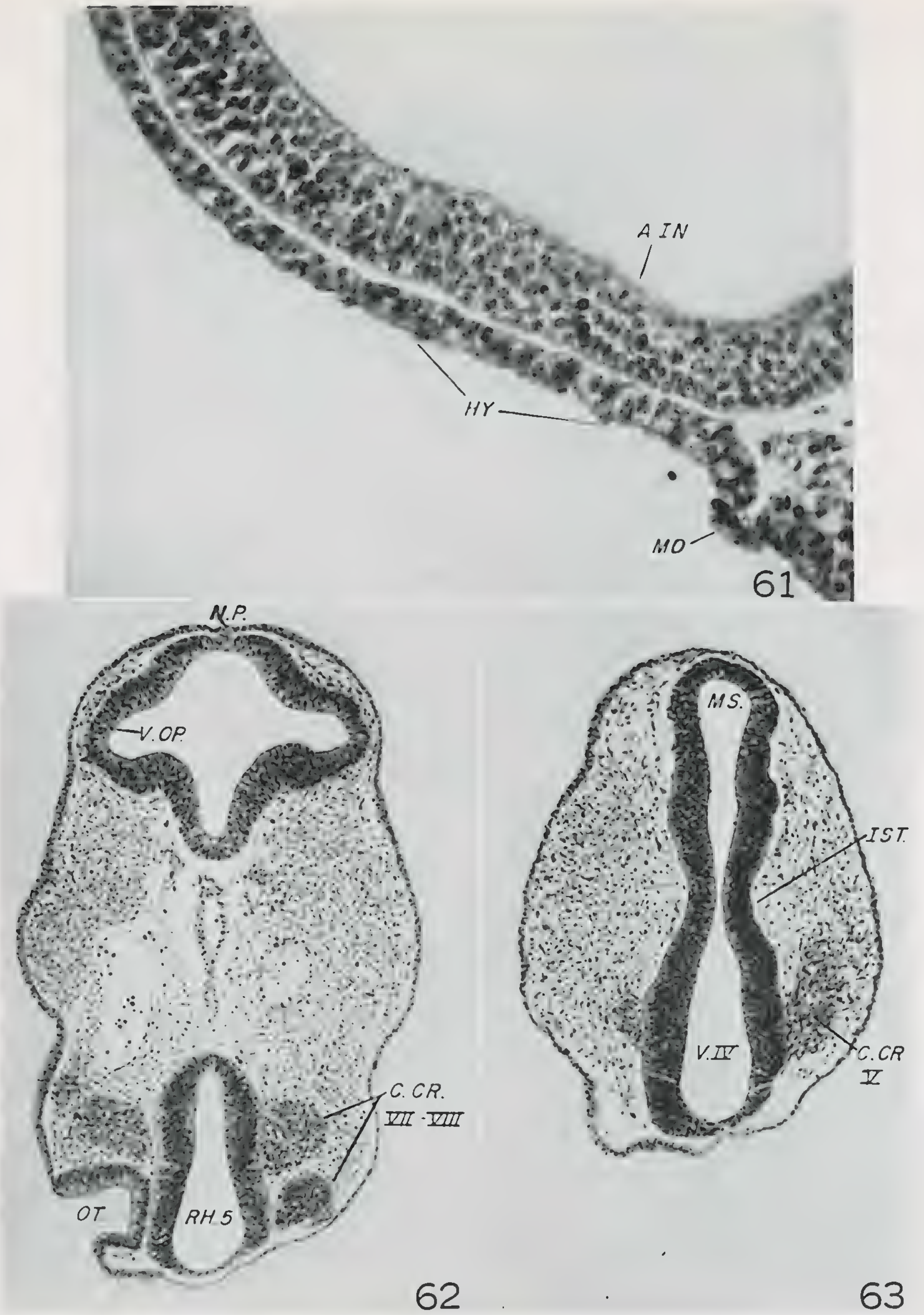

Photomicrographs from brain of embryos. Figure 61 is from sagittal section 3-3-5 of embryo 8944, showing differentiation of oral hypophysis. × 300. Figure 62 represents section 2-3-2 of embryo 8943. × 75. Level of section shown by arrows in figure 60. Figure 63 represents section 1-5-4 of head of embryo 8943. × 75.

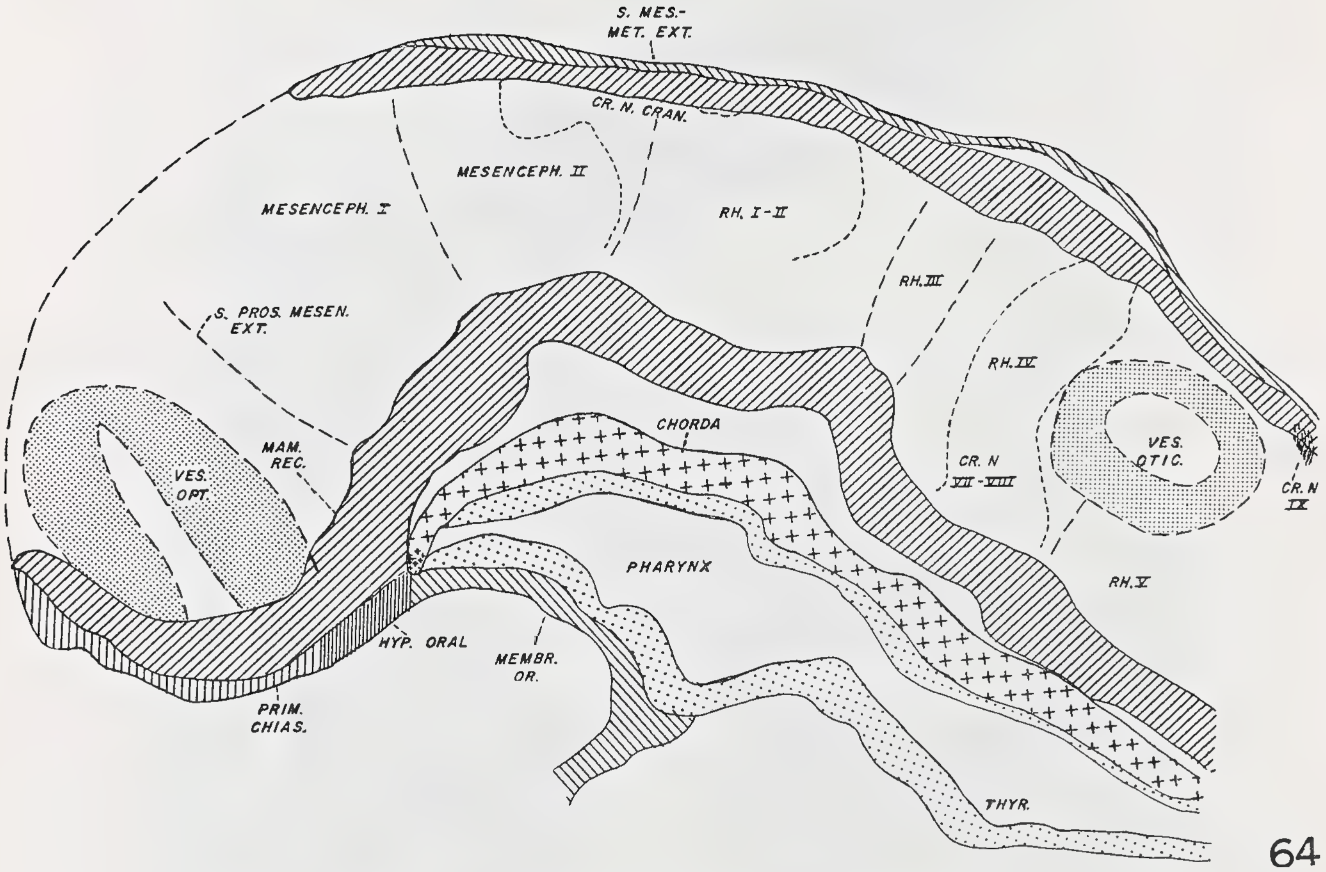

64

Fig. 64. Midsagittal projection reconstruction of brain of embryo 7665, horizon xi (4.3 mm. G. L., 19 somites). × 137.

Abbreviations

CR. N. CRAN., Crista neuralis cranialis
CR. N. VII–VIII, IX, Cristal neuralis VII, VIII, IX
HYP. ORAL, Hypophysis oralis
MAM. REC., Recessus mamillaris
MEMBR. OR., Membrana oralis
MESENC., Mesencephalon
MESENCEPH. I, II, Mesencephalon I, II
PRIM. CHIAS., Primordium chiasmatis
RH. I, II, III, IV, V, VI, Rhombomeres 1–6
S. MES.-MET. EXT. (S. MES.-MET.-ENCEPH. EXT.), Sulcus mes-metencephalicus externus
S. PROS. MESEN. EXT. (S. PROS.-MESEN.), Sulcus pros-mesencephalicus externus
THYR., Glandula thyroidea
VES. OPT., Vesicula optica
VES. OTIC., Vesicula otica

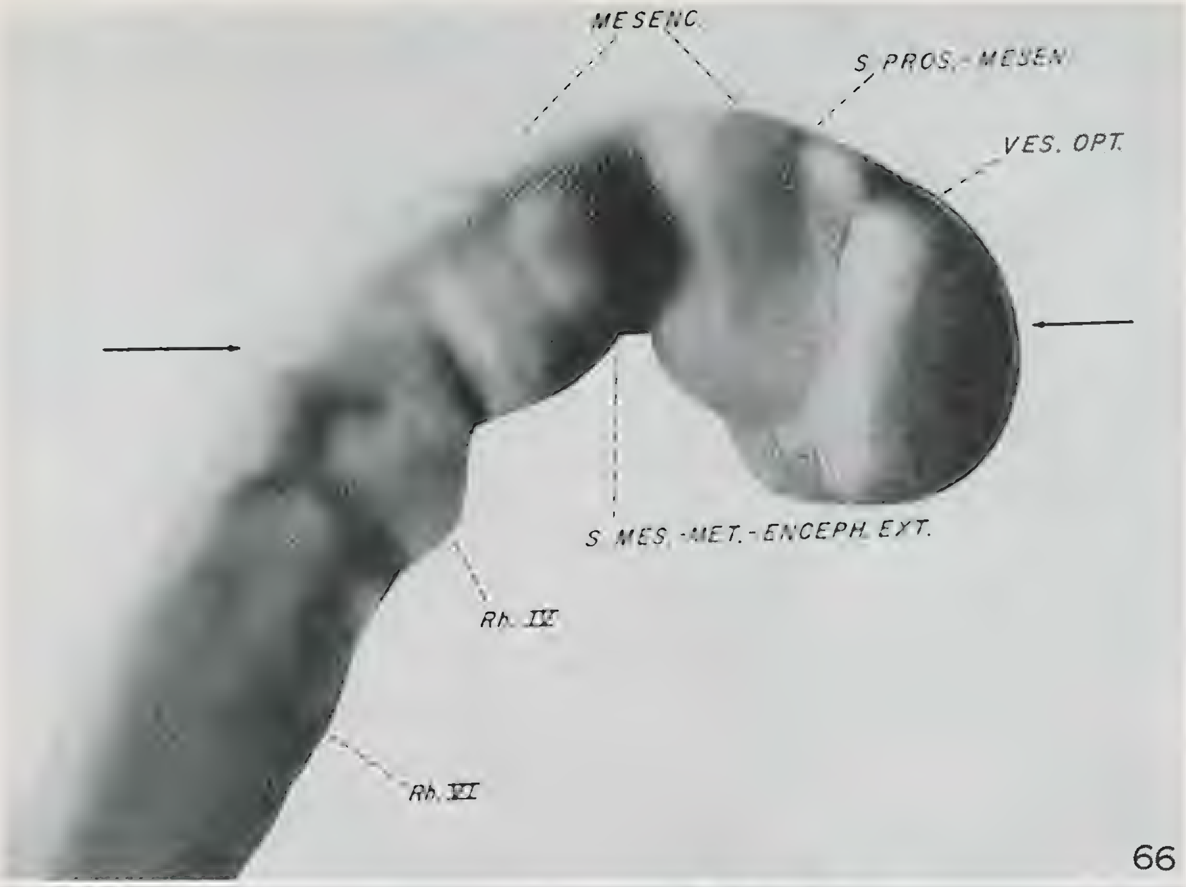

66

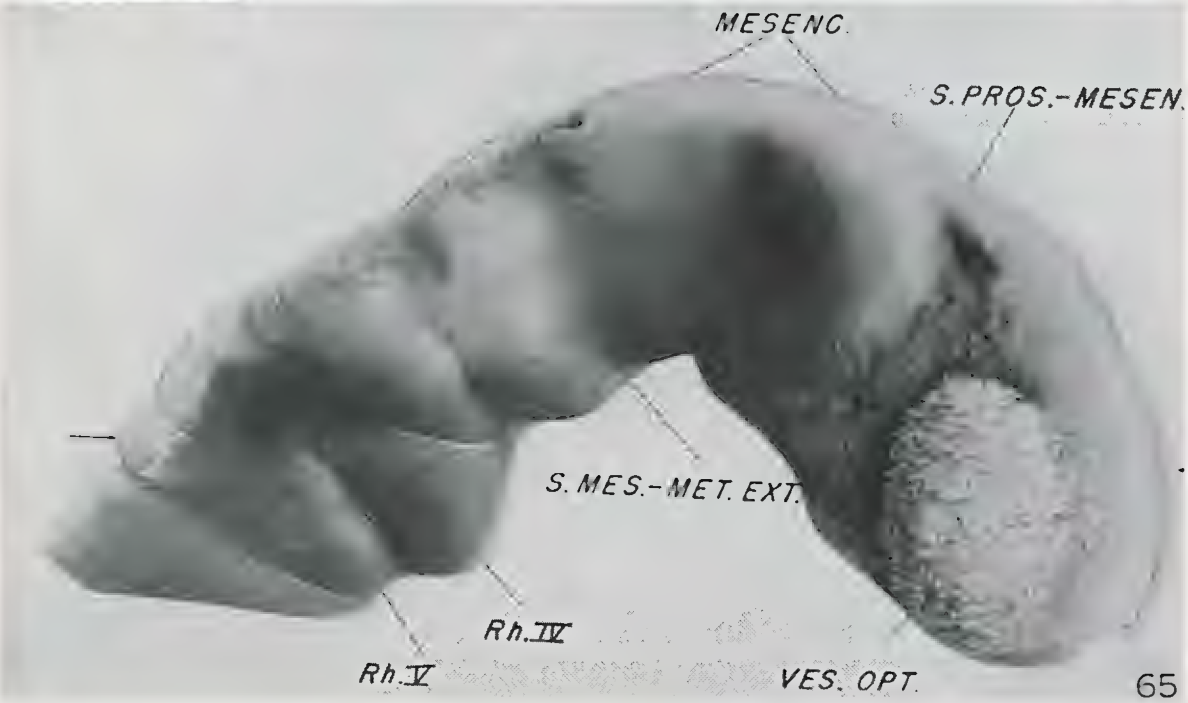

65

Fig. 65. Drawing of model of brain of embryo 8943. × 83. Arrows indicate plane of section. (See fig. 60.)

Fig. 66. Drawing of model of brain of embryo 7665. × 96.

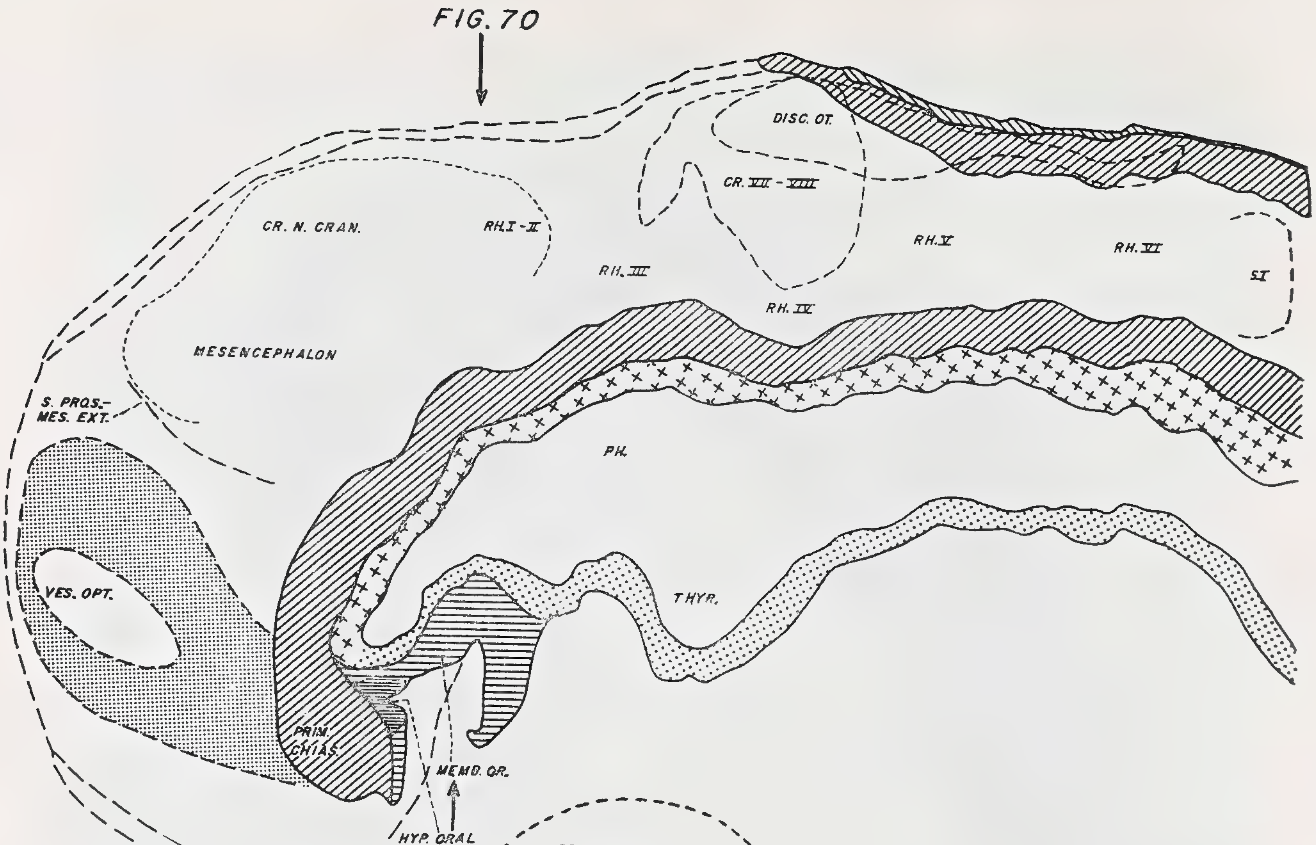

67

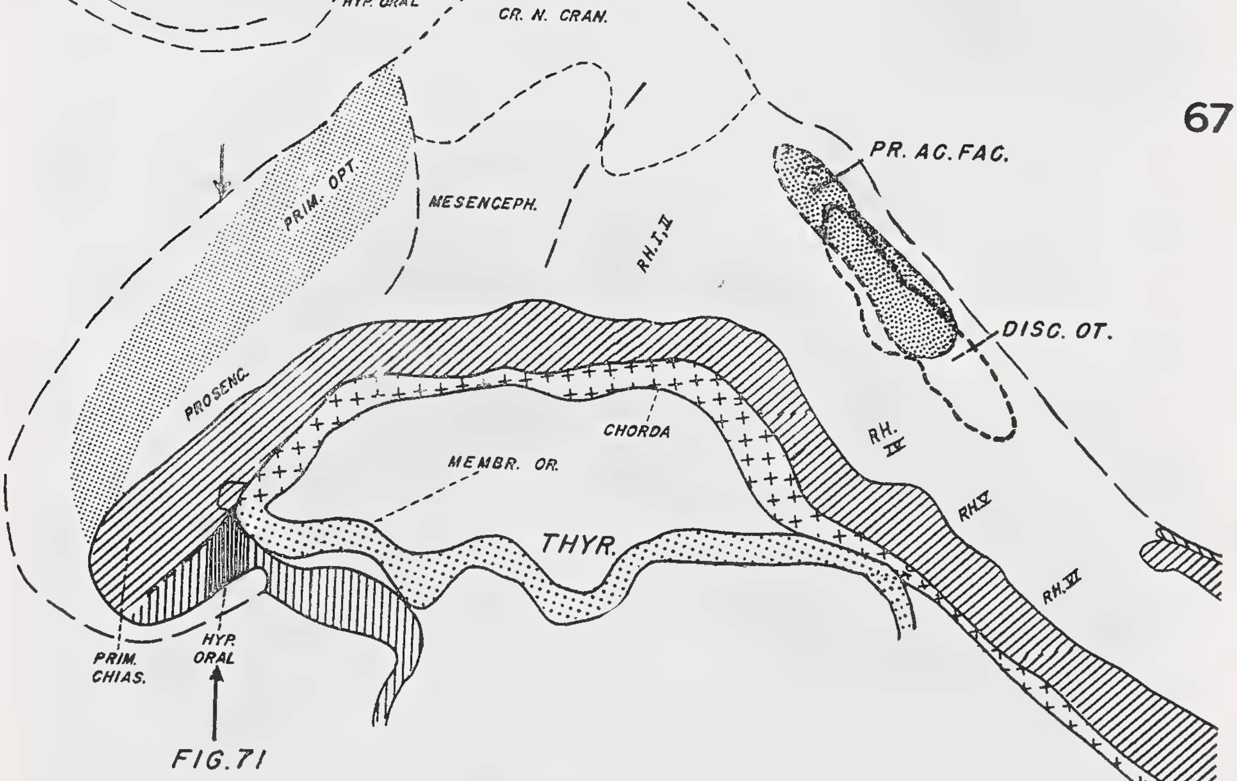

68

Fig. 67. Midsagittal projection reconstruction of brain of embryo 5074, horizon x (3 mm. G. L., 10 somites). ×161. Double broken line indicates extent of surface ectoderm on neural folds (see E. S., figs. 70, 71, pl. 30).

Fig. 68. Midsagittal projection reconstruction of brain of embryo 1201, horizon x (2 mm. G. L., 8 somites). ×236.

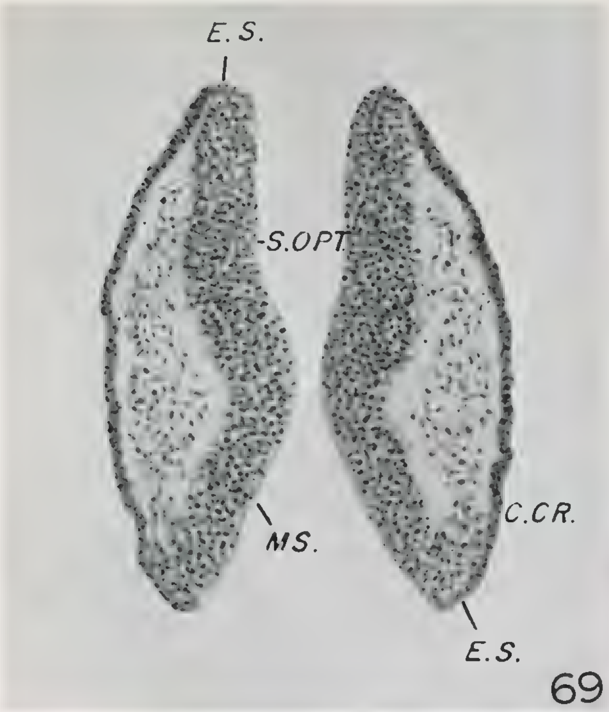

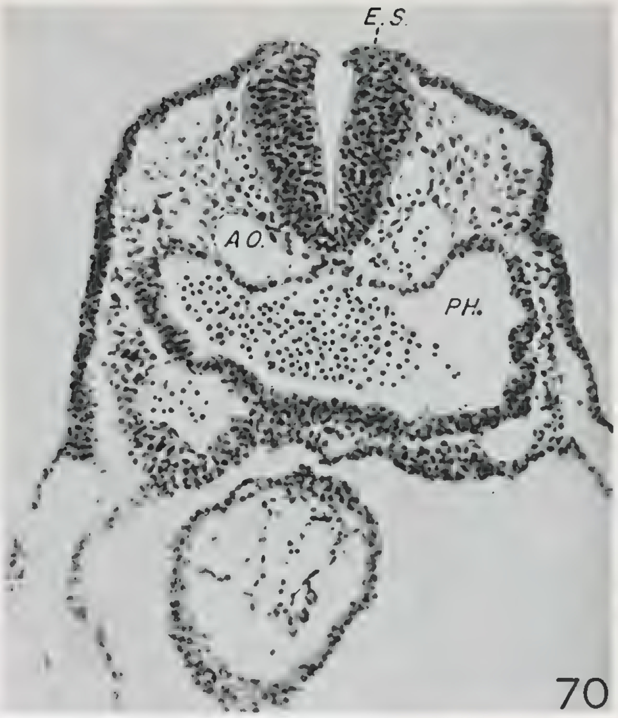

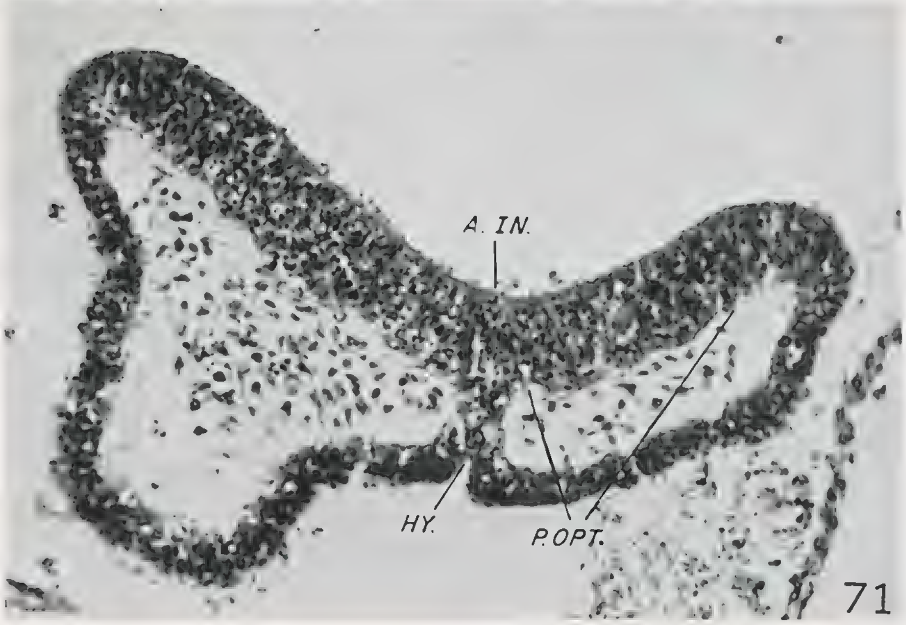

Figure 69 represents photomicrograph of brain of embryo 5074, section 1-3-1, × 125; figure 70, embryo 5074, section 1-5-5, × 125; figure 71, embryo 1201, section 3-1-2, × 250.

Abbreviations

A. IN., Area infundibularis
AO., Aorta
C. CR., Crista neuralis
CR. N. CRAN., Crista neuralis cranialis
CR. VII, VIII, Crista neuralis VII, VIII
DISC. OT., Discus oticus
E. S., Ectoderm superficialis
HYP. ORAL (HY.), Hypophysis oralis
MEMBR. OR., Membrana oralis
MESENCEPH. (MS.), Mesencephalon
PH., Pharynx
PRIM. CHIAS., Primordium chiasmatis
PR. AC. FAC., Primordium acustico-faciale
PRIM. OPT. (P. OPT.), Primordium opticum
PROSENC., Prosencephalon
RH. I, II, III, IV, V, VI, Rhombomeres 1–6
S. I, Somite 1
S. OPT., Sulcus opticus
S. PROS.-MES. EXT., S. pros-mesencephalicus externus
THYR., Glandula thyroidea
VES. OPT., Vesicula optica

CONTRIBUTIONS TO EMBRYOLOGY, NO. 254

ANATOMICAL ANALYSIS OF RABBIT TROPHOBLAST INVASION

Bent G. Böving

Department of Embryology, Carnegie Institution of Washington, Baltimore, Maryland

With fifteen plates and one text figure

CONTENTS

PAGE

INTRODUCTION 35

PART I. LOCATION OF INVASION 35
- Invasions as Histological Pointers 35
- Local Trophoblastic Factors 35
- Local Uterine Factors 35
- Section 1. Relation of Invasions to Sites of Storage 36
  - Glycogen Depots 36
  - General Evaluation 37
- Section 2. Quantitative Relation of Invasions to Sites of Transfer 37
  - Materials 38
  - Observation Criteria 38
  - Measurements 39
  - Calculations 39
  - Results and Discussion 40
    - Proximity between Attachments and Vessels 41
    - Cause of Proximity 41
    - Tropism Hypothesis Evaluation 41
- Section 3. Three-Dimensional Relation of Invasions to Sites of Transfer 43
  - Reconstruction and Mapping Method 43
  - Results and Discussion 43
    - Parallax Error 43
    - Comparison with Quantitative Analysis 44
    - Conclusion 45
- Section 4. Relation of Invasions to Endometrial Contours and Secretions 45

PART II. STAGES OF INVASION 46
- Conflicting Interpretations 46
- Adhesion 47
- Partial Penetration 48
- Complete Penetration 48

PART III. REGULATION OF INVASION 48
- Spread of Invasions in the Plane of the Epithelium 49
- Endocrine-Regulated Anatomical Control of Path of Chemical Transfer 49
- Endocrine-Regulated Enzymatic Aid to Chemical Transfer 49
- Endocrine-Regulated Endometrial Convolution as Source of New Invasion Sites 49

PART IV. MECHANISM OF INVASION 50
- Epithelium Pushed Aside by Trophoblast 50
- Loss of Epithelium 51
- Ingestion and Digestion 51
- Differential Dissociability 52

PHYSIOLOGICAL INTERPRETATION 52

SUMMARY 53

ACKNOWLEDGMENTS 54

LITERATURE CITED 54

ANATOMICAL ANALYSIS OF RABBIT TROPHOBLAST INVASION

INTRODUCTION

When a rabbit blastocyst attaches to the uterus and begins to form the placenta, there is trophoblastic invasion of the uterine mucosa which resembles cancerous invasion, at least superficially. However, cancerous invasion begins unpredictably and becomes spontaneously inhibited only rarely, whereas trophoblastic invasion both starts and stops according to a rapid and predictable schedule. The trophoblast and uterus system, therefore, has important advantages for studies of invasion and the inhibition of invasion.

One may hope that exploration of the mechanisms of trophoblastic invasion and identification of their stimuli and inhibitors will contribute to the understanding of implantation and, perhaps, to improved control of it, but considerable reservation must be attached to the related hope of contributing to eventual therapeutic imitation of the spontaneous arrest of malignant invasion until both systems become understood sufficiently to let it be judged whether the resemblance between trophoblastic and malignant invasion is more than superficial. Anatomical analysis of trophoblastic invasion can provide part of the necessary information by testing whether specific structures and substances, or categories of them, promote trophoblastic invasion, inhibit it, or are indifferent.

In the rabbit, trophoblastic invasion begins about 7 days *post coitum,* or a little before. Within the next 12 hours, several hundred aggregates of trophoblastic syncytium (the "knobs" of Assheton, 1895) on the abembryonic hemisphere (fig. 2, pl. 1) of the blastocyst come in contact with antimesometrial uterine epithelium, adhere to it (Schoenfeld, 1903), penetrate it, and spread slightly in the plane of the epithelium (figs. 3–11, pls. 2–5). Next, the epithelium becomes syncytial, the trophoblast between knobs adheres to it, and fusion becomes general in the antimesometrial hemisphere about 8½ or 9 days *post coitum* (fig. 13, pl. 6). Even while this yolk sac placenta is thus being completed it begins to degenerate, and the definitive placenta is initiated at the opposite pole of the blastocyst (fig. 12, pl. 6).

PART I. LOCATION OF INVASION

Invasions as histological pointers. This study is restricted to the yolk sac placentation—in fact, to only the beginning of it—in order to utilize the invasions as histological pointers while they are discrete and small and, therefore, most precise. This is merely prudent use of the assumption that, where invasions have occurred, all the requirements for invasion have been met, and where there is no invasion, not all requirements have been met. It remains, then, to discern what structures or substances are distinctively characteristic of such sites, and at what time they are so. If they are present before and during invasion, they may be considered favorable for invasion; if present only after invasion they cannot be requirements but must be consequences and may possibly be inhibitors of invasion. Conversely, available factors that are typically avoided by invasions would be considered unfavorable. Factors that are not present at all are certainly unnecessary, and factors that are present and localized but randomly related to invasions must be unnecessary at the site of attachment and able to influence invasion only in a general or indirect way, if at all. Anatomical analysis of the type proposed cannot distinguish favorable, indifferent, or unfavorable effects of factors that are not localized. Such general factors are therefore omitted from the principal analysis. Nevertheless, the possibility that they may be helpful or necessary for attachment is in no way precluded, and is considered in subsidiary analysis (part III, p. 49) and discussion (p. 46).

The discrete invasions may be given a logical sense of direction distinct from the biological direction of invasion. Since they merely mark the locations where all needs for invasion have been met, they point to individual invasion-promoting factors in the trophoblast when one looks there, and they point in the opposite direction when one searches in the uterus.

Local trophoblastic factors. Localized trophoblastic specialization for invasion is indicated by both positive and negative evidence. The trophoblast develops aggregates of syncytium or knobs before it adheres to and invades the uterine epithelium (Assheton, 1895; Schoenfeld, 1903). The knobs invade (Schoenfeld, 1903); the intervening, attenuated trophoblast does not, and this is so in spite of equally close contact with uterine epithelium and even adhesion to it (figs. 2, pl. 1; 6, pl. 3; 18, pl. 8; and 27*g,* pl. 13). Thus, only knobs have all the trophoblastic factors necessary for antimesometrial invasion.

Local uterine factors. Localized uterine facilitation of invasion is also indicated by both positive and negative evidence. Some knobs have become attached, while their apparently similar, except usually smaller, neighbors have not (figs. 2, pl. 1; 4, pl. 2; 18, pl. 8). Very early in implantation, such a difference in behavior may be exhibited even by parts of a single knob (figs. 4, pl. 2; 7, 8, and 9, pl. 4; and 28, pl. 15). Therefore, at least initially, the parts of the uterus where all requirements for invasion have been met are even smaller than the knobs of the trophoblast. The attachments, and hence the susceptible sites, are of the order of 10 to 20 microns across (table 1, C). Evidently, the histological pointers show the effective dimension as well as the location of the uterine invasion-promoting factor. The effective dimension, however, would be the actual dimension of an invasion-promoting factor only if the factor did not spread. If it did spread, the manner of spread would influence the distribution and effective dimension in an interpretable way. For this reason, identification by size, in addition to time and place, can be carried as far as possible if the unknown factors are sought by anatomical categories that reflect a mode of operation or distribution. The local uterine facilitation of invasion must operate either chemically or physically, or both. In anatomical terms, a chemical factor would be expected to operate at (1) a site of storage, (2) a site of transfer, or (3) a site of production. A physical factor, the epithelial contours, might be expected to influence (4) the site of contact between trophoblast and endometrium. Each of these four categories will be considered.

Section 1. Relation of Invasions to Sites of Storage

Since antimesometrial invasions are first local (about 10 to 20 microns across), then spread, and then arrested, one might expect to find an invasion-promoting substance first stored in accessible antimesometrial depots 10 to 20 microns across, then spread more widely in the epithelium, and finally dissipated without replacement. (Static depots are conceivable, but cannot be reconciled with the changing contours of invasion.)

Glycogen depots. Glycogen has been regarded as a possible nutriment for implanting embryos, and so it will be considered specifically before the role of stored substances is evaluated in a general way. At 5, 6, 6¾, 7, and 8 days *post coitum* (7 rabbits), segments of uterus were fixed with 10 per cent formalin in absolute alcohol saturated with picric acid. Sections of various thicknesses were stained by the Bauer-Feulgen procedure. Controls were treated with diastase or saliva before staining. This proved particularly important, because Feulgen-positive materials that remained undigested were found in the lumen, in cilia, in the epithelium, in stromal connective tissue, and in perivascular muscle. Perivascular muscle in addition had true glycogen at 8 days *post coitum.* In the myometrial muscle, glycogen was present on each of the days, and there was no undigested Feulgen-positive material with which it could have been confused. Glycogen was probably present in the epithelium on each of the days, but undigested Feulgen-positive materials, some of them apparently cross sections of cilia, imitated glycogen and introduced some uncertainty when the amount was very small. This occurred at 5 and 6 days *post coitum,* when the epithelium was free of glycogen except for a rare cell or small group of cells.

At 6¾ and 7 days, with implantation imminent or begun, the epithelium generally was still free of glycogen, but there was a moderate amount near each conceptus. Most of that moderate amount was in the basal parts of epithelium deep in mesometrial glands (fig. 14, pl. 7). These depots were regional; their extent was a portion of a single gland up to two dozen or more adjacent glands. The antimesometrial epithelium contained occasional granules of glycogen, but they were generally distributed rather than in depots the size of invasions (fig. 15, pl. 7). They were more abundant in the epithelium of glands and at the base of the epithelium than in the superficial parts of epithelium accessible to the trophoblast. At 8 days *post coitum,* glycogen was more abundant and widespread than earlier, and it was closer to the free surface of the epithelium, or even in the lumen, but the predominance mesometrially and the privileged occurrence near a conceptus persisted (figs. 16, 17, pl. 7). There was no support for Chipman's impression (1903) that glycogen first appears deep in the mesometrial stroma in specimens "of 8 days."

The accentuated epithelial glycogen near each conceptus was first pointed out to me by Dr. B. Goldberg of the Johns Hopkins University in a specimen 8 days *post coitum* that he had prepared by a rapid freezing technique. It was confirmed in my chemically fixed specimens of 6¾, 7, and 8 days. Quantitatively, too, at 8 days *post coitum,* there are a number of instances of more endometrial glycogen at large implantations than in portions of empty uterus between them, and also more at large implantations than at small ones of identical age (Lutwak-Mann, 1954*a*). Lutwak-Mann avoided a general conclusion, and this was very wise, for there were exceptions and the differences were not all beyond question of statistical significance, so far as may be judged from the published data, which were pooled. Therefore, the quantitative evidence is considered consistently related but neither conclusively contradictory nor confirmatory of the histochemical evidence for glycogen accumulation near conceptuses.

Thus, it is certain that glycogen in general appears and accumulates rather than disappears during antimesometrial attachment. It is likely that it is augmented near each blastocyst and in response to it. On the other hand, glycogen is certainly not a highly localized response (or stimulus) to invasion, because most of the glycogen is mesometrial (fig. 14, pl. 7), whereas the first invasion is antimesometrial, and because what antimesometrial glycogen there is occurs over an area much larger than any individual beginning trophoblastic attachment yet in granules much smaller than any such attachment (fig. 15, pl. 7).

The preceding conclusions based on general observations may be derived even more pointedly from considerations of specific invasions. Some have glycogen in the adjacent epithelium but none in the trophoblast (fig. 17, pl. 7); others have glycogen in the trophoblast but none in the epithelium (fig. 18, pl. 8); others have glycogen in both places; and still others have glycogen in neither. Glycogen cannot be considered a prerequisite for invasion, because invasion occurred where it was absent from epithelium, from trophoblast, or from both. Conversely, the unattached knob in figure 18 has much accessible glycogen (or possibly mucopolysaccharide), yet it has not been stimulated to invade. Epithelial glycogen probably should not be considered able to prevent invasion, for many invasions have occurred through epithelium that presumably contained considerable amounts of glycogen before invasion, if one may judge from a rather uniform distribution of it in a substantial region of the remaining epithelium. Neither is it likely that glycogen is a consistent local result of an invasion which, in turn, inhibits that invasion. In the first place, in spite of some suggestive situations, glycogen cannot be locally dependent on invasion, because it may appear where there is no invasion. In the second place, synchronous invasions with and without involved glycogen are not obviously different in their progression.

An amusing although exceptional natural experiment refuting a local glycogen effect on invasion was seen in 4 consecutive 7-micron sections of a knob 13 sections in extent. Epithelium and trophoblast on one side had glycogen and on the other side had none or almost none, yet the invasion had progressed symmetrically (fig. 19, pl. 8).

It is concluded that, in antimesometrial placentation of the rabbit, endometrial glycogen is frequently but inconstantly taken up by trophoblast that has invaded, that the invasion probably facilitates the uptake, but that the function of endometrial glycogen in implantation is unknown; glycogen is neither a local stimulus nor a local inhibitor of invasion.

General evaluation. If not glycogen, then perhaps it is some other stored substance that promotes antimesometrial invasion. Since such a substance might be either unknown or nonexistent, further pursuit of it by specific tests could be endless yet inconclusive. A general evaluation employing an anatomical dichotomy is more practicable.

It is unlikely that any substance stored *within the stroma* stimulates invasion. Intervening epithelium about 50 microns thick makes the stroma inaccessible to the trophoblast before invasion. Moreover, after the trophoblast has reached the stroma, the trophoblast does not penetrate it deeply but, instead, spreads a little in the plane of the epithelium or just below (figs. 11, pl. 5; 18, pl. 8).

On the other hand, it is unlikely that depots *within the epithelium* stimulate invasion. Trophoblast invades from the uterine lumen to the base of the epithelium, yet, immediately after having done so, it does not fulfill the implication that there should be further invasion from base to lumen where that would appear possible (figs. 10, pl. 5; 20, pl. 9). Moreover, considerations of the mechanism of epithelial penetration (pp. 50–52) make it prudent to recognize and question the presupposition that the trophoblast has contact with any substance stored in the epithelial cytoplasm before, or even during, its penetration of the epithelium.

It is concluded that the local uterine facilitation of trophoblast invasion is very probably caused by no agent stored in either endometrial stroma or epithelium and certainly not by glycogen.

One may reflect that the idea of invasion toward a substance stored in an adjacent, intact, cell is not only inconsistent with observations; it also suffers from the teleological implication that the site for invasion is selected by trophoblastic foresight of something to be gained after invasion. It seems much more likely that the site is selected by the mechanical adhesion (Böving, 1959*a*) that initiates invasion. Since this occurs before the trophoblast and endometrium are related more intimately than by contact, the uterine localizing factor, if it is chemical, must pass from one tissue to the other. The factor could either be produced and secreted by the uterine epithelium, or it could originate elsewhere and merely be transferred through the epithelium. The second possibility appears to be the more reasonable. Since implantation outside the uterus occurs occasionally (fig. 21) (Eales, 1932), it is unlikely that any necessary factors occur exclusively in the uterus. But, since ectopic pregnancies fail much more frequently than intrauterine pregnancies of the same species (Nicholas, 1934; Waterman, 1934), it may be presumed that the necessary factors are especially abundant or accessible in the uterus.

Section 2. Quantitative Relation of Invasions to Sites of Transfer

If the local uterine facilitation of invasion depended on a chemical that originated remote from the uterine epithelium (such as a food, hormone, ion, or respiratory gas), one would expect the substance to be carried by the circulatory system and transferred to or from the uterine epithelium where a capillary touches it. That anatomical combination may be spoken of as a "transfer site" (figs. 22, 23, pl. 10), and the capillaries in contact with the epithelium will be called "hypo-epithelial" to distinguish them succinctly from the other subepithelial or stromal vessels with which they are continuous but which do not touch the epithelium. The latter will be excluded from consideration, because they do not transfer a diffusible substance effectively to or from the epithelium and the trophoblast on the other side of it, whereas the hypo-epithelial vessels do (fig. 22) (Böving, 1954, 1959*b*). Thus, testing of the hypothesis that trophoblast attachment is promoted at sites of chemical transfer may begin with the question: Are attachments associated with hypo-epithelial vessels? They appear so by inspection (figs. 3–9, pls. 2–4; 15, pl. 7; 18, pl. 8; 20, pl. 9; 28, pl. 15) (Schoenfeld, 1903), and the impression deserves rigorous test.

Materials

Two rabbit blastocysts, with the portion of uterus containing them, were fixed at 7 and 8 days *post coitum* in Zenker's fluid and Susa, respectively. In an effort to retain normal amounts of blood in the vessels, the former specimen was clamped off before it was excised and fixed. The two specimens were embedded in paraffin, cut into serial sections 7 microns thick, and stained with hematoxylin and eosin, and azan, respectively. (Other specimens injected intravascularly with India ink were excluded after it was found that superimposed stains could reveal many vessels that the ink did not.)

Advantage was taken of the fact that a dozen or so sections yield enough data. Cross sections cut reasonably near the greatest diameter (fig. 26, pl. 12) were used so that the plane of section would coincide most nearly with the general centrifugal direction of trophoblast invasion, and so that uterine stretching would be greatest and most uniform. Only one specimen was used for each stage to avoid scattering the data by individual variations in uterine stretching, vascularity, and response to hormones, differences in conceptus size and genetics, and inconsistencies in technical preparation.

Note that the resultant data (tables 1, 2, 3) permit rigorous testing of certain relations only within each specimen; they will be so used in parts I and IV. In particular, it should be realized that, in spite of derivation from specimens considered normal, the data permit no reliable estimate of the dimensions typical of the ages of the two specimens that happened to be used. Quantitative comparison between the specimens is, therefore, avoided as far as possible, and, where its introduction proved irresistible, it is segregated (part III) and qualified. Throughout, the reliability of interpretations will be indicated by designating the less certain as suggestions and the more certain as conclusions.

Observation Criteria

Antimesometrial attachments were identified easily and with certainty as the discrete connections, pointed by tension, which remained after the blastocyst and endometrium elsewhere were separated by the shrinkage accompanying histological preparation. Where overlap of tissues left doubt about attachment, no datum was taken. Such omissions, and any attachments that might have been torn loose or unobserved, would not affect the conclusions, whereas those attachments that persisted could be depended on to have maintained their original anatomical relations to hypo-epithelial vessels by means of common attachment to the continuous uterine epithelium or by attachment to the vessel itself. Each attachment was classified as (*a*) an adhesion, (*b*) a partial penetration, or (*c*) a complete penetration of uterine epithelium, according to its greatest progress in the single section being viewed.

The identification of hypo-epithelial vessels was more complicated and less certain than the identification of trophoblastic attachments. For the analytical method employed, ideal hypo-epithelial vessels were blood-filled capillaries lying at the base of and slightly indenting uterine epithelium accessible to the blastocyst.

It was usually easy to decide whether or not the vessel was in contact with epithelium. In fact, for vessels that touched epithelium through only part of their extent within the section, it was possible to decide within a few microns which parts to accept or ignore (fig. 20, pl. 9, extreme left).

It was slightly more difficult to determine whether a vessel supplied epithelium that was accessible to the blastocyst. Judgment was aided by the decision to consider inaccessible any epithelium that was depressed below adjacent protruding portions of epithelium more than 45° from the general plane of the near-by endometrium (fig. 26, pl. 12, extreme left of lower panel). The 45° criterion may seem more precise than it truly is; the accuracy of decisions based on it suffers from uncertainty in choosing the plane of reference. Nevertheless, selection for accessibility and employment of the 45° criterion are considered worthwhile improvements over the methods used in preliminary studies (Böving, 1952, 1954). The recognition of effects of epithelial contours (see p. 46) excluded many data that were irrelevant and that had avoided being seriously discrepant only for a rather special reason (see p. 49).

Lack of blood made a substantial number of capillaries difficult to detect and distinguish from stromal tissue spaces. A risk of bias entered because vessels at invasions seemed to be somewhat more filled with blood than vessels elsewhere, and an inadvertent tendency to miss empty vessels not related to attachments conceivably could have led to a spurious demonstration of proximity between attachments and vessels. Primarily as a precaution against that error, but useful in deciding a crucial aspect of interpretation, it was ascertained statistically (pp. 41, 48) that accidental omissions, if any, were insufficient to influence the conclusions.

Measurements

In the invaded antimesometrial region of each section, the distance from the center of each accessible hypo-epithelial blood vessel to the center of the next was determined by a series of ocular micrometer measurements (fig. 26, pl. 12, lowest panel). The mean separation is designated B.

At trophoblastic attachments to the epithelium, the distance between the hypo-epithelial vessels under, or on each side of, that attachment (fig. 26) was recorded in sequence with the aforementioned vessel-to-vessel distances, but it was given a distinguishing mark. The mean of these distances between hypo-epithelial vessels at sites of invasion is designated B_i.

A concurrent record was made of the shortest distance between the center line of the attachment and the center of the nearest vessel (fig. 26). (The center line was drawn through the center of the attachment in the prevailing direction of the adjacent columnar epithelial cells). The mean of these distances, which may be called "invasion inaccuracy," is designated I when applied to all stages of invasion collectively. Separately, the mean inaccuracies of adhesions, partial penetrations, and complete penetrations are designated I_a, I_b, and I_c, respectively.

The widths of adhesions and complete penetrations were measured in the plane of the epithelium. The mean width is designated W_a for adhesions and W_c for complete penetrations.

At each attachment, the extent of contact between the related or nearest vessel and the epithelium (or trophoblast, in the case of complete penetration) was measured in the plane of the epithelium. For vessels cut transversely, it was usually their diameter. The mean contact dimension is designated D_i.

Calculations

If the hypo-epithelial vessels occurred at random distances from each other, and if trophoblast attachments entered the sequence at random, then the mean invasion inaccuracy should equal[1] one-half the mean blood vessel separation, or $I=B/2$. Under these ideal conditions, unusual proximity and presumably a causal relationship between vessels and attachments would be revealed by an I significantly less than $B/2$.

A correction must, however, be introduced, because the distances between vessels were not perfectly random.

---

[1] The relation $I=B/2$, its correction,

$$I=\frac{B}{4}\left[1+\left(1-\frac{a}{B}\right)^2\right]$$

and the rigorous justification for setting $a=B[1-(s/B)]$ were pointed out to the author by Dr. Franklin Hutchinson, Biophysics Department, Yale University. Of several derivations which he demonstrated, the following are the briefest.

If the blood vessels are arranged at random, the chance of finding a given number, n, of blood vessels in a distance, x, is given by the Poisson equation. [See, for example, Margenau and Murphy (1943), p. 422.] In particular, the probability of finding no blood vessels in traveling a distance x to the right of a randomly selected point is $e^{-(x/b)}$. The same expression holds for the probability of no blood vessels within a distance x to the left, so the probability that there is no blood vessel within the distance x is the product of the two separate probabilities, or $e^{-2(x/B)}$. The mean distance from a randomly selected point to the nearest blood vessel is then

$$\frac{\int_0^\infty xe^{-2(x/B)}dx}{\int_0^\infty e^{-2(x/B)}dx}=\frac{B}{2}$$

If the vessels whose mean separation is B are never found closer than a but are randomly arranged wherever the separation is greater than a, then there is a parameter $b=B-a$ which is random. According to Poisson statistics, in random cases the chance of finding no vessels in a distance x is $e^{-x/b}$. The chance of finding one in distance $x+dx$ is $e^{-(x+dx)/b}$, so the chance of finding a vessel between x and $x+dx$ is $e^{-x/b}dx/b$. Then, since $B=a+b$, the probability of vessels being separated by a distance that is between $a+x$ and $a+x+dx$ is $e^{-x/b}dx/b$. The probability that a random invasion will be centered in that interval is proportional to $(a+x)e^{-x/b}dx/b$. The mean distance to the nearest end of the interval, the center of the nearest vessel, then becomes

$$\frac{\int_0^\infty \frac{a+x}{4}(a+x)e^{-x/b}dx/b}{\int_0^\infty (a+x)e^{-x/b}dx/b}=\frac{1}{4}\,\frac{a^2+2ab+2b^2}{(a+b)}$$

$$=\frac{B}{4}\left[1+\left(1-\frac{a}{B}\right)^2\right]$$

Since random spacing was specified by b (and uniform spacing by a), and the standard deviation, s, is defined by

$$s^2=\frac{\Sigma(B-B_j)^2}{n_j}$$

where B_j are the individual measurements of n_j separations between vessels,

$$s^2=\frac{\int_0^\infty[a+b-(a+x)]^2e^{-x/b}\,dx/b}{\int_0^\infty e^{-x/b}dx/b}$$

$$=\frac{\int_0^\infty(b^2+x^2-2bx)e^{-x/b}dx/b}{\int_0^\infty e^{-x/b}dx/b}$$

$$=\frac{b^3+2b^3-2b^3}{b}=b^2$$

Thus, $s/B=b/B=(B-a)/B$, and $B(s/B)=B-a$, and so $a=B-B(s/B)=B[1-(s/B)]$.

For example, with random arrangement, one would occasionally have zero separation, but a microscopist cannot distinguish two vessels from one, or measure their separation, until there is a certain distance, *a*, between their centers. If the assumption that vessels are spaced at random is amended with the exception that no vessel separation is less than this limit of anatomical resolution, *a*, then[1] attachments entering the sequence at random would give

$$I=\frac{B}{4}\left[1+\left(1-\frac{a}{B}\right)^2\right]$$

This equation is only partially corrected, because it still ignores the possibility of ordering effects other than *a*, and it encounters practical complications because *a* is different for vessels of different diameters and angles of section, and they vary considerably. Therefore, the equation is neither inclusive nor convenient enough for the purpose at hand. However, it can lead to a suitable, generally corrected equation.

The expected value of I would vary from $B/2$ to $B/4$ as hypo-epithelial vessel arrangement varies from random ($a=0$) to even ($a=B$), if *a*, the resolution limit, were the only factor contributing toward reducing the randomness of the vessel separation data. If we assume it to be so, and determine how such a restricted *a* is related to the randomness of samples in general, we should be able to reason backward from a determination of the randomness of a particular sample to a value that could be substituted for the unrestricted *a* in the preceding equation, yet represent the net effect of all factors contributing either to the randomness or to the regularity of the spacing data.

The degree of evenness or randomness may be expressed by a simplified coefficient of variation,

$$V=\frac{\text{Standard deviation of } B}{B}$$

whereby perfectly even spacing is reflected by $V=0$, and samples of random dummy data have a mean near 1.00 (Böving, 1956). Thus, for random data, we have $a=0$ and may assume $V=1.00$; and, for the special "string of beads" situation of perfectly even spacing of vessels at a mean distance equal to their diameter, we have $a=B$ and $V=0$. These extreme values suggest that we may substitute $a=B(1-V)$. The estimate was first checked empirically with dummy data derived from a table of random numbers (Fisher and Yates, 1953) by plotting the V that resulted from assuming various values of *a*. Agreement was sufficiently close, particularly when *a* was considerably less than *B*, as it was for the actual data, so that no serious error was to be expected from assuming that $a=B(1-V)$. The assumption has since been shown to follow rigorously.[1]

Substitution of the above into the partially corrected equation gives[2]

$$(B/4)(1+V^2)$$

which avoids the awkward limit of resolution, *a*, and the uncertainty about unrecognized other factors that might reduce or augment randomness; it provides a general estimate of the net effect of all factors, known or unknown, that have reduced or augmented the randomness of the particular body of data being studied. Consequently, if I is significantly less than $(B/4)(1+V^2)$, it is satisfactory evidence that trophoblastic attachments are more closely associated with hypo-epithelial vessels than is likely to have occurred by chance.

An estimate of the importance of individual factors that may contribute to regularity is justified only after the preceding general evaluation. For completeness, the importance of the limit of anatomical resolution, *a*, was estimated. The average vessel dimension touching and parallel to the base of the epithelium at invasions, D_i, was substituted for *a* in the partially corrected equation, and the resultant estimate of I was compared with that from the generally corrected equation.

Results and Discussion

In the specimen fixed at 7 days *post coitum,* hypo-epithelial vessels were separated an average of 99.1 microns (table 1, A). Their arrangement was more nearly random than even, since their V of 0.73 was closer to 1.00 than to zero (table 1, A). Invasions entering at random would be expected to have an average distance of 37.9 microns to the nearest vessel (table 1, B).

That distance, the mean inaccuracy of invasion, would be estimated to be 49.5 microns (table 1, B) by the equa-

---

[2] Since $B[1-(s/B)]=a$, and $s/B=V$, one may substitute:

$$I=\frac{B}{4}\left[1+\left(1-\frac{a}{B}\right)^2\right]=\frac{B}{4}\left[1+\left(1-\frac{B(1-V)}{B}\right)^2\right]$$
$$=\frac{B}{4}\{1+[1-(1-V)]^2\}=\frac{B}{4}[1+(+V)^2]$$
$$=\frac{B}{4}(1+V^2)$$

The following form for the equation, though less expressive and compact, may be more convenient in use:

$$I=\frac{B}{4}\left(1+\frac{s^2}{B^2}\right)$$

This equation, though derived for a specific purpose, would appear to have wider usefulness in testing for association between items in parallel sequences of space or time, because it lifts the requirement and often untested assumption of randomness by introducing a simple quantitative expression that measures and compensates for the degree of randomness actually characteristic of the particular sample under consideration. This automatic correction not only avoids the labor and uncertainty of introducing estimates based on extraneous assumptions or measurements; it also safeguards against drawing unwarranted conclusions from samples whose randomness may have been altered to unknown degrees by unsuspected causes.

tion which simply assumes random vessel distribution; 41.3 microns (table 1, B) would be the estimate of the equation which partially corrects for nonrandomness by the use of average vessel dimensions at invasions, D_i (table 1, C), as a limit of resolution, *a*. The 49.5-micron estimate is significantly larger than 37.9 microns; the 41.3-micron estimate is not quite. However, exactly the same amount of difference (3.4 microns) occurred in the comparable data from the 8 days *post coitum* specimen and in that case it was significant. Therefore, it seems unwise to interpret the statistics as proof that the limit of resolution, *a,* is the only factor that keeps the hypo-epithelial vessel distribution data from being random, but it is clearly the most important one, since it accounts for most of the difference between the fully corrected and the uncorrected estimates:

$$(50\mu - 41\mu)/(50\mu - 38\mu) = 71 \text{ per cent}$$

The main conclusions that follow would have been qualitatively the same regardless of the equation used, but their statistical significance would have been exaggerated by both the uncorrected and the partially corrected equations. Thus, the generally corrected equation is the most conservative of the three as well as the most theoretically complete. Its prediction, $I = 37.9$ microns for random invasion, conveys those advantages.

Proximity between attachments and vessels. In the specimen fixed at 7 days *post coitum,* all stages of invasion were closer to hypo-epithelial vessels than is likely to have occurred by chance (table 1, B) (fig. 1). The most advanced invasions, those that had completely penetrated the epithelium, were centered on a vessel with a mean inaccuracy (I_c) of only 5.9 microns. Intermediate stages of invasion had a mean inaccuracy (I_b) of 19.8 microns, and that of adhesion (I_a) appeared similar, 20.1 microns. The median inaccuracy of all stages combined was only 5.2 microns, and, because of parallax errors (see p. 47), the median rather than the mean gives the most realistic estimate of the typical relationships. In anatomical terms, it lets one conclude that, as judged from sections, over half of all the trophoblastic attachments were centered over a vessel with an error less than the diameter of a uterine epithelial cell.

Cause of proximity. The precise relationship suggests that the invasions may have been directed toward individual vessels, presumably by chemical interaction across the intervening epithelium. Yet several plausible alternatives to this tropism hypothesis must be considered.

1. Pre-invasion vessel concentration: Invasion may have been facilitated in regions with more than the average number of vessels, as, for example, the preformed implantation areas of certain bats (Wimsatt, 1944; Marshall, 1953) and the elephant shrew (Van der Horst and Gillman, 1942). G. W. Bartelmez of the Department of Embryology, Carnegie Institution, has suggested that an increased coiling of vessels could also increase the number seen in the histological section, and this might occur locally.

2. Post-invasion vessel concentration: New hypo-epithelial vessels may have grown into the neighborhood of an invasion, perhaps as part of an inflammatory response, but, in any event, secondary to the invasion. The deeper subepithelial vessels, deliberately ignored in the present study, were described by Parry (1950) as behaving in this way in the rabbit from 7½ to 9 days *post coitum.* Again, as suggested above, there might be an apparent increase in the number of vessels wherever their coiling had increased.

3. Technical vessel concentration: Shrinkage during histological preparation opens uterine glands. (See p. 46.) Vessels on opposite sides of each gland are separated, and vessels between glands are brought slightly closer. If invasions had a tendency to avoid gland openings, they would passively become related to epithelium that would acquire vessel concentration as an artifact.

This must be considered, because the human blastocyst has been said to avoid glands and lodge near vessels as a result (Hertig and Rock, 1951). For the rabbit, however, testing of the hypothesis is more a formality than a necessity, because rabbit trophoblast invades at random with respect to gland openings (table 2) and, consequently, offers no basis for technical vessel concentration.

4. Spurious vessel concentration: Vessels near invasions were usually dilated and easily seen. Some vessels in uninvaded regions remained quite constricted, and it is conceivable that still others were so constricted that they were missed by the microscopist during the measuring procedure.

In contrast to the tropism hypothesis, all four alternative hypotheses imply vessels near invasions to be unusually close together. Actually, they were not; B_i was not significantly less than B (table 1, A). Therefore, the four alternatives are disproved, and, of the hypotheses at hand, only tropism deserves further consideration.

Tropism hypothesis evaluation. The mean widths of adhesions (W_a) and of penetrations (W_c) were not significantly different from D_i, the mean extent of contact with epithelium by the vessels nearest to attachments (table 1, C). Since the uterine epithelium is simple columnar, and since all measurements were made with due respect for the direction of the long axis of its cells, it may be concluded that adhesions and penetrations in the 7-day-old specimen were related in extent, as well as in centration, to uterine epithelial cells with a blood vessel at their base. To the degree that this shows that invasions failed where there was no vessel and succeeded only where there was a vessel, its negative import extends the positive evidence of proximity to a tentative proof and

TABLE 1. Trophoblast Attachments and Hypo–epithelial Vessels

		7 days *post coitum*							8 days *post coitum*						
	Symbol	Mean S.E.	Compared with	Difference	N	t	$P<$*		Mean S.E.	Compared with	Difference	N	t	$P<$*	
A. Distribution of vessels															
Separation, all hypo-epithelial vessels	B	99.1±3.1μ			554				97.3±2.6μ			685			
Standard deviation	s							±72.1μ							±67.5μ
Coefficient of variation (=s/B)	V							0.73							0.69
Separation, vessels at all attachments	B_i	105.2±7.3	B	6.1μ	96	0.78	.5		116.7±7.1	B	19.4	130	2.66	.01	
Separation, vessels at complete penetrations	B_c	91.8±7.7	B	7.3	45	0.72	.5		113.9±7.1	B	16.6	110	2.34	.02	
B. Inaccuracy of attachment															
Calculated															
from observed vessel distribution	$\frac{B}{4}(1+V^2)$	37.9±1.2			554				36.0±1.0			685			
corrected for limit of resolution	$\frac{B}{4}[1+(1-D_i/B)^2]$	41.3±1.3	$\frac{B}{4}(1+V^2)$	3.4	554	1.93	.06		39.4±1.0	$\frac{B}{4}(1+V^2)$	3.4	685	2.42	.02	
assuming vessels randomly spaced	$B/2$	49.5±1.6	$\frac{B}{4}(1+V^2)$	11.6	554	5.81	.001		48.7±1.3	$\frac{B}{4}(1+V^2)$	12.7	685	7.75	.001	
Observed															
all attachments	I	14.5±2.6 (5.2)†	$\frac{B}{4}(1+V^2)$	23.4	94	7.68	.001		24.6±2.9 (13.8)	$\frac{B}{4}(1+V^2)$	11.4	126	4.42	.001	
adhesion only	I_a	20.1±5.8 (5.2)	$\frac{B}{4}(1+V^2)$	17.8	40	3.84	.001		27.8±9.9 (17.3)	$\frac{B}{4}(1+V^2)$	8.2	19	1.40	.2	
partial penetration	I_b	19.8±3.8 (22.4)	$\frac{B}{4}(1+V^2)$	18.1	17	2.69	.01		0 (0)	$\frac{B}{4}(1+V^2)$	36.0	1	1.44	.2	
complete penetration	I_c	5.9±1.7 (3.5)	$\frac{B}{4}(1+V^2)$	32.0	37	7.01	.001		24.1±3.0 (13.8)	$\frac{B}{4}(1+V^2)$	11.9	106	4.41	.001	
C. Dimensions of attachment and site															
Extent of contact with epithelium by vessels nearest attachments	D_i	17.9±1.5	8 days	2.3	81	1.18	.3		20.2±1.4	7 days	2.3	138	1.18	.3	
Width of adhesions	W_a	15.1±1.7	D_i	2.8	40	1.15	.3		45.9±3.6	D_i	25.7	19	6.56	.001	
Width of penetrations	W_c	16.9±1.9	D_i	1.0	37	0.39	.7		71.2±1.4	D_i	51.0	83	24.34	.001	

* The nearest round number greater than P is given, except that .001 is listed instead of any smaller value.

† The median is given in parentheses.

extension of the tropism hypothesis. Trophoblastic attachments are not merely favored in the general vicinity of hypo-epithelial vessels and the epithelial cells which rest on them, but this very restricted anatomical complex, this site of chemical transfer, is a necessary uterine part of the adhesion and penetration mechanism.

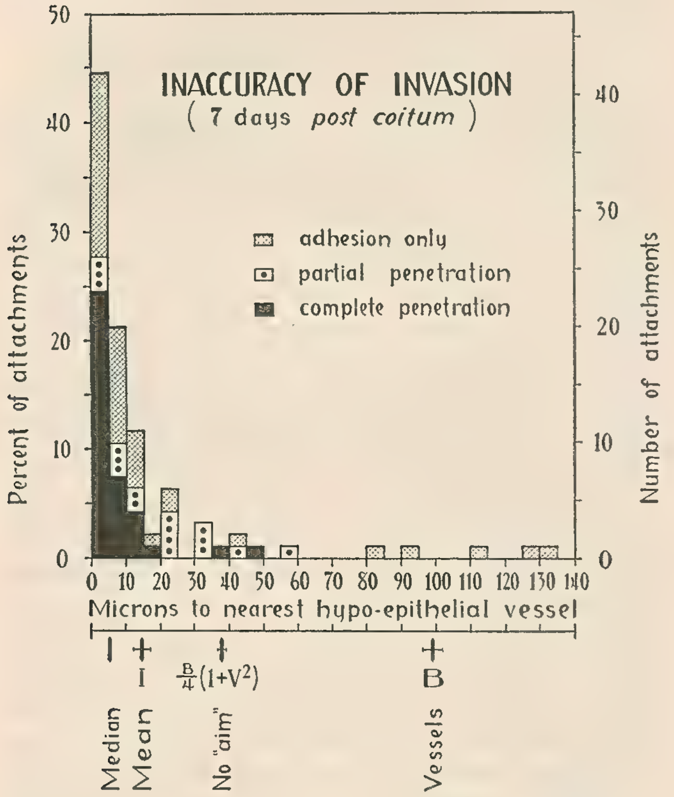

Fig. 1. The frequency distribution of the inaccuracy of invasion is shown in 5-micron categories for the three histological stages of invasion. Below the horizontal scale are graphic representations of the statistics which demonstrate that, at all stages, invasions are more accurately "aimed" for vessels than is likely to have occurred by chance. The tipped horizontal bars extend 1 standard error in each direction from each mean.

SECTION 3. THREE-DIMENSIONAL RELATION OF INVASIONS TO SITES OF TRANSFER

Information obtained by the statistical procedure conceivably could be criticized for being derived from one-dimensional measurements of two-dimensional preparations and being assumed without adequate justification to describe a three-dimensional relationship. This aspect as well as the reliability, sensitivity, and interpretation of the statistical analysis was checked by graphic reconstruction.

Reconstruction and Mapping Method

Sequential and partly overlapping camera-lucida tracings were made of the same part of the 7-day-old specimen that had been analyzed quantitatively (fig. 26, pl. 12), proceeding through one section at a time. All the tracings from each section were then combined into one drawing on a sheet of transparent plastic. The twelve such sheets representing the twelve histological sections were then piled up to provide a model of the entire material that had been analyzed. Such a model, when viewed by transmitted light, gives an impression of the three-dimensional relationships. Unfortunately, however, it can be viewed only from points near the plane of the epithelium, whereas the question of trophoblast aim for vessels could be answered much better if we could look in the same direction as the trophoblast does when it aims for the vessels, that is to say, perpendicularly to the epithelium. To attain that objective, as well as to represent the three-dimensional relations in a manner that could be published, a map of the model was prepared by procedures like those for making a contour map from a series of hill profiles. The resulting map was so long and narrow that it was necessary to divide it into a series of ten panels, *a–j*, in order to publish it (fig. 27, pls. 13, 14). The relation of these panels to the specimen as a whole and the derivation of the symbols used on the map are shown by figure 26 (pl. 12).

Results and Discussion

The analysis by mapping agreed with and amplified the conclusions of each step of the quantitative study of the 7-day-old specimen.

Hypo-epithelial vessels were about as far apart as the measurements indicated, and those near invasions were not unusually close together or tortuous (fig. 27).

Attachments appeared to be related to hypo-epithelial vessels at all stages of invasion. Many of the attachments were centered over a hypo-epithelial vessel, and most of those that were not centered had at least some part overlying a vessel.

Parallax error. There were four exceptions. Two "misses" were adhesions so small that they extended through no more than single, 7-micron sections. The first (fig. 27*e*, pl. 13), while missing a vessel, was thought not to have attached randomly, because it was within a few microns of overlying a vessel and within 10 microns of being centered on it. The second (fig. 27*a*, extreme right), which was much farther from a vessel, suggested the reason for its own and the preceding apparent miss; we may call it "parallax error." Unlike the first, it was the only attachment of a small knob. Its restriction to one side of that knob suggested that the direction of invasion passed from the knob toward the vessel just "north" or "above" on the map, instead of coinciding with our line of sight perpendicular to the general plane of the epithelium. Since invasions usually follow the long axis of the columnar epithelial cells (p. 47), the different direction of invasion by the aberrant attachment could be explained if it involved epithelium that was oblique. One may deduce that the epithelium was oblique, because it was at the edge of a gland opening. Histological inspection in several planes of focus showed that the epithelium was, indeed, oblique.

The interpretation that obliquity caused the parallax error was confirmed in another way too. The small adhesion shared with the adherent portion of a larger adjacent knob a similar position on the edge of the gland opening, and from this position, both were related to the same vessel "above," as judged by the correspondence of their direction of elongation with that of the vessel. The distance to the vessel was also similar for the two areas of adhesion, and, if one allows for the thickness of the epithelium, that distance may be recognized as quite reasonable. (It is as if adhesion had occurred below the number "75" at the edge of the gland opening in fig. 26, pl. 12. See also fig. 28, pl. 15.) The remaining exceptions were two partial penetrations at edges of the material mapped (fig. 27*c*, pl. 13). Reference to the preceding but unmapped histological section, number 1, showed that the partial penetration farthest to the right was a slightly more advanced version of the adhesion just described; it was invading at the edge of a gland opening, toward the vessel "above" it on the map, and almost in the plane of the map instead of perpendicular to it. Section 1 also showed that the left attachment was only an apparent miss; the mapped portion was a peripheral part of a complete penetration that was well centered on the next section of the vessel which appears nearest at the bottom of the map.

In view of the preceding examination, it is believed that in no case of adhesion or partial penetration from the present material need the missing of a vessel be attributed to random attachment. Every complete penetration touched a vessel. Thus, the map suggests that the relation of attachments to vessels is a consistent structural feature and not just a vague statistical tendency.

Comparison with quantitative analysis. A direct confirmation of the statistical analysis requires, however, an estimate of P, the probability that the mapped relationships could occur by chance. It is difficult to do so in a unified and simple way for the complete map, because knob dimensions and the mesh size of the vascular net are so irregular. But it is convenient, instructive, and sufficient to estimate a maximum value of P from the map of a single trophoblast knob, its several attachments, and the vessels near it.

For this purpose the most complicated knob was chosen (fig. 27*e*, pl. 13). We may regard that knob as having 6 centers of attachment. (There are 2 small, isolated adhesions, and there are 4 complete penetrations which are distinct, although their peripheral areas of adhesion merge tenuously at two points.) Since vessels underlie about ¼ of the area of the knob in question (estimated from comparison of the weights of cut-out corresponding parts of the map), the probability of any one random attachment having its center over a vessel is about ¼. The probability that 4 of 6 will do so is

$$\frac{6!}{4!\ (6-4)!} \times (\tfrac{1}{4})^4 \times (\tfrac{3}{4})^2 = 135/4096 = 0.03$$

and the probability that 5 of 6 will do so is

$$\frac{6!}{5!\ (6-5)!} \times (\tfrac{1}{4})^5 \times (\tfrac{3}{4})^1 = 18/4096 = 0.004$$

(Kuhn and Weaver, 1935). If we conservatively reject the 2 adhesions as being not centered on vessels, the remaining 4 well centered penetrations indicate that $P = 0.03$, and that is small enough to be within acceptable limits for statistical significance. If we admit the one actually borderline adhesion, we obtain $P = 0.004$, and this value is close to the statistical estimate that $P < 0.001$ that the observed proximity, I, between attachments of all stages and hypo-epithelial vessels could occur by chance. Moreover, if we restrict the confirmatory test to complete penetrations, we find that, for all 4 of the 4 penetrations to have been centered over vessels, $P = (\tfrac{1}{4})^4 = 1/256 = 0.004$. This value is close to $P < 0.001$, the similarly restricted statistical estimate that the observed proximity, I_c, between complete penetrations and vessels could have occurred by chance. Thus, reconstruction and mapping confirm the statistically derived conclusions that the observed proximity between vessels and either attachments generally or complete penetrations is very unlikely to have been the result of chance.

A direct confirmatory test of the agreement between the width of penetrations and the width of the related vessels is, in part, less satisfactory. There does appear to be agreement, not only with respect to the order of magnitude but even to the association of wider penetrations with wider vessels, or even wider parts of vessels; but the estimation of P is difficult. Pursuing first the agreement in order of magnitude, one might estimate crudely that, since the width of the knob (potentially invasive trophoblast) varies from about 5 to 30 times the width of the vessels and complete penetrations, the probability that penetrations are not wider than vessels lies between $P = 0.2$ and $P = 0.03$. This admits of but does not establish statistical significance; but neither does it benefit from including the other half of the picture, the probability that penetrations are not significantly narrower than vessels. No means of deriving that probability from the map is obvious, so this approach is abandoned short of completion. The very local agreement of width variation will be pursued instead.

If wider vessels or portions of vessels are indeed reflected by wider penetrations, as they seem to be, then a vessel that appears narrow because it has been cut transversely would be expected to have associated with it a correspondingly narrow penetration. On the other hand, one would expect a long portion of vessel lying in the plane of section to be reflected by a wide expanse of penetration in that section. Consequently, penetrations should reflect the course of the associated vessels. The map shows that they do so. Three of the four attachments were elongated, and one might expect to perceive any difference of more than 30° between the direction of elongation and the direction of the associated vessel. If an attachment were located by chance, its axis of elongation would have an equal probability of extending in any of 360° of rotation with respect to the underlying vessel. Consequently, the probability that any one penetration would have chanced to align with the vessel beneath it is about $30^\circ \times 4/360^\circ = \frac{1}{3}$. The probability of all three doing so is $(\frac{1}{3})^3 = 1/27$, and so $P < 0.04$. If the somewhat triangular penetration at the bifurcation of vessels is also considered to correspond (and consideration of the shapes of surrounding partial penetration and adhesion supports the idea), then the probability of the observed agreements' occurring by chance is 1/81, or $P < 0.02$.

Chance occurrence of the coincidence of centration, width, and axis of elongation to the degree observed is so ridiculously improbable ($P = 0.03 \times 0.2 \times 0.04 = 0.0002$ maximum, and possibly only $0.004 \times 0.2 \times 0.02 = 0.000014$) that one may infer confirmation of the statistical method and its conclusions that trophoblastic attachments are precisely related to vessels in both location and width, and one may do so in spite of having tested it with only a small part of the material that was analyzed quantitatively. Since confirmation is mutual, it suggests that the attachments of the single knob just studied were probably a fair sample in spite of being a small one.

Conclusion. It is evident that the statistical method is more suitable for describing a large sample, expressing random or inverse relations as well as associations, stating conclusions in numerical terms, and estimating the certainty of these conclusions. On the other hand, a three-dimensional reconstruction and mapping procedure is a great deal more efficient in extracting information from a very small amount of material. In addition, it describes the gaps between attachments as well as the attachments. This somewhat subtle advantage is a logically important one, for it is the negative evidence that there was no invasion where there was no vessel (with due allowance for adjacent spread and obliquities of section), which promotes the positive evidence of association between invasions and vessels to the definite conclusion that: in the 7-day-old specimen, invasions occurred *only* where the epithelium had a vessel at its base. Such epithelium with its vessel, a privileged site for chemical transfer, is a localized anatomical unit of the uterus which is essential for abembryonic rabbit trophoblast adhesion and penetration.

SECTION 4. RELATION OF INVASIONS TO ENDOMETRIAL CONTOURS AND SECRETIONS

The selective adhesion of trophoblast to epithelium with an underlying vessel has been attributed to a specific chemical reaction that occurs almost exclusively at exactly such transfer sites at 7 days *post coitum* (Böving, 1959*a*, *b*, *c*). It remains to be considered whether additional local uterine factors either mediate the adhesion at those sites or facilitate it in a less restricted but still somewhat localized manner. In particular, the role of epithelial depressions and elevations must be evaluated.

TABLE 2. Trophoblast Attachments and Gland Openings

7 days *post coitum*

	Symbol	S.E.	Diff.	N	t	$P<$
Distribution of glands						
Mean separation between glands	G	400 ± 27		135		
Standard deviation	s	310				
Coefficient of variation ($= s/G$)	V	.78				
Inaccuracy of attachment						
Calculated mean	$(G/4)(1 + V^2)$	160 ± 11		135		
Observed mean	I_g	176 ± 14	16	94	.93	.4

Measurements, calculations, and mapping analogous to the procedures used to test for a relation between invasions and vessels showed that invasions were randomly related to gland openings (table 2 and fig. 27, pls. 13 and 14). The mean separation between gland openings, G, is analogous to the mean separation between blood vessels, B. However, the gland openings shown on the map do not all correspond to those whose separation was measured. In order to focus attention on major sources of possibly stimulatory uterine secretion, only the larger epithelial depressions or "glands" were recognized for measurement. The map includes all these large depressions but adds many minor ones to show why certain vessels or parts of vessels were judged inaccessible.

If the large depressed regions are truly gland openings, one must conclude that glands exert no local stimulation or inhibition of invasion. If they are not gland openings, as there is some reason to believe (see p. 50), the same conclusion follows although for a different reason. This is not to say that uterine secretion can have no role at all in blastocyst attachment. A helpful generally distributed secretion or one restricted to cells with a vessel at their base is not precluded. An example of the former is the uterine secretion of the gloiolemma, a membrane which covers the blastocyst and takes part in attachment by becoming sticky (Böving, 1954, 1957). An example of restricted secretion, although in an atypical direction, would be provided if what has been called chemical transfer through epithelial cells over vessels is considered to be secretion because it involves modification of the substance transferred (Böving, 1959*b*, 1959*c*) rather than just the passage of it.

Since most epithelial protrusions have a vessel at their core, it could be supposed that the proximity of invasions to vessels was caused by a high probability of contact (and hence of adhesion and invasion) where the epithelium was most elevated and a low probability of contact where depressed. That idea was probably disproved quantitatively when the relation of invasions to glands was found to be random rather than inverse, and it was disposed of graphically by the observation that some attachments are at the brink of glands (fig. 27*a, j,* pls. 13, 14) and one even bridged a gland opening (figs. 27*g,* 28, pls. 13, 15). Nevertheless, in the present material, no invasion was ever found deep in a gland, and in other specimens where it has seemed to be suggested there was evidence of considerable concurrent tissue shrinkage and distortion (fig. 5, pl. 3).

The lack of invasion into glands is explained by frozen sections. Trophoblast and endometrium are in practically continuous contact; there are no appreciable epithelial projections, and the lumina of glands and their mouths are, with few exceptions (fig. 29, pl. 15), not large. *In vivo,* even where no blastocyst is pressed against the soft endometrium to flatten it, gland openings are no more than shallow funnels (Böving, 1960*b*). Evidently, the general and wide gaping of glands is a histological artifact. It has been found less severe in perfused specimens than in those fixed by immersion (Böving, 1959*a*). The essentially spherical blastocyst cannot be expected to gain any attachments deep within glands or even minor depressions which are closed to it during life. This fact was recognized in the measuring procedures (p. 38) by ignoring the hypo-epithelial vessels which supplied epithelium that was depressed below adjacent accessible epithelium more than 45° from the general plane of the epithelium (fig. 26, lower left, pl. 12).

It was an understatement to say (p. 41) that the proximity between attachments and vessels was not attributable to histotechnical shrinkage pulling vessels on either side of gland openings unusually far apart and pushing the intervening vessels closer together than in the fresh state. The fact that B_i was no less than B (table 1, A) actually showed that the distortion did not even exaggerate the estimate of proximity. The random relation between attachments and gland openings explains why no bias was introduced by the distortion, and gives another assurance that no adjustment is required for that distortion. Taken together, these quantitative considerations justify the assumption made intuitively at the outset: that the invasions and hypo-epithelial vessels were either attached to each other or both attached to and carried along with the epithelium during its displacements, and their relationships were thereby maintained.

In conclusion, at 7 days *post coitum,* no localized promotion or inhibition of invasions can be attributed to uterine "glands" or epithelial prominences. Nevertheless, in spite of a certain triteness, contact between trophoblast and epithelium must be listed as a requirement for invasion, because there is no invasion where there is no contact. These conclusions are spared conflict, because contact is so nearly universal in the abembryonic hemisphere of the blastocyst that it can be expected to have no localizing influence on invasion.

The denial of specific glandular promotion of invasion should by no means be considered a general denial of the usefulness of the extreme endometrial convolution attending progestational proliferation, which is characteristic of implantation time (Bouin and Ancel, 1910) and progesterone domination (Corner, 1928; Corner and Allen, 1929), but discussion of its probable function will be deferred until the data from 8 days *post coitum* are introduced (pp. 49–50).

PART II. STAGES OF INVASION

The demonstration of where the trophoblast adhered and penetrated in the 7-day-old specimen raises the question of how it did so. The life history of an individual attachment cannot, of course, be followed in fixed material. It cannot even be directly estimated from a sequence of timed specimens, because many stages of invasion coexist during the critical period. It can be estimated, to some extent, from appearances and mutual checking with the preceding quantitative analysis.

Conflicting interpretations. In figure 27 (pls. 13 and 14), the few entire, separate attachments which consist only of adhesion are seen to be usually smaller than those whose center has penetrated the epithelium. Intuitively, this and the idea of tropism suggest that the "implantation cone," as the invading part of the trophoblast has been called, has a straightforward, wedge-like progression of adhesion, penetration, and spread, with a trophoblastic point picking the site for attachment by adhesion and leading the way through the epithelium to the blood vessel (by means not directly evident but probably related to the same chemical mechanism as adhesion, since directed toward the same target).

This appears to be contradicted by the fact that complete penetrations had significantly better aims for vessels (I_c=5.9±1.7μ) than did adhesions (I_a=20.1±5.8μ) or partial penetrations (I_b=19.8±3.8μ). The implication that precision of aim is greatly improved during penetration of the basal part of the epithelium is inconsistent, in turn, with the observed contours of invasion. No case was seen of the sudden 14-micron basal deviation which the quantitative data from the same material imply to be typical. Where present at all, obliquities or basal deviations toward near-by vessels were subtle. Typically, penetrations were directly in line with the long axis of the columnar epithelial cells all the way through the epithelium.

The conflict might be explained in several ways:

1. Probing by trophoblast: Adhesion and penetration might become reversed in unfavorable locations and progress only where there is a vessel.

2. Selective "mortality": Perhaps only adhesions that are nearly perfectly aimed for vessels proceed promptly to complete penetration, whereas less well aimed ones lag or fail to penetrate at all.

3. Faulty or incomplete analysis of data: The data may reflect something that is not recognized.

Both the first and second explanations imply that the inaccuracy data of greatest magnitude should have come from arrested and presumably small adhesions. A frequency distribution chart (fig. 1) showed that the five most discrepant data were indeed from adhesions. The sources of these data were next tracked down to the camera-lucida tracings and map. Contrary to implication, only one aberrant datum came from a small, isolated adhesion. It was the one on the edge of a gland (fig. 27*a*, pl. 13) that was discussed on pages 43–44. The other four discrepant data came from peripheral parts of two larger attachments. One of these attachments was the neighbor that shared the gland edge with the adhesion just mentioned (fig. 27*a*); the other was the large attachment in figure 27*j* (pl. 14), and it too was near a gland opening. Thus, involvement of oblique epithelium near a gland opening is the common feature which both analytical methods reflect as unusually great inaccuracy of aim.

The way in which the obliquity affects the reconstruction and mapping has been discussed (p. 43). The effect on the measuring procedures is more subtle. The map showed that the larger attachments were well aimed as a whole and that the peripheral parts which gave the aberrant adhesion data had merely fallen into histological sections which did not include the vessels to which they were related. Instead of reflecting that relationship, the measuring procedures had registered the distance from each of these adhesions to the nearest unrelated vessel in the same 7-micron section. The *loss* of the true data of small magnitude can have distorted the estimate of typical relations only slightly, but one would expect considerable distortion from the *introduction* of the random data whose mean is much larger than the mean inaccuracy of invasion.

If, accordingly, the five most discrepant and misrepresentative adhesion data are ignored, it may be seen from the graph (fig. 1) that the inaccuracies of adhesion and penetration are very similar. A less forthright but more sophisticated way of de-emphasizing extreme values is to use the median (5.2μ) instead of the mean (I_a=20.1±5.8μ) as a measure of central tendency. Its great difference from the mean shows that it did, indeed, avoid the influence of some discrepantly high values. The median inaccuracy of adhesion (5.2μ) was almost identical with the median inaccuracy of penetration (3.5μ). With reservations, this similarity suggests that, in the 7-day-old specimen, the aim of trophoblastic invasions for hypoepithelial vessels was established at the time of adhesion and was maintained but not improved during penetration.

The reservations are not due to any evidence against the suggestion; they stem from the small proportion of the adhesion data that represent adhesions that assuredly are early invasions which are independent of other attachments. When the source of each of the 40 adhesion data was checked on the map, only 4 were found to have come from knobs that surely had nowhere progressed beyond adhesion (fig. 27*a, b*, pls. 13, 14). One additional datum came from an adhesion of thin trophoblast at, or possibly beyond, the edge of a knob which had adhered in the adjacent (unmapped) section and not beyond (fig. 27*c*). An additional 2 data came from adhesions that were on the same knob as more advanced attachments, although distinctly separated from them (fig. 27*e, i*). Of the remaining data (which almost certainly are not relevant to the argument), 31 represented peripheral parts of attachments which elsewhere had invaded more deeply, and 2 represented adhesions that did not involve knobs but only thin trophoblast which is not capable of penetrating the epithelium (fig. 27*g, j*). The map shows 3 additional, minute adhesions that were excluded from the data, because there was some doubt whether the trophoblast and epithelium adhered or merely overlapped (fig. 27*e, g, j*).

Adhesion. It is concluded that "adhesion only" is a multiple category, and the microscopist who identifies it in a single section is considerably less likely to be observing a beginning attachment of a knob than a peripheral part of an attachment that has gone deeper in another section. It is not certain that the distinction was appreciated by Schoenfeld (1903), who first noted adhesion and thought of it as the first stage of attachment; it is certain that I previously missed the distinction myself and chose for an illustration of the adhesive stage of attachment (Böving, 1954) what three-dimensional review now proves to be a questionably separate spot of adhesion at the edge of a penetration. However, when three-dimensional identification is practiced, and if allowance is made for parallax error, it may be said that the few true beginning attachments in the present 7-day-old material are as accurately aimed for vessels as the complete penetrations. Thus, the evidence, though not abundant, is entirely consistent with the suggestion that the site for hemotropic trophoblast invasion is chosen by the adhesion which precedes and initiates it.

Partial penetration. Among partial penetrations, there were several cases of parallax error, but they happened to be less extreme than the adhesion discrepancies. The median (22.4μ) and mean (19.8±3.8μ) inaccuracies of invasion were not significantly different, but both were high. The map showed that "partial penetration" at 7 days *post coitum* was a double category. Of the 17 data, 14 referred to intermediate portions of larger attachments whose better-aimed parts had completed penetration and whose peripheral parts were merely adhering. There were only 3 data, representing 3 separate invasions (but only 2 knobs), which had progressed to partial penetration and no further. The knob with 2 partial penetrations is shown in figure 27*j*; the other is at the lower right of figure 27*c*.

Complete penetration. Complete penetrations formed a single category, and there were many examples. The median (3.5μ) and mean (5.9±1.7μ) inaccuracies of invasions were small and not significantly different. Thus, they were not significantly affected by parallax error. The reason became clear when the data were traced back to the camera-lucida drawings and it was recognized that all the data, even those with greatest inaccuracy, represented invasions that had reached a vessel in the same section. Thus, the data on complete penetrations avoided the introduction of random values from measurements to unrelated vessels. The fact that parallax error was essentially eliminated when epithelium no longer intervened between trophoblast and vessel confirmed the previous explanation of the parallax error. The fact that such unequivocal data were the standard with which the adhesion data agreed when they were compared, either by medians or after adjustment by the discarding procedure, gave increased confidence both in the procedures and in the resulting suggestions: that penetration follows at sites selected by adhesion but does not significantly improve the attachments' aim for vessels.

It is apparent from the map (fig. 27) that most attachments had penetrated the epithelium completely and very few were merely adherent or partly penetrating. It might be inferred that the specimen was simply fixed too late to show a larger proportion of the earlier stages. Such is probably not the case, because about as many knobs were unattached as were attached. It seems more likely that the individual attachment passes through the stage of adhesion quite rapidly and that penetration of the epithelium is still faster and possibly almost instantaneous.

In summary of part II, the 7-day *post coitum* specimen suggests that: adhesion between a knob and epithelium with a vessel at its base establishes the individual attachment's aim for that hypo-epithelial vessel; wherever it occurs, adhesion by a knob is followed promptly by penetration; penetration is itself rapid; penetration follows at a site of prior adhesion without significantly improving the aim for the related vessel; penetration is progressive rather than probing, but the progress is somewhat faster through epithelium overlying a vessel than through adjacent epithelium. Some invasions had also spread widely in the plane of the epithelium at 7 days *post coitum* (fig. 10, pl. 5), but spread is best described by introducing the specimen from 8 days *post coitum*.

PART III. REGULATION OF INVASION

In the specimen fixed at 8 days *post coitum,* as in the younger one, the tropism hypothesis was supported, because invasions in general were related to hypo-epithelial vessels more closely ($I=24.6\pm2.9\mu$) than would be expected for random invasion (36.0±1.0μ), and there was no attendant vessel concentration (table 1, A, B).

Of the sections of knobs that appeared in the sample, 72 per cent had attached to the epithelium, whereas only 51 per cent had done so in the younger specimen. Of the sections of attachments that appeared in the sample, 84 per cent showed complete penetration of the epithelium, whereas only 39 per cent did so in the younger specimen. By these two anatomical criteria as well as size and age, the two specimens represent successive stages, and, to the extent that one may judge from only two specimens, they demonstrate progress of invasion between 7 and 8 days *post coitum*.

Paradoxically, that progress was accompanied by an increased mean inaccuracy of aim for vessels. Complete penetrations were seriously affected but were still unquestionably associated with vessels. Adhesions and the single partial penetration were no longer even significantly related to vessels (table 1, B). That the mean inaccuracy of invasion was greater for adhesions and partial penetrations than for complete penetration was reminiscent of the parallax errors examined in part II, but the fact that the complete penetrations as well as the other categories had lost accuracy between 7 and 8 days showed that an additional factor was operating. It was thought to be a spreading-out of the invasions.

Spread of invasions in the plane of the epithelium. There was, indeed, considerable spread. The mean width of penetrations was 17 microns at 7 days and 71 microns at 8 days (table 1, C). Not only had attachments spread far beyond related vessels and introduced random quantities instead of data actually reflecting the central aim of the attachment-as-a-whole, but many of the attachments appeared to have either spread over several vessels or merged from several attachments in such a way that the center of the resulting attachment was somewhere between vessels (fig. 11, pl. 5). Evidently, by 8 days, trophoblastic attachments had become so blunt as histological pointers that they could no longer point to individual blood vessels. This is a reasonable consequence and confirmation of what may now be considered the conclusion that trophoblastic aim for vessels is established by adhesion about 7 days *post coitum* and is not improved during subsequent invasion.

Endocrine-regulated anatomical control of path of chemical transfer. It is curious that invasion, which was so narrowly restricted to epithelial cells over vessels at 7 days, should have spread so widely by 8 days. On the two days, the hypo-epithelial vessels in general were not significantly different in separation, in randomness, or in extent of contact with epithelium (table 1, A, C). Thus the change in tropism cannot be attributed to the vessels. The fact that the vast majority of invasions (the complete penetrations) still corresponded to vessels in location, although not in extent, suggests that the spreading of the invasions was stimulated by a diffuse invasion-promoting factor. It is not precluded that the diffuse factor is a new one different from the localized one that promoted hemotropism, but it seems simpler to begin with the supposition that the same one is still operating and that spread of invasion between 7 and 8 days is caused by only a change in the pathway of chemical exchange, between trophoblast and maternal blood, from the narrow channel characteristic of 7 days to general diffusion at 8 days. Accordingly, such a change in pathway was looked for between 7 and 8 days; it was found, and it was attributed to the disappearance of intercellular membranes from the accessible uterine epithelium during that time (Böving, 1955, 1959*a*). The epithelial transformation to a syncytium or symplasma was known to Duval (1892), and was found by Bouin and Ancel (1910) to depend on the corpus luteum.

Endocrine-regulated enzymatic aid to chemical transfer. Identification of the adhesion- and invasion-promoting substance transferred over this changing pathway as a bicarbonate from the blastocyst, and discussion of its action through local induction of alkalinity where it is removed to the maternal circulation (Böving, 1954, 1959*a, b, c*), are beyond the scope of the present anatomical analysis, except for pointing out that there is now experimental support for the originally anatomical inference that the invasion-promoting substance is blood-borne and diffusible through uterine epithelium. This is in agreement with the inference from ectopic implantation mentioned earlier (p. 37): that maternal factors essential for implantation occur outside the uterus as well as in the endometrium. There is less obvious agreement with the second part of the inference: that the essential factors are more accessible or abundant in the uterus than ectopically. Whereas vessels are abundant in the endometrium, the uterine epithelium is certainly thicker than, for example, the peritoneum. Admittedly, there may be factors other than chemical exchange which make the ectopic sites unfavorable, but it would be foolish to ignore the clear hint that the transfer of bicarbonate across the uterine epithelium is somehow facilitated. The dependence of implantation on progesterone (Allen and Corner, 1929) suggested the facilitation to be progesterone-dependent. The progesterone-dependence of carbonic anhydrase in the rabbit endometrium, the appropriateness to implantation in the timing of the rise, peak, and fall of its activity (Lutwak-Mann, 1954*b,* 1955), its specificity of function, the chemical evidence of its function in epithelium overlying blood vessels (Böving, 1959*b*), and the covariable inhibition of bicarbonate transfer and implantation by a specific carbonic anhydrase inhibitor (Böving, 1960*a*) combine to suggest that it is the progesterone-augmented enzyme, carbonic anhydrase, which makes uterine vessels peculiarly accessible to the blastocyst's bicarbonate by facilitating carbon dioxide conversion in and removal from the intervening uterine epithelial cells (Böving, 1959*c*).

Endocrine-regulated endometrial convolution as source of new invasion sites. Progesterone is better known for its induction of the extreme endometrial convolution known as progestational proliferation (Corner and Allen, 1929). A role in implantation for some of those convolutions is suggested by another guarded comparison of the 8 days *post coitum* specimen with the one a day younger. The difference in diameter between the two specimens suggested that the uterus was considerably more stretched at 8 days than at 7. The mean distance between the most outlying invasions suggested that the arc of the uterus involved in invasion had about doubled in length (from 4550 to 8340 microns, table 3). From that ratio, one might expect the older uterus to show the presumed stretching by an approximate doubling of the mean distance between accessible hypo-epithelial vessels. Instead of that, the mean distance was not significantly changed (from 99.1 ± 3.1μ to 97.3 ± 2.6μ, table 1, A). The spacing was kept constant only because the number of accessible hypo-epithelial vessels in the involved part of the uterus had increased from a mean of 46.2 to 85.7 per section (table 3). Where did they come from? One thinks of Parry's (1950) report that new "subepithelial" or stromal vessels grow into sites of "fusion" or invasion, but it seems unlikely that many of these meet the criteria for accessible hypo-epithelial vessels, or that, if they do, enough arise in a day to account for the doubling of vessel number, or that the increase of vessels near invasions is accomplished without an accompanying decrease (rather than the observed statistically significant increase, table 1, A) in the mean distance between them.

TABLE 3. Comparison of 7 and 8 Days *Post Coitum* Specimens

	7 Days Mean	8 Days Mean
Placental arc,* microns	4550	8340
Accessible vessels per section	46.2	85.7
Gland openings per section	11.3	9.8

* By "placental arc" is meant the distance between the two most lateral (or mesometrial) points of trophoblastic attachment, measured around the antimesometrial periphery of the uterine lumen.

It seems more likely that the additional hypo-epithelial vessels were supplied by an unfolding of the accordion-pleated endometrium that simply carried the additional vessels with it as it unfolded. Such folding, rather than stretching, is suggested to be the mechanism for increasing endometrial perimeter, because the uterine epithelium was not attenuated to half its original thickness between the two stages (figs. 10, 11, pl. 5). Seeking to check that interpretation, I looked for a decrease in the number of endometrial folds or "glands" between the two stages. Although no claim of statistical significance is justified, there was apparently a slight decrease from 11.25 to 9.75 glands per section (table 3). The unsophisticated inference that about 1.5 glands per section provided the additional 40 new vessels in the section was then recognized as ridiculous. It seems more reasonable to suggest that the 10 or so "glands," which each section cuts across, unfold simultaneously but only a little at a time, each yielding an average of about 4 newly accessible vessels during the 1-day interval. Perhaps 10 per cent of the "glands" unfold completely during the process. With hypo-epithelial vessels about 100 microns apart, the average "gland" would be required to yield 400 microns of newly accessible epithelium, 200 microns coming from each side of its opening. The dimensions of typical epithelial depressions are consistent both with a yield of that order of magnitude and with the complete unfolding of a small proportion of the depressions.

Such unfolding of preplicated endometrium seems a singularly appropriate means for accommodating the extremely rapid blastocyst expansion and the accompanying invasions. The concentration of vessels accessible to the blastocyst for the maintenance of its metabolism is kept constant, yet the number of vessels accessible to its trophoblastic invasions is doubled and the new vessels are supplied at locations that are random with respect to the attachments that have already been established. Since the location of the still unattached knobs is governed, so far as one may judge, by the geometrically different mechanism of simple stretching or growth of the blastocyst surface, one may infer that the unfolding epithelium provides the unattached knobs a slowly changing array of accessible vessels. That would offer the knobs a better prospect for eventually overlying a vessel and consummating invasion than would any mechanism, such as stretching, that maintained constant geometrical proportions. The latter could provide only ever-increasing separation between a knob and even the nearest transfer site and vessel that, initially, was just beyond effective range.

In summary, part III suggests that progesterone regulates abembryonic implantation in the rabbit through three mechanisms: (1) the endometrial enzymatic regulation of bicarbonate discharge from the blastocyst to the maternal circulation, (2) the anatomical regulation of the dimensions of the pathway available for that discharge, and (3) the anatomical provision of moving and ever more numerous accessible sites for the bicarbonate discharge and consequent knob attachment.

PART IV. MECHANISM OF INVASION

The studies of the location, sequence, and regulation of invasion raise and help to answer questions about the mechanism by which trophoblast penetrates the uterine epithelium. The 8-day-old specimen suggested two aspects, a loss of epithelium and a pushing aside of epithelium.

Epithelium pushed aside by trophoblast. The mean separation between all hypo-epithelial vessels, B, was 97.3±2.6 microns, yet the mean separation between those of them nearest complete penetrations, B_c, was 113.9±7.1 microns. (The slight difference from B_i in table 1, A, is due to the exclusion of 20 data that were related to adhesions and partial penetrations.) Thus, vessels at complete penetrations were 16.6 microns farther apart than vessels generally ($P<0.02$), and, since epithelium and vessels are joined, one may suggest that the epithelium was pushed aside an average of that amount at each complete trophoblastic penetration. The suggestion falls short of a conclusion, because other explanations are not excluded. The alternatives that come to mind, such as destruction or occlusion of vessels at invasions, are less consistent with the measurements and with typical histological appearances. The vessels at invasions are only slightly farther apart, not twice the general average, and they tend to be somewhat more rather than less dilated. Nevertheless, the alternatives must be taken seriously, for a few vessels near invasions showed definite degeneration even in the 7-day-old specimen (the central vessel in figs. 10, pl. 5, and 27*f*, pl. 14, and the narrowed vessels in 27*a* and *i*, pl. 13), and I refer to changes which differ, at least in the absence of erythrocytes, from the disappearance of vessel walls which lets maternal blood flow through trophoblast-lined spaces (figs. 11, pl. 5; 13, pl. 6) (Chipman, 1902, 1903; Parry, 1950). It would be prudent to consider that the slightly increased separation of hypo-epithelial vessels at invasions may have more than one cause.

Loss of epithelium. Epithelium at invasions must have been not only displaced but also destroyed, for the mean width of the penetrations ($W_c=71.2\pm1.4\mu$) was much greater than the mean epithelial displacement (16.6μ). The difference (54.6μ) is the average extent of epithelial loss at each invasion. With the columnar epithelial cells 5 to 10 microns across their short dimension, an average penetration of the 8-day specimen must have destroyed and substituted itself for a zone of epithelium about 5 to 10 cells wide.

A similar study of the 7-day-old specimen was performed to learn, by comparison with the preceding data, whether the epithelial displacement and destruction occur in sequence or together. The idea was entertained that it might be possible to distinguish or preclude sequentially different mechanisms for the sequential phenomena of penetration and spread. However, the epithelial separations and the penetration width were so small, and the variations were so great, that a statistically significant distinction between displacement and destruction could not be made with the present body of data from 7 days *post coitum.*

Ingestion and digestion. The attempt to distinguish sequential mechanisms for penetration and spread, therefore, came to depend principally on nonquantitative morphological methods. A knob that presumably had completed its spread at 8 days *post coitum* (fig. 11, pl. 5) contained a number of epithelial cell nuclei but not epithelial cells. Since the loss of epithelium at invasions and the spread of invasions occur between 7 and 8 days *post coitum,* a more promising place to look for the processes in operation (rather than completed) would be in that knob whose invasion had spread the most at 7 days *post coitum* (fig. 27*f*, pl. 14). In a section of that knob (fig. 10, pl. 5) the trophoblast was seen to contain only rare epithelial cell nuclei but numerous rounded-up epithelial cells and even groups of them. Without violating convention, one might infer that the loss of epithelial cells and the accompanying spread of invasions are accomplished by trophoblastic ingestion and digestion of the epithelial cells.

On the other hand, the fact that many of the epithelial elements that had been ingested were not yet digested (fig. 10, pl. 5) suggested that digestion did not begin until well after penetration and ingestion. If that is so, then ingestion as well as digestion must have been preceded by penetration. (It would be impossible for trophoblast to surround epithelial cells while it was still entirely on one side of an intact epithelium.) Thus, one may deduce that, if ingestion and digestion do account for the spread of invasions and occur in sequence, they do not account for the preceding penetration of uterine epithelium. The paradoxical lack of biological economy implied by that interpretation suggests the even less conventional but more reasonable possibility that we have identified ingestion and digestion from morphological appearances that have actually been caused by phenomena somewhat different from what we usually think of when we use those terms.

If the loss of a zone of epithelium 5 to 10 cells wide at each invasion follows an initial penetration which is isolated, the loss would be beside rather than below the penetration, and it would probably be more or less divided between the two sides of the penetration. Epithelial changes of an appropriate extent have been observed beside some but not all penetrations. The best example is from an 8-day *post coitum* specimen that was fixed, not just by immersion, but also by injection of fixing fluid directly into the uterine lumen (fig. 6, pl. 3). Here, as in figure 10, plate 5, the presumably doomed epithelial cells are certainly abnormal in appearance, but it is not certain that their changes are the result of digestion. They have, after all, been cut off from their normal food and respiratory supply as they have become loosened from the stroma, and they have rounded up as they have become loosened from their neighbors. But in spite of these degenerative and dissociative changes there is nothing anywhere in the whole knob that can be taken as evidence that the trophoblast (which has already completed its penetration) has ingested any epithelial cell; neither is there any indication that it later will ingest the altered epithelial cells. It is at least equally likely that such adjacent loosened cells will be shed into the uterine lumen, and a few cells thought to be of such origin have, in fact, been found in the lumen of several rabbit uteri at this stage of pregnancy.

Where a number of penetrations proceed from a single knob (figs. 7, 8, pl. 4; 27*e*, pl. 13), it is unavoidable that both loosened and intact epithelium below the knob and among the penetrations would be trapped there. Subsequent spreading and merging of the penetrations (fig. 9, pl. 4) with progressive loosening and envelopment of all the trapped epithelium would give the picture (fig. 10, pl. 5) that was interpretable as ingestion and digestion, would avoid the inconsistent implications that ingestion precedes digestion in figure 10 but follows it or fails to occur in figure 6 (pl. 3), and would allow penetration and spread to be explained by one continuous set of phenomena rather than two inconsistent ones.

Differential dissociability. Histological impressions, such as the ones that have been discussed, suggest that trophoblastic penetration depends on differential dissociability, that is to say, that the epithelial cells in the target area over a vessel suffer dissociation while the trophoblast knob there, being syncytial, does not dissociate and therefore prevails. (The intrusion of trophoblast among the loosened cells suggests that there is also an as yet unexplored mechanism that provides a push.)

If the differential dissociability hypothesis is correct for penetration, one would expect to see evidence for epithelial dissociation after the adhesive stage but before penetration. There is such evidence (fig. 5, pl. 3). If the hypothesis applies also to spread, one would expect evidence that the spread of invading trophoblastic syncytium occurs while the epithelium is in transition from cellular to syncytial but stops after the epithelium too becomes syncytial. The spread does occur during the transition period between 7 and 8 days *post coitum,* and there is some unquantitated evidence (figs. 13, pl. 6; 17, pl. 7; 18, pl. 8) that it does not continue thereafter. Also consistent is the loss of endothelium from the portions of vessels adjoined or surrounded by trophoblast (figs. 11, pl. 5; 13, pl. 6).

Tempering the preceding hypothesis is the recent experience from the more critical studies, especially part II, which taught that direct histological interpretation may be as deceptive as it is inviting. Moreover, it is not just that interpretations may be insecure unless three dimensions and quantitative analysis are employed; there remains the problem that, even if they are employed, one cannot usually depend on histological evidence to describe a continuous process, such as the loss of cells, because no individual cell with an identified alteration can be followed to confirm its estimated fate. Though it is acceptable "common sense," it is not rigorously logical to assume that the completely lost epithelium once looked like and functioned like the near-by epithelium that was *not* completely lost—and that applies not only to intact epithelium but also to that which is in a presumably intermediate state of degeneration. The assumption is not just formally contradictory; it can prove treacherous. It presupposes one of many possible conclusions, namely, that the agent that destroyed the epithelium spread and acted gradually, harming more distant cells exactly as it did the lost ones, except later or less severely. That presupposed conclusion is so plausible that it may have blinded one to alternative possibilities such as: (1) uterine facilitation of invasion by a limited number of epithelial cells which differ, at least in function, from those that remain; (2) all-or-none loss of epithelial cells, or groups of them; (3) epithelial loss by means that are not of a typical ingestive or digestive type. All these alternative possibilities have been given various degrees of credence by the studies described.

Except in the matter of epithelial dissociation, the conclusions of one descriptive histological method were set against those of another to reveal some of the strengths and weaknesses of various means of histological analysis as well as to ensure or improve the reliability of the conclusions. The hypothesis of dissociation lacks such a check by another descriptive histological method applied to normal material, but it has been confirmed by experimental procedures. That check and similar checking of other conclusions from histological analysis with information from other disciplines are either accomplished or contemplated, and they may be understood most readily in the light of a working hypothesis, or physiological interpretation, which relates the histological phenomena to each other and to pertinent phenomena from those other disciplines.

PHYSIOLOGICAL INTERPRETATION

One may discern a definite chain of mechanisms responsible for antimesometrial rabbit trophoblast invasion. An increase of progesterone causes an increase of carbonic anhydrase in the endometrium (Lutwak-Mann, 1954*b;* 1955; Lutwak-Mann and Adams, 1956), and it is believed that this, in turn, speeds carbon dioxide release from carbonic acid and transfer to maternal blood, thereby indirectly facilitating the transfer of accumulated bicarbonate from the blastocyst, through the epithelium, to the maternal circulation (Böving, 1959*b, c*). The transfer and conversion are thought to be accompanied by a rise in *p*H which makes the blastocyst adhesive but causes the epithelial cells to lose cohesion (fig. 5, pl. 3) (Böving, 1954, 1959*a*). At 7 days *post coitum*, the chemical transfer is restricted, by the intercellular membranes of the uterine epithelium, to those cells having a capillary at their base. The invasion (adhesion followed by epithelial dissociation, and then trophoblastic penetration among the loosened cells) is, consequently, restricted to the same location and thus "aimed" for a hypo-epithelial vessel. Under the influence of the corpus luteum (Bouin and Ancel, 1910) the intercellular membranes disappear from most of the accessible epithelium between 7 and 8 days *post coitum* (Duval, 1892), and do so perhaps a little sooner near invasions than elsewhere (figs. 11, pl. 5; 20, pl. 9) (Böving, 1959*a*). During that interval invasions spread. By 8 days *post coitum,* chemical transfer across the epithelium has become diffuse (Böving, 1955, 1959*a*), and, soon thereafter, abembryonic attachment becomes general, not by continued spreading of invasions (fig. 13, pl. 6), but by a general adhesion of the thin trophoblast between knobs.

If the interplay of mechanisms has been discerned correctly, the arrest of abembryonic trophoblast invasion may be correlated with no specific inhibitor but with two anatomical and one chemical relationship. (1) The penetration, or "vertical" phase of invasion, stops when the trophoblast has reached its physiological objective, a maternal vessel. (2) The spread, or "horizontal" phase of invasion, appears to stop after the epithelium, like the trophoblast, has become syncytial and is no longer susceptible to dissociation. (3) The gradually falling concentration of bicarbonate in the blastocyst reaches the maternal serum level at about the same time (Lutwak-Mann and Laser, 1954).

In most general terms, trophoblastic invasion of the antimesometrial endometrium of the rabbit may be described as the anatomical (physical) results of chemical transfer and associated reactions which are aided by a hormone-controlled enzyme and directed by hormone-controlled anatomical changes. This easily studied type of invasion, therefore, invites further exploration by anatomical, physical, chemical, enzymological, and endocrinological means.

SUMMARY

1. The attachment of the abembryonic hemisphere of the rabbit blastocyst to the antimesometrial part of the uterus is proposed as a tool for studying invasion and its arrest.

2. An anatomical analysis employs the many discrete trophoblastic invasions of uterine epithelium as histological pointers to sites where all factors necessary for invasion are available.

3. Factors characteristically associated with invasion are distinguished from incidental and inhibitory ones by a quantitative method. The method can have other applications for testing the relationship of items in parallel sequences of either time or space; and it avoids an untested and unjustified assumption of randomness by determining and compensating for the degree of randomness or regularity actually characteristic of the sample.

4. The conclusions of the quantitative method are confirmed and extended by those of reconstruction and mapping. The combination of methods is superior to either alone. The quantitative method can demonstrate inverse and random relations as well as associations, and it can express the reliability of the conclusions. The graphic reconstruction is more sensitive, less susceptible of misinterpretation, and logically superior in that it supplies negative information coupled with the positive.

5. (*a*) In a specimen 7 days *post coitum,* both trophoblast and uterus had sharply localized anatomical factors that were not merely favorable but necessary for invasion. Trophoblast invaded only where it had an aggregate of syncytium or "knob." Uterine epithelium was invaded only where it had a capillary at its base. Contact between the two tissues was, of course, also necessary. (*b*) The localized promotion of invasion was not associated with a local increase in the number of hypo-epithelial vessels and could not be attributed to epithelial contours, to endometrial glands or secretions, or to any substance, including glycogen, stored in the epithelium or stroma. (*c*) No localized inhibitor of invasion was identified.

6. The sequential stages of the individual attachment cannot be learned directly from specimens fixed in a time sequence, because almost all stages coexist. However, various considerations suggest that the sequence is: contact, adhesion, penetration, and spread.

7. Contact is favored generally except in the depths of glands; glands are closed in the fresh state. Attachment was neither promoted nor inhibited near gland mouths in the 7-day-old specimen.

8. (*a*) Adhesion, in the 7-day-old specimen, occurred preferentially but not exclusively where abembryonic trophoblast touched uterine epithelium overlying a capillary. Sections of adhesions were centered over hypo-epithelial vessels with a median inaccuracy of 5.2 microns. (*b*) Most of the adhesion data represented lagging peripheral parts of attachments whose more deeply penetrating regions were in other sections. When also the related vessel was in another section for this reason, or because of epithelial obliquity, "parallax error" was introduced. (*c*) A few data represented adhesions of trophoblast not destined to invade, because no knob was present. (*d*) The remaining few adhesions that were truly beginning attachments may be considered very accurately aimed for hypo-epithelial vessels, if allowance is made for one case of parallax error.

9. (*a*) Penetration, in the 7-day-old specimen, occurred essentially only through uterine epithelium with a vessel at its base. Penetrations were directed toward such vessels with a median inaccuracy of 3.5 microns and a mean inaccuracy of 5.9 ± 1.7 microns, and the mean width of the penetrations (16.9 ± 1.9μ) was not significantly different from the mean extent of the related vessels in the plane of the base of the epithelium (17.9 ± 1.5μ). (*b*) Penetrations always reached the related vessel and thereby avoided the aberrations from epithelial obliquities which complicated the adhesion data. (*c*) Penetration occurred only where there was a trophoblast knob, but only about half of the knobs had attached by 7 days *post coitum.*

10. Certain aspects of the course and mechanism of invasion in the 7-day *post coitum* specimen may be interpreted with reasonable but unmeasured security. (*a*) Since the few attachments that had progressed to adhesion and no further were smaller than their contemporaries that had penetrated, adhesion probably precedes penetration in the individual attachment. (*b*) Since such adhesive beginning attachments not only precede penetration but are about as accurately aimed for vessels, the selection of sites for invasion may probably be attributed entirely to adhesion. (*c*) Since accessible epithelium with a vessel at its base defines a local site for chemical transfer as well as the typical site of adhesion, one may infer that adhesion is induced there by a reaction that attends chemical transfer. (*d*) Since penetrations occurred exclusively at such sites, penetration is probably also promoted chemically, and probably by the same reaction that induces adhesion. (*e*) Since most knobs are either unattached or all the way through the epithelium, adhesion and penetration are probably rapid and progressive rather than probing. Though invasion is not reversed in unfavorable locations, outlying regions of individual attachments do tend to lag behind the regions nearest a hypo-epithelial vessel.

11. A nonglandular role for endometrial convolutions was suggested in which they supply unattached knobs with newly accessible and moving sites for attachment.

12. (*a*) In the specimen of 8 days *post coitum,* as in the younger, invasions were restricted to knobs and were related to hypo-epithelial vessels. The mean extent of the vessels in the plane of the base of the epithelium was similar to that at 7 days, but the attachments were many times wider. (*b*) The spread of invasions was attributed to the broadening of the pathway of chemical transfer through uterine epithelium as intercellular membranes disappear between 7 and 8 days *post coitum.* (*c*) The mean width of complete penetrations was 71.2±1.4 microns. Hypo-epithelial vessels near such sites were 16.6 microns farther apart than vessels generally. Thus, the invading trophoblast may push aside the epithelium to that extent (or destroy some vessels), but it is accommodated principally by a loss of epithelium at the locus of invasion. (*d*) The mechanism of that local epithelial loss cannot be determined with certainty by histological inspection alone. Digestion may account for the ultimate destruction of epithelial cells that become enveloped by trophoblast after being trapped among several penetrating invasions, but it is unlikely that ingestion and digestion in the usual sense are the mechanisms primarily responsible for the initial penetration or even the subsequent spread of trophoblast through uterine epithelium. A hypothesis of differential dissociation was derived.

13. A physiological interpretation was offered which suggested the functional relations among the anatomical features examined and a few pertinent conclusions from other studies.

ACKNOWLEDGMENTS

The study reported was begun with support from T. L. Montgomery, Department of Obstetrics and Gynecology, Jefferson Medical College, in laboratory space provided by A. E. Rakoff of the same department. It was extended during tenure of a U.S.P.H.S. National Cancer Institute fellowship under W. U. Gardner, Anatomy Department, Yale University, and it was given its mathematical basis principally by F. Hutchinson, Biophysics Department, Yale University. M. Merrell, formerly of the Biostatistics Department, Johns Hopkins University, was also consulted. At the Department of Embryology, Carnegie Institution of Washington, the previously studied material and new material were analyzed by improved criteria, and the mapping was extended to include the entire 7-day material. The photography is the work of R. D. Grill, and the histological preparations (other than my own L-1, L-25, and L-29) were made by W. H. Duncan, both of Carnegie Institution. To all these people and institutions, and to others who have helped in less specific or direct ways, I express my very deep thanks.

LITERATURE CITED

Allen, W. M., and G. W. Corner. 1929. Physiology of the corpus luteum. III. Normal growth and implantation of embryos after very early ablation of the ovaries, under the influence of extracts of the corpus luteum. *Am. J. Physiol., 88,* 340–346.

Assheton, R. 1895. On the causes which lead to the attachment of the mammalian embryo to the walls of the uterus. *Quart. J. Microscop. Sci., 37,* 173–190.

Bouin, P., and P. Ancel. 1910. Recherches sur les fonctions du corps jaune gestatif. I. Sur le déterminisme de la preparation de l'utérus à la fixation de l'oeuf. *J. physiol. et pathol. gén., 12,* 1–16.

Böving, B. G. 1952. Rabbit trophoblast invades uterine epithelium overlying blood vessels (abstract). *Anat. Record, 112,* 12.

Böving, B. G. 1954. Blastocyst-uterine relationships. *Cold Spring Harbor Symposia Quant. Biol., 19,* 9–28.

Böving, B. G. 1955. Uterine epithelial cells guide trophoblast hemotropism (abstract). *Anat. Record, 121,* 426.

Böving, B. G. 1956. Rabbit blastocyst distribution. *Am. J. Anat., 98,* 403–434.

Böving, B. G. 1957. Rabbit egg coverings (abstract). *Anat. Record, 127,* 270.

Böving, B. C. 1959*a*. Implantation. *Ann. N. Y. Acad. Sci., 75,* 700–725.

Böving, B. G. 1959*b*. Endocrine influences on implantation. In *Recent Progress in the Endocrinology of Reproduction,* C. W. Lloyd, ed., pp. 205–226. Academic Press, New York, N. Y.

Böving, B. G. 1959*c*. The biology of trophoblast. *Ann. N. Y. Acad. Sci., 80,* 21–43.

Böving, B. G. 1960*a*. Invasion mechanisms in implantation (abstract). *Anat. Record, 136,* 168.

Böving, B. G. 1960*b*. L'interaction entre les mécanismes physiologiques intervenant dans l'implantation du blastocyste chez la lapine. Translated by J. Van Campenhout. In *Les fonctions de nidation utérine et leurs troubles,* pp. 103–124. Masson et Cie, Paris.

Chipman, W. 1902. Observations on the placenta of the rabbit, with special reference to the presence of glycogen, fat and iron. *Studies from the Royal Victoria Hospital, Montreal, 1,* 3–261.

Chipman, W. 1903. Same title and content. *Lab. Repts. Roy. Coll. Physicians, Edinburgh, 8,* 227–485.

Corner, G. W. 1928. Physiology of the corpus luteum. I. The effect of early ablation of the corpus luteum upon embryos and uterus. *Am. J. Physiol., 86,* 74–81.

Corner, G. W., and W. M. Allen. 1929. Physiology of the corpus luteum. II. Production of a special uterine reaction (progestational proliferation) by extracts of the corpus luteum. *Am. J. Physiol., 88,* 326–339.

Duval, M. 1892. Le placenta des rongeurs. (Extrait du *J. anat. et physiol.,* 1889–1891.) Ancienne Librarie Germer Baillière et Cie, Paris.

Eales, N. B. 1932. Abdominal pregnancy in animals, with an account of multiple ectopic gestation in a rabbit. *J. Anat., 67,* 108–117.

Fisher, R. A., and F. Yates. 1953. *Statistical Tables for Biological, Agricultural and Medical Research.* Hafner Publishing Co., New York, N. Y.

Hertig, A. T., and J. Rock. 1951. The implantation and early development of the human ovum. *Trans. Intern. 4th Am. Congr. Obstet. Gynecol., Am. J. Obstet. Gynecol., 61A,* 8–14.

Kuhn, H. W., and J. H. Weaver. 1935. *Elementary College Algebra.* The Macmillan Co., New York, N. Y.

Lutwak-Mann, C. 1954*a*. Some properties of the rabbit blastocyst. *J. Embryol. Exptl. Morphol., 2,* 1–13.

Lutwak-Mann, C. 1954*b*. The occurrence of carbonic anhydrase in the rabbit uterus. *J. Endocrinol., 11,* xi.

Lutwak-Mann, C. 1955. Carbonic anhydrase in the female reproductive tract. Occurrence, distribution and hormonal dependence. *J. Endocrinol., 13,* 26–38.

Lutwak-Mann, C., and C. E. Adams. 1956. Carbonic anhydrase in the female reproductive tract. II. Endometrial carbonic anhydrase as indicator of luteoid potency: correlation with progestational proliferation. *J. Endocrinol., 15,* 43–55.

Lutwak-Mann, C., and H. Laser. 1954. Bicarbonate content of the blastocyst fluid and carbonic anhydrase in the pregnant rabbit uterus. *Nature, 173,* 268–270.

Margenau, H., and G. M. Murphy. 1943. *The Mathematics of Physics and Chemistry.* D. Van Nostrand Co., Princeton, N. J.

Marshall, A. J. 1953. The unilateral endometrial reaction in the giant fruit-bat (*Pteropus giganteus* Brunnich). *J. Endocrinol., 9,* 42–44.

Nicholas, J. S. 1934. Experiments on developing rats. I. Limits of fetal regeneration; behavior of embryonic material in abnormal environments. *Anat. Record, 58,* 387–413.

Parry, H. J. 1950. The vascular structure of the extraplacental uterine mucosa of the rabbit. *J. Endocrinol., 7,* 86–99.

Schoenfeld, H. 1903. Contribution à l'étude de la fixation de l'oeuf des Mammifères dans la cavité utérine, et dans les premiers stades de la placentation. *Arch. Biol., Paris, 19,* 701–830.

Van der Horst, C. J., and J. Gillman. 1942. Pre-implantation phenomena in the uterus of *Elephantulus*. *S. African J. Med. Sci., 7,* 47–71.

Waterman, A. J. 1934. The differentiation of entire young rabbit embryos in omental grafts. *Am. J. Anat., 54,* 347–381.

Wimsatt, W. A. 1944. An analysis of implantation in the bat, Myotis lucifugus lucifugus. *Am. J. Anat., 74,* 355–411.

PLATES

PLATE 1

Fig. 2. A rabbit uterus, transversely sectioned, contains an implanting blastocyst. The mesometrium is upward, corresponding to its dorsal origin. Toward it, in typical orientation, is directed the embryonic pole of the blastocyst which is identifiable here by its three layers, variously separated by artifact. The opposite, or abembryonic, hemisphere of the blastocyst is essentially two-layered, and is attached by its outer, or trophoblastic, layer to the attenuated antimesometrial region, or "dome," of the uterus. Attachment occurs at a number of discrete points; they are the histological pointers on which the anatomical analysis depends and of which most of the subsequent illustrations are greatly magnified examples.

The orientation of the subsequent illustrations will be related to the orientation of this figure to the extent that antimesometrial subjects will be shown with endometrium below trophoblast or uterine lumen, and mesometrial subjects will be the reverse. 8 days *post coitum* (L-1-5/35-3) × 20.

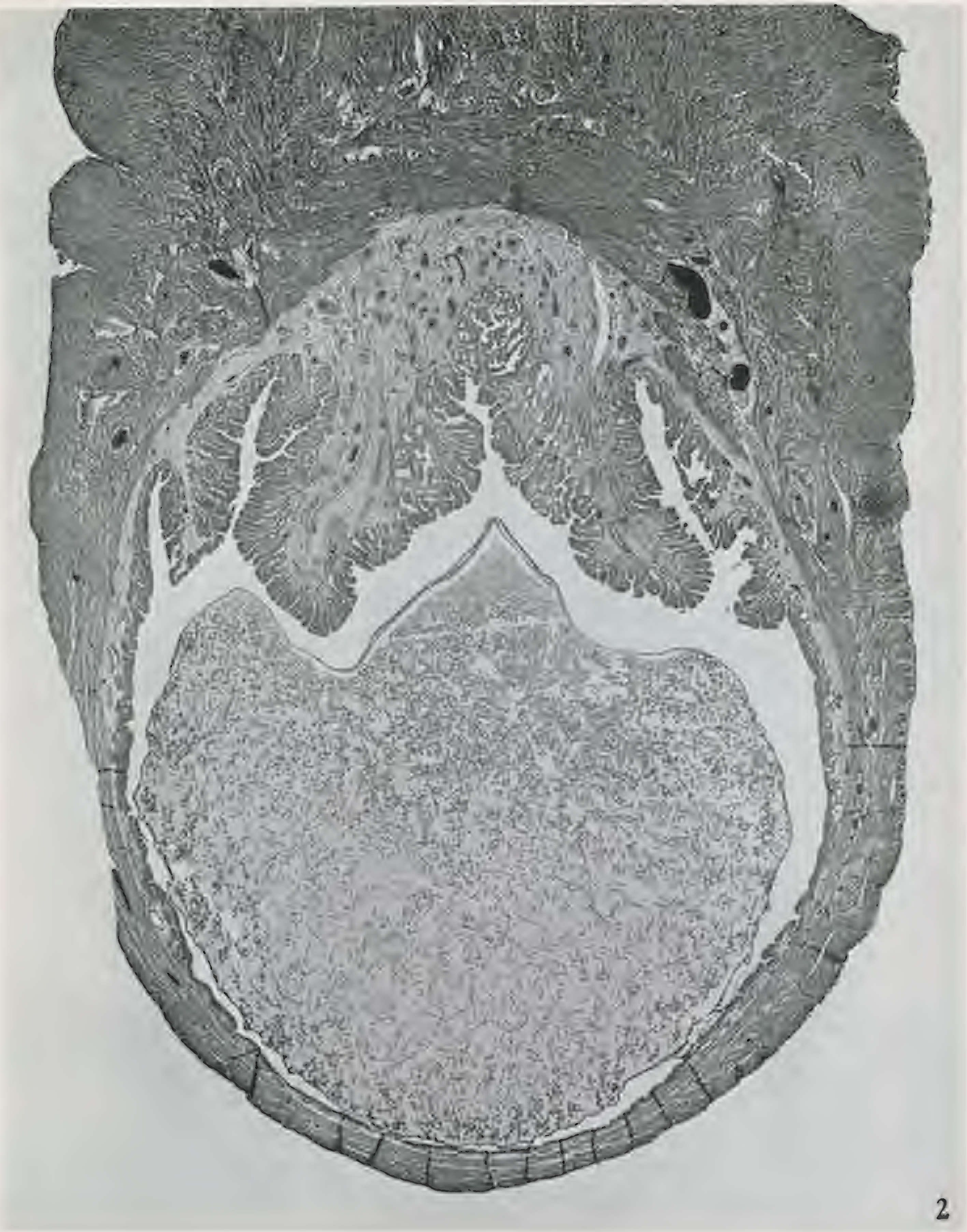

2

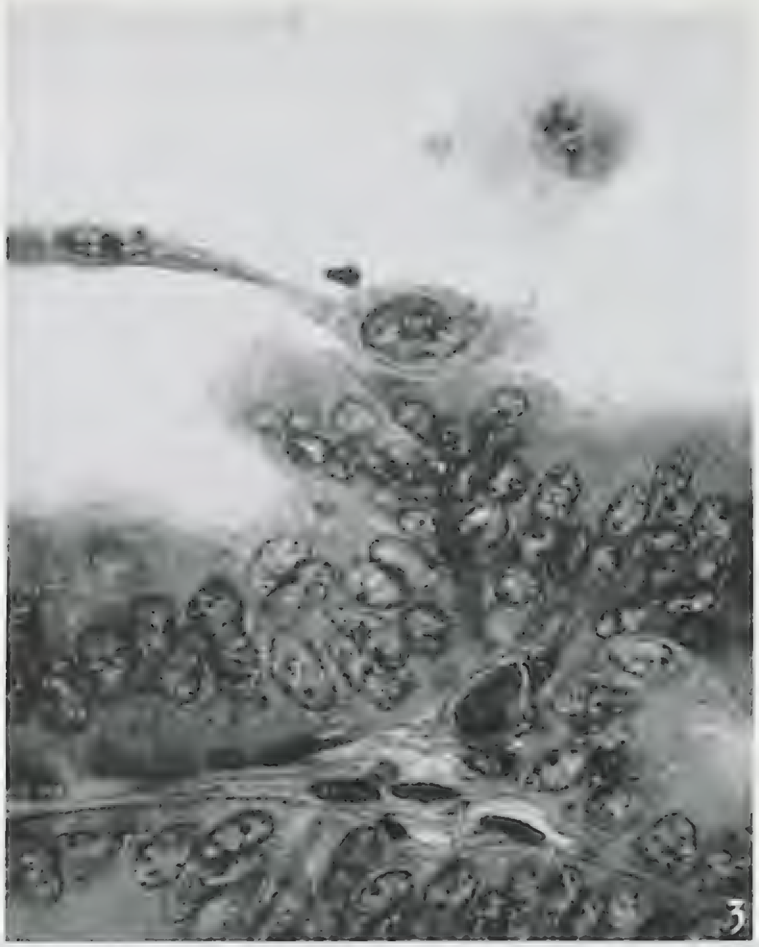

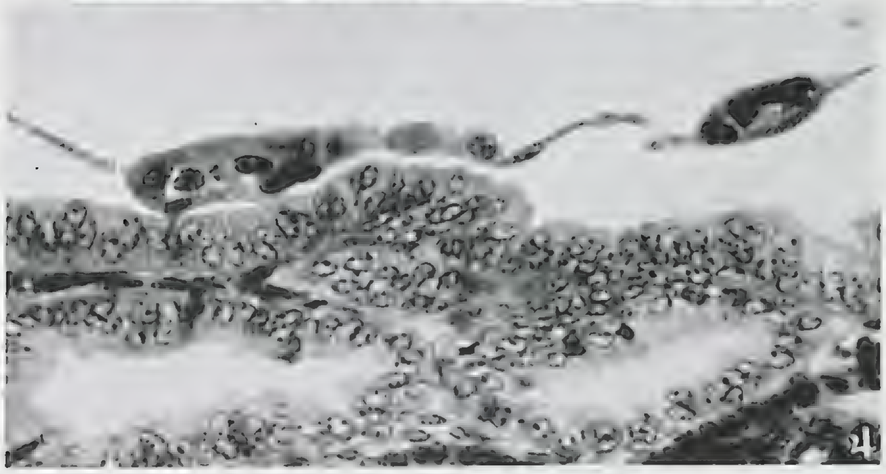

Fig. 3. A small knob is beginning to attach. It is joined to the epithelium by adhesion only. The adhesion extends through two sections and part of a third. In each section the adhesion is closely related to a hypo-epithelial vessel. The three corresponding measurements are the only data which unequivocally represent a knob's beginning attachment. The photograph shows the most central of the three sections. That and other three-dimensional relations may be visualized with the aid of the map (fig. 27, pls. 13, 14). A reference to the map is provided by the suffix to the identification number of this and other photographs of specimen L-25/slide 25; 3*b* refers to section 3, in map panel *b*. 7 days *post coitum* (L-25/25-3*b*) × 1000.

Fig. 4. A knob appears to be attached to the epithelium by two adhesions. Neither is the beginning attachment of the knob as a whole. The right attachment is in an early stage; it extends through two sections and has nowhere progressed beyond adhesion. The left adhesion, however, is adjoined by a complete penetration in the next section.

Invasion occurs only where there is a knob, but the occurrence of separate attachments smaller than the knob indicates the fact, the location, and the extent of local facilitation of invasion by the uterus. The attachments involve epithelium with a vessel at its base. (Retouching has been used to intensify pale areas.) 7 days *post coitum* (L-25/25-4*e*) × 400.

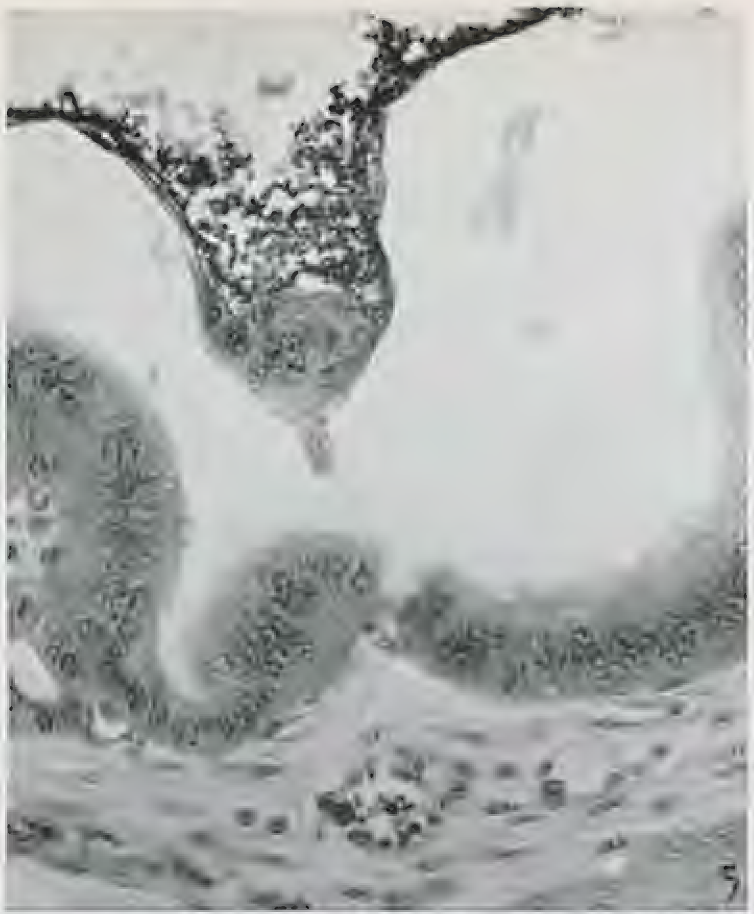

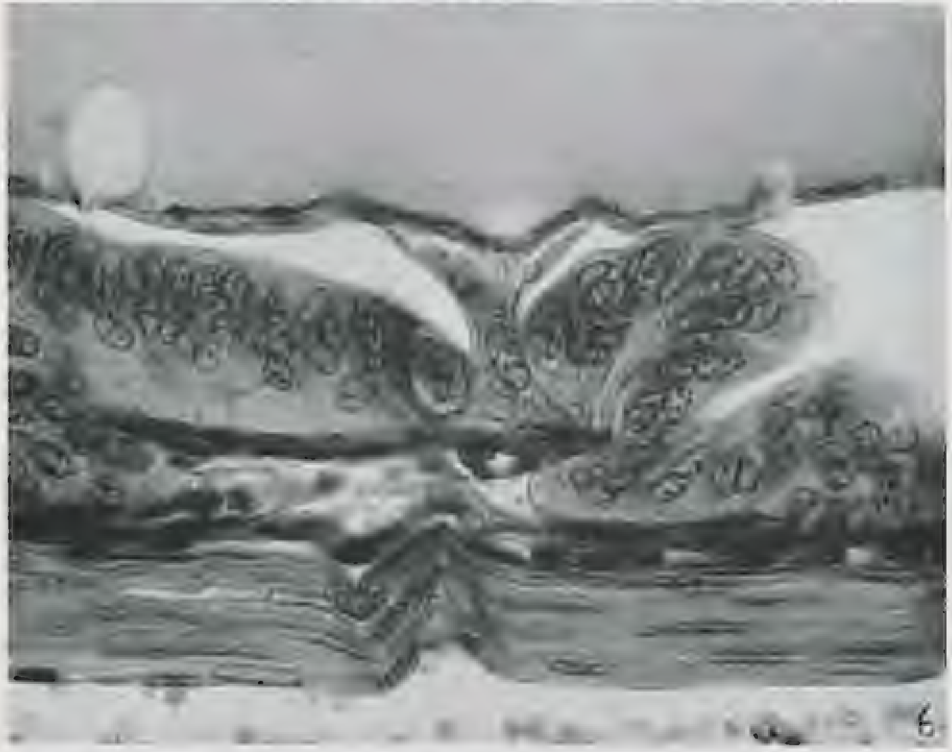

Fig. 5. An unusual artifact suggests that the trophoblast knob adhered to a uterine epithelial cell with a vessel at its base, and that the adhesive bond remained firm while the cohesive bonds between the epithelial cell and its neighbors did not. Since these relations occurred before the trophoblast penetrated the epithelium, they are consistent with the interpretation that local epithelial dissociation follows adhesion but precedes penetration. (Retouched.) 8 days *post coitum* (L-1-1/43-3) × 400.

Fig. 6. Trophoblast has completely penetrated uterine epithelium directly over a vessel. This narrow penetration was restricted to essentially a single section, and nowhere was there evidence that epithelium had been ingested. However, the epithelium had been altered for a short distance on both sides of the penetration. On the right was a small pocket of debris; on the left a group of pale epithelial cells had separated slightly from the stroma and had rounded up. Attention is directed to the intercellular membranes of the epithelium; they are better preserved than is usual for this age, and the unusual narrowness of the invasion correlates better with this state of the epithelium than with the gestation age. 8 days *post coitum* (L-29/12-11) × 600. (Figures 5 and 6 reproduced from Böving, Implantation, *Ann. N. Y. Acad. Sci., 75,* art. 2, 1959, by permission.)

PLATE 4

Figs. 7 and 8. The same field is shown in two planes of focus to point out that the fact and location of attachments are usually rather easily determined, but that errors may enter unless all planes of focus are studied carefully. The edge of an adhesion, at the center of figure 8, was missed in taking the measurements for the quantitative analysis, but during mapping it was "pointed out" by a portion of it in an adjacent section. The completeness of penetration by the left invasion is much more evident at one plane of focus than at another.

The section is adjacent to the one of figure 4 (pl. 2), and it is the two left attachments that correspond to the two adhesions in figure 4. Such considerations of three-dimensional relations allow the left attachment to be identified as a very small, and presumably recent, complete penetration, whereas the attachment whose edge is barely perceptible in this section has progressed nowhere more deeply than adhesion. On the other hand, the penetration on the right is the edge of a substantial penetration that extends through four complete sections plus part of this section and another (fig. 9). (Figure 8 was retouched to outline the pale adhesion.) 7 days *post coitum* (L-25/25-5*e*) × 1000.

Fig. 9. Two sections beyond the field shown in figures 7 and 8. The same knob has a well developed central penetration directly to a vessel and two partial penetrations at the sides. The left partial penetration is the peripheral part of the small and presumably recent penetration at the left of figure 8. The stout central penetration was represented in figure 8 by the dubiously classified complete penetration at the right. The partial penetration at the right of figure 9 was not represented in the preceding illustrations but continued through a number of subsequent sections as a complete penetration.

It is apparent from figures 7, 8, and 9 that a single knob not only may have a number of separate attachments but they may invade at slightly different times or rates. Between these attachments epithelial cells exhibit various degrees of separation from the stroma and from each other. 7 days *post coitum* (L-25/25-7*e*) × 1000.

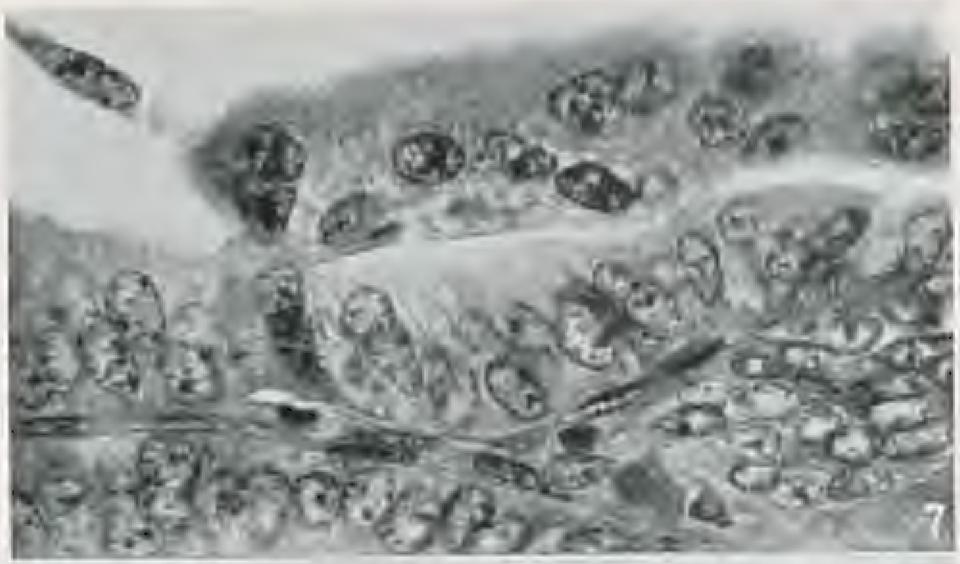
7

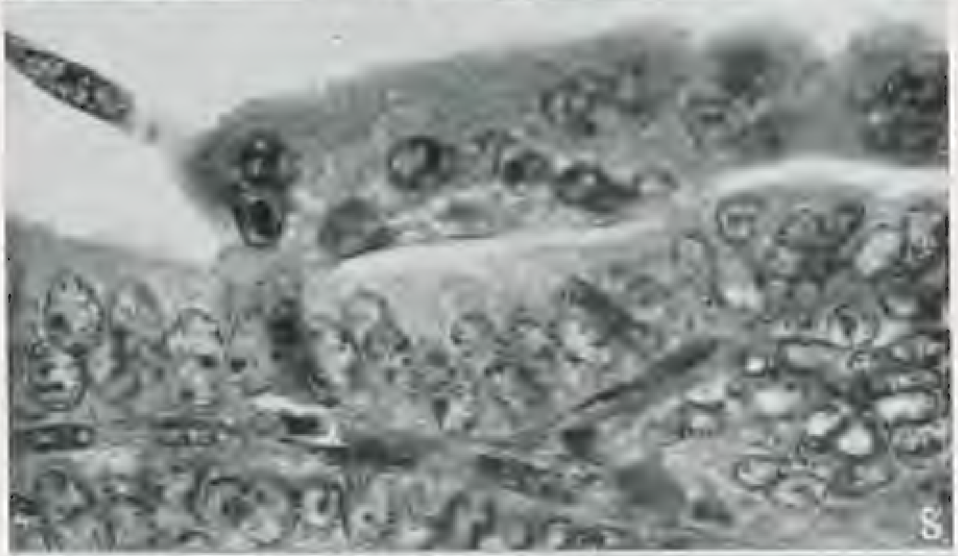
8

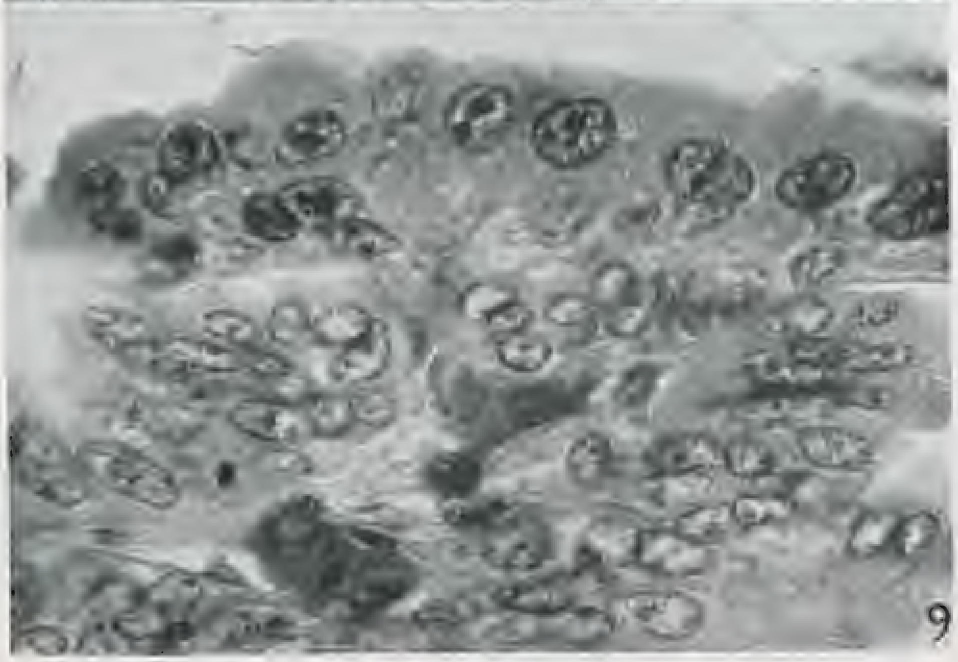
9

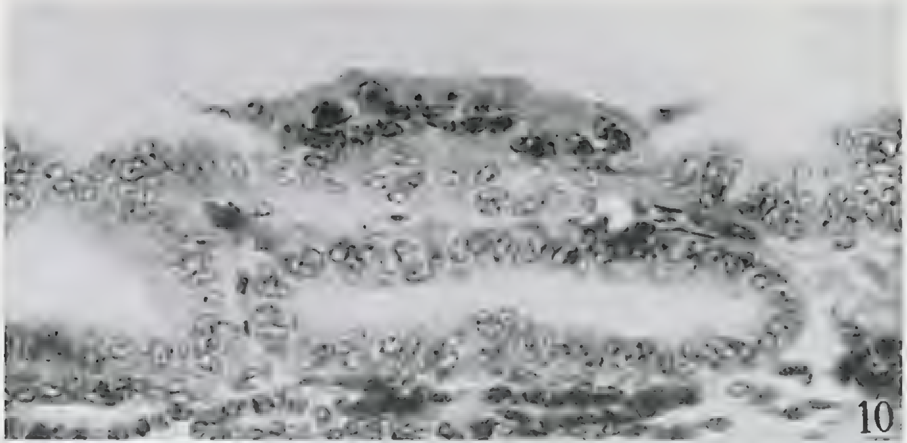

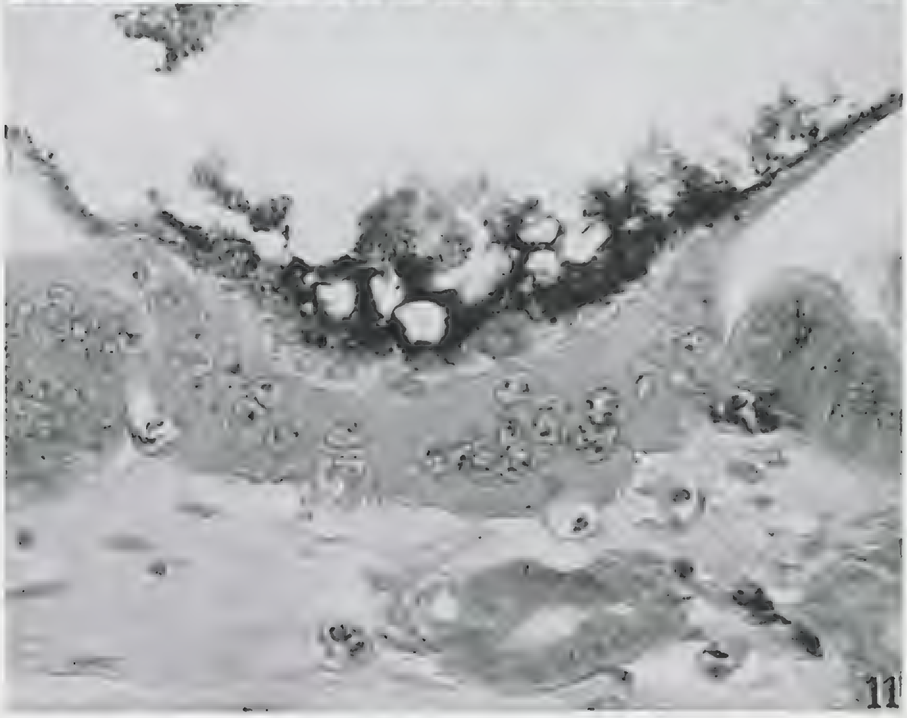

Fig. 10. Complete penetration of epithelium by trophoblast is becoming widespread, apparently through coalescence of previously isolated invasions. The knob still rides above the plane of the epithelium, but trophoblast has replaced epithelium throughout most of the region below the knob. Enveloped by the trophoblast that has invaded lie small clumps of epithelial cells, isolated epithelial cells (rounded and in abnormal orientations), and cellular debris, such as nuclei. Most of these inclusions are easily distinguished from the dark nuclei of the trophoblast. The epithelial cell at the extreme left of the invasion has separated slightly from its neighbor, but more remote epithelial cells are not obviously altered. Below the invasion is an altered vessel of which faint but consistent traces (sometimes no more than a "phagocytized" erythrocyte) are found in successive sections (fig. 27*f*, pl. 14). 7 days *post coitum* (L-25/25-2*f*) × 400.

Fig. 11. Invasion has spread, and the knob has come to rest in the plane of the epithelium. It overlies a number of vessels, and it is difficult to discern "aim" for individual vessels. There is, however, a tendency to envelop vessels, at least partially, and the vessel on the left has had part of its endothelium replaced by trophoblast. Whether that replacement may be attributed to differential dissociability is uncertain, for now there is evidence also of trophoblastic ingestion and digestion. An erythrocyte appears caught on a trophoblastic protrusion into the vessel mentioned. Slightly to the right of center, just above the lowest vessel, an erythrocyte is passing from the vessel to the trophoblast, and the adjacent trophoblast contains two erythrocytes and a number of small droplets. Whole epithelial cells are not seen, but some of the smaller nuclei may be remnants of them. The functioning of the yolk sac placenta is suggested by the greater abundance of proteinaceous material within the 8-day-old blastocysts than within the 7-day specimens. Intercellular membranes have disappeared from some parts of the epithelium. 8 days *post coitum* (L-1-5/35-3) × 400.

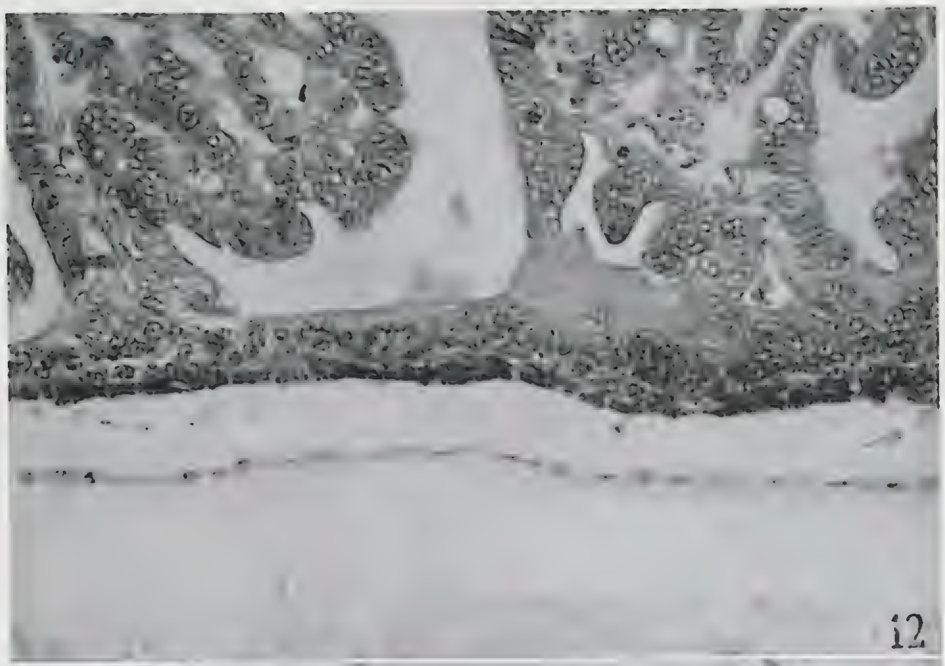

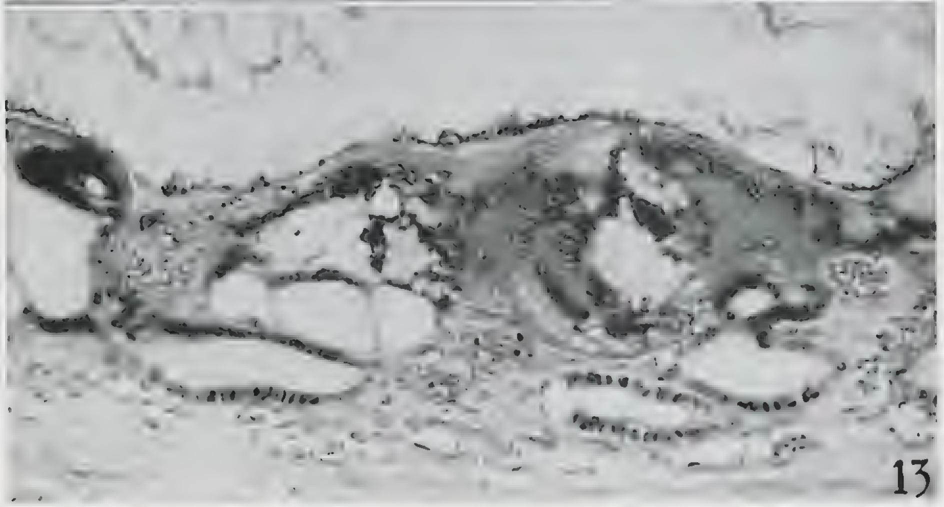

Fig. 12. Mesometrial invasion, initiating the definitive placenta, begins after most of the antimesometrial knobs have completed their penetration and spread. The mesometrial invasion proceeds on a broad front, from one continuous aggregate of trophoblastic syncytium rather than from separate knobs. Whether uterine placentation mechanisms also have differences in this hemisphere has not been thoroughly explored. 8 days and 20 hours *post coitum* (L-80-B/1-9) × 200.

Fig. 13. The yolk sac placenta may be considered completed when the epithelium is converted into a syncytium or symplasma and the trophoblast between knobs adheres to it generally. Toward the left, blood flows through spaces lined at least partly by trophoblast. Degeneration is also evident; the epithelial symplasma has become vacuolated. (In parts of the same specimen beyond those shown, necrotic epithelium has sloughed.) 8 days and 20 hours *post coitum* (L-80-B/1-6) × 200.

PLATE 7

Fig. 14. Significant amounts of glycogen appear first in the epithelium of deep regions of mesometrial glands. Not all glands have glycogen, but those that do are often in small groups. The glycogen is predominantly near the base of the epithelium. 6¾ days *post coitum* (L-309-C/2-10) × 200.

Fig. 15. Occasional granules of glycogen occur in the antimesometrial epithelium at the time of implantation. Of those that might be considered sufficiently superficial to be accessible to the trophoblast, two lie slightly more than a centimeter apart, at the right of the invasion. Perhaps half a dozen smaller ones, difficult to distinguish, are at the epithelial surface just to the left of the invasion. Only one granule is evident at the site of invasion, and it lies deep, between the two hypo-epithelial vessels that are directly below the knob. An association between invasion and glycogen is not evident. 6¾ days *post coitum* (L-309-C/2-10) × 400.

Fig. 16. At 8 days *post coitum,* as on the previous day, most glycogen is deep in mesometrial glands, but the amount is greater and much of it has passed to the distal part of the cells and even into the lumen of the glands. (L-322/2-10) × 200.

Fig. 17. Antimesometrially, glycogen is more abundant at 8 than at 6¾ or 7 days *post coitum.* It may appear as granules or as diffuse staining of the frothy epithelial symplasma. A depot of the second type is shown near the base of the epithelium toward the left. The attachment of the trophoblast knob to the right of the depot is considered inconsistent with invasion promotion by glycogen.

The syncytial structure of the epithelium is particularly evident. It may be observed that the knob was unable to penetrate such epithelium in spite of having widespread intimate contact with it through many successive sections and even indenting it in the section shown. The two syncytia are not confluent. A complete boundary may be distinguished by varying the plane of focus, but in the photograph it appears only in the right quarter of the knob. 8 days *post coitum* (L-313/3-20) × 400.

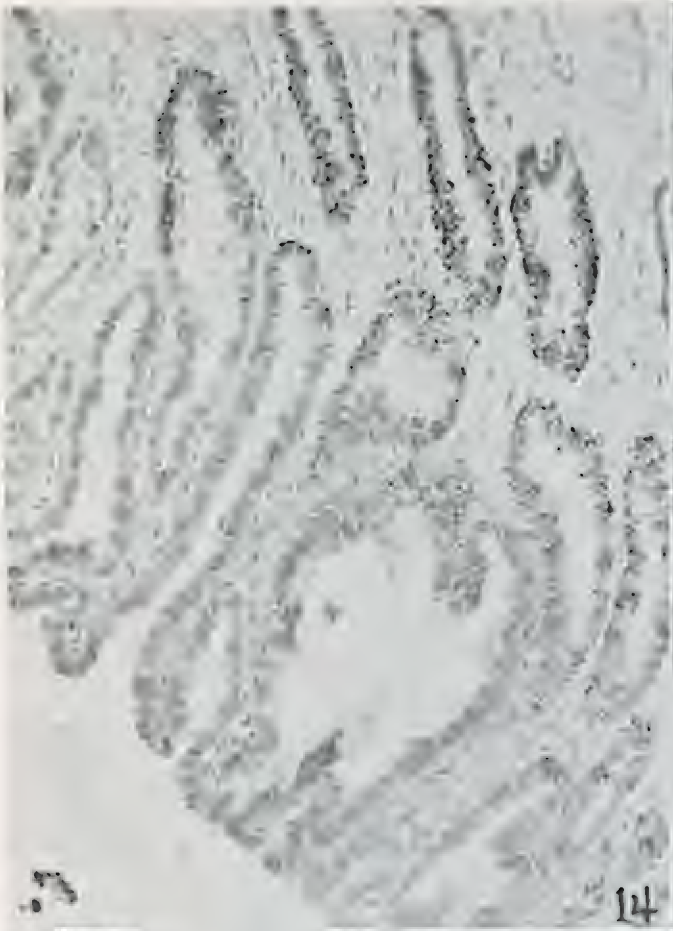
14

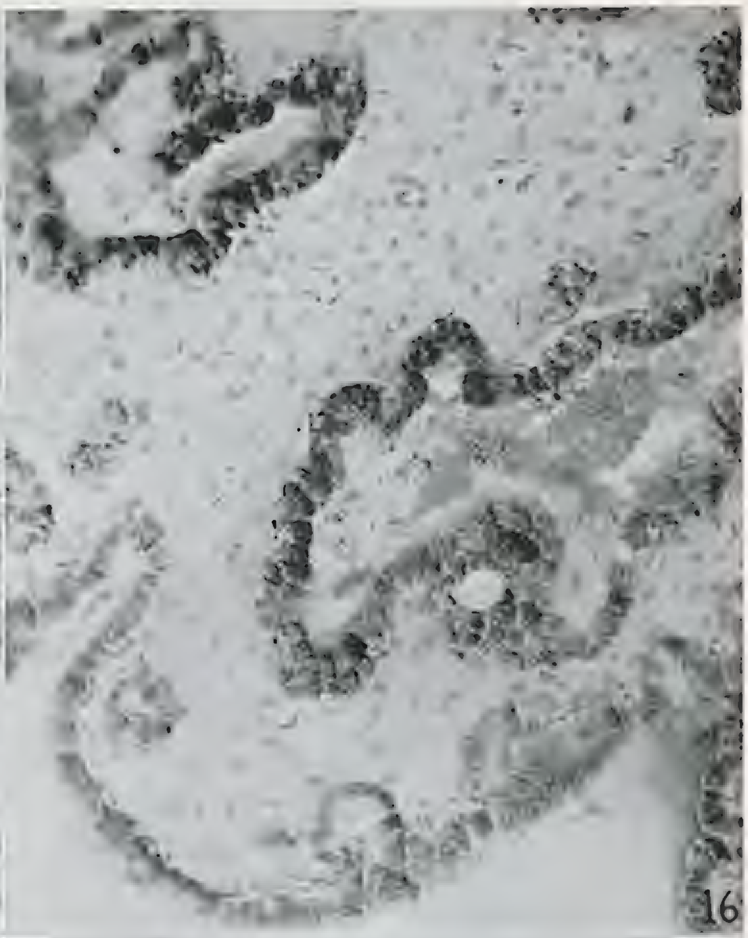
16

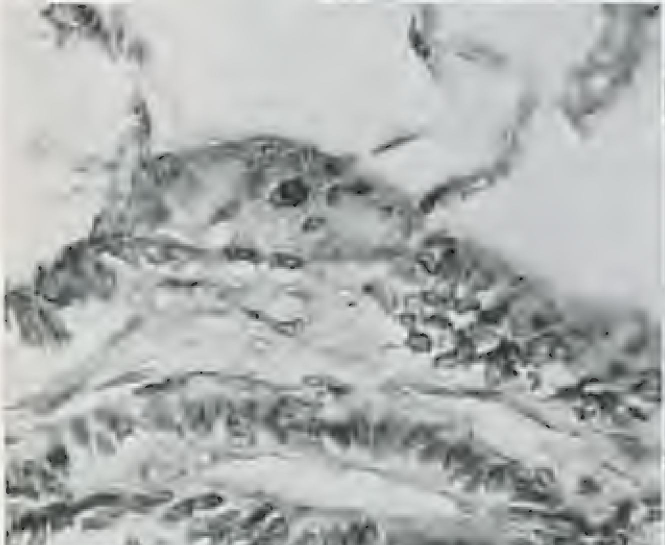
15

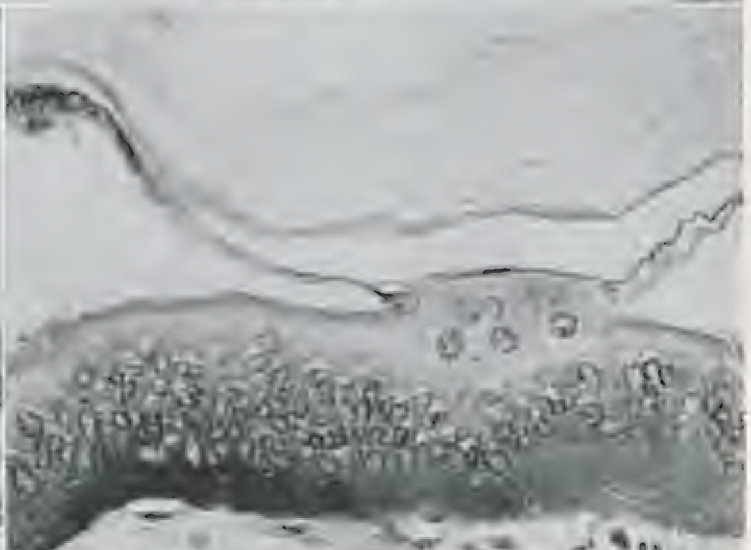
17

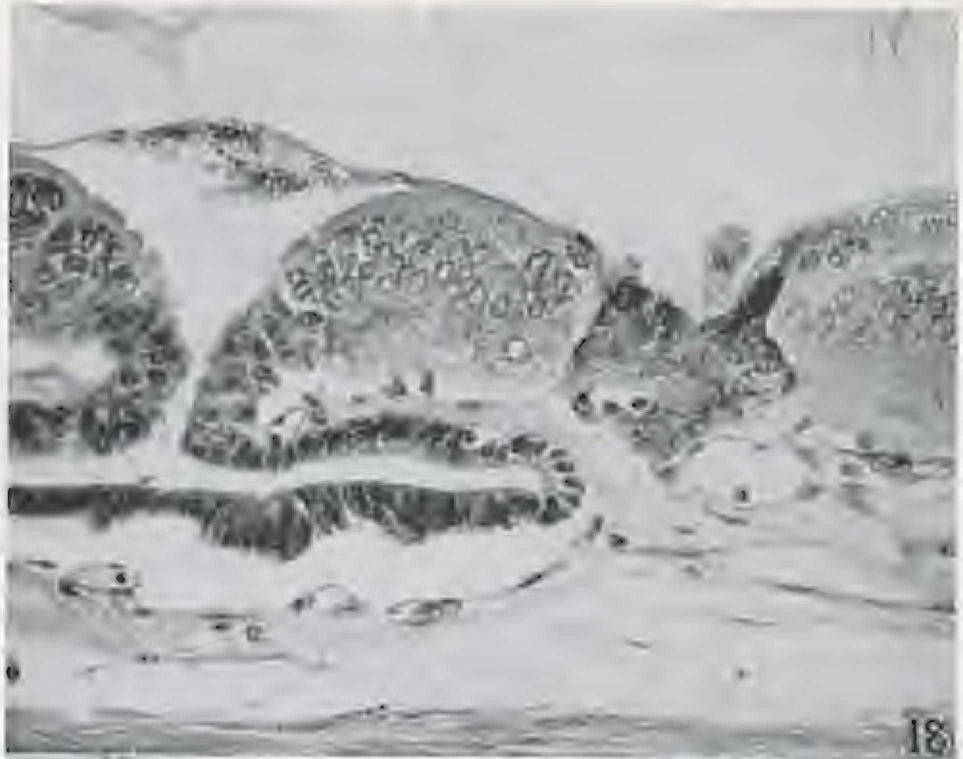

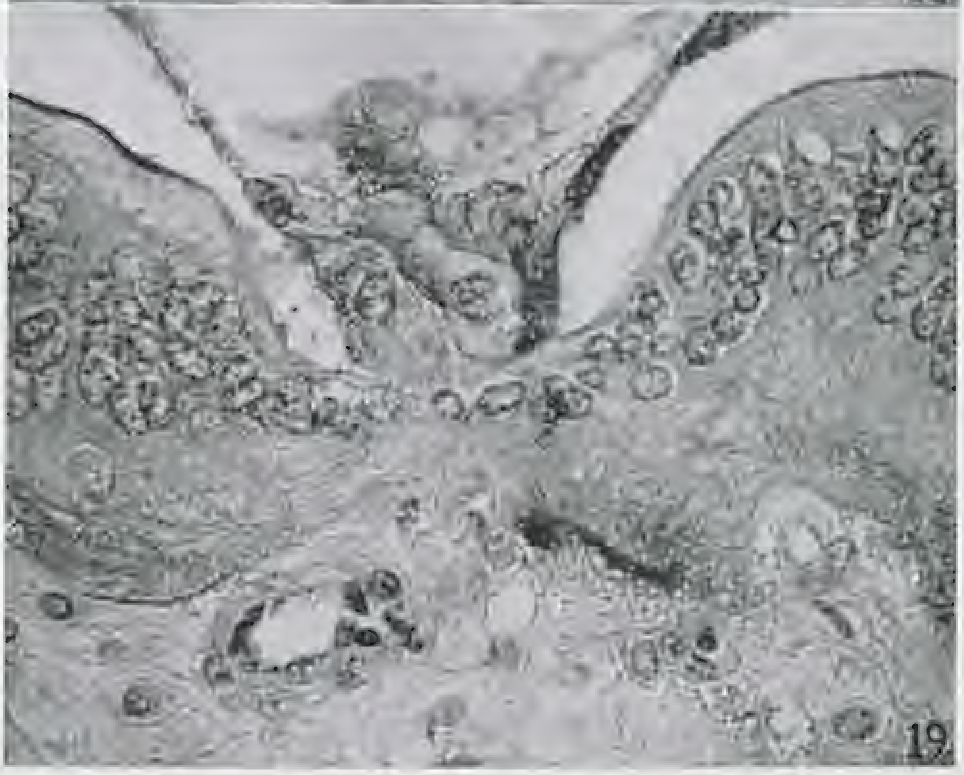

Fig. 18. A knob containing much glycogen has penetrated and spread through epithelium that has essentially no glycogen. The source of the glycogen is not apparent. A knob containing no glycogen, but with abundant glycogen (or mucopolysaccharide?) accessible to it, lies unattached in a gland opening. Trophoblast between the knobs adheres to the syncytial epithelium, and, at the right, above the epithelium, is some trophoblastic syncytium that adhered but did not invade. 8 days *post coitum* (L-313/3-9) × 400.

Fig. 19. A trophoblast knob attached at one side of an epithelial glycogen depot has a large amount of glycogen on the side nearest that depot. A train of granules in the epithelium joins the two accumulations. (The largest granules are somewhat obscured by lying next to an epithelial nucleus.) In spite of the evidence for glycogen passage from the epithelium to the trophoblast, the invasion, elsewhere a complete penetration, had not deviated or accelerated either toward or away from the glycogen depot. The transfer of incidental glycogen may be favored by invasion, but it is unlikely that invasion is favored by glycogen. 8 days *post coitum* (L-313/2-17) × 600.

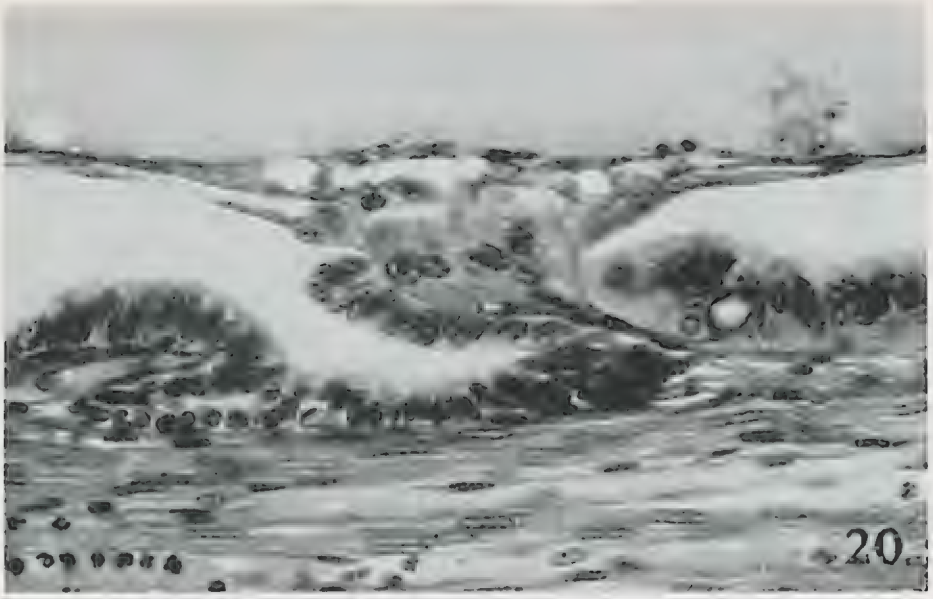

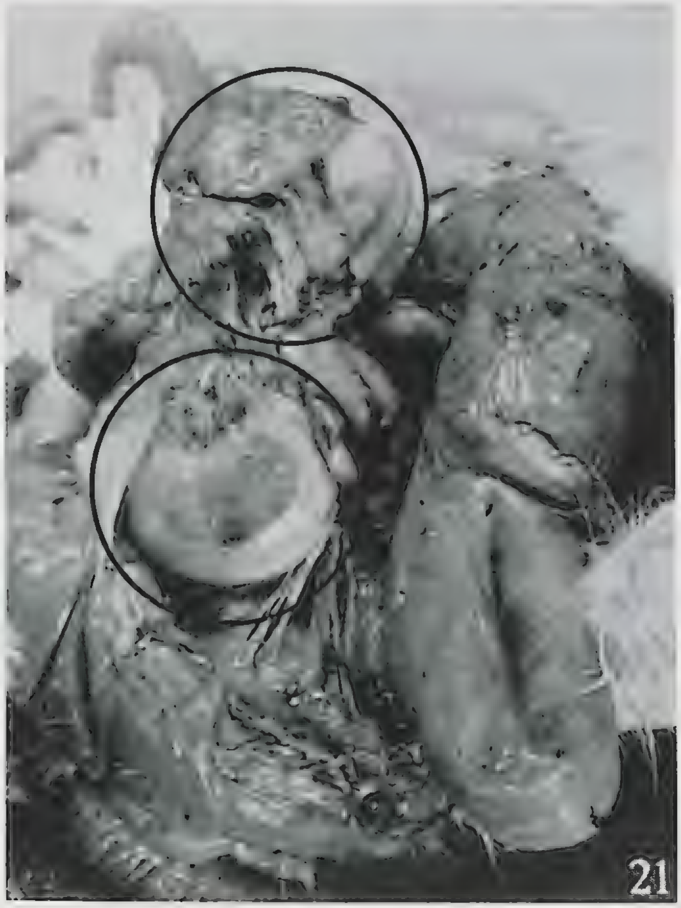

Fig. 20. A trophoblast knob has completely penetrated uterine epithelium and has come in contact with the base of epithelium of an underlying gland. There is no evidence that the trophoblast has attacked that epithelium, yet it must have been at the site for considerable time, because the knob has spread to almost its full extent. Intercellular membranes have disappeared from the epithelium for a short distance to the right of the invasion, but they remain in most of the rest of the epithelium shown, including that whose base is adjoined by trophoblast. The invasion is directly centered on a hypo-epithelial vessel. The vessel farthest left shows transition from stromal to hypo-epithelial. 8 days *post coitum* (L-29/12-11) × 400.

Fig. 21. The remains of two fetuses encased in fibrous tissue and bound with adhesions lie within the peritoneal cavity of a rabbit. They may represent either ectopic gestation or uterine rupture during labor. (L-334) × 2/3.

PLATE 10

Fig. 22. When silver nitrate solution is perfused through a uterus with implanting blastocysts, precipitates are formed within the blastocyst (outside the picture, owing to shrinkage) and within adjacent uterine epithelium that has a vessel at its base. Epithelium inaccessible to the blastocyst, such as that deep in glands, does not exhibit such a precipitate, nor typically does accessible epithelium which has no vessel at its base—even where a vessel dips away from the epithelium for only a very short distance (lower left of center). The vessels themselves are stained by silver, but they do not exhibit massive precipitates. The massive black precipitate is a reaction product of bicarbonate coming from the blastocyst and silver nitrate supplied by perfusion. Its restricted appearance in epithelial cells with a vessel at their base is considered to identify that anatomical complex as a privileged site for the transfer of chemical substances between the blastocyst and the maternal circulation. 7 days *post coitum* (L-143-D/2-1) × 300.

Fig. 23. As in figure 22, silver precipitates reveal the pathway of chemical exchange across uterine epithelium. The pathway is sharply bounded by intercellular membranes of the epithelium. Consequently, there is at the surface of the epithelium what may be considered a chemical image of the vessel at the base. The image has the same center as the vessel and the same lateral extent. In L-25/25, of the same gestation age, trophoblastic adhesions and complete penetrations were found also to be centered on hypo-epithelial vessels and to have the same lateral extent. Taken together, the observations indicate that trophoblastic adhesion and penetration are promoted at such sites of chemical exchange, very possibly by a reaction accompanying the transfer of bicarbonate from the blastocyst to the maternal circulation. 7 days *post coitum* (L-143-A/1-2) × 500. (From *Cold Spring Harbor Symposia Quant. Biol., 19,* 1954, with the permission of the publisher.)

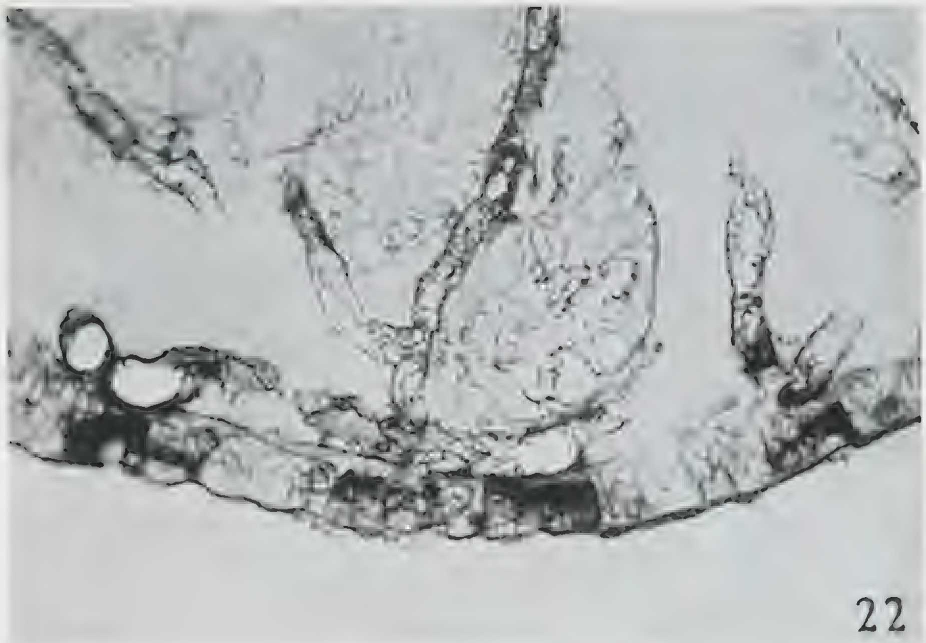

22

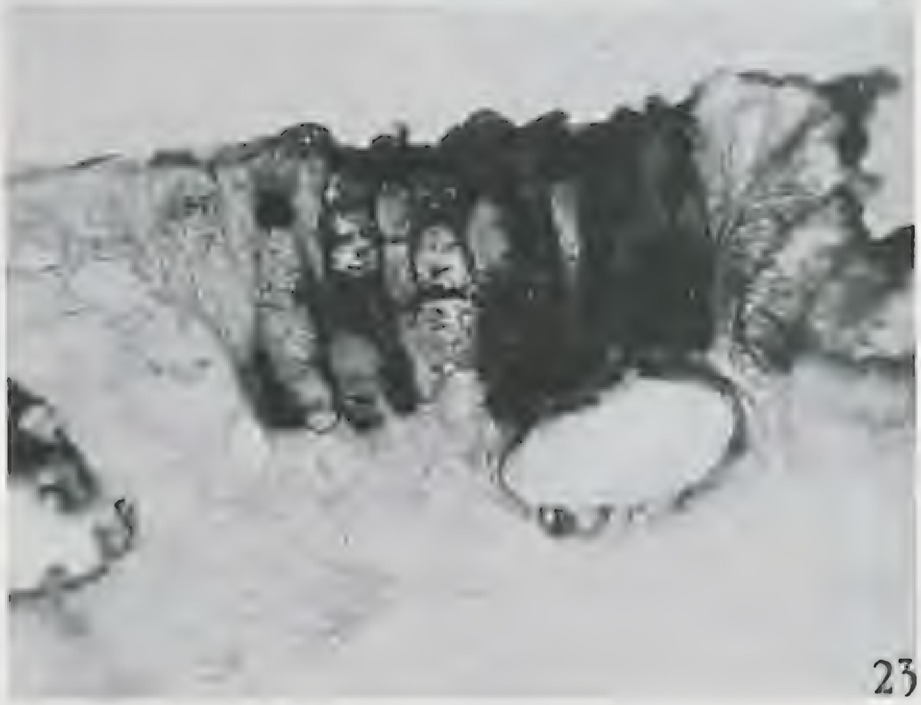

23

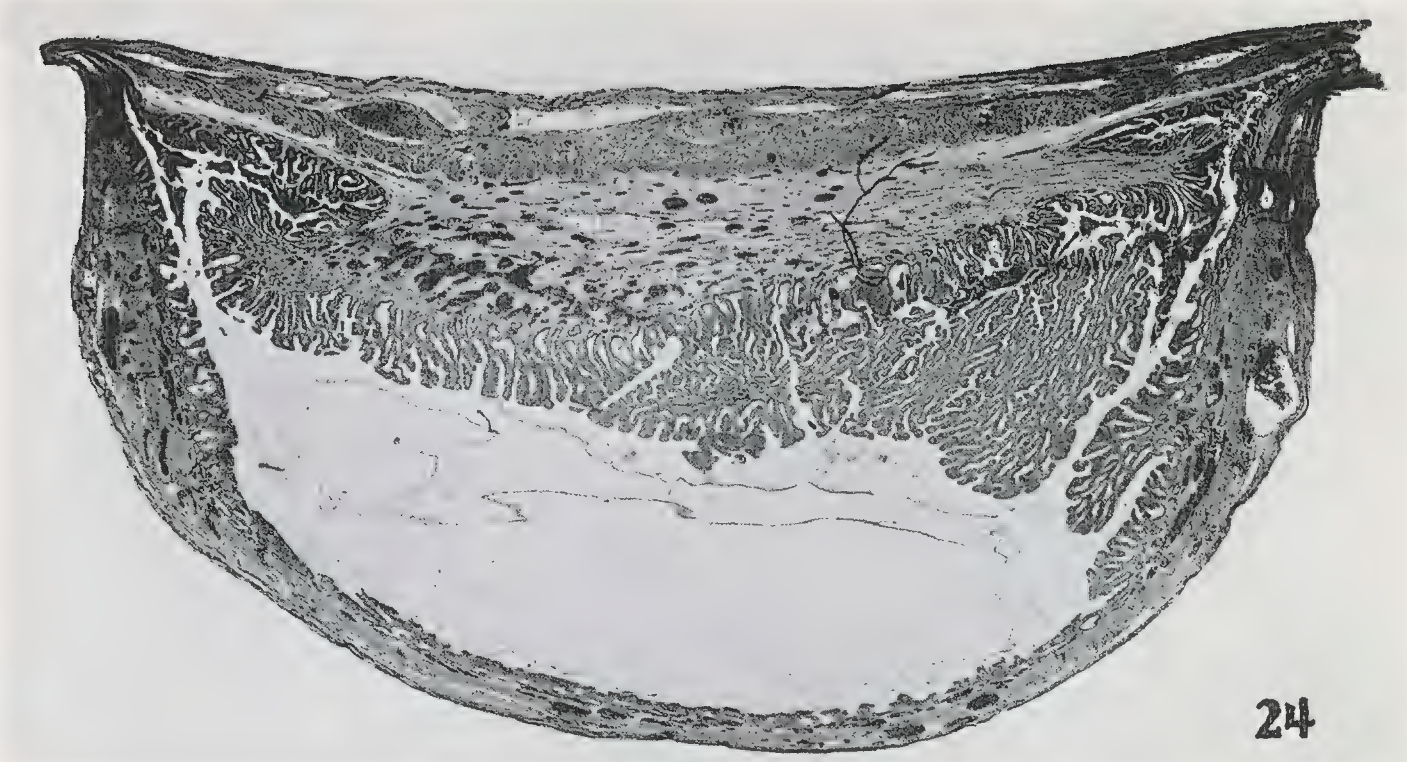

Figs. 24, 25, and 26. The analysis of the 7 days *post coitum* specimen, L-25, is illustrated. A segment of uterus containing a blastocyst was cut transversely into serial sections (fig. 26, top). The pertinent part of one of the sections (L-25/25-3) is shown in figure 24 at the same magnification (× 20) as figure 1. The antimesometrial region analyzed is at the bottom; it has 7 attachments, about a dozen "gland" openings, and about 50 accessible hypo-epithelial vessels. The extreme right region, panel *j*, from the adjacent section 2, is shown in figure 25 at the magnification (× 322.5) used for the quantitative analysis. The map was constructed at × 645 and was reduced one-half for publication. The lowest panel of figure 26, in comparison with the one just above and with figure 25, shows that vessels were recognized (red) only if they touched epithelium accessible to the trophoblast; vessels or parts of vessels were excluded if they did not touch epithelium or touched epithelium judged to be inaccessible because it was depressed more than 45° from the general plane of the epithelium near by. Not all recognized hypo-epithelial vessels contained erythrocytes.

The quantitative analysis examined the sections separately (fig. 26, bottom). The mean, *B*, was derived from the number of microns between vessels (60, 126, and 102), B_i from just the separations nearest invasions (the underlined 102), and I or I_c from invasion inaccuracy (5). The mean, *G*, represents the separation of gland openings (235), and I_g the inaccuracy of invasion toward them (75).

The analysis by mapping proceeded from the same material, but reassembled sections 2 through 13 to develop a view looking down on the long, narrow area of epithelium (black) (fig. 26, near top). The extreme right sector, *j*, is shown at higher magnification in the center of figure 26. The map (on the upper surface) was obtained by drawing projections from significant items in camera-lucida tracings of each section (of which one is shown on the front surface) to the space between the 2 of 13 lines that represented the thickness and position (shown by number) of that section. One such section-thickness line is drawn completely across the map; the rest are indicated by ticks at the edges, as at the left in figure 27*a* (pl. 13).

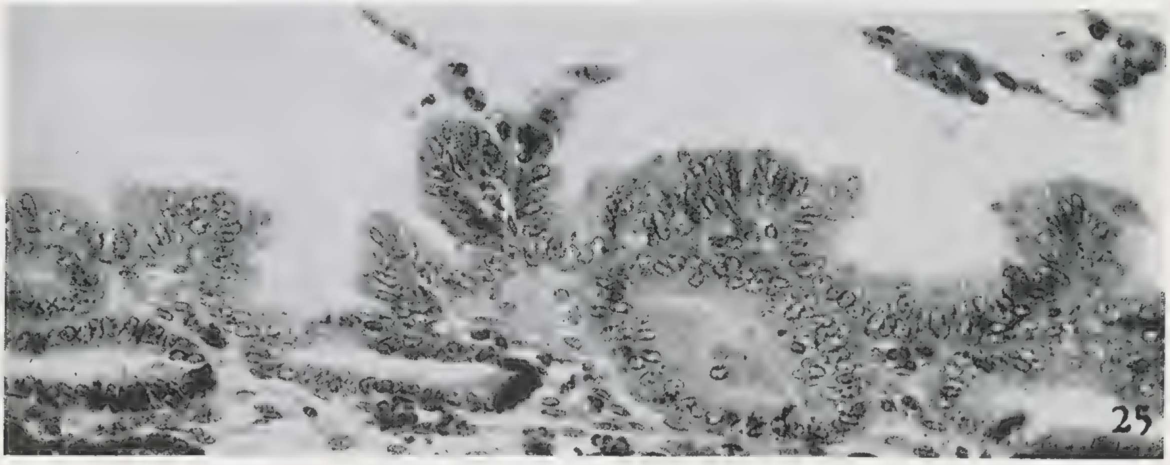

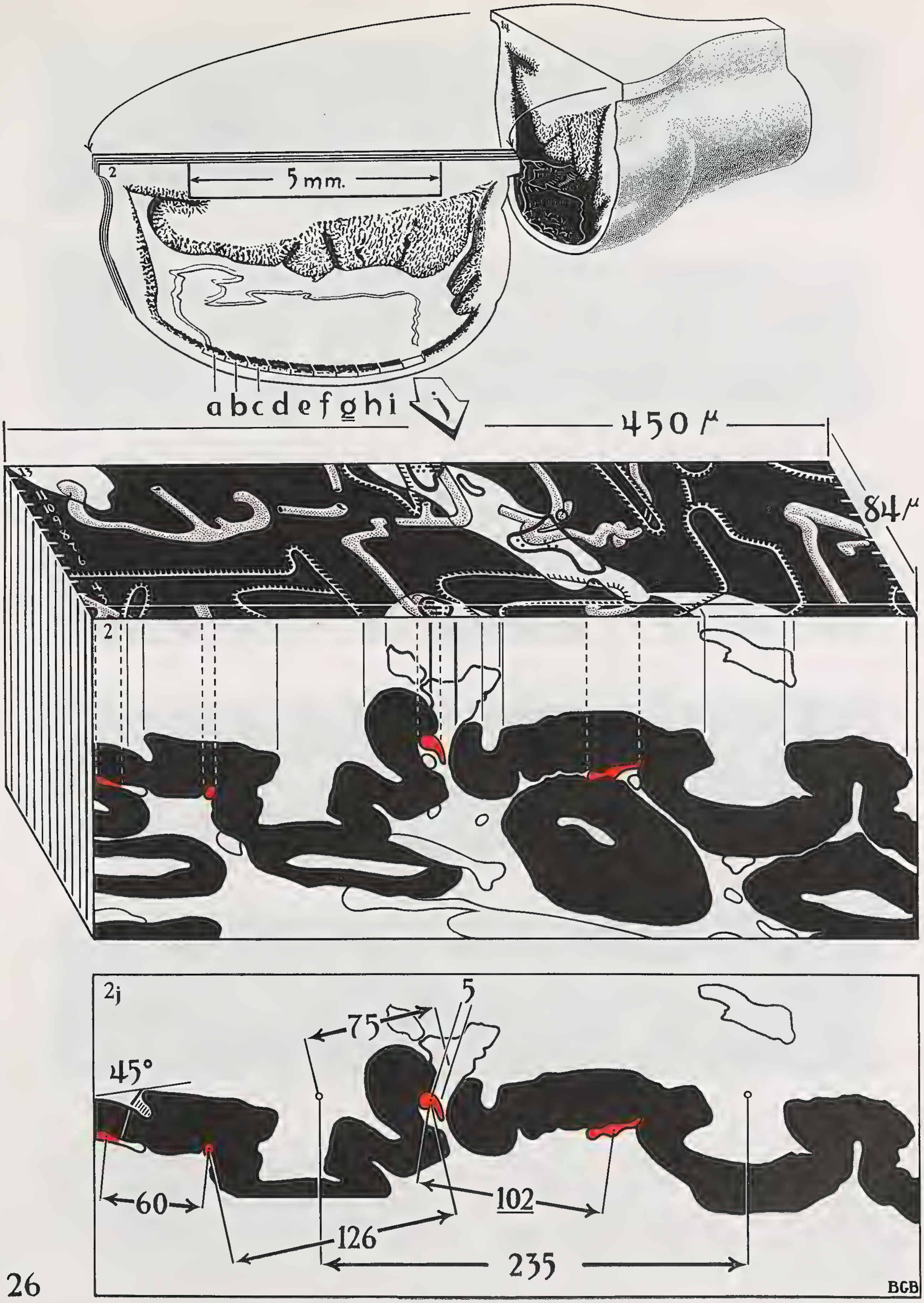
14
2
5 mm.
a b c d e f g h i j
450 μ
84 μ
13
11 10 9 8 7 6
4 3
2
2j
75
5
45°
60
102
126
235
BGB

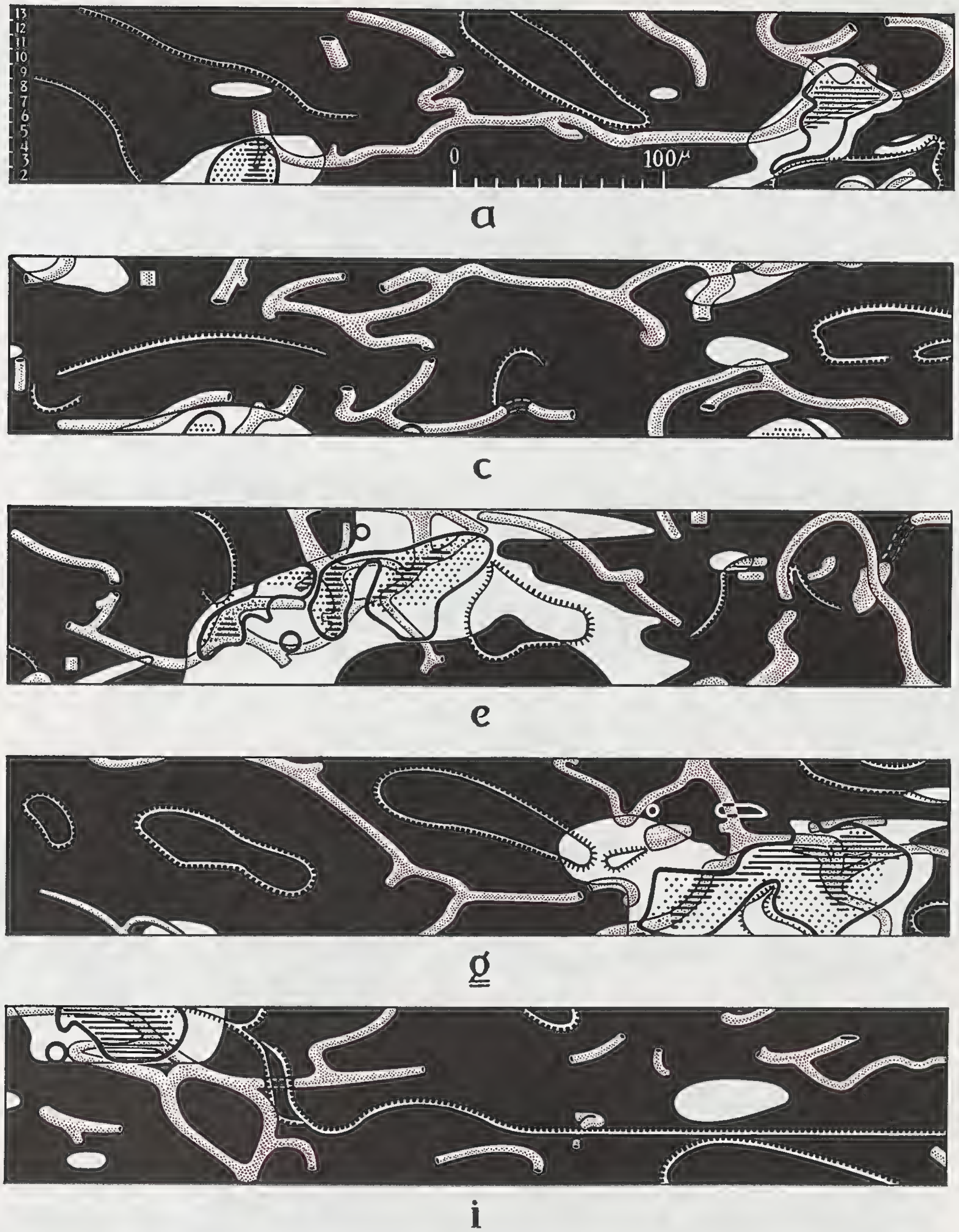

Fig. 27. The area of attachment between a rabbit blastocyst and antimesometrial endometrium is represented by a map of the consecutive sections numbered 2 through 13. The location of each section is shown by the scale at the left of panel *a*. The panels are consecutive alphabetically in the lengthwise direction. Endometrium is shown in black; gland openings and additional smaller depressions are indicated by toothed lines with the teeth pointing outward and upward at the edges of the depressions. Accessible hypo-epithelial vessels are stippled red; widely spaced red dots are used where the vessel was ill defined. Vessel ends

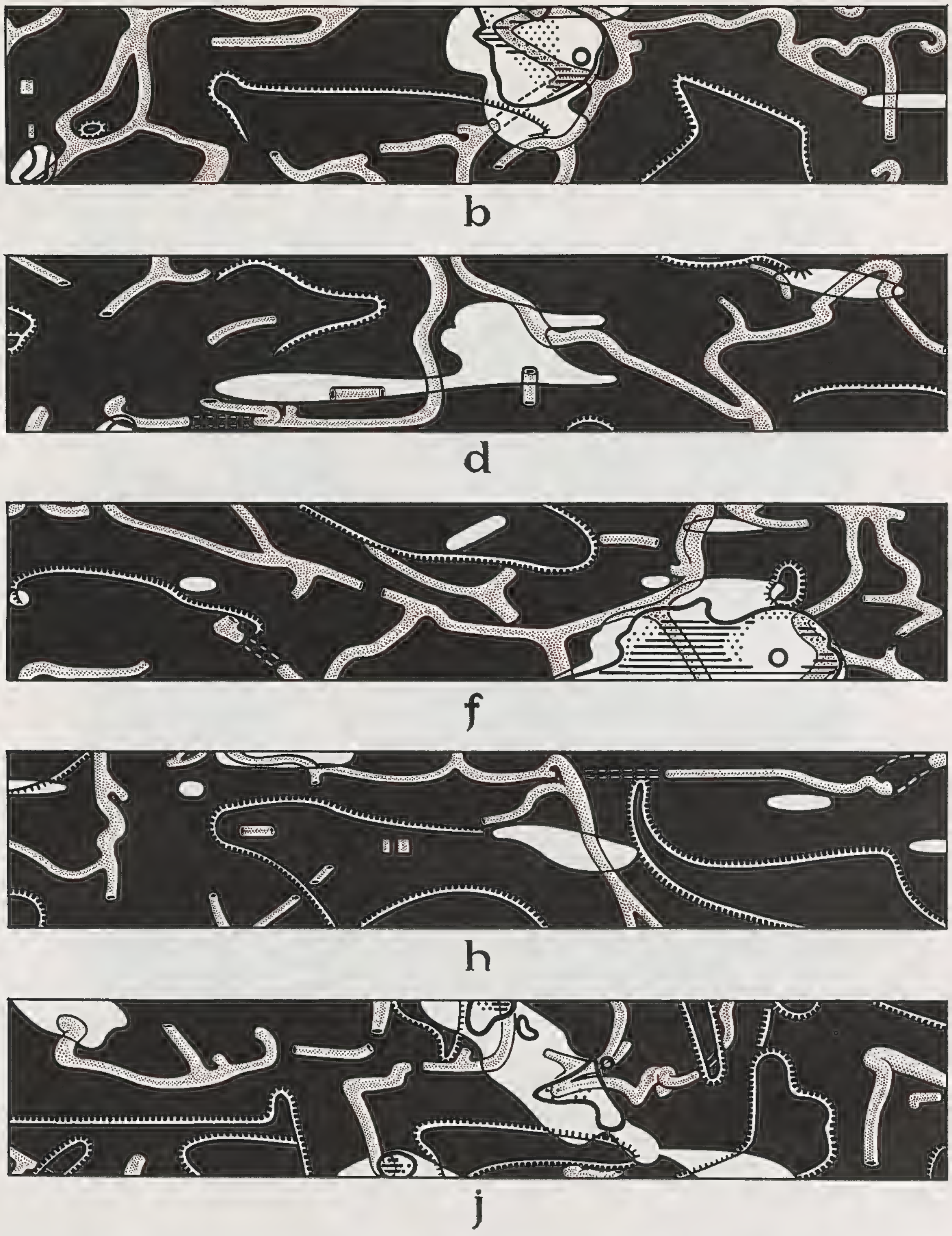

shaded to suggest a cut indicate points beyond which no trace of the vessel was found. Blunt ends of vessels indicate points at which the overlying epithelium becomes inaccessible or where the vessel loses contact with epithelium. Such deeper vessels were originally mapped, but they were omitted from the published map except for a few, shown by dashes, that were thought to contribute more understanding than confusion. Trophoblast knobs are white; areas of adhesion are bounded by a bold line; partial penetration is shown by black dots, and complete penetration by horizontal black lines. 7 days *post coitum* (L-25/25) × 322.5 (scale in panel *a*).

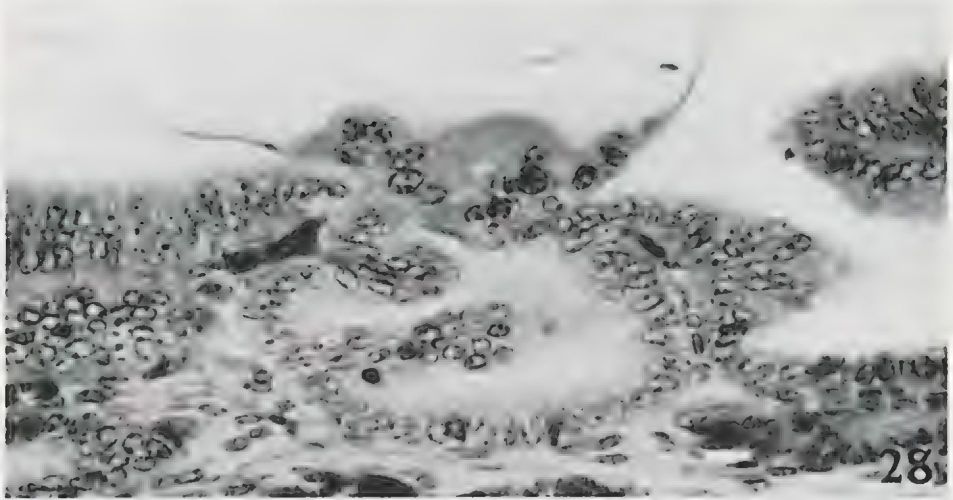

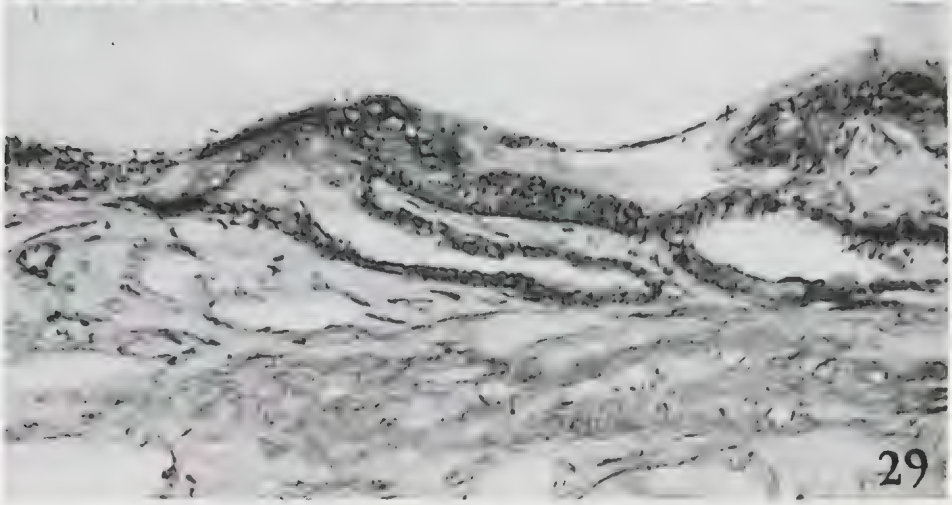

Fig. 28. A knob that bridges a gland opening is attached at each side to epithelium overlying a vessel. It has not penetrated deeply into the gland. The direction of invasion at the left is almost in the plane of the epithelium, but, since the trophoblast barely reached the vessel, the relationship is clear. The direction of invasion at the right is similar, and one might consider the relation to the vessel to be similar, but since the penetration was not complete, the map (fig. 27) can record only a rather remote relationship. 7 days *post coitum* (L-25/25-2g) × 400.

Fig. 29. A fresh frozen section shows that glands do not gape as widely as in fixed sections and that the blastocyst does not intrude into what gland openings there are. General apposition of trophoblast and epithelium is shown to be characteristic of the fresh and presumably also the living state.

CONTRIBUTIONS TO EMBRYOLOGY, NO. 255

ON THE CHICK SPLEEN: ORIGIN; PATTERNS OF NORMAL DEVELOPMENT AND THEIR EXPERIMENTAL MODIFICATION

L. E. DeLanney and J. D. Ebert
In Collaboration with C. M. Coffman and A. M. Mun
Department of Biology, Wabash College, and Department of Embryology,
Carnegie Institution of Washington

With fourteen plates and one text figure

CONTENTS

PAGE

INTRODUCTION 59
- I. Morphogenesis and Cytogenesis of the Chick Spleen 60
- II. The Impact of Implanted Fragments of Homologous Adult Spleen 60
  - A. On the Host's Spleen 60
  - B. On the Chorioallantoic Membrane 60
  - C. Graft-versus-Host and Host-versus-Graft Reactions 61
- III. Selective Uptake of Subcellular Fractions by the Chick Embryo and Modification of Patterns of Synthesis in the Host 61

ACKNOWLEDGMENTS 62

MATERIALS AND METHODS 62

I. MORPHOGENESIS AND CYTOGENESIS OF THE CHICK SPLEEN 62

II. THE IMPACT OF IMPLANTED FRAGMENTS OF HOMOLOGOUS ADULT SPLEEN 65
- Impact on the Host's Spleen 65
  - Recovery at Nine Days: Two Days Postimplantation 66
  - Recovery at Eleven Days: Four Days Postimplantation 66
  - Recovery at Twelve Days: Five Days Postimplantation 66
  - Recovery at Thirteen Days: Six Days Postimplantation 68
  - Recovery at Fifteen Days: Eight Days Postimplantation 68
  - Recovery at Seventeen and Eighteen Days: Eight to Eleven Days Postimplantation 68
- Impact on the Chorioallantoic Membrane 69
  - Recovery at Eight Days: One Day Postimplantation 69
  - Recovery at Nine Days: Two Days Postimplantation 69
  - Recovery at Eleven Days: Four Days Postimplantation 70
  - Recovery at Twelve Days: Five Days Postimplantation 70
  - Recovery at Thirteen Days: Six Days Postimplantation 71
  - Recovery at Fifteen Days: Eight Days Postimplantation 71
  - Recovery at Seventeen and Eighteen Days: Ten and Eleven Days Postimplantation 72
- Graft-versus-Host and Host-versus-Graft Reactions 72
  - Manifestations in the Host's Spleen 72
  - Manifestations at the Site of Implantation 73
  - Manifestations at Other Sites 73
  - Second- and Third-Set Phenomena 73

III. SELECTIVE UPTAKE OF SUBCELLULAR FRACTIONS BY THE CHICK EMBRYO AND MODIFICATION OF PATTERNS OF SYNTHESIS IN THE HOST 74

LITERATURE CITED 81

APPENDIX 83

ON THE CHICK SPLEEN: ORIGIN; PATTERNS OF NORMAL DEVELOPMENT AND THEIR EXPERIMENTAL MODIFICATION

INTRODUCTION

"Science is a search for truth and its pattern is that of a mountain rather than of a tree. At times it may seem that research spreads out like growing branches which are separating ever further from one another; but it is truer to speak of explorers on different ridges, of exciting meetings followed by mapping of intervening areas" (Uttley, 1959). Our objective is to map in detail one such intervening area, the "ridges" being two of the more provocative ideas in the field of developmental biology. Both these ideas spring from studies of the impact on the chick embryo of grafts of immunologically competent tissues of adult chickens.

We shall consider the idea that not only may such a graft react against its host (Dempster, 1951, 1953; Simonsen, 1953, 1957; Ebert and DeLanney, in Ebert, 1957; DeLanney, 1958; Ebert and DeLanney, 1960; Billingham, 1959) but also the host embryo may mount an incomplete reaction against the graft. The spleen of an embryo bearing a graft containing immunologically competent cells may serve as the principal "battleground" in a competition between donor and host cells, and, depending on several factors to be discussed, the outcome may be in either direction: either the graft-versus-host or the host-versus-graft reaction predominating.

Such reactions are intriguing; yet we shall present evidence demonstrating that the response of the embryo and its membranes cannot be explained fully on the basis of these immune mechanisms. We offer, as a working hypothesis, the idea that macromolecular or particulate biosynthetic units of the graft are incorporated by the host; this phenomenon of epigenetic recombination, we believe, differs significantly from the building-block hypothesis (Ebert, 1954) and from other hypotheses of the regulation of differentiation and growth of a cell strain by a balance of cell-type-specific molecules (Lenicque, 1959; Paschkis, 1958; Polezhaev, Akhabadze, Sakharova, and Mantieva, 1959; Rose, 1958; Weiss, 1947, 1955; Weiss and Kavanau, 1957).

We shall deal largely with research of the past decade, yet the basic problems to be considered are not new, having been formulated, in different terms, some forty years ago. They hark back to Danchakoff (1916, 1918), Murphy (1916), and Willier (1924), who demonstrated that the transplantation of a fragment of adult chicken spleen to the chorioallantoic membrane of a chick embryo is followed by a dramatic splenomegaly in the recipient. These pioneering works are, in fact, noteworthy accomplishments, but it is difficult to assess the extent to which they have contributed to the development of current thinking. In them are embodied a number of astute observations and provocative conjectures; indeed, an historical study of the development of the problem might itself prove rewarding. It is not our intent, however, to trace in detail the antecedents of our work, which have been treated fully elsewhere (Ebert, 1955, 1957, 1958, 1959*a*; Ebert and DeLanney, 1960). At this time, only a brief résumé of the principal findings will be given, to provide perspective for a discussion of the new directions that the research has taken.

We shall attempt in these pages to answer the question whether experiments based on the administration to embryos of constituents of adult tissues, in the form of grafts, cell suspensions, homogenates, or particulate fractions, have fulfilled their projected role in evaluating the hypothesis of selective chemical coordination among cells of identical type by direct exchange of type-specific compounds, or whether the principal rewards have been by-products, albeit significant ones, in elucidating the graft-versus-host reaction and in revealing the extent to which the chick embryo is capable of responding to an antigenic stimulus.

In approaching this question it is necessary to consider first the specificity of the reaction. It should be made clear that the introductory statement that transplantation of homologous adult spleen to the coelom or extraembryonic membranes of the chick embryo evokes an increase in the size of the host's spleen is no longer adequate. It must be said, first, that a fragment of any homologous tissue containing immunologically competent cells is capable of producing some, if not all, of the reactions ascribed initially to spleen. In the past we have used the expression "quantitatively organ-specific" to describe the reaction, for Ebert (1951 *et seq.*) found at least three tissues to be effective, spleen, thymus, and liver, the degree of effectiveness decreasing in that order. Evidence has been advanced of the ability of grafts of small intestine (Van Alten and Fennell, 1959) and skin (Billingham and Silvers, 1959) to affect the host's spleen. Each of these organs may contain immunologically competent cells; hence it appears more consistent to state that the reaction is functionally (or tissue, in the broad sense) specific, leaving open the possibility that we may be able eventually to define the cell specificity of the reaction. Evidence has been advanced (Terasaki, 1959) indicating that splenomegaly resulting from injection into embryos of suspensions of blood cells taken from adult chickens may be attributed to lymphocytes; suspensions of monocytes and thymocytes were found to be ineffective.

What is the specificity with respect to the *response?* Here we find fewer data, fewer detailed descriptions, and clearly less agreement. The evidence to be presented demonstrates that in the chick spleen the initial response is increased myelogenesis, that response being followed frequently by the destruction of the host's spleen; among the effects on other tissues of the host is widespread breakdown of the vascular bed. The thymus also is affected, but whether the destructive phase is preceded by a proliferative phase has not been established.

We may treat briefly the question of class- and species-specificity. In his analysis of the graft-versus-host reaction in the chick, Simonsen (1957) found that, in contrast to the ability of adult chicken leucocytes to cause destruction of the host embryo's spleen, leucocytes of two other avian species, pigeon and turkey, did not cause splenic damage in the chick. Although this observation is difficult to reconcile with the graft-versus-host hypothesis, there is ample precedent for it, in addition to partial verification from later studies. For example, Ebert (1951 *et seq.*) pointed out that grafts of mouse spleen had no effect on the spleens of chick-embryo recipients; transplanted duck spleen was less effective than homologous spleen. Mun, Kosin, and Sato (1959) have implanted fragments of turkey, pheasant, rat, and guinea pig spleen on the chick chorioallantois. The mammalian spleens were completely ineffective; the turkey and pheasant spleens were only slightly effective in producing splenomegaly.

As Chargaff (1945) put it (cf. Ebert, 1952), in its development a scientific problem passes through four periods: formulation, oversimplification, "anarchy," and solution, or partial solution, for solution inevitably leads to a restatement of the problem and the cycle is resumed. When a problem has passed through several such cycles, as have the problems under consideration, it is possible to begin an analysis by entering one of the cycles at any point, taking up the findings chronologically. We have elected to follow another course, proceeding from descriptive to experimental studies, attempting, as far as possible, to synthesize our own findings with those of others. The specific objectives of the research are stated in the following *outline* under three principal headings:

I. *Morphogenesis and Cytogenesis of the Chick Spleen*

Danchakoff (1916) outlined the sequence of events that occur in the normal development of the spleen, but her generalizations are too sweeping to permit accurate comparisons of normal and experimental spleens with reference to specific stages of development. Such comparisons are the foundation stones of our study. Sandreuter (1951) has presented a detailed account of hematopoiesis in the chicken and starling, in which she compares blood-cell formation in bone marrow, liver, and spleen. Her important study, focused as it is on cytogenesis, fails to provide the information necessary for an understanding of morphogenesis of the spleen. It became necessary, therefore, to attempt to integrate splenic morphogenesis with the sequence of changes in cell populations. Thus we shall present normal stages of splenogenesis in the chick with reference to the Hamburger-Hamilton (1951) stages of normal development.

II. *The Impact of Implanted Fragments of Homologous Adult Spleen*

A. *On the host's spleen.* In analyzing the effects of chorioallantoic grafts of adult chicken tissues on the differentiation and growth of the homologous organs of the recipient, Ebert and DeLanney (in Ebert, 1957) observed that, after grafts of adult spleen, the hosts' spleens frequently undergo striking degenerative changes characterized by intense granulopoiesis, the destruction or modification of the vascular bed, the formation of cystic masses in the spleen, and, often, the eventual death of the embryo or hatched chick. The cystic condition of the spleen occurs with a frequency approximating that of the death of chicks at or shortly after hatching. The time course of the reaction and the conditions resulting in its expression led Ebert and DeLanney to postulate that the transplanted adult spleen produces an immune response directed against its host, with the primary locus of action the vascular bed (cf. Billingham and Brent, 1957; Simonsen, 1957).

Emphasis has been centered previously on the terminal stages of the reaction following prolonged exposure to grafts (8 to 11 days post-implantation). Attention is now focused on progressive changes in the host's spleen, with emphasis on the initial stages and on the course of granulopoiesis (cf. Boyer, 1960). There is a precocious granulopoiesis by the fourth day after implantation of a homologous graft of adult spleen, followed by a spectrum of changes, not all of which are observed necessarily in each embryo: extreme granulopoiesis, accumulation of mucopolysaccharide, breakdown of the vascular bed, and the appearance of necrotic and fibrotic foci.

Taken as a whole, the findings lead to the postulation that the changes observed embrace at least three phenomena; i.e., the effects of splenic grafts are *more than a graft-versus-host reaction.* Possible mechanisms of balance and interplay among these reactions will be discussed.

B. *On the chorioallantoic membrane.* The epithelial and mesenchymal cells of the chorioallantoic membrane are labile, being capable of keratinization (Moscona, 1959), striated muscle formation (Ebert, 1959*b*), and other metaplastic modifications (Moscona, 1960). Changes in the chorioallantoic membrane have been studied at closely timed intervals after implantation of homologous adult spleen. Both the epithelium of contact and mesenchyme respond rapidly to the implant, the former by varying degrees of thickening; changes in the latter include the formation of spindle cells and a shift toward myelogenesis. We will emphasize the cytology of the graft and adjacent chorioallantoic membrane.

Previously, what we have described as the graft-versus-host reaction has been transferred serially by intracoelomic and chorioallantoic transplantation of embryonic host spleen after a primary graft of adult spleen. We now examine in detail the findings of experiments involving serial transfer through three transplant generations of this reaction by fragments of chorioallantoic membrane in contact with a primary implant of adult spleen. The transplantation to the membrane of 7- or 9-day-old embryos of fragments of chorioallantoic membrane taken from reactive sites surrounding the original spleen implant results in intensified reactions in second and third transplant generations, characterized by extreme conditions of vascular breakdown. These grafts effect a rapid destruction of large areas of the chorioallantoic membrane surrounding them. The striking contrast between the appearance of the membrane after a primary implant of spleen and a secondary graft of chorioallantoic membrane will be described.

C. *Graft-versus-host and host-versus-graft reactions.* We shall summarize our findings on the sequence of events culminating in graft-host interactions and compare them with the findings of others. Our primary focus will be the cytogenesis of the affected spleens and membranes; attention will be paid to the genetic relationship between donor and recipient. We will not attempt a detailed comparative study of these phenomena as they occur in other species; brief reference will be made to pertinent findings in amphibians and mammals.

III. *Selective Uptake of Subcellular Fractions by the Chick Embryo and Modification of Patterns of Synthesis in the Host*

Viewing our own findings within the framework of those of Billingham and Brent, and Simonsen, there can be no doubt that grafts of immunologically competent tissues may react against their hosts, contributing to the formation of cysts and other pathological lesions in their spleens and other organs and ultimately to their death. Perhaps the most vexing question concerns the extent to which cells leave the graft and enter not only the extraembryonic membranes but also the embryo itself, at least some of them taking up residence in the homologous organ of the host. It is clear that, when suspensions of adult chicken spleen cells, whole chicken blood, or suspensions of chicken lymphocytes are administered to the embryo intravenously, some of the cells colonize the organs of the host (Simonsen, 1957; Terasaki, 1959; Biggs and Payne, 1959). There can be no doubt that some of the cells of the chorioallantoic grafts become distributed throughout the membrane, often at considerable distances from the site of the graft (Tardent, Mun, and Ebert, in Ebert, 1960). Moreover, it is now clear that some cells leave chorioallantoic grafts and become localized in the organs of the host (Mun, Errico, and Ebert, in Ebert, 1960).

It has not been established unequivocally, however, even in experiments with cells injected intravenously, that the increase in size of the host's spleen is due only to the proliferation of adult cells populating it, the proliferation being the result of antigenic stimulus. In fact, recent findings have shown not only that an appreciable component of the splenic enlargement after the injection of whole blood may be provided by host embryo cells but also that the persistence of immunologically active donor cells may not be necessary for homologous stimulation (Biggs and Payne, 1959; Simonsen and Jensen, 1959).

Whether tissues transplanted to the embryo emit complex matter including intracellular particulates and large molecules which operate in regulating the synthesis of macromolecules in the host is another question. Can the modification of the patterns of synthesis in the host be achieved as a consequence of the predominant localization of particles or molecules in the homologous organ? If so, to what extent are such interactions involved in the normal course of embryogenesis? Croisille (1958) has reported that the intravenous inoculation of a cell-free extract of adult chicken spleen into the chick embryo results in a significant increase in the size of the recipient's spleen. No evidence of cysts or lesions indicative of the graft-versus-host reaction was reported. Similarly, extracts of liver stimulate embryonic liver growth when injected *in ovo*. Croisille reports, however, that attempts to demonstrate similar effects *in vitro* failed.

Van Haeften (1958) implanted cell-free homogenates of adult spleen, thymus, and striated muscle on the chorioallantoic membranes of 9-day-old embryonic hosts. The spleen homogenate provoked a strong myeloid reaction in the chorioallantoic stroma as well as marked hypertrophy of the host's spleen. Histologically the enlarged spleens were said to be normal. After inoculation of spleen homogenate, there is also an increase in all cell types in the circulating blood; after thymus homogenate, lymphocytosis and eosinophilia.

These findings prompted a re-examination of our own earlier results, which had demonstrated predominant localization, but not stimulation, with microsome preparations. It seemed particularly important since Croisille's data on stimulation by extracts paralleled quantitatively our own findings using membrane filters. Experiments have been described in which the inoculation of a splenic microsome fraction has resulted in a significant increase in the weight of the host's spleen. An effort will be made to relate the results to our current information about the role of ribonucleoprotein granules in protein synthesis, particularly in antibody formation.

ACKNOWLEDGMENTS

L. E. DeLanney's research is supported in part by grants from the National Science Foundation (G-1381) and U. S. Public Health Service (RG-5619). During 1957 he was a Fellow of Carnegie Institution of Washington in the Department of Embryology. Some of the findings reported by J. D. Ebert and A. M. Mun were obtained in an experimental program initiated at Brookhaven National Laboratory and Indiana University. It is a pleasure to thank Richard D. Grill for photographic services, and to acknowledge the technical assistance of William Duncan, Edward Johnson, and W. D. McCleary. Several undergraduate and graduate students have participated in these studies, notably James Duncan, Arturo Fontanes, John Goffinet, and Robert Tolman. We thank Drs. A. M. Mun and P. J. Van Alten, who permitted us to read manuscripts before publication; Dr. R. F. Ruth, whose criticisms and suggestions have been helpful; and Drs. Bayard Clarkson and Brian Solomon, with whom exchange of information and materials has been rewarding.

MATERIALS AND METHODS

Embryos and tissues have been obtained from eggs and adults of both sexes of three varieties of domestic fowl: New Hampshire Red, a "synthetic" dominant white, and White Leghorn. Unless it is stipulated to the contrary, donor-host combinations are intrabreed combinations. It must be emphasized, however, that they are homologous (not isologous) combinations, the fowl not being highly inbred. Significant differences attributable to differences in breed have not been observed.

The technique of chorioallantoic transplantation was that of Willier (1924; cf. Hamburger, 1942, and Ebert, 1951). Recently, the modification described by Zwilling (1959) has proved to be helpful. Intracoelomic grafting has been done by the technique of Dossel (1954). Other experimental techniques will be described as they are introduced.

Observations have been made on several thousand embryonic spleens. Most of the specimens used in this report were fixed in the solutions described by Maximow and Helly; other fixatives include 10 per cent formalin, Bouin's solution, Allen's B-15, and Feulgen's solution. Most of the spleens have been sectioned at 6 microns. Although a number of staining procedures have been employed, we have relied heavily on the triple stain of Himes and Moriber (1956), toluidine blue, *p*H 4, and the Dominici stain.

I. MORPHOGENESIS AND CYTOGENESIS OF THE CHICK SPLEEN

The splenic primordium appears at *stage 22* of the Hamburger and Hamilton (1951) series (3½-day-old embryo) as a slight swelling dorsal to the duodenum and dorsal pancreas. The coelomic epithelium in this region is several cells thick, with individual elliptical nuclei arranged approximately perpendicular to the surface of the epithelium. A definite inner border sets off the coelomic epithelium from the general mesenchyme that makes up the bulk of the splenic ridge. The mesenchyme itself bears no special characteristics; the nuclei are large, clear, and polynucleolar, the cytoplasm being less basophilic and less dense than the cytoplasm of the overlying epithelium. Numerous venous capillaries appear between the splenic mesenchyme and the dorsal pancreas; they contain round and elliptical young erythrocytes. Mitotic figures are observed in the mesenchyme but with a lower frequency than in the adjacent pancreas or liver. As shown in figure 1 (pl. 1) the splenic primordium may be identified at this stage topographically, yet it cannot be distinguished cytologically from other embryonic mesenchyme.

At *stage 23* (3½–4 days) the splenic mesenchyme appears more dense when stained with iron hematoxylin; consequently it can be distinguished readily from the mesenchyme around it (e.g., the dorsal pancreas). Also the venous pattern first seen at *stage 22* associated with the portal vein has become more evident. The coelomic epithelium has not changed.

At *stage 24* (4 days) the spleen is observed as a pronounced dome. The coelomic epithelium and the mesenchyme have essentially the same characteristics as in previous stages. Mitotic figures in the mesenchyme are numerous but are observed infrequently in the overlying epithelium. The venous capillaries that are seen to penetrate to the apex of the dome or ridge, as it is in reality, are now lined by the elongated thin endothelial cells characteristic of veins. Figure 2 (pl. 1) illustrates the splenic anlage. Danchakoff (1916) stated that at this stage the mesenchyme cells are syncytial; to dispute her statement would require electron microscopy, despite our observation of scattered, clearly demarcated individual cells with a thin rim of dense cytoplasm (such as Danchakoff illustrated as hemocytoblasts).

At *stage 25* (4½ days) the mesenchyme of the rounded crest of the splenic rudiment is clearly more dense than the mesenchyme lying immediately ventral to it but dorsal to the pancreas (fig. 3, pl. 1). The characteristics of the coelomic epithelium and the mesenchyme remain unchanged. Mitotic activity is increased; e.g., 15 mitotic figures can be observed in a single high-power field. The red blood cells seen within the endothelially lined blood vessels and sinuses cannot be distinguished from those seen in the heart, liver, or dorsal aorta.

By *stage 26* (4½–5 days) there has been sufficient rotation of the gut to place the proventriculus and gizzard lateral to the splenic ridge when seen in cross section; nevertheless, the apex of the ridge or dome is still directed dorsally. The following changes are to be noted in the spleen itself: (1) the nuclei of the coelomic epithelium, which no longer lie at several levels, are round rather than elliptical; they are aligned more or less in a single irregular row. (2) The mesenchyme itself now contains sinusoidal areas.

The spleen at *stage 27* (5 days) is also directed dorsally at its apex. Depending on the level of the cross section, whether anterior or posterior, the tip of the apex may be pointed and tongue-like or blunt and rounded. The coelomic epithelium is thinner, and smooth along its outer edge, the nuclei being oriented parallel to the surface. The internuclear cytoplasmic areas are almost as wide as the nuclei themselves. It may be conjectured that the mitotic activity in the mesenchyme, increasing the splenic mass, leads to a stretching of the epithelium. Near the junction of the base of the primordium with the mesentery, the epithelium contains rounded nuclei, suggesting that the stretching has not affected the area.

At *stage 28* (5½ days) the spleen does not depart significantly from the description given for stage 27. Mitotic activity continues unabated; well developed sinuses containing numerous erythrocytes are observed; and the epithelium is composed of a single layer of cells.

By *stage 29* (6 days), the spleen has been shifted in its orientation: it bulges laterally from the general mesentery and begins to assume its definitive morphology, illustrated in figures 4 (pl. 1) and 5 (pl. 2). The epithelium is stretched and thin; there may be distances equivalent to 3 or 4 nuclear lengths between adjacent nuclei in the cytoplasm. The sinusoidal nature of the spleen is prominent, accompanied by a widespread distribution of erythrocytes. The mesenchyme retains many of the qualities of Danchakoff's "mesenchyme syncytium."

As illustrated in figure 6 (pl. 2), two further changes are recorded at *stage 30* (6½ days): (1) The nuclei of the erythrocytes in the splenic sinuses are dense; dense nuclei also are observed in the systemic circulation, but their incidence in the spleen is greater. (2) For the first time a difference between arteries and veins associated with the spleen is noted. The major splenic vessels associated with what is to become the gastrosplenic ligament are defined clearly. The endothelium of the vein is more squamous than that of the artery, a distinction seen clearly only where the vessels are large. It is not possible to distinguish arteries and veins within the spleen itself. In fact, even at *stage 32* (7½ days) it is possible clearly to distinguish artery from vein within the splenic mesenchyme only where the principal vessels penetrate it. A study of *stage 33* (ca. 7½ days) and *stage 34* (7½–8 days) contributes very little new information. Mitosis continues; the spleen remains sinusoidal. Beginning at *stage 35,* spleens no longer were sectioned *in situ* but were removed and sectioned separately. Between *stages 32* and *35* granulocytic differentiation is initiated. It is impossible, however, to state with certainty the point in time at which granulopoiesis begins. It can be said only that by *stage 35* (8–9 days) a definite population of granulocytes exists in the spleen. Sandreuter (1951) states that eosinophilic granulocytes make their appearance in the spleen between days 10 and 12, whereas basophilic granulocytes appear first at day 12. These cells are few in number; even so, careful examination discloses that the granulocytes themselves contain granules that vary in number, shape, and size. With the Dominici stain, some cells have granules that resemble large, orange or bluish red lipoidal droplets; a few cells contain elongate or comma-shaped granules, but this type of granule is not so pronounced as it is in later stages.

By *stage 36* (10 days), although granulocytes are in the minority, one does not have to search laboriously for them (fig. 7, pl. 3). Mitotic figures are observed frequently in the mesenchyme. At this stage also, as in the preceding stage, hemocytoblasts are a characteristic feature (fig. 8, pl. 3), being observed frequently in the sinuses as well as occasionally in the splenic mesenchyme.

Our understanding of the response of the developing spleen to the implantation of a fragment of mature spleen containing immunologically competent cells turns on our ability to define the granulocyte and to delineate its life history, i.e., on our understanding of the normal course of granulopoiesis (see, also, Boyer, 1960). It seems important, therefore, before leaving *stages 35* and *36,* which herald a major surge of granulocytogenesis, to reflect on the definition of the granulocyte.

When stained by the Dominici technique, the embryonic spleen contains a population of cells having as "granules" blunt and slightly curved rods or highly refractile spheres. The mature "granule" of the heterophilic granulocyte in the chicken is a long rod or spindle. During embryogenesis the granules are pleomorphic; by and large, however, the description "blunt rod" is appropriate. Whether these cells are but intermediate steps in the transformation of granuloblasts to mature granulocytes is not clear. Although we are unable to distinguish in the developing spleen the several stages in the development of the granulocyte (myelocyte) figured by Sandreuter (1951, p. 61), we believe that the term "granulocyte" is appropriate.

Stage 37 (11 days) is marked by additional changes in the spleen. Not only are hemocytoblasts prominent in the sinuses (in agreement with Danchakoff) but also erythropoiesis is increased, especially at the periphery of the spleen. It is not possible to distinguish a "cortical" area of erythropoiesis; on the contrary, in fact, erythropoietic sites appear randomly in the periphery. One may argue either that erythroblasts have accumulated in already formed sinuses or that sinuses form around erythroblastic centers.

Even at this stage, arteries are observed only infrequently. Arteries can be distinguished from veins, however: the endothelial cells of arteries instead of being flattened as in the veins tend to be "ruffled" and to project into the lumen of the vessel. Usually it is possible to see also that the mesenchyme cells surrounding the endothelium and the lumen are set apart from the rest of the mesenchyme. Descriptive criteria are difficult to establish, but the following is an attempt. The nuclei of the arterial endothelium are more consistently round-oval than elongate-oval as in the venous endothelium; there are few erythrocytes in the lumina of the arteries. It is convenient to distinguish two categories of mesenchyme: the general mesenchyme of the spleen, described as nonarterial mesenchyme; and the mesenchyme immediately around the endothelium of an arterial lumen, as arterial mesenchyme. The tangential orientation of mesenchyme cells around the developing artery sets off this group of cells from the general nonarterial mesenchyme (fig. 9, pl. 2). The thickness of the arterial mesenchyme associated with the vascular wall is variable. It may span as much as 5 nuclear diameters. Mitotic activity continues uninterruptedly, and the appearance of the general mesenchyme and granulocytes is unchanged.

At *stage 38* (12 days), the spleen is richly endowed with erythroblasts and erythrocytes, as is clearly seen in figure 10 (pl. 3). At this stage, too, the arteries first appear prominently; the foregoing description of endothelial cells, arterial mesenchyme, and generalized nonarterial mesenchyme is most apt. By *stage 38* it would be difficult to confuse a small artery with a vein or a splenic sinus. In fact, an artery can be seen and distinguished clearly even though its lumen may be so small that it is filled by one erythrocyte. Also, there can be no doubt that there is an increased population of granulocytes, which are distributed randomly throughout the splenic mesenchyme. Hemocytoblasts with large clear nuclei, large and sometimes metachromatic nucleoli, and a rim of basophilic cytoplasm are observed more frequently in the mesenchyme; they, too, are randomly distributed. There is greater variation in the shape of the granules themselves in the granulocytes; they range from bluish red large "droplets" through bluntly elongate to almost mature thin spindle or rod shapes. Even the last, however, have blunted or bulbous ends in contrast to those to be seen later. Comparison of figure 11 (pl. 3) at *stage 37* and figure 10 (p. 3) at *stage 38,* both at the same magnification, reveals the granulocytic increase. At *stage 38,* then, there is a pronounced increase in granulocytic differentiation; this point is reiterated in view of the observations to be reported on the time of impact on the host embryo and its membranes of grafts of homologous adult spleen.

During the next day, *stage 39* (13 days), another major change is visible, the initiation of follicle formation, which is unmistakable although not pronounced. The arterial channels, which now consist of a "ruffled" endothelium in addition to an ordered mesenchymatous sheath presumably destined to provide the musculature and possibly the connective-tissue tunics of the artery, are set off from the granulocytic pulp.

Figure 12 (pl. 3) illustrates the pattern at *stage 40* (14 days): Granulopoiesis continues unabated in the pulp; follicular development becomes more pronounced. Hemocytoblasts are prominent. The illustration shows clearly the close association of granulocytes with sinuses, a condition comparable to their association with veins but in contrast to their absence from the vicinity of well established arteries, as is illustrated for the next stage in figure 13 (pl. 2). Most of the erythrocytes are mature. It has been reported (Sandreuter, 1951; Romanoff, 1960) that erythropoiesis begins in the bone marrow on the 15th day of incubation; apparently, therefore, the spleen has fulfilled its erythropoietic function by this time. Figure 14 (pl. 3), which is illustrative of *stage 40* at higher magnification, demonstrates hemocytoblasts as well as a broad spectrum of granule types ranging from spheres through blunt spindles to elongate rods in the granulocytes.

By the next day, *stage 41* (15 days), in contrast to the foregoing account, the granulocytes may be aggregated around arterial channels, provided that the arteries are small. Despite variations from spleen to spleen, the pattern is apparent both in cross sections and in longitudinal sections containing arteries. The description that follows is for a pronounced example, and it is emphasized that some spleens show this phenomenon less intensively. In the case in point (a cross section) the artery has a small lumen lined by four to six endothelial cells and with erythrocytes visible in the lumen. The endothelial cells, except for their position and the definite cytoplasmic outline as they project into the lumen, have the staining characteristics of the hemocytoblasts, the cytoplasm being basophilic, the nuclei being large and clear and having prominent nucleoli. Just outside the endothelial cells are similar cells oriented with their nuclei tangential to the lumen so that collectively they form a conspicuous ring. Often this ring is no more than 1 or 2 nuclear diameters wide; peripheral to it is a striking congestion of granulocytes. In sections parallel to lengths of arteries the pattern is more dramatic, for the granulocytes on each side of the section are crowded in lines like the spectators at a parade (fig. 13, pl. 2). On the other hand, the pattern is not observed around sinuses or recognizable venous channels, where granulocytes may abut the lumen but are distributed randomly, similar to their appearance in the pulp. In the region of larger arteries the granulocytes are not tightly packed around the loose outer tunic. However, when sections show a large artery branching to smaller arteries consisting only of endothelium and dense inner circumferentially oriented tunic the granuloblasts appear packed against the walls. The granulocytic line shows the several variations of granule or rod formation, the large refractile droplet type being the most prominent. Small lymphocytes have not been recognized with certainty either in the splenic tissue or in the channels, in contrast to earlier accounts in which they are described as early as day 14 or 15 (Sandreuter, 1951; Romanoff, 1960).

At *stage 42* (16 days) the spleen does not deviate significantly from its appearance at *stage 41* except that the mass of arterial tissue is increased and, under low power, the follicular nature of the organ is more prominent.

Figure 15 (pl. 3) shows the status of the spleen on the next day (17 days, *stage 43*), at which time the architecture is essentially the same as at *stage 42*. The illustration is selected to show not only the nature of the arteries and the pattern of follicular development but also the numerous heterophils. The heterophilic leucocytes have, on the whole, thin, rodlike granules characteristic of the mature heterophil. Nevertheless, there is still a broad spectrum of granule types ranging from the "oily" refractile spheres reminiscent of the basophilic leucocytes described by Olson (1937) through blunt rods, boat-shaped rods, and elongate rods destined to emerge from the particular cells seen here. Figure 16 (pl. 3) illustrates the spleen of a 17-day-old embryo stained with the Himes and Moriber triple stain. In the general proteinaceous background of yellow of the cytoplasm, the mucopolysaccharide, which gives a reddish cast to the granules of the granulocytes, can be seen.

Stage 44 (18 days) clearly illustrates follicular enlargement, the pulp between the follicles being principally granulocytic and hemocytoblastic. *Stage 45* (19–20 days), and the terminal stage, *stage 46* (days 20–21; new hatched), are so like *stage 44* as to make any further description unnecessary.

In summarizing the normal development of the spleen, there are three principal periods: (1) The appearance of the splenic primordium from the region dorsal to the duodenum and dorsal pancreas; there the undifferentiated mesenchyme is gradually infiltrated by venous vessels and sinuses. This phase begins at Hamburger and Hamilton stage 22 (3½ days) and continues through stage 34 (8 days), during which time the primordium itself shifts from its initial position to its characteristic site along the left side of the dorsal mesentery. During this period gradual changes appear that anticipate the next phase of development. Some of them are: the establishment of an endothelial lining in the venous channels; infrequent granulocytic differentiation; and finally the establishment of early arterial channels distinguishable from the venous channels by the character of the endothelium—venous endothelium being somewhat squamous, arterial endothelium being irregularly columnar. (2) The phase of granulocytic differentiation, during which a variety of granule types become distinguishable in the cytoplasm; eventually a gradual increase in the number of rodlike granules that characterize the chicken heterophil. Small lymphocytes have not been identified with certainty. This phase begins at about stage 35 and continues until about stage 39, i.e. between days 8 or 9 and 13. (3) The third phase, beginning at about stage 39, shows even under low power the separation of follicles and the pulp, and, up to hatching, the phase is principally an elaboration of the theme of follicle formation.

II. THE IMPACT OF IMPLANTED FRAGMENTS OF HOMOLOGOUS ADULT SPLEEN

Impact on the Host's Spleen

Having described the morphogenesis and cytogenesis of the spleen, we may examine next the changes in the host's spleen after transplantation of a fragment of spleen from a homologous adult chicken (cf. Danchakoff, 1916, 1918; Murphy, 1916; Willier, 1924; Ebert, 1951; Mun, Kosin, and Sato, 1959).

The dramatic splenomegaly in the host embryo as a consequence of such a graft is so well known that additional documentation would not be required were it not for the fact that earlier accounts have emphasized only the terminal stages of the reaction; neither the time at which the reaction first can be observed nor that at which it reaches its maximal effectiveness has been stated. To provide this information a series of experiments was carried out in which adult chicken spleen was implanted on the chorioallantois at the 7th day of incubation and recovered at 2-day intervals through the 19th day, the spleens of the recipients being weighed at recovery. The findings are presented in figure 17*a,* which presents the average per cent weight increase at each recovery, spleens from 532 hosts being compared with spleens from 226 sham-operated control embryos. Figure 17*b* illustrates not only the distribution of deviations from the mean of the control series but also the degree to which the experimental series deviated from the control mean.

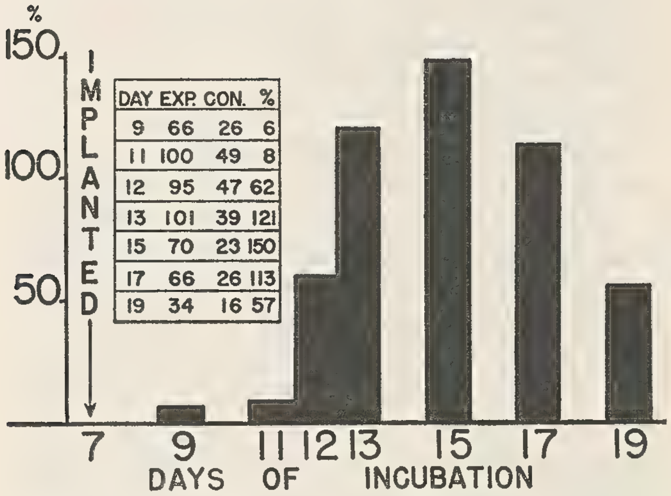

DAY	EXP.	CON.	%
9	66	26	6
11	100	49	8
12	95	47	62
13	101	39	121
15	70	23	150
17	66	26	113
19	34	16	57

Fig. 17*a*. Impact of grafts of homologous adult spleen on spleens of embryonic hosts, expressed as average per cent weight increase above average control weights.

It is clear that during the first 4 days after implantation the increase in average spleen weights in the experimental groups is only nominal, being 6 and 8 per cent, respectively, at the 9th and 11th days of incubation. At the 13th day of incubation a dramatic rise in the average weights is seen, that increase continuing at the 15th day of incubation when the average weights of the experimental series exceeds the average weights of the controls by 150 per cent. These findings indicate that the effect of the graft becomes pronounced between the 11th and 13th days of incubation; to pinpoint the time more precisely additional experiments were performed with recovery at day 12, five days after implantation. The data speak for themselves: it is at day 12 that significant effects, at least as judged by average weights, first become apparent. But what of the drop in percentage increase observed at days 17 and 19? We believe that it may be explained by the death of large numbers of affected hosts 10 to 12 days after implantation of the graft. Large numbers of dead embryos have been recovered; although their spleens were enlarged significantly, they were not included in the data because of uncertainty as to the time of death. To this extent, therefore, the average per cent weight increases at days 17 and 19 are biased.

But changes in weight are a crude yardstick, although they do parallel changes in protein and total nitrogen (Ebert, 1954); what are the cytologic and histologic changes preceding and accompanying splenomegaly? Again, earlier investigations have been focused on the terminal stages of the reaction following the prolonged exposure of the host to the graft; we now propose to analyze the progressive changes leading to them. Normal and experimental spleens have been compared, using principally the Dominici stain, Himes and Moriber triple stain, and toluidine blue, *p*H 4; appropriate modifications, e.g. diastase and ribonuclease digestion, have also been employed. Several thousand embryonic spleens accumulated by both authors in previous studies have been re-examined in addition to the 758 spleens derived from the experiment just described.

Recovery at nine days: two days postimplantation. Figure 18 (pl. 4) illustrates a 9-day-old normal embryonic spleen stained with toluidine blue. Aside from the general mesenchyme of the spleen only a few hemocytoblasts and a few mitotic figures can be seen. According to Sandreuter (1951), assuming that the hemocytoblasts illustrated here are normally destined to form granulocytes, the presence of the large nucleolus suggests that these cells are destined to give rise to neutrophilic leucocytes. By the 2nd day after implantation of a graft, however, as shown in figure 19 (pl. 4), there is clearly an increase in the number of hemocytoblasts. Comparing figures 18 and 19 one is impressed also by the larger hemocytoblasts in the affected spleen. Moreover, thick, rod-shaped nucleoli may be identified readily in the hemocytoblasts in figure 19. One day earlier, at the 8th day of incubation, 24 hours after implantation we have been unable to observe a similar differential in numbers of hemocytoblasts in affected and normal spleens, nor have significant differences in cell size been noted.

Recovery at eleven days: four days postimplantation. Figures 20 and 21 (pl. 4) again show dramatically that hemocytoblasts are more abundant in the spleen after implantation than in the normal spleen. Figure 22 (pl. 4) demonstrates that on the 4th postoperative day granulocytes are present in significant numbers; moreover, the granulocytic population consists principally of mature neutrophils. There is little evidence of the intermediate promyelocyte stages, which according to Sandreuter (1951) are observed commonly at day 11 in the normal embryo. Instead, the population of granulocytes is comparable to that usually found in the 12-day-old embryonic spleen; hence, the first impact of the graft on the host's spleen appears to be the stimulation of myelogenesis, evidence of which becomes clearer as the time between implantation and recovery is increased.

Recovery at twelve days: five days postimplantation. Figure 23 (pl. 4) reintroduces the reader to the third principal stain employed, the Himes-Moriber stain. This photograph of a section of a normal 12-day-old embryonic spleen illustrates the three characteristics that make the technique useful: nuclear deoxyribonucleic acid (DNA) is stained blue; proteinaceous material, e.g. of erythro-

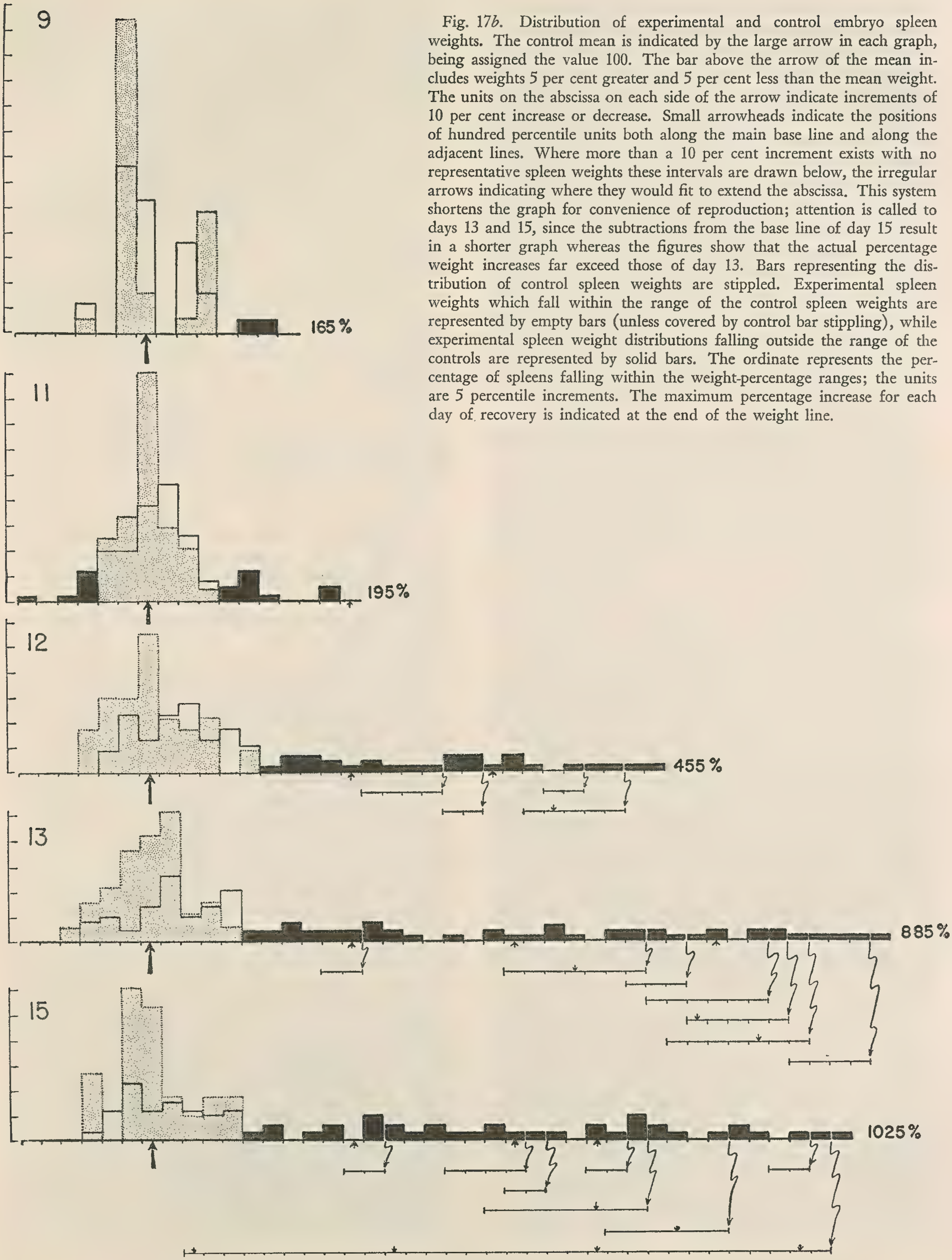

Fig. 17*b*. Distribution of experimental and control embryo spleen weights. The control mean is indicated by the large arrow in each graph, being assigned the value 100. The bar above the arrow of the mean includes weights 5 per cent greater and 5 per cent less than the mean weight. The units on the abscissa on each side of the arrow indicate increments of 10 per cent increase or decrease. Small arrowheads indicate the positions of hundred percentile units both along the main base line and along the adjacent lines. Where more than a 10 per cent increment exists with no representative spleen weights these intervals are drawn below, the irregular arrows indicating where they would fit to extend the abscissa. This system shortens the graph for convenience of reproduction; attention is called to days 13 and 15, since the subtractions from the base line of day 15 result in a shorter graph whereas the figures show that the actual percentage weight increases far exceed those of day 13. Bars representing the distribution of control spleen weights are stippled. Experimental spleen weights which fall within the range of the control spleen weights are represented by empty bars (unless covered by control bar stippling), while experimental spleen weight distributions falling outside the range of the controls are represented by solid bars. The ordinate represents the percentage of spleens falling within the weight-percentage ranges; the units are 5 percentile increments. The maximum percentage increase for each day of recovery is indicated at the end of the weight line.

cytes and granulocytes, is stained yellow; and the granulocytes can also be identified by the slight periodic acid–Schiff reaction of the granules, which indicates that these cytoplasmic inclusions contain a mucopolysaccharide. Moreover, it will be seen that there are several mitotic figures in the field. Attention is called to the metaphase figure in the center of the photograph: a granulocyte in mitosis. Usually it is stated that granulocytes do not undergo mitosis. For example, in attempting to identify *the* type of blood cell responsible for the graft-versus-host reaction, Terasaki (1959) eliminates the polymorphonuclear leucocyte from consideration because Simonsen (1957) had been able to propagate the reaction serially, and, as Terasaki puts it, the polymorphonuclear leucocyte is generally thought not to reproduce. However, the photograph denies the generalization that granulocytes do not undergo mitosis. Later we shall question the obligatory relation between hemocytoblastic stem cells and granulocytic differentiation.

The acid hydrolysis employed in the Himes-Moriber stain is not compatible with the demonstration of hemocytoblasts. Nevertheless, with experience one can often identify hemocytoblasts because of the partial shadowing of the large nucleolus by condensed chromatin. (The condensation apparently is not a property of DNA, since the intense blue color of azure A is absent, as seen in fig. 23, pl. 4.)

We have observed (p. 72) that, after a graft of adult spleen, the host's spleen frequently undergoes a striking degenerative change characterized by destruction or modification of the vascular bed and the appearance of cystic masses. The 5th day after implantation is the first day on which the cystic condition is observed clearly. Figure 24 (pl. 5) shows a longitudinal section of a spleen in the center of which a large lesion can be identified. The events that mark the 5th postoperative day are not only a continued rise in the granulocytic population but also, as illustrated in figure 34 (pl. 7), the aggregation, both intracellularly and extracellularly, of periodic acid–Schiff positive droplets. Moreover, the architecture of the spleen has changed; it is less syncytial, the cells being more sharply delimited. We have been unable to identify any pattern of distribution of the mucopolysaccharide droplets. The illustrations for day 12 have been chosen to emphasize the most pronounced reactions observed at this time. It is true that probably one more often sees simply a large increase in cells undergoing mitosis, hemocytoblasts, and granulocytes, and that ordinarily neither necrotic areas nor droplets of periodic acid–Schiff positive material are observed; occasionally, in addition to mucopolysaccharide in association with the granulocytes, it is observed lining some of the sinuses.

Recovery at thirteen days: six days postimplantation. Between day 12 and day 13, the average per cent weight increase nearly doubles; concomitantly the cytologic changes observed at day 12 are intensified. The shift toward granulopoiesis continues, mucopolysaccharide concentration is increased, cysts and necrotic loci are increased in number. Degenerative changes are the more prominent events, as illustrated in figures 26 and 27 (pl. 5). In figure 26 there is a prominent necrotic area near the edge of the spleen, the rest of the section appearing relatively homogeneous. In figure 27 there is a random loss of ribonucleic acid (RNA) or of affinity of RNA for the stain; where it remains there are concentrations of hemocytoblasts.

Recovery at fifteen days: eight days postimplantation. Figures 28 and 29 (pl. 6), sections of the same spleen prepared by the Himes-Moriber stain and toluidine blue, respectively, reveal multiple necrotic foci and an almost complete lack of RNA staining. These figures illustrate the progressive nature of the destructive condition.

Recovery at seventeen and eighteen days: eight to eleven days postimplantation. In figures 30 and 31 (pl. 6) are compared 17-day-old normal and affected spleens, the graft having been made at day 9 rather than at day 7. Note the "homogeneity" of the enlarged spleen: well defined follicles are absent, and arteries, which are identified readily in the normal, are almost entirely lacking. These photographs illustrate also the magnitude of the splenomegaly. By contrast figure 32 (pl. 7) shows an alternative extreme in which the affected host spleen is riddled with cysts.

These figures, 31 and 32, reinforce our earlier statement that not all the spectrum of changes—extreme granulopoiesis, accumulation of mucopolysaccharide, and necrotic foci—occurs invariably in every affected spleen. One of the principal questions yet to be answered concerns the nature of the granulocytic response. A comparison of normal and affected spleens reveals that there is no fixed pattern of response so far as the type of granulocyte, as defined by granule shape, is concerned. For example, one might select a group of affected spleens containing granulocytes which, because of the spherical, refractile nature of their granules, would be marked as acidophilic. Only a few heterophils (neutrophils) with their spindle- or rod-shaped granules could be seen. Yet such a conclusion would be unsound, for several techniques must be brought to bear to demonstrate the variability of the response. With the Dominici stain the granules are predominantly eosinophilic; viewed under phase contrast, granules stained by this technique appear brilliant blue-green. With the Himes-Moriber stain (figs. 23, pl. 4; 33, pl. 7) the granules can be identified by a slight periodic acid–Schiff positive "overcast." With this stain, the granules appear light brown under phase contrast. With toluidine blue, *p*H 4, the difference between hemocytoblasts and granulocytes is striking. The latter lack the accumulations of RNA that mark the former. The granulocyte can be recognized only by the "frothy" appearance of the cytoplasm which indicates the position of the granules, as can be demonstrated by examining the same slides under phase contrast.

A second major question concerns the relation between the granulocytic response and the increase in mucopolysaccharide concentration that has been apparent since the 5th day postimplantation. The origin of this material has not been determined. The presence of mucopolysaccharide in association with the granules of the granulocyte and the association in time of increasing numbers of granulocytes with an increasing concentration of periodic acid–Schiff reactive materials have been noted, yet it is clear (cf. fig. 33, pl. 7) that the mucopolysaccharide may appear as extracellular droplets or aggregates; it may not be associated specifically with the degradation of granulocytes in the immediate vicinity. Moreover, both grafts and chorioallantoic membrances at the site of implantation contain concentrations of mucopolysaccharide, not infrequently concentrated at the zone of junction.

Impact on the Chorioallantoic Membrane

Grafts have been made by two modifications of the chorioallantoic grafting technique (Willier, 1924; as modified by Zwilling, 1959) into hosts incubated either 7 or 9 days. We have been unable to discern any significant differences in the findings in the several groups; hence the discussion will be based largely on data derived from grafts made at day 7 by the original chorioallantoic transplantation procedure (Willier, 1924) and drawn chiefly from the experimental series described on page 66.

It will be well to recognize at the outset the variability in the relation between the graft and the subjacent membrane. The sources of the variability are not fully understood. Inasmuch as highly inbred lines of chickens have not been employed, the success or failure of grafts cannot be correlated with the genetic relations between donor and host (cf. Burnet and Burnet, 1960). It is clear, however, that viable grafts may reside on the membrane, which itself appears normal, without even a suggestion of an untoward or unusual reaction between them. Other viable grafts may evoke a marked reaction in the membrane, and still other grafts and membranes may interact to the ultimate destruction of either or both. Initially, attention will be centered on the evidence for an interaction between graft and membrane, the presence of the graft being accompanied by alterations of the membrane. We emphasize, however, that this approach is for convenience only; we shall return to a consideration of experiments in which viable grafts can reside on the surface of membranes without reactions in the subjacent tissue. Figure 25 (pl. 5) illustrates just such a graft in which there is little evidence of interaction between graft and membrane.

Recovery at eight days: one day postimplantation. Figure 35 (pl. 7) shows that the union between the graft and the underlying membrane can be accomplished within 24 hours. The slight edema in the membrane is typical. Usually grafts have a "rind" of apparently viable mesenchyme-like cells; although the thickness of this peripheral region varies, it may be as much as 30 nuclear diameters. This region may be present also in the interzone immediately between graft and membrane. Not infrequently the center of the graft contains seemingly moribund cells, while its outer, apparently more viable, border may contain structurally intact segments of small arteries. At the junction between graft and membrane there is an erosion of the chorionic epithelium sometimes accompanied by hyperplasia, seen in figure 35 as a slight thickening, giving the appearance of a syncytium of epithelial cells. Cells which probably originate in the graft (their nuclei show the denser blue stain characteristic of the graft mesenchyme cells, in contrast to the lighter color of the nuclei of the mesenchyme cells of the membrane) have mingled with the adjacent mesenchyme of the membrane. Although studies employing tritium thymidine–labeled grafts have shown invasion of the adjacent membrane by donor cells (Tardent, Mun, and Ebert, in Ebert, 1960), we are unable to distinguish at the junction between the graft and membrane significant numbers of mature cells, e.g. small lymphocytes or granulocytes. Sections stained with toluidine blue reveal that the periphery of the graft retains a higher concentration of RNA than the center of the graft.

Recovery at nine days: two days postimplantation. Forty-eight hours after implantation a graft may remain supported as a distinct "button" on the surface of the membrane (fig. 36, pl. 8), or it may sink into the thickened membrane (fig. 37, pl. 8). What the circumstances are that lead to this difference we do not know. Mun, Kosin, and Sato (1959) refer to the graft that sinks into the membrane as a "well incorporated graft." We may note that the character of the membrane differs, depending on the position of the graft, although the membrane invariably expands dramatically. Let us consider the graft that lies deeply embedded in the membrane. Its position does not appear to be the result of mechanical depression of the edematous membrane, because the depressed chorionic epithelium is seen only at the edges of the site of invasion and there for only a short distance. Deeper in the membrane, there is no evidence of intact chorionic epithelium, and the graft itself lies in direct contact with mesenchyme of the membrane. That arteries from the graft can retain their integrity through this period is evident from figure 38 (pl. 8), which illustrates principally the graft showing the membrane only at one border. The characteristic reaction for mucopolysaccharide associated with arteries is evident. Some of the cells at the periphery of the graft also begin to show faint positive reactions for mucopolysaccharide (fig. 37, pl. 8). Mesenchyme cells of the membrane elongate and become spindle-like. The pattern is not obligatory, but these cells tend to lie roughly parallel to the graft, suggesting a positive orientation of host cells under the impact of the graft. Mucopolysaccharides may accumulate precociously in the cytoplasm of the surface epithelium of the allantoic side of this membrane. They are observed normally in this part of the membrane at day 12. Although erythrocytes and hemocytoblasts may be observed in the graft or the membrane adjacent to it, granulocytes in either graft or stimulated membrane are extremely rare. Also, small lymphocytes have been observed rarely, usually at the edge of the graft rather than in the membrane. We have not been able to identify plasma cells. Sandreuter (1951) observed that plasma cells can be found in spleens of chickens by the 20th day after hatching.

Recovery at eleven days: four days postimplantation. The conditions to be described at this stage are illustrated in figure 39 (pl. 8). Attention is called to the location of the graft on the surface of the membrane and the extremely thickened area in the membrane beneath the graft containing a dense aggregation of cells. This dense aggregation within the membrane appears to have a volume (suggested by cross-sectional area) as large as or greater than that of the graft. It is not uniform in its cellular make-up. The largest single population of cells is composed of hemocytoblasts, with densely basophilic cytoplasm, large clear nuclei, and usually two very prominent nucleoli. There are small foci containing multinucleate giant cells. The reaction with Dominici stain, surprisingly, does not reveal granulocytic cells, but, by employing phase contrast microscopy with the Dominici technique, granules characteristic of granulocytes are evident in the cytoplasm of cells that would otherwise be interpreted as hemocytoblasts and also in cells (usually nearer the margins of the dense aggregations) that might otherwise be interpreted as fibroblasts.

What is the origin of these aggregations of hemocytoblasts in the membrane? The multiplication of graft cells? The differentiation of cells of the membrane? Or the migration to the membrane of immature granulocytes from other regions of the embryo? These questions are asked now to focus attention on the body of evidence that suggests a response by the host to the graft. The several possible interpretations of this reaction will be deferred until the description of reactions at later stages is completed. It is of interest, however, to note that Boyer (1960) concurs with the argument advanced previously (DeLanney and Ebert, 1959*a*) that localized reactions can be observed in the membrane. She, too, calls attention to the occurrence of granulocytes in the membrane and in the embryo as well, but interprets them as arising by proliferation of immunologically competent donor cells in response to antigenic stimulation by components of the embryo.

The dense aggregates of cells within the membrane do not contain mitotic figures in abundance. On the other hand, in one part of the membrane mitotic figures are observed with ease: the *allantoic epithelium,* which is populated heavily by hemocytoblasts containing numerous mitotic figures. Hemocytoblasts are often associated with the blood vessels of the membrane also.

To this point we have advanced a body of evidence suggesting that a significant part of the increase in cell population arises in the membrane itself. On the other hand, figure 40 (pl. 9), which is a photograph of a different section of the graft and membrane in figure 39, shows the graft, which is necrotic, to be continuous with the characteristic dense aggregate of cells beneath it, the "bridge" consisting of a vertically oriented section of artery. The mechanism of "invasion" of the artery into the membrane is intriguing. It appears possible that cells of the graft originally adjacent to the membrane may have moved into it during its early edematous phase, thus baring the vessel so that the weight of the graft above it pushed it into the interior. The artery looks more like arteries found in the adult spleen than like those in the embryonic spleen or membrane; hence an adult origin appears likely.

Recovery at twelve days: five days postimplantation. The reader will recall that it is at 5 days after implantation of a graft that a significant increase in weight is observed in the host's spleen. Yet significant changes have occurred in the adjacent membrane within 48 hours. By the 5th postoperative day, extreme reactions occur in the membrane, as shown in figure 41 (pl. 9). This section does not show the graft itself. It does include several large blood vessels adjacent to the affected area of the membrane, as well as a necrotic or cystic region in the center of the membrane. Note, too, that areas of the allantoic epithelium can be seen to be highly positive with the periodic acid–Schiff stain.

Figure 42 (pl. 9) illustrates another type of response on the part of the membrane, this time to a necrotic graft lying in a small depression in an edematous but otherwise unaltered membrane. The chorionic epithelium is intact at all points under the graft and has a maximum thickness of about four cells immediately subjacent to the graft. A zone of mucopolysaccharide separates the graft from the membrane, and "fingers" of mucopolysaccharide penetrate into the chorionic epithelium but not through it. The mesenchyme cells of the membrane are spindle-like or oriented parallel to the surface of the membrane. Blood vessels in the membrane immediately under the graft are not surrounded by hemocytoblasts; mitotic figures are observed only in unspecialized mesenchyme or in the endothelium of the blood vessels. The chorionic epithelium is squamous and only one or two cells thick apart from the site of implantation; the allantoic epithelium opposite the site of implantation is a single-layered squamous sheet which is strongly positive for periodic acid–Schiff stain along its entire outer surface.

By contrast with the description just given for a relatively unaffected membrane, membranes such as that in figure 41 (pl. 9) show not only a mucopolysaccharide border between the chorionic epithelium and the graft but also droplets or irregular clumps of mucopolysaccharide distributed throughout the thickened chorionic epithelium. Figure 43 (pl. 9) shows intact epithelium remaining between graft and membrane. Thin lines of mucopolysaccharide at the borders of viable graft cells are in contact with the dense band of mucopolysaccharide.

The generalized area of stimulation contains numerous mesenchyme cells, many of which are spindle-shaped and contain numerous mitotic figures; cells containing mucopolysaccharide are presented in figure 44 (pl. 10); they include scattered cells with irregular nuclei which are heavily laden with large droplets of mucopolysaccharide. The question may be raised whether these cells are phagocytic. Slides stained with toluidine blue show that there are great concentrations of hemocytoblasts; many of these cells lie in the allantoic epithelium. The last observation is of interest in relation to the observations of Ackerman and Knouff (1959), who conclude, "It is almost universally accepted at the present time that lymphocytes develop from the mesenchymal cells or their derivatives in all places in the vertebrate body. . . . Although we have been highly skeptical of theories suggesting that lymphocytes may develop from sources other than mesodermal derivatives our observations on the bursa of Fabricius leave us in little doubt that the lymphocytes originally develop from undifferentiated, endodermal epithelial cells in this organ." Whether the hemocytoblasts that we see here are stem cells, precursors of lymphocytes, is not our primary concern. We wish to point out only the possibility that when conditions are favorable allantoic epithelium too can form hematopoietic stem cells (see also Ruth, 1960).

Granulocytes are found at the 5th postoperative day in significant concentrations throughout the adjacent membrane. Their irregularly shaped, spindle-shaped, and rod-shaped granules are characteristic of neutrophils (heterophils). Mature granulocytes are present also in the blood vessels in some of the affected embryos. The distribution of the granulocytes is as random as that of the hemocytoblasts. We have been unable to correlate the differentiation of granulocytes with a decrease in number of hemocytoblasts or to obtain direct evidence of such a transformation. Observations of acidophilic regions suggest that such regions are localized aggregations of immature progranulocytes in which typical granules are developing. Study of them suggests that granulocytic aggregations may contribute to cyst formation. We may reiterate that the irregular shape of the granules of some of the first leucocytes to appear as the result of graft-membrane interactions identifies them as neutrophils (heterophils), which, it will be recalled, occur normally at this stage. Yet we have also described granulocytes having large, spherical granules such as those described by Sandreuter (1951) for eosinophilic (acidophilic) leucocytes. Sandreuter reports the first appearance of eosinophilic leucocytes at the 14th day. We have observed these cells in the normal spleen as early as the 13th day of incubation, but more important is the fact that, at least as early as day 12, granulocytes of the eosinophil line are evoked in the membrane; they may be associated with foci destined for necrosis.

Recovery at thirteen days: six days postimplantation. The findings on the 6th day are so variable that it is impossible to present one set of characteristics as typical. It is possible for the affected region of the membrane to reach dimensions as large in cross section as 3½ by 5 mm. In some specimens this enlarged area blends into the unaffected part of the membrane; in others it may be a rounded and pendant mass suspended below the rest of the membrane by a narrow isthmus as illustrated in figure 62 (pl. 14). Necrotic and cystic areas are frequently present, and mucopolysaccharide is distributed widely in large droplets. Some of the affected membranes consist primarily of fibrocytes with debris and generalized necrosis throughout. Granulocytes are present in large numbers, often being associated with cysts. They may be aligned in rows between densely staining affected regions and the unaffected regions of the membrane. The cysts will be examined in detail in our consideration of graft-versus-host and host-versus-graft reactions. Attention is called, however, to the large cyst in figure 62 (pl. 14), which shows a region of necrotic tissue encapsulated by epithelium. Study of figure 46 (pl. 10) suggests that, in invading the membrane, the graft follows a route from the lower right-hand corner diagonally across the photograph. Near the blind end of this channel the epithelium appears to disperse, some of the epithelial cells becoming fibrous and entering the general mesenchymatous mass. The lower part of this photograph is achromatic, containing a localized necrotic region.

Recovery at fifteen days: eight days postimplantation. The conditions at this stage are so much like those described for the 13th day, i.e., large numbers of hemocytoblasts and granulocytes, necrotic regions, that, were it not for one finding of unusual interest, it would be unnecessary to consider it in detail. The consistency of these observations permits us to describe them by referring to a typical example. In the membrane shown as figure 47 (pl. 10), the blood vessels of the affected region are filled not with erythrocytes but with what appear to be bare nuclei, irrespective of the staining procedures used. Furthermore, many of these so-called nuclei appear to have left the channels, being distributed widely throughout the affected region. A re-examination of the large blood vessel lying adjacent to the affected region revealed that the "nuclei" were, in fact, erythrocytes (not small lymphocytes) but that they were so pressed together that they were abnormal in shape. Also, numerous fractured and degenerating erythrocytes are seen. These observations are important, for the characteristics of the residual nuclei of these modified erythrocytes have a consistency that makes possible their identification throughout the membrane, so that the nuclei can be traced to cysts where they are accumulated.

Recovery at seventeen and eighteen days: ten and eleven days postimplantation. It is now appropriate to turn to the dramatic changes associated with cyst formation; before doing so it is necessary only to illustrate the range of reactions possible at the 10th or 11th postoperative day by a comparison of figures 48 and 49 (pl. 11). In figure 48, remnants of the graft lie on the surface, over an affected membrane containing dense accumulations of hemocytoblasts and numerous granulocytes. At least three necrotic regions may be observed; these pale areas are relatively devoid of RNA staining. The graft itself has an outer covering of mesenchyme cells and some hemocytoblasts; closer to the membrane is seen only the pale, lightly staining material resembling the core of an intramembranous cyst, and finally immediately adjacent to the membrane a relatively clear region suggests a fibrous meshwork.

Figure 49, on the other hand, shows what appears to be a healthy graft resting on a membrane that is only mildly affected, although quite edematous, but contains a few nests of hemocytoblasts. A more careful examination of the graft itself, however, reveals that it contains not normal cell types but rather aberrant erythrocytes tightly packed together. The border between the graft and the membrane is made up of polynucleate giant cells. In the graft, remnants of arteries can be seen; the arterial walls have not undergone major changes. The nuclei of the erythrocyte-like cells of the graft, however, are often pycnotic.

We may summarize the consequences of interactions between the chorioallantoic membrane and grafts of adult spleen: (1) The graft attaches to the membrane within 24 hours, attachment being accompanied by an edema in the subjacent membrane. (2) By the end of the 2nd day, some grafts lie embedded within the membrane while others may remain on the surface. Changes in the histology of the mesenchyme of the membrane are observed first at this time in association with embedded grafts. (3) By the 4th postoperative day the adjacent membrane is modified, being characterized by dense aggregations of hemocytoblasts exceeding the volume of the original graft itself; granulocytes can be identified clearly. (4) At 5 days postimplantation (the 12th day of incubation) and later, an additional reaction is observed marked by clearly identifiable necrotic regions. Variations in the population of hemocytoblasts and granulocytes are apparent.

Graft-versus-Host and Host-versus-Graft Reactions

From the foregoing description of the differentiation and growth elicited in the chorioallantois and embryonic spleen after a graft of homologous adult spleen, it is evident that the reactions of both the membrane and the host's spleen embrace several common features, the reactions of the membrane occurring before those in the spleen, owing to its immediate relation to the graft. Reactions in both sites culminate in the destruction of the tissues; it will be recalled that DeLanney and Ebert (in Ebert, 1957) advanced the idea, as a working hypothesis, that the graft of immunologically competent adult spleen mounted an immune reaction against its host. Evidence has accumulated steadily favoring the idea that the reaction is, at least in large part, an immune reaction, but whether graft-versus-host or host-versus-graft, or whether both types of responses must be evoked, has not been clear until recently. It is necessary to consider possible alternatives to the graft-versus-host reaction; the possibility of an abortive, or incomplete, host-versus-graft reaction has been raised (Ebert and DeLanney, 1960; Ebert and Wilt, 1960). Before attempting to evaluate the evidence, which springs from several approaches, we propose to illustrate these reactions to provide a firm cytological and histological base for the discussion to follow.

Manifestations in the host's spleen. Figure 32 (pl. 7) will recall the appearance of the multiple foci of necrosis in the embryonic spleen 11 days after implantation of a graft of adult spleen. At recovery these necrotic cysts appear as knobbed, usually blanched, occasionally hemorrhagic, areas on the surface of the spleen. In figure 50 (pl. 11) a cross section of one of these cystic areas is seen. The center of the cyst is always filled with an acidophilic aggregation containing dense basophilic spots suggesting pycnotic nuclei. The border of the cyst is composed of a ring of giant cells. Figure 50*a* (pl. 11) is a higher magnification of the giant-cell region showing the necrotic central cystic aggregation on one side and the poorly defined host mesenchyme on the other. We have described necrosis in the host's spleen as early as the 12th day of incubation, 5 days after implanting a graft of homologous spleen. Usually the foci at this stage are small aggregates of damaged cells, but only 1 day later the typical cystic reaction (fig. 51, pl. 12) can be seen clearly; a central basophilic mass, presumably of nuclear origin, is surrounded by giant cells. The organization of the cysts suggests, in contrast to the interpretation advanced by Boyer (1960), that first a localized center of destruction arises, which elicits a response on the part of the host; as the cells in the center of the cyst become moribund the host contributes to the outer giant-cell zone from the surrounding mesenchyme.

We must reiterate that the splenomegaly with which we are concerned is not invariably accompanied or followed by cyst formation; on the other hand, it does almost invariably involve enhanced granulocytopoiesis (Danchakoff, 1916). Is the myelogenous trend also symptomatic of a graft-versus-host reaction, or is it a host reaction to the graft? Clarkson and Karnofsky (see Ebert and DeLanney, 1960) have elicited splenomegaly by intravenous injections of mouse ascites tumor cells; no necrotic infarcts were observed, yet several of their slides that we have been privileged to examine contain more granulocytes than the controls. Croisille (1958) reported a significant increase in the weight of the spleen of the host after injection of cell-free extracts of spleen but made no mention of cystic regions. Van Haeften (1958) also observed splenomegaly in the host after introducing a cell-free homogenate of spleen in the chorioallantoic membrane, and, although a myelogenous trend was observed within the membrane, the spleens of the host embryos were found to be normal, no mention being made of cystic or necrotic centers. As we shall see, the question of a possible host reaction is raised also by Van Alten and Fennell (1959) and DeLanney and Ebert (1959*a, b*).

Manifestations at the site of implantation. Figure 52 (pl. 12) shows a chorioallantoic membrane, harvested 10 or 11 days after implantation of adult spleen, in which cystic regions identical in appearance to those found in the spleens of host embryos of comparable age are observed. Figure 53 (pl. 12) is an enlargement of the cyst seen at the extreme edge in the previous figure. The surrounding rim of giant cells is laden with acidophilic droplets. The cystic region is connected to the thickened epithelial surface as shown in figure 54 (pl. 12). A few granulocytes are found within this region.

In contrast to the degeneration and encapsulation found in the membranes of older embryos, the first sign of graft-host antagonism is similar to that observed in the spleen (fig. 24, pl. 5): a small disorganized region of necrosis. This condition was described for the membrane of the 12-day-old embryo, 5 days postimplantation, in figure 41 (pl. 9). Boyer (1960), having Burnet's (1959) clonal selection hypothesis in mind, postulates for these cysts that each lesion may arise as a result of the effective implantation of a single donor cell, a postulate that cannot be supported on the basis of the present study of the architecture and cytology of the cyst.

Manifestations at other sites. Figure 55 (pl. 13) shows a cross section of 16-day-old embryo thymus 9 days after implantation of a fragment of adult spleen to the chorioallantoic membrane. The concentration of acidophilic material in the center of the section is not found in the normal thymus at this stage, but pending completion of an intensive examination of thymus we can conclude only that it is a departure from the normal under the impact of a graft of immunologically competent tissue. Boyer (1960) indicated that lesions form not only in thymus but also in liver, proventriculus, bone, muscle, and subcutaneous tissue. It would be interesting to know whether her statement that "widespread granulopoiesis occurred" applied to the thymus.

Ebert (1957) has described the consequences of implanting pieces of adult spleen into the coelom of 4-day-old chicks according to the technique of Dossel (1954) and recovering 6 days or more later. By this procedure adult spleen is introduced to the host before the host's own spleen has more than just begun to appear as a small mesenchymatous ridge; the graft causes not only a marked splenomegaly but also a breakdown of the vascular bed leading to hemorrhage and massive areas of stasis in the extremities.

Second- and third-set phenomena. Previously the graft-versus-host reaction (or what we now believe to be a complex of graft-host, host-graft reactions) has been transferred serially by intracoelomic and chorioallantoic transplantation of embryonic host spleen after a primary graft of adult spleen (Ebert, 1957). In addition, Simonsen (1957) has been able to propagate the reaction serially by intravenous injection of spleen cells or whole blood. In view of the pronounced effects observed in the chorioallantoic membrane, including cyst formation, the question was raised whether a fragment of the affected membrane could, in turn, upon implantation to a second membrane, evoke a reaction in the new membrane or the host's spleen (DeLanney and Ebert, 1959*a, b*).

Figure 56 (pl. 13) illustrates a section of host's spleen after such a second-set implantation of chorioallantoic membrane. Two features are noteworthy: there is a precocious appearance of heterophilic granulocytes; and it is difficult to identify hemocytoblasts with certainty. In fact, as can be seen in figure 57 (pl. 13), staining with toluidine blue reveals only a few hemocytoblasts. This 11-day-old spleen by comparison with either an 11-day-old control or an 11-day-old first-set host spleen (figs. 20, 21, pl. 4) is almost entirely devoid of RNA. The question may be raised whether under these conditions hemocytoblasts are the precursors of granulocytes. Evidence of precocious granulocytopoiesis, coupled with other evidence including an average weight increase at the 11th day of 18 per cent instead of the 8 per cent observed in first-set reactions, necrosis which in first-set reactions does not appear until the 12th day, and mucopolysaccharide droplets at the 11th rather than the 12th day, suggests that the splenic mesenchyme cells are channeled in the direction of granulocytes.

The second-set reaction is clearly identifiable in the chorioallantoic membrane having characteristics similar to those in the spleen. Figure 58 (pl. 13) shows a fragment of previously affected membrane now in residence as a graft in a newly affected membrane which contains a large necrotic zone on the 4th postoperative day. Figure 59 (pl. 14) is a section of the same membrane stained with toluidine blue. Attention is called to the achromatic zone directly below the graft; this region is separated from the edematous but otherwise mesenchymatous membrane by heterophilic leucocytes.

Figure 60 (pl. 14) illustrates a third-set implantation of affected chorioallantoic membrane to chorioallantoic membrane; figure 61 (pl. 14) is a view of the same graft stained by the Himes-Moriber technique. Immediately opposite the graft, close to the allantoic epithelium, there is a dense region suggestive of early cyst formation.

III. SELECTIVE UPTAKE OF SUBCELLULAR FRACTIONS BY THE CHICK EMBRYO AND MODIFICATION OF PATTERNS OF SYNTHESIS IN THE HOST

We turn next to the question, raised earlier, whether experiments based on the administration to embryos of constituents of immunologically competent adult tissues, in the form of grafts, cell suspensions, homogenates, or particulate fractions, contribute effectively to the hypothesis of selective chemical coordination among cells of identical type by exchange of type-specific compounds, or whether such experiments must be viewed apart from such tissue-specific regulation of differentiation and growth. After assessing our own findings, in relation to those of others, we are inclined to answer the latter question in the negative. We believe that the evidence available demonstrates a reaction on the part of the host. The reaction of the host which we view as a tissue-specific reaction may be masked by the graft-versus-host reaction or by an incomplete host-versus-graft reaction; nevertheless, it must be considered significant. The difficulty in interpretation stems from the fact that the responses to both nonspecific antigenic stimuli and specific stimuli are essentially the same; they must be distinguished by differences in the extent and the time course of the reaction.

It is clear that the proper setting or framework for opening the discussion is the field of immunology, and, at least at the outset, more specifically the field of transplantation or cellular immunity. This conclusion is dictated by the following lines of evidence:

1. Recent work using spleens from inbred lines (Mun, Kosin, and Sato, 1959) demonstrates that interstrain grafts produce a greater effect than intrastrain grafts, a finding expected if the reaction was an immunological one. Adult spleen grafts from donors of the S line (selected for leucosis susceptibility) affected spleens in embryos of the same line to a lesser extent than in embryos of the R line (selected for leucosis resistance); the converse experiment produced the same results, although the effect of R spleen on S hosts was not so marked. S line donor spleens implanted to F_1 (R×S) hosts produced an effect similar to interline S into R grafts, but R donor line spleens to the F_1 produced an effect comparable to the intraline combination. These findings agree essentially with those of Cock and Simonsen (1958), who also used inbred White Leghorn lines. In their study, when blood from adult birds of line I was injected into newly hatched F_1 chicks (C×I), the host livers and spleens were affected drastically, but when F_1 blood was injected into F_1 chicks only a slight effect was observed.

2. The ability of splenic grafts to affect the host varies with the age of the donor; grafts of spleen from embryonic donors have little or no effect, the effectiveness of grafts increasing with progressively older donors up to several weeks after hatching, roughly corresponding with the attainment of "immunological maturity" (DeLanney, unpublished findings; Mun, Errico, and Ebert, in Ebert, 1960; Solomon, 1960).

3. X irradiation of adult chicken spleen removes its ability to affect the homologous organ of the embryo. According to Mun, Kosin, and Sato (1959), after irradiation at 205 to 810 r, splenic grafts retain their effectiveness; at higher doses, between 1230 and 1640 r, a significant decrease in effectiveness is observed; and at doses above 1845 r all activity is lost. Kryukova (1959) also showed that, whereas nonirradiated homologous spleen cells and cells X-irradiated at 300 r caused approximately sixfold enlargement of the embryo spleen, cells irradiated with 900 and 1200 r had little or no effect.

4. The reaction is quantitatively organ-specific and class-specific, but not species-specific. Of 11 donor tissues studied by Ebert, only spleen, thymus, and liver (in that order) were effective, but Van Alten and Fennell (1959) and Billingham and Silvers (1959) respectively have shown that grafts of small intestine and skin also affect the host spleen. Each of these organs contains immunologically competent cells; hence, it appears consistent to

state that the reaction is tissue-specific. Perhaps the quantitative organ specificity reflects the proportion of immunologically competent cells a tissue contains. Spleen of other avian species (duck, turkey, and pheasant) produces some effect on the host's spleen, but never as much as homologous spleen. Yet mouse spleen (Ebert, 1951) and guinea pig spleen (Mun, Kosin, and Sato, 1959) are completely ineffective.

Clearly, the first line of evidence may be regarded as basic, the others providing mutual support; X irradiation may destroy capacities of cells other than immunological competence, and the association of immunologically competent cells in the graft and the resultant splenomegaly offers only indirect evidence. Although points 2, 3, and 4 are not fully meaningful alone, they acquire more significance when the experiments with inbred lines of animals are considered.

Accepting the argument that splenomegaly after a graft of adult spleen encompasses immune reactions, we may take up next the nature and site of those reactions. The effective factors can be transferred serially by intracoelomic and chorioallantoic transplantation of embryonic host spleen following a primary graft of adult chicken spleen. For example, Ebert (1957) found that grafts made to the coelom of the chick embryo before the appearance of the spleen affect the host's spleen by the 10th day. The question was raised whether such a stimulated 10-day embryonic spleen (normally not an effective donor) might be a competent donor. Grafts were made to a number of 4-day-old embryos, which were permitted to develop until the 10th day, when the host spleens were harvested and used as donors for the second-set graft, the experiment being carried through four transplant generations. The activity was not diluted by serial passage, but was maintained relatively constant. DeLanney and Ebert (1959*a;* Ebert and DeLanney, 1960) have reported also the serial transfer of the reaction through three transplant generations by fragments of chorioallantoic membrane previously in contact with a primary adult graft. As we have seen, the transplantation to the membrane of 7- or 9-day-old embryos of fragments of chorioallantois taken from reactive sites surrounding the original spleen implant results in intensified reactions in second and third generations characterized by extreme conditions of vascular breakdown, widespread pycnosis, and aggregates of giant cells.

Simonsen (1957) demonstrated a comparable deleterious effect on the host spleen by intravenous injection of juvenile or adult chicken leucocytes or spleen cells to the 18-day-old chick embryo, a reaction which he serially transferred without dilution for nine generations. According to Simonsen the recipients have to be of an age in which tolerance of homologous cells can be induced; the donors must be old enough for an immune response.

Moreover, serial transfer experiments appear to argue for the transfer of viable cells. Simonsen suggested initially that the increase in size of the host spleen is due solely to the proliferation of adult donor cells populating the embryonic spleen, the proliferation being the result of antigenic stimulus (cf. pp. 61–62). Terasaki (1959) has offered evidence which indicates that the splenomegaly following injection into embryos of blood cell suspensions may be attributed to lymphocytes, not to monocytes or thymocytes. Yet, although the authors have long recognized that colonization and proliferation of donor cells account for some of the effects of splenic grafts, they are not convinced that they are the sole cause of the splenomegaly. The interpretation is made difficult, in part, by the fact that others (Simonsen, 1957; Billingham, 1959) have equated the effects of intravenously inoculated cells with those of chorioallantoic grafts. But perhaps the greatest difficulty in accepting colonization and proliferation as the sole cause of splenomegaly stems from our own studies.

The cellular nature of the response which has been documented here points to the host as the principal source of proliferating cells. Moreover, earlier studies using radioactively labeled grafts, though not decisive, revealed a predominant localization of material in the homologous organ but precluded a massive transfer of cells. That our earlier skepticism of the hypothesis of colonization and proliferation is justified is borne out by recent experiments that are beginning to clarify the contributions of donor and host cells. Biggs and Payne (1959) have presented significant preliminary findings in a study in which they identify proliferating donor cells in chick embryos injected with adult chicken blood. In the chicken the fifth largest chromosome is paired in the male, unpaired in the female. Cockerel blood was injected into 14-day-old embryos which were sacrificed at day 18, demecolcine being administered 3 hours before sacrifice. In enlarged spleens taken from female embryos, male chromosomes can be identified, proving the localization of some donor cells. The relatively high number of dividing female cells, however, suggests to Biggs and Payne that an appreciable component of the splenomegaly is provided by cells of the host. Moreover, Simonsen and Jensen (1959) have reported cases in which immunologically active donor cells are not necessary for homologous stimulation. Their conclusion is based on an analysis of splenomegaly in transplantation chimeras in the mouse, in some of which donor cells could not be detected in enlarged spleens, while other donor cells appeared to have lost or never acquired reactivity against the recipient. The evidence available, therefore, suggests that, after the intravenous injection of blood or spleen cell suspensions, donor cells may or may not colonize the host's spleen. Moreover, such colonization need not result invariably in splenomegaly, which may result in whole or in large part from proliferation of cells of the host. Hence, in agreement with Simonsen and Jensen, we believe that, after administration of spleen cells by intravenous inoculation, the embryonic spleen may serve as a "battleground" and that either or both graft-versus-host and host-versus-graft reactions can occur. Tardent, Mun, and Ebert (in Ebert, 1960) have completed the initial stages of a large-scale investigation in which grafting and intravenous inoculation approaches are being compared, tracing the donor cells by labeling them with tritium thymidine. To date the findings after inoculation lend strong support to the view just enunciated, i.e., that colonization may occur, and that the contribution of donor cells is highly variable. On the other hand, these authors have been unable to detect substantial numbers of donor cells in the embryo's spleen after the incorporation of labeled chorioallantoic grafts, even at 24 and 48 hours after grafting. These negative findings are difficult to assess, especially in the light of evidence of colonization presented by Mun, Errico, and Ebert (in Ebert, 1960). In their experiments, spleen cells from an original 14-day-old embryonic donor were propagated serially through eight weekly passages by chorioallantoic grafting. The immunological competence of these cells to produce a graft-versus-host reaction matured progressively even though they were being maintained in an embryonic environment. Taken as a whole, the evidence from these two lines of research supports the conclusions of Biggs and Payne (1959); although splenic grafts must contribute some cells to the host, a major contribution by the host is required.

Further evidence for a response on the part of the host stems from the following experiments reported by Ebert and DeLanney (1960). In exploring the relation between the age of the donor and the effectiveness of the graft, fragments of 17- and 18-day-old embryonic spleen were implanted on the chorioallantoic membrane. Although the findings in DeLanney's and Ebert's laboratories differed slightly with respect to the presence or absence of splenomegaly, they were consistent in that degenerative or necrotic changes in the host's spleen were not observed. Figure 45 (pl. 10) shows a well vascularized tissue mass on the allantoic surface of the chorioallantoic membrane; although this mass superficially resembles affected membrane, it is in reality one half of a 17-day-old embryonic spleen which after being grafted to the membrane was displaced to the interior. Figure 63 (pl. 14) shows a cross section of membrane into which an entire 17-day-old embryonic spleen has penetrated. Other than a slight edema there has been no effect on the membrane, which has expanded to permit intramembranous residence of the graft. It will be recalled that the predominant cell type seen in 17- and 18-day-old normal embryonic spleens is the granulocyte. Granulocytes can be seen in considerable number in the graft; there is some pycnosis.

The ineffectiveness of embryonic spleen cells to affect the host led us to question whether the failure results from their inability to receive an antigenic stimulus or from their inability to respond. In exploring this question we grafted fragments of adult chicken heart to the chorioallantoic membrane, ventricle being selected because it lacks immunologically competent cells. First-set grafts were, in fact, completely ineffective. But, when second-set grafts were made in which fragments of spleen and chorioallantoic membrane from the first-set recipients were transplanted, positive reactions were observed. Second-set grafts of spleen from "heart-stimulated" hosts produced spleens in the second hosts averaging 16.1, 18.8, 16.9, 19.8, and 12.2 mg., respectively (8, 8, 8, 8, and 6 days of exposure to stimulus, respectively) by comparison with mean host-spleen weight of 12.7 mg. after grafts of normal 17-day embryonic spleens (Appendix, table 2). Nine spleens were found to be cystic. When "heart-stimulated" chorioallantoic membrane was used as a second-set graft, the mean weights of host spleens differed from the controls, but not strikingly. Fifteen of 55 spleens in one series, and 16 of 77 in another, exceeded the maximum weight attained by the appropriate controls. Earlier, we asked whether these results could be explained on the basis of the graft-versus-host reaction. Is there a transfer of a small population of immunologically competent cells from the heart graft? Only 4 embryos out of many hundreds have shown a first-set reaction attributable directly to grafts of heart; moreover, it appears unlikely that a longer period is required for the proliferation of a few active cells of the immune series from the heart, that period being afforded by transfer to a second embryo. Spleens from hosts which carried heart grafts are consistent; they do not differ from the controls; there is no suggestion of the proliferation of even a small population of donor cells. The effect of second-set grafts of spleen is greater than the effect of second-set fragments of chorioallantoic membrane.

Furthermore, Clarkson and Karnofsky (see Ebert and DeLanney, 1960), by means of a fluorescent antibody technique, arrive at a similar conclusion: mouse ascites tumor cells injected into the chick embryos cannot account for the splenomegaly that results; a host response is required.

Finally, in a brief article embodying findings of unusual interest, Burnet and Boyer (1960) argue that immunologically competent cells lose specificity after passage in the chick embryo; the findings, however, might be interpreted as revealing a response on the part of the host. They first reaffirm and extend the earlier statement by Boyer (1960) that when leucocytes are placed on the chorioallantois they form focal lesions within 4 to 7 days, 2×10^4 leucocytes giving rise to lesions as large as 2 to 4 mm. in diameter. Next they compare isologous and homologous combinations using two inbred strains of chicken, designated A and B. In isologous combinations (A into A, B into B) the production of lesions by leucocytes varies considerably, the ratio of embryos bearing full numbers of foci, to those with few foci, to those with no foci, being of the order of 20:2:14, 1:4:11, and 2:1:23. However, when cells of either strain A or strain B are placed in embryos of the opposite strain or of other random stock, the ratios shift markedly, for example 26:3:1, 14:0:1, 16:0:0. In other words, the incidence of lesions increases sharply. Burnet and Boyer assume, as do Burnet and Burnet in a later article (1960), that the cells in these foci are of donor origin. When embryos are inoculated, nodular lesions occur also in the spleen (less regularly in other organs). When suspensions of cells from the spleens of these recipient embryos are now transferred to the membranes of secondary hosts, they produce focal lesions.

Burnet and Boyer reiterate that the simplest explanation holds that the cells are descendants of those that were originally inoculated. But when the specificity of these cells is tested employing the inbred stocks, specificity is seen to have been lost, irrespective of the type of embryos used for passage. The data may be summarized: original donor A in recipients A 8:2:0, in recipients B 4:0:0; original donor A in recipients A 20:1:0, in recipients B 6:1:1; original donor B in recipients A 21:0:0, in recipients B 21:3:6.

Burnet and Boyer, who find that they can maintain the reaction through only three to five passages, in contrast to Simonsen's nine passages (p. 75), attribute the loss of specificity to the first step in a series of changes in which cells lose the capacity for the graft-versus-host reaction. The possibility that the initial response is on the part of the host embryo is not considered likely enough even to be mentioned by Burnet and Boyer. They do not describe the lesions in the host's spleen in this article, referring to Boyer's (1960) earlier description of granulocytopoiesis.

In view of several lines of evidence summarized above and the granulocytic nature of the response indicated by Boyer, we may ask whether the findings of Burnet and Boyer may reflect not a loss of specificity of colonized donor cells but rather a host response.

What significance can be attributed to the granulocytes? This question is, indeed, significant in view of the intense granulocytic response to grafts of homologous spleen. Yet a fully meaningful answer cannot be given. From time to time eosinophils have been credited with a role in immune reactions (Speirs, 1958), but whether they may be concerned with the problem of recognition or uptake of antigenic material or with the response, *per se,* is not understood. We have described the precocious appearance of both heterophils and eosinophils in affected spleens. The heterophils appear before the eosinophils just as they do in the normal development of the spleen. Granulocytes are believed ordinarily to be derived from hemocytoblasts, and in the affected spleens increasing numbers of hemocytoblasts and increasing numbers of granulocytes are concomitant. On the other hand, in second-set reactions, especially in the chorioallantoic membrane but also in the host's spleen, few hemocytoblasts are seen, although granulocytes occur frequently. Are the granulocytes simply marshaled from other sites in the embryo? The occurrence of granulocytes in the apparent absence of hemocytoblasts does suggest that the relation between hemocytoblast and granulocyte may not be obligatory. It is clear also that, under the conditions described, granulocytes are capable of mitotic activity. Granulocytes in mitosis have been seen not only in the spleen but also in the membrane.

It is pertinent to ask also whether the allantoic epithelium of the chorioallantoic membrane may be stimulated to produce hemocytoblasts, leading to granulocytopoiesis. Evidence of activity in the allantoic epithelium has been presented, and it may be that this tissue, too, is altered and precocious in its functional relationships. The evidence advanced by Ackerman and Knouff (1959) for the endodermal origin of hemocytoblasts leading to lymphocytes is cogent (see also Ruth, 1960). It may be recalled that we have described the aggregation of substantial numbers of hemocytoblasts, not adjacent to the graft, but rather closely associated with the allantoic endoderm. Until labeling experiments have been completed, either cytologic or radiologic, the origin of the granulocytes in the membrane cannot be regarded as established, but we favor the view that at least a substantial contribution may be the result of differentiation of cells in the membrane itself.

A few words need to be said about other cell types.

The possible role of the *small lymphocytes* in these reactions is enigmatic. The status of the small lymphocyte is a matter for debate, ranging from Medawar's (1957) belief that the lymphocyte is a terminal cell to the opinion of Taliaferro (1949) that lymphocytes can develop into macrophages or plasma cells, and Burnet's (1959) view that a small lymphocyte may differentiate variably. In grafting adult spleen we are contributing a rich source of lymphocytes; we should expect plasma cells to be present also. Yet we have been unable to identify in the host's spleen cells even resembling small lymphocytes. In the adjacent membrane, however, in first-, second-, and third-set implantations, we have observed small lymphocytes both normal and aberrant; possibly the latter are transitional stages in their further differentiation, but whether such differentiation occurs is a matter of conjecture.

Plasma cells have not been observed. We have been unable to see cells with the cytocentrum making a halo to one side of the nucleus. Further attempts to identify plasma cells or other pyroninophilic cells are in progress.

[*Note added in proof:* Mori has now succeeded in identifying plasma cells in both the chorioallantoic membrane adjacent to grafts of homologous spleen and the host's spleen (Carnegie Inst. Wash. Year Book *60,* 1961).]

To what extent are *erythrocytes* involved in the reactions described above? Danchakoff (1916) contended that localized conditions of anoxia produce sites of erythropoiesis, which she described in the host's spleen. We are unable to confirm her observations of erythropoiesis despite the fact that the affected spleen is marked by a lack of arterial channels which should lead to anoxia and should allow erythropoiesis if stem cells are present.

In our opinion, erythrocytes are involved only in the sense that they appear to be "targets" of immune reactions, judging by the frequency with which agglutinated and fragmented cells occur in the chorioallantois adjacent to grafts of adult spleen.

Further evidence of a response on the part of the host is afforded by a consideration of the relations of multinucleate *giant cells* to cystic areas in the chorioallantois and spleen. When the giant cells are oriented around a cyst, their inner edges appear to be "frayed out" into the cyst itself, whereas the outer surface is usually rounded. The architecture of the cyst in relation to these giant cells makes it difficult to conceive of the cyst's resulting from centrifugal expansion, i.e. from continued proliferation of descendants of a single donor cell; instead, these relations point strongly to a reaction of the host (cf. Isacson, cited by Boyer, 1960).

In the discussion to follow, we shall assume that the splenomegaly under consideration is more than a graft-versus-host reaction. In fact, we suggest that it may embrace at least three discrete reactions: (1) graft-versus-host (whether the immune reactions of the graft are cell-mediated or mediated by antibodies in the conventional sense is not clear); (2) an incomplete host-versus-graft reaction, in which the host spleen may recognize an antigenic stimulus, yet fail to react during the initial period of the stimulus, only to react when challenged a second time; and (3) a specific precocious differentiation of granulocytes from indifferent cells of the host's membranes, possibly the allantoic endoderm, and the host's spleen and other organs.

We have only touched on the distinction between (2) and (3). Having abandoned the "economical" hypothesis of colonization and proliferation as the sole mechanism, to focus attention on the host, why can we not argue, again "economically," that the host's reaction is a simple proliferation in response to antigenic stimuli? Obviously we cannot, for that argument is denied by all the evidence bearing on the tissue specificity of the reaction, aside from the experiments of Clarkson and Karnofsky, which were discussed above.

Perhaps the principal consideration that cannot be reconciled with the argument that the host's cells are stimulated to proliferate by antigens of the graft springs from experiments of others using a variety of tissues, e.g. those of Andres (1955), which indicate the stimulatory effectiveness of frozen, thawed, triturated tissues. In fact, devitalization has been shown to improve specificity and stimulatory effectiveness. In an effort to define more precisely the nature of the substances transported from graft to host tissue and the manner in which they act, tissues of adult chickens were labeled, as in earlier experiments, by the injection of methionine labeled with sulfur 35. These organs were stored in the frozen state, after which they were homogenized, and a small amount of the homogenate was injected directly into the chorioallantoic vessels of the 9-day embryo. The results of these experiments, in which labeled kidney and spleen homogenates were injected on either the 9th or 10th day of incubation with recovery after 24 hours, show that the exposure of the embryo to a very small quantity of tissue homogenate for only 24 hours results in a differential incorporation of the label in the homologous organ. The differential is not of the same order as that obtained with living transplants, acting over several days, but it is consistent and reproducible.

The next step was the fractionation of the homogenate following standard (sucrose) procedures for the separation of nuclear, mitochondrial, microsomal, and supernatant fractions. The findings show clearly a selective localization only of the microsomal and supernatant fractions, and not of the nuclear and mitochondrial fractions (Appendix, table 3). The properties of the microsomal and supernatant fractions that determine the specificity or are essential to the localization are nondialyzable, and are destroyed by heating at 80°C. for 5 minutes, and by ashing. These experiments dealt with only one aspect of the problem, namely, predominant localization; they did not contribute to an understanding of how the homologous organ is stimulated. The small quantities of these subcellular fractions tolerated by the embryo do not result in a significant growth stimulation. It was suggested that a continuing supply of injected materials may be necessary in order to bridge the gap between the transplantation and the injection experiments.

Experiments employing filters which preclude cellular transfer from graft to host have not yet been fully convincing. In these experiments, initiated with the advice and aid of Dr. J. Mulnard, splenic grafts encased in membrane filters evoked a significant increase in the size of the homologous organ of the host. The increase was of the order of 30 per cent, significant, but far less than the several hundred per cent increase attained by grafts in the absence of any filter (Appendix, table 4).

At this point, it was questioned (Ebert, 1958, 1959*a*) whether, in view of the ultimate destruction of the host tissues, the use of organs like spleen for further tests of the hypothesis of tissue-specific regulation of differentiation and growth was advisable. Recent developments demonstrate that this note of skepticism was premature. Croisille (1958) has reported that the intravenous inoculation, in a series of three injections, of a cell-free extract of adult chicken spleen into the chick embryo beginning on the 3rd day of incubation results in a significant increase of 25 per cent in the size of the host spleen. The recipients were recovered at 12, 14, 16, 17, and 18 days of incubation; no evidence of cysts or lesions related to the "graft-versus-host" reaction was reported. Similarly extracts of liver stimulate embryonic liver growth when injected *in ovo*. Croisille reports, however, that attempts to demonstrate similar effects *in vitro* failed. Van Haeften (1958) implanted cell-free homogenates of adult spleen, thymus, and striated muscle on the chorioallantoic membranes of 9-day-old embryonic hosts. The spleen homogenate provoked a strong myeloid reaction in the chorioallantoic stroma as well as marked hypertrophy of the host spleen. Histologically the enlarged spleens were said to be normal. After inoculation of spleen homogenate, there is also an increase in all cell types in the circulating blood; after thymus homogenate, lymphocytosis and eosinophilia.

These findings prompted Ebert and DeLanney to reexamine their own earlier results, which had demonstrated predominant localization, but not stimulation, with microsome preparations. It seemed particularly important since Croisille's data on stimulation by extracts paralleled quantitatively the findings using membrane filters. It was decided to examine the efficacy of a fraction prepared according to the procedure described by Moloney (1956) for purification of the Rous sarcoma virus, which one of us had been employing (Ebert, 1959*b*) in experiments in which combinations of the Rous sarcoma virus and a tissue-specific microsome fraction have been shown to be effective homoiogenetic inductors. In the experiments described (Ebert and DeLanney, 1960), it must be reiterated, the virus was not included; the technique commonly applied for virus purification was employed for the extraction of spleen and other organs. The method employs preliminary hydrolysis of the tissues by hyaluronidase, the addition of protamine sulfate, followed by tryptic digestion, and separation of the microsome fraction by differential centrifugation. Tissue fractions obtained by this procedure were administered to the embryo by two routes, intravenous injection (Terasaki and Cannon, 1957) and inoculation directly to the chorioallantoic membrane. The former route is highly effective. The inoculation of 0.1 to 0.15 ml. of a splenic microsome fraction on the 9th or 11th day resulted in a highly significant increase in the weight of the host spleen (Appendix, table 5), as compared with the sham-operated controls and with embryos receiving microsome fractions from other organs.

Should one attempt a synthesis of findings of granulocytopoietic splenomegaly after grafting with the stimulation after administration of cell-free extracts? Perhaps the two phenomena are completely different; obviously the former is the more complex. Like spleen (and related) cells, however, splenic microsomes have the capacity of predominant localization and of stimulating granulocytic proliferation in the homologous centers of the host. They appear to differ in that (at least thus far) the less dramatic, but significant, splenomegaly after microsomal administration has not resulted in the characteristic deleterious cystic reaction. Although there is no evidence for serial transfer of activity of microsomes and it is premature to argue that they are "infective," *sensu strictu*, it is becoming increasingly clear that the "building block" hypothesis offered by Ebert (1954), in which it was suggested that the graft provided a supply of specific materials which contributed to the growth of the homologous organ, is oversimplified. It appears more likely that the observed splenic growth includes a phenomenon of epigenetic recombination in which adult particles are carrying on synthesis in the homologous embryonic environment. By epigenetic recombination (cf. Ebert, 1959*b*; Ebert and Wilt, 1960) we mean the exchange of functional biochemical units.

Ebert has reported that the exposure of the chorioallantoic membrane of the 11-day-old chick embryo to a mixed inoculum composed of a microsomal fraction of adult or late embryonic cardiac muscle and the Rous sarcoma virus, extracted together by the technique of Moloney (1956), results in the formation of tumorous masses indistinguishable grossly from those produced by the inoculation of the Rous sarcoma virus. Contractions have not been observed in these masses. A study of sections reveals differences in the two groups. Inoculation with Rous sarcoma virus evokes the ectodermal and mesodermal lesions characteristic of the tumor. Inoculation of the mixture evokes masses which contain to a varying degree, intermingled among the mesodermal sarcoma cells, muscle and muscle-like elements. Of 603 masses recovered from membranes inoculated with the mixture, 167 (27 per cent) contain muscle to some degree. These findings may be contrasted with the absence of muscle in 291 masses after the inoculation of Rous sarcoma virus. The implantation on the chorioallantois of a cardiac microsome fraction alone failed to produce tumor masses; in fact, the only response was an occasional example of keratogenic metaplasia in the chorionic epithelium. Masses resulting from the combined inoculum were cut into fragments which were in turn transplanted to the membranes of new 11-day-old embryonic hosts, in an effort to enhance the differentiation of muscle. On the contrary, however, the extent and frequency of muscle formation were reduced drastically in these secondary tumors.

The complexity of the system employed requires that these findings be interpreted cautiously. Although the findings are not altogether consistent, taken as a whole they must be considered meaningful. The contrast between the findings when either the cardiac microsome fraction or Rous sarcoma virus alone is employed and those when the combined inoculum is used is striking and compels consideration. Yet it must be pointed out that there exists in the literature at least one report of the formation of myocytes in the chorioallantois after inoculation of a cell-free muscle extract without the addition of virus.

Van Haeften (1958) added to the membrane a saline homogenate, said to be free of intact cells, of striated muscle of the adult chicken. He reported that within 2 days spindle-shaped cells showing the characteristics typical of myoblasts appear, which after another 10 days acquire the features of more mature mononuclear myocytes. They lack cross striations, yet are believed by van Haeften to be muscular in nature. In the experiments reported by Ebert (1959*b*) cardiac microsomes alone evoked nothing more than an occasional keratogenic metaplasia.

Another report bearing on the last-mentioned study is one by Oker-Blom and Standström (1956), who added to the chorioallantois Rous sarcoma virus mixed with either crude fresh muscle extract derived from the suckling mouse or a mouse muscle extract partially purified with bentonite. The experiments were performed with another goal in mind, as controls for mixtures of Rous and coxsackie viruses, and only a passing comment is made about the masses that were recovered, to the effect that they were typical of the tumor.

Let us consider briefly other examples which suggest that epigenetic recombination by RNA or RNA-protein may be meaningful. Reiner and Goodman (1955) reported that during induction of gluconokinase in *E. coli* the rate of formation of the enzyme could be increased by an extract prepared from cells that already contained gluconokinase. This cell-free extract could also elicit enzyme formation in noninduced cells in the absence of inducer. Hunter and Butler (1956) have reported similar results with the inducible β-galactosidase of *B. megatherium*. Addition of RNA extracted from cells grown on lactose to cells growing exponentially on glucose stimulated enzyme formation by a factor of 2.5 over control levels; the nucleic acid had no inherent enzyme activity. Kramer and Straub (1956) examined the inducible penicillinase of *B. cereus:* a heated 1 *M* NaCl extract of a strain containing constitutive enzyme specifically induced a transient (20 minutes) and rapid penicillinase formation in cells of inducible strain in the absence of inducer. The receptor cells were pretreated with ribonuclease and subsequently washed; ribonuclease treatment of the extract, which had no inherent enzyme activity, abolished the effect.

The role of microsomal particles in protein synthesis has been treated in a number of reviews (Roberts, 1958); only recently, however, has clear-cut evidence of net synthesis of specific protein been advanced. Webster (1959) cites several species of microorganisms in which net synthesis of protein (as contrasted with simple amino acid incorporation) has been achieved in crude preparations. More conclusive, however, are the experiments of Webster himself (*op. cit.*), who has demonstrated the synthesis of soluble protein by ribonucleoprotein particles isolated from peas. When these particles are incubated with a mixture of amino acids, energy sources, and a polynucleotide fraction, the soluble protein in the medium increases appreciably. The cytoplasmic polynucleotide is required for net synthesis. The soluble protein is composed of several components and has enzymatic activity in hydrolyzing adenosine triphosphate.

None of the studies employing particles from animal tissues are fully satisfactory. Evidence stemming from studies of albumin synthesis are reviewed by Ebert (1958). Schweet, Lamfrom, and Allen (1958) have described the synthesis of soluble protein, mainly hemoglobin, in a system containing microsomal particles from rabbit reticulocytes plus soluble enzymes. Kern, Helmreich, and Eisen (1959) have shown the presence of antibody activity on microsomes. The activity induced in lymph nodes draining sites of injection of 2,4-dinitrophenylbovine γ-globulin into guinea pigs was specific for the DNP group. The presence of antibody on the microsomes (which cannot of course be taken as proof of its synthesis there) suggests a possible explanation for the finding of Sterzl and Hrubesova (1957) that the injection of nucleoprotein from adult animals immunized against *Salmonella* into unimmunized 5-day-old rabbits results in the rapid production of anti-*Salmonella* antibodies in these normally unresponsive young rabbits. As Ebert and Wilt (1960) have pointed out, both van Doorenmaalen (in Ebert and DeLanney, 1960) and Jankovic, Isakovic, and Horvat (1959) have failed in attempts to extend these findings to another system, the chicken precipitin system.

Were the experiments based only on the observation that anti-*Salmonella* antibodies can be detected in the recipients, one would be inclined to conclude that antibody was in fact transferred with the ribonucleoprotein. Yet the recent finding of splenomegaly coupled with an increase in γ-globulin (Hrubesova, Askonas, and Humphrey, 1959) does argue that synthesis has been initiated in the recipients. In this respect the findings are in agreement with our own observation that the inoculation of homologous spleen microsomes into the chick embryo stimulates the growth of the host's spleen. It would seem wise to leave open the question of possible transfer of antibody-forming capacity by RNA or RNA-protein.

It is clear, then, that we regard the interaction between graft and host as more than the sum of possible homograft reactions (graft-versus-host and host-versus-graft); it appears to involve the transfer, to the host embryo, its spleen and membranes, of particulate or macromolecular components which act not merely as building blocks but also as centers of synthesis, redirecting the course of differentiation and growth. It happens that the direction of this differentiation is granulocytopoiesis; unfortunately, the incomplete response of the embryonic spleen upon secondary antigenic challenge results in a similar cytological reaction, which tends to make interpretation difficult until one realizes that the latter reaction requires a secondary response, whereas the first can be achieved directly by grafts, cell suspensions, or subcellular particles.

The hypothesis just advanced is amenable to experimental attack; we may confidently expect that, through recombination experiments at particulate and molecular levels, the roles of RNA and RNA-protein may be elucidated. Yet the ideas advanced spring largely from experiments with subcellular units; they bear only indirectly on some of the questions arising from the complex interactions, observed in the grafting experiments, for which no satisfactory explanations are yet in sight.

First, we may reiterate our opinion that the granulocytic population elicited in second- and third-set reactions differs from that observed after primary grafts. In the former reactions, the granulocytes found in the interzone between the achromatic region of the affected membrane and the adjacent intact membrane deviate from the normal, having properties intermediate between those of mesenchyme cells and those of definitive granulocytes. Moreover, hemocytoblasts are absent, giving rise to the question, posed earlier, whether granulocytic or "granulomimetic" cells may differentiate directly from cells of the chorioallantois.

Second, we need only restate our conviction, arising out of our description of the architecture of the cyst in relation to the multinucleate giant cell, that the membrane lesions are not simply clones of proliferating donor cells as postulated by Burnet and Boyer (1960) and Burnet and Burnet (1960).

Third, we wish to raise again the several questions stemming from the repeated demonstration of an association between a mucopolysaccharide and the spectrum of cytologic changes described. Earlier (Ebert and DeLanney, 1960) we admitted that we had no clues about the role or significance of these striking inclusions. We can add nothing to that statement. Nevertheless we should point out that this observation presents a series of experimental targets, among them being the question of the possible role of mucopolysaccharide as a transplantation antigen (Haskova and Hrubesova, 1958), and the possible relation between the mucopolysaccharide and the definitive granules of the granulocytes.

Finally, and possibly most important, are the differences in the effects of second- and third-set grafts on both the chorioallantois and the host embryo itself. The membranes are affected profoundly, losing their ability to stain, at *p*H 4, with toluidine blue, suggesting a loss of RNA or at least such a change in it as to result in loss of its staining properties. In the host embryo itself, the spleen is affected in much the same way; there may be a marked destruction of the vascular bed, resulting in the accumulation of blood in the extremities. In this respect the embryos resemble those described by Ebert (1957) following intracoelomic spleen grafts. It would appear, then, that in second and third transplant generations the immune reactions of graft and host override the other reactions postulated.

LITERATURE CITED

Ackerman, G. A., and R. A. Knouff. 1959. Lymphocytopoiesis in the bursa of Fabricius. *Am. J. Anat., 104,* 163–205.

Andres, G. 1955. Growth reactions of mesonephros and liver to intravascular injections of embryonic liver and kidney suspensions in the chick embryo. *J. Exptl. Zool., 130,* 221–250.

Biggs, P. M., and L. N. Payne. 1959. Cytological identification of proliferating donor cells in chick embryos injected with adult chicken blood. *Nature, 184* (*suppl. 20*), 1594.

Billingham, R. E. 1959. Reactions of grafts against their hosts. *Science, 130,* 947–953.

Billingham, R. E., and L. A. Brent. 1957. Acquired tolerance in newborn mice. *Ann. N. Y. Acad. Sci., 69,* 678–680.

Billingham, R. E., and W. K. Silvers. 1959. The immunologic competence of chick skin. *J. Immunol., 82,* 448–457.

Boyer, G. 1960. Chorioallantoic membrane lesions produced by inoculation of adult fowl leucocytes. *Nature, 185,* 327–328.

Burnet, F. M. 1959. *The Clonal Selection Theory of Acquired Immunity.* 208 pp. University Press, Cambridge, England.

Burnet, F. M., and G. Boyer. 1960. Loss of specificity on passage of immunologically competent cells in the chick embryo. *Nature, 186,* 175–176.

Burnet, F. M., and D. Burnet. 1960. Graft versus host reactions on the chorioallantoic membrane of the chick embryo. *Nature, 188,* 376–379.

Chargaff, E. 1945. The coagulation of blood. *Advances in Enzymol., 5,* 31–65.

Cock, A. G., and M. Simonsen. 1958. Immunological attack on newborn chickens by injected adult cells. *Immunology, 1,* 103–110.

Croisille, Y. 1958. Action de différents extraits d'organes sur l'embryonen de poulet et sur des organes embryonnaires cultivés *in vitro. Arch. anat. microsc. et morphol. exptl., 47,* 360–400.

Danchakoff, V. A. 1916. Equivalence of different hematopoietic anlages (by method of stimulation of their stem cells). *Am. J. Anat., 20,* 255–327.

Danchakoff, V. A. 1918. Equivalence of different hematopoietic anlages (by method of stimulation of their stem cells). II. Grafts of adult spleen on the allantois and response of the allantoic tissues. *Am. J. Anat., 24,* 127–189.

DeLanney, L. E. 1958. Influence of adult amphibian spleen on the development of embryos and larvae: an immune response? In *The Chemical Basis of Development,* edited by W. D. McElroy and B. Glass, pp. 562–568. Johns Hopkins Press, Baltimore, Md.

DeLanney, L. E., and J. D. Ebert. 1959*a*. Reactions of the chorioallantoic membrane to serial transplantation of fragments of extraembryonic membrane following initial contact with adult spleen. *Anat. Record, 134,* 552–553.

DeLanney, L. E., and J. D. Ebert. 1959*b*. Analysis of progressive changes in embryonic chick spleen following extraembryonic grafting of homologous adult spleen. *Anat. Record, 134,* 552.

Dempster, W. J. 1951. Problems involved in the homotransplantation of tissues, with particular reference to skin. *Brit. Med. J., 2,* 1041–1049.

Dempster, W. J. 1953. Kidney homotransplantation. *Brit. J. Surg., 40,* 447–465.

Dossel, W. E. 1954. New method of intracoelomic grafting. *Science, 120,* 262–263.

Ebert, J. D. 1951. Ontogenetic change in the antigenic specificity of the chick spleen. *Physiol. Zoöl., 24,* 20–41.

Ebert, J. D. 1952. Appearance of tissue-specific proteins during development. *Ann. N. Y. Acad. Sci., 55,* 67–84.

Ebert, J. D. 1954. The effects of chorioallantoic transplants of adult chicken tissues on homologous tissues of the host chick embryo. *Proc. Natl. Acad. Sci. U. S., 40,* 337–347.

Ebert, J. D. 1955. Some aspects of protein biosynthesis in development. In *Aspects of Synthesis and Order in Growth,* edited by D. Rudnick, pp. 69–112. Princeton University Press, Princeton, N. J.

Ebert, J. D. 1957. Annual Report of the Director of the Department of Embryology for 1956–1957. *Carnegie Inst. Wash. Year Book 56,* 297–356.

Ebert, J. D. 1958. Immunochemical analysis of development. In *The Chemical Basis of Development,* edited by W. D. McElroy and B. Glass, pp. 526–545. Johns Hopkins Press, Baltimore, Md.

Ebert, J. D. 1959*a*. The acquisition of biological specificity. In *The Cell,* vol. I, edited by J. Brachet and A. Mirsky, pp. 619–693. Academic Press, New York.

Ebert, J. D. 1959*b*. The formation of muscle and muscle-like elements in the chorioallantoic membrane following inoculation of a mixture of cardiac microsomes and Rous sarcoma virus. *J. Exptl. Zool., 142,* 587–622.

Ebert, J. D. 1960. Annual Report of the Director of the Department of Embryology. *Carnegie Inst. Wash. Year Book 59,* 353–414.

Ebert, J. D., and L. E. DeLanney. 1960. Ontogenesis of the immune response. *Natl. Cancer Inst. Monograph 2,* Symposium on Normal and Abnormal Differentiation and Development, pp. 73–111.

Ebert, J. D., and F. H. Wilt. 1960. Animal viruses and embryos. *Quart. Rev. Biol., 35,* 261–312.

Hamburger, V. 1942. *A Manual of Experimental Embryology.* 213 pp. University of Chicago Press, Chicago, Ill.

Hamburger, V., and H. L. Hamilton. 1951. A series of normal stages in the development of the chick embryo. *J. Morphol., 88,* 49–92.

Haskova, V., and M. Hrubesova. 1958. Part played by deoxyribonucleic acid in transplantation immunity. *Nature, 182,* 61–62.

Himes, M., and L. Moriber. 1956. A triple stain for deoxyribonucleic acid, polysaccharide, and protein. *Stain Technol., 31,* 67–70.

Hrubesova, M., B. A. Askonas, and J. H. Humphrey. 1959. Serum antibody and gamma globulin in baby rabbits after transfer of ribonucleoprotein from adult rabbits. *Nature, 183,* 97–99.

Hunter, G. D., and J. A. V. Butler. 1956. Stimulation by ribonucleic acid of induced beta galactosidase formation in *B. megatherium. Biochim. Biophys. Acta, 20,* 405–406.

Jankovic, B. D., K. Isakovic, and J. Horvat. 1959. Failure of ribonucleoprotein to transfer antibody formation. *Nature, 183,* 1400–1401.

Kern, M., E. Helmreich, and H. N. Eisen. 1959. A demonstration of antibody activity on microsomes. *Proc. Natl. Acad. Sci. U. S., 45,* 862–867.

Kramer, M., and F. B. Straub. 1956. Role of specific nucleic acid in induced enzyme synthesis. *Biochim. Biophys. Acta, 21,* 401–403.

Kryukova, I. N. 1959. The effect of *in vitro* irradiation of spleen cells on induced splenomegaly in chick embryos. *Folia Biol. Prague, 5,* 29–31.

Lenicque, P. 1959. Studies on homologous inhibition in the chick embryo. *Acta Zool. Stockholm, 40,* 141–202.

Medawar, P. B. 1957. Transplantation immunity and subcellular particles. *Ann. N. Y. Acad. Sci., 68,* 255–267.

Moloney, J. B. 1956. Biological studies of the Rous sarcoma virus. V. Preparation of improved standard lots of virus for use in quantitative investigations. *J. Natl. Cancer Inst., 16,* 877–888.

Moscona, A. 1959. Squamous metaplasia and keratinization of chorionic epithelium of the chick embryo in egg and in culture. *Developmental Biol., 1,* 1–23.

Moscona, A. 1960. Metaplastic changes in the chorioallantoic membrane. *Transpl. Bull., 26,* 120–124.

Mun, A. M., I. L. Kosin, and I. Sato. 1959. Enhancement of growth of chick host spleens following chorioallantoic membrane grafts of homologous tissues. *J. Embryol. Exptl. Morphol., 7,* 512–525.

Murphy, J. B. 1916. The effect of adult chicken organ grafts on the chick embryo. *J. Exptl. Med., 24,* 1–6.

Oker-Blom, N., and H. Standström. 1956. Effect of coxsackie virus on the growth of the Rous sarcoma in embryonated chicken eggs. *Ann. Med. Exptl. et Biol. Fenniae Helsinki, 34,* 293–300.

Olson, C. 1937. Variations in the cells and hemoglobin content in the blood of the normal domestic chicken. *Cornell Vet., 27,* 235.

Paschkis, K. E. 1958. Growth promoting factors in tissues: a review. *Cancer Research, 18,* 981–991.

Polezhaev, L. V., L. V. Akhabadze, N. A. Sakharova, and V. L. Mantieva. 1959. Stimulation of myocardium regeneration in mammals. *Folia Biol. Prague, 7,* 29–59.

Reiner, J. M., and F. Goodman. 1955. The role of polynucleotides in induced enzyme formation. *Arch. Biochem. Biophys., 57,* 475–490.

Roberts, R. B., editor. 1958. *Microsomal Particles and Protein Synthesis.* 168 pp. Pergamon Press, New York.

Romanoff, A. L. 1960. *The Avian Embryo.* 1305 pp. The Macmillan Company, New York.

Rose, S. M. 1958. Failure of self-inhibition in tumors. *J. Natl. Cancer Inst., 20,* 653–664.

Ruth, R. F. 1960. Ontogeny of the blood cells. *Federation Proc., 19,* 579–585.

Sandreuter, A. 1951. Vergleichende Untersuchungen über die Blutbildung in der Ontogenese von Haushuhn und Star. *Acta Anat., 11, suppl. 14,* 1–72.

Schweet, R., H. Lamfrom, and E. Allen. 1958. The synthesis of hemoglobin in a cell-free system. *Proc. Natl. Acad. Sci. U. S., 44,* 1029–1034.

Simonsen, M. 1953. Biological incompatibility in kidney transplantation in dogs. *Acta Pathol. Microbiol. Scand., 32,* 36–86.

Simonsen, M. 1957. The impact on the developing embryo and newborn animal of adult homologous cells. *Acta Pathol. Microbiol. Scand., 40,* 480–500.

Simonsen, M., and E. Jensen. 1959. The graft versus host assay in transplantation chimeras. In *Biological Problems of Grafting. Colloque de l'Université de Liège, 12,* 1–23.

Solomon, J. B. 1960. Onset of the ability of spleen cells to evoke the "graft versus host" reaction in chicken. *Exptl. Cell Research, 20,* 223–225.

Speirs, R. S. 1958. Advances in the knowledge of the eosinophil in relation to antibody formation. *Ann. N. Y. Acad. Sci., 73,* 283–306.

Sterzl, J., and M. Hrubesova. 1957. Transfer by nucleoprotein fractions of antibody-forming capacity into unimmunized recipients. *J. Microbiol. Epidemiol. Immunobiol. U. S. S. R., 28,* 503–510.

Taliaferro, W. H. 1949. The cellular basis of immunity. *Ann. Rev. Microbiol., 3,* 159–194.

Terasaki, P. I. 1959. Identification of the type of blood-cell responsible for the graft-versus-host reaction in chicks. *J. Embryol. Exptl. Morphol., 7,* 394–408.

Terasaki, P. I., and J. A. Cannon. 1957. A technic for cross-transfusion of blood in embryonic chicks and its effect upon hatchability. *Proc. Soc. Exptl. Biol. Med., 94,* 103–107.

Uttley, A. M. 1959. The reasoning machine. *The Sunday Times,* London, June 21, p. 23.

Van Alten, P. J., and R. A. Fennell. 1959. The effects of chorioallantoic grafts on the developing chick embryo. I. *J. Embryol. Exptl. Morphol., 7,* 459–475.

Van Haeften, F. F. 1958. Differentiation induced by chorioallantoic grafting of tissue homogenate. *Acta Physiol. Pharmacol. Neerl., 7,* 1–34.

Webster, G. C. 1959. Protein synthesis by isolated nucleoprotein particles. *Arch. Biochem. Biophys., 85,* 159–170.

Weiss, P. 1947. The problem of specificity in growth and development. *Yale J. Biol. Med., 19,* 235–278.

Weiss, P. 1955. Specificity in growth control. In *Biological Specificity and Growth,* edited by E. G. Butler, pp. 195–206. Princeton University Press, Princeton, N. J.

Weiss, P., and J. L. Kavanau. 1957. A model of growth and growth control in mathematical terms. *J. Gen. Physiol., 41,* 1–47.

Willier, B. H. 1924. The endocrine glands and the development of the chick. I. The effect of thyroid grafts. *Am. J. Anat., 33,* 67–103.

Zwilling, E. 1959. A modified chorioallantoic grafting procedure. *Transpl. Bull., 6,* 115–116.

APPENDIX

In the course of this investigation, which has extended over several years, preliminary accounts have appeared, often in the Annual Reports of the Director of the Department of Embryology, published in the Carnegie Institution of Washington Year Books, 56 to 59, inclusive. Some of the findings have been presented in tabular form, others have not. In this appendix are collected many of the findings from the laboratories of both authors. The data in tables 1 and 4 have not been published. Some of the data in tables 2, 3, and 5 have appeared previously, but each table is supplemented with newer findings. For each table, reference is made to the original citation.

TABLE 1. Splenomegaly Following Transplantation of Fragments of Adult Chicken Spleen to Normal Chick Embryos and to Embryos Hypophysectomized by Partial Decapitation

(*Carnegie Inst. Wash. Year Book 56,* 325–327)

	Wet Weight of Host's Spleen, mg.	
Operation Performed	At 16 days	At 18 days
None	8.1 ± 0.3	10.3 ± 0.4
Optic vesicles removed	8.8 ± 0.4	10.0 ± 0.4
Partial decapitation	10.8 ± 0.3	14.7 ± 0.6
Chorioallantoic transplantation of adult spleen at 9th day	26.7 ± 2.9	33.8 ± 3.2
Partial decapitation followed by chorioallantoic transplantation of adult spleen at 9th day	22.4 ± 3.0	35.6 ± 3.4

TABLE 2. Effect on the Host Embryo of Chorioallantoic Grafts of 17-Day-Old Embryonic Spleen Previously Exposed to the Stimulus of Adult Heart Grafts

(*Carnegie Inst. Wash. Year Book 58,* 397)

Series	Age of Host at Operation, days	Donor Tissue	No. Recovered/ No. Attempted	Mean Weight of Host Spleens at 17 Days, mg.	Range, mg.
S-59-1	9	Sham	117/120	10.2	7.9– 11.3
S-59-2	9	Normal 17-day embryo spleen	59/60	12.7	7.4– 17.8
S-59-3	9	Unimmunized adult spleen	42/60	22.9	8.0– 69.0
S-59-4	9	Adult heart	59/75	9.9	6.1– 12.0
S-59-5	9	Adult heart	32/50	10.3	7.4– 11.7
S-59-6	11	Adult heart	25/40	8.8	6.3– 13.2
S-59-7	9	17-day embryo spleen recovered in S-59-3	39/100	39.6	11.0–102.0
S-59-8	9	17-day embryo spleen recovered in S-59-4	41/57	16.1	6.0– 44.0
S-59-9	9	17-day embryo spleen recovered in S-59-5	53/64	18.8	7.4– 40.0
S-59-10	9	17-day embryo spleen recovered in S-59-6	21/48	12.2	8.8– 40.3
S-59-11	9	Adult heart	29/36	10.6	8.0– 13.1
S-59-12	9	Adult heart	27/36	9.8	7.8– 11.7
S-60-1	11	17-day embryo spleen recovered in S-59-11	47/58	16.9	6.9– 37.0
S-60-2	11	17-day embryo spleen recovered in S-59-12	40/54	19.8	7.3– 46.7

TABLE 3. Relative Specific Activities of Host Tissues after Injection of Tagged Organ Fractions

Injection day 9, recovery day 10

(*Carnegie Inst. Wash Year Book 56,* 328)

Experiment No.	Host Tissue	Kidney Fraction Injected			
		Nuclear	Mitochondrial	Microsomal	Supernate
1	Spleen	1.05	1.00	0.49	0.61
	Kidney	1.00	1.00	1.00	1.00
2	Spleen	1.02	0.97	0.53	0.76
	Kidney	1.00	1.00	1.00	1.00
3	Spleen	1.04	0.94	0.56	0.69
	Kidney	1.00	1.00	1.00	1.00
4	Spleen	0.98	1.01	0.52	0.70
	Kidney	1.00	1.00	1.00	1.00
5	Spleen	1.03	0.97	0.48	0.81
	Kidney	1.00	1.00	1.00	1.00
6	Spleen	0.99	1.01	0.59	0.73
	Kidney	1.00	1.00	1.00	1.00
		Spleen Fraction Injected			
1	Spleen	1.00	1.00	1.00	1.00
	Kidney	0.97	1.04	0.44	0.80
2	Spleen	1.00	1.00	1.00	1.00
	Kidney	0.96	0.95	0.61	0.84
3	Spleen	1.00	1.00	1.00	1.00
	Kidney	0.99	1.01	0.51	0.73
4	Spleen	1.00	1.00	1.00	1.00
	Kidney	1.01	1.03	0.49	0.89
5	Spleen	1.00	1.00	1.00	1.00
	Kidney	0.98	1.01	0.53	0.77
6	Spleen	1.00	1.00	1.00	1.00
	Kidney	1.02	0.97	0.60	0.90

TABLE 4. Splenomegaly Following Transplantation on the Chorioallantoic Membrane of Fragments of Adult Chicken Spleen Encased in Membrane Filters * †

(*Carnegie Inst. Wash. Year Book 57,* 346)

Operation Performed	Number of Embryos	Wet Weight of Host's Spleen at 17 Days, mg.	Range, mg.
None	36	9.7	7.3–13.0
Inserted membrane filter alone	33	10.1	7.9–12.6
Inserted fragment of homologous adult spleen alone	29	46.2	8.3–95.6
Inserted fragment of homologous spleen encased in membrane filter	43	13.9	6.9–18.6

* Millipore Filter Corporation, Watertown, Massachusetts, filters designated TH and TV. Differences were not observed in effectiveness of these filters.

† The authors were introduced to this technique by Dr. Jacques Mulnard, who employed filters of several porosities kindly supplied by Dr. Clifford Grobstein.

TABLE 5. Mean Weights of Spleens of 17-Day-Old Chick Embryos after Inoculation of "Microsome Fractions" of Adult Organs (*Carnegie Inst. Wash. Year Book 58,* 405)

Series	Age at Inoculation, days	*,†,‡	Source of Inoculum							
			Sham	Spleen	Liver	Kidney	Heart	Brain	Ovary	Testis
MF 59, 1 + 2	9	*	51	50	48	50	30	x	x	x
		†	11.1	19.6	10.9	9.9	10.7	x	x	x
		‡	8.9–14.0	13.1–28.4	7.6–12.9	8.9–13.6	8.0–13.6	x	x	x
MF 59, 3 + 5	9	*	53	52	56	51	x	23	x	x
		†	10.2	14.1	13.0	10.7	x	10.9	x	x
		‡	8.2–13.1	11.3–19.3	8.3–14.9	9.3–15.1	x	8.6–17.1	x	x
MF 59, 6	9	*	33	67	31	40	x	x	25	25
		†	10.8	16.7	13.9	11.0	x	x	11.1	10.7
		‡	9.0–13.3	15.6–19.6	9.1–18.2	8.4–13.0	x	x	7.2–15.0	6.9–14.6
MF 59, 9	11	*	25	31	50	x	25	24	x	x
		†	9.7	14.3	12.2	x	9.6	10.8	x	x
		‡	7.6–14.3	10.9–16.3	8.9–16.1	x	8.7–11.3	8.0–14.1	x	x
MF 59, 11	11	*	12	29	25	30	26	25	x	x
		†	10.3	13.9	11.9	8.9	11.1	10.0	x	x
		‡	8.9–11.0	11.1–18.7	11.0–14.6	6.1–13.6	6.7–13.4	8.3–12.7	x	x
MF 59, 13	11	*	12	33	26	29	x	x	20	18
		†	10.7	15.2	12.4	10.1	x	x	9.4	10.9
		‡	9.3–12.1	11.9–20.1	9.3–16.8	8.3–11.6	x	x	8.6–10.2	8.1–13.1
MF 59, 15	9	*	33	39	x	x	24	24	27	19
		†	10.2	18.1	x	x	10.3	10.9	9.8	10.2
		‡	7.8–13.1	8.3–31.0	x	x	8.3–13.0	7.9–14.2	6.7–12.9	8.2–12.8
MF 59, 17	9	*	29	36	33	37	x	x	x	x
		†	10.9	15.6	12.9	10.2	x	x	x	x
		‡	8.3–12.9	9.1–23.7	7.9–16.3	6.8–12.7	x	x	x	x
MF 59, 21	9	*	40	36	30	x	18	31	20	20
		†	9.9	12.4	12.4	x	9.7	9.6	10.1	10.8
		‡	6.9–13.6	8.0–19.1	6.9–17.0	x	8.7–11.9	8.1–11.7	7.9–13.1	8.2–13.6
MF 59, 22	9	*	15	24	19	22	x	x	x	x
		†	9.9	16.0	13.6	9.8	x	x	x	x
		‡	7.3–14.0	9.0–21.3	7.8–18.1	7.6–13.1	x	x	x	x
MF 59, 23	9	*	15	24	26	20	17	18	x	23
		†	10.4	19.3	12.0	10.4	10.0	9.4	x	10.4
		‡	8.9–12.0	8.4–29.6	9.0–17.1	8.3–12.6	8.6–11.4	7.9–14.1	x	7.8–12.9

* Number of embryos.
† Mean weight in milligrams.
‡ Range in milligrams.

PLATES

PLATE 1

Fig. 1. Hamburger and Hamilton stage 22 (3½ days). Initial appearance of splenic ridge dorsal to developing dorsal pancreas. × 100.

Fig. 2. Hamburger and Hamilton stage 24 (4 days). Elevated splenic ridge showing venous capillary in conjunction with the portal circulation. × 100.

Fig. 3. Hamburger and Hamilton stage 25 (4½ days). Splenic mesenchyme pervaded with venous capillaries. × 100.

Fig. 4. Hamburger and Hamilton stage 29 (6 days). Section through embryo to illustrate left-lateral orientation of spleen. × 15.

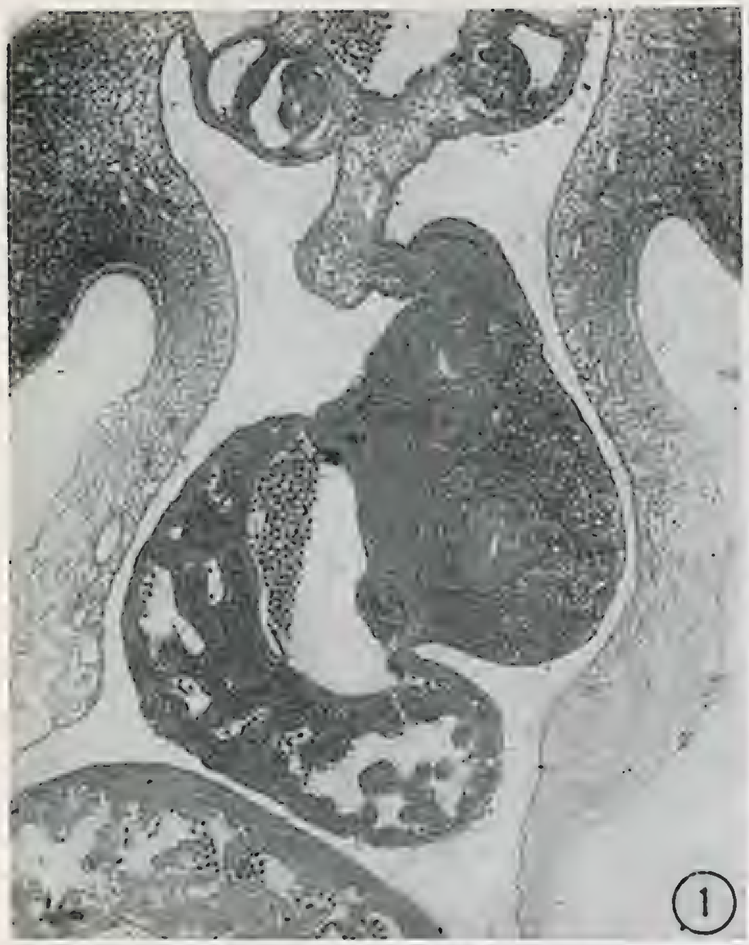

①

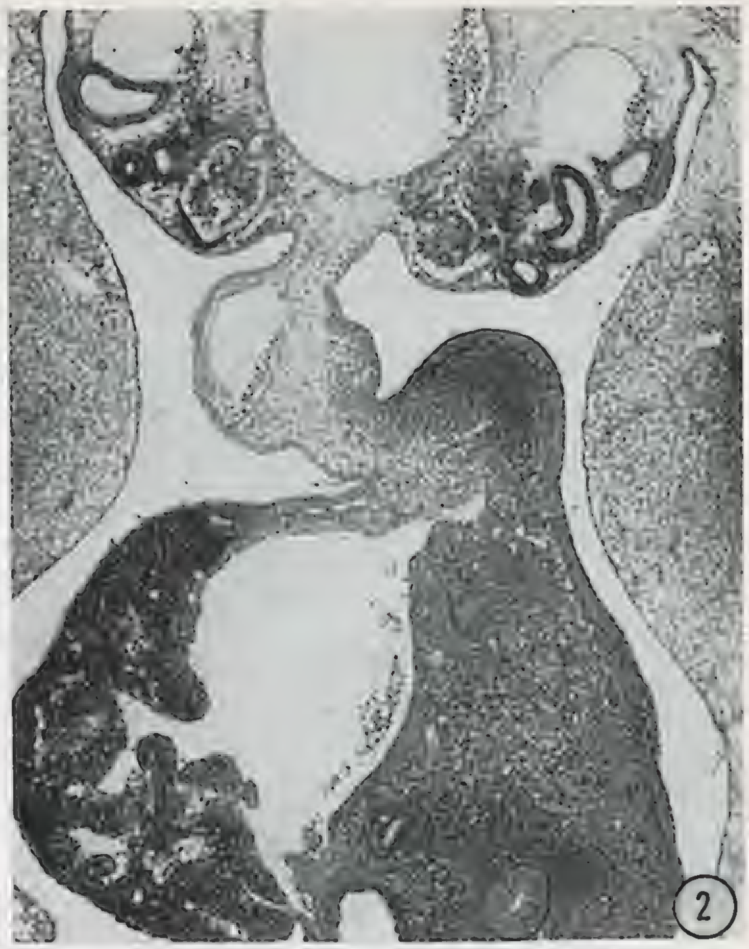

②

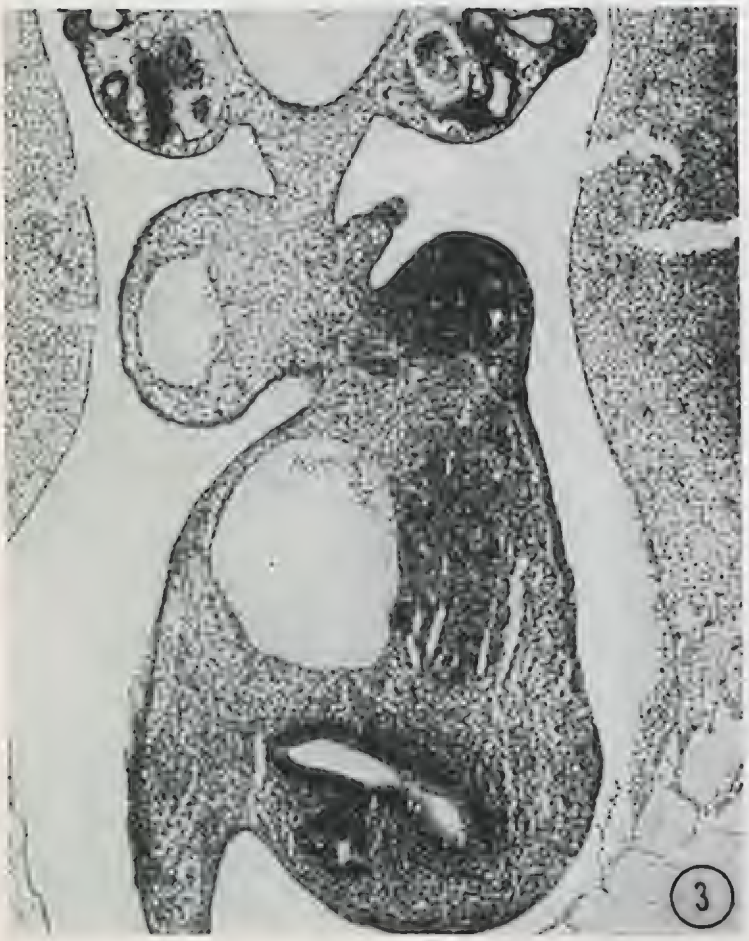

③

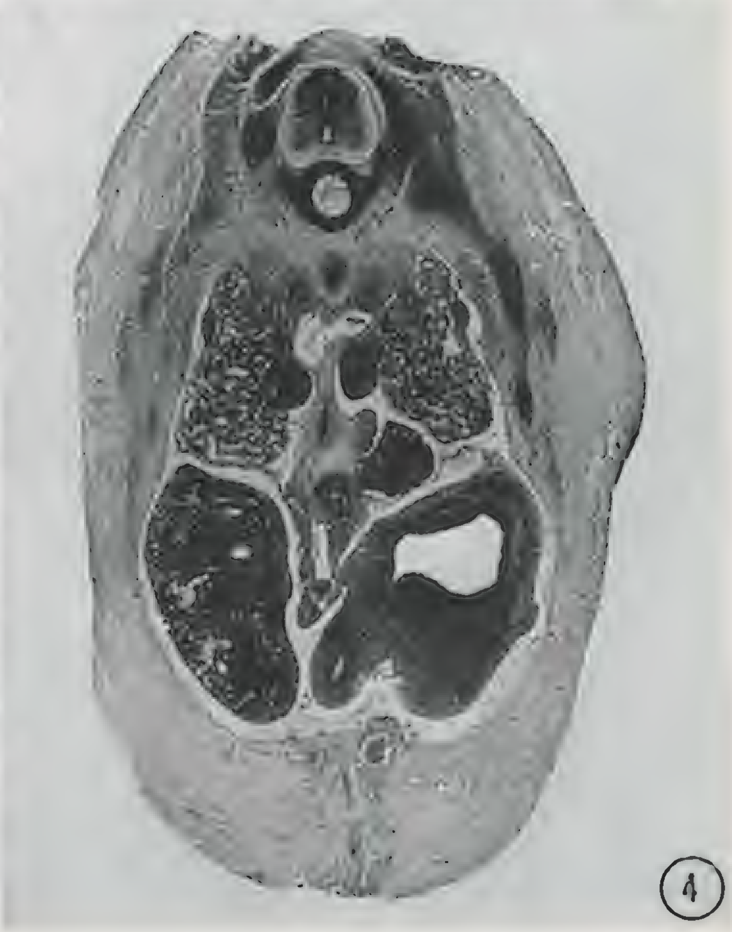

④

PLATE 2

Fig. 5. Higher magnification of spleen in figure 4. × 100.

Fig. 6. Hamburger and Hamilton stage 30 (6½ days). Erythrocytes with densely stained nuclei clearly seen in venous sinuses of spleen at right. × 400.

Fig. 9. Hamburger and Hamilton stage 37 (11 days). An artery with round-oval endothelial cells and circumferentially oriented arterial mesenchyme of the developing tunics. × 600.

Fig. 13. Hamburger and Hamilton stage 41 (15 days). Orientation of granulocytes in arterial and venous channels. Granulocytes rarely penetrate the tunic to approach the lumen in the artery, but can be seen in juxtaposition to the lumen of a venous sinus. × 600.

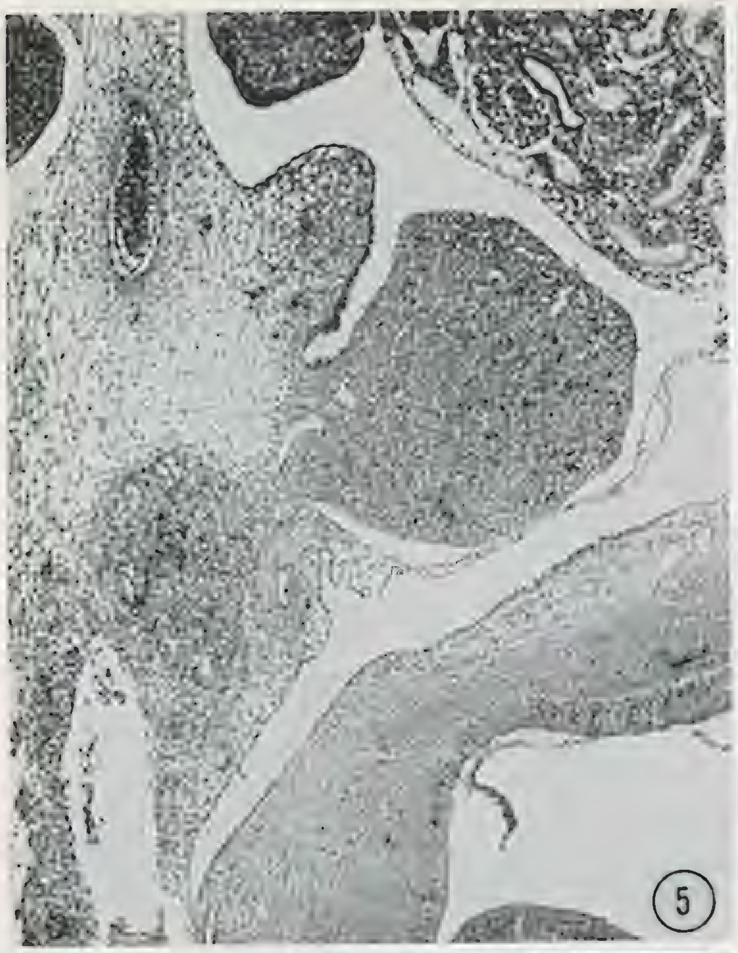
5

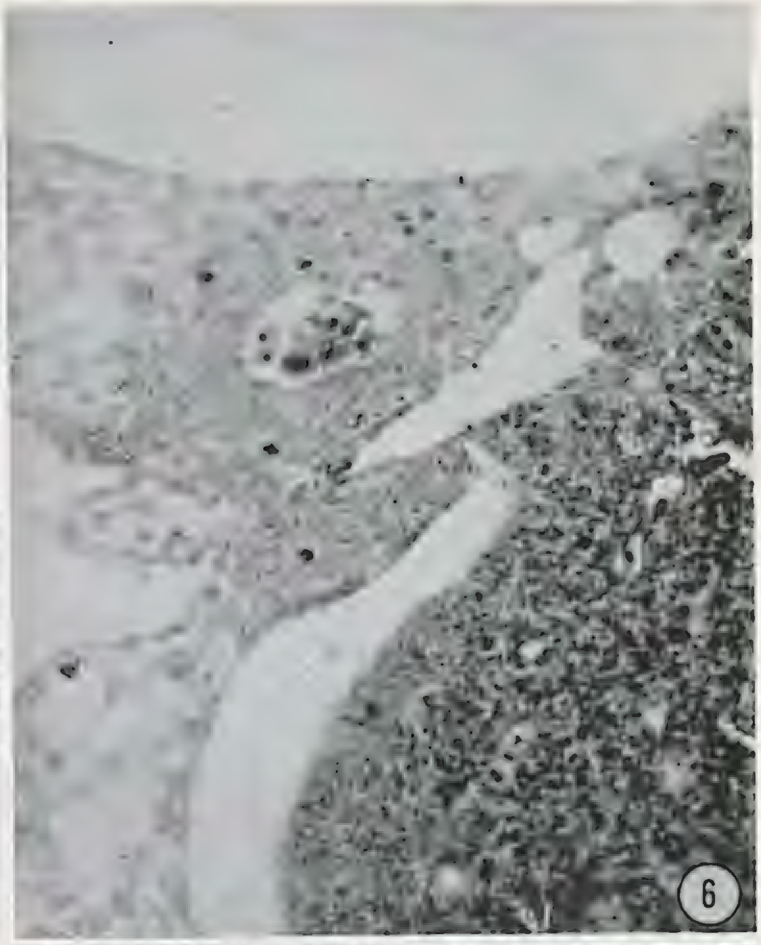
6

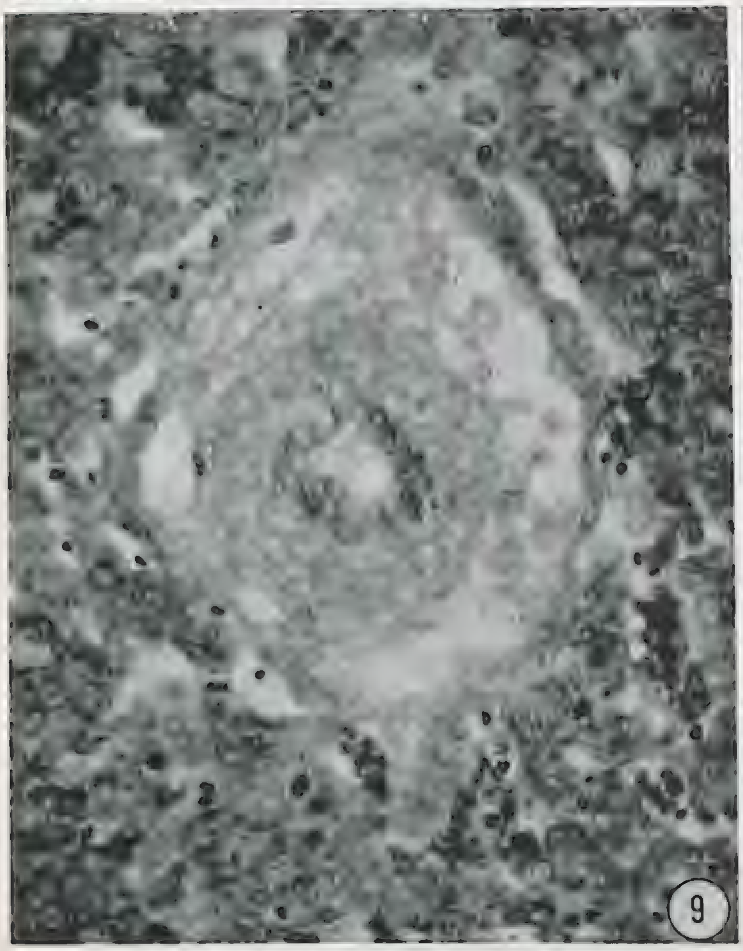
9

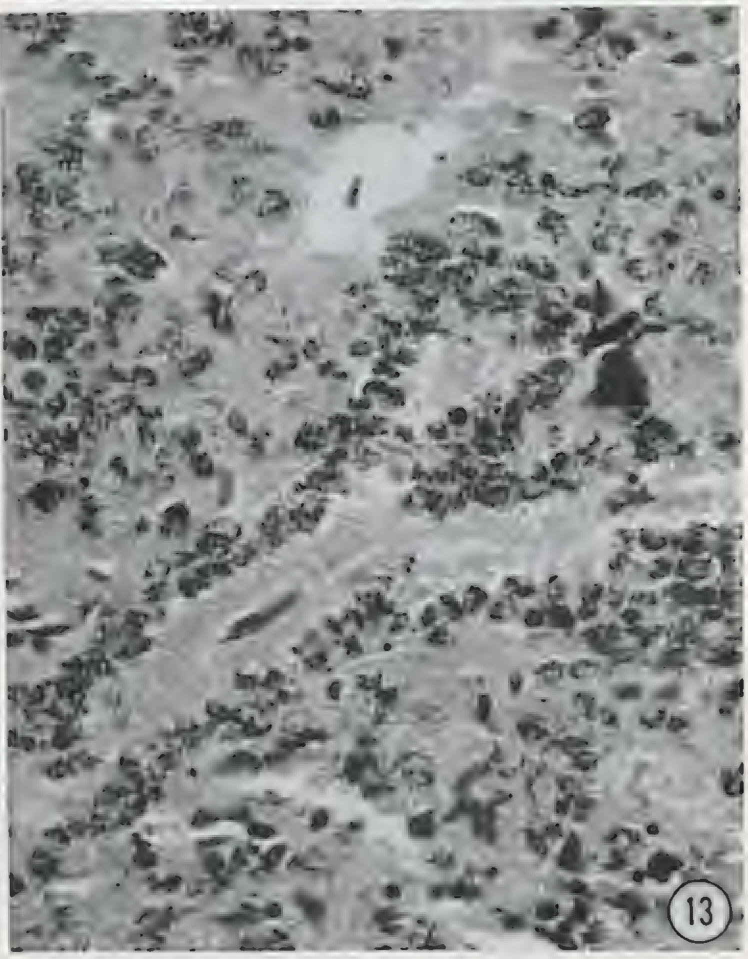
13

PLATE 3

Fig. 7. Hamburger and Hamilton stage 36 (10 days). Hemocytoblasts with large, densely basophilic nucleoli. Dominici technique. × 1000.

Fig. 8. Same as figure 7. Splenic mesenchyme with immature neutrophilic (heterophilic) leucocyte. Dominici technique. × 1000.

Fig. 10. Hamburger and Hamilton stage 38 (12 days). Erythrocytes, granulocytes, and splenic mesenchyme. The granulocytes that show achromatic granules are destined to become acidophils; metachromatic and eosinophilic granules of the remaining leucocytes indicate immature stages of neutrophilic leucocytes. Dominici technique. × 1000.

Fig. 11. Hamburger and Hamilton stage 37 (11 days). Compare with figure 10 for quantitative difference in young granulocytes. Granulocytes illustrated are immature neutrophils. Dominici technique. × 1000.

Fig. 12. Hamburger and Hamilton stage 40 (15 days). Neutrophilic (heterophilic) granulocyte in close association with large numbers of hemocytoblasts. The clarity of the binucleolate condition of the hemocytoblasts indicates blast cells destined to differentiate into neutrophils. Slender rod- and spindle-shaped granules indicate some neutrophils approaching maturity (metamyelocytes of Sandreuter). Dominici technique. × 1000.

Fig. 14. Hamburger and Hamilton stage 40 (15 days). Granulocytes primarily of the neutrophil (heterophil) line illustrating a wide spectrum of granule types ranging from metachromatic spheres through spindle form to elongate rods. Size of hemocytoblasts in relation to the splenic mesenchyme is noteworthy. Dominici technique. × 1000.

Fig. 15. Hamburger and Hamilton stage 43 (17 days). The general architecture of the spleen is shown to illustrate arteries, white and red pulp areas, the red pulp being populated primarily by neutrophilic leucocytes. Dominici technique. × 100.

Fig. 16. Same as figure 15. Himes and Moriber triple stain. The granules of the leucocytes have a reddish "overcast" as they lie in the protein (yellow) matrix of the cytoplasm, suggesting an association of mucopolysaccharide with granule architecture. The presence of identifiable nucleoli indicates condensation of chromatin material on the surface of the nucleoli. × 1000.

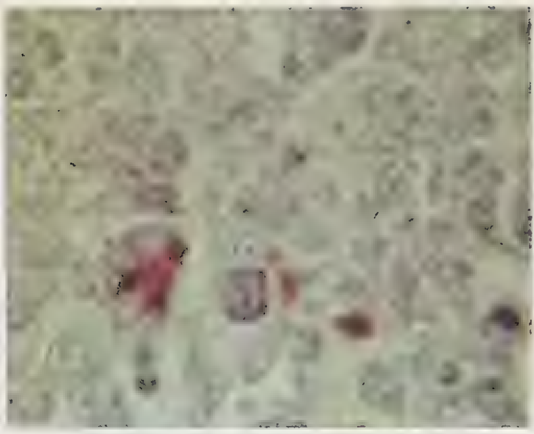
7

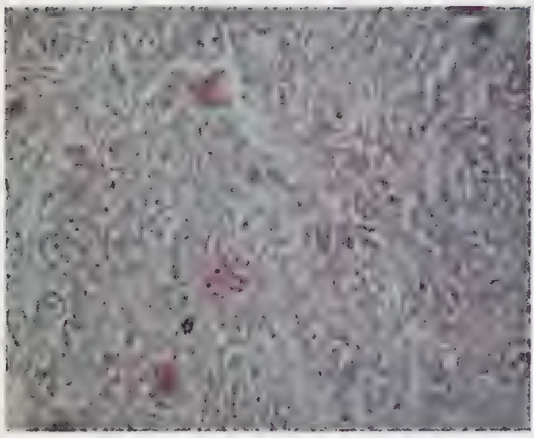
8

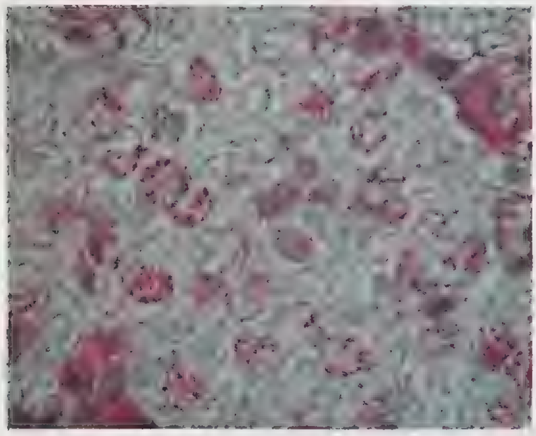
10

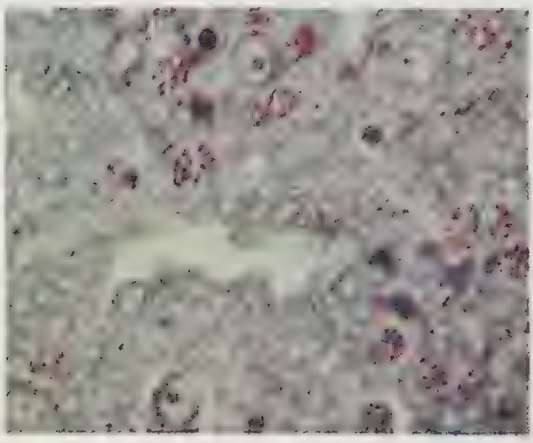
11

12

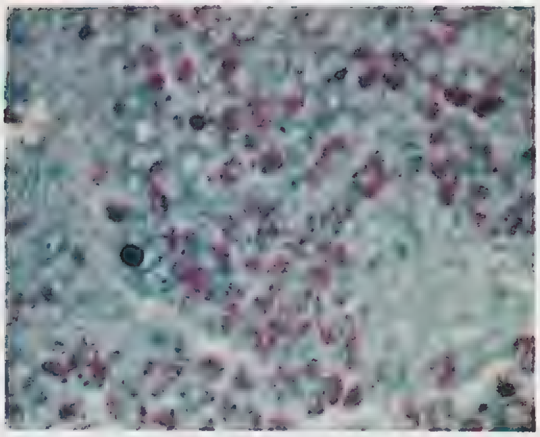
14

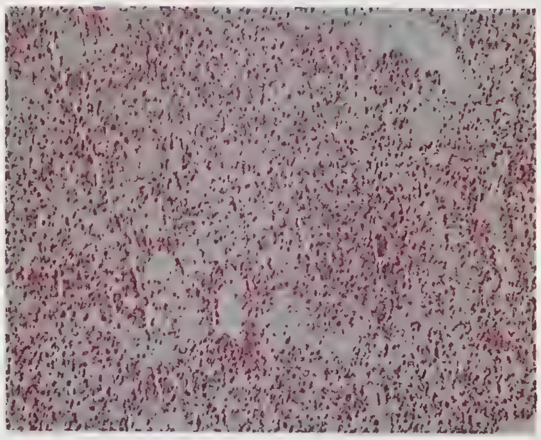
15

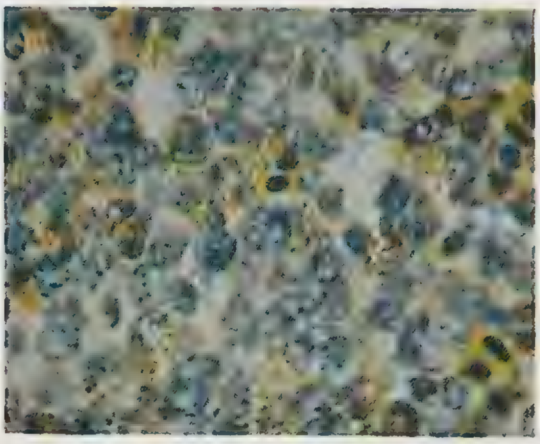
16

PLATE 4

Fig. 18. Normal spleen of 9-day embryo, showing generalized mesenchyme, rare hemocytoblasts, mitotic figures, venous sinuses. Toluidine blue, *p*H 4. × 600.

Fig. 19. Spleen of 9-day embryo after chorioallantoic graft of adult spleen at day 7. Note striking increase in number of hemocytoblasts in comparison with figure 18. Toluidine blue, *p*H 4. × 600.

Fig. 20. Normal spleen at 11 days. Developing artery, generalized mesenchyme, relatively few hemocytoblasts. Toluidine blue. × 600.

Fig. 21. Spleen of 11-day embryo after implantation of graft of adult spleen at day 7. Compare with figure 20. Increase in hemocytoblasts is evident. Toluidine blue. × 600.

Fig. 22. Same as figure 21. Generalized mesenchyme, granulocytes with irregularly shaped granules signifying heterophils. Dominici technique. × 600.

Fig. 23. Normal spleen at 12 days. Generalized mesenchyme and granulocytes predominate; hydrolysis reduces visibility of hemocytoblasts. Note proteinaceous cytoplasm (yellow) of granulocytes and faintly periodic acid–Schiff positive granules. Note also granulocyte in mitosis. Himes and Moriber triple stain. × 1000.

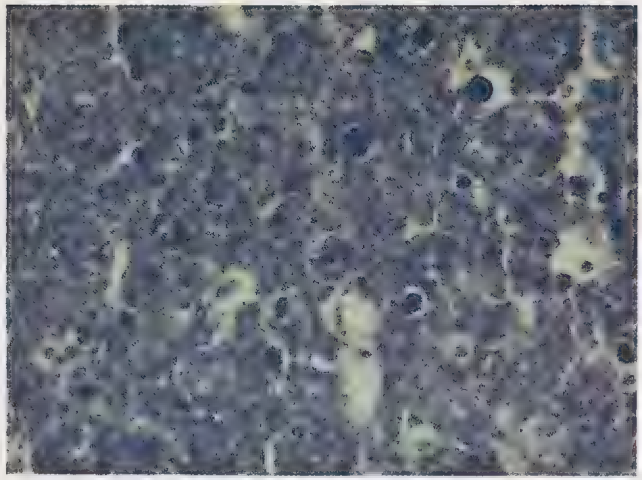

18

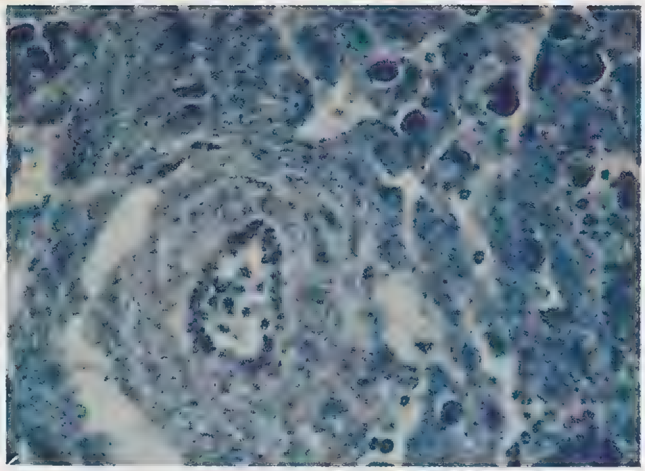

21

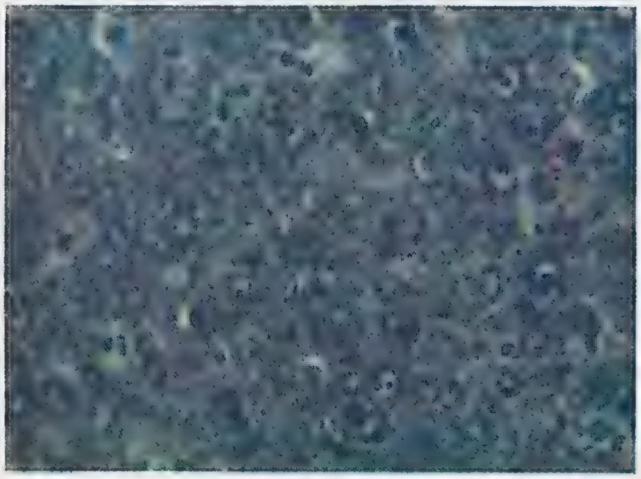

19

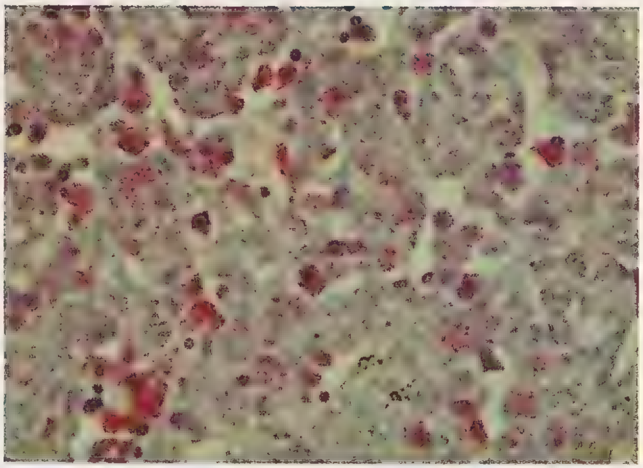

22

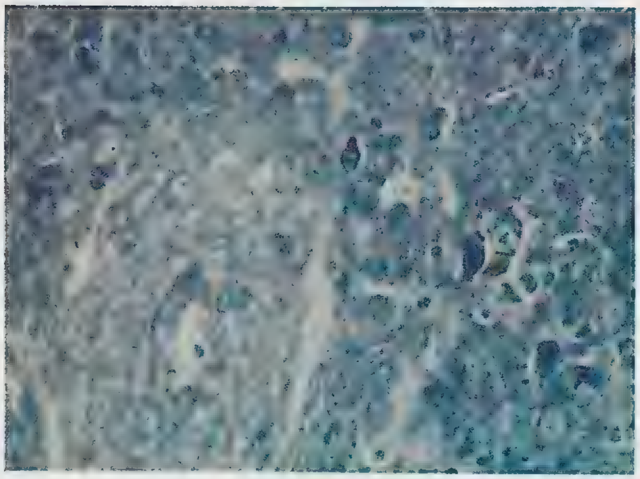

20

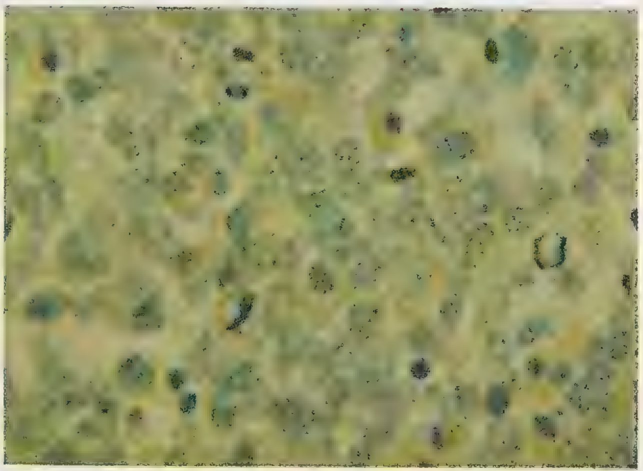

23

PLATE 5

Fig. 24. Twelve-day-old embryonic spleen, 5 days after implantation of adult spleen to chorioallantoic membrane. Center of spleen necrotic. Himes and Moriber triple stain. × 40.

Fig. 25. Adult spleen on surface of chorioallantoic membrane. Meager evidence of reaction in membrane adjacent to graft. The section of the membrane that lies above the graft is not in its natural position, being an artifact of preparation. Hematoxylin and eosin. × 10.

Fig. 26. Spleen of 13-day-old embryo, 6 days after implantation of adult spleen to chorioallantoic membrane. Note a few venous sinuses; no evidence of arteries. Achromatic necrotic region near edge of spleen. Dominici technique. × 25.

Fig. 27. Spleen of 13-day-old embryo, 6 days after implantation of adult spleen to chorioallantoic membrane. Some areas retain hemocytoblasts with the characteristic basophilia associated with RNA. Most of area necrotic, failing to stain with toluidine blue, *p*H 4. × 40.

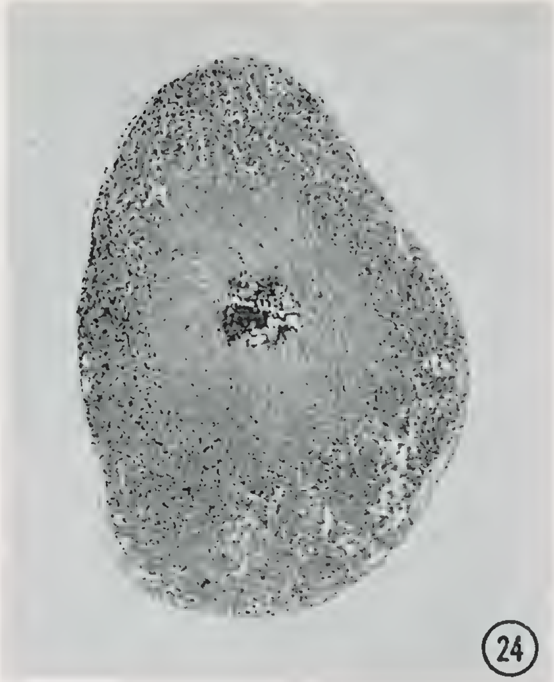

24

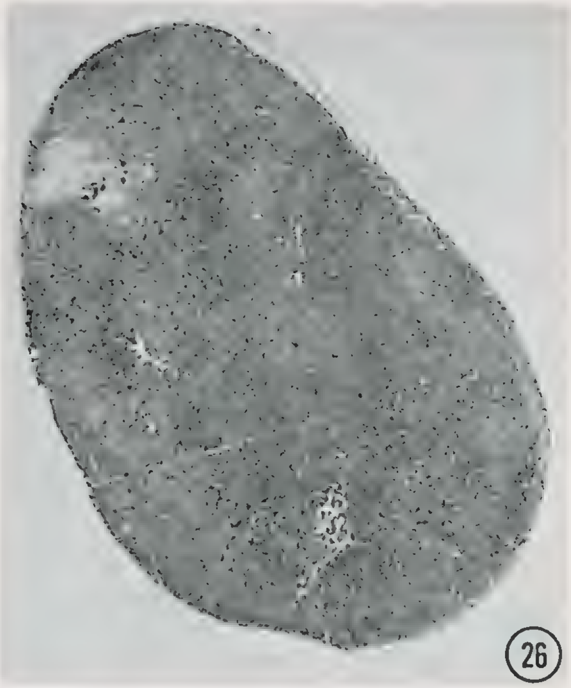

26

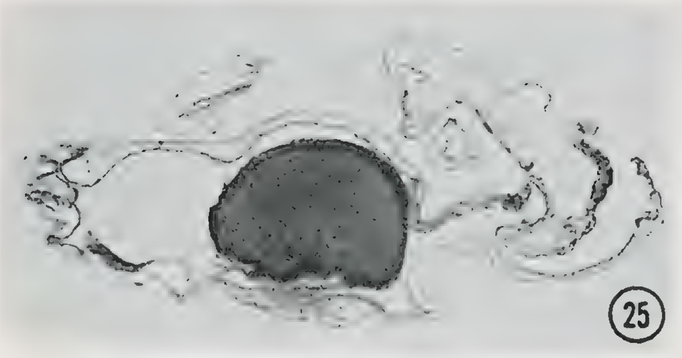

25

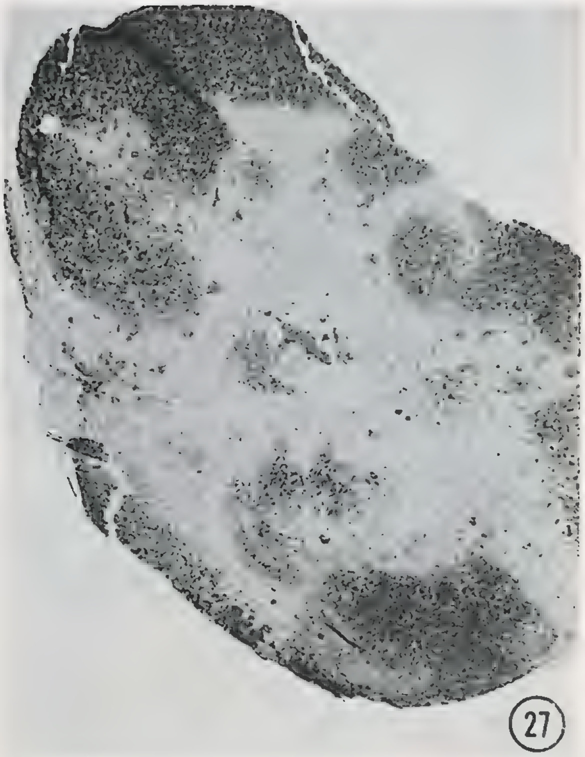

27

PLATE 6

Fig. 28. Fifteen-day embryonic spleen, 8 days after implantation of adult spleen to chorioallantoic membrane. Numerous degenerative foci are evident throughout the spleen. Himes and Moriber triple stain. × 25.

Fig. 29. Another section of the spleen shown in figure 28. Note randomly distributed achromatic regions of degeneration and poor staining reaction of remaining, as yet nonnecrotic, cells. Toluidine blue, *p*H 4. × 25.

Fig. 30. Normal spleen of 17-day-old embryo. Cross section of spleen to show arteries; follicular distinctions between red and white pulp evident. Hematoxylin and eosin. × 20.

Fig. 31. Spleen of 17-day-old embryo, 8 days after implantation of adult spleen to the chorioallantoic membrane. Compare with figure 30. Note presence of some venous sinuses, poorly defined arteries, size increase by comparison with control. Necrotic regions absent. Hematoxylin and eosin. × 20.

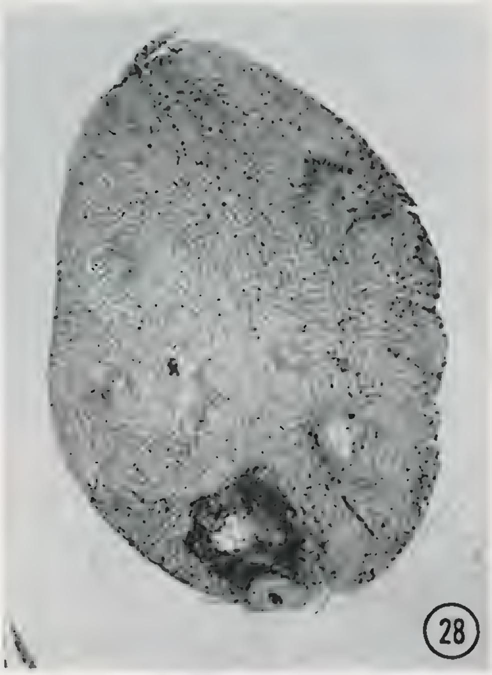

28

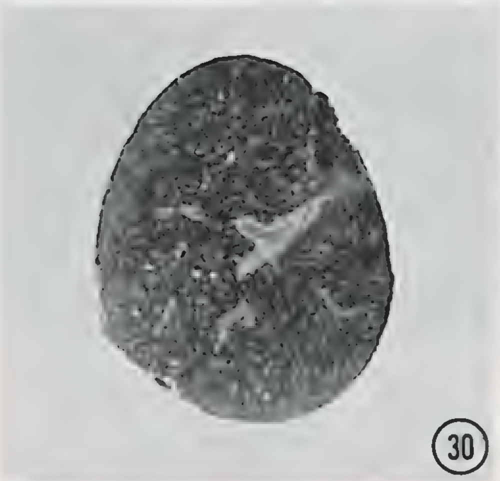

30

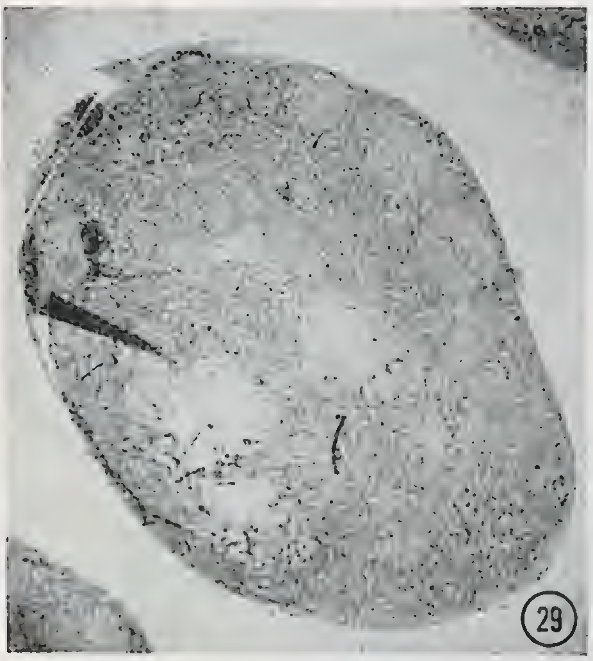

29

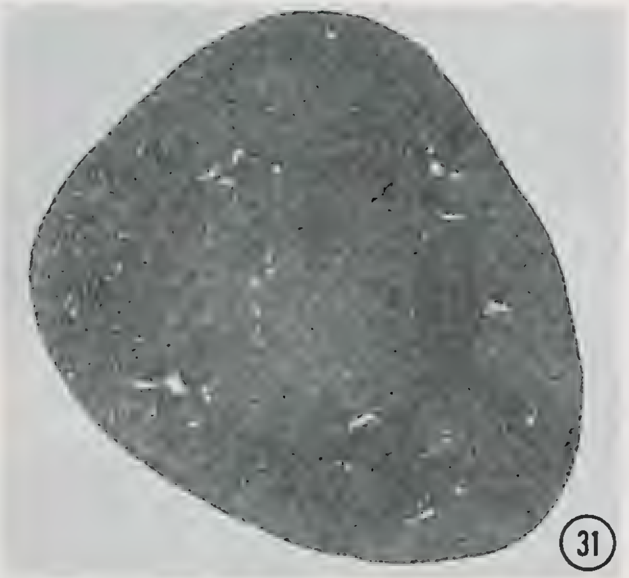

31

PLATE 7

Fig. 32. Eighteen-day-old embryonic spleen, 11 days after implantation of adult spleen to chorioallantoic membrane. Contrast with figure 31. Extremely cystic and necrotic spleen. Dominici technique. × 15.

Fig. 33. Seventeen-day-old embryonic spleen, 10 days after implantation of adult spleen to chorioallantoic membrane. High concentration of periodic acid–Schiff positive material. Himes and Moriber triple stain. × 1000.

Fig. 34. Twelve-day-old embryonic spleen, 5 days after implantation of adult spleen to chorioallantoic membrane. Aggregations of mucopolysaccharide. Many cells appear somewhat fibrotic. A few poorly defined granulocytes. Himes and Moriber triple stain. × 1000.

Fig. 35. Portion of chorioallantoic membrane at 8th day of incubation, with graft of adult spleen implanted 24 hours earlier. Epithelial erosion has occurred, permitting the mesenchyme of the two organs to be in continuity. Note generalized thickening of membrane. Dominici technique. × 30.

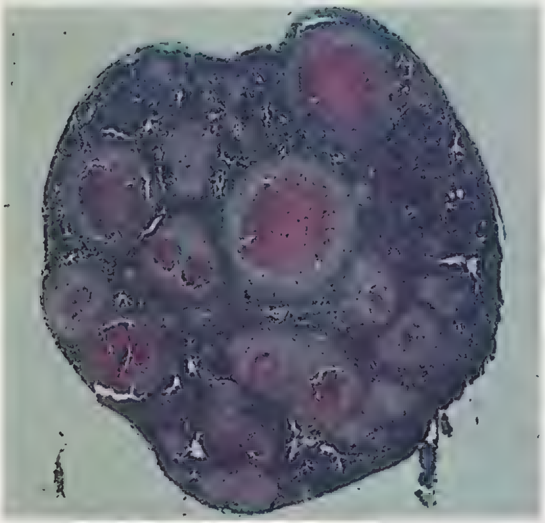

32

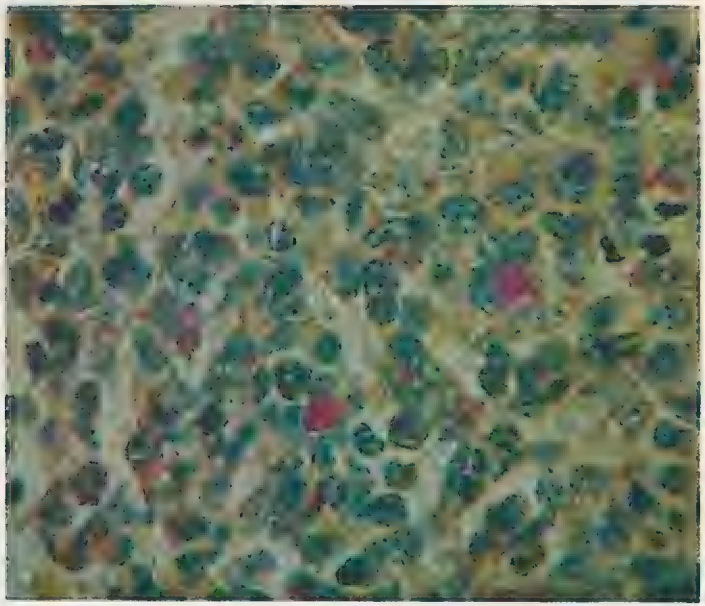

33

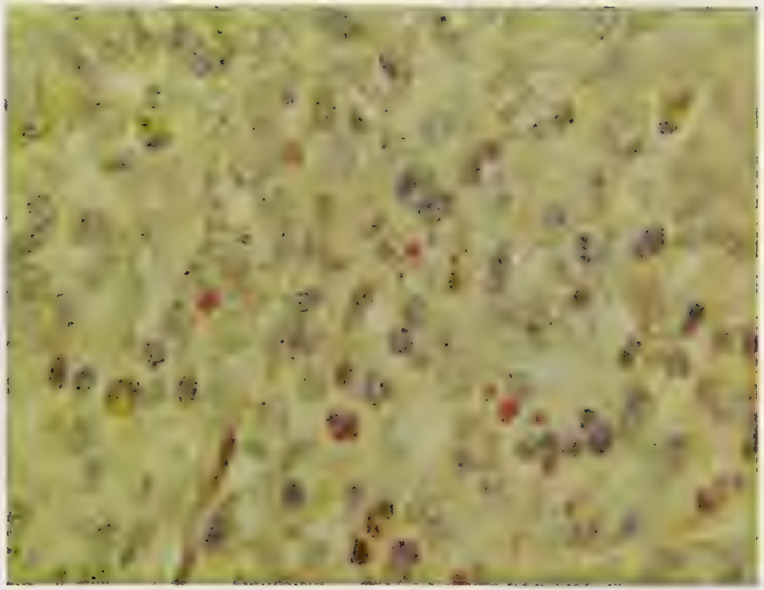

34

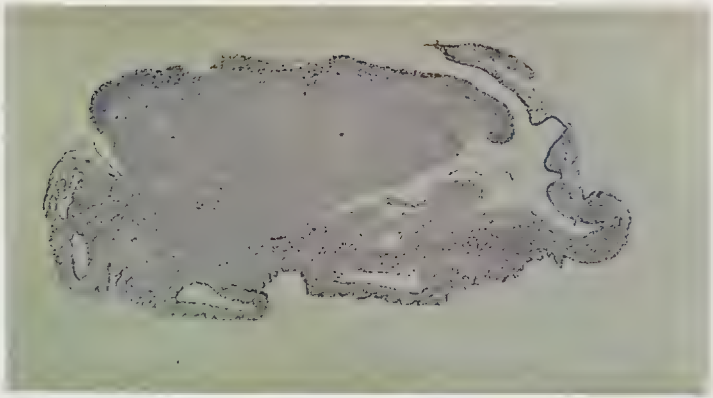

35

PLATE 8

Fig. 36. Chorioallantoic membrane at 9th day of incubation, bearing a graft of adult spleen 2 days earlier. Note edema of the membrane; normal cross-sectional dimensions of membrane are illustrated in the reflected piece lying above the graft. Himes and Moriber triple stain. × 40.

Fig. 37. Chorioallantoic membrane at 9th day of incubation, 2 days after implantation of adult spleen. Contrast with figure 36. Nearly all the graft has become incorporated within the membrane. Himes and Moriber triple stain. × 100.

Fig. 38. Higher magnification of figure 37 to show remnants of adult blood vessels in the graft. Himes and Moriber triple stain. × 500.

Fig. 39. Chorioallantoic membrane at 11th day of incubation, 4 days after implantation of adult spleen. Graft of approximately original dimensions lies on the surface of the membrane. Subjacent membrane highly edematous. Aggregation, primarily of hemocytoblasts, in the lower part of the stimulated area. Toluidine blue, *p*H 4. × 30.

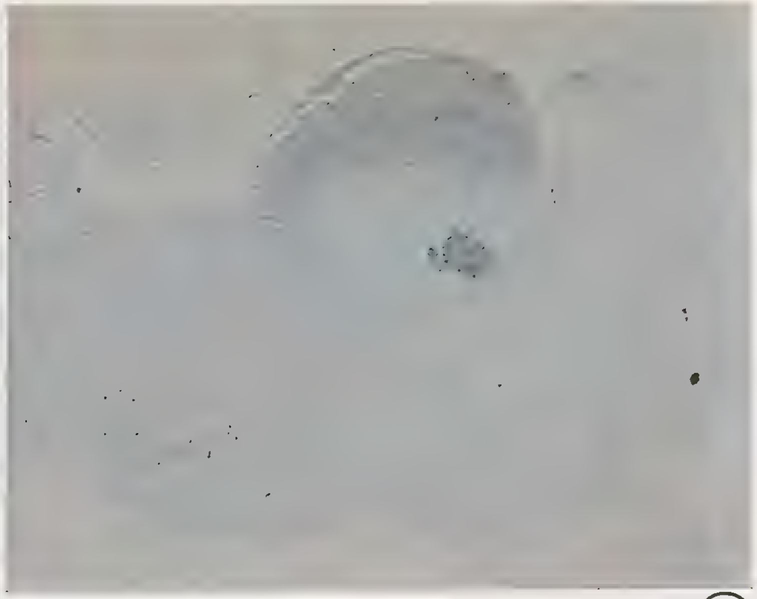

36

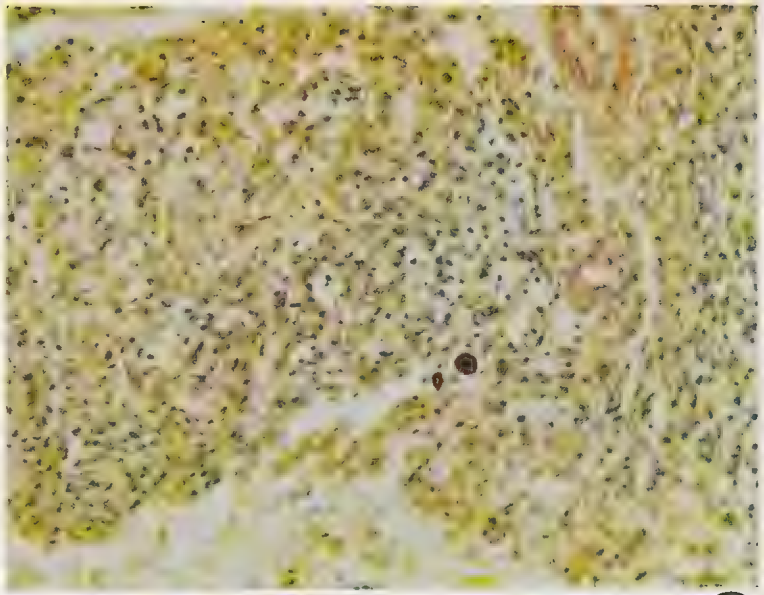

38

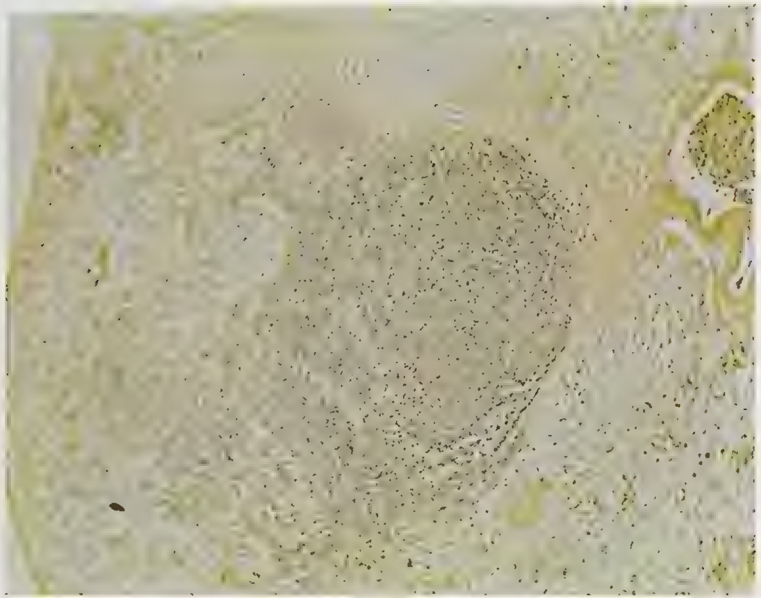

37

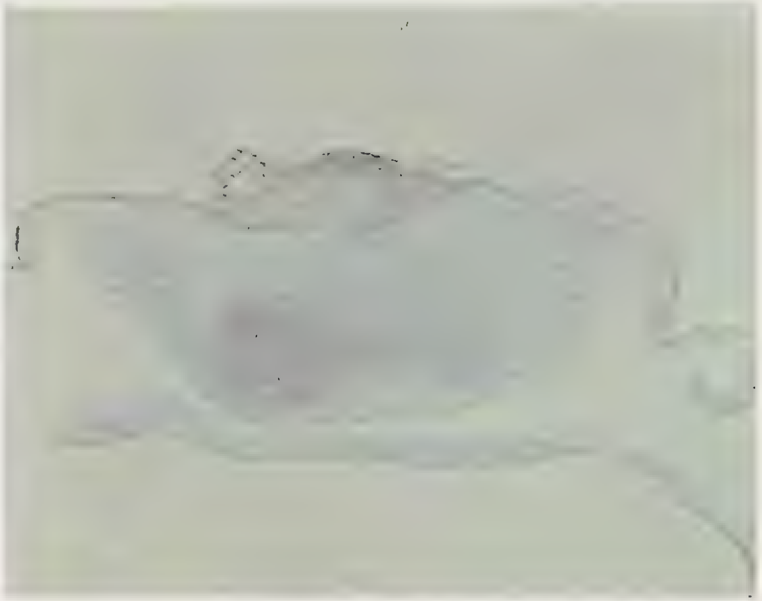

39

PLATE 9

Fig. 40. Inverted section of the splenic graft shown in figure 39. Himes and Moriber triple stain. × 40.

Fig. 41. Chorioallantoic membrane at 12th day of incubation, 5th day after implantation of adult spleen. Note nodule with large allantoic blood vessel. Edema does not explain the intramembranous condition; hemocytoblasts are prominent, granulocytes are present; necrotic region surrounded by giant cells creates cyst in the center. Himes and Moriber triple stain. × 25.

Fig. 42. Chorioallantoic membrane at 12th day of incubation, 5 days after implantation of adult spleen. The chorionic epithelium is unbroken at the region of contact with the graft. Note the periodic acid–Schiff positive inner rind, which appears to push fingers of polysaccharide between the epithelial cells. Himes and Moriber triple stain. × 25.

Fig. 43. Zone of union between chorioallantois of 12-day-old chick and adult graft, showing periodic acid–Schiff positive aggregation at the line of junction and droplets of periodic acid–Schiff positive material within the chorionic epithelium. × 500.

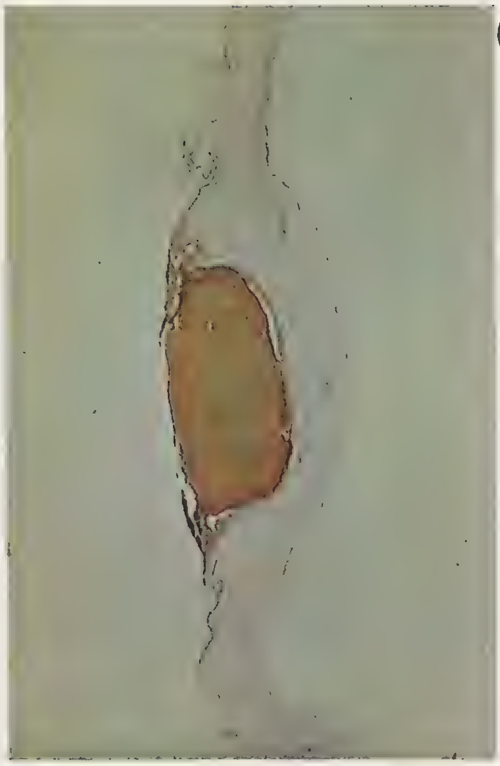
㊷

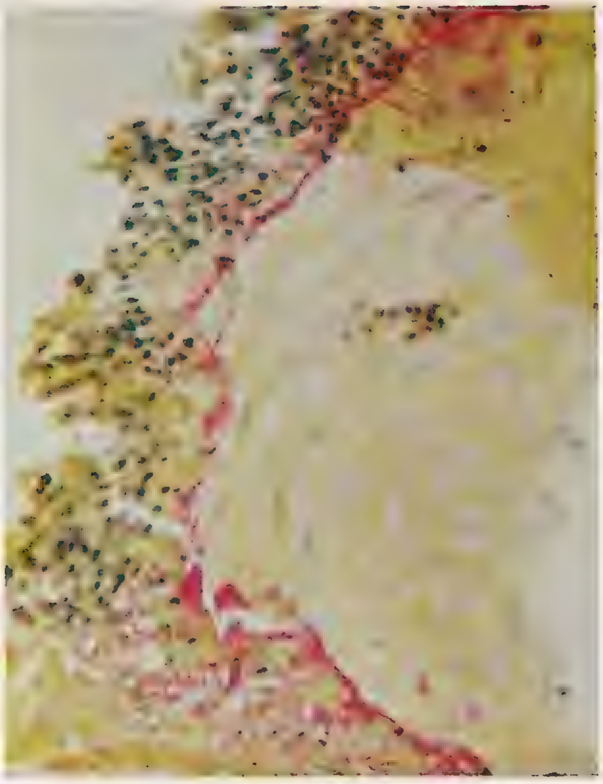
㊸

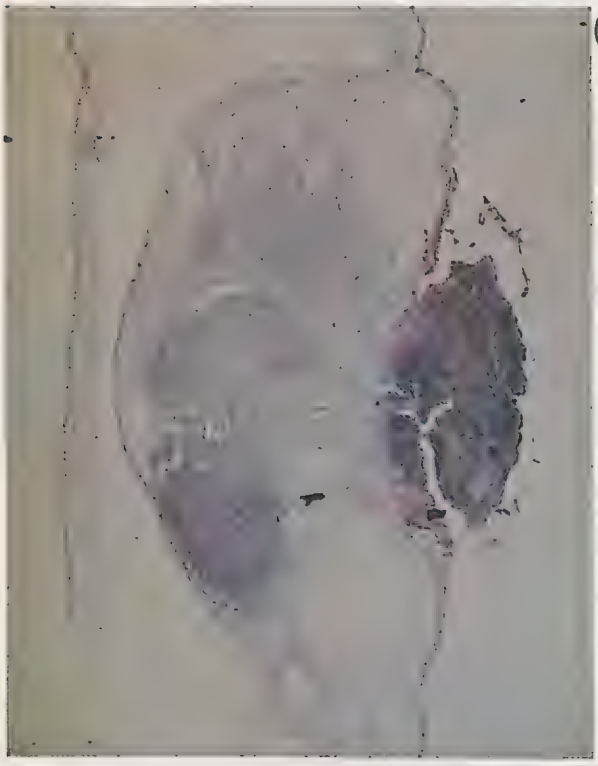
㊵

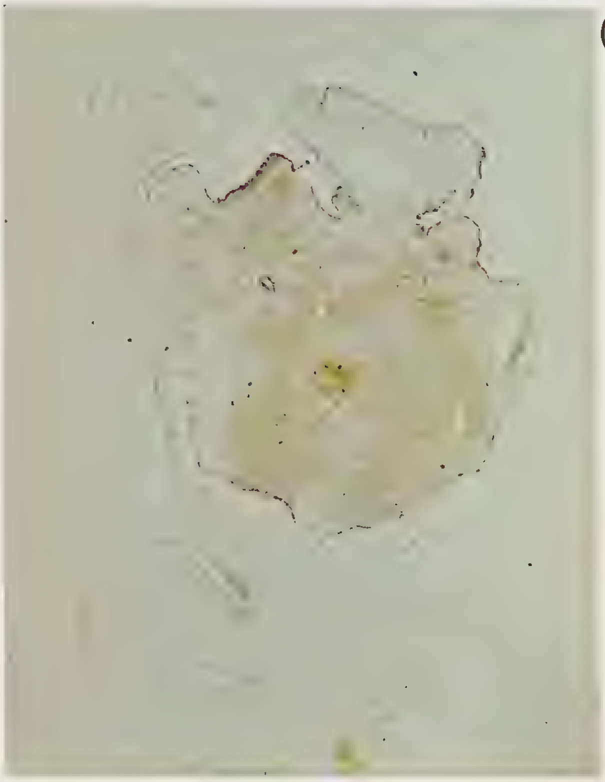
㊶

PLATE 10

Fig. 44. Allantoic edge of affected region of chorioallantoic membrane at 12th day of incubation. Postitive periodic acid–Schiff reaction; mesenchyme cells are fibrotic; some are laden with periodic acid–Schiff positive material. Himes and Moriber triple stain. × 500.

Fig. 45. Chorioallantoic membrane seen from allantoic side; white nodule is half a 17-day-old spleen incorporated into the membrane without affecting it. × 5.

Fig. 46. Section of membrane at 13th day of incubation, 6 days after implantation of graft. Route of incorporation of cells from graft is at the lower right-hand corner. Upper section of photograph shows an achromatic zone containing localized region of necrosis. Toluidine blue, *p*H 4. × 25.

Fig. 47. Chorioallantoic membrane at 15th day of incubation, 8 days after implantation of graft. Extreme effects on the membrane are evident. Several foci of necrosis exist within the membrane. Himes and Moriber triple stain. × 15.

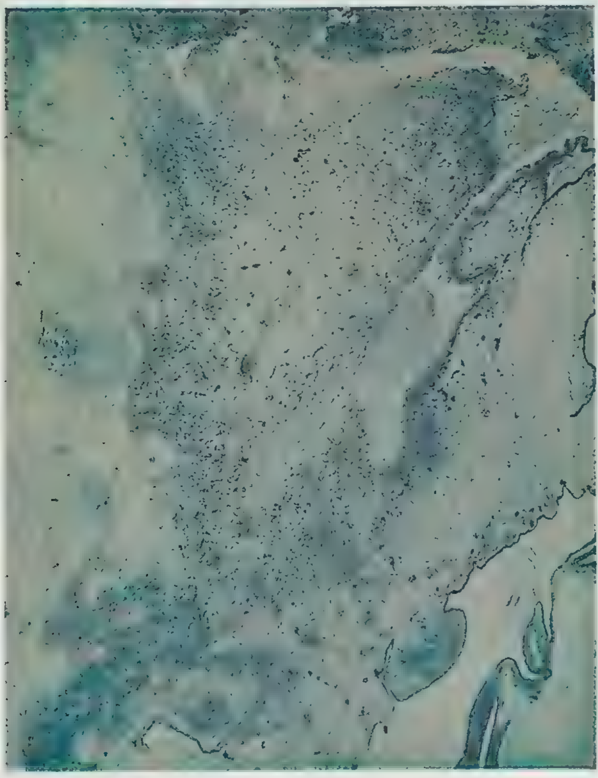

46

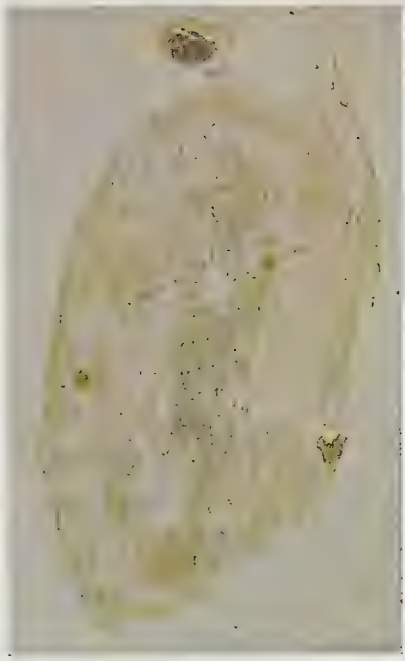

47

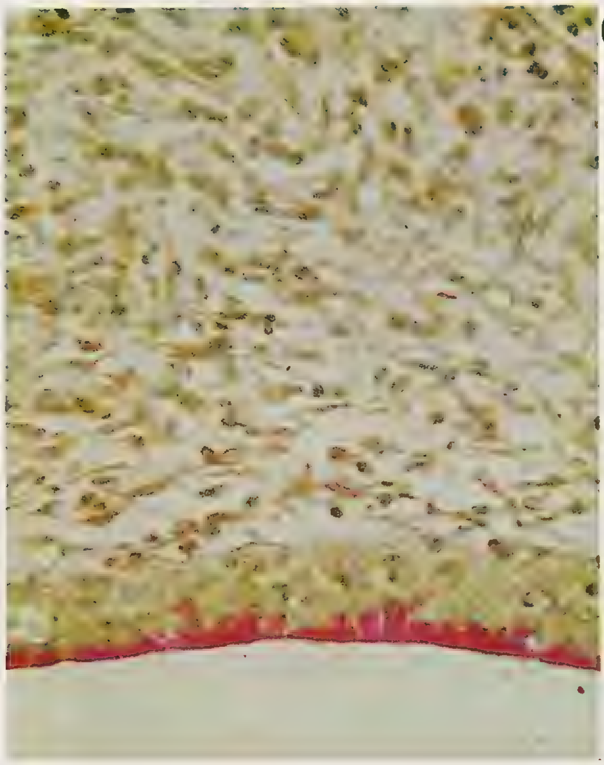

44

45

PLATE 11

Fig. 48. Chorioallantois at 17th day of incubation, 10 days after implantation. Note the original graft lying on the surface of the inverted membrane. At least three necrotic regions are evident, one of which lies in an area of the membrane which is nearly normal in thickness (left). Note also an aggregation of hemocytoblasts between the two major necrotic regions. Toluidine blue, *p*H 4. × 15.

Fig. 49. Chorioallantoic membrane at the 17th day of incubation, 10 days after implantation. The graft has not evoked a strong response within the membrane; there are some hemocytoblasts, but the principal reaction is a generalized edema. Hematoxylin and eosin. × 10.

Fig. 50. Cystic aggregation from 18-day-old embryonic spleen, 11 days after implantation of adult spleen to chorioallantoic membrane. Note dense acidophilia in the center and numerous giant cells around the periphery. Dominici technique. × 200.

Fig. 50*a*. Higher magnification of figure 50, to show details of giant cells at cystic border. Dominici technique. × 600.

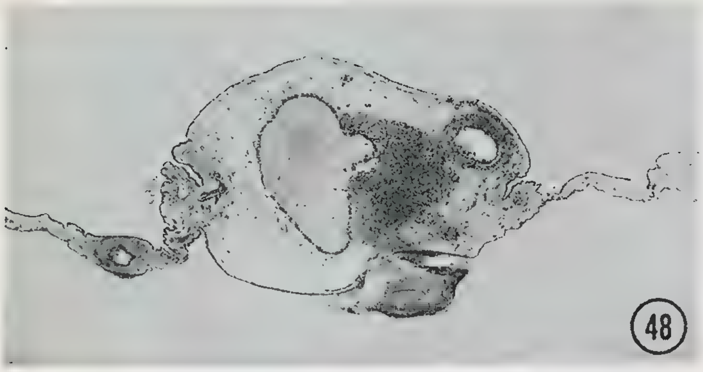
48

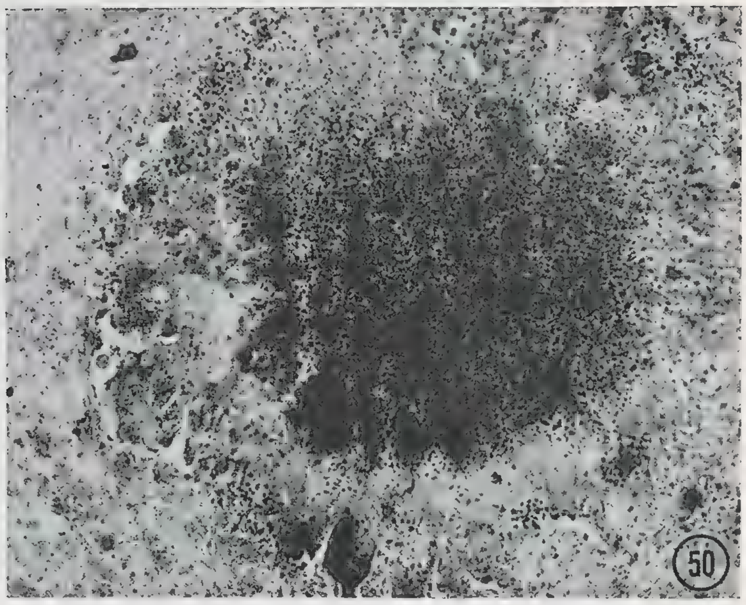
50

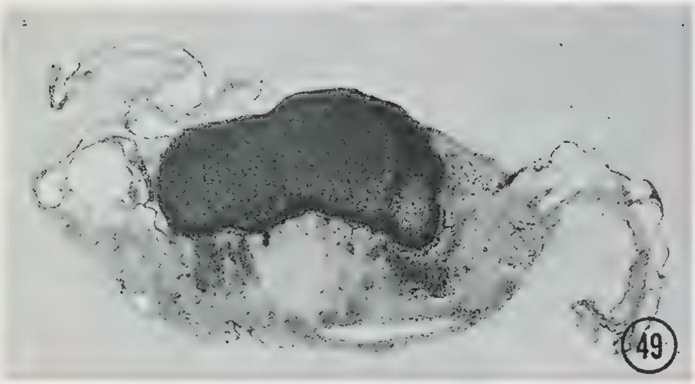
49

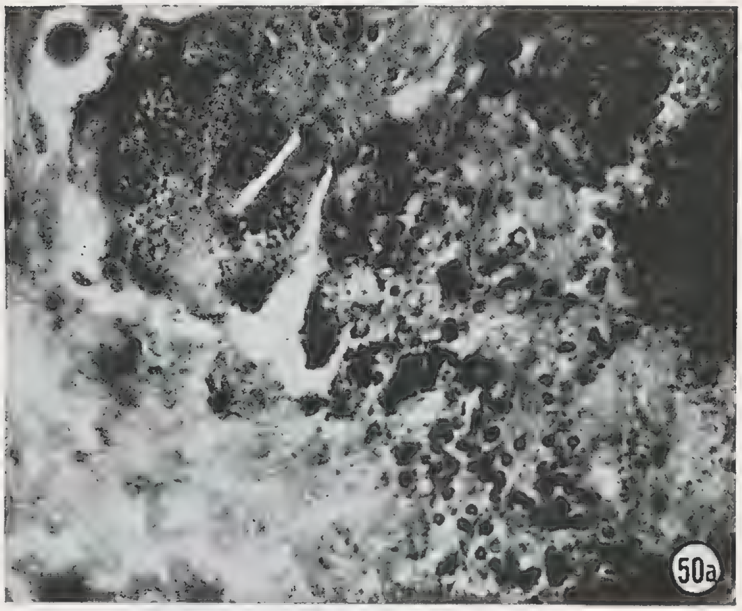
50a

PLATE 12

Fig. 51. Small cyst in 13-day-old embryonic spleen, 6 days after implantation of adult spleen on chorioallantoic membrane. Necrotic aggregation in center of spleen; giant cells at periphery. Toluidine blue, *p*H 4. × 400.

Fig. 52. Cystic chorioallantoic membrane at 18th day of incubation, 11 days after implantation of graft. Note cyst at extreme left. Dominici technique. × 12.

Fig. 53. Higher magnification of figure 52, to show cystic aggregation adjacent to the surface epithelium. Dominici technique. × 100.

Fig. 54. Higher magnification of figures 52 and 53, to show epithelioid connection with cyst. Note small number of granulocytes in epithelioid area. Dominici technique. × 400.

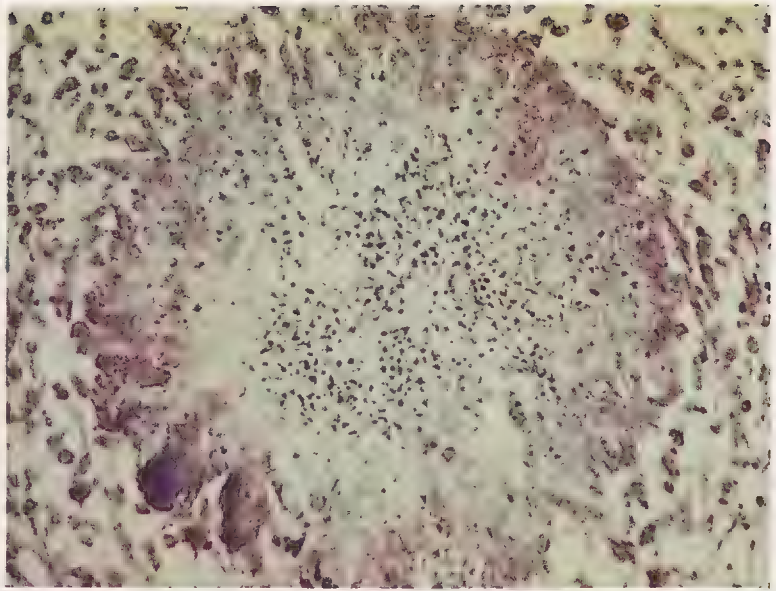

51

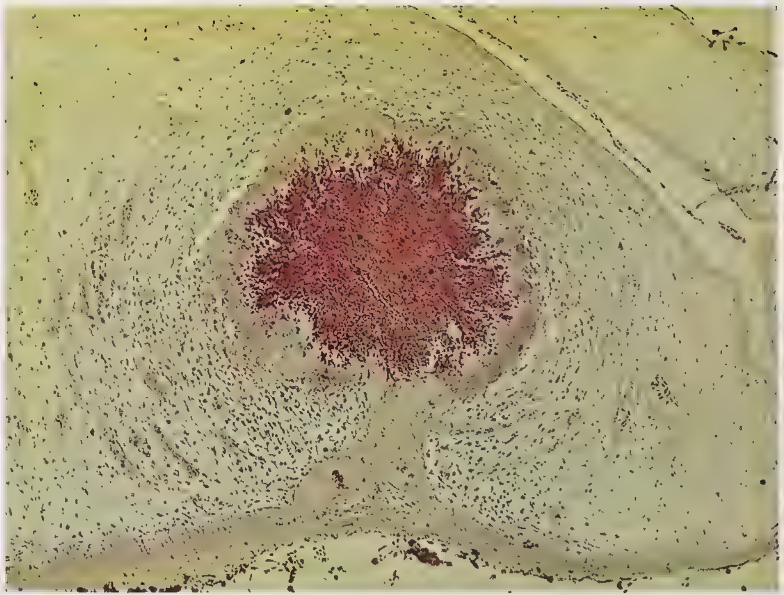

53

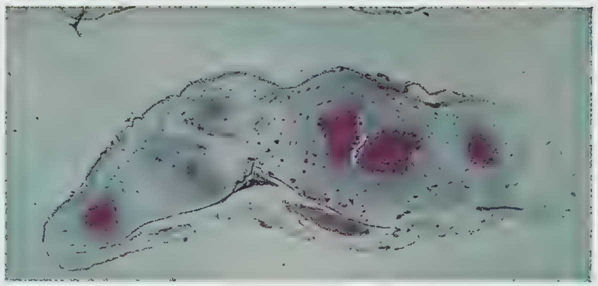

52

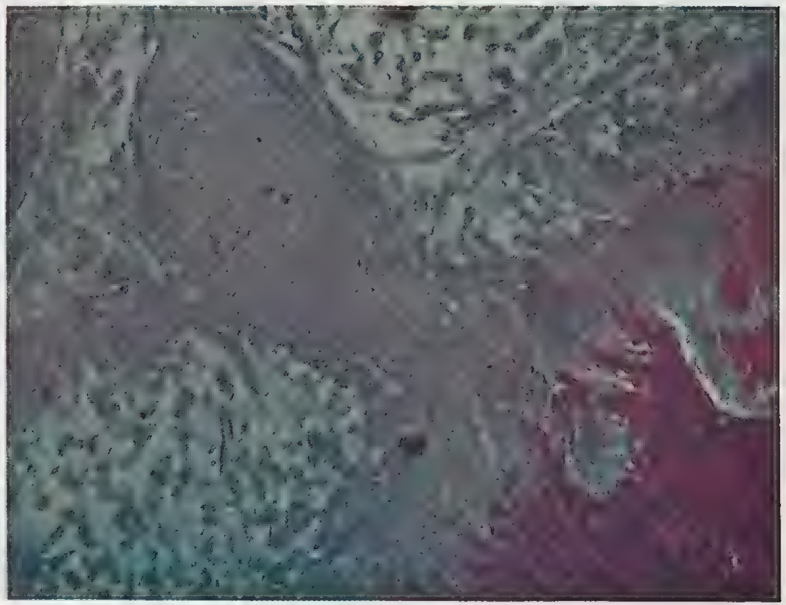

54

PLATE 13

Fig. 55. Cross section of 16-day-old embryo thymus, 9 days after implantation of adult spleen to chorioallantoic membrane. Dominici technique. × 35.

Fig. 56. Eleven-day-old embryonic spleen after second-set implantation of previously affected membrane. Note heterophilic leucocytes. Dominici technique. × 600.

Fig. 57. Eleven-day-old embryonic spleen 4 days after implantation of second-set graft of membrane. RNA staining reduced. Toluidine blue, *p*H 4. × 600.

Fig. 58. Second-set implantation of membrane to membrane of new host on 7th day of incubation, recovered on 11th day. Note boundary dividing region of host membrane undergoing degenerative changes from peripheral membrane. Himes and Moriber triple stain. × 40.

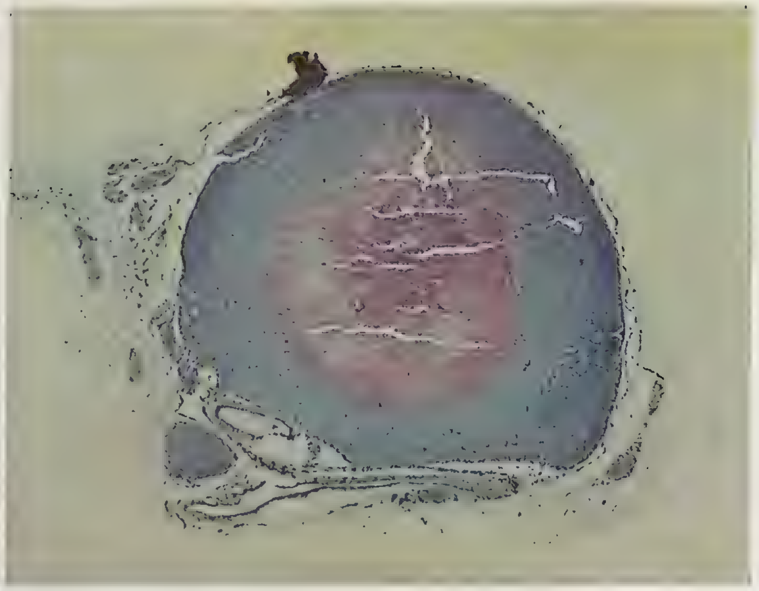

55

57

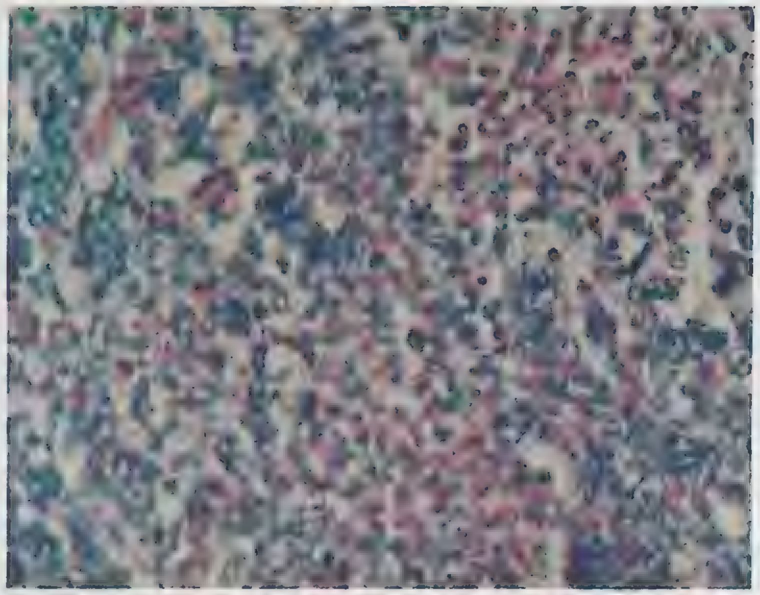

56

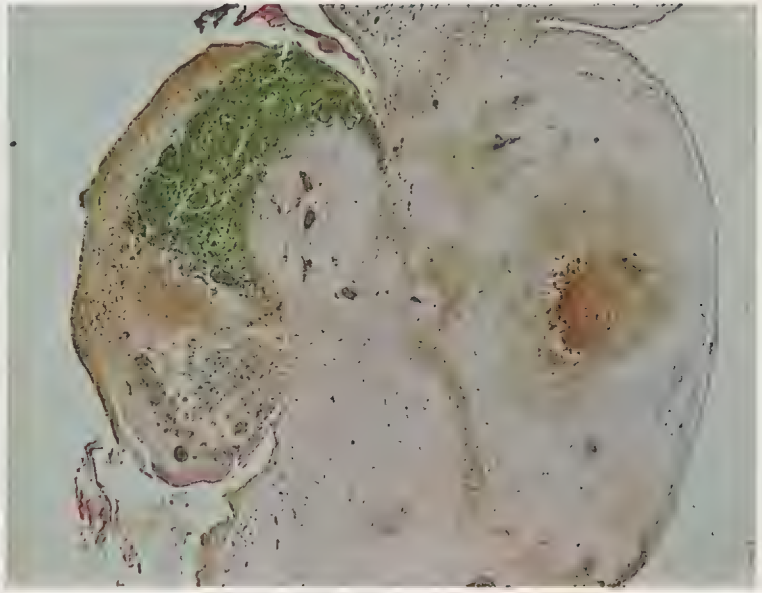

58

PLATE 14

Fig. 59. Achromatic region of host chorioallantois below second-set graft of membrane. Note the zone of junction between achromatic and necrotic region and lateral mesenchyme. Toluidine blue, *p*H 4. × 40.

Fig. 60. Third-set implantation of membrane to membrane of new host at 7 days with recovery at 11 days. Note beginning cystic areas in lower part of host's thickened membrane immediately below graft. Himes and Moriber triple stain. × 40.

Fig. 61. Section of membrane shown in figure 60. Note effect on host's membrane. Dense areas in membrane indicate hemocytoblasts. Toluidine blue, *p*H 4. × 40.

Fig. 62. Chorioallantoic membrane at 13th day of incubation, 6 days after implantation of adult spleen. A nodule bearing a cyst with a dense, necrotic center. The original graft does not show on the surface in the section. Dominici technique. × 25.

Fig. 63. Cross section of chorioallantoic membrane bearing a whole spleen from a 17-day-old embryo embedded within the membrane but without affecting the membrane itself. Himes and Moriber triple stain. × 12.

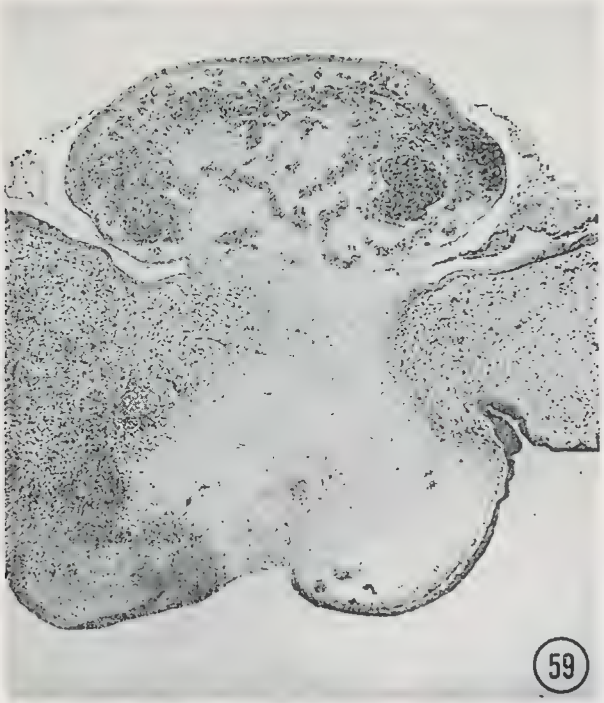
59

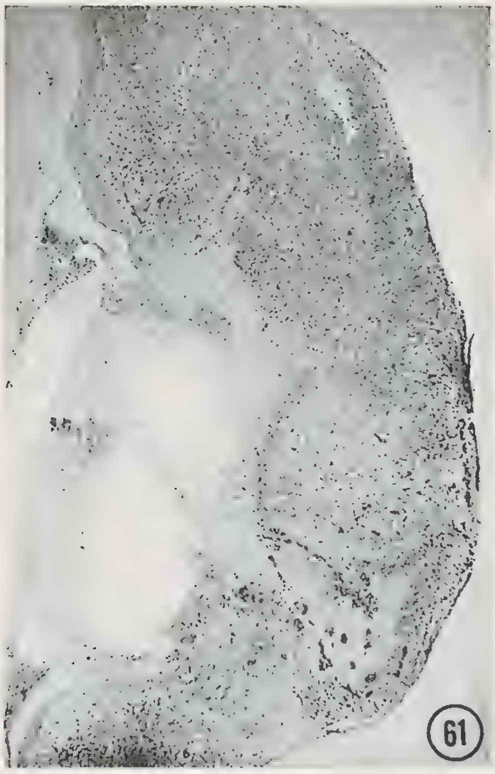
61

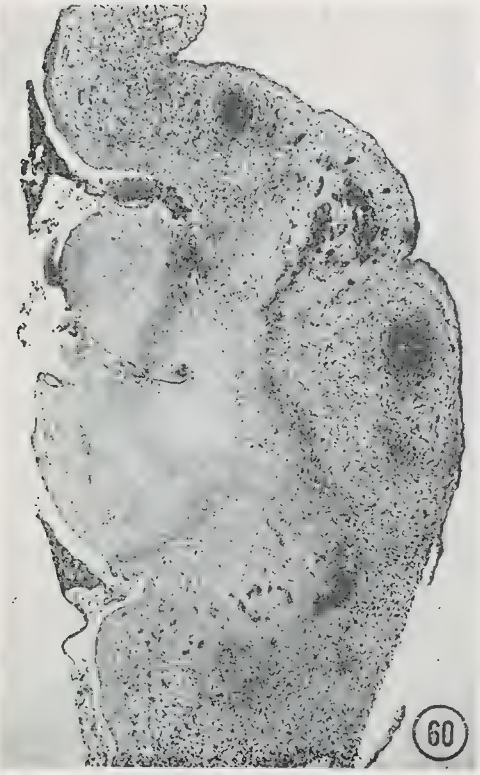
60

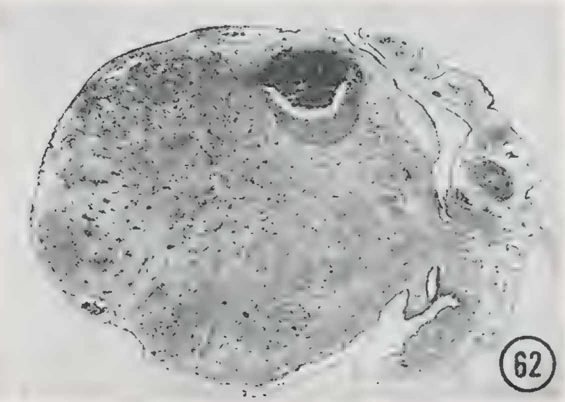
62

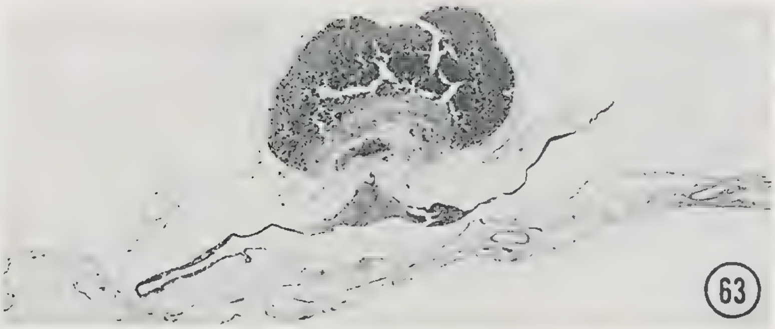
63

CONTRIBUTIONS TO EMBRYOLOGY, NO. 256

DEVELOPMENT OF THE VENTRICLES AND SPIRAL OUTFLOW TRACT IN THE HUMAN HEART

A Contribution to the Development of the Human Heart from Age Group IX to Age Group XV

Pieter A. de Vries and John B. de C. M. Saunders
University of California School of Medicine
San Francisco, California

With nine plates and nine text figures

CONTENTS

PAGE

INTRODUCTION 89
  Terminology 89
  Fluid Dynamics in Spiral Septation of the Heart 90

MATERIAL AND METHODS 91

AGE GROUPS IX AND X 92
  Embryo 5080 93
  Embryo 3709 93
  Embryo 1878 94
  Embryo Klb 95
  Embryo 4216 95
  Embryos of 8 to 12 Somites 96

AGE GROUP XI 96
  Figure 3*C, D;* Figure 5 96

AGE GROUP XII 97
  Figure 6; Plates 2, 3, 4 97
  Embryo 8944, 25 Somites 97
  Embryo 5923, 28 Somites 100

AGE GROUP XIII 101
  Figures 6, 7, 8; Plates 6, 7 101
  Embryo 836, 30 Somites 102
  Embryo 8066 103

AGE GROUP XIV 104
  Embryo 6502 104

AGE GROUP XV 106
  Figures 7 and 9*C, D;* Plates 2, 9 106

DISCUSSION 107

LITERATURE CITED 112

DEVELOPMENT OF THE VENTRICLES AND SPIRAL OUTFLOW TRACT IN THE HUMAN HEART

A Contribution to the Development of the Human Heart from Age Group IX to Age Group XV

INTRODUCTION

The purpose of this paper is to present the morphological findings[1] in a study of the developing heart in human embryos from age group ix to age group xv inclusive, and to correlate these findings with the physical forces that, from our observations on fluid dynamics, we believe are important in influencing cardiac development.

The study was initiated by an inquiry about the mechanisms of change in cardiogenesis, for the purpose of gaining some insight into the manner in which certain cardiac anomalies developed. A review of the literature on the subject of normal and abnormal development confirmed our impression that the numerous conflicting opinions encountered are, in large part, due to insufficient data on normal development. The number of early embryos available for study in previous reports has been small; some stages in which significant changes occur have not been described. In fact, there has been no illustrated description, based on a closely graded series of human embryos belonging to age groups xii to xv, inclusive, of that portion of the developing human heart extending from the atrioventricular junction to the arterial arches. This omission is surprising, because it is in these age groups that the spiral outflow tract of the heart is undergoing its development. This study attempts to repair the deficiency in our knowledge of this period of development.

The first enlightening account of the development of the heart, based on a study of human embryos serially sectioned but not reconstructed with precision, was made by His and reported in detail in 1885. He described five hearts belonging to what we would now designate as age groups xi to xv, illustrating his interpretation of the changes by means of freehand drawings of questionable accuracy. In this publication, which has served as an important source of reference on the development of the human heart, His expressed his indebtedness to a contemporary, F. T. Schmidt (1870), for his studies on developing human hearts.

Born's description of the development of the mammalian heart, based on wax-plate reconstructions, established a new standard of accuracy and, in consequence, has been held in the highest regard since its publication in 1889. His descriptions and illustrations were derived almost entirely from studies of rabbit embryos. Tandler (1912), because of an inadequacy of human material, which consisted of only three embryos (R. Mayer, age group xii; Hal 2, age group xiv; Hal 6, age group xv), used Born's descriptions to develop his account of cardiogenesis in man, which appeared in the text by Keibel and Mall (1912) and was illustrated sparsely in the age groups under discussion. More complete descriptions and illustrations of cardiac development in man were advanced by Waterston (1918), Davis (1927), and Streeter (1942, 1945, 1948). Waterston made scattered accurate observations in age groups x to xv, but, owing to the incompleteness of material, he was unable to provide a comprehensive account. Davis's superb report was restricted to embryos falling within age groups ix, x, and xi.

Terminology

In discussing the region between the atrioventricular junction and the arterial arches of the developing heart, many authors have been confronted with the problem of terminology. In studies of cardiogenesis, this problem results not only from too few observations of the developing heart but also from conflicting interpretations, both phylogenetic and ontogenetic. To resolve these conflicts, theoretical ideas must be related to observations of changes in form. Later in this article we shall identify the several descriptive terms that are, or have been, in common usage and attempt to clarify and simplify this terminology. In the meantime, however, we shall employ the terminology outlined below:

Following the direction of blood flow, we shall refer to the venous end of the heart tube as proximal, and the end associated with the arterial arches as distal. We prefer the term arterial arches to branchial arches or aortic arches, because "arterial" does not embody controversial connotations of homology but allows for more specific descriptive terminology as developmental change brings into being one or another pattern of mature structure. The most distal portion of the heart, which Davis

---

[1] These studies were aided by grants from the New York Crippled Children's Association and the San Francisco Heart Association.

Definition of developmental horizons and age groups is presented by Streeter (1942). Descriptions of the age groups may be found in the publications by Streeter (1942, 1945, 1948).

For the sake of uniformity, the descriptions and illustrations of the developing heart by other authors prior to Streeter's work have been brought into accord with Streeter's age-group classification with as much precision as the data of these authors would permit.

(1927) designated the "aortic bulbar portion," appears, according to our studies of age groups ix, x, and xi, to be the precursor of the truncus arteriosus, and we shall so designate it. We have divided Davis's cardiac bulbar portion, which is usually referred to by others as the bulbus cordis, into the trabeculated right ventricle proximally and infundibulum distally, at such times as these structures appear; this is done on the basis of serial observations which include age groups ix through xv.

In normal development the infundibular region appears to contribute, for the most part, to the right ventricle of the fully developed heart, being incorporated into it in the same sense that the sinus venosus is incorporated into the right atrium.

Before Streeter's (1945) use of the term primary heart tube for that part of the developing heart between the atrioventricular junction and the arterial arches, the term, in general usage, had also included the atria and the sinus venosus. Streeter's restricted usage has the advantage of allowing one to describe two general areas of the developing heart: the venous part, proximal to the atrioventricular junction; and the arterial part, or primary heart tube, distal to the atrioventricular junction. We shall use the term as defined by Streeter (1948), for we can then stipulate the regions of the developing trabeculated ventricles and forego (at certain stages of development) the use of the ambiguous term ventricle for the region between the infundibulum and the atrioventricular junction. However, we do not subscribe to Streeter's view that the arterial part of the heart is sufficiently different from the venous part, in genesis and in the nature of its myoendocardial layers, to warrant his restriction. It will be shown that between age groups x and xv the gelatinous myoendocardial layer is not restricted to the arterial part of the heart.

The terms employed are illustrated in figure 1, which presents a synopsis of the changes in the heart chambers in age group ix through xv. The arrows denote the directions of growth and migration of areas between successive stages.

Fluid Dynamics in Spiral Septation of the Heart

Correlation of the morphological findings with our observations on the nature of fluid patterns resulting from intersecting streams led to a theory of the development of spiral septation, which requires exposition before the data are presented.

It has long been recognized that vertebrates with a double circulation, i.e., lesser or greater separation of blood into pulmonary and systemic circuits, have, at some time during the development of the heart, a spiral structure in the heart's outflow tract. It is generally accepted that in all mature normal mammals the blood is

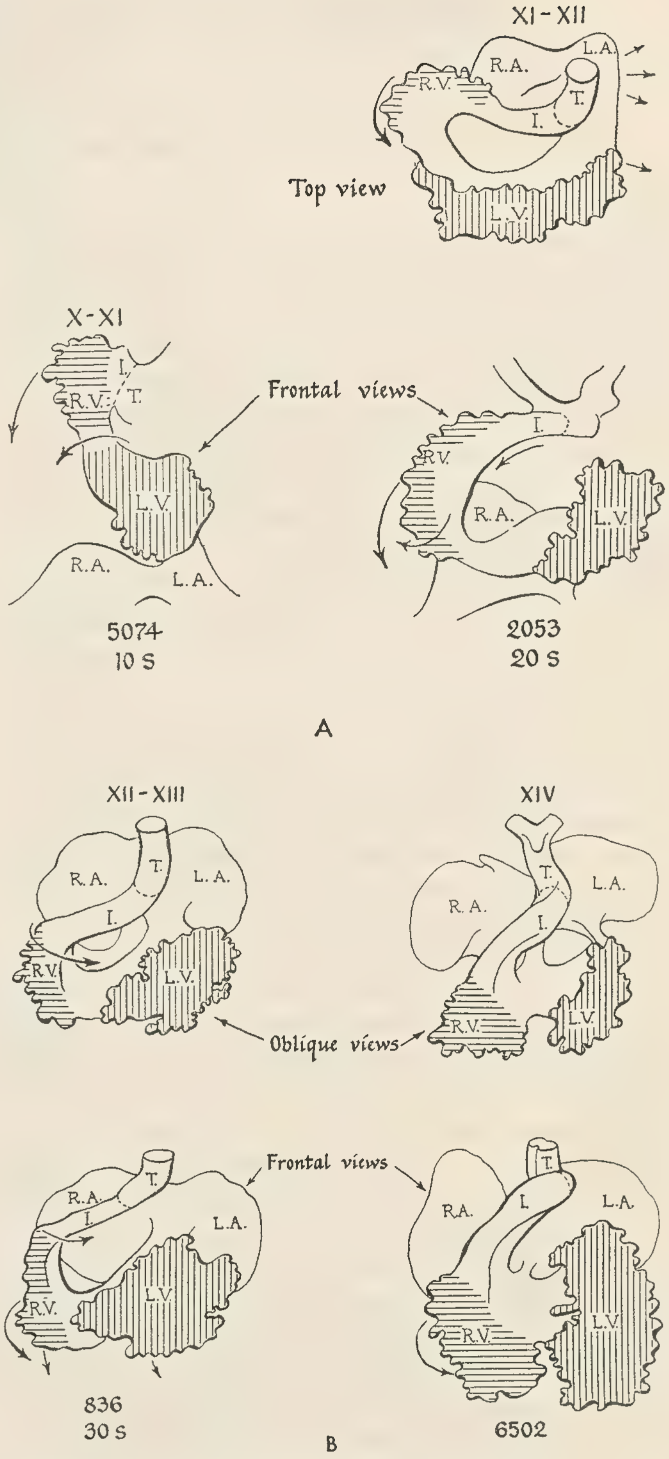

Fig. 1. Tracings of photographs of reconstructions of heart lumina of embryos. *A:* 5074, 10 somites, age group x, frontal view; 2053, 20 somites, age group xi, top and frontal views. *B:* 836, 30 somites, age group xiii, oblique and frontal views; 6502, age group xiv, oblique and frontal views. The arrows indicate the directions of expansion of the lumen and the changes in position which occur in each stage. The regions described in the text are labeled as follows: *R. A.*, right atrium; *L. A.*, left atrium; *L. V.*, left trabeculated ventricle; *R. V.*, right trabeculated ventricle; *I.*, infundibulum; *T.*, truncus arteriosus.

pumped into pulmonary and systemic circuits by hearts in which blood flows from the right ventricle into a sixth arterial arch, and from the left ventricle into a fourth arterial arch, with intact walls separating the streams of flow. The manner in which this separation is accomplished, however, has remained a subject of controversy.

We will reserve for later discussion a comparison of our views with those of others.

We shall demonstrate that the outflow tract, between the trabeculated ventricles and the arterial arches of the developing human heart, develops spiral ridges between age groups xii and xv, which, we suggest, result from a molding of the endothelial-lined gelatinous layer of the infundibulotruncal region by a spiral fluid stream coursing through its lumen. In our hypothesis a spiral fluid stream, the shape of which in cross section is that of a dumbbell, modulates the gelatinous cylinder of the outflow tract to form two channels, eventually resulting in two separate lumina. The spiral fluid stream is viewed as the product of two junctioning blood flow vectors, one derived from the left ventricular pump and the other from the right ventricular pump.

We studied fluid shapes derived from junctioning streams and experimentally produced fluid configurations which revealed that the direction of a fluid spiral is dependent on the relation of the planes of junction of the two streams. For example, if two cylindrical fluid streams (surrounded by air), whose axes are in the same plane, join with each other, the resultant configuration will be that of perpendicularly alternating, flattened nodes. The amplitude of the nodes is dependent on the velocity of the streams and the angle of junction within the plane. The two streams, though fused, remain largely discrete and lateralized except for progressive diffusion (pl. 1*A, B*).

Two junctioning streams, the axes of which are not within the same plane, form a spiral in which the original two components remain separated and revolve about each other.

If two streams are made to junction from the right and left, and the axis of the left cylindrical stream is fixed, the direction of the spiral can be changed from counterclockwise to clockwise by shifting the plane of axis of the right stream from a position partly behind the left stream to one partly in front. In so doing a nodal pattern develops at the mid-point of transit where the axes of the streams lie within the same plane. These fluid configurations are shown in plate 1*C, D*. The basic patterns persist whether or not the streams are pulsatile, and differences in volume or velocity between the two streams distort but do not destroy the patterns. When two streams were made to junction within the lumen of a cylinder having a thick, plastic (gelatin or silicon) internal layer, ridges and depressions in the plastic layer, similar to those seen in the heart's outflow tract, were observed if the flow vectors of the intersecting streams were controlled as described.

The development of spiral septation can be viewed, then, not only as a result of the action of a spiraling stream molding the plastic subendothelial tissue but primarily as a function of the morphological development of two ventricles so located as to produce flow vectors which will join in a specific manner. The ventricular relation required for the genesis of a fluid form, spiraling clockwise in a distal direction, is that of a left ventricular stream which joins dorsally with a right ventricular stream.

If our theory is correct, no evidence of developing spiral septation should be found prior to the development in appropriate relations of the ventricles; further, when such relations come into existence the elaboration of spiral ridges should become manifest.

Our findings will be presented in descriptions of cardiogenesis by age groups, after which theoretical views on the development of anomalous form, as related to the effects of blood flow, will follow in the Discussion.

MATERIAL AND METHODS

Most of the human embryos in our study are from the collection of the Department of Embryology, Carnegie Institution of Washington. They were made available by the director, Dr. James D. Ebert. This collection, studied under the tutelage of one of its principal contributors, Dr. G. W. Bartelmez, provided more well preserved early embryos than were available to earlier authors. The late Dr. Carl L. Davis gave generously of his thought, and supported with great enthusiasm the reevaluation of early cardiac development including many of the specimens described in his notable contribution on cardiogenesis (1927).

Study of serial sections was aided by the availability of excellent photographs of the intact embryos. After fixation, many of the embryos had been photographed from several views, often stereoscopically; some of the specimens had been photographed while fresh, hence the extent of shrinkage and distortion could be evaluated. The photographs were valuable also in evaluating the relation of the heart to other structures in the embryo.

Plaster casts of wax-plate reconstructions of hearts and of whole embryos made by Mr. O. O. Heard were used also. These are:

Age group ix: Embryos 5080, 1 somite; 1878, 2 somites.
Age group x: Embryos 3709, 4 somites; Klb, 6 somites; 4216, 7 somites; 391, 8 somites; 4439, 9 somites; 1201, 8 somites; 4251, 9 somites; 5074, 10 somites; 3707, 12 somites.

Age group xi: Embryos 6344, 14 somites; 4529, 14 somites; 470, 17 somites; 6050, 19 somites; 2053, 20 somites.
Age group xii: Embryo 5923, 26 somites.
Age group xiii: Embryo 836, 30 somites.
Age group xv: Embryo 3385.
Age group xvi: Embryo 6510.
Age group xvii: Embryo 6520.

Most of the reconstructions of the hearts had been made with reference to the external form of the embryos and were controlled by accurate profiles of the intact specimen. Such controls are important for the early stages especially; only the Lewis-Heuser method of reconstruction makes it possible to obtain with precision the form of an internal organ. The reconstructions were examined, checked against the serial sections, and photographed anew in specific orientations: ventral, right and left profile, and from above. Special care was exercised in determining the correct plane and axis of such photographs. In addition, graphic reconstructions of some of the specimens (age group x to age group xv, inclusive) were made for purposes of orientation during the study of serial sections and as a further check on the accuracy of the reconstructions.

Reconstructions of the hearts of five embryos were made specifically for the present study, with the technical assistance of Miss C. Barth. Four of these embryos were from the Carnegie Collection: embryos 8944, 25 somites, age group xii; 5923, 28 somites, age group xii; 8066, age group xiii; and 6502, age group xiv; the fifth reconstructed specimen, from the collection of the authors, will hereafter be referred to as embryo S. It fulfills Streeter's criteria for age group xv.

At least three models were made of each of the five hearts: One of the endothelial tube, or cavities; one of the myoendocardial layer, showing developing cushions or ridges; and one of the myoepicardium. In embryos 8066, 6502, and S, inlays of different colored wax were added to the reconstructions of the myoendocardium. Reconstructions of the pericardium with various layers of the heart suspended within, together with photographs of the intact embryos, were used for orientation. The cut-outs of the poured wax plates were made by tracing on the wax the transilluminated direct-contact image of an underlying thin paper or stripping film photograph. This method is more accurate than tracing an image obtained by optical means, since it avoids errors due to the distortion of parallax. A photograph of each section was made at a magnification of 100× in embryos 8944, 5923, and 6502; 125× in embryo S. Bromides with orientation lines on the sections were available in embryos 5923, 100×; 6502, 50×; 836, 100×; and 8066, 50×.

The text figures are either tracings of photographs of wax-plate reconstructions or tracings of graphic reconstructions made from photographs of individual sections of an embryo.

Most of the serially sectioned embryos studied, other than those noted above, are listed in Developmental Horizons in Human Embryos (Streeter, 1942, 1945, 1948). Other embryos, added to the Carnegie Collection subsequent to Streeter's listings, which proved valuable for this study are: 8941, 25 somites; 8943, 22 somites; 8505(a), 24 somites; 8505(b), 23 somites; and 9154, 24 somites.

A few embryos in our own collection, staged in age groups xi through xiv, were sectioned and variously stained for identification of the nature of the myoendocardial tissue.

AGE GROUPS IX AND X

It was our original intent merely to refer to Davis's (1927) work on the development of the heart from its first appearance to its form in embryos having 20 pairs of somites, and to go on to descriptions of age groups xii to xv, inclusive. However, we found it necessary to correlate the findings in age groups xii to xv with those in the earlier age groups ix, x, and xi. Consequently, these earlier age groups have been re-examined.

Several studies of the structure of the early embryonic mammalian heart have been published, including those of Wang (1917–1918), on the ferret; Schulte (1914), on the cat; Strahl and Carius (1899) and Yoshinaga (1921), on the guinea pig; Streeter (1927) and Patten (1931), on the pig; Girgis (1930, 1933) and Murray (1919), on the rabbit; Burlingame and Long (1939) and Goss (1938, 1952), on the rat. A review of early cardiac development in Mammalia as well as in other classes of vertebrates revealed significant differences of observation and interpretation between species as to the mode and time of development of an unpaired tubular heart. It is not within the scope of this paper to discuss all the conflicting views about these earliest stages.

It has usually been stated by those who have written on early cardiogenesis that fusion of lateral primordia first takes place in the region referred to as the bulbus or conus, although it is often not stipulated whether reference is made to myocardial or endocardial elements alone. Very early fusion of partially connected lateral myocardial elements appears to be supported by DeHaan's (1959) experimental studies in chick embryos. By chemically or surgically treating the endoderm of chick blastoderms at pre- or early-somite stages, he was able to produce separately beating double hearts, which often were joined in the middle at the anterior ends in the region of the "conus or ventral aorta."

We should like to point out that the use of the terms conus or bulbus cordis, in describing spatial relationships in the very early developing heart, connotes a sequential knowledge of the evolving morphology at later stages. Such knowledge of the human heart has been lacking.

Davis (1927) described and illustrated five developing hearts within the period, 1 to 7 somites, during which fusion of lateral cardiac elements occurs. These specimens, which we have restudied, are, in order of their increasing cardiac development: embryos 5080, first somite forming; 3709, 4 somites; 1878, 2 somites; Klb, 6 somites; and 4216, 7 somites.

Embryo 5080. In the youngest specimen of this series, the primordial heart developing in the precephalic mesoderm is represented by a layer of cells bounded dorsally by the horseshoe-shaped developing pericardial cavity and ventrally by the endoderm of the yolk sac. This layer is the so-called cardiogenic plate, a term first used by Mollier (1906) to describe cardiac primordia in the embryos of reptiles and birds. The plate, roughly U-shaped, consists of an irregularly thickened layer of cells (splanchnic mesoderm) separated from the thinner somatic mesoderm by the cystic pericardial cavity. It is the precursor of the myoepicardial mantle, which includes the paired cardiogenic folds. The angioblasts which appear to be proliferating from the ventral side of the mesodermal cardiogenic plate are the primordial cells of the endothelium, and lie between the cardiogenic plate and the endoderm of the yolk sac.

In this specimen, where the heart primordium is dorsal to the yolk sac, there is no evident morphological differentiation denoting the site of future cardiac chambers.

Embryo 3709. Figure 2*A* and *B*. This second specimen, with 4 pairs of somites, shows marked advances in the development of the heart. The cardiac primordium, having undergone rotation, now lies ventral to the developing foregut. Within the now ventrally placed pericardial sac, the myoepicardial mantle encloses ventrally and laterally the endothelial plexi which lie surrounded by cardiac jelly on the ventral endoderm of the foregut. Bilaterally the mantle is roughly symmetrical, with paired cardiogenic folds diverging at an acute angle rostrally and at an obtuse angle caudally. There is a mid-sagittal groove in the caudal half of the ventral surface of the mantle, which is presumed to be the line of fusion of lateral folds. In the rostral half there is a median bulge between the lateral folds, which, in the absence of intervening stages, may represent the site of primary myocardial continuity between the two otherwise separated lateral cardiogenic folds, seen in the earlier stage as the central portion of the cardiogenic plate below the median transverse pericardial limb. (See Yoshinaga [1921] on early development in the guinea pig for greater detail concerning the earlier stages of development in Mammalia.)

There are three ectal grooves and corresponding ental ridges traversing each of the myocardial folds. These grooves or sulci are most prominent laterally, and diminish in depth as they approach the mid-ventral area of fusion cephalically or the medial unfused border of each of the two folds in their caudolateral extensions.

Davis used the terminology of earlier investigators, which stemmed from studies of cardiac development in forms other than man. Although our observations confirm the presence of the landmarks described by Davis, his terminology is acceptable only in a very limited sense since it presents difficulties in its implications of the developmental fates of the regions concerned.

The most prominent pair of sulci divide the myoepicardial mantle into a cephalic half and a caudal half. Davis designated these as the right and left bulboventricular sulci. We shall substitute the term interventricular for Davis's bulboventricular, for we believe that these sulci divide the right ventricular primordia from those of the left. There is ample evidence for this contention. As we shall see in the serial observations which follow, and as was noted by His (1885, 1886*a, b*), the right and left ventricles arise in series rather than in parallel. The right ventricle of embryo 3709 is distal or toward the arterial arch, whereas the left ventricle is proximal or toward the atria. Davis's designations of right ventricle and left ventricle refer to regions which we consider to be paired primordia of the left ventricular region of the primary heart tube. To designate these areas of the right and left folds as right ventricle and left ventricle leads to confusion, and supports the erroneous concept that originally paired parallel ventricles fuse to form a common ventricle, which somehow divides again, along the old line of fusion of the folds, to create right and left ventricles. We cannot accept Girgis's conclusion, "Each half of the adult mammalian heart arises from the cardiac tube of the corresponding side" (Girgis [1930], p. 780).

The mantle rostral to these interventricular sulci Davis termed the bulbus. He divided the bulbus on the basis of a less well demonstrated pair of ectal sulci (the right and left interbulbar sulci), and corresponding ental ridges, into two regions: (1) the bulbus cordis, the small areas of the ventrally fused lateral folds lying between the interbulbar and bulboventricular sulci or ridges; and (2) the bulbus aorta, the much larger rostral segments of the lateral folds together with the connecting mid-ventral protuberant area. We have substituted the term infundibulotruncal for interbulbar, since it appears to us, by virtue of serial observations which continue through subsequent age groups, that the so-called aortic bulb is, in fact, the primordium of the truncus arteriosus, and that the so-called bulbus cordis is actually the primordium of the right ventricle and infundibulum.

The myoepicardial mantle caudal to the interventricular sulcus is comprised of the diverging portions of the lateral folds and a flat, intervening myocardial area, referred to as the middle cardiac plate. A sulcus is seen on the ectal surface of each of these divergent folds. These two sulci divide the caudal half of the mantle into paired right and left ventricles and smaller caudolaterally placed right and left atria. The paired longitudinal endothelial plexi are joined beneath the middle cardiac plate in the ventricular area, and this Davis called the "interventricular anastomosis." We shall refer to it as the left ventricular anastomosis. Two more slender transverse communications of endothelial strands above this level, which Davis termed the interbulbar anastomosis, we shall call the right ventricular anastomosis.

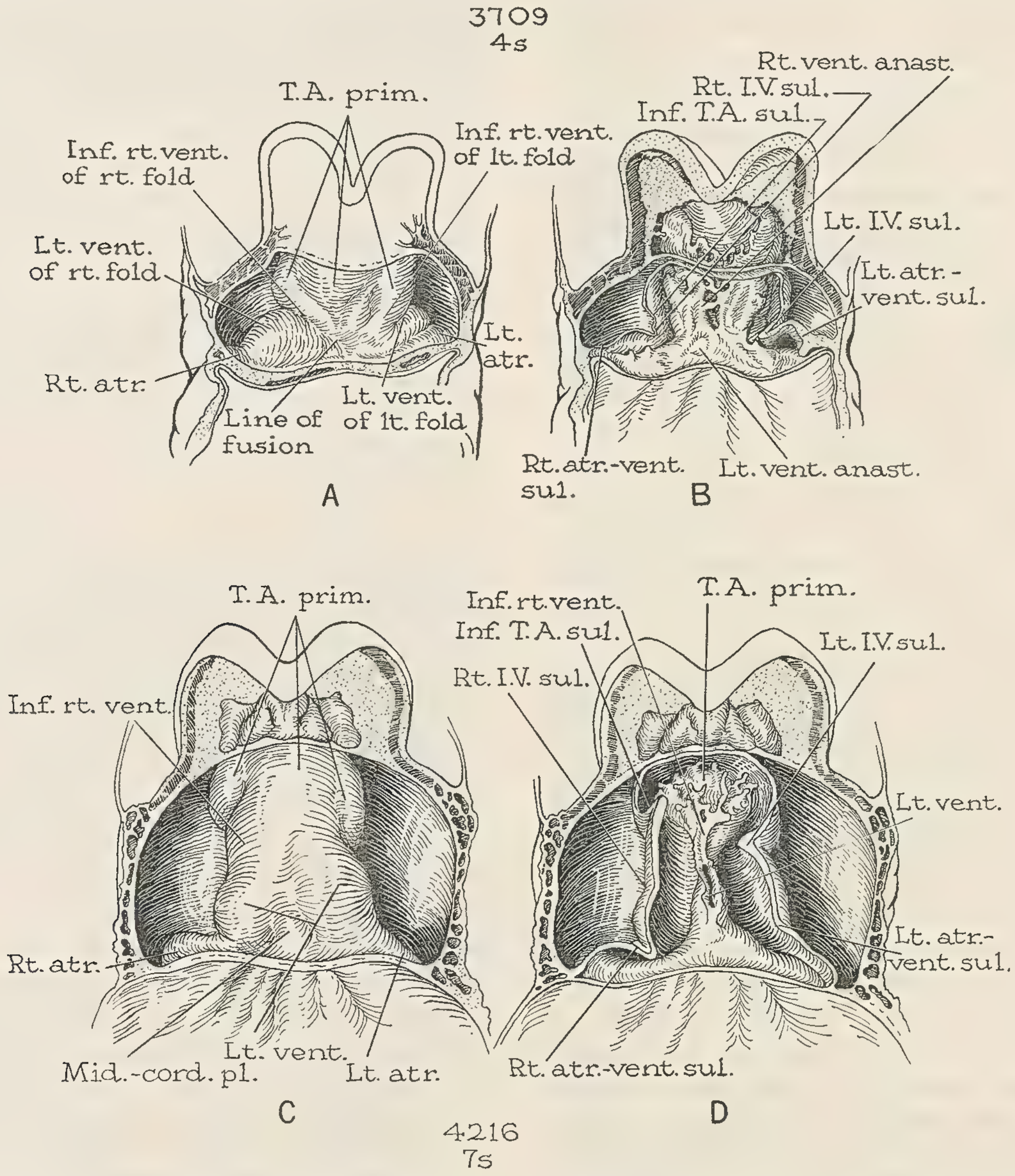

Fig. 2. *A.* Embryo 3709, 4 somites viewed from in front with ventral pericardium removed showing the myoepicardial mantle. Labeling denotes our interpretation of the identifiable landmarks.

B. Same view as *A,* following removal of ventral myoepicardium.

C and *D.* Similar views of embryo 4216, 7 somites. Note the increased length of the right half of the right ventriculoinfundibular segment which we suggest has been derived from the right ventricular fold. *A* and *B* were redrawn from figures 11 and 12, plate 1, and *C* and *D* from figures 17 and 18, plate 2, Davis (1927), after examination of reconstructions and embryo sections.

Embryo 1878. This 2-somite embryo contributes little to the changing picture of cardiac development. Two points of interest are: (1) Davis interpreted this embryo as a distorted specimen, while Ingalls (1920) believed it was possibly a heart showing situs inversus. If we accept Davis's interpretation of an unusual extracardial fold "pressing directly against this side of the heart, in such a manner as to push the bulbar end of the heart to the right," we cannot escape the fact that the folds and prominences of the myoepicardial mantle are subject to considerable variation from distortion. (2) The developmental stage of the embryo as determined by the number of somites may be only roughly correlated with the degree of development of an organ, as this embryo has two fewer pairs of somites than embryo 3709, whose heart is in a slightly earlier stage of development.

Embryo Klb. Progressing to this 6-somite embryo, we find much the same external picture of bilateral symmetry as seen in the heart of embryo 3709. However, the left ventricular region is larger than the right. These significant changes are associated with a more prominent left interventricular crest.

Embryo 4216. Figure 2*C, D;* figure 4. The heart of this 7-somite specimen demonstrates unequivocally beginning rotation of the developing ventricular loop, which is composed of the partially fused pairs of right and left ventricular elements. The myocardial and endocardial elements of the right and left ventricular primordia have undergone displacement. The more cephalic right ventricular primordium is displaced to the right,

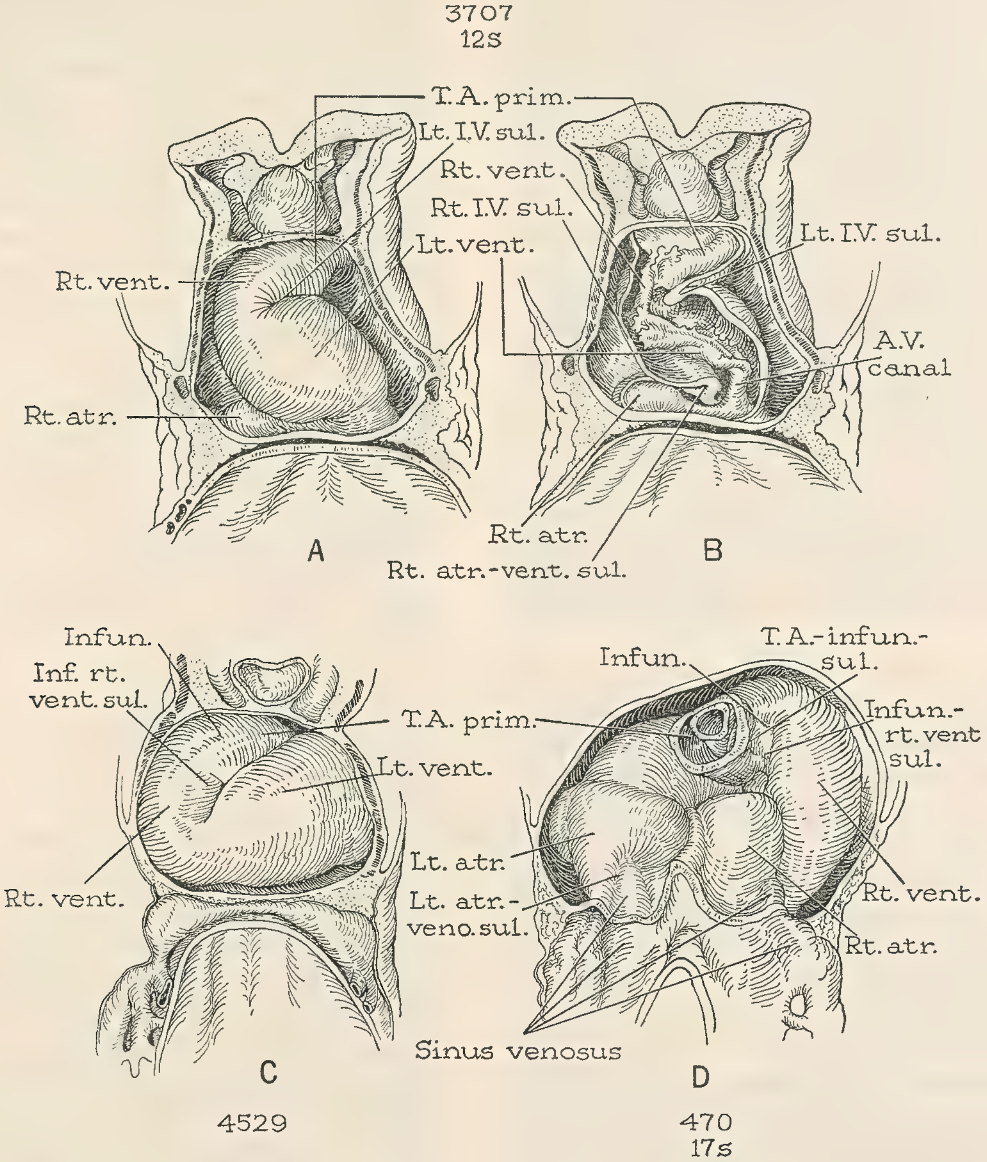

Fig. 3. *A.* Embryo 3707, 12 somites, viewed from in front with ventral pericardium removed, showing the myoepicardial mantle.

B. Same view as *A,* after removal of the ventral myoepicardium. Note the increased length of the right atrium, shift of the atrioventricular canal to the left, and increased depth of the left interventricular sulcus.

C. View from in front of embryo 4529 with ventral pericardium removed. Note the further deepening and rotation toward the vertical of the cleft between the right and left ventricular areas as rotation of the ventricular loop has continued in a counterclockwise direction relative to the ventral view.

D. Dorsal view of the heart of embryo 470, 17 somites. Note the presence of an evolving infundibular limb distinguished by its horizontal axis and delimited by the infundibulo-right ventricular sulcus proximally and the truncus arteriosus-infundibular sulcus distally. Redrawn from figures 23, 24, and 25, plate 4; figure 29, plate 5, Davis (1927).

there are significant differences which foretell the pattern of change which will continue through this age group, and which indicate the manner whereby rotation of the developing ventricular loop is accomplished.

The right cardiogenic fold in the atrial region is of greater length than the left; the left cardiogenic fold in while the left ventricular primordium is displaced to the left. As a result of these changes, the direction in which the ventricular loop rotates appears to be counterclockwise when viewed from in front.

The dorsal borders of the cardiogenic folds have fused at the level of the interventricular sulcus but diverge slightly rostral and caudal thereto. As a result of the fusion and of linear growth which has taken place in this embryo representing the changes during a developmental interval between embryos Klb and 4216, the ventricular myocardium is approaching the shape of an elongated tubular structure. The heart has become ventrally bowed, with the apex at the interventricular junction. The specific area evidencing the greatest growth during this interval is the infundibulo-right ventricular portion (bulbus cordis) of the right cardiogenic fold. The formerly paired lateral endothelial tubes have apparently fused in the ventricular loop, except in the distal left ventricular region, where there is a narrow gap. The great width of the endothelial plexus in the region of the left ventricular anastomosis (Davis's interventricular anastomosis), seen in embryo 3709, 4 somites, has narrowed, as fusion of the paired endothelial elements has progressed cephalically and caudally and the flattened plexus of cells has become tubular.

Embryos of 8 to 12 somites. Figures 3, 4. In embryos from 7 somites through the end of age group x, 12 somites, there is a progressive increase in size of the right side of the atrial and infundibulo-right ventricular regions of the heart which appear to be derived from the right cardiogenic fold. This apparent asymmetrical growth very likely accounts for the increasing depth of the left interventricular sulcus, migration of the proximal or venous end of the left ventricular segment to the left of the mid-sagittal line, and increasing depth of the right atrioventricular sulcus. The right interventricular and left atrioventricular sulci become progressively difficult to identify. The ventral bowing and counterclockwise rotation of the ventricular segments progress, as a result of the continuing differential regional growth, described above, within the over-all linear growth of the heart tube.

The middle cardiac plate disappears as an observable entity, and the atrioventricular canal comes into existence by the dorsal approximation and fusion of the cardiogenic folds in the region of the atrioventricular sulci. The atrioventricular canal is displaced to the left, apparently as a result of the great right atrial growth. After 7 somites, the endothelium is seen as a single tube except in the regions of the divergent, proximal atrial limbs. The endothelial tube becomes relatively narrow within the atrioventricular myocardial junction, expands in the left ventricular area, narrows at the interventricular isthmus, and expands again in the right ventricular area.

The infundibular segment is barely distinguishable from the right ventricular segment at the end of this age group and is poorly defined. The two ventricles, particularly the left, and the right atrium are most conspicuous in their growth.

AGE GROUP XI

Figure 3C, D; figure 5. Starting at the venous end of the heart, the significant cardiac developments during this age group can be summarized as follows:

The development of the atria continues, largely as a result of the contribution being made by the beginning elaboration of a sinus venosus.

The endothelial tube of the atrioventricular canal leading from the left atrium elongates, principally because of the accumulation of cardiac jelly surrounding it. This effect can be seen in the outlines of the endothelial tubes in figure 5.

Better differentiation of the trabeculated ventricles within the primary heart tube can be visualized as a result of an increase in number and size of the irregular outpouchings of the endothelium along the ventral wall of the left ventricular segment and dorsolateral wall of the right ventricular segment of the primary heart tube.

Beginning differentiation of an infundibular segment from the right trabeculated ventricle effects the establishment of a fourth limb or segment in the primary heart tube.

In age group xi, the second arterial arches are more fully developed. These arches made their appearance in age group x.

Cardiac contraction is believed to commence at the beginning of age group x, and it is generally accepted that peristaltic flow begins during age group xi. However, there have been no direct observations as to the time of onset of cardiac contraction in human embryos, and we must rely largely on knowledge of the time of onset in other mammalian species. Goss (1938) first noted beginning myocardial contraction at the 3-somite stage of the rat. Observations on the mode of progress in contraction of the rat heart would appear to correspond closely with the many observations that have been made on the development of the heart beat in the chick. However, Patten and Kramer (1933) and others have noted that heart contraction in chicks first occurs at the 9- to 10-somite stage.

The fixation of the distal primordium of the truncus arteriosus from which the arterial arches arise, and the continued growth of the caudal end of the myoepicardial mantle at the atrio-sinus junction, bring about progressive diminution of the dorsal, longitudinal interval separating the venous and arterial ends of the heart. This change, described by Davis (1927) as the ascent of the atria, can be noted in the profile views of the endothelial tubes of developing hearts of age group xi (fig. 5).

During age group xi, the development of the intrapericardial portion of the sinus venosus increasingly separates the caudal portion of the atria from the broad base of vitelline veins to which they were connected at the end of age group x. In this manner, the atria come to lie more within the pericardial cavity.

The atrioventricular canal was vertical at the beginning of age group x. However, the development of a ventricular bow has rotated the canal in the sagittal plane about 45° toward a dorsoventral orientation. During age group xi, the canal is seen to rotate further in this direction, so as to lie practically dorsoventrally in the 20-somite embryo 2053.

The heart of embryo 4529 has the so-called compound S configuration. This embryo was described by Davis (1927) as having 11 to 12 somites and later by Streeter (1942) as having 14 somites. We find 11 separated somites on the left and 12 separated somites on the right. The most cephalic and caudal somites are not separated from the mesenchyme at their cephalic and caudal limits respectively. The heart in some respects appears older than that of embryo 6344, 14 somites, and should therefore be placed in age group xi. The heart's configuration can be seen from a ventral view in figure 3*C*.

The development of the truncus arteriosus and infundibulum during age group xi is certainly of as great significance as the developmental changes at the venous end of the heart. In embryo 470, 17 somites, a dorsocephalic sulcus in the myoepicardium at the infundibulo-right ventricular junction can be observed; it is demonstrated in figure 3*D*. This shallow sulcus and the infundibulotruncal sulcus, on the right wall of the heart tube, identify the boundaries of the evolving infundibular segment which is differentiating from the common infundibular-right ventricular segment. By 20 somites, the elongating infundibular segment is more recognizable as a segment distinct from the right ventricular segment. The circumference of the infundibulum externally is smaller than that of the trabeculated right ventricular region, and the extremely narrow lumen is a reflection of the great thickness of the myoendocardial jelly layer relative to the circumference of the myoepicardial tube.

It would be desirable to subject these ideas of early chamber differentiation, based on morphological findings in different fixed specimens at various stages, to vital dye-marking experiments so that the elaboration of the parts in a single specimen could be traced. A few such experiments have been carried out in amphibians, but there is great need of more extensive studies in mammals, preferably primates.

AGE GROUP XII

Figure 6; plates 2, 3, 4. The general flexion curvature of the total embryo, seen, in profile view, to start in age group xi, becomes much more pronounced in age group xii, the ventral concavity of the curve deepening markedly and thus exaggerating the dorsal convexity. By 28 to 29 somites, the curve (exclusive of the caudal segments of the tail) is so pronounced as to achieve a semicircle. Arterial arches I and II are generally present, and arch III in the more advanced embryos is in varying stages of development.

Embryo 8944, 25 somites. When the heart is viewed externally, the right atrium is observed to lie ventral to the intrapericardial part of the sinus venosus; there is no sulcus at the junction of their confluent right lateral walls. The atrioventricular junction is ventral to the left atrium. No sulcus is observed in the left lateral wall of the cardiac tube at the junction.

The primary heart tube, commencing at the atrioventricular junction, courses transversely from left to right across the ventral aspect of the embryo, and making a turn of 90° ascends on the right within the pericardial sac. The heart tube distal to this, the ascending limb, turns once again through 90° and passes transversely from right to left toward the mid-line. At the mid-line, the tube makes a final turn through almost 90° to become the terminal limb, which runs dorsally, leading into the arterial arches.

Thus, the primary heart tube may be divided at this stage into four limbs, the roughly right-angled bends associated with sulci serving to demarcate the divisions. The proximal transverse, ascending, and distal transverse limbs lie roughly in the frontal plane, and the terminal limb in the sagittal plane.

The first sulcus is on the right wall of the atrioventricular junction; the second is on the cephaloventral wall of the primary heart tube, at the junction of the proximal transverse limb with the ascending limb; the third is at the junction of the ascending and distal transverse limbs on the caudal wall; and the fourth is on the right wall of the junction of the distal transverse limb with the terminal limb. (Variations in the depth of the sulci observed in the several photographs of specimens from 20 to 25 somites appear to result from differences in the state of preservation of the specimen. However, in even the best-preserved specimen where the cardiac loop appears circular the sulci are observable grossly.)

The first or right atrioventricular sulcus is the site of an acute bend to the right of the cardiac tube, and is associated with an area of apposition between the ventral wall of the right atrium and the dorsal wall of the primary heart tube's proximal transverse limb. There is no sulcus along the left wall of the atrioventricular junction, the left atrioventricular sulcus having disappeared toward the end of age group x. The proximal part of the first limb of the primary heart tube lies ventral to the left atrium and has a relatively large circumference. It is the site of the developing left trabeculated ventricle. As the proximal transverse limb courses to the right, approaching the ascending limb, its outer circumference gradually diminishes, to become the interventricular canal. This junctional region of the two limbs curves through an angle of about 90°, and a sulcus is seen on the cephaloventral surface. The sulcus, derived from the interventricular sulcus of the left cardiogenic fold, appears now as the inferior portion of a hollow which is bounded by the proximal transverse, ascending, and distal transverse limbs of the primary heart tube. The infolding of myocardium at the site of this sulcus, referred to in the literature as the bulboventricular or conoventricular flange or spur, has been said by others (Keith, 1906; Kramer, 1942; de la Cruz and da Rocha, 1956) to interfere with the egress of blood from the left ventricle. Our studies of the interior of the developing heart reveal no evidence for support of such a contention. The descriptions of an obstructive spur located in a position which would interfere with blood flow from the left ventricle appear to us to be errors both of observation and of interpretation.

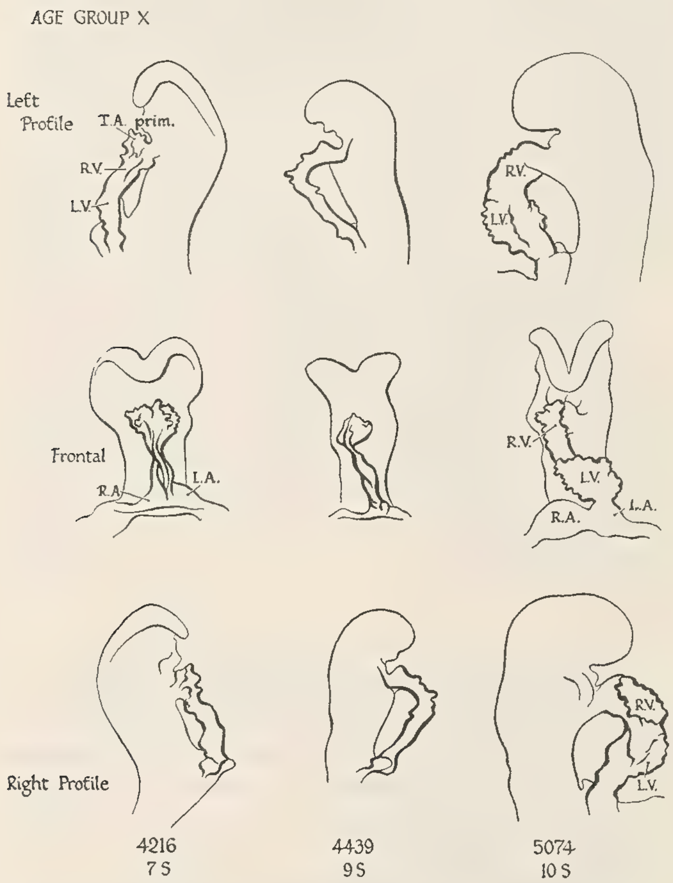

Fig. 4. These line drawings, traced from photographs of reconstructions, show the configuration of the heart lumen from left profile, frontal, and right profile views in each of three embryos in age group x, of increasing age: 4216, 7 somites; 4439, 9 somites; 5074, 10 somites. The beginning of the ventricular loop is best seen on the profile view. × 27.5.

The left interventricular sulcus is represented on the internal surface of the cardiac tube by a fold in the myocardium, but our reconstructions show that this fold does not impinge on, or obstruct, the lumen of the endothelia-lined tube of the interventricular canal. The fold is, in fact, the forerunner of the ventrocephalic portion of the interventricular septum.

The primary heart tube expands again as it curves into the ascending limb, and the dorsolateral wall of this limb is the region of the growing right trabeculated ventricle. The circumference and length of this limb are somewhat less than those of the one containing the left trabeculated ventricle, as the development of the right trabeculated ventricle lags behind that of the left.

The third or infundibulo-right ventricular sulcus, that between the ascending limb and the distal transverse limb or infundibulum, is situated on the caudal surface of the primary heart tube and cannot be seen from a ventral or right profile view of reconstructions or photographs of embryos. It first appeared at the close of age group xi, with the development of an infundibular limb.

The junction of the distal transverse limb with the terminal limb has been named by previous authors the fretum, bulbotruncal, conotruncal, and infundibulotruncal junction; the last is in accord with our views. It is situated on the right wall of the junctional area, and this sulcus is believed to be a derivative of that which Davis referred to as the right interbulbar sulcus. The junctional angle on the right surface between the two limbs at this infundibulotruncal sulcus is slightly obtuse.

Of particular note, and well demonstrated in this specimen, is the sulcus on the caudal or inferior surface of the atrioventricular junction. This sulcus has been referred to by Davis, in embryos of 17 to 20 somites (embryos 470 and 2053), as part of the right atrioventricular sulcus. Davis attributed the presence of this sulcus seen in the earlier stages to the bending of the heart tube to the right. During age group xii, however, the liver primordium in the septum transversum projects upward into this sulcus at the atrioventricular junction. The expansion of the left atrium and left ventricle, on either side of the atrioventricular junction, results in the heart tube's draping itself over a wedge-shaped projection of liver primordium, to hang on either side like a pair of saddlebags. Photographs of whole embryos in this age group from a left profile view show this relationship nicely (pl. 2*A*), as do parasagittal sections through the atrioventricular canal (pl. 2*B*).

When the interior of the heart is viewed, it can be seen in this, as well as in all younger specimens, that a thick, almost acellular layer of jelly separates the endothelium from the myocardium of the primary heart tube. This cardiac jelly has been stained blue with colloidal iron stain in some of our embryos, after prompt fixation with neutral buffered formalin. If the sections are treated with hyaluronidase before colloidal iron staining the jelly is unstained. Differential staining with acid aldehyde and PAS suggests the absence of sulfonated groups in the mucopolysaccharide contained in this layer. Very likely it is the same one found in umbilical cord and intercellular spaces, namely, hyaluronic acid.

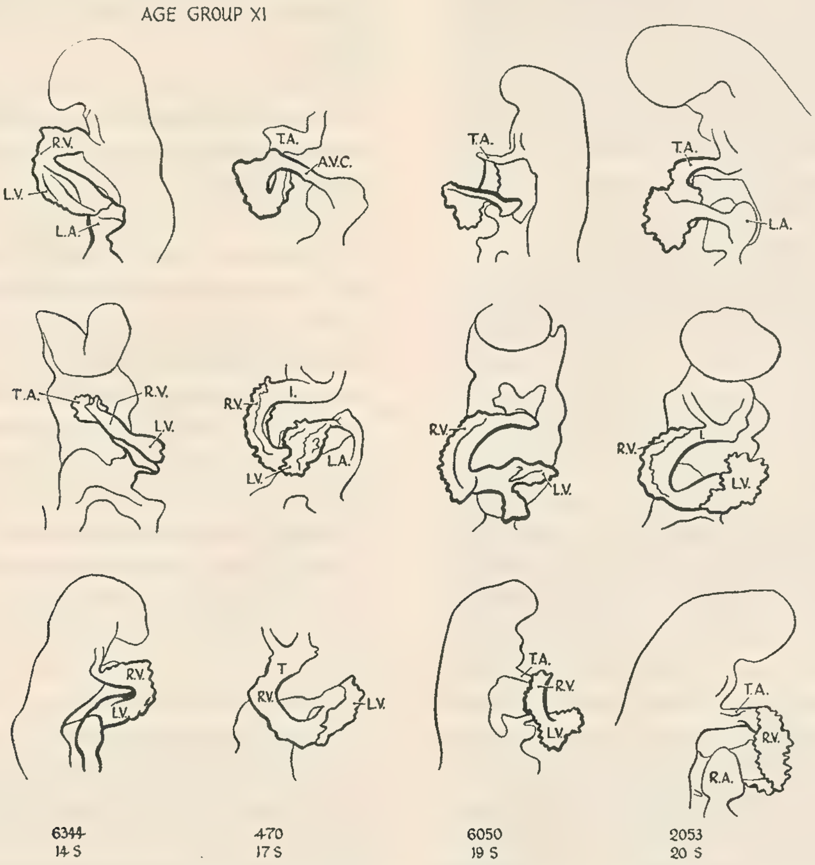

Fig. 5. Same views as in figure 4 of embryos in age group xi. 6344, 14 somites; 470, 17 somites; 6050, 19 somites; 2053, 20 somites. The rotation of the ventricular limbs with the apex of the loop at the interventricular area is seen, together with the shift of the atrioventricular junction to the left. × 27.5.

The configuration of the endothelial tube varies significantly from that of the myocardial tube, reflecting the varying thickness of the intervening plastic layer. The myoendocardial space of the left atrium in this specimen is still of note, as it is in the later age group xi and earlier group xii specimens, whereas, in the right atrium, the jelly has almost vanished as a layer. The thickness of the gelatinous layer in the left atrium, as contrasted with the virtual absence of this layer in the right atrium, accounts for the smaller size of the left atrial cavity relative to the right, although they appear to be of equal size when viewed externally. The layer is thickest over the entire cephalic wall of the left atrium and interatrial region, and extends downward through the atrioventricular canal into the primary heart tube as the precursor of the ventral atrioventricular cushion. Caudally, it is thickest over the internal transverse myocardial eminence or ridge at the atrioventricular sulcus. Jelly in this area becomes the dorsal atrioventricular cushion. Much of the cephalocaudal flattening of the lumen constituting the atrioventricular canal results from the distribution of the jelly in the myoendocardial space rather than from the shape of the surrounding myoepicardial tube.

There is a relatively thin gelatinous layer in the areas of the expanding trabeculated ventricles. It otherwise extends as a layer of greater but varying thickness from the interatrial junction to, and even around, the proximal part of the developing arterial arches.

In the region where the proximal transverse limb of the myoepicardial tube narrows down to its junction with the ascending limb, the endothelial tube comes to lie almost in contact with the myocardium dorsally. The thin myoendocardial layer that we observe dorsally is in contrast to the thick layer seen ventrocephalically. Because of this distribution of jelly at the interventricular region, the cephaloventral ridge formed by the infolding of the myocardium (represented externally by the interventricular sulcus) does not project as a spur into the lumen, since jelly surrounds the ridge (pl. 2*C, D*). The lumen of the developing heart in the interventricular region, although of less diameter than that of the trabeculated ventricular areas, does not appear to be obstructed in any manner. The endothelial tube constituting the luminal surface is dorsally placed within the myoepicardial tube in the region of the interventricular canal.

The trabeculated ventricle is developing predominantly on the dorsolateral surface of the ascending limb. Here the myoepicardium is thicker, and, as in the left ventricle, a trabecular layer is internal to the myoepicardial layer. At this stage, it resembles a thin latticework, with myoendocardial jelly between the loosely meshed cells. One-cell-thick endothelial outgrowths account for the irregularity of the lumen in this region.

On the anteromedial side of the ascending limb, and from the distal end of the trabeculated right ventricle to the arterial arches, the myoendocardial layer is relatively thick. The endothelial tube is flattened cephalocaudally through the infundibulum and truncus arteriosus.

The configuration of the lumen of the endothelial tube in this age group is difficult to reconstruct mentally from the serial sections alone. The difficulty is particularly apparent when one attempts to determine the presence or absence of longitudinal or spiral ridges in the gelatinous layer of the infundibulum and/or truncus found in hearts of older age group embryos. Not infrequently, apparent projections of the endothelium into the lumina of the hearts in this age group, when viewed in serial section, were at first mistakenly accepted as evidence of a longitudinal ridge system, but studies of graphic and wax-plate reconstructions of this and other specimens in age group xii have failed to reveal any longitudinal or spiral ridges. This failure does not preclude the possible presence of a ridge or ridges in the living state, as the sol or gel state of the subendocardial layer could conceivably conform to a lateralized intraluminal flow pattern if one were present.

Fixation artifacts in many, if not all, of the sectioned embryos, particularly of the myoendocardial layer, add to the difficulty of determining the presence or absence of ridges.

Rosenbauer's (1955) well illustrated description of the heart of a 24-somite embryo corresponds closely with our morphological findings in embryo 8944.

In plate 3, figures *H–L* show transverse sections through the heart of embryo 8943, 22 somites, a younger specimen than the reconstructed 8944. The cardiac jelly can be seen in the right atrium in *K* and *L* as well as in the left atrium in contradistinction to embryo 8944. *I, J,* and *K* show well the endothelial diverticula of the right and left trabeculated ventricle areas.

Embryo 5923, 28 somites. Several illustrations of this excellent 28-somite embryo were presented by Streeter (1942) in his description of age group xii. They included illustrations of the reconstructed endothelial heart tube and a study of the venous end of the heart. We chose to reconstruct the heart of this beautifully preserved embryo anew, for the purpose of correlating the myocardial and myoendocardial configurations with those of the endothelial cavities.

We were unable to verify the presence of a left third arterial arch, as illustrated by Streeter (1942, fig. 4, p. 238).

Between 25 somites (embryo 8944) and this 28-somite embryo, there has been expansion of the left atrium and left trabeculated ventricle. The bulging of the left wall of the myocardial heart tube on either side of the atrioventricular junction has resulted in the reappearance of a left atrioventricular sulcus, at the left lateral border of the atrioventricular canal (fig. 6).

The myoepicardial tube of the atrioventricular canal has not increased significantly in circumference, but it is more medially positioned relative to the lateral heart borders. This apparent migration results from the abovementioned growth of the left atrium and the left trabeculated ventricle, which has led to the formation of a left atrioventricular sulcus together with a decrease in the depth of the right atrioventricular sulcus. The dorsal wall of the primary heart tube's proximal transverse limb has not grown as rapidly as the cephalic, ventral, and caudal areas, the site of the expanding trabeculated left ventricle. Therefore, the area of apposition between the proximal transverse limb of the primary heart tube and the ventral wall of the atria has diminished relative to the surface areas of the segments concerned, and the right atrioventricular sulcus has become less prominent. The depths of the two atrioventricular sulci have been, and in future stages will be, influenced in addition by increases in the total length of the primary heart tube. This increase in length progressively displaces the left trabeculated ventricle to the left and dorsally.

Davis's "left atrio-venous sulcus" should not be confused with the above-described, newly appearing left atrioventricular sulcus. The former could be seen first in embryo 3707, 11 somites, and marked the junction of the left atrium with the sinus venosus. It migrated dorsomedially during age group xi and in the earlier members of age group xii. In the specimen under discussion it lies to the right of the mid-line, at the left wall of the now lateralized sinoatrial foramen.

Returning our attention to the primary heart tube of embryo 5923, we find that the line of the left interventricular sulcus has changed from the more or less vertical to the horizontal. Linear growth of the left ventricular, infundibular, and truncal limbs has forced a dorsal displacement of the right ventricular limb within the restrictive pericardial sac. The circumferential growth of these limbs has obliterated the hollow between the proximal three limbs seen in embryo 8944.

At first glance, there appears to have been a progressive cephalodorsal compression of the heart tube during age group xii, from constriction between the branchial region above, and septum transversum and yolk sac below, as increasing flexure of the embryo has taken place. This presumptive compression was considered as a cause of the increased prominence of the left interventricular sulcus. On further examination, however, it appears that the linear growth together with circumferential growth of the two ventricular limbs has led to a coaptation of the cephalic wall of the proximal transverse limb with the left wall of the ascending limb and consequent deepening of the left interventricular sulcus.

The caudal infundibulo-right ventricular sulcus, seen in embryo 8944, is obscured within the interventricular sulcus in embryo 5923. Its prominence, it would appear, is diminished as a result of the lesser growth of the lesser curvatures of the right ventricular and infundibular limbs.[1]

The right ventricular limb extends still further dorsomedially between the right pericardial wall and the right atrium. The earlier obtuse angle of junction between the infundibular and truncal limbs becomes acute around 28 somites, as a result of medial displacement of the distal end of the elongating infundibulum, together with the linear growth of the truncus arteriosus. Expansion of the right trabeculated ventricular limb, immediately proximal and to the right of the infundibulum, also contributes to the medial displacement of the infundibulotruncal junction. With the caudal descent of the right ventricle, the acute angle on the right at the infundibulotruncal junction seen at 28 somites becomes, at the end of age group xii, more obtuse again. As a consequence the junction of the infundibulum and truncus arteriosus is thereafter poorly defined morphologically. In embryo 5923, the infundibulotruncal junction cannot be defined histologically. This junction, we believe, is the site of future semilunar valve development, as was first suggested by von Haller (1758).

The rapidly enlarging right atrium impinges upon the laterally situated right ventricle. The ventral wall of the right atrium projects cephaloventrally into the concavity of the dorsal wall of the primary heart tube.

Between 25 and 28 somites, there is no significant alteration in the distribution of jelly in the myoendocardial space.

We have been unable to identify any longitudinal or spiral ridges in the gelatinous myoendocardial layer. The thickness of this layer at the junctures of the several limbs could easily act as "valves" in peristaltic unidirectional flow, as suggested by Patten, Kramer, and Barry (1948).

AGE GROUP XIII

Figures 6, 7, 8; plates 6, 7. The profile contour of embryos in age group xii was seen to be C shaped, but in age group xiii the contour changes, with the establishment of a dorsal neck bend and a ventral cervical sinus of the branchial region, so as to resemble a fish hook. As the result of the rapid enlargement of the brain, in association with flexion of the neck, the olfactory region of the forebrain approaches the pericardium and, in older specimens of the group, actually makes contact with it. The heart, viewed from either profile of the embryo, lies on a plane midway between horizontal and frontal, so that a line drawn on a profile photograph of an embryo, from the ventral border of the ventricles to the apex of the neck bend dorsally, very nearly bisects all the heart chambers.

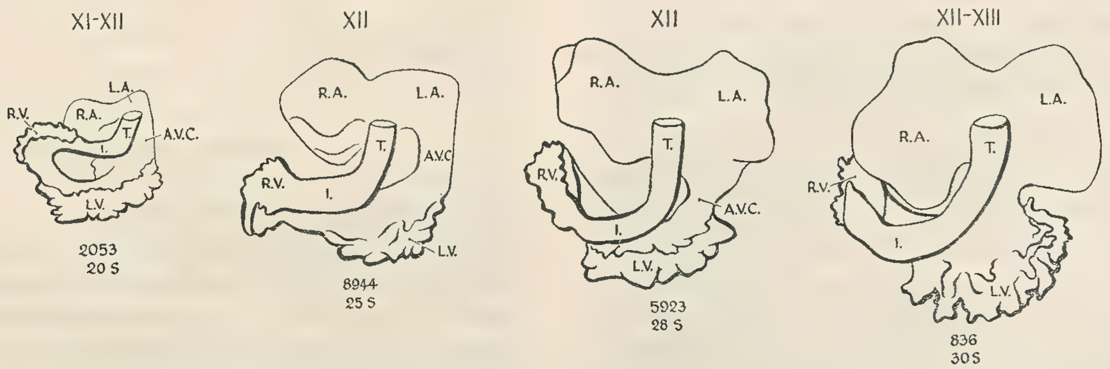

Fig. 6. Line tracings of photographs from reconstructed heart cavities of embryos 2053, 20 somites, age group xi; 8944, 25 somites, age group xii; 5923, 28 somites, age group xii; 836, 30 somites, age group xiii. The drawings show particularly well from this top view the progressive expansion of the left atrial cavity, the elongation of the infundibulum and truncus arteriosus, and the relation of right and left trabeculated ventricles to each other. The so-called shift to the right of the atrioventricular canal can be seen. × 32.5.

---

[1] If homologies are to be drawn, these two limbs, the infundibular and right ventricular together, at this stage, correspond to the bulbus cordis of reptiles, as described by Langer (1894) and Greil (1903*a*). Waterston (1918) was of a similar opinion.

Large third arterial arches are characteristic of age group xiii. The first arches disappear, the second grow smaller, and the fourth develop.

Embryo 836, 30 somites. This specimen, with 30 pairs of somites, represents a transitional stage from age group xii to age group xiii, and the fourth arterial arches are incomplete. Streeter (1942) acknowledged the inevitability of overlapping in the adjacent age groups. The heart of this youngest specimen studied in age group xiii differs from the heart of the 28-somite embryo in several significant features. The right atrium has expanded ventrally and laterally. Concomitantly, and probably as a result of the expansion of the right atrium, the infundibular limb, which at 28 somites was transverse in position, at 30 somites has partially rotated toward the vertical, a rotation completed in older embryos. The right border of the infundibulum, together with the truncus arteriosus, describes a crescent diagonally upward and to the left, across the ventral surface of the right atrium. The right ventricle, having descended in a caudal direction, impinges on the lateral and inferior surfaces of the right atrium. With the further expansion of the left atrium and ventricular, the left atrioventricular sulcus has deepened, which accounts for the further apparent or relative shift of the atrioventricular junction to the right. The truncus arteriosus lies in an interatrial sulcus of increasing depth. This sulcus is situated on the ventrocephalic surface of the interatrial junction. The descent of the right trabeculated ventricle results largely, we believe, not only from direct displacement of it by the expanding right atrium, but also from growth in length, and change in axis of the infundibulum, which allows the descent to take place.

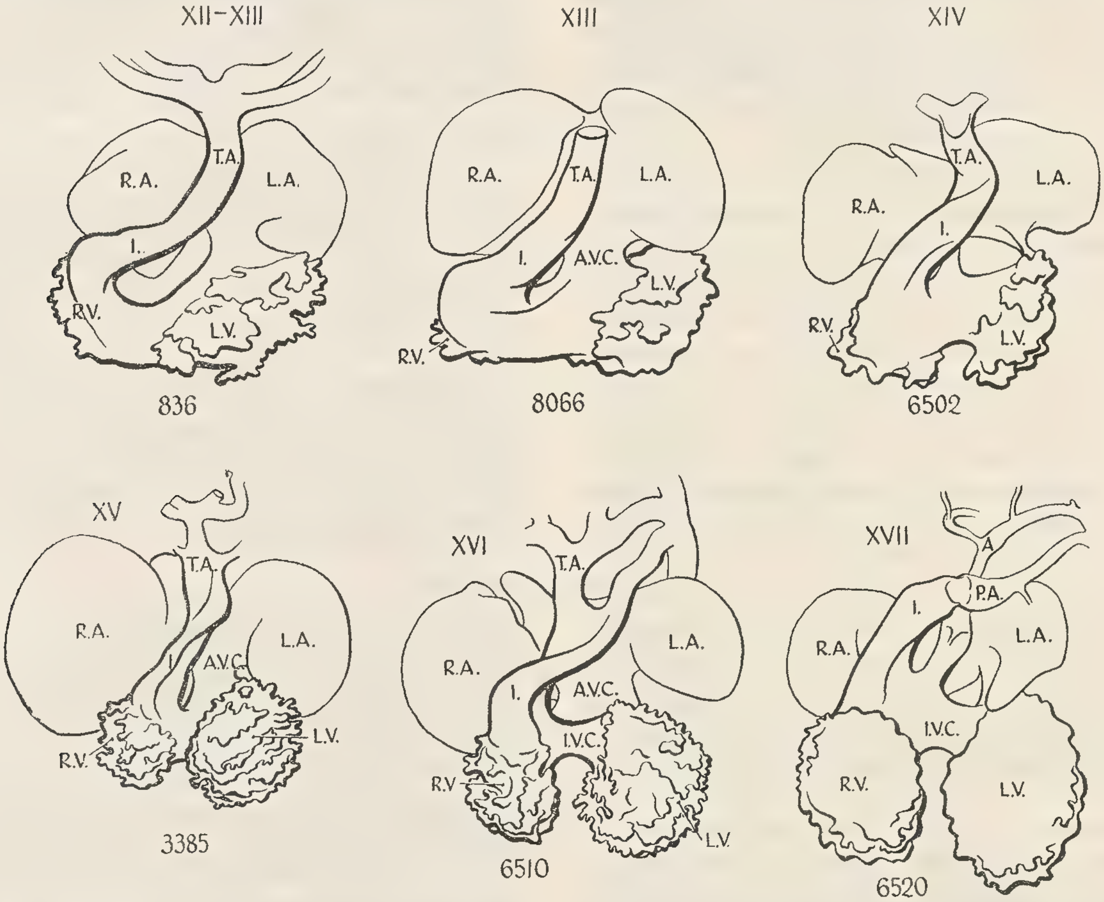

Fig. 7. Line tracings of photographs of endothelial heart tubes viewed obliquely, one-half between frontal and top views. From the beginning of age group xiii, 836, top left, through age group xvii, 6520, lower right, the progressive ventromedial rotation of the right trabeculated ventricle can be observed. The spiral indentations in the infundibulotruncal outflow tract are first easily noticeable in age group xiv, 6502, top right, although they are evident in reconstructions of 8066, age group xiii. They are pronounced in age group xv, 3385, lower left. Illustrations have been reduced to same size so as to compare changes in configuration rather than changes in size.

The gelatinous myoendocardial layer of the heart in embryo 836 is virtually acellular, but it becomes progressively more cellular in specimens of advancing age and toward the end of age group xiii; thereafter it will be referred to as a reticulum of myoendocardial or subendocardial tissue. The source of the cells forming this layer has been a subject of controversy upon which we can shed little light. Tentatively, we subscribe to the view that (as has been noted by others) the endothelium is the source of these cells, on the slender evidence that the cells resemble those of the endothelium.

Embryo 8066. Embryo 8066, somewhat older than 836, viewed externally reveals further growth and change in position of the parts of the heart. The right and left atria have enlarged except at their junction. The truncus arteriosus courses across the roof of the interatrial junction in a rather deep groove. The left atrioventricular sulcus has deepened, to become a cleft in the interval between the expanded left atrial and left ventricular walls. The atrioventricular orifice at this time lies only slightly to the left of the mid-line. The marked enlargement of the right atrium has further displaced the infundibulum medially.

The right ventricle, which was inferior and lateral to the right atrium in embryo 836, has become ventral as well as inferior in 8066. The change represents the beginning of a ventromedial rotation of the right ventricle toward the left, a rotation that will be seen to continue throughout the subsequent age groups (fig. 7).

The more-expanded infundibulum overlaps, ventrally, the interatrial region, a portion of the right atrium, and the right half of the atrioventricular canal. The left wall of the infundibulum apposes the right (formerly cephalic) wall of the left ventricle, so that a vertical cleft appears between them in ventral view. Inferiorly and in line with the vertical cleft or left border of the infundibulum is the left interventricular sulcus, which extends with decreasing depth to the caudal juncture of the ventricles. Expansion of the myocardial walls of the infundibulum and right ventricle, together with the descent and medial rotation of the right ventricle, have led to the change in direction from diagonal to vertical of the infundibuloventricular cleft and interventricular sulcus.

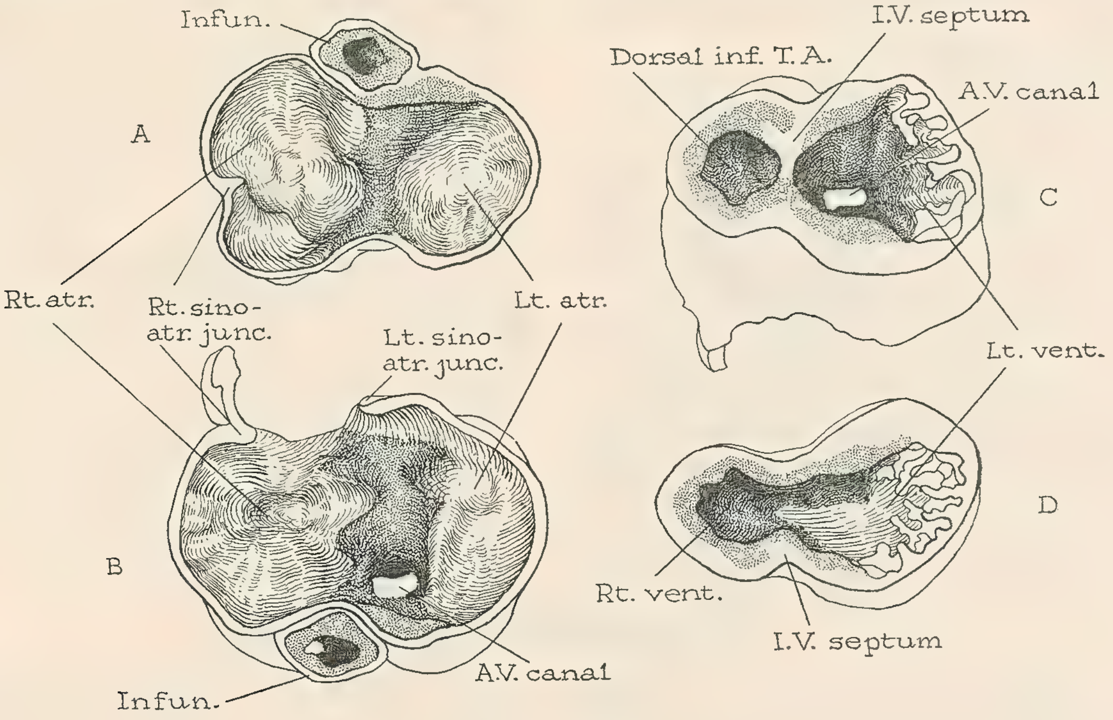

8066

Fig. 8. These figures were drawn from graphic reconstructions and transected wax-plate reconstructions of embryo 8066, age group xiii. The stippled areas represent the distribution of myoendocardial jelly. The top and bottom of the horizontally transected heart through the atria and infundibulum are seen in *A* and *B*. *A* shows the atrial roof and distal infundibulum; *B* shows the proximal infundibulum, atrial floor, and atrioventricular canal. *C* and *D* are of the horizontally transected heart at the level of the top of the interventricular canal. *C* is a view toward the atrioventricular canal and infundibulum; *D* is toward the apex of the ventricle. The distribution of jelly in relation to the developing interventricular septum and trabeculated ventricles can be noted, as can the beginning spiraled elevations and depressions in the infundibulum.

In embryo 8066, an increased number of cells in the gelatinous layer of the myoendocardial space first appears adjacent to the endothelium. It is noteworthy that increasing numbers of cells first appear directly beneath the endothelium of the atrioventricular canal and infundibulum, in regions where the gelatinous layer is thickest, and hence project into the once cylindrical lumen.

In the atria, the gelatinous layer has become restricted to a sagittal ring around the interatrial junction (fig. 8*A*). The ring varies in width and thickness. Ventrocephalically, it extends into the left atrium and through the atrioventricular orifice. Dorsocaudally, the ring of jelly surrounds the left lip of the sinoatrial junction and continues across the floor of the atrium and through the atrioventricular orifice (fig. 8*B*). This area within the atrium, as was mentioned previously, might well be considered as constituting the primary heart tube on the venous end of the heart, to distinguish it from the expanded portions of the atria which are devoid of a gelatinous layer, were it not for the confusion in terms that would result. In the expanded trabeculated portions of the primary heart tube (i.e., the left trabeculated ventricle and right trabeculated ventricle), the gelatinous material is reduced to a very thin layer, whereas, in the less expanded portions of the primary heart tube, the layer remains of considerable thickness.

The ventromedial rotation of the right ventricular limb of the primary heart tube results in an infolding of the myocardium, which increases the depth of the interventricular sulcus externally and the height of the myocardial crest internally. This crest was recognizable earlier as the beginnings of the interventricular septum. To the right of this interventricular septal crest the gelatinous layer is thick and, in effect, blunts what would otherwise be a sharp ventral projection of myocardium into the lumen (fig. 8*C, D*). This thickened region of the gelatinous layer is the forerunner of the large ventral cushion or "bulbar cushion," which comparative anatomists have referred to as the "proximal swelling B." The gelatinous layer to the left of the septum is the primordium of the ventricular component of the ventral atrioventricular cushion; the thick gelatinous layer on the dorsal wall of the primary heart tube is the primordium of the ventricular component of the dorsal atrioventricular cushion.

Embryo 8066 is the youngest specimen in our series to show evidence of two longitudinal spiral ridges of the infundibulotruncal outflow tract, embryo 836 having shown none. From the infundibular region to the middle of the truncus arteriosus, the myoendocardial gelatinous layer has, on its luminal surface, paired depressions and elevations which spiral distally in a clockwise direction. These elevations and depressions are interpreted as arising from a conformation of the plastic gelatinous layer about a spiral stream of fluid coursing through the lumen of the infundibulotruncal portion of the heart tube. A spiraling of the blood stream, we believe, results from the junction of two columns or streams of blood in the proximal infundibulum. These streams are brought about by the ejection of blood from contraction of the two pumps, the right and left trabeculated ventricles, both of which are proximal to the infundibulum at this stage of development and therefore now more in parallel than in series. The ejection stream from the left ventricle is dorsal to that of the right. This relationship of the ventricles satisfies the criteria necessary for the elaboration of fluid streams which will junction and form a clockwise spiral distal thereto (pl. 1*C*).

AGE GROUP XIV

Embryo 6502. Figures 7, 9A, B; plates 3, 8. Embryo 6502, one of the older specimens in age group xiv, demonstrates the changes between mid age group xiii (embryo 8066) and late age group xiv. The four principal heart chambers, left and right atria and left and right ventricles, have continued their expansion. The ventromedial rotation of the right ventricle has continued. The infundibulotruncal outflow tract leads into arterial arches III, IV, and VI. The mid-portion of the combined infundibular and truncal segments extends across the mid-sagittal plane of the embryo, to the left, returning to the mid-line at the junction of the truncus arteriosus with the arterial arches.

Within the heart, the distribution of the myoendocardial reticular layer has become more restricted. The expansion of the myocardial and endothelial tubes, in the atrial and ventricular outpouchings, has not been accompanied by any significant increase of the myoendocardial reticulum in these areas. In the atrium, the myoendocardial reticular layer is confined to a sagittal, crescent-shaped area. The open region, in what was previously a ring, is dorsal at the sinoatrial junction. This crescent of reticulum is broad ventrally at the atrioventricular canal and vanishes dorsally where the myocardial spur, the septum primum, is developing. The endothelial tube of the atrioventricular canal is clearly divided into two channels (fig. 9*A*), whereas in embryo 8066, age group xiii, there was but a single channel (fig. 8*C*). The narrow right and left canals result from an approximation, rather than fusion, of the dorsal and ventral atrioventricular cushions. These cushions we view as accumulations of the plastic jelly, or increasingly cellular mesenchymal tissue, occupying the interval between the endothelium and myocardium, and capable of being molded somewhat by the hydrodynamic forces that develop in association with the moving columns of blood from the contracting right and left atria.

In age group xiii, and younger specimens of age group xiv, the flow of blood through the atrioventricular canal in living embryos is presumably at least partially separated to the right and to the left by the progressive bulging, during development, of the myoendocardial gelatinous tissue into the center of the canal. In about half of the specimens in age group xiv, the atrioventricular cushions are approximated centrally in the more distal part of the canal.

We pointed out that in age group xii the dorsal wall of the primary heart tube's proximal transverse limb, i.e., that confluent with the right wall of the atrioventricular canal, was not keeping pace with the growth of the left or ventral wall of the proximal transverse limb wherein the left trabeculated ventricle was developing. It can be seen, on reviewing the course of development during age groups ix, x, and xi, that this dorsal wall in embryos of age groups xii to xiv appears to be derived from the left ventricular part of the right cardiogenic fold, which during those early age groups failed to keep up with the growth of the left ventricular portion of the left cardiogenic fold from which we believe the left trabeculated ventricle largely develops.

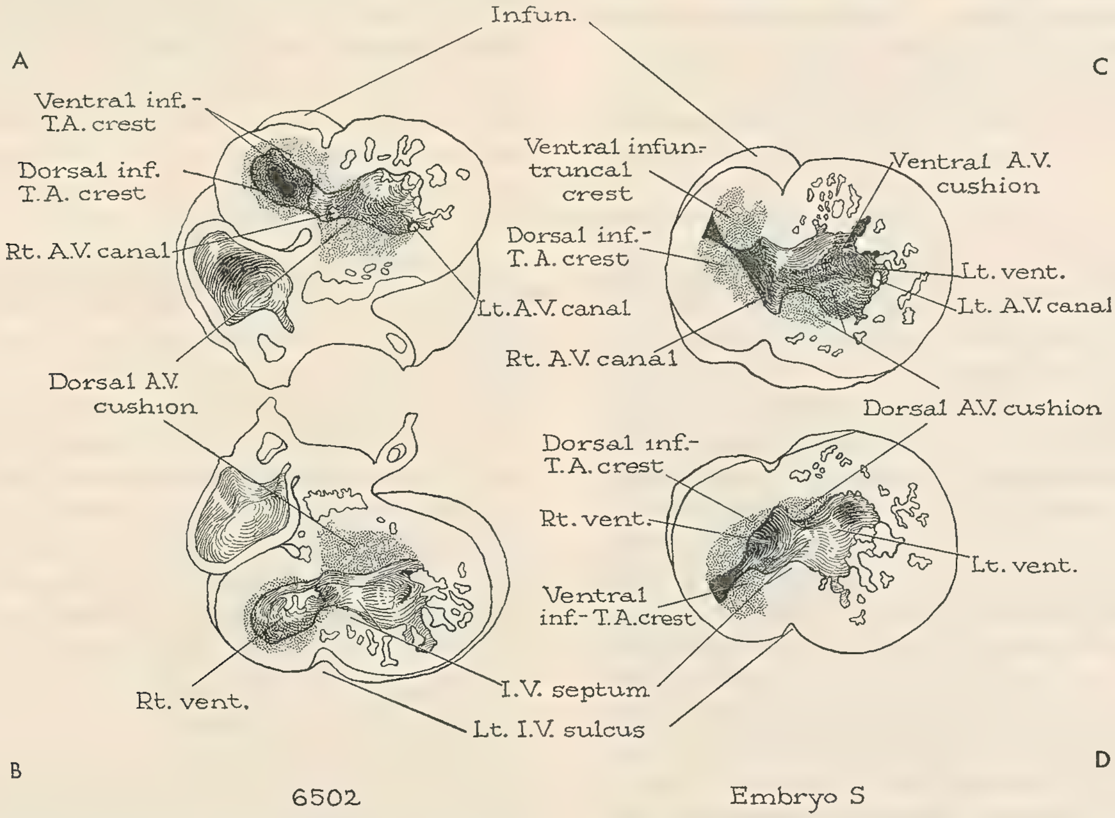

Fig. 9. *A* shows the top half and *B* the bottom half of the horizontally transected ventricular part of the heart of embryo 6502, age group xiv. *C* and *D* are similar views of the heart of embryo S, age group xv. The progressive elaboration of the infundibulo-truncal cushions or ridges can be seen. In 6502 the atrioventricular canal is divided, by approximation of the myoendocardial reticulum or cushions, into right and left atrioventricular canals. The progressive ventromedial rotation of the right trabeculated ventricle and increasing depth in the ventral part of the interventricular septum are remarkable.

The relatively short dorsal wall of the primary heart tube opposite the left trabeculated ventricle, seen in embryo 8066 of age group xiii, becomes the lateral wall of the right atrioventricular canal in embryo 6502 of age group xiv. This alteration has been brought about by the participation of the dorsal wall of the proximal transverse limb in the ventromedial rotation of the right ventricular limb of the primary heart tube. The right wall of the heart tube at the atrioventricular junction acts as a hinge upon which the rotation takes place.

The lag in growth, and ventral rotation of this dorsal wall, are accompanied during age group xiv by a bulging into the lumen of the cephalic (ventral) and caudal (dorsal) myoendocardial reticulum (cushions) in the center of the relatively narrow primary heart tube inlet (atrioventricular canal).

The above developmental changes occurring in age groups xiii and xiv account for the establishment of right and left atrioventricular canals, seen in 6502. The right canal empties ventrocaudally into the interventricular isthmus, toward the ventro-inferiorly positioned right trabeculated ventricle; and the left canal empties into the primary heart tube, toward the left trabeculated ventricle. The junction of the infundibulum with the right trabeculated ventricle is just to the right of the ventricular ostium of the newly formed right atrioventricular canal. This is the result of the restriction in growth of the right ventricular limb's lesser curvature which we believe is derived from the right ventricular (proximal bulbus cordis) portion of the left cardiogenic fold.

The endothelial tube of the interventricular canal or isthmus lies, as was previously observed, in a dorsal position within the myocardial tube. It is cephalodorsal to the developing muscular portion of the interventricular septum. Dorsocaudally, the developing muscular interventricular septum commences at the caudal limit of the dorsal atrioventricular cushion, and appears to be primarily the product of a fusion of trabeculae at the junction between the enlarging right and left trabeculated ventricles. The more ventral portion of the interventricular septum is formed by the buckling-in of the myocardial tube at the junction of the right and left trabeculated ventricles, brought about by the ventromedial rotation of the right ventricular limb of the primary heart tube and fusion of coapted walls of the expanded right and left trabeculated ventricles. The ventral atrioventricular cushion terminates on the ventrocephalic crest of the interventricular septum. Transverse sections through embryo 8967, plate 3*A–G,* show the developing septa in a younger specimen of this age group.

In embryo 6502, there is a thick layer of myoendocardial reticulum on the ventral wall of the right ventricle, to the right of the interventricular septum. It is continuous with the thick reticular layer of the infundibulum and truncus, and is observed to be the base of one of the paired crests that constitute the spiral "ridge system." The paired crests and troughs have become higher and deeper respectively in the infundibulum and truncus, but there is no evidence that one of the paired crests in the infundibular region is more prominent than the other at this stage.

If one were to accept the thesis of Robertson (1913–1914) in regard to the formation of the outflow tract and its septation, one would expect to find a great predominance, at any stage in development, of the ridge that arises ventrally at the infundibulo-right ventricular junction.

AGE GROUP XV

Figures 7 and 9C, D; plates 2, 9. During age group xv, the paired spiral elevations and depressions within the lumen of the infundibulum and truncus arteriosus undergo further development. In embryo S, late age group xv, the elevations or ridges of myoendocardial reticulum are approximated in the distal infundibulum and proximal truncus arteriosus. The muscular interventricular septum has become very prominent, as a result of continued ventral infolding and coaptation of the ventricular walls and caudal fusion of trabeculae associated with further expansion of the trabeculated ventricles. In both embryo S and embryo 3385, the right trabeculated ventricle is not yet ventral in position to the left trabeculated ventricle. The left ventricle is significantly more voluminous and thicker-walled than the right ventricle.

The so-called aorticopulmonary spur or septum of extracardial mesoderm between the fourth and sixth arterial arches does not meet the evolving reticular septum dividing the infundibulum and truncus arteriosus. The elevations and depressions of the myoendocardial reticulum are much less prominent in the terminal truncus, a fact that accounts, at this stage, for the discontinuity of the developing septum between the partially divided spiral outflow tract proximally and the arterial arches distally. However, the right ventricle can now eject blood distally through a largely separate channel which spirals clockwise, approximately 270°, through the infundibulum and truncus arteriosus, wherein blood may course directly into the dorsally placed orifice of the sixth arterial arch. The left ventricle may eject blood distally and to the right, through the dorsally placed interventricular canal into the dorsal portion of the proximal infundibulum, whence it passes in a spiral path through the infundibulum and truncus, to arrive at the ventrocephalically placed orifice of the third and fourth arterial arches.

The so-called descent of the aorticopulmonary spur or septum between the fourth and sixth aortic arches does not primarily contribute to the spiral of septation in the outflow tracts. In age groups xvi and xvii the extracardial tissue between the fourth and sixth arterial arches meets the infundibulo-truncal septum to complete the distal division of the double outflow tract (fig. 7).

A study of the serial sections of several embryos in age group xv, in addition to embryos S and 3385, fails to reveal a clear line of histological demarcation between the truncus arteriosus and the infundibulum, a fact previously noted by Tandler (1912) and Kramer (1942).

At this stage of development the dorsal bend of the outflow tract is the presumed site of the infundibulo-truncal junction and the future site of semilunar valve formation. Examinations of cross sections of the heart tube at this level reveal accumulations of cells in the myoendocardial reticular layer between the two elevations of the spiral ridges. These have been referred to by Kramer (1942) as intercalated valvular cushions. Proximal and distal to this region, the histological difference between infundibulum and truncus becomes more distinct. Proximally in the infundibulum, the myoendocardial reticulum has about the same cell concentration as that seen in the atrioventricular cushions (pl. 2*F*). The myocardium stains lightly with hematoxylin. Distally in the truncus, the reticular layer has become more cellular (pl. 2*E*). The tissue of the outer wall of the truncus arteriosus previously referred to as myoepicardium stains darker than the myocardium of the ventricles and infundibulum; it resembles more the noncardiac splanchnic mesoderm lining the coelom.

It has been generally held that the spiral ridge commencing ventrally in the right ventricle is more prominent than the one commencing dorsally, as a result of phylogenetic predetermination. In embryos S and 3385, this ridge or crest is the more prominent of the two in the mid-infundibulum. We believe that this difference in size is most likely the result of fluid forces molding the reticular layer, rather than a predetermined cellular growth pattern within the reticular tissue, regardless of the validity of a phylogenetically predetermining cause.

The accumulation of reticular tissue to the right of the interventricular septum has been seen in the earlier age groups. In age group xv embryos, expansion of the right trabeculated ventricle and, we believe, fluid dynamic forces have led to greater relative restriction of this layer than was seen in age group xiv. It is situated, however, as before, ventrally in the concavity, to the right of the interventricular septum.

The flow of blood through the atrioventricular canal is almost certainly divided into right and left streams, despite the lack of fusion of dorsal and ventral cushions. About half of the embryos in this age group, as in age group xiv, show apposition of the cushions at least in the distal part of the canal. Those specimens in which the atria and ventricles are engorged with blood, for example 3385, show the greatest separation of the cushions. It is perhaps significant, however, that all but a few have blood in the right and left canals lateral to the cushions while blood cells are infrequently seen medially between the cushions despite the absence of approximation. There is further presumptive evidence that before fusion of the cushions a separation of blood into two lateral streams occurs. Patten's slow-motion moving pictures of the living heart in the chick show cushion approximation and division of the blood streams emerging from the atrioventricular canal at an earlier stage of development. Shrinkage of the reticular layer during fixation probably accounts for some of the variation seen in different specimens.

Fusion of the cushions appears to take place in many specimens of age group xvi. An occasional specimen from late age group xvii still shows slight separation of the dorsal and ventral atrioventricular cushions.

DISCUSSION

Our studies of the developing heart in human embryos from age group ix to age group xv, inclusive, provide a reasonably continuous picture of certain aspects of cardiogenesis in man which has previously been lacking.

The limited number of specimens during age group ix and early age group x fail, however, to provide a satisfactory morphological picture of events before and during the time of presumed fusion of originally lateralized ventricular primordia. Our present definitions of chambers and descriptions of their evolution beyond 4 somites are based on static morphological observations, which, despite close grading of successive specimens, leave something to be desired. For instance, we can only infer the presence of regional variation in tissue growth by virtue of change in size of specific areas delimited by morphological landmarks such as ridges or grooves, and we cannot rule out the possibility of cellular migrations. Observations of the heart in living mammalian embryos with tissue markers could help resolve these uncertainties.

Within the limitations of periodic observation of fixed embryos it appears likely that the more distal right cardiogenic fold contributes more to the right trabeculated ventricle and infundibulum than the distal left cardiogenic fold, and that the more proximal part of the left cardiogenic fold contributes most to the left trabeculated ventricle. There is either growth dominance or cellular tropism within the ventricular segments distally to the right and proximally to the left.

The lateralization of the atrioventricular canal to the left during the last half of age group x appears to result from a greater linear growth of the right atrium than that occurring in the left atrium. Here, again, however, tissue migration rather than displacement from a growth center cannot be ruled out.

Changes in relationships during age groups xii to xv, inclusive, such as the so-called migration of the atrioventricular canal back to the mid-line, and descent and ventromedial rotation of the right ventricular and infundibular segments appear more certainly to result from the mechanics of regional tissue growth and chamber displacements.

Widespread acceptance of reports based on isolated observations between age groups xii and xv has led to the prevalence of some erroneous views. We will, therefore, recapitulate and elaborate on some of the important differences of observation and interpretation between our work and that of others.

The inherent distortion in even the best-preserved specimens accounts for some differences in observation, these difficulties increasing geometrically in poorly fixed material. Further, interpretation of living form from preserved structures has significant limitations, and the best drawings of meticulously faithful reconstructions are subject to interpretive error. These limitations apply particularly to interpreting function. However, some of the current concepts about the development of the heart, which we believe to be erroneous, appear to be the result, in part, of the misuse of schematic drawings, often from a secondary source.

A case in point is Kramer's (1942) view of the "conoventricular flange," which was described as a flap of tissue allegedly obstructing the egress of blood from the left ventricle on its course to the arterial arches. Kramer has used a drawing entitled "Heart of an embryo, about

4 to 5 mm., based, in part, on figure 532 in *Buchanan's Manual of Anatomy* (1927)" to illustrate his discussion of this critical period in cardiac development. Since Kramer did not cite any personal observations of hearts at this stage of development, we must conclude that he relied on this illustration and descriptions in the literature. The dangers of this practice are emphasized by the fact that J. E. Frazer, who provided the figures of the developing heart in *Buchanan's Manual of Anatomy,* stated that they were made to reflect the process of change rather than to present the actual state of affairs in specific specimens. For this reason, a brief survey of the works of other authors cited by Kramer appears indicated.

Keith (1909), writing on malformations of the bulbus cordis, used the freehand illustrations of His (1866*b*) for his exposition of the embryology of the human heart between 4 and 5 mm. Keith, however, in support of his theoretical concept of the role of the bulbus cordis in human heart development, departed from the descriptions of the developing heart by His. He illustrated diagrammatically, and quite erroneously, first the presence and then the atrophy of an obstructing spur derived from the lesser curvature of the "bulbus" and "ventricle." He was apparently attempting to describe the evolution of the mammalian heart from the selachian heart, within the confines of Haeckel's biogenetic law or theory of recapitulation. In a later work, Keith (1924) substituted the illustrations of Frazer (1916) for those of His, still preserving his own diagrammatic illustrations based on a theoretical conviction. Frazer (1916, p. 19) had stated, in regard to the illustrations subsequently used by Keith, "I had determined at an early stage that the purpose with which the work had been undertaken would be served best by constructing 'schematic' models—made with a free hand, founded on actual reconstructions, but showing only the general and main conditions." He warned that these figures should not be misconstrued as representing morphological fact at any one stage of development. Frazer (1931), in his *Textbook of Embryology,* illustrated and described the heart of a "4.5 millimeter embryo," similar to his earlier freehand illustrations. The figure in Frazer's textbook appears to be the same illustration that was used in *Buchanan's Manual of Anatomy,* and employed by Kramer for his extensive interpretations. Of this illustration, Frazer said, "These drawings show this heart with the front wall removed from the ventricle and bulb; the cavities of these two hearts are seen to be separated, partly, by a prominent bulbo-ventricular spur or angle which, by its presence, causes the opening into the bulb to lead out of the right extremity of the ventricular cavity to the right, in front of and rather below the auriculo-ventricular aperture."

Kramer (1942, p. 358) stated, "There is one relationship suggested by Keith's diagrams which, regardless of what one may feel as to its possible phylogenetic implications, seems of considerable importance in connection with partitioning of the conus. This is the position of the extensive flange found internally at the cono-ventricular sulcus. The location of this flange makes it necessary for blood from the left ventricle to negotiate a sharp reverse turn through the interventricular foramen into the right ventricle, before it can leave the chest by way of the truncus."

There followed, in Kramer's article, a discussion of the differences observed between what he believed to be human morphology and his own observations of living chick hearts. Interestingly, he concluded (p. 359), "Nevertheless, with all due allowance made for such possible differences between the living and fixed hearts, this flange certainly lies across the most direct route for the outlet which must eventually be established from the left ventricle into the aortic part of the truncus. It becomes, therefore, a matter of some theoretical interest whether this flange is reduced entirely by differential growth in its vicinity, or whether there may be some actual resorption of its tissues." He followed with a debate on the subject of reabsorption versus differential growth, with reference to the afore-mentioned illustrations of Keith, and concluded by favoring the concept of differential growth as the cause of disappearance of the flange. In a survey of the subject, he then stated (p. 360), "The mesial shift of the conus and reduction of the cono-ventricular flange, together with the coincident shortening, widening, and straightening of the exit from the ventricles, all combine in paving the way for the final steps in the partitioning process."

The mesial shift of the conus or, as we have termed it, the infundibulum, does appear, from our studies, to be of importance to septation. However, the concept of an obstructing structure between the proximal transverse and ascending limbs of the primary heart tube, variously referred to as conoventricular flange, bulboventricular spur, and bulboauricular spur, appears to us to be largely the result of speculations on developmental changes in the absence of supportive serial observations.

The speculations by Keith, Frazer, and Kramer have apparently resulted from concern about the manner in which the right atrioventricular orifice comes to open into the right ventricle, and how the blood from the left ventricle eventually leads directly into the aorta. A description of the former has been given in the text of age groups x to xv. As for the latter, we have presented a picture of events to and including age group xv. The remainder of the story must be based on serial descriptions of older age groups.

The origin of the right ventricle and interventricular septum in Mammalia has been a controversial subject ever since the descriptions by His in 1885. Waterston (1918) briefly reviewed the subject in his magnificent but often-overlooked work. Waterston derived the right ventricle in its entirety from the bulbus cordis. He concluded that the infundibular region of the right ventricle arose from the distal part of the bulbus, and the trabeculated region from the proximal part. He subscribed to and verified to his own satisfaction the concept that the bulboventricular furrow or groove, externally, represents the site of the interventricular septum internally. Mall (1912) and Murray (1919) held a similar view. Waterston's description of the division of the atrioventricular canal was limited by his material, which jumped from a 28-somite embryo in age group xii to a 6-mm. embryo which we would stage late in age group xiv. Lacking human material, he accepted the descriptions by Born of the rabbit heart as pertaining to man, and emphasized the significant concept that approximation of the myoendocardial tissue within the ventricular portion of the atrioventricular canal, beyond the atrioventricular junction, results in the development of a right atrioventricular canal which empties directly into the bulbus cordis or right ventricle. Our study on human embryos confirms this concept.

Despite Waterston's paper, Kramer subscribed to the more traditional but ambiguous views of Tandler and Frazer on the genesis of the right ventricle and interventricular septum. Frazer (1931) stated some 12 years after Waterston, in regard to a 4.5-mm. embryo, "The ventricular cavity is already showing an early stage of division into right and left ventricles, for a low septum is visible extending back to the inferior atrioventricular cushion. This septum is really little more than the original floor of the cavity persisting at its original level, the two subdivisions of the cavity enlarging downwards on each side of it. Thus, the right ventricle starts its existence as a bulging of the common ventricle. This bulging can be seen on the surface view of the heart." He went on, "Turning now to the 10 mm. embryo, it is to be noticed that the bulbo-ventricular spur has decreased markedly in prominence. This is due to actual atrophy and disappearance of the dorsal and left wall of the bulbus, so that the bulbar opening is now above the level of the right-hand end of the atrioventricular aperture which, with its cushions, is plainly seen." It should be noted that Frazer skipped from a description of what we consider an age group xiii embryo heart to one that we would place in age group xvi. His pen-and-ink illustrations of these two hearts do not coincide either with our observations or with his own descriptions. One can only speculate as to whether these illustrations of 1931, like those in his earlier work, are not, in fact, interpretive drawings. It is clear, however, that Kramer's (1942) widely accepted opinions and often-used illustrations of human heart development prior to age group xv must be viewed as unverified secondary source material.

We should like here to examine the historical origin of some of the terms and ideas relating to the development of the outflow tract of the heart.

Von Haller (1758) divided the aortic part of the heart, that portion between the ventricle and arterial arches, into: "le détroit, le bulbe et le bec." Later, embryologists Kölliker and von Baer considered von Haller's designation of a specific region, "le détroit," or strait, as superfluous. They apparently overlooked the fact that von Haller, in studying the hearts of living chick embryos, had said (p. 116): "L'onde de sang qui parcourt le détroit est plus effilée," and, further (p. 84), "le sang sort du ventricule par un orifice plus étroit que le bulbe de l'aorte." This region, where the wave of blood is slender, von Haller described as the site of development of the semilunar valves. Kölliker, concerned primarily with the external form of the heart, referred to the region between the ventricle and the arterial arches simply as bulbus arteriosus or bulbus aortae and derived the two ventricles from a division of a single ventricular precursor. His (1885, 1886*a, b*), the first to work with a relatively large group of serially sectioned human embryos, divided the primitive heart tube into three main parts: bulbus, ventricle, and atrium. The ventricle, in turn, was divided into three components: the left shank or conus venosus, the middle piece, and the right shank or conus arteriosus. The bulbus was divided into the "fretum Halleri" (i.e., "le détroit"), a proximal narrowed area, and the truncus arteriosus, a distal, more expanded segment. The former was described as separated from the right ventricle or conus arteriosus by a groove, and the latter represented a segment between the fretum Halleri and the aortic arches. In other words, the "détroit" or "fretum Halleri" was recognized by His, whereas von Haller's "le bulbe et le bec" became the equivalent of the truncus arteriosus. His derived from the conus venosus the left ventricle, and from the conus arteriosus the right ventricle. The middle piece, he believed, contributed a part to each of the two ventricles.

Born (1889), describing the development of the rabbit heart, followed the terminology employed in Kölliker's earlier descriptions of avian and mammalian hearts, namely: ventricle and bulbus arteriosus.

Earlier, Gegenbauer (1866) had used the term conus arteriosus to designate that portion of adult selachian and ganoid hearts which lies beyond the ventricle, whose wall is composed of circular striated muscle. The selachian and ganoid conus arteriosus he differentiated from a similar region in the bony fishes, termed the bulbus arteriosus, the wall of which is composed of smooth muscle. Boas (1880, 1882), with greater specificity, extended the use of the term conus arteriosus to define a clearly separated, independent part of the heart in dipnoids and amphibians. He considered the conus arteriosus of amphibians to be homologous with the conus arteriosus described by Gegenbauer in ganoids. Langer (1894), confronted with these conflicting terms, solved the dilemma by coining the name bulbus cordis to designate in amphibians and reptiles the part of the developing heart that he regarded as homologous with the bulbus aortae of the mammalian heart, as described by Born, and the conus arteriosus, as described by Boas and Gegenbauer. Thereafter, Born and others accepted and used the term bulbus cordis.

Born believed the right ventricle of Mammalia, in at least its upper part, to be derived from the bulbus cordis. Greil (1903*a, b,*), in his publications on reptiles, described the proximal part of the bulbus cordis as the precursor of the cavum pulmonale, a chamber that we consider to be a ventrally placed right ventricle. Keith's (1906) interpretations of Born's and Greil's work, together with his study of cardiac malformations, led him to conclude that, "In the human heart, the bulbus cordis is the precursor of the infundibular portion of the right ventricle only." Hochstetter (1903) and Tandler (1912) followed, in general, the terminology and interpretations of Born. Nevertheless, they divided the bulbar swellings into proximal and distal. In what appears to us to be a contradiction in terminology, Tandler described the distal bulbar swellings: extending through the truncus arteriosus, a region that he believed was not, in fact, a part of the heart. Robertson (1913) divided the bulbus cordis, in *Lepidosiren* embryos, into three definite parts: proximal, transverse, and distal. She emphasized the role of torsion or kinking of the heart tube in approximating discontinuous ridge primordia of each of the segments, to form a spiraled ridge system, and related this concept to the genesis of the spiraled ridge system in reptile and mammalian hearts and human congenital anomalies. Pernkopf and Wirtinger (1933) divided the common ventricular cavity into a "proampule" (proximal part of the primitive ventricle) and "metampule" (distal part of the primitive ventricle), but continued the use of the terms bulbus and truncus for the more distal segments. From the "proampule" they derived the left ventricle, from the "metampule" the right ventricle.

Kramer (1942) recommended the substitution of "conus" for "bulbus cordis." He accepted the continuous nature of spiral septation as described by Waterston (1918) but, at the same time, rationalized Tandler's conflicting description of discontinuous bulbar septae. In regard to the chambers, Kramer, to compound the confusion, had apparently accepted the views of Tandler, ignoring the fact that Waterston had divided the bulbus cordis into a "conical" portion, the precursor of the right ventricular cavity, and a "tubular" portion, eventually representing the infundibulum.

In 1945, Streeter abandoned his previous use of the terms ventricle, bulbus cordis, and truncus arteriosus. Henceforth, he referred to that portion of the heart occupying the interval between the atrioventricular junction and the arterial arches as the primary heart tube, from which there develop right and left outpouchings called ventricular sacs or pouches, ventricular redundancies.

Implicit in much of the terminology utilized in describing the development of the human heart are its supposed comparative relationships to the hearts found in other classes of vertebrates. Congdon (1922) illustrated fully the error of interpreting too strictly the transformation of the human aortic-arch system in terms of the theory of phylogenetic recapitulation. These strictures receive further emphasis from Patten and Kramer's (1933) studies on contraction in the embryonic chick heart. They clearly demonstrated the discrepancy between the morphological tradition of early preformed chambers and their own findings of the simultaneous evolution of function and form in the development of the chick heart.

The rather rigid phylogenetic concepts based on the theory of recapitulation, which are inherent in the views of Keith (1906, 1909, 1924), Robertson (1913–1914), and Spitzer (1923, 1951), are not acceptable substitutes for serial observations of the changes in structure and function of the developing human heart. Most of the hypotheses based on recapitulation theory are inadequate as explanations for anomalous conditions, lack confirmation in static morphology, and preclude direct proof of the causative factors involved.

We do not yet possess adequate information on the precise phylogenetic precursors of the various regions, nor is there sufficient experimental evidence about centers of growth and the intrinsic or extrinsic forces that change the simple cardiac tube into a mature organ. We do believe, however, that greater understanding of the many variations that result in congenital anomalies has, and will, come about through a clearer comprehension of ontogenetic processes.

De la Cruz and da Rocha (1956) and de la Cruz et al. (1959) offer "a new ontogenetic theory" for the explanation of congenital malformations involving the truncus and conus based upon Davis, Streeter, and Kramer's "modern school of embryology." Our reservations about the acceptance of de la Cruz's work coincide with those we have expressed in regard to the embryology she cited.

It is not within the scope of this paper to discuss at length all the various theoretical views that have been put forth about the normal and abnormal development of the human heart in the regions under discussion, but Spitzer's "phylogenetic theory" of the development of normal and malformed hearts in Mammalia must be discussed and evaluated here because of its widespread acceptance. It relies for support on Haeckel's biogenetic law and unrestrained teleology. Spitzer's point of view is shown in his argument on the transposition type of cardiac malformation. At the beginning of his argument, Spitzer labeled as "fantastic" Meckel's phylogenetic theory of parallelism, and with this we heartily concur. He rejected also, however, all the ontogenetic theories of transposition, concluding that their shortcomings were "quite self-evident," while at the same time accepting that "simple malformations" such as patent foramen ovale, patent ductus arteriosus, defects of ventricular septum, ordinary truncus arteriosus communis, and arrest in an embryonic aortic arch were nothing more than inhibition in development, being the remains of transitional stages in the normal developmental period. He contended (p. 75) that "Their presence does not constitute a marked departure from normal cardiac architecture, since they represent structures originally present in a transitional stage. It is easy to interpret their presence in the definitive completed heart, and their incorporation into the general structure of the heart typical of an earlier phase, as a simple inhibition of ontogenetic development. However, a revolutionary departure from the normal cardiac architecture, like that found in transposition, cannot be explained as simple effects of evolutionary inhibitions, for not even a suggestion of such atypical formation is present as a transitional stage of normal development." Continuing (p. 76), Spitzer said: "In short, these [ontogenetic] theories do not give sufficient information concerning either the presence or the reasons for the assumed aberrant factors in the malformations. Even the theory of Rokitansky fails in this manner, although it constitutes a definite advance because it explains the various types of transposition from the standpoint of a common denominator. However, the theory of Rokitansky, on heart malformations, still rules the accepted teaching of today. And although the theory does not give us a satisfactory explanation, we cling to it, because, as expressed by Vierordt and Herxheimer, we have nothing better to substitute for it."

Spitzer, unable to postulate any ontogenetic event which could bring about an anomaly such as transposition, concluded (p. 77), "Therefore, we must assume that transposition is founded on a phylogenetic basis, but it is suppressed and concealed ontogenetically until it is only a latency, and that disturbances in ontogenesis make manifest this latency." Spitzer's improbable theory and questionable interpretations of morphology cannot be accepted by us in their entirety.

The suggestion that the flow of blood influences the architecture of the developing heart is by no means a new idea. In the nineteenth century, it was considered a molding force in the development of cupped valves. Both Spitzer (1951) and Bremer (1932) presented at length their ideas of the effect of streaming blood on the development of septation. Streeter (1948, p. 159) stated, "One naturally associates the formation of two separate channels with the growth and activity of the two ventricular pouches, . . . as one can see in horizon xvi, as they become larger and their positions prove favorable for producing directional thrusts or currents toward the pulmonary and aortic outlets, respectively. Consideration of the wide variety of anomalies that occur in these large arteries warns one, however, that ventricular thrusts, if a factor at all, may be only one of many in the development of this, our most important organ."

The theoretical ontogenetic fluid dynamic forces outlined at the beginning of this paper have not been ruled out by our morphological findings.

The human heart before age group xii is, we believe, a propulsal pump; and, although two streams appear to be lateralized, in the living chick heart, as they emerge from the atrioventricular junction early in heart development, it appears likely to us that discontinuity of the streams occurs in the ventricular portions of the heart tube by virtue of the position and function of the trabeculated areas. Our view of the origin and function of the spiral stream, therefore, varies from that presented by Bremer (1932). Bremer's (1928) concept of a torsion of the elongating heart tube also lacks confirmation in our work. Between age group xii and age group xvi, a pair of spiral elevations and depressions appear on the endothelia-lined surface of the plastic gelatinous layer in the outflow tract of the human heart, distal to the trabeculated right ventricle, following the period of peristaltic contraction and coincident with the development of the two ventricular pumps. These spiral elevations and depressions become progressively higher and deeper, as a result, we believe, of continuing hemodynamic forces. The elevations are largely approximated before the descent of the spur between the fourth and sixth aortic arches. Spiral septation of the outflow tract precedes its histological segmental differentiation but follows considerable morphological differentiation of the two pumps: the trabeculated ventricles. By age group xvi, the flow of blood from the right ventricle to the sixth arches, and from the left ventricle to the fourth arches, in the "normal" heart, is a fait accompli.

Our studies of junctioning streams reveal that a left stream, slightly behind, junctioning with a right stream, slightly in front, will form a clockwise spiral—as is the case in normal cardiogenesis. The morphological positioning of the ventricles during age group xiii would, in the normal course of development, allow (and, we believe, does account for) the junctioning of streams in such a manner as to produce a clockwise spiral. Reverse positioning of junctioning streams, in regard to the plane of their axes, on the other hand, will cause a reverse spiral; and junction in a frontal plane results not in a spiral but a lateralization of streams with nodes in alternating perpendicular planes. We believe that various anomalies of the heart, including transposition of various degrees, may be better understood by further analysis of the interdependent factors of ontogenetic segmental growth potential and the physical forces involved in function, including fluid mechanics.

Before our morphological study, we had observed the effects of intersecting streams on one another, and demonstrated that a spiral stream coursing through a gelatinous or plastic tube, in the manner described above, would produce spiral ridges in a cylinder similar to those seen in the heart. It, therefore, seems reasonable to us to assume that, regardless of other factors, the fluid dynamics of blood streams and consideration of their configurations within the heart, as well as the effects of flow on the luminal surfaces, cannot be ignored in an evaluation of the development of form and function of the heart. Further, we are convinced that the task of documenting morphology must continue hand in hand with physical and chemical studies.

After the completion of this article we were referred to the recent experimental studies by Rychter (1959) and Rychter and Lemež (1957, 1958, 1959, 1960) on the chick heart. They appear to support the idea that the function of the ventricles and blood flow within the heart effects the development of ridges and the eventual septation of the outflow tract. A detailed discussion of this important work in relation to our theories and findings concerning human heart development cannot be presented at this time, but these reports appear to support our belief that experimental studies of blood flow in embryo hearts will lead to better understanding of the evolution of anomalous forms.

LITERATURE CITED

Atwell, W. J. 1930. A human embryo with seventeen pairs of somites. *Carnegie Inst. Wash. Publ.* 407, *Contribs. to Embryol., 118,* 1–24.

Bernays, A. C. 1876. Entwicklungsgeschichte der Atrioventricularklappen. *Morphol. Jahrb., 2,* 478–518.

Boas, J. E. V. 1880. Über den Conus arteriosus bei Butirinus und bei anderen Knochenfischen. *Morphol. Jahrb., 6,* 527–534.

Boas, J. E. V. 1882. Über den Conus arteriosus und die Arterienbogen der Amphibien. *Morphol. Jahrb., 7,* 488–572.

Born, G. 1889. Beiträge zur Entwicklungsgeschichte des Säugetierherzens. *Arch. mikroskop. Anat., 33,* 284–378.

Bremer, J. L. 1928. An interpretation of the development of the heart. The left aorta of reptiles. *Am. J. Anat., 42,* 307–369.

Bremer, J. L. 1932. The presence and influence of two spiral streams in the heart of the chick embryo. *Am. J. Anat., 49,* 409–440.

Buchanan's Manual of Anatomy. 1927. Chapter 12, vol. 2, pp. 986–1114. C. V. Mosby Co., St. Louis.

Burlingame, P. L., and J. A. Long. 1939. The development of the heart in the rat. *Univ. Calif. Publs. Zoöl., 43,* 249–320.

Congdon, E. D. 1922. Transformation of the aortic-arch system during the development of the human embryo. *Carnegie Inst. Wash. Publ.* 277, *Contribs. to Embryol., 14,* 47–110.

Copenhaver, W. M. 1939. Initiation of the beat and intrinsic contraction rates in different parts of the Amblystoma heart. *J. Exptl. Zool., 80,* 193–224.

Davis, C. L. 1923. Description of a human embryo having twenty paired somites. *Carnegie Inst. Wash. Publ.* 332, *Contribs. Embryol., 15,* 1–51.

Davis, C. L. 1924. The cardiac jelly of the chick embryo. *Anat. Record, 27,* 201–202.

Davis, C. L. 1927. Development of the human heart from its first appearance to the stage found in embryos of 20 paired somites. *Carnegie Inst. Wash. Publ.* 380, *Contribs. Embryol., 19,* 245–284.

DeHaan, R. L. 1959. Cardia bifida and the development of pacemaker function in the early chick heart. *Developmental Biol., 1,* 586–602.

De la Cruz, M. V., and J. P. da Rocha. 1956. An ontogenetic theory for the explanation of congenital malformations involving the truncus and conus. *Am. Heart J., 51,* 782–805.

De la Cruz, M. V., *et al.* 1959. An embryologic explanation for the corrected transposition of the great vessels: additional description of the main anatomic features of this malformation and its varieties. *Am. Heart J., 57,* 104–117.

Foxon, G. E. H. 1954. Problems of the double circulation in the vertebrates. *Biol. Revs., Cambridge Phil. Soc., 30,* 196–226.

Frazer, J. E. 1916. The formation of the pars membranacea septi. *J. Anat. Physiol., 51,* 19–29.

Frazer, J. E. 1931. *Textbook of Embryology.* Baillière, Tindall and Cox, London.

Gegenbauer, C. 1866. Zur vergleichenden Anatomie des Herzens. *Jenaische Z. Med. u. Naturwissensch., 2,* 365–383.

Girgis, A. 1930. The development of the heart in the rabbit. *Proc. Zool. Soc. London,* part 3, pp. 755–782.

Girgis, A. 1933. A further contribution on the development of the heart in the rabbit. *Proc. Zool. Soc. London,* part 2, pp. 421–450.

Goss, C. M. 1938. The first contractions of the heart in rat embryos. *Anat. Record, 70,* 505–524.

Goss, C. M. 1952. Development of the median coordinated ventricle from the lateral hearts in rat embryos with three to six somites. *Anat. Record, 112,* 761–796.

Greil, A. 1903*a*. Über die Entwicklung des Truncus arteriosus der Anamier. *Ergänzungshefte Anat. Anz., 23,* 91–105.

Greil, A. 1903*b*. Beiträge zur vergleichenden Anatomie und Entwicklungsgeschichte des Herzens und des Truncus arteriosus der Wirbeltiere. *Morphol. Jahrb., 31,* 123–310.

Heuser, C. H. 1930. A human embryo with 14 pairs of somites. *Carnegie Inst. Wash. Publ.* 414, *Contribs. Embryol., 22,* 135–153.

His, W. 1885. *Anatomie menschlicher Embryonen.* Leipzig.

His, W. 1886*a*. Über die Entwicklung der Form und der Abteilungen des Herzens. *Congrès period. intern. des sci. méd. C. R. 1884 Copenhague 1886,* I. Section d'anatomie, pp. 32–34.

His, W. 1886*b*. *Beiträge zur Anatomie des menschlichen Herzens.* F. C. W. Vogel, Leipzig.

Hochstetter, F. 1903. Die Entwicklung des Blutgefässystems. *Hertwigs Handb. d. vergl. u. exptl. Entwickl. d. Wirbeltiere, 3,* 1906.

Ingalls, N. W. 1920. A human embryo at the beginning of segmentation, with special reference to the vascular system. *Carnegie Inst. Wash. Publ.* 274, *Contribs. Embryol., 11,* 61–90.

Keith, A. 1906. Malformation of the bulbus cordis. In *Studies in Pathology,* edited by William Bullock. *Aberdeen University Studies, 21,* 57–74.

Keith, A. 1909. The Hunterian lectures on malformations of the heart. *Lancet, 2,* 519–523.

Keith, A. 1924. Schorstein lecture on the fate of the bulbus cordis in the human heart. *Lancet, 2,* 1267–1273.

Keibel, F., and F. P. Mall. 1912. *Manual of Human Embryology.* J. B. Lippincott Co., Philadelphia.

Kölliker, A. von. 1861–1879. *Entwickelungsgeschichte des Menschen und der löheren Thiere, 2,* 903. Leipzig.

Kramer, T. V. 1942. The partitioning of the truncus and conus and the formation of the membranous portion of the interventricular septum in the human heart. *Am. J. Anat., 71,* 348–370.

Langer, A. 1894. Über die Entwicklungsgeschichte des Bulbus cordis bei Amphibien und Reptilien. *Morphol. Jahrb., 21,* 40–67.

Langer, A. 1895. Zur Entwicklungsgeschichte des Bulbus cordis bei Vögeln and Säugethieren. *Morphol. Jahrb., 22,* 99–112.

Lev, M., and O. Sophir. 1945. A theory of transposition of the arterial trunks based on the phylogenetic and ontogenetic development of the heart. *Arch. Pathol., 39,* 172.

Lindes, G. 1865. Ein Beitrag zur Entwicklungsgeschichte des Herzens. Dissertation, Heinrich Loakmen Dorpat. *60,* 696–700.

Mall, F. P. 1912. On the development of the human heart. *Am. J. Anat., 13,* 249–298.

Mollier, S. 1906. Die erste Anlage des Herzens bei den Wirbeltieren. *Hertwigs Handb. d. vergl. u. exptl. Entwickl. d. Wirbeltiere, 1,* 1020–1051.

Murray, H. A. 1919. The development of the cardiac loop in the rabbit with special reference to the bulbo-ventricular groove and origin of the interventricular septum. *Am. J. Anat., 26,* 29–39.

Patten, B. M. 1922. The formation of the cardiac loop in the chick. *Am. J. Anat., 30,* 373–397.

Patten, B. M. 1931. *The Embryology of the Pig,* p. 83. P. Blakiston Co., Philadelphia.

Patten, B. M., and T. C. Kramer. 1933. The initiation of contraction in the embryonic chick heart. *Am. J. Anat., 53,* 349–375.

Patten, B. M., T. C. Kramer, and A. Barry. 1948. Valvular action in the embryonic chick heart by localized apposition of endocardial masses. *Anat. Record, 102,* 299–312.

Pernkoff, E., and W. Wirtinger. 1933. Die Transposition der Herzostienein. Versuch der Erklärung dieser Erscheinung, *Z. Anat. Entwicklungsgeschichte, 100,* 561–711.

Rathke, H. 1843. Über die Entwicklung der Arterien, welche bei den Säugetieren von dem Bogen der Aorta ausgehen. *Arch. Anat.,* pp. 276–302.

Robertson, Jane I. 1913. The development of the heart and vascular system of *Lepidosiren paradoxa. Quart. J. Microscop. Sci., 59,* 53–132.

Robertson, Jane I. 1913–1914. The comparative anatomy of the bulbus cordis with special reference to abnormal positions of the great vessels in the human heart. *J. Pathol. Bacteriol., 18,* 191–210, 211–217.

Robertson, Jane I. 1941. Congenital abnormality of the heart. *Lancet, 1,* 872–875.

Rokitansky, C. von. 1875. *Die Defecte der Scheidewände des Herzens.* W. Brausmuller, Wien.

Rosenbauer, K. 1955. Untersuchung eines menschlichen Embryos mit 24 Somiten, unter besonderer Berücksichtigung des Blutgefäss systems. *Z. Anat. Entwicklungsgeschichte, 118,* 236–276.

Rychter, Z. 1959. Cévní soustava zárodku kurete. III. K problému septace srdecního bulbu a trunku u zárodku kurete. *Českoslov. morfol., 7,* 1–20.

Rychter, Z., and L. Lemež. 1957. Experimentelle Untersuchung über die Entstehung sowie über die Lage und Grösse von Kammerseptumdefekten am Herzen von Hühnerembryonen. *Verhandl. anat. Ges., 54,* 97–102.

Rychter, Z., and L. Lemež. 1958. Experimenteller Beitrag zur Entstehung der Transposition von Aorta in die rechte Herzkammer der Hühnerembryonen. *Verhandl. anat. Ges., 55,* 310–315.

Rychter, Z., and L. Lemež. 1959. Cévní soustava zárodku kurete. IV. Popisná morfogenesa pokusne vyvolaných defektú mezikomorové prepárzky. *Českoslov. morfol., 7,* 21–32.

Rychter, Z., and L. Lemež. 1960. Cévní soustava zárodku kurete. V. Vývoj a pokusná morfologie proximálního intersticiálniho polstárku srdecního bulbu. *Českoslov. morfol., 8,* 32–49.

Schmidt, F. T. 1870. Bidrag till kundskaben om hjertets utviklingshistorie. *Nord. Med. Arkiv Stockholm,* 2, N:r *23,* 1–47.

Schulte, H. von W. 1914. Early stages of vasculogenesis in the cat, with special reference to the mesenchymal origin of endothelium. *Mem. Wistar Inst. Anat. Biol., 3.* Philadelphia.

Schulte, H. von W. 1916. The fusion of the cardiac anlages and the formation of the cardiac loop in the cat (*Felix domestica*). *Am. J. Anat., 20,* 45–72.

Spitzer, A. 1923. Über den Bauplan des normalen und missgebildeten Herzens. Versuch einer phylogenetischen Theorie. *Virchows Arch. pathol. Anat. u. Physiol., 243,* 81–201.

Spitzer, A. 1951. *The Architecture of Normal and Malformed Hearts.* A phylogenetic theory of their development. With a summary and analysis of the theory by Maurice Lev and Aloysius Vass. Charles C Thomas, Springfield, Ill.

Strahl, H., and F. Carius. 1889. Beiträge zur Entwicklungsgeschichte des Herzens und der Körperhöhlen. *Arch. Anat. u. Entwick.,* pp. 231–248.

Streeter, G. L. 1927. Development of the mesoblast and notochord in pig embryos. *Carnegie Inst. Wash. Publ.* 380, *Contribs. Embryol., 19,* 73–92.

Streeter, G. L. 1942. Developmental horizons in human embryos. Description of age group xi, 13 to 20 somites, and age group xii, 21 to 29 somites. *Carnegie Inst. Wash. Publ.* 541, *Contribs. Embryol., 30,* 211–245.

Streeter, G. L. 1945. Developmental horizons in human embryos. Description of age group xiii, embryos about 4 or 5 millimeters long, and age group xiv, period of indentation of the lens vesicle. *Carnegie Inst. Wash. Publ.* 557, *Contribs. Embryol., 31,* 27–63.

Streeter, G. L. 1948. Developmental horizons in human embryos. Description of age groups xv, xvi, xvii, and xviii, being the third issue of a survey of the Carnegie Collection. *Carnegie Inst. Wash. Publ.* 575, *Contribs. to Embryol., 32,* 133–203.

Tandler, J. 1912. The development of the heart. In F. Keibel and F. P. Mall, *Manual of Human Embryology, 2,* 534–570. J. B. Lippincott Co., Philadelphia.

von Baer, K. E. 1828. Über Entwicklungsgeschichte der Tiere, *1,* 56; Beobachtung und Reflexion, *1,* 271. Gebrüder Bornträger, Königsberg.

von Haller, A. 1758. *Sur la formation du coeur, 1,* 116; 2, 84. Lausanne.

Wang, C. 1917–1918. The earliest stages of development of the blood vessels and the heart in ferret embryos. *J. Anat., 52,* 107–185.

Waterston, D. 1918. The development of the heart in man. *Trans. Roy. Soc. Edinburgh, 52* (part II), 257–302.

West, C. M. 1930. Description of a human embryo of eight paired somites. *Carnegie Inst. Wash. Publ.* 407, *Contribs. Embryol., 21,* 25–35.

Yoshinaga, I. 1921. A contribution to the early development of heart in Mammalia, with special reference to the guinea pig. *Anat. Record, 21,* 239–308.

PLATES

Plate 1. Fluid configurations resulting from intersecting streams. Direction of the flow is upward. *A,* two cylindrical streams whose axes join in the same vertical plane, forming a model pattern in which fluid from each side remains on the same side. The proximal (lower) node is seen edge on; the distal (upper) node shows the horizontal amplitude. *B,* the same two streams and their joined pattern viewed laterally, or 90° from *A*. *C* shows the two streams from the same view as *A,* but with the left stream shifted to a position slightly in front (toward the viewer) of the right stream. This change in position results in a clockwise spiral. If one imagines looking at a heart from in front the streams would be coming from the ventricles and would course through the infundibulum and truncus arteriosus. Cross sections show the configuration of the streams through the infundibulum and truncus arteriosus as seen in age group xv. *R* is lumen of stream from right ventricle; *L* is lumen of stream from left ventricle. *D* shows a reversal of the front and back relationship of the two streams with a reversal of the direction of the spiral.

A

B

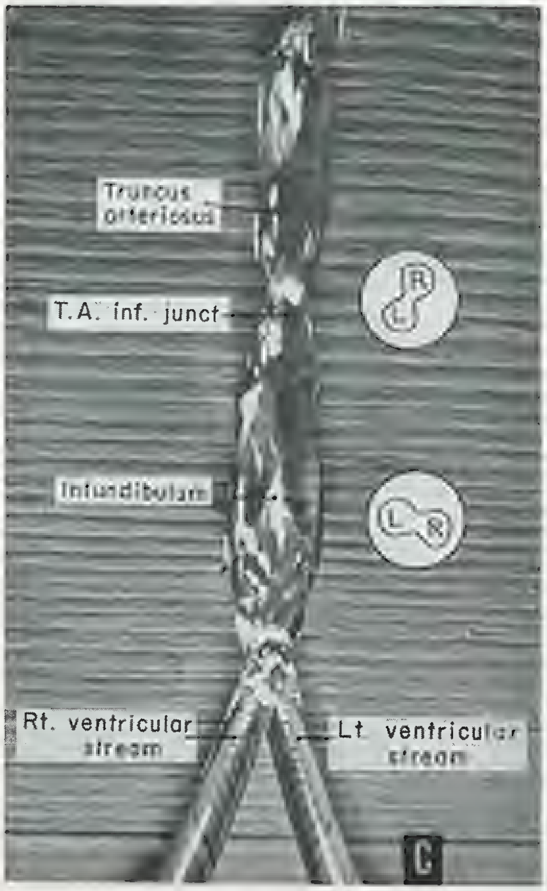
Truncus arteriosus
T.A. inf. junct
R
L
Infundibulum
L
R
Rt. ventricular stream
Lt. ventricular stream
C

D

Plate 2. *A,* left lateral view of age group xii, embryo 5923, 28 somites. Liver is seen projecting into caudal surface of atrioventricular junction.

B, Age group xii, embryo 8944, 25 somites, parasagittal section through the left atrium, atrioventricular canal, and left ventricle. The liver projects up into the caudal surface of the atrioventricular junction.

C, parasagittal section of embryo 8944 where the left ventricle approaches the interventricular isthmus. *C. J.,* cardiac jelly.

D, parasagittal section of embryo 8944, showing the position and configuration of the endothelial tube within the myoepicardial tube at the interventricular isthmus. Note the dorsal position of the endothelial tube and the accumulations of jelly ventrally in both *C* and *D.*

E, embryo S, cross section of the truncus arteriosus. *R* is the lumen through which the stream from the right ventricle is ejected, and *L* is that through which the left ventricle stream is ejected.

F, embryo S, cross section at the level of the distal infundibulum. Note the rotation of the ridges between *E* and *F.*

All figures are × 68.5.

PLATE 2

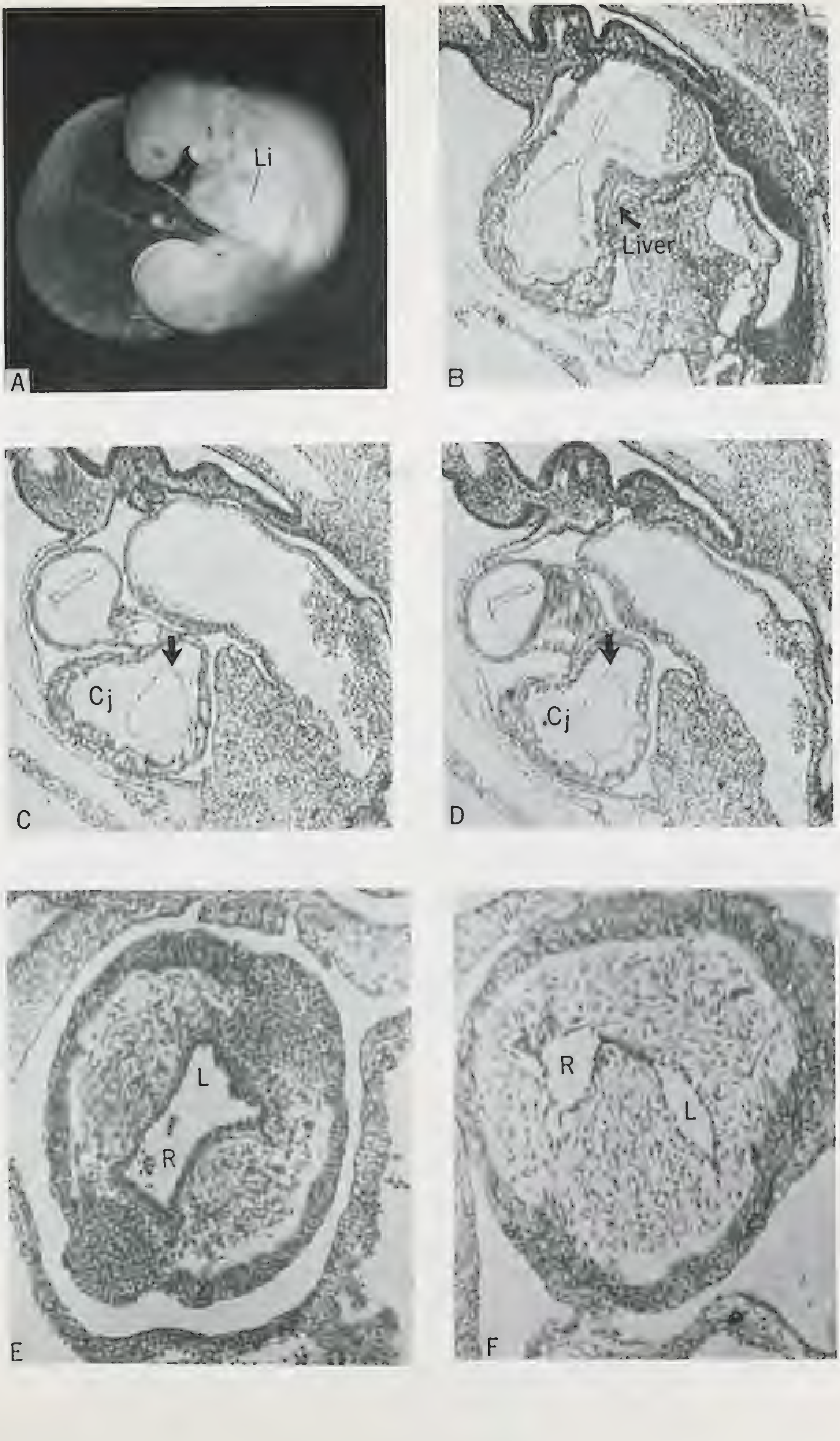

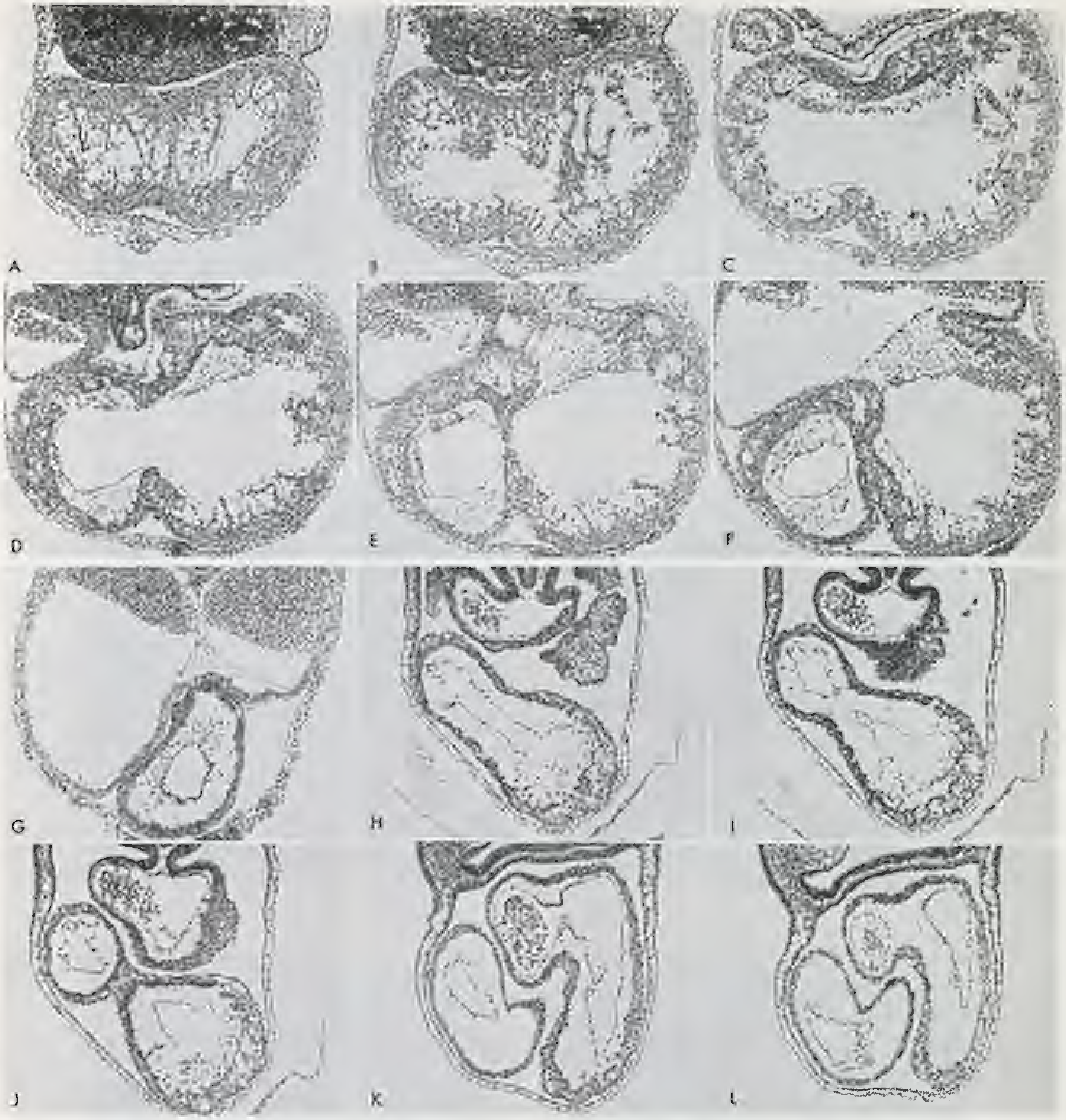

Photomicrographs of sections from embryo 8967, age group xiv, *A–G,* and embryo 8943, 22 somites, age group xii, *H–L. A,* section 6-2-11, transversely through the trabeculated ventricles, shows ventrally the interventricular sulcus near the apex. *B,* section 6-4-2, demonstrates the fusion of the septal trabeculae to the left of the invaginated ventral portion of the interventricular septum. *C,* section 6-6-4, and *D,* section 5-6-12, show the left ventricle, interventricular canal, and right ventricle just below the level of the infundibulum. *E,* section 5-6-4, shows the left ventricle at the level of the dorsal atrioventricular cushion and the right ventriculoinfundibular junction. *F,* section 5-5-3, shows the beginning pair of myoendocardial reticular layer elevations in the proximal infundibulum. *G,* section 4-1-7, is through the infundibulotruncal junction and the cephalically divided atria. Note the muscular interatrial septum dorsally growing into the myoendocardial layer, which primarily divides the cephalic portion atrial cavities. Comparing figures *A-F* one can note the continuity of line from the ventral interventricular sulcus to the cleft between the infundibulum and left ventricle. *H,* section 4-182-7; *I,* section 4-182-2; *J,* section 4-172-7; *K,* 4-152-4; and *L,* 3-42-8, of embryo 8943 correspond roughly in orientation and plane of section with those of the older embryo 8967 seen in figures *B, C, E, F,* and *G.* All figures × 53.

XII
25S
8944

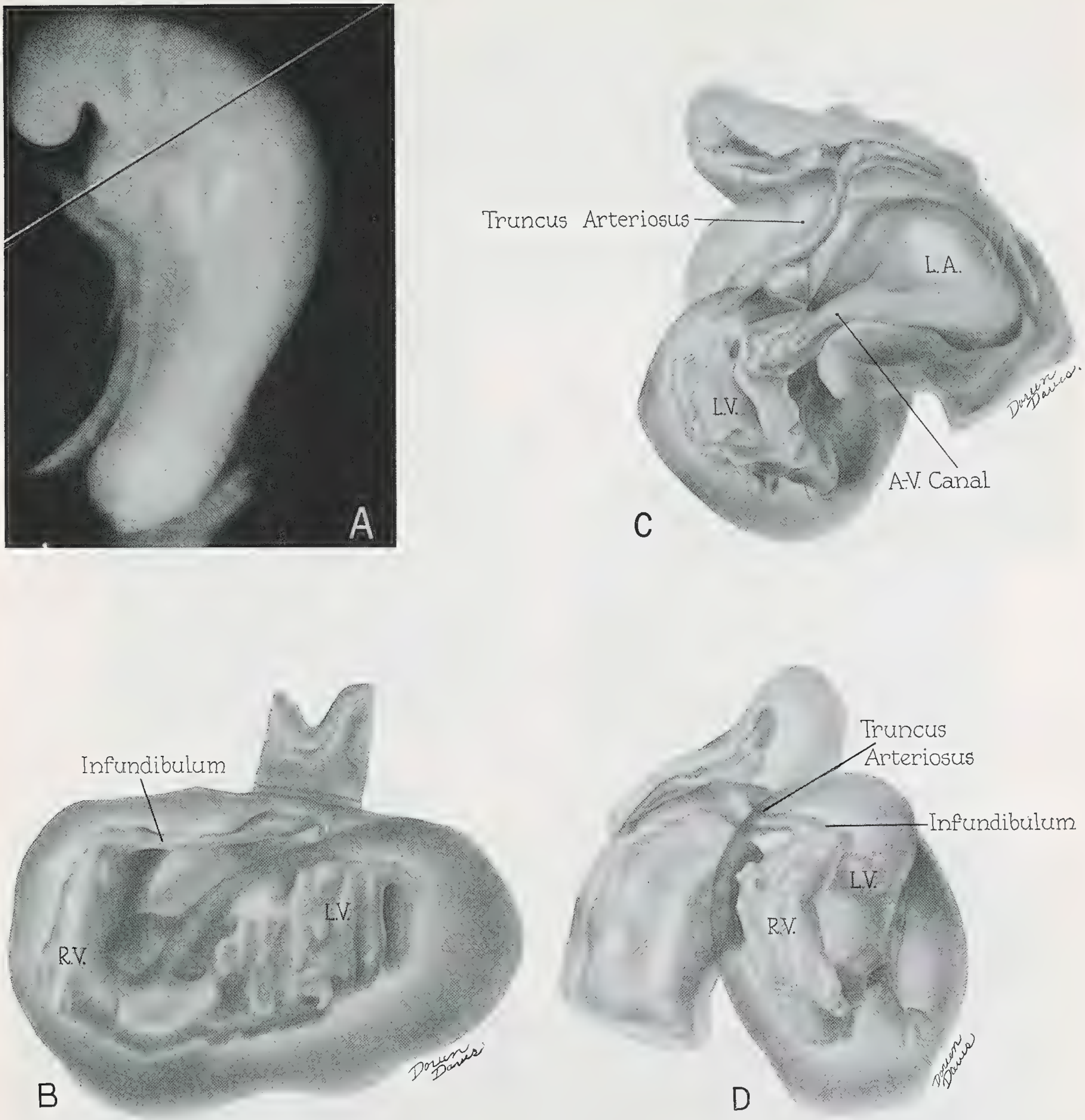

A, left profile photograph of middle age group xii, embryo 8944, 25 somites, with a line indicating the angle of view of the illustrated heart reconstruction as seen in *B;* from in front.

C, left profile, *D,* right profile, views of the heart reconstructions. Heart cavities are shown through the transparency of outside form.

XII
5923
28S

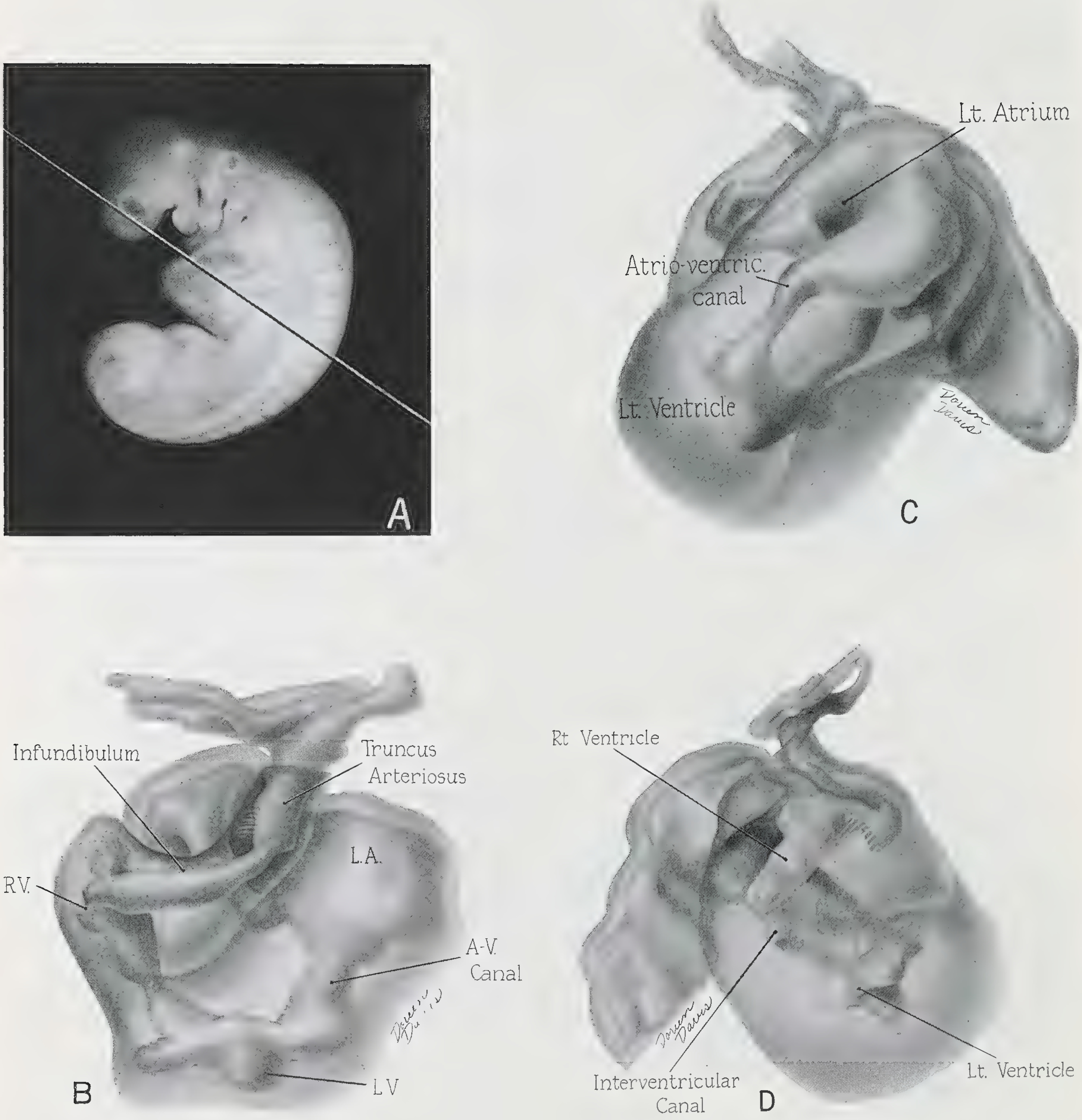

A, left profile view of late age group xii, embryo 5923, 28 somites, with a line indicating the angle of view of the heart as seen from *B* (almost top view). *C,* left profile; *D,* right profile.

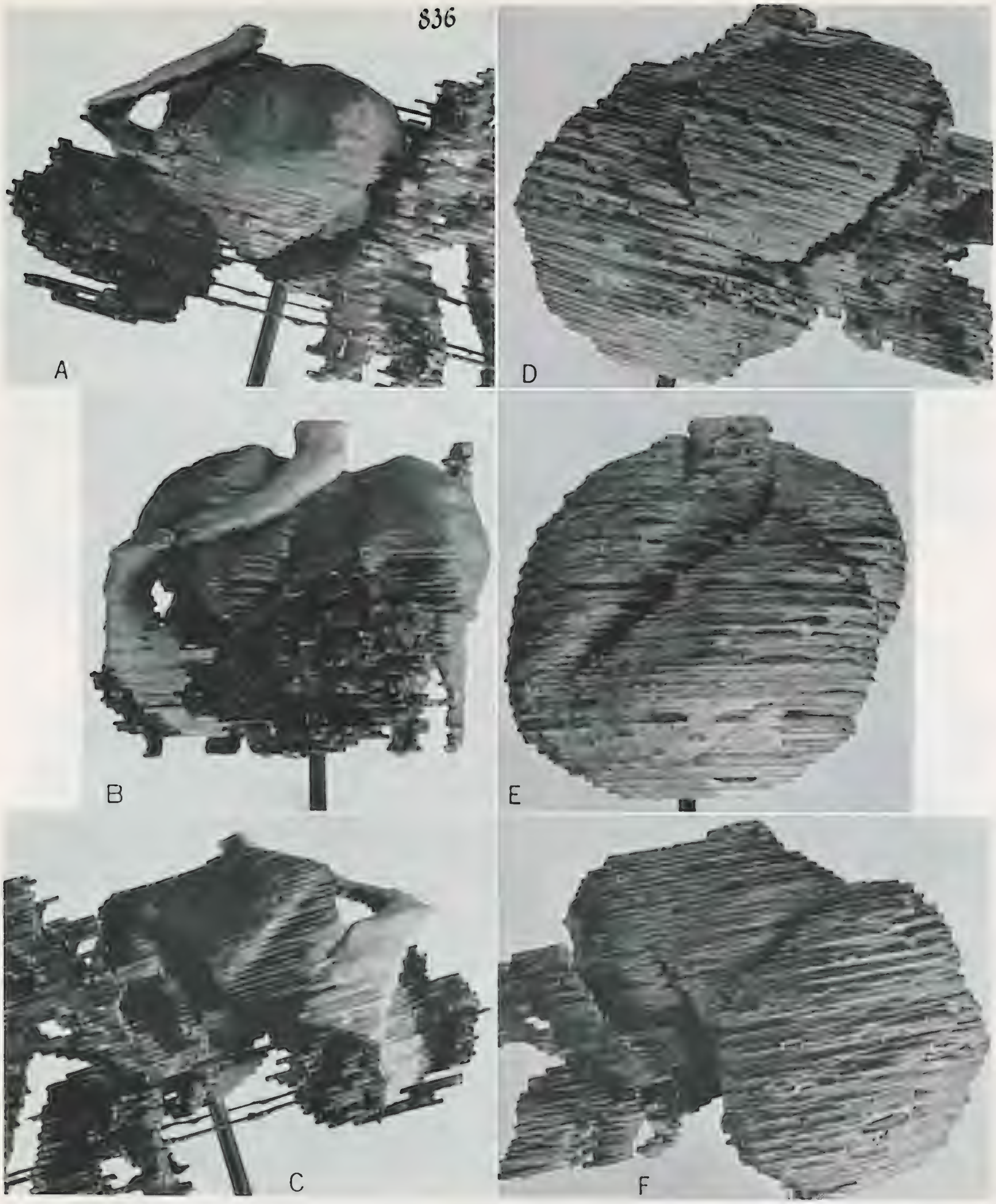

Views of the plaster casts of wax-plate reconstructions of embryo 836, earliest of age group xiii specimens. *A,* left profile, *B,* frontal, *C,* right profile, views of a reconstruction of the inside or lumen of the heart; *D, E,* and *F* show the corresponding views of a reconstruction of the heart's external form. × 70.

XIII
8066

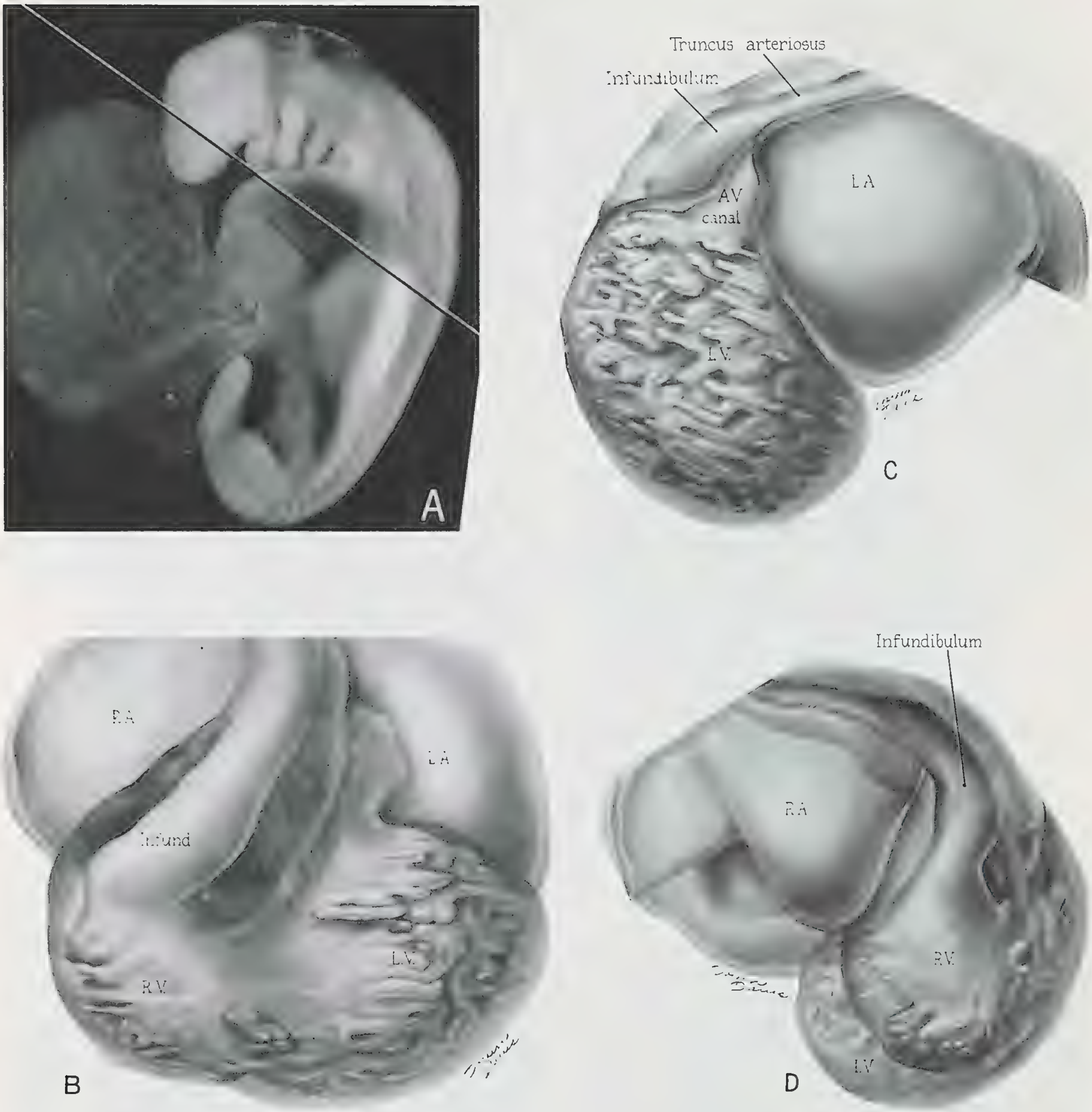

A, left profile view of embryo 8066, age group xiii, with a line indicating the direction of the view of the heart as seen *B,* from in front. *C,* left, and *D,* right, profile views of the heart.

XIV
6502

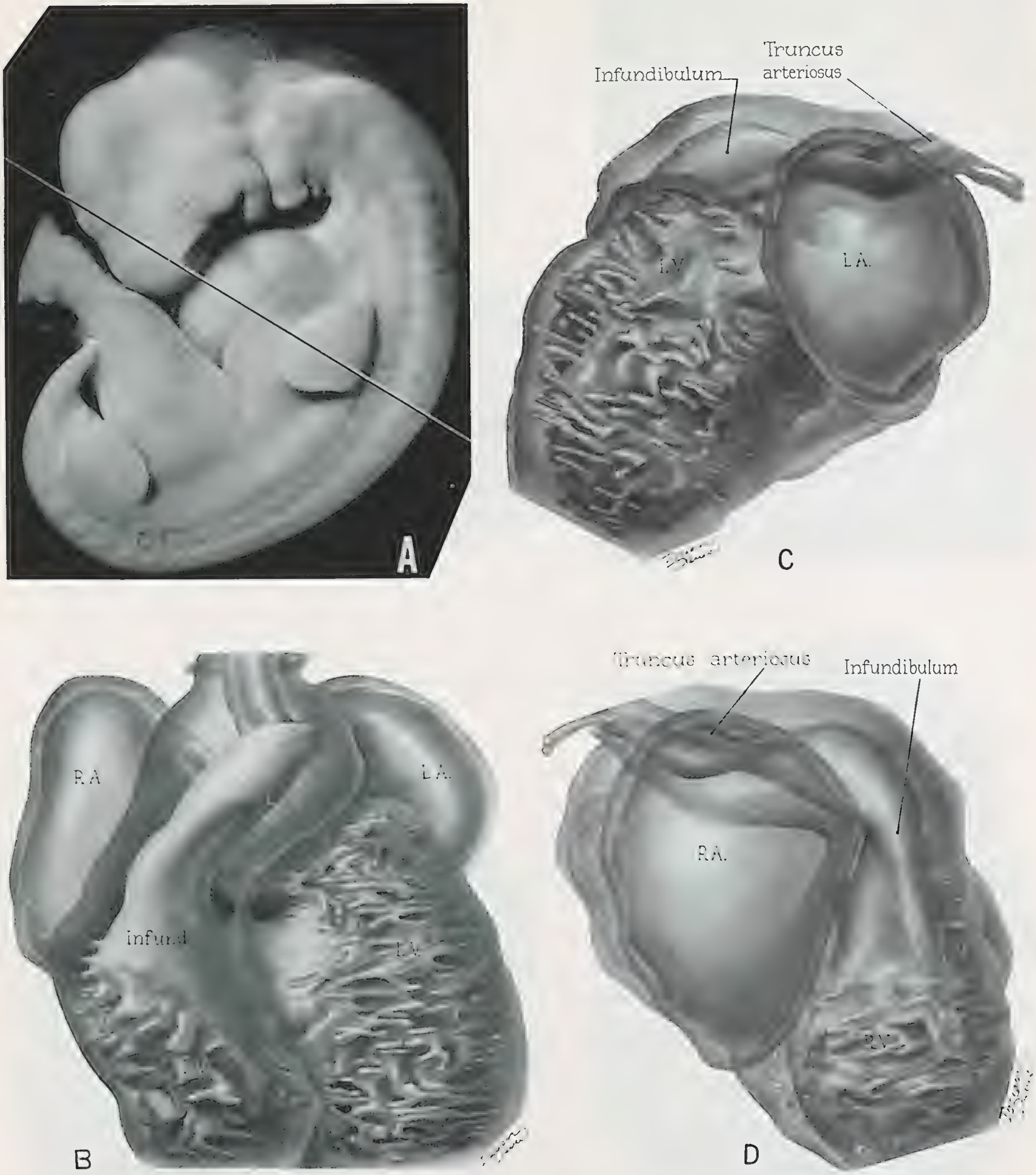

A, left profile view of embryo 6502, age group xiv, with a line indicating the direction of the view of the heart as seen *B,* from in front. *C,* left, and *D,* right, profile views of the heart.

XV
"S"

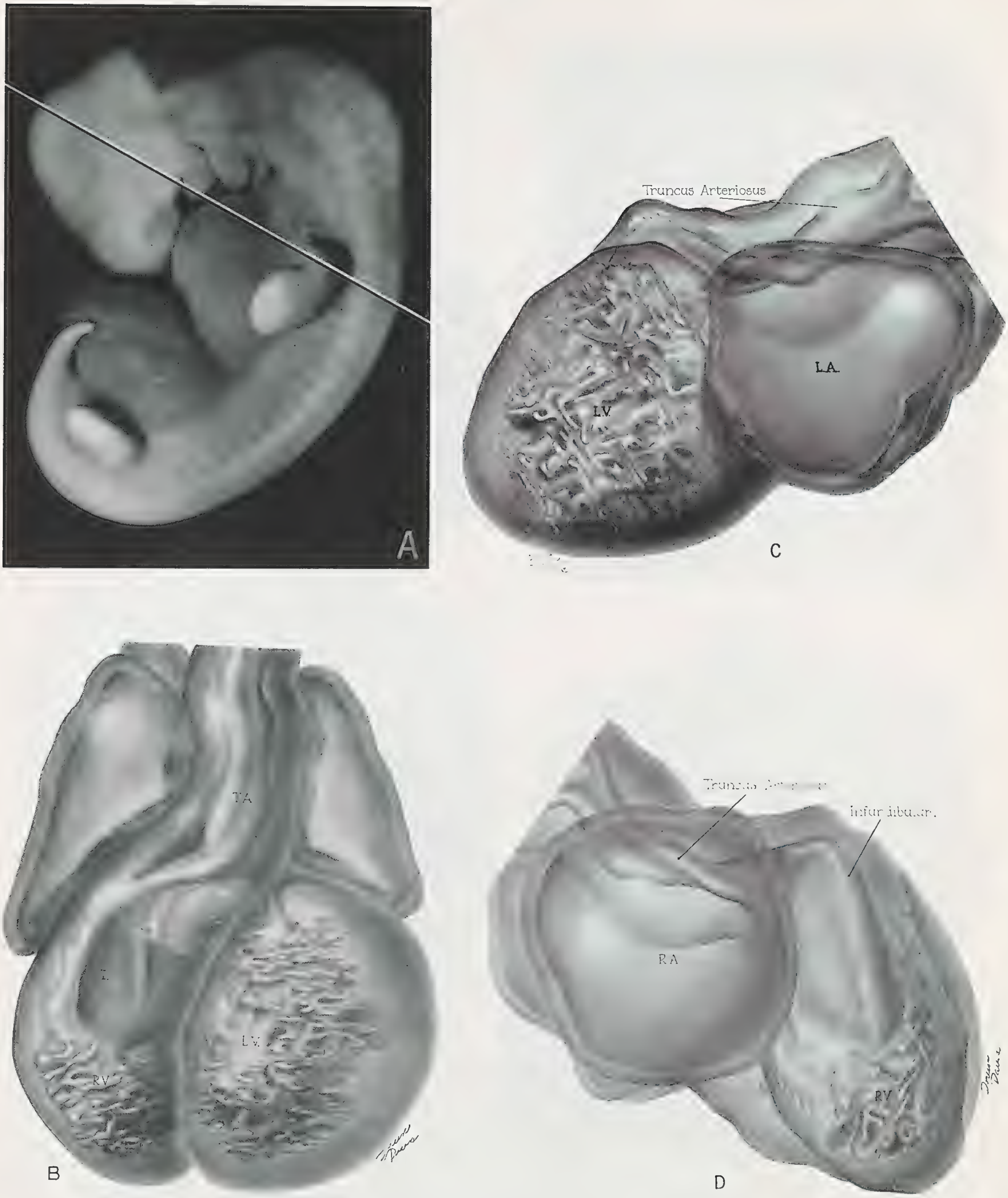

A, left profile view of embryo S, age group xv, with a line indicating the direction of the view of the heart as seen *B,* from in front. *C,* left, and *D,* right, profile views of the heart.

CONTRIBUTIONS TO EMBRYOLOGY, NO. 257

THE PRIMORDIAL GERM CELLS IN THE MALE HUMAN EMBRYO

Roberto Narbaitz
Department of Embryology, Carnegie Institution of Washington
Baltimore, Maryland

With five plates

CONTENTS

PAGE
Introduction 117
Material and Methods 117
Results 118
Discussion and Conclusions 118
Summary 118
Acknowledgment 118
Literature Cited 119

THE PRIMORDIAL GERM CELLS IN THE MALE HUMAN EMBRYO

INTRODUCTION

Perhaps no single question has had a greater impact on the evolution of theories of differentiation than that of the continuity of the germ line. That the origin and fate of germ cells have captured the imagination and interest of embryologists is attested by a steady flow of publications over the past sixty years. The background and development of the concept of the germ line need not be reviewed here, the reader being referred to the works of Everett (1945), Gillman (1948), Tyler (1955), and Witschi (1948).

In the human species, these problems have both theoretical and practical importance because on their solution rests our understanding of a number of anomalies in gonadal development, which are attracting increasing attention of the clinicians.

The study of human material presents several difficulties. Not only are experimental procedures excluded, but also the embryonic material obtained is not always as well preserved as required for adequate histological study; finally, the developmental study of human gonads must embrace not only a long embryonic period but also a much longer period of immaturity which does not end until puberty, when the gonads at last reach their final stage of development. As a consequence of these difficulties, the studies made on human material have been few and refer to limited periods of development.

The early works of Kohno (1925) and Simkins (1928) were based on only a few embryos; the latter, which presents arguments against the theory of the continuity of the germ cell line, contains serious errors, the principal one being the confusion of the fetal Leydig cells with the germ cells.

In an important study based on the examination of twenty-three serially sectioned human embryos of the Carnegie Collection, Witschi (1948) concluded that the germ cells migrate from the endoderm of the yolk sac to the gonadal ridges. Embryos ranging from 13-somite to 8-mm. stages were studied; in the youngest, all the germ cells are found in the endoderm of the yolk sac near the allantoic evagination; in later embryos, up to 20 somites, the germ cells are found largely in the hind gut, a variable number remaining temporarily in the endodermal epithelium. Finally, in embryos of more than 25 somites, germ cells are found progressively in positions which enabled Witschi to chart their course through the mesentery toward the mesonephric folds, and led him to conclude that they migrate actively by movements of individual cells.

McKay, Hertig, Adams, and Danziger (1953) confirmed Witschi's conclusions using histochemical techniques. Their findings on individual embryos are clear and convincing, although some might wish that the number of embryos studied were larger.

Mancini, Narbaitz, and Lavieri (1960) followed the germ cells in the testis of the late fetus and in children of all ages from birth to puberty and found that they are always present.

From these works one might conclude that the continuity of the germ line, demonstrated experimentally in many animals, holds also for the human. Yet one important discrepancy must be noted: Gillman (1948) failed to observe these cells in male human embryos of the second and third month. Gillman, whose studies also were based on a study of embryos in the Carnegie Collection, concluded that, whereas in female embryos the germ cells can be seen at all stages, in male embryos these cells lose their identity after the 15-mm. stage. They can again be distinguished, however, much later in embryonic life, in embryos of 132-mm. crown-rump length.

The need for re-examining the question of the continuity of the germ cell line in the male human embryo is apparent, for, if Gillman's findings are found to be correct, a re-evaluation of the basic concept would be required. This important question has been reopened using embryos ranging in length from 15 to 115 mm. C. R. from the Carnegie and University of Michigan Collections.

MATERIAL AND METHODS

The Carnegie Collection contains 174 embryos between 15 and 60 mm. (C. R. length) in grades I, II, and III. All female embryos were omitted in this study, as were those male embryos in which the sections were more than 25 microns thick, in which very little histological detail could be observed. Hence a total of 44 embryos of the Carnegie Collection was used.

The University of Michigan Collection includes 23 male embryos ranging from 15 to 115 mm. (C. R. length). All were sectioned at less than 20 microns and were included in the study.

Three embryos (9203, 9712, 9721) recently incorporated in the Carnegie Collection were dissected, the gonads being refixed in Bouin's solution and sectioned alternately at 10 and 30 microns. The sections studied were stained routinely with hematoxylin and eosin, Masson's stain, Mallory's triple stain, or carmin.

Among the embryos ranging from 15 to 20 mm. some had testicular cords and could be classified as males; the rest were considered sexually undifferentiated. All embryos over 20 mm. were considered sexually differentiated, and only the males were studied.

The criteria used to identify the germ cells were morphological, the main characteristics being the presence of a round, clear nucleus and a very large, well delimited cytoplasm (cf. Witschi, 1948).

RESULTS

Witschi (1948) stated that germ cells were recognized clearly only when sections were cut at 10 microns or less; since nearly all the embryos available for study were sectioned at greater thicknesses, it was necessary to study first the relation between the thickness of the section and the appearance of the germ cells. This aspect of the study can be summarized as follows:

Germ cells can be seen with difficulty in sections cut at 15 and 20 microns; they have not been seen in sections of more than 20 microns, although they are distinguished readily in embryos of the same ages, provided that the sections are cut at 10 microns or less. The explanation is simple: in thick sections, the overcrowding of the nuclei in the testicular cords does not permit the visualization of the clear cytoplasmic area that surrounds the nucleus of the germ cell.

That the germ cells can be identified with ease in excellent preparations is illustrated in figure 1 (pl. 1). Figures 2 (pl. 1) and 3 (pl. 2) show clearly the difference between thick and thin sections of the testis in embryos of approximately the same age.

Next, a systematic study of the gonads of embryos of both collections was conducted, attention being focused on the presence, number, and "distinguishability" of the germ cells. The gonads were classified as follows:

—	No germ cells are seen.
+	Some germ cells are present, but they are few, and can be distinguished with difficulty.
++	Many germ cells are present, although some are distorted or seen with difficulty.
+++	Many germ cells are present; they can be recognized readily.

The histological condition of each embryo was classified as poor, fair, or good in relation to the prevalence of artifacts and shrinkage, dependent on the state of preservation of the embryo.

The findings, which are presented in table 1, and illustrated in figures 4 to 10 (pls. 2 to 5), may be summarized as follows: (1) Twenty-nine embryos, comprising 11 of the second month and 18 of the third and fourth months of development, which were preserved adequately, were found to have a large number of germ cells. (2) Twenty-five embryos, comprising 19 of the second month and 6 of the third and fourth months, were preserved poorly or sectioned thickly; in them only a few germ cells could be identified wtih difficulty. (3) Sixteen embryos were preserved or sectioned so badly that germ cells could not be identified in them after careful examination.

DISCUSSION AND CONCLUSIONS

The fact that Gillman did not observe the germ cells in male human embryos older than 15 to 17 mm. must be explained not by changes in their size or appearance, as he supposed, but simply by the fact that the embryos older than 15 mm. available for study at that time were sectioned very thick (30 to 40 microns), primarily for anatomical studies. The best embryos of these ages now in the Carnegie Collection were incorporated after Gillman's study was completed. Although no measurements have been made, it may be said that no striking change in size or appearance of the germ cells occurs at these ages.

Additional work should be done; cell counts should be made, and the application of histochemical methods also is in order. Yet we may conclude, for the present, that the observations support clearly the theory of the continuity of the germ cell line in the male human embryo.

SUMMARY

Seventy human embryos of the Carnegie and University of Michigan Collections were studied to determine the presence or absence of germ cells in embryos of 15- to 115-mm. crown-rump length. Twenty of them were sexually undifferentiated, the rest being males.

The germ cells are seen clearly and in large numbers in embryos adequately preserved and sectioned. In embryos poorly preserved or sectioned thickly the germ cells are few or not seen at all.

These observations favor the view of the continuity of the germ cell line and provide a reasonable explanation for previous statements of other authors in disagreement with it.

Acknowledgment. During the course of this study in the Department of Embryology, the author was a Fellow of the Consejo Nacional de Investigaciones Científicas y Técnicas of Argentina.

TABLE 1

Embryo	Size, mm.	Preser- vation	Thickness of Sections, microns	Sex	Germ Cells *	Embryo	Size, mm.	Preser- vation	Thickness of Sections, microns	Sex	Germ Cells *
M 707	15	Good	10	Und.	++	C 240	20	Poor	20	Male	—
M 644	15	Fair	10	Und.	+	C 8157	20.8	Fair	20	Male	++
C 841	15	Fair	20	Und.	—	M 380	22	Fair	10	Male	+
C 8355	15	Poor	10	Und.	—	C 7254	22.5	Poor	20	Male	+
C 9247	15	Fair	8	Und.	++	M 419	23	Fair	20	Male	+
C 8097	15.5	Fair	10	Und.	+	C 4638	23.4	Poor	15–20	Male	+
C 4405	15.8	Poor	10	Und.	—	C 7864	24	Poor	20	Male	+
C 74	16	Fair	10	Und.	+	C 3167	24.5	Fair	20	Male	+
C 317	16	Poor	20	Und.	—	M 589	26.5	Fair	15	Male	—
C 8235	16	Fair	10	Und.	+++	C 5621-A	27	Poor	20	Male	—
C 43	16	Poor	?	Male	—	M 882	29	Fair		Male	+
C 256	16	Poor	?	Male	—	C 4525	30	Fair	20	Male	+
C 8092	16.3	Good	20	Und.	++	C 9226	31	Good	10	Male	+++
C 8172	16.5	Fair	10	Male	+	M 523	36	Good	15	Male	++
C 6150	17	Poor	15	Und.	+	C 4415	37	Poor	20	Male	+
C 9325	17	Poor	20	Male	—	M 829-C	37	Fair		Male	++
C 296	17	Fair		Und.	+	C 4021	38	Poor	15	Male	+
C 907	17	Fair	15		++	M 909-E	40	Fair	15	Male	+
C 576	17	Fair	15	Male	+	C 301	44	Good	20	Male	++
C 7900	17.4	Fair	20	Male?	++	C 4921	47	Poor	20	Male	—
M 650	18	Good	10	Und.	+	C 105	48	Fair	20	Male	++
C 4501	18	Fair	15	Male	+	C 9484	49	Good	20	Male	+++
C 7274	18	Fair	20	Und.	+	M 370-a	53	Good	15	Male	++
C 8226	18	Good	10	Male	+++	C 3990	54	Fair	20	Male	++
C 17	18	Poor		Und.	—	C 4229	58	Good	20	Male	++
C 1390	18	Poor	20		—	M 541-E	65	Good	15	Male	+++
C 409	18	Poor	20	Und.	—	M 269-A	67	Good	10	Male	++
C 432	18.5	Good	20	Und.	+	M 25-B	85	Fair	15	Male	++
C 6824	18.5	Poor	12	Male	—	M 300-J	89	Fair	15	Male	++
C 9113	18.5	Poor		Und.	—	M 536-L	94	Good	15	Male	++
M 358	19	Fair	15	Male	+	M 20-E	95	Good	15	Male	+++
M 521	19	Fair	15	Und.	+	M 922-T	100	Fair	15	Male	++
C 431	19	Fair	20	Male	+	M 181-A	105	Fair	15	Male	++
C 8965	19.1	Good	20	Male	+++	M 145-L	105	Good	15	Male	+++
C 7906	19.5	Good	20	Male	+++	M 364-A	115	Fair	15	Male	++

* Explanation in text.

LITERATURE CITED

Everett, N. B. 1945. The present status of the germ cell problem in vertebrates. *Biol. Rev., 20,* 45–56.

Gillman, J. 1948. The development of the gonads in man with a consideration of the role of fetal endocrines and the histogenesis of ovarian tumours. *Carnegie Inst. Wash. Publ.* 575, *Contribs. Embryol., 32,* 81–131.

Kohno, S. 1925. Zur Kenntnis der Keimbahn des Menschen. *Arch. Gynäkol., 126,* 310–326.

McKay, D. G., A. T. Hertig, E. C. Adams, and S. Danziger. 1953. Histochemical observations on the germ cells of human embryos. *Anat. Record, 117,* 201–219.

Mancini, R. E., R. Narbaitz, and J. C. Lavieri. 1960. Origin and development of the germinal epithelium and Sertoli cells in the human testis. *Anat. Record, 136,* 477–490.

Simkins, C. S. 1928. Origin of the sex cells in man. *Am. J. Anat., 41,* 249–272.

Tyler, A. 1955. Gametogenesis, fertilization and parthenogenesis. In *Analysis of Development,* B. H. Willier, P. Weiss, and V. Hamburger, editors, pp. 170–212. W. B. Saunders Co., Philadelphia.

Witschi, E. 1948. Migration of the germ cells of human embryos from the yolk sac to the primitive gonadal folds. *Carnegie Inst. Wash. Publ.* 575, *Contribs. Embryol., 32,* 69–80.

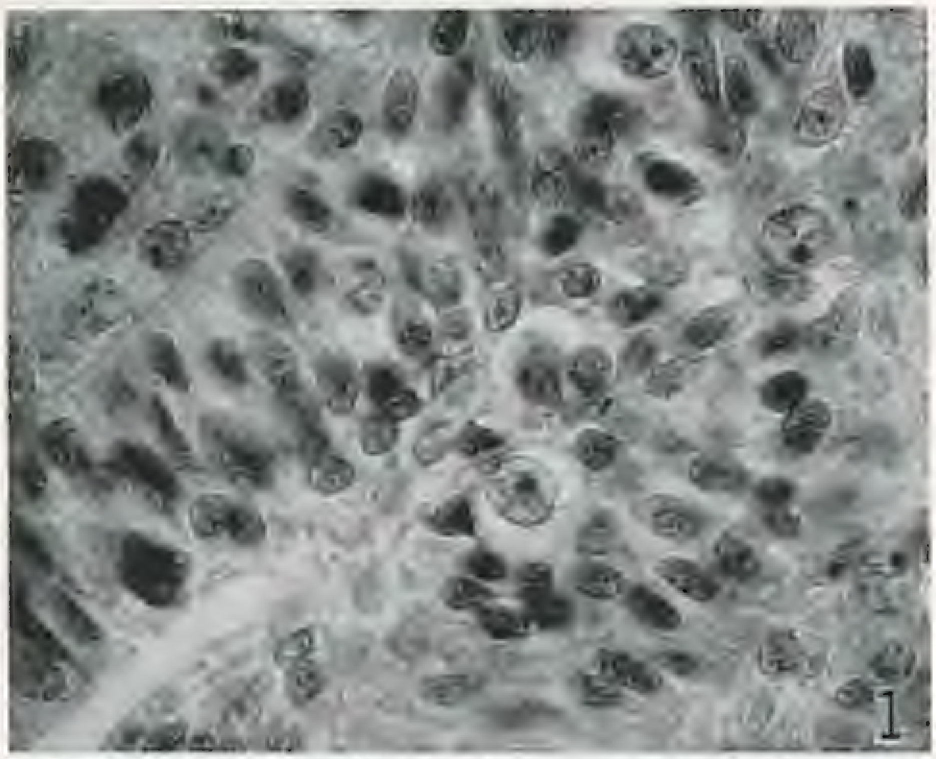

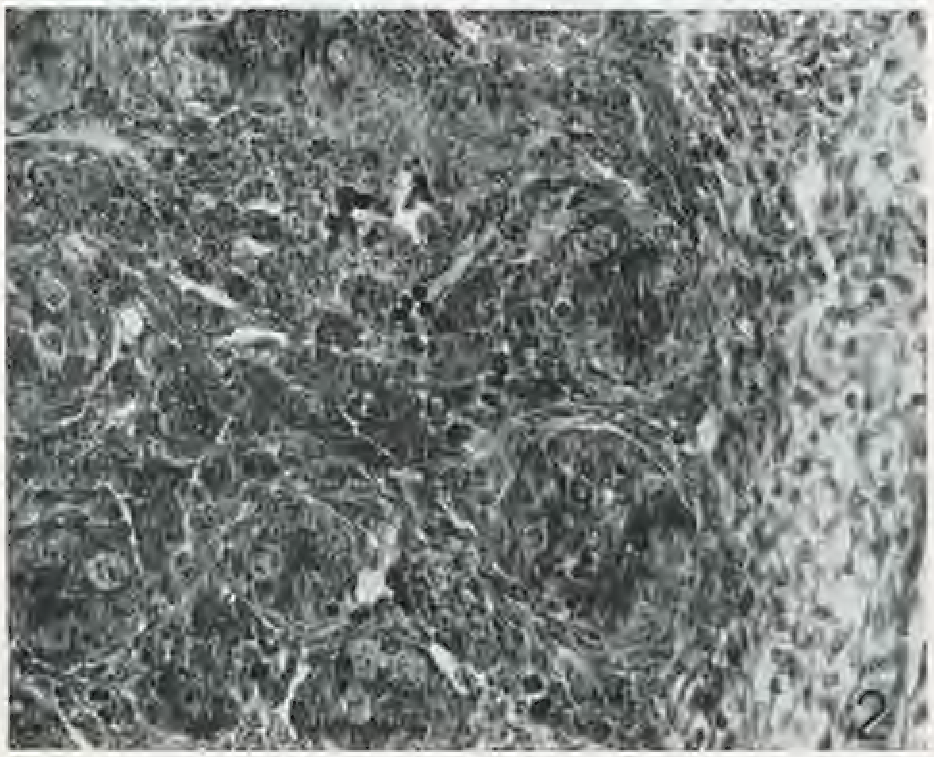

Fig. 1. Embryo Carnegie 9226. (31 mm.) Germ cells are recognized clearly by their rounded nuclei and their clear and well delimited cytoplasm, characteristics described by previous authors. × 1000.

Fig. 2. Embryo Michigan 269-A. (67 mm.) Gonad sectioned at 10 microns. Germ cells are seen clearly. × 400.

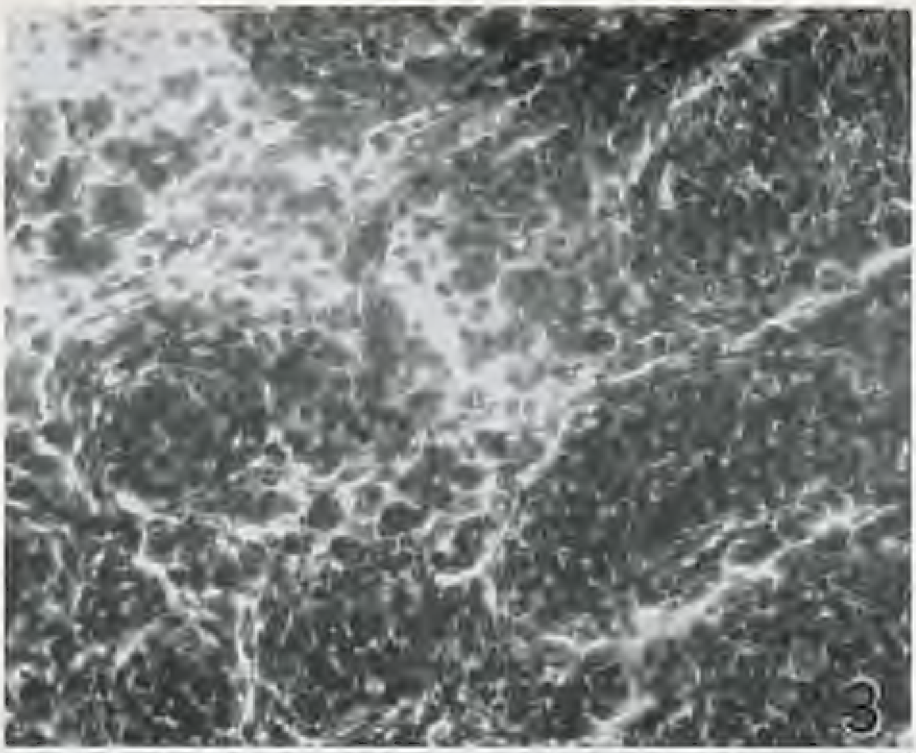
3

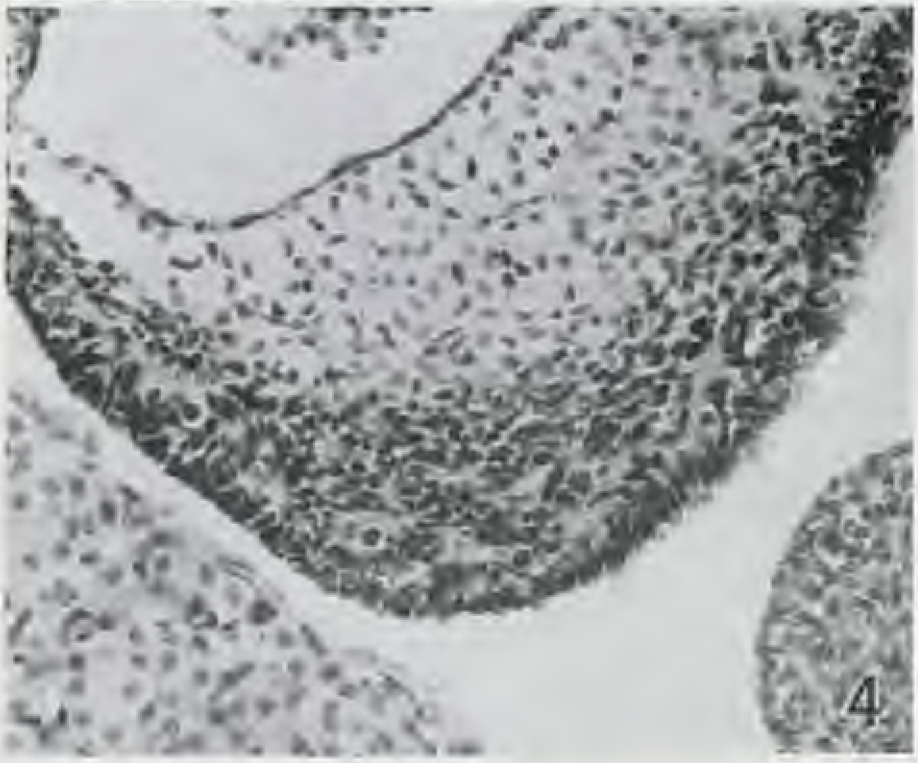
4

Fig. 3. Embryo Michigan 541-E. The embryo is of approximately the same age as in figure 2 (65 mm.), but the sections are cut at 15 microns. The germ cells are seen with difficulty. × 400.

Fig. 4. Embryo Michigan 56. (10 mm.) Germ cells have arrived at the urogenital ridge. × 400.

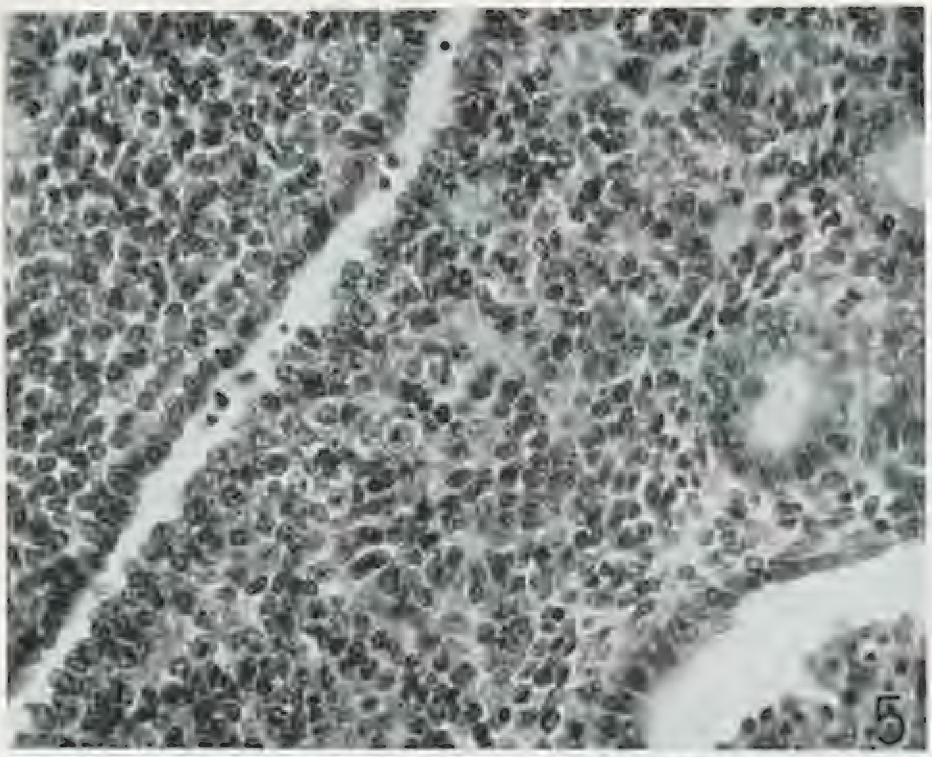

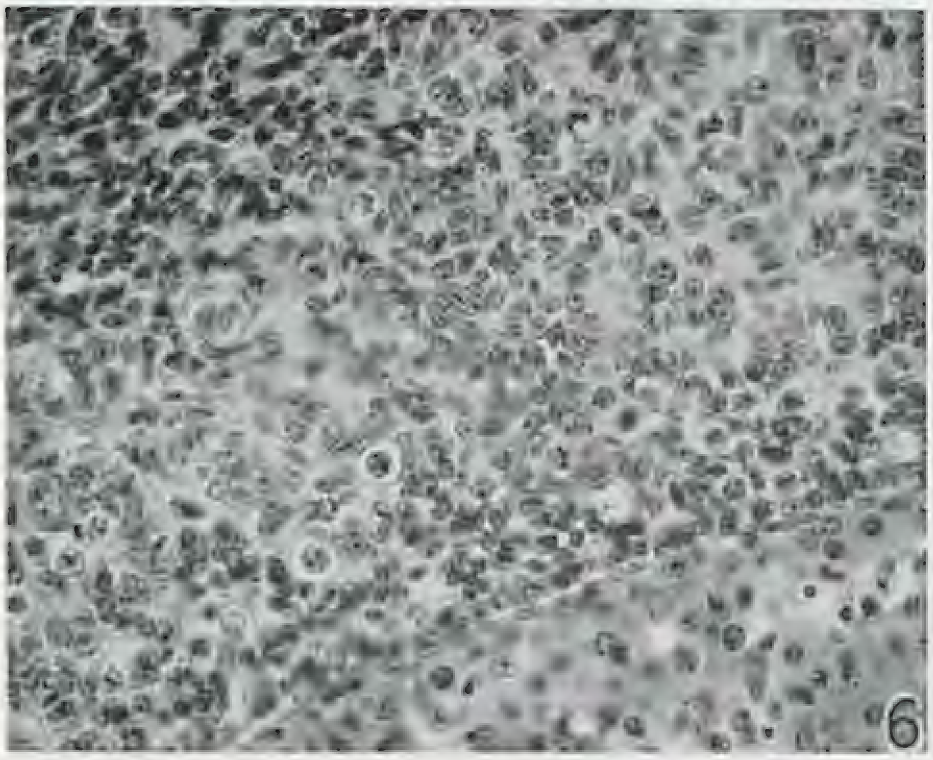

Fig. 5. Embryo Carnegie 8235. (16 mm.) Undifferentiated gonad. × 400.
Fig. 6. Embryo Carnegie 8226. (18 mm.) Male. × 400.

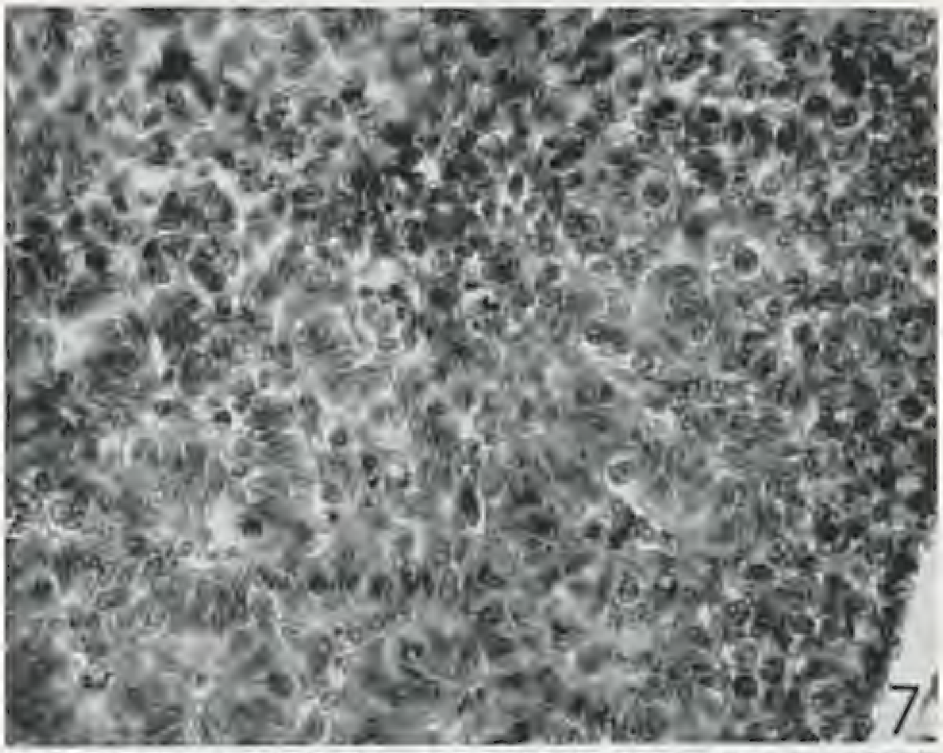
7

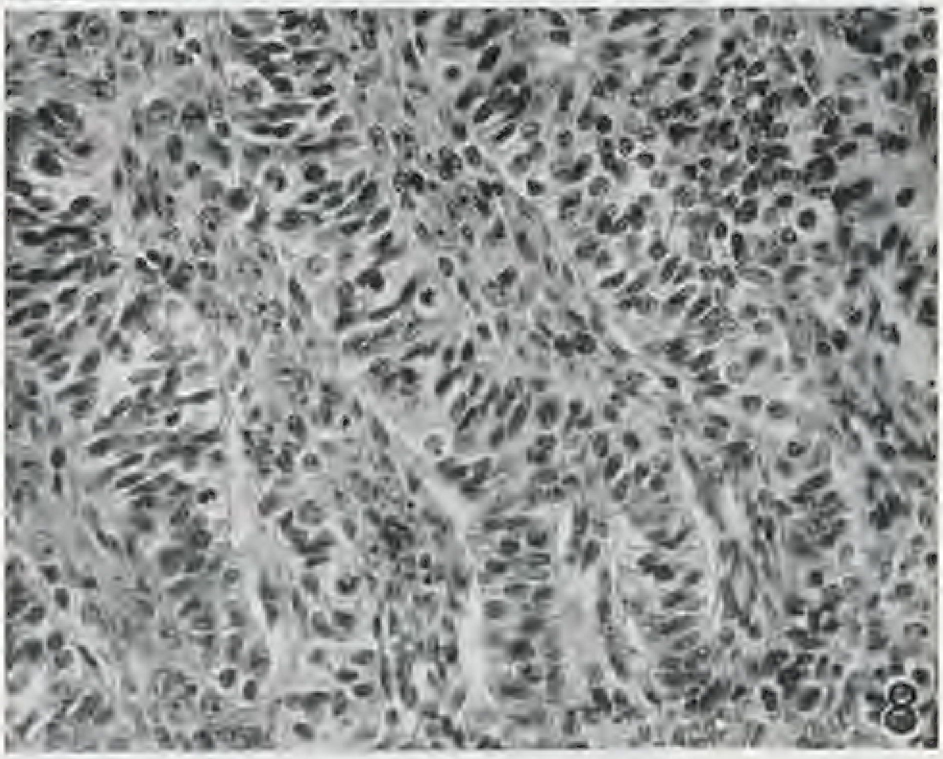
8

Fig. 7. Embryo Carnegie 7906. (19.5 mm.) Male. × 400.
Fig. 8. Embryo Carnegie 9226. (31 mm.) Male. × 400.

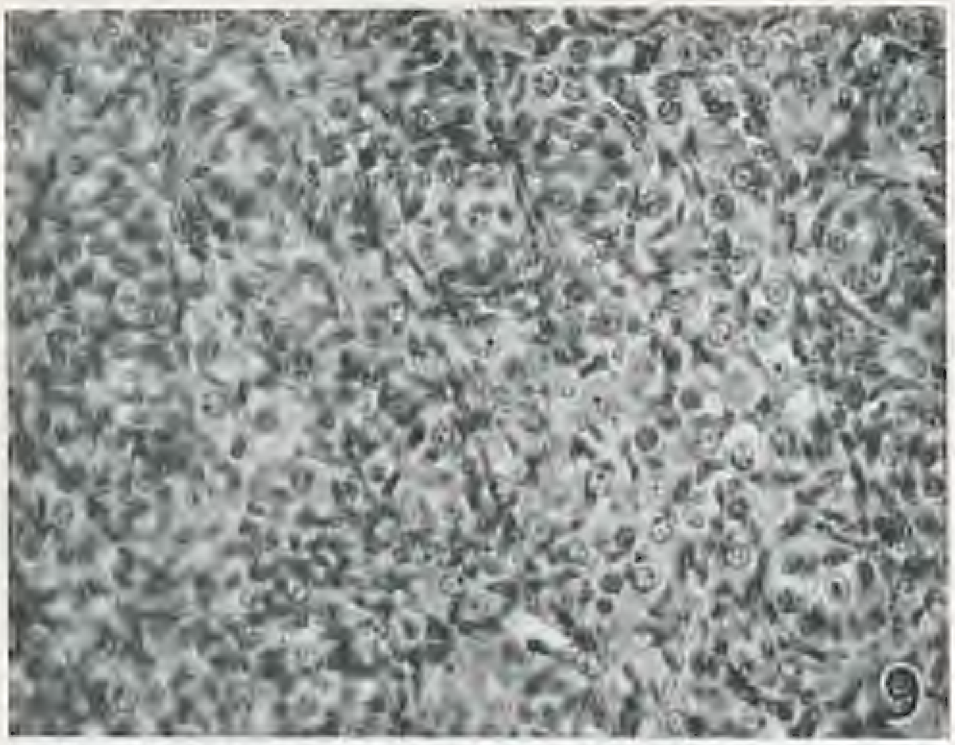

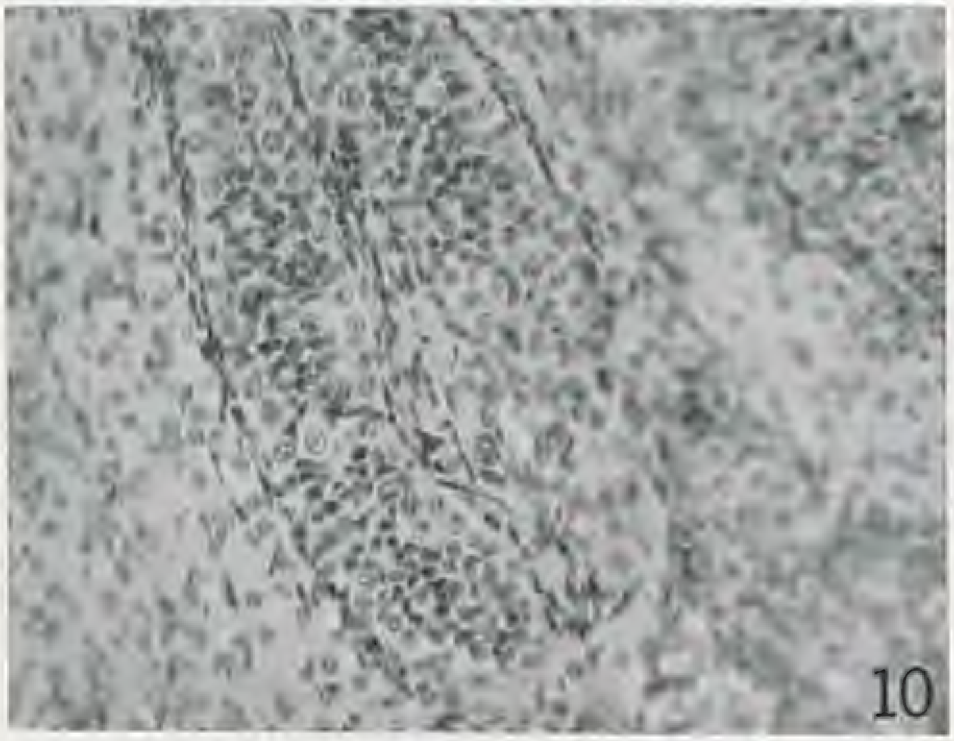

Fig. 9. Embryo Carnegie 9484. (49 mm.) Male. × 400.
Fig. 10. Embryo Michigan 145-L. (105 mm.) Male. × 400.

CONTRIBUTIONS TO EMBRYOLOGY, NO. 258

THE DEVELOPMENT OF THE STERNOMASTOID AND TRAPEZIUS MUSCLES

J. McKenzie

Department of Embryology, Carnegie Institution of Washington, and
Department of Anatomy, University of Aberdeen, Scotland

With thirteen plates and two text figures

CONTENTS

PAGE

INTRODUCTION 123

MATERIALS AND METHODS 124

OBSERVATIONS 124
- Embryo 2841, xiv, 4.85 mm., plate 1 124
- Embryo 7829, xiv, 7 mm., plate 2 125
- Embryo 3216, xv, 6.5 mm., plate 3 125
- Embryo 8929, xv, 6.35 mm., plates 4*A* and *B* 125
- Embryo 7333, xiv, 6.3 mm., plate 5 126
- Embryo 3385, xv, 8.3 mm., plate 6 126
- Embryo 6517, xvi, 10.56 mm., plate 7 126
- Embryo 1836, xvi, 11 mm., plate 8 126
- Embryo 6258, xvii, 14 mm., plate 9 126
- Embryo 8969, xvii, 11.2 mm., plate 10 126
- Embryo 6520, xvii, 12.9 mm., plate 11 127
- Embryo 6524, xviii, 11.76 mm., plate 12 127
- Embryo 4430, xviii, 13.95 mm., plate 13 127

DISCUSSION 127

LITERATURE CITED 128

ABBREVIATIONS IN PLATES 129

THE DEVELOPMENT OF THE STERNOMASTOID AND TRAPEZIUS MUSCLES

INTRODUCTION

In spite of innumerable and persistent attempts to explain the dual innervation of the sternomastoid and trapezius muscles, few, if any, anatomists would hazard an unequivocal answer today. There was an awareness of the problem even in the last century, and various approaches were evolved in attempts at solution.

Cuvier's illustrations (1849) showed that it would be difficult to arrive at a simple conclusion in view of the comparative anatomy of these muscles, especially the sternomastoid; in no sense could the composition of the sternomastoid or the trapezius be regarded as consistent even in the mammals. Confusion in terminology still exists in the definition of the heads of the sternomastoid, some authorities including an obvious omocervicalis without comment; the absence of the clavicle in other species might be a misleading factor, or the fusion of the two muscles to form the cucullaris, or the occasional subdivision of the trapezius into component parts.

On the other hand, closer attention to the detail depicted by Cuvier might have prevented the confusion emanating from the accumulated results of experimental procedures: the simple observation of whether the sternomastoid had an integral portion deep to the accessory nerve might have rationalized these results. Chauveau (1891) claimed that, in the horse, while the sternomastoid was supplied by the eleventh cranial and a branch from the second cervical nerves, pain fibers from the muscle were present only in the cervical contribution, and the cranial portion was the only source of motor fibers. Lesbre and Maignon (1908) found the same state of affairs in the horse and cow but were not happy with the outcome of their experiments in the dog. Windle and DeLozier (1932), working with the cat, obtained results in agreement with those of Chauveau. In the case of the monkey there has been as much doubt and confusion; Sternberg (1898), for instance, claimed that the sternomastoid did not receive motor fibers through the cervical nerves but that the trapezius did; Russell (1897) and Sherrington (1898) found evidence of cervical efferents to both muscles. Straus and Howell (1936) had a major degree of success in stimulating the cervical nerves supplying the musculature in dogs and showed that "the sternomastoid receives a more cranial cervical motor innervation than does the trapezius. . . . The cervical motor nerves to the trapezius, on the other hand, may reach the muscle via any of the three nerves mentioned (C2, 3 and 4)." With one chimpanzee, these workers found, on stimulating the spinal nerves to the accessory musculature, "weak though definite action of the trapezius." No mention was made of the sternomastoid, and their conclusion was "that in this animal spinal nerves carry motor fibres to the XI field."

If there be uncertainty in the field of mammalian accessory musculature, then it is several times greater for fishes, amphibians, and reptiles. There, the initial problem may be to decide what is homologous with the mammalian form, and in fish the difficulty arises in differentiating the "accessory" muscles from those of the gill arches. Straus and Howell (1936) are satisfied that there is a trapezius or a representative, but there is no unanimity regarding its nerve supply. Opinion is divided with a bias toward those who claim no more than a cranial (vagal) innervation for the trapezius. In the amphibian, the "accessory" musculature of *Siren,* according to Norris (1913), is also innervated by the first and second spinal nerves, but so little work has been done that no generalizations can be made on this point. The data for reptiles are more plentiful; a sternomastoid and a trapezius can be identified, but their innervation is still a bone of contention. Howell's (Straus and Howell) experiments on the iguana revealed in some specimens no motor fibers in the spinal contribution to the sternomastoid-trapezius, suggesting that this portion is merely sensory, whereas in another very large specimen there were unequivocal signs of a motor supply from the third and fourth cervical nerves. These writers held the view that the phylogenetic development of efferent spinal nerve fibers to the accessory musculature involved neurobiotaxis whereby first the sensory and later the motor fibers chose the more direct route to reach the sternomastoid and the trapezius. Probably it has been the insistence on this or a similar principle that led to the according of so much study to the central connections and components of the accessory nerve.

Great argument has raged, for example, on the origin of the bulbar part of the accessory nerve, e.g. Kappers (1912, 1920), Addens (1933), and the same authors have been divided on the origin of the cells of the spinal part of the nerve; even their position seems to be in doubt, Bruce (1901). Generally, however, it has come to be accepted that they are visceral in origin.

Numerous writers have produced evidence more pertinent to the problem under consideration here, especially in the light of the hypothesis that there is a phylogenetic and ontogenetic migration first of the sensory fibers within the accessory circuit and later of the motor element to the shorter spinal nerve course. Windle (1931*a* and *b*) and Ranson, Davenport, and Doles (1932) claim that afferents from the sternomastoid and trapezius reach the tractus solitarius both from the spinal accessory and from the spinal nerves. Streeter (1905) and Fahmy (1927) suggest a translation of sensory ganglia from the accessory nerve to the cervical nerves during development.

Lewis (1910) claimed that "the accessory motor-nerve supply from the cervical region to the trapezius and sternocleidomastoid is secondary and does not indicate a myotomic origin for any part of the muscles." Perhaps it was this categorical statement and his earlier work (Lewis, 1901) which inspired so much collateral investigation and discouraged further detailed study of the human embryo in serial section, but, with the more extensive range of material at our disposal today compared with fifty years ago, we should not hesitate to verify these claims. Furthermore, we should not be hidebound in our allegiance to the reconstruction techniques for information on the development of mesodermal derivatives; there is, with all such methods, the necessity or at least the tendency to define a border to a premuscle mass in circumstances where it might be more accurate to declare a tenuous link or even continuity with adjacent masses that are equally ill defined. In this investigation, therefore, instead of reproducing artificial models of embryonic stages in muscle development, extensive photographic illustration has been preferred.

MATERIALS AND METHODS

All the specimens examined during this investigation are in the Collection of Human Embryos, Department of Embryology, Carnegie Institution of Washington, Baltimore. Each embryo is denoted by its serial number, and the group or horizon to which it was allocated by Streeter (1945, 1948) is stated. Although only 13 specimens have been described here with their relevant photomicrographs, a total of 32 embryos from groups xiv to xviii, all in transverse serial section, have been investigated. Each embryo was examined serially, and the representative photographs were taken at intervals from above (cranial to) the level of the sternomastoid-trapezius premuscle mass to the point where it could be presumed to have ended (in the younger embryos) or to its attachment to the shoulder girdle and vertebral column (in older specimens).

Recognition of a well established sternomastoid-trapezius mass was relatively easy (*a*) from its position lateral to the anterior cardinal vein and (*b*) from the presence of the accessory nerve piercing the mass. Of these the former was the more useful in the younger embryos because of the uncertainty of identifying the nerve. Reference should be made initially to figure 1, where the plane of the sections and the positions of the relevant structures are indicated diagrammatically, and to figure 2, a composite diagram of a horizontal section through the region of the muscles in question.

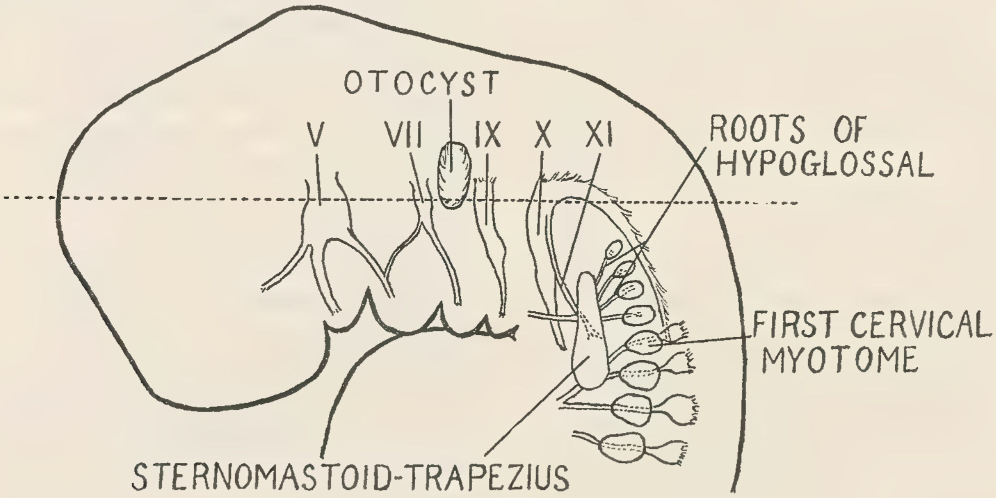

Fig. 1.

OBSERVATIONS

Embryo 2841, xiv, 4.85 mm., plate 1. Figure 1, plate 1, lies above the level of the sternomastoid-trapezius: it shows the vagal ganglion ventral to the anterior cardinal vein and a tongue of condensed mesoderm reaching ventrally from the myotome region to touch the dorsal surface of the vein. In figure 2 this tongue of mesoderm is shown in direct continuity with the sternomastoid-trapezius mass on the lateral aspect of the vein. Throughout its whole length (figs. 3 to 6) the accessory musculature (the nerve itself cannot be identified) maintains close contact with the myotome mass on its dorsal aspect without even a hint of separation from it.

Embryo 7829, xiv, 7 mm., plate 2. Lateral to the vein (fig. 1, pl. 2), there is a faint condensation of mesoderm —the cranial tip of the sternomastoid-trapezius mass; ventral to the vein is the ganglion of the vagus, and dorsally lie the roots of the hypoglossal nerve on the medial aspect of a condensation reaching forward from the myotome mass. In figure 2, the sternomastoid-trapezius mass is now well defined and the roots of the hypoglossal nerve are positioned immediately dorsal to the vein; medial to the myotome condensation is an oblique section of a cervical nerve. It would be difficult to define accurately or honestly a plane of cleavage between the sternomastoid-trapezius mass and the myotome material, although variations in density do indicate the two masses. Were it not for the presence of a small vein entering the anterior cardinal vein in figure 3 the difficulty of separating sternomastoid-trapezius from myotome material would be even greater, and this is the case above and below such vessels. The extension of myotome premuscle tissue along the lateral side of a cervical nerve is a prominent and constant feature in all specimens.

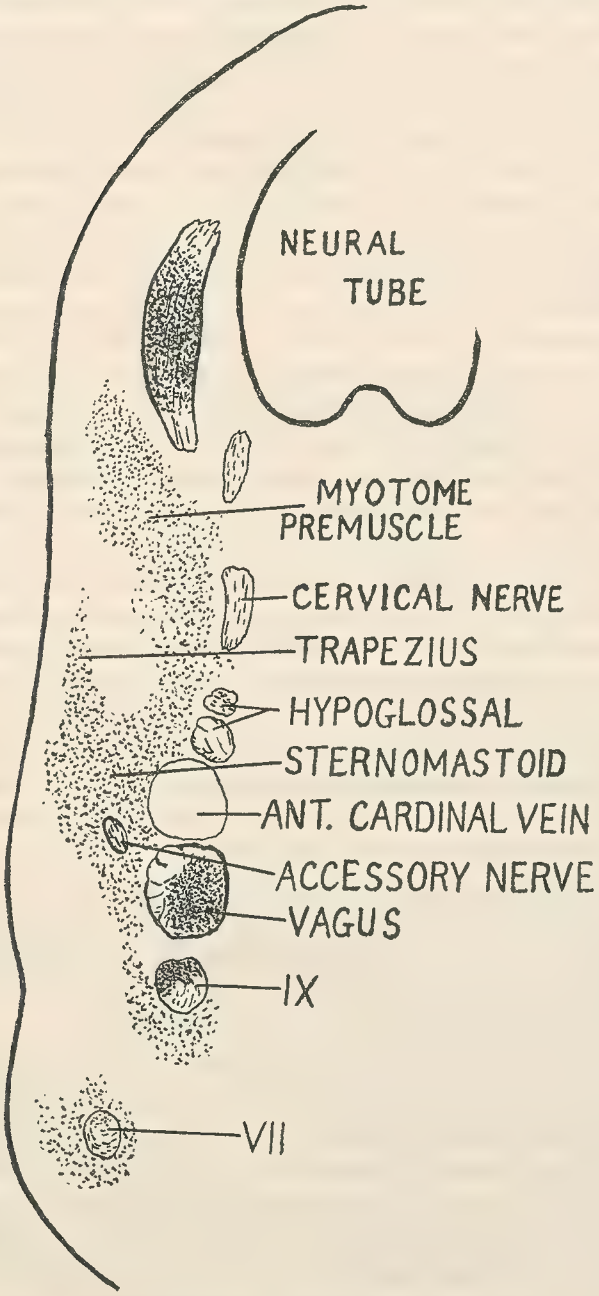

Fig. 2.

Figures 4, 5, 6, and 7 show, at successive levels, the increase and then the decrease in the size of the sternomastoid-trapezius mass and finally its virtual disappearance, the movement of the hypoglossal nerve around the outside of the vein, and the position of the cervical nerves and their accompanying prolongations of compact mesoderm.

Embryo 3216, xv, 6.5 mm., plate 3. Although this embryo does not illustrate so clearly the development of the muscle masses in which we are interested, it does emphasize the variability occurring from specimen to specimen; longer than embryo 8929, and allocated to group xv on account of its more salient features, it nevertheless possesses premuscle masses at an earlier stage of differentiation. Figure 1, plate 3, shows the first evidence of the sternomastoid, and even here it is joined to myotome material; figure 2 corroborates this. Figures 3, 4, 5, and 6 (a matter of 100 microns in depth) bridge the whole length of the sternomastoid-trapezius mass; the features worthy of note are the persistence of the union between sternomastoid-trapezius and the mesodermal condensation alongside the cervical nerves, the failure to define the accessory nerve, and the absence of subdivision into a sternomastoid and a trapezius.

Embryo 8929, xv, 6.35 mm., plates 4A and B. Figures 1 and 2, plates 4*A* and 4*B*, depict sections above the level of the sternomastoid-trapezius mass but illustrate the position of the hypoglossal rootlets, the first indication of the cervical nerves, and the mesodermal condensation lateral to these two groups. The upper end of the sternomastoid-trapezius appears in figure 3 without demarcation from the myotomic mesodermal condensation. Figures 4, 5, 6, and 7 demonstrate that this state of affairs persists throughout a thickness of 200 microns. Traced as far as the stage of separation of the accessory nerve from the vagus (fig. 7), there is no sign of a break in this link, and only after the nerve has plunged into the sternomastoid and reached the deep surface of the trapezius rudiment (fig. 9) can one safely draw the line of separation between sternomastoid and the musculature lateral to and accompanying the cervical nerves. In figures 8 and 9, a new feature appears; with the severance of the sternomastoid-myotome link there seems to be a fusion or intimate association on a more dorsal plane between the trapezius and the cervical musculature, the dorsal tip of the trapezius losing its identity on the lateral surface of a projecting myotome premuscle mass (figs. 9 to 12).

Embryo 7333, xiv, 6.3 mm., plate 5. Although it belongs to an earlier group than the previous specimens, this embryo is described here because the unusual feature it demonstrates is nevertheless consonant with the picture taking shape at this stage in the series. Figure 1, plate 5, is a section above the level of the sternomastoid-trapezius but shows mesodermal condensation of myotomic origin dorsal to the anterior cardinal vein; in figure 2, a small portion appears to separate itself from this general mass, and, when traced through successive sections, its course takes it lateral to the vein (figs. 3 and 4), where it merges with the deep surface of the sternomastoid and entirely loses its identity (figs. 5 and 6). Meanwhile the outer part of the sternomastoid-trapezius forms a tenuous link on a more superficial plane with the mesoderm from the myotomes (figs. 5 and 6). Although the accessory musculature persists for at least another 200 microns it reverts to a localized condensation clinging to the side of the anterior cardinal vein (figs. 7 to 9).

Embryo 3385, xv, 8.3 mm., plate 6. In figure 1, plate 6, the vagus-accessory nerve complex appears in the middle of the anterior cardinal vein. If the accessory premuscle mass is present lateral to the vein at this level it cannot be distinguished within or from the mesodermal condensation pushing around from the dorsal aspect of the vein. When the accessory nerve eventually identifies the sternomastoid-trapezius mass in figure 2, there is quite a distinct "forking" posteriorly in that premuscle condensation; the medial limb curls around the back of the vein to meet the myotome mass associated with the hypoglossal rootlets and later with the cervical nerve roots; this link persists in greater or lesser degree throughout figures 3 to 7 (depth of 400 microns); the lateral limb of the fork tries hard to reach the main mass of myotomic mesoderm by its progressive increase in size throughout the same series of sections. The accessory nerve on the deep surface of this latter extension (figs. 6 and 7) indicates that it is the future trapezius muscle.

Embryo 6517, xvi, 10.56 mm., plate 7. The tip of the sternomastoid-trapezius mass appears first in figure 1, plate 7, as a broad condensation spreading laterally from the edge of the vein just before the accessory nerve leaves the vagus. There is no more than a suggestion of any link with the myotome condensation dorsally. By the time the nerve has entered the muscle (figs. 2 and 3) there is a definite bridge alongside the cervical and hypoglossal rootlets between the two muscle masses, and it is at its best in figure 5 when the hypoglossal nerve begins to push its way forward between the vein and muscle. In figures 6 and 7 it is possible to define a posterior border to the sternomastoid muscle and to recognize the dorsal prolongation of the trapezius by virtue of the presence of the accessory nerve. However, first in figure 5 and later in figures 6 and 7, there spreads out from the tongue of mesoderm accompanying the cervical nerves a broad fan of mesoderm which meets and fuses with the deep surface of the trapezius; and curving around the ventral border of this extension is a cervical nerve heading for the interval between the sternomastoid and trapezius muscles (fig. 8).

Embryo 1836, xvi, 11 mm., plate 8. It is not of major importance to decide at this stage whether the condensation present on the lateral side of the vein and continuous around on to its lateral border (figs. 1 and 2, pl. 8) is the tip of the sternomastoid or not; the muscle or more correctly its anlage has appeared 60 microns later (fig. 3). What is of greater significance is the gradual dissolution of this dorsal bridge during the first three figures and thereafter, when the accessory nerve enters the mass, the increased definition of that tongue of mesoderm linking the muscle with the myotomes over a depth of 150 microns (figs. 4, 5, and 6). The trapezius is not easily defined, partly because of the disruption of the sections, but its position can be recognized as well as its association with the lateral projection from the myotomes alongside the cervical nerves.

Embryo 6258, xvii, 14 mm., plate 9. This specimen is not so far advanced in development as its size suggests in comparison with embryos 1836 and 6517. In figure 1, plate 9, there is no sign of the sternomastoid-trapezius, although the mesodermal condensation continuous with myotome material is pressing against the dorsal border of the vein. One hundred microns farther down (fig. 2) the sternomastoid can just be discerned, and it is obvious in figure 3. The link between myotomes and accessory musculature is poor throughout (figs. 4, 5, and 6), partly because of the presence of small veins cutting across it to reach the anterior cardinal vein. Nevertheless, even when the nerve is traversing the muscle (fig. 6) there is a dorsal projection from the deeper part of the mass, but by this stage the most obvious and interesting feature is the development of a well defined condensation of myotome material which, in figures 6 and 7, cannot be demarcated with assurance from the trapezius. Only with increased concentration of tissue in its deeper part (fig. 8) is there the likelihood that two separate muscle masses may in the end arise in this region.

Embryo 8969, xvii, 11.2 mm., plate 10. In this specimen the projections from the mesodermal condensations dorsal to the anterior cardinal vein, and the bridges between them and the sternomastoid-trapezius premuscle masses, display a more definite pattern. In figures 1 and 2, plate 10, it is very doubtful that any part of the sternomastoid is present, and at this juncture the question arises whether the mesodermal condensation along the dorsal edge of the anterior cardinal vein, at this level in the embryo, presages the bone of the skull. Figure 3 (135 microns distant) has the first real suggestion of any accessory musculature, though still poorly defined. There can be no doubt of its presence in figure 4, nor of its link with the myotome material. One hundred and twenty microns caudal to this section, just before the entrance of the accessory nerve (fig. 5), the sternomastoid is beginning to acquire a separate identity, and, with the nerve in the middle of it (fig. 6), its posterior border is distinct and remains so. Figures 7 and 8 demonstrate the intimate association between myotome musculature and the deep surface of the trapezius.

Embryo 6520, xvii, 12.9 mm., plate 11. Figures 1 and 2, plate 11, demonstrate the mesodermal condensation around the lateral and dorsal aspects of the anterior cardinal vein, and, with the establishment of the sternomastoid mass in figure 3, there is only a faint link between it and the myotome musculature. As the definition of the sternomastoid-trapezius improves (figs. 4 and 5) so is there greater separation until these muscles are bounded dorsally by a wide space of loose mesenchyme (fig. 6). In figures 7, 8, and 9 the most prominent feature is the wide lateral sweep of the myotome musculature into the path of the developing trapezius.

Embryo 6524, xviii, 11.76 mm., plate 12. In some respects an older embryo and in others a different presentation of the development of its musculature, this specimen is particularly valuable in the present study.

The wide band of condensed mesoderm along the side of the anterior cardinal vein (fig. 1, pl. 12) reveals itself to be part of the skull, an entirely different entity from the developing sternomastoid and trapezius, which can be seen at a lower level (figs. 2 and 3) pushing laterally and backward into the superficial tissues of this region. The bridge between sternomastoid and myotomic musculature, seen so well in the younger specimens before the entry of the accessory nerve, has resolved itself into a gradually increasing condensation situated behind the sternomastoid; in figures 4 to 8 it is apparently undecided whether to throw in its lot with the sternomastoid or the trapezius, but eventually it shakes itself free of the former and joins forces with the other; in figures 8 and 9 the myotomic premuscle appears to stand in the path of the trapezius as that muscle pushes dorsally, but in figures 10 and 11 it has become overlain by it and the accompanying accessory nerve.

Embryo 4430, xviii, 13.95 mm., plate 13. Recorded as being the oldest in its group, this specimen provides definition of the trend shown by the rest of the series. In figure 1, plate 13, the sternomastoid is still poorly delineated, and even in figure 2, when it begins to divide into two parts, it retains an affinity with the large muscle mass lying behind it. By the stage shown in figure 3 the whole sternomastoid has a distinct posterior border, as also has the deep surface of the trapezius. Figures 4, 5, and 6 illustrate the difficulties confronting the dorsal edge of the trapezius; stopped by a condensation of myotomic material, the future rhomboideus, it slowly overlaps this muscle as it is traced downward (figs. 5 and 6).

In the adult rhesus monkey the accessory nerve lies entirely deep to the sternomastoid, and, as in most other mammals, there is a muscle, normally absent in man, stretching from the upper cervical transverse processes to the acromion, called the omocervicalis. A study of the macaque material in the Carnegie Institution Department of Embryology revealed only one specimen comparable in age and plane of section with the present series of human embryos, corresponding in fact to the stage of an age group xviii embryo. Mesodermal condensation representing the omocervicalis, verified by tracing the muscle mass to its insertion, lay dorsal to the sternomastoid, showing no tendency to join with it at any level. In conformity with the adult condition, the accessory nerve, in this monkey embryo, passed deep to the sternomastoid muscle.

DISCUSSION

The dangers of accepting a categorical statement derived initially from material considered by present-day standards to be inadequate have been thrown into relief during this investigation. It is no reflection on the integrity or ability of any observer for later investigators to seek confirmation of detail in a collection of human embryos such as those early embryologists visualized and strove to create. Perhaps it was the desire to define each muscle mass in every reconstruction plate that perpetuated the view in regard to the sternomastoid and trapezius, but even casual observation of serial sections raises doubt whether these muscles have no myotomic contributions to their final form.

The first suggestion, derived from the study of human material, that myotomes might be involved in the development of the sternomastoid-trapezius musculature was based on the examination of only one human embryo (McKenzie, 1955); this hypothesis has been verified and elaborated. The continuity of dorsally placed myotome premuscle material with the accessory premuscle condensation is present dorsolateral to the anterior cardinal vein in the earliest embryos described here. Only as it is traced throughout the series does this connection resolve itself into two distinct parts, an upper one representing the base of the skull around the anterior cardinal vein and separated by a variable interval from the lower one, which, associated rather with the sternomastoid portion of the premuscle mass, is most pronounced at the level of origin of the upper cervical nerves just before the entry of the accessory nerve.

The inference to be drawn from these observations and the comparable findings in the monkey and rabbit (McKenzie, 1955) is that, at least, there is an element of myotome material in the sternomastoid, and that, at most, the deep part of the sternomastoid corresponds to an omocervicalis.

The situation in regard to the trapezius is very similar; there is, although of later development, a bridge of mesodermal condensation between the same myotome premuscle mass and its deep surface, but, in the last two specimens of the series described, the impression is of the trapezius progressively separating or delaminating itself from the underlying musculature as it pushes backward to reach its adult attachment. In other words, we do not find a trapezial muscle developing from the original accessory premuscle mass and extending dorsally as a discrete lamella superficial to and distinct from the remaining muscles of the neck; accordingly, it would not be presumptuous to argue that the trapezius, too, contains myotome elements.

So far in this work, the terms myotomic material and myotomic premuscle mass have been used to designate the anlagen of all muscles except those of known or accepted branchial origin. Recently, however, the belief expressed by His (1868) has been revived, viz., that the lateral plate mesoderm gives rise to the abdominal musculature, in opposition to the more widely held view that they are entirely of somite (myotome) origin. Straus and Rawles (1953), using the carbon-marking technique in the developing chick and intracoelomic grafts of lateral plate material, conclude that "in the domestic fowl the ventral parts of the three lateral abdominal muscles, the whole of m. rectus abdominis, the ventral part of the intercostal muscle complex, the ventral parts of the ribs, and the sternum are not derived from somites but developed from mesodermal cells of the lateral plate (somatopleure)."

Although the results of these experiments are not directly applicable to the present study of the neck region, there are obvious implications especially in relation to the trapezius. Embryos 6258, 6520, 6524, and 4430 show how this muscle sweeps laterally from the region of the anterior cardinal vein into the superficial tissues, becoming closely associated there with the remaining musculature of the shoulder; it would not be pushing analogy too far to regard the lateral and ventral parts of the neck as lateral plate mesoderm and therefore to assume that muscle tissue appearing there develops as much *in situ* as from a migration either from the myotomes or from the branchial region. The appearance presented by the trapezius as if it were being "peeled off" the underlying muscles supports this view, viz., that there is an original element of entirely branchial origin extending dorsally and caudally by increments from the myotomes or the lateral plate mesoderm and that the muscle, in addition to its branchial innervation, will adopt the nerve supply of the newly acquired musculature.

It is not difficult to identify the somatic muscle or group of muscles so closely associated with the accessory musculature. In embryo 4430 the trapezius is separating itself from the muscular sheet immediately deep to it, namely, the rhomboids; this deduction and the homology of the deep head of the sternomastoid with the whole or part of the omocervicalis are in keeping with Giebel's (1874-1900) suggestion that the omocervicalis, levator scapulae, and rhomboideus are ontogenetically and phylogenetically the same muscle group.

In view of these findings, it would be surprising if the human sternomastoid and the trapezius muscles did not have a substantial motor as well as sensory innervation from the cervical nerves. If the nerve supply to a sternomastoid lying entirely superficial to the accessory nerve also comprises motor fibers in the spinal nerves, and this has not yet been satisfactorily demonstrated, then and then only need we take refuge in postulating a phylogenetic and/or ontogenetic migration of innervation.

LITERATURE CITED

Addens, J. L. 1933. The motor nuclei and roots of the cranial and first spinal nerves. Part 1. Introduction. Cyclostomes. *Z. Anat. Entwicklungsgeschichte, 101,* 307–410.

Bruce, A. 1901. *A Topographical Atlas of the Spinal Cord,* 16 pp. Williams and Norgate, London.

Chauveau, A. 1891. On the sensorimotor nerve-circuit of muscles. *Brain, 14,* 145–178.

Cuvier, G. 1849. *Anatomie comparée.* Chez Dusacq, Libraire Agricole de la Maison Rustique, Paris.

Fahmy, N. 1927. A note on the intracranial and extracranial parts of the ninth, tenth and eleventh nerves. *J. Anat., 61,* 298–301.

Giebel, C. G. 1874–1900. In Bronn's *Klassen und Ordnungen des Thier-reichs* (*Säugethiere*), *1,* 731. C. F. Winter'sche Verlagshandlung, Leipzig.

His, W. 1868. *Untersuchungen über die erste Anlage des Wirbelthierleibes. Die erste Entwickelung des Hühnchens im Ei.* F. C. W. Vogel, Leipzig.

Kappers, C. U. A. 1912. Weitere Mitteilung über Neurobiotaxis. VII. Die phylogenetische Entwicklung der motorische Wurzelkerne in Oblongata und Mittelhirn. *Folia Neurobiol., 6,* 1–142.

Kappers, C. U. A. 1920. Die vergleichende Anatomie des Nervensystems der Wirbelthiere und des Menschen. *Haarlem, 1.*

Lesbre, F. X., and F. Maignon. 1908. Contribution à la physiologie du pneumogastrique et du spinal. *Ann. soc. agric. sci. ind. Lyon* (1907), 332–350.

Lewis, W. H. 1901. The development of the arm in man. *Am. J. Anat., 1,* 145–183.

Lewis, W. H. 1910. The development of the muscular system. In Keibel and Mall, *Manual of Human Embryology, 1,* 454–522. J. B. Lippincott Co., Philadelphia.

McKenzie, J. 1955. The morphology of the sternomastoid and trapezius muscles. *J. Anat., 61,* 526–531.

Norris, H. W. 1913. The cranial nerves of *Siren lacertina. J. Morphol., 24,* 245–338.

Ranson, S. W., H. K. Davenport, and E. A. Doles. 1932. Intramedullary course of the dorsal root fibres of the first three cervical nerves. *J. Comp. Neurol., 54,* 1–12.

Russell, J. S. R. 1897. An experimental investigation of the cervical and thoracic nerve roots in relation to the subject of wry-neck. *Brain, 20,* 35–55.

Sherrington, C. S. 1898. II. Experiments in examination of the peripheral distribution of the fibres of the posterior roots of some spinal nerves. Part II. *Phil. Trans. Roy. Soc. London, B, 190,* 45–186.

Sternberg, M. 1898. Über den ausseren Ast des Nervus accessorius Willisii. *Pflügers Arch. ges. Physiol., 71,* 158–175.

Straus, W. L., and A. B. Howell. 1936. The spinal accessory nerve and its musculature. *Quart. Rev. Biol., 11,* 387–405.

Straus, W. L., and Mary E. Rawles. 1953. An experimental study of the origin of the trunk musculature and ribs in the chick. *Am. J. Anat., 92,* 471–509.

Streeter, G. L. 1905. The development of the cranial and spinal nerves in the occipital region of the human embryo. *Am. J. Anat., 4,* 83–116.

Streeter, G. L. 1945. Developmental horizons in human embryos. Description of age groups xiii and xiv. *Carnegie Inst. Wash. Publ.* 557, *Contribs. Embryol., 31,* 27–63.

Streeter, G. L. 1948. Developmental horizons in human embryos. Description of age groups xv, xvi, xvii, and xviii. *Carnegie Inst. Wash. Publ.* 575, *Contribs. Embryol., 32,* 133–203.

Windle, W. F. 1931*a.* The neurofibrillar structure of the spinal cord of cat embryos correlated with the appearance of early somatic movements. *J. Comp. Neurol., 53,* 71–113.

Windle, W. F. 1931*b.* The sensory component of the spinal accessory nerve. *J. Comp. Neurol., 53,* 115–127.

Windle, W. F., and L. C. DeLozier. 1932. The absence of painful sensation in the cat during stimulation of the spinal accessory nerve. *J. Comp. Neurol., 54,* 97–101.

ABBREVIATIONS IN PLATES

a, accessory nerve
a c v, anterior cardinal vein
c, (roots of) upper cervical nerves
h, (roots of) hypoglossal nerve
m, myotome (pre)muscle mass
s, sternomastoid
st, sternomastoid-trapezius premuscle mass
t, trapezius
v, ganglion of vagus

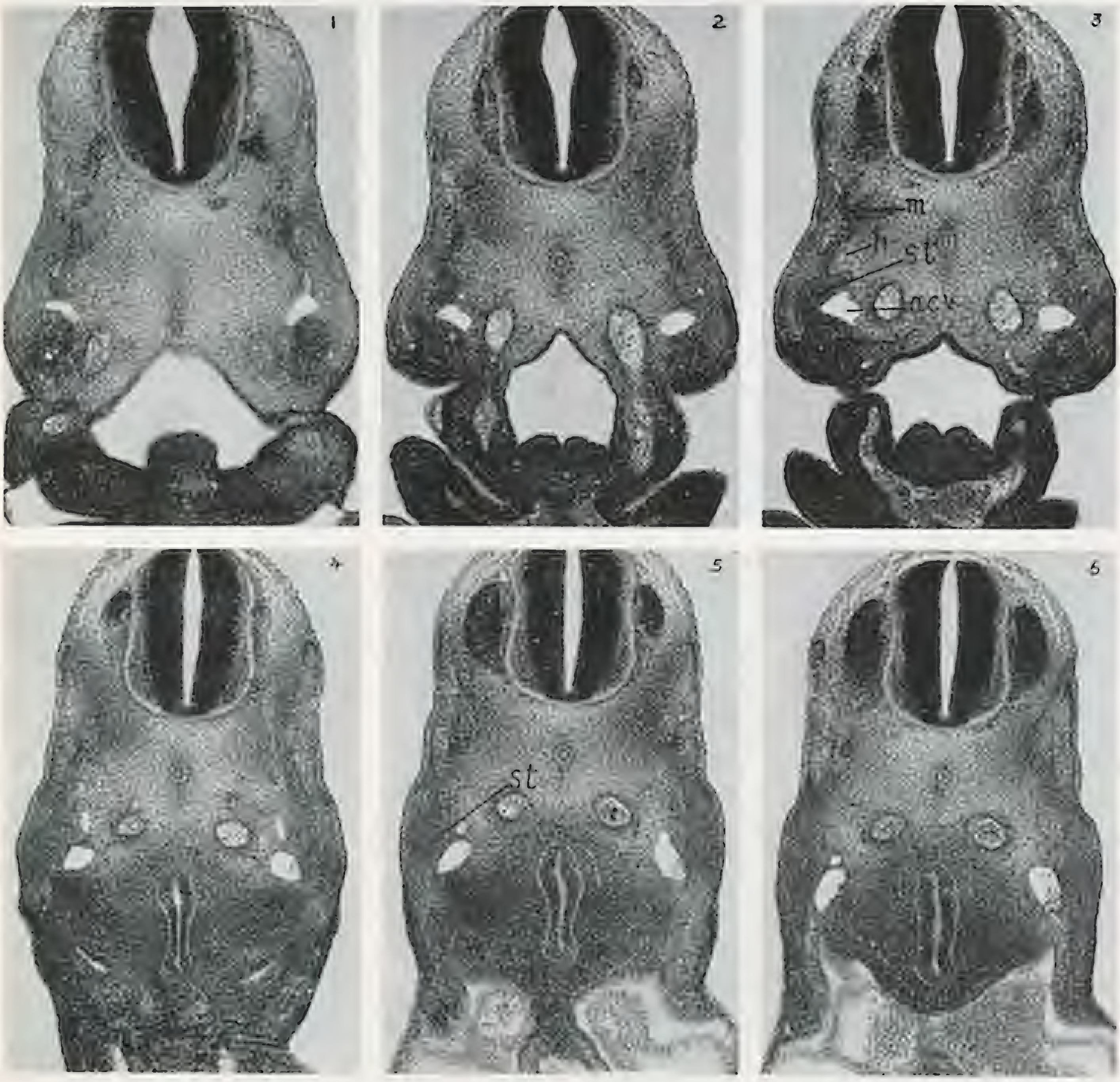

Embryo 2841, xiv, 4.85 mm. Sections cut at 20 μ. Serial numbers: figure 1, 2-5-6; figure 2, 3-1-6; figure 3, 3-2-2; figure 4, 3-3-2; figure 5, 3-3-6; figure 6, 3-4-1.

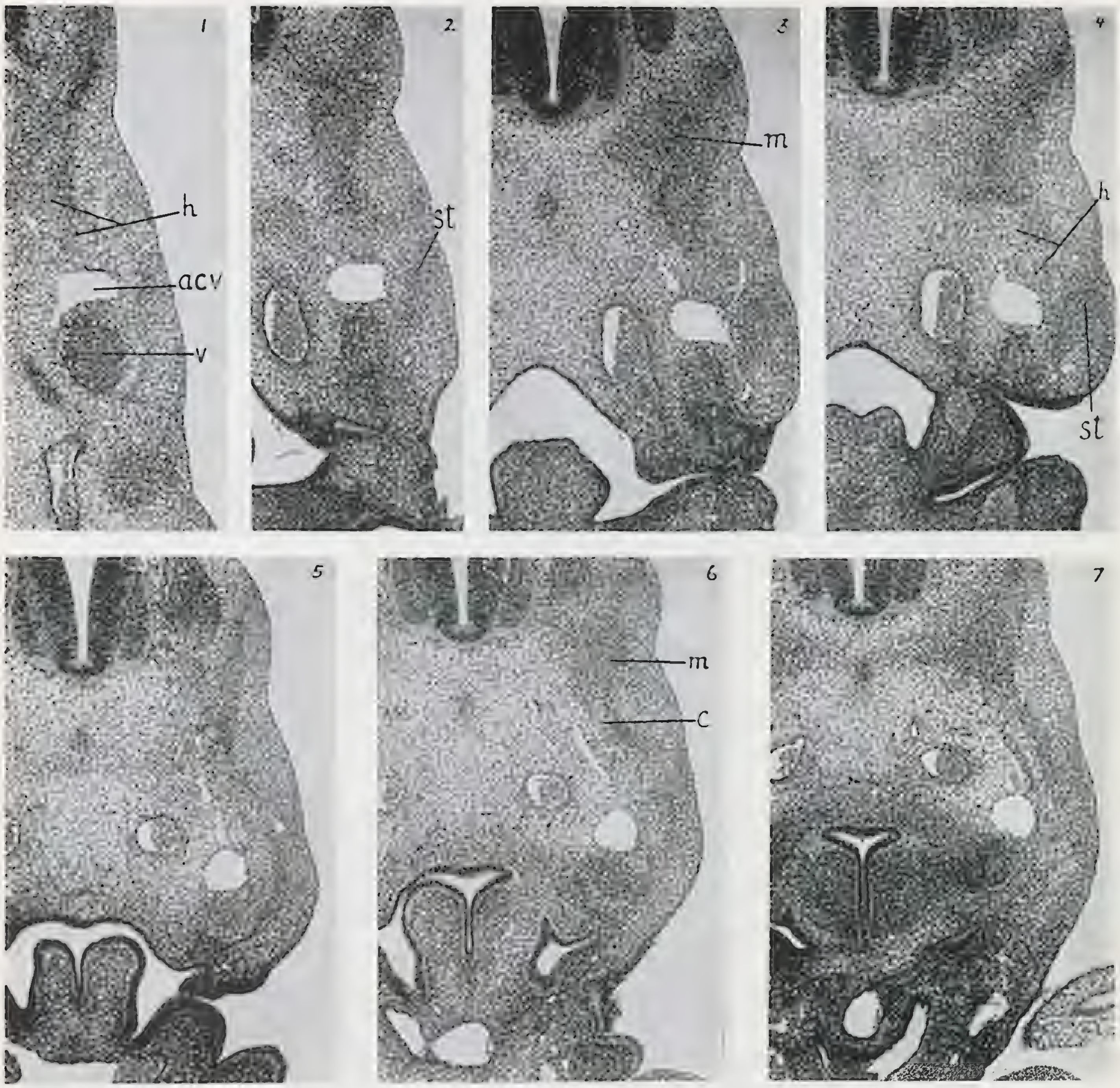

Embryo 7829, xiv, 7 mm. Sections cut at 8 μ. Serial numbers: figure 1, 5-3-2; figure 2, 5-5-2; figure 3, 5-5-8; figure 4, 6-2-1; figure 5, 6-4-2; figure 6, 6-5-2; figure 7, 7-1-4.

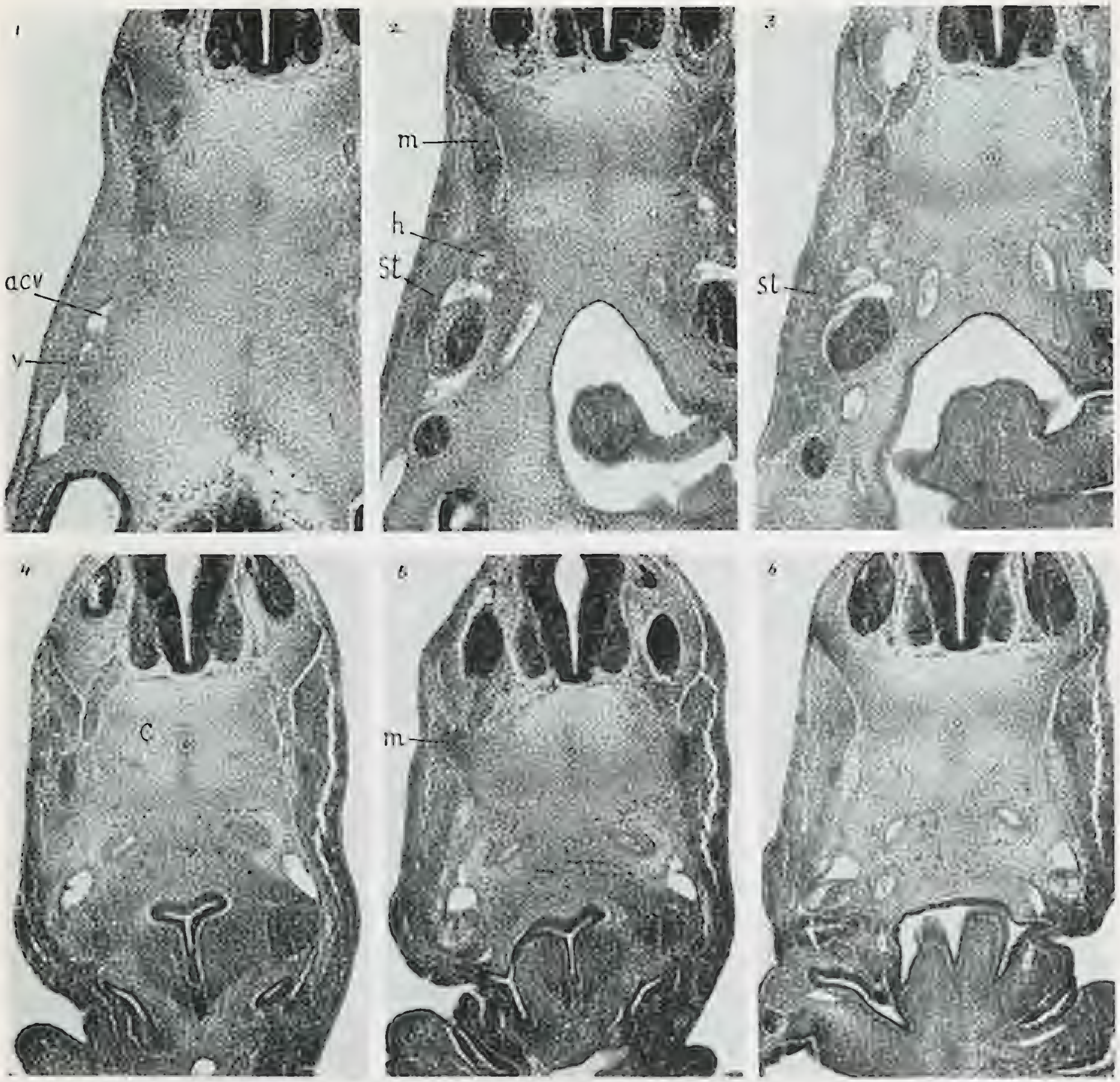

Embryo 3216, xv, 6.5 mm. Sections cut at 20 μ. Serial numbers: figure 1, 2-3-2; figure 2, 2-3-8; figure 3, 2-4-4; figure 4, 2-5-1-; figure 5, 2-5-6; figure 6, 3-1-1.

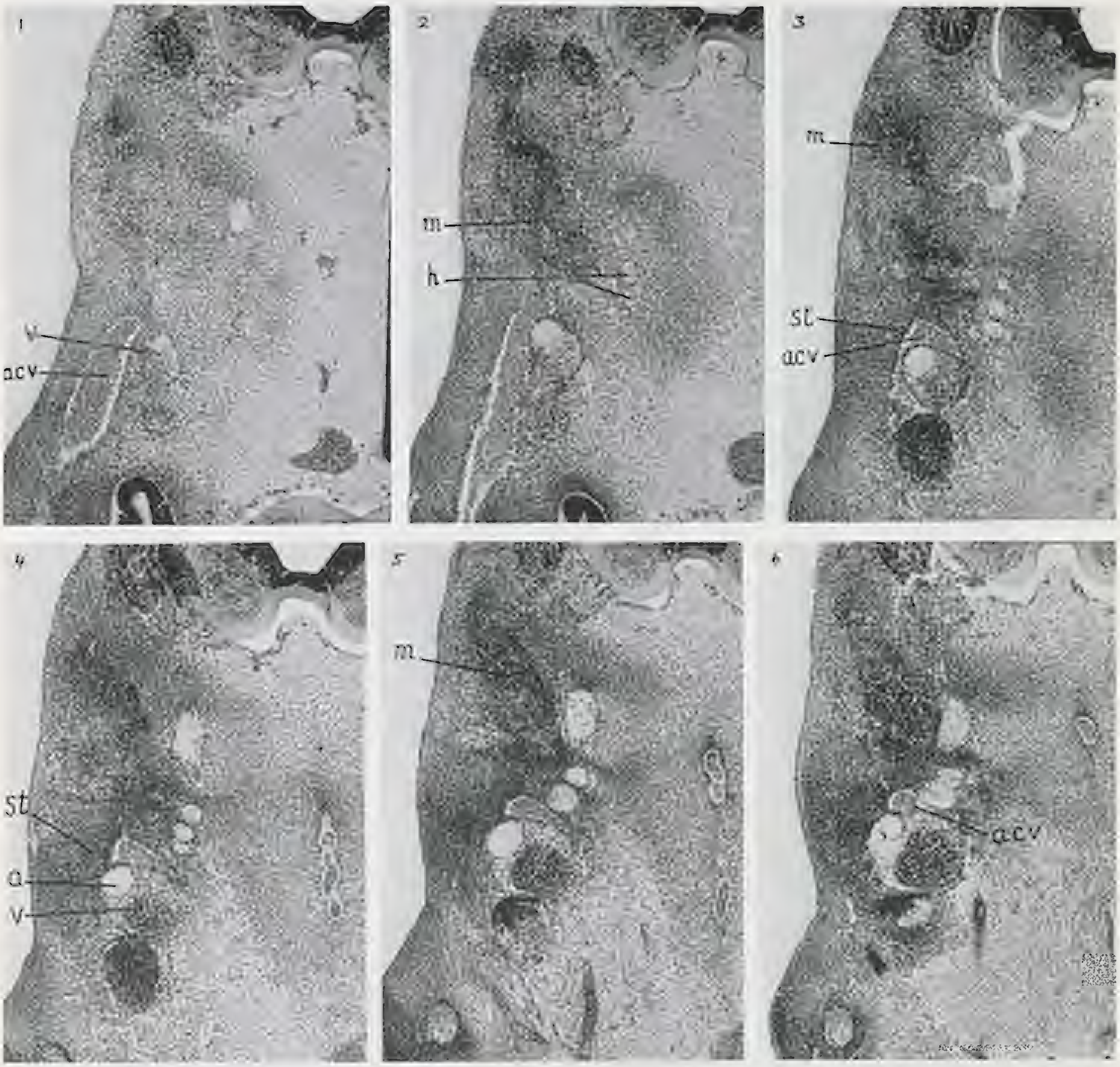

Embryo 8929, xv, 6.35 mm. Sections cut at 10 µ. Serial numbers: figure 1, 3-2-1; figure 2, 3-3-1; figure 3, 3-4-1-; figure 4, 3-4-7; figure 5, 3-5-1; figure 6, 3-5-5.

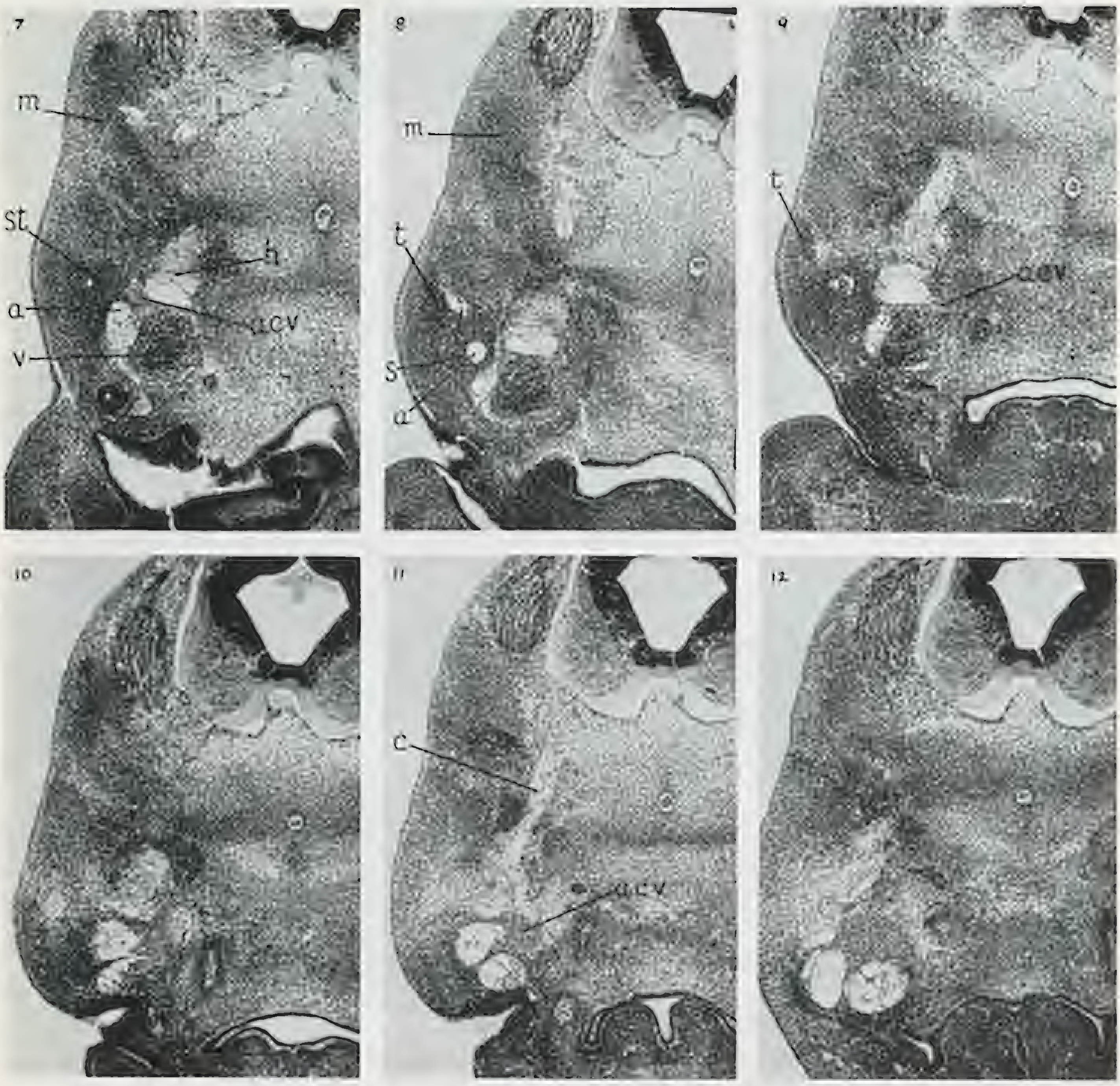

Embryo 8929, xv, 6.35 mm. Sections cut at 10 µ. Serial numbers: figure 7, 3-6-1; figure 8, 3-6-7; figure 9, 4-1-6; figure 10, 4-2-5; figure 11, 4-3-2; figure 12, 4-4-1.

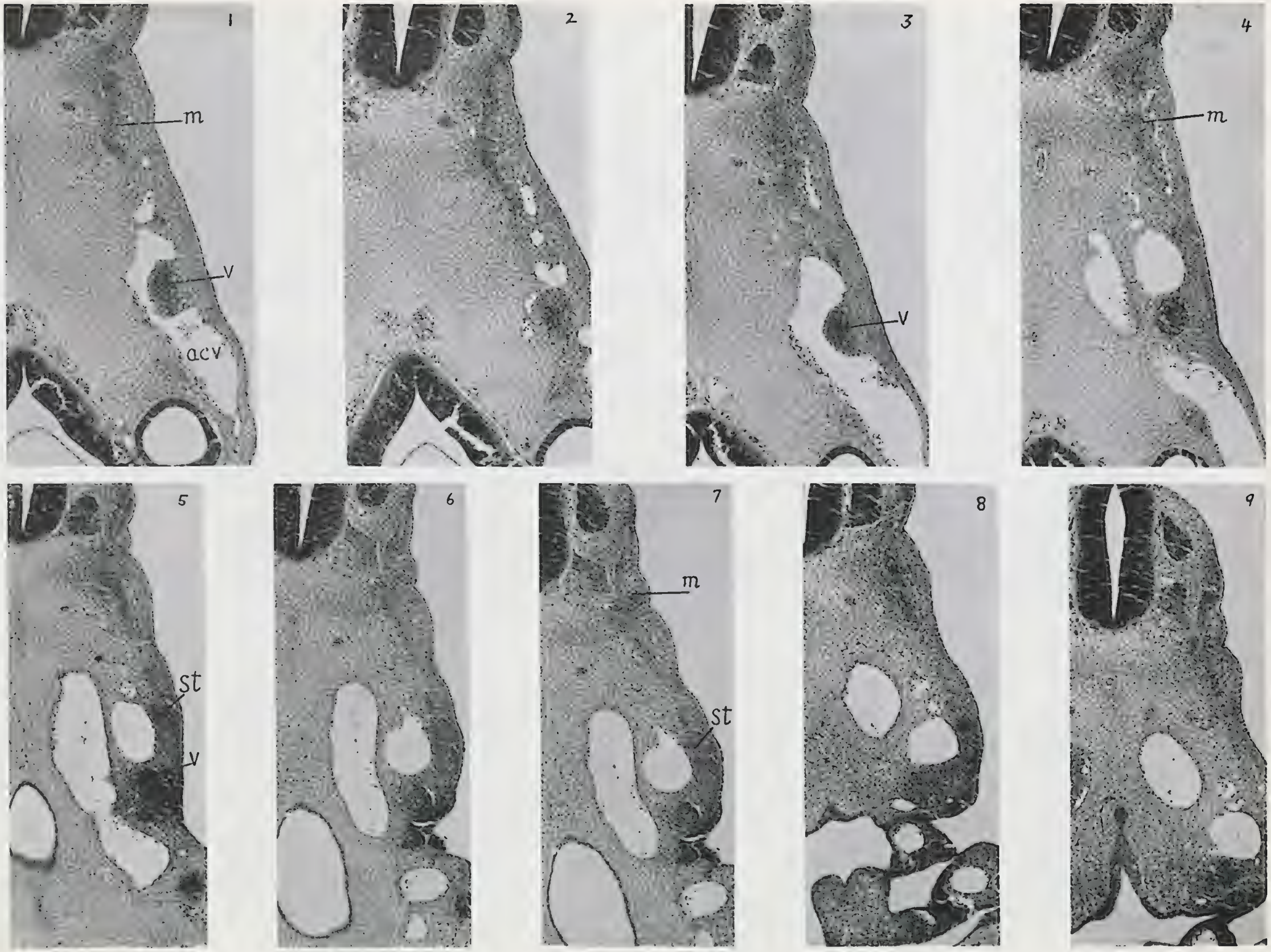

Embryo 7333, xiv, 6.3 mm. Sections cut at 8 µ. Serial numbers: figure 1, 3-1-12; figure 2, 3-2-3; figure 3, 3-2-7; figure 4, 3-3-2; figure 5, 3-3-8; figure 6, 3-3-12; figure 7, 4-1-3; figure 8, 4-1-12; figure 9, 4-2-7.

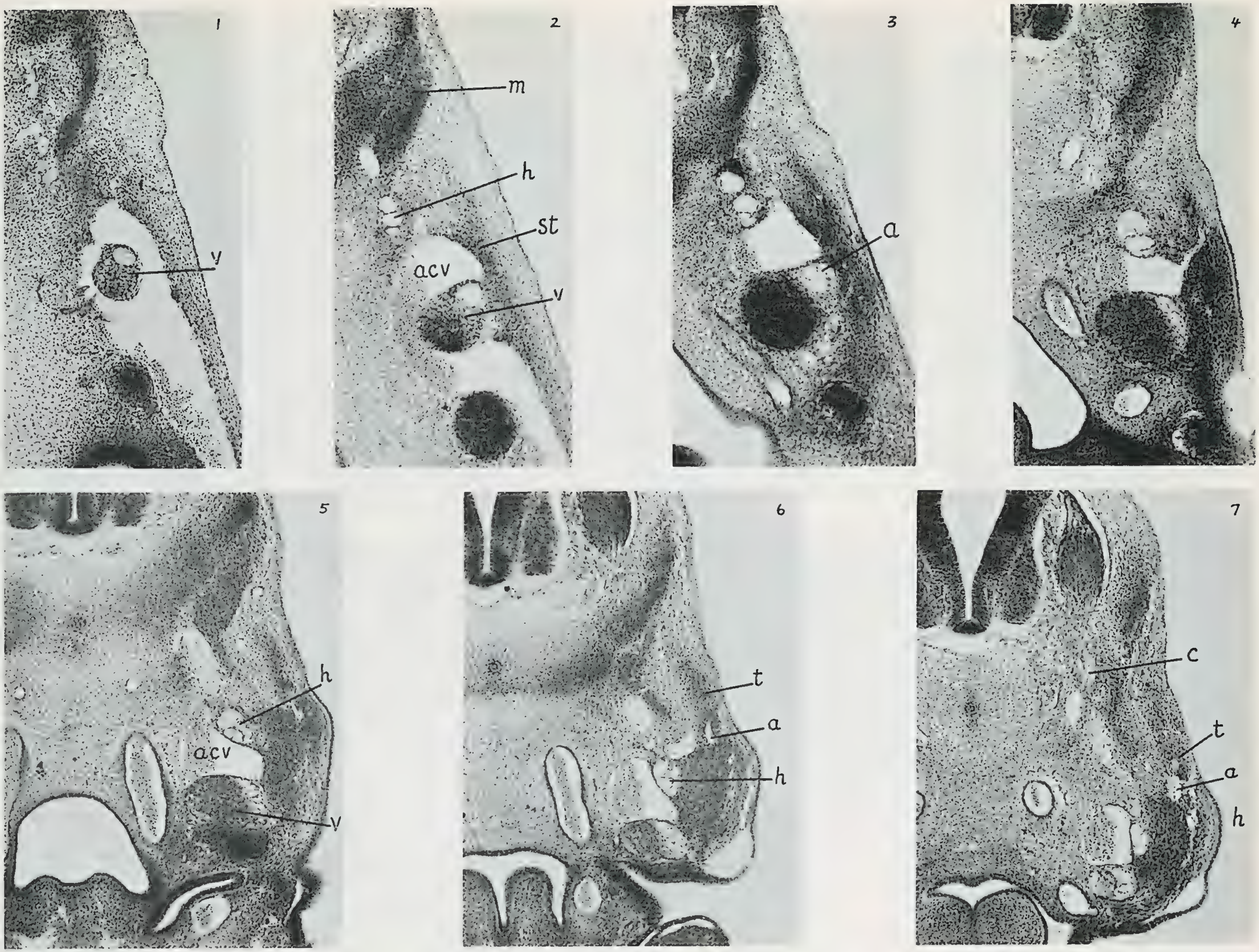

Embryo 3385, xv, 8.3 mm. Sections cut at 20 μ. Serial numbers: figure 1, 5-3-5; figure 2, 6-1-5; figure 3, 6-2-5; figure 4, 6-3-5; figure 5, 7-1-5; figure 6, 7-2-5; figure 7, 7-3-5.

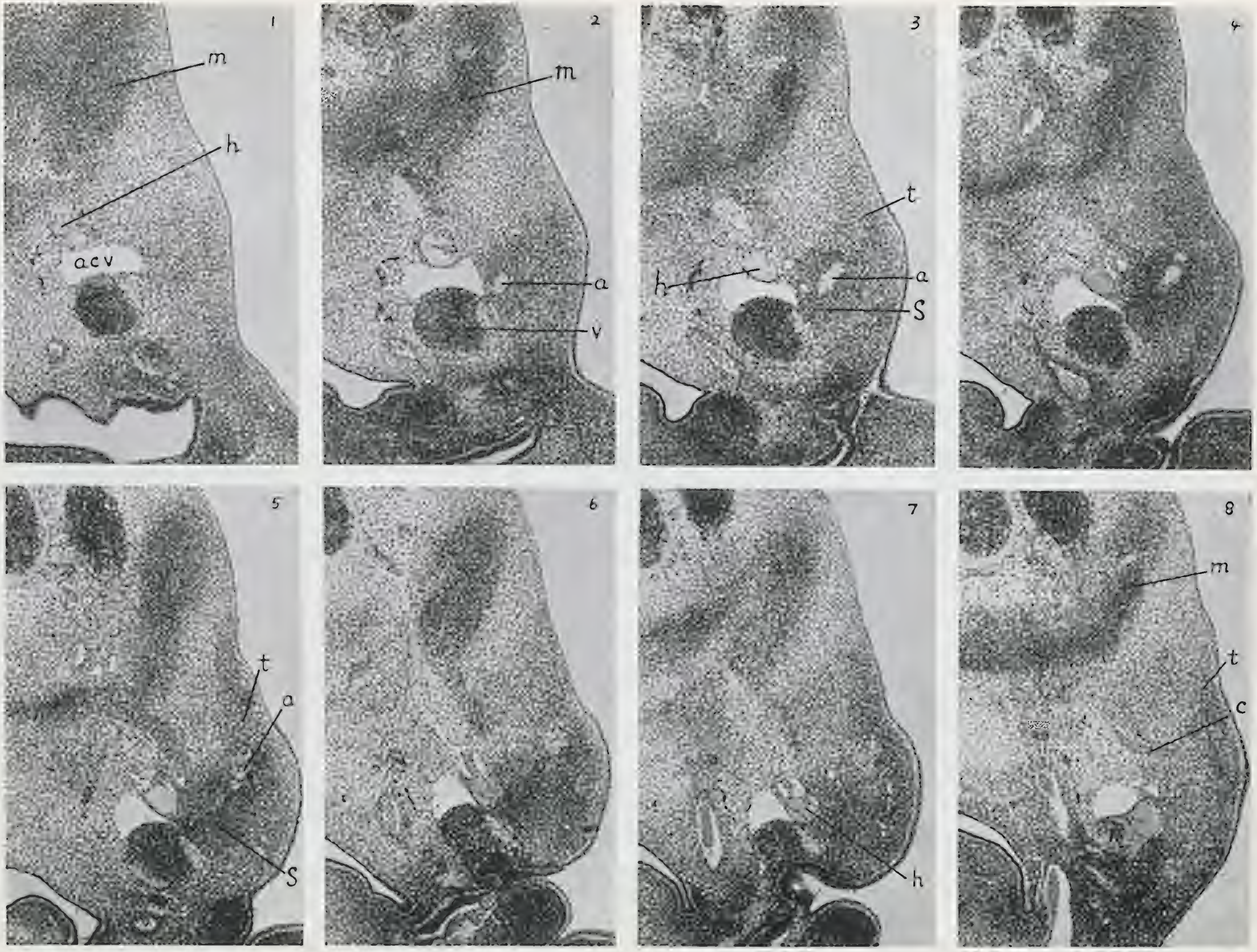

Embryo 6517, xvi, 10.56 mm. Sections cut at 20 µ. Serial numbers: figure 1, 13-4-1; figure 2, 14-2-6; figure 3, 14-3-6; figure 4, 14-4-6; figure 5, 15-1-5; figure 6, 15-3-6; figure 7, 15-4-6; figure 8, 16-3-5.

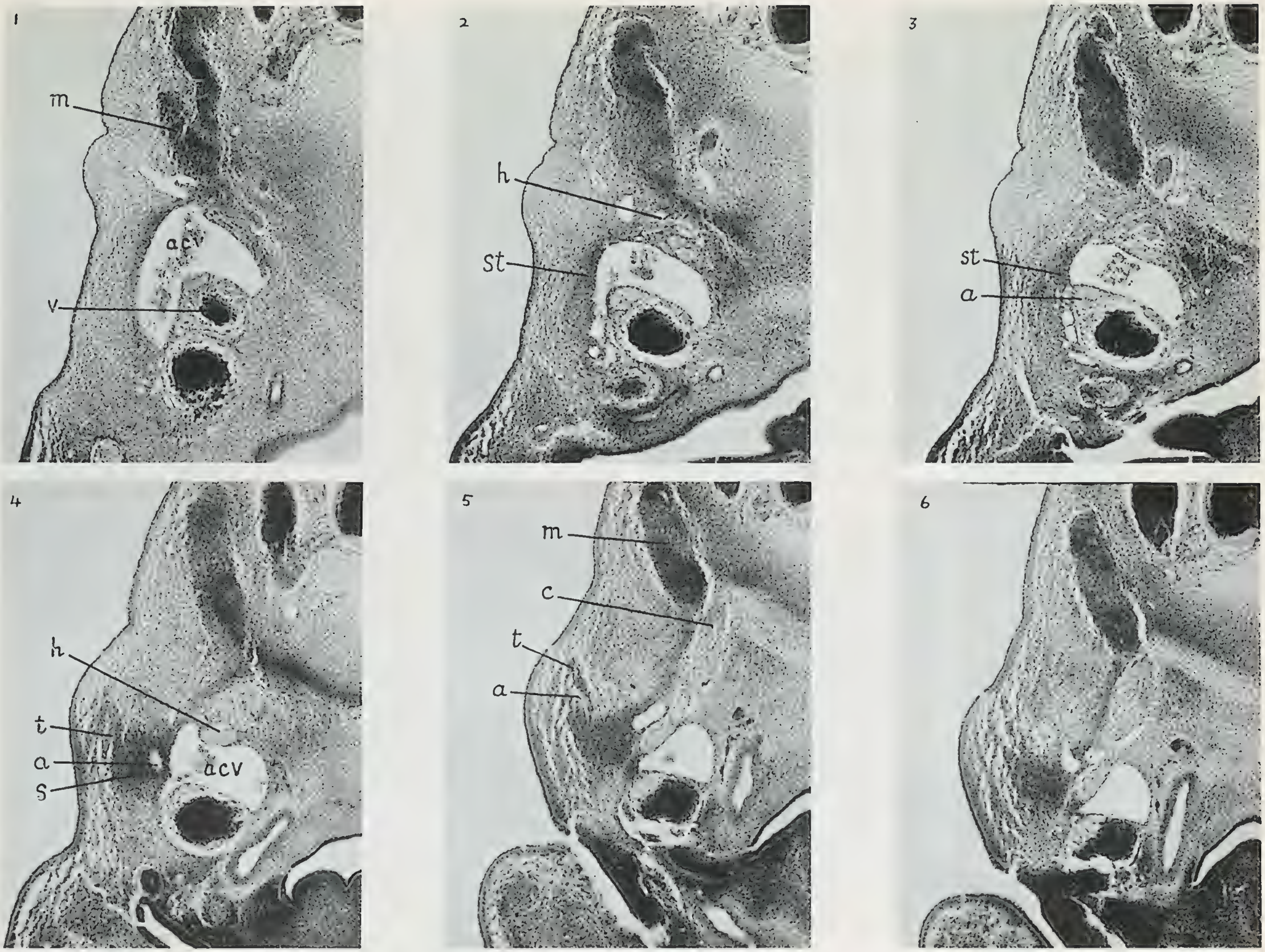

Embryo 1836, xvi, 11 mm. Sections cut at 20 μ. Serial numbers: figure 1, 9-1-1; figure 2, 9-2-1; figure 3, 9-2-4; figure 4, 10-1-1; figure 5, 10-2-3; figure 6, 10-2-5.

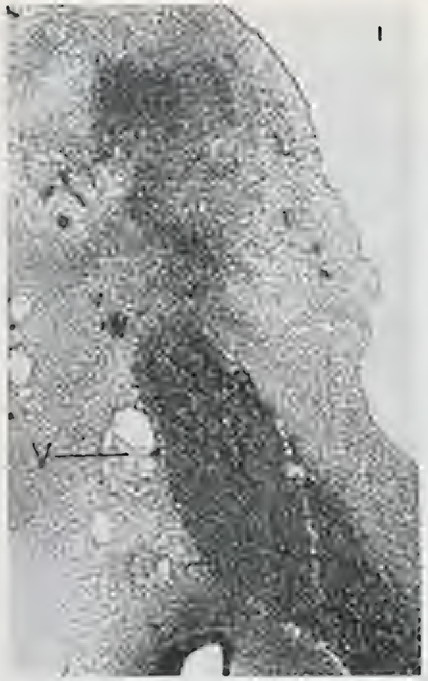

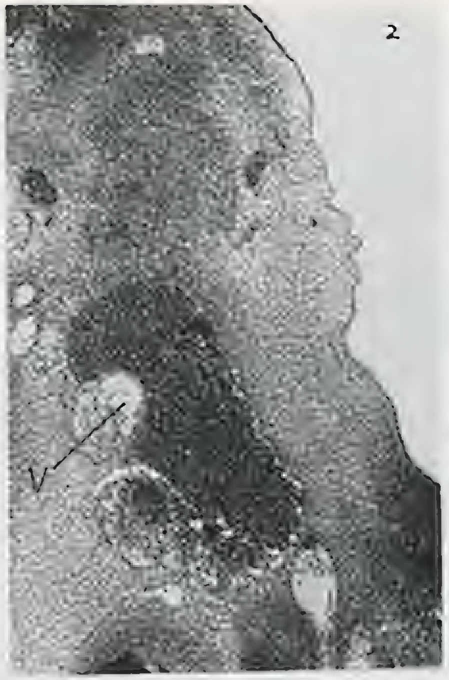

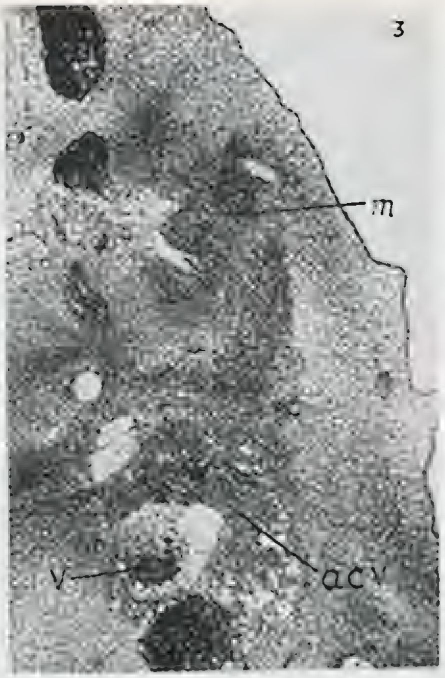

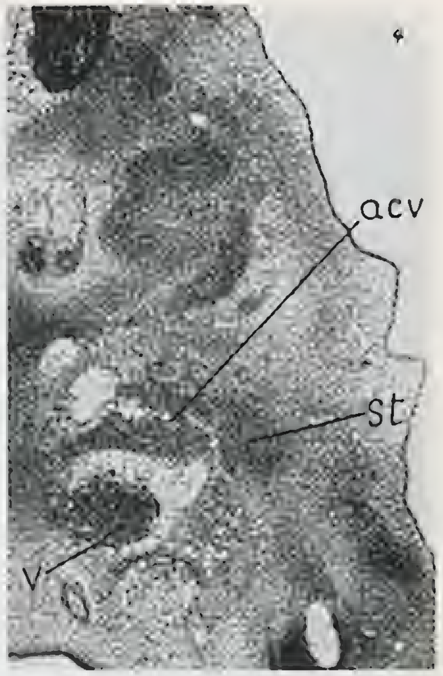

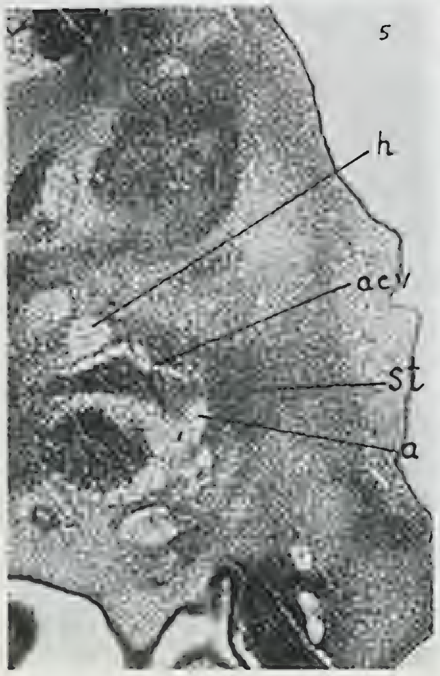

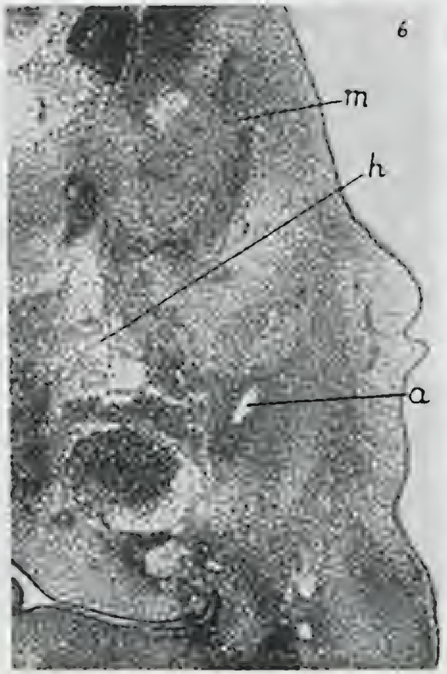

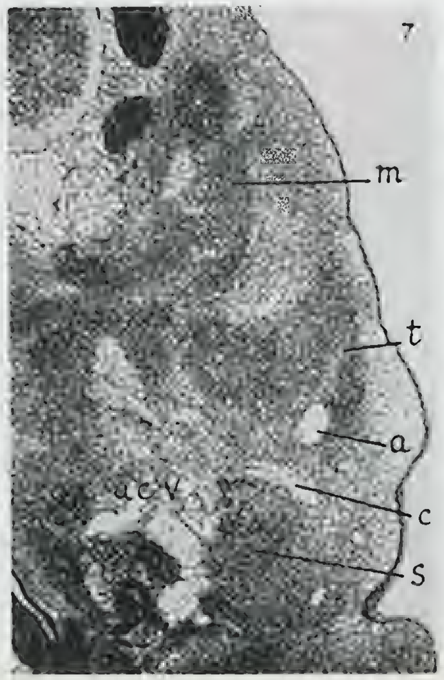

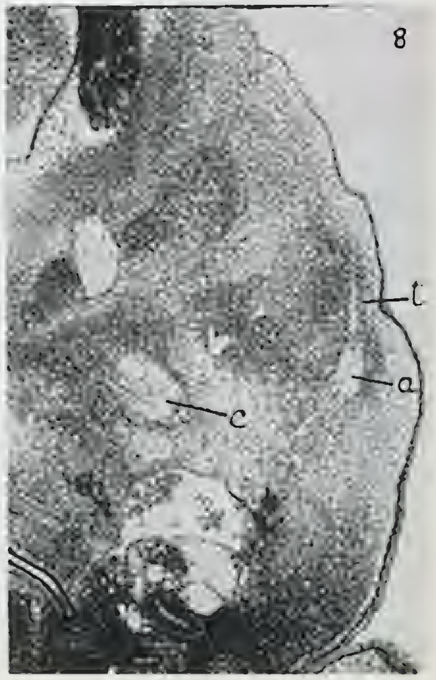

Embryo 6258, xvii, 14 mm. Sections cut at 10 μ. Serial numbers: figure 1, 9-1-6; figure 2, 9-4-4; figure 3, 10-3-2; figure 4, 10-4-4; figure 5, 11-1-3; figure 6, 11-2-6; figure 7, 12-3-4; figure 8, 13-1-5.

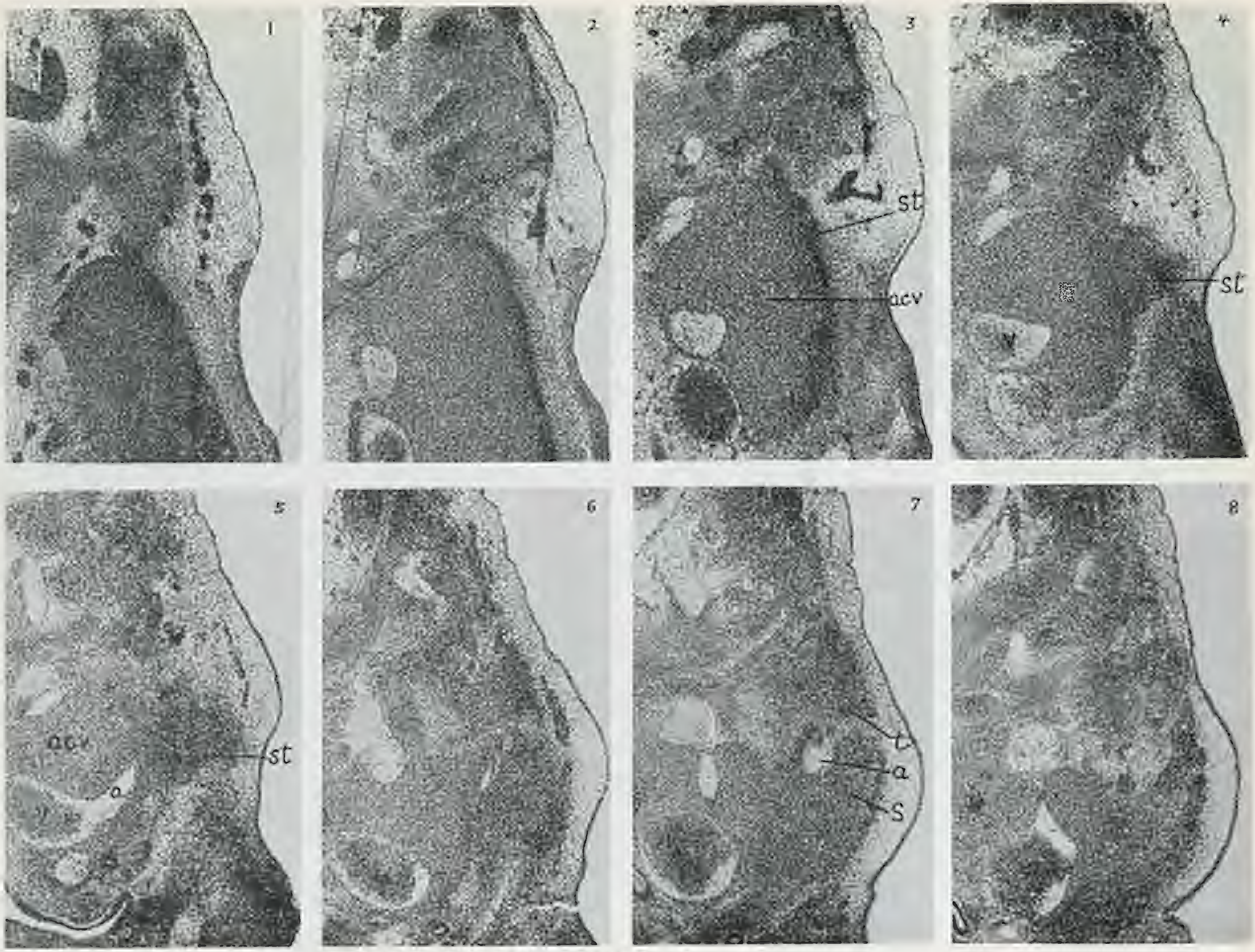

Embryo 8969, xvii, 11.2 mm. Sections cut at 15 μ. Serial numbers: figure 1, 6-1-5; figure 2, 6 3 3, figure 3, 6-4-3; figure 4, 7-1-1; figure 5, 7 1 9, figure 6, 7 2 7, figure 7, 7-3-4; figure 8, 7-4-3.

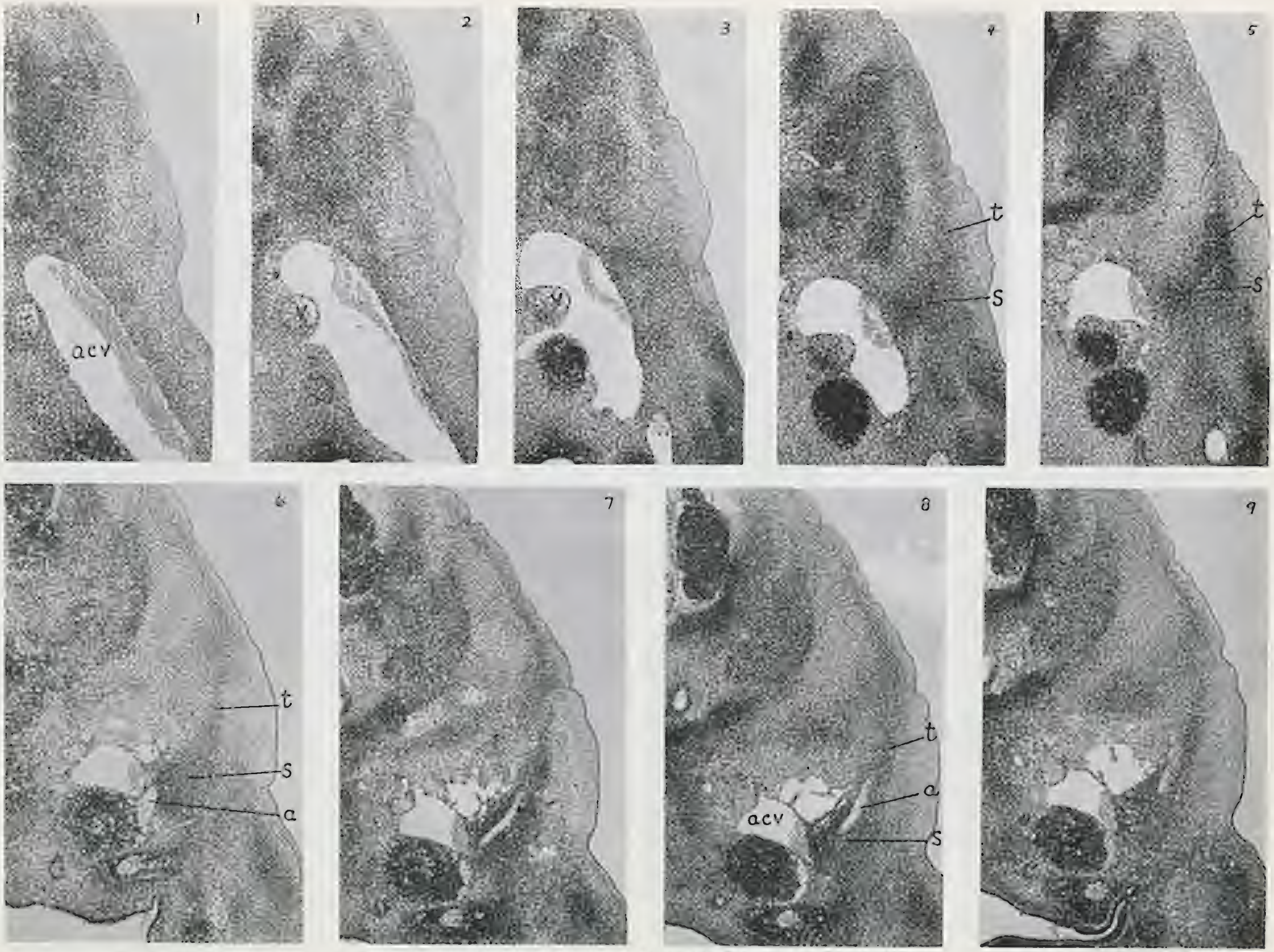

Embryo 6520, xvii, 12.9 mm. Sections cut at 10 µ. Serial numbers: figure 1, 16-1-2; figure 2, 16-3-4; figure 3, 17-2-3; figure 4, 17-3-3; figure 5, 18-2-4; figure 6, 19-3-4; figure 7, 20-2-1; figure 8, 20-2-4; figure 9, 20-3-1.

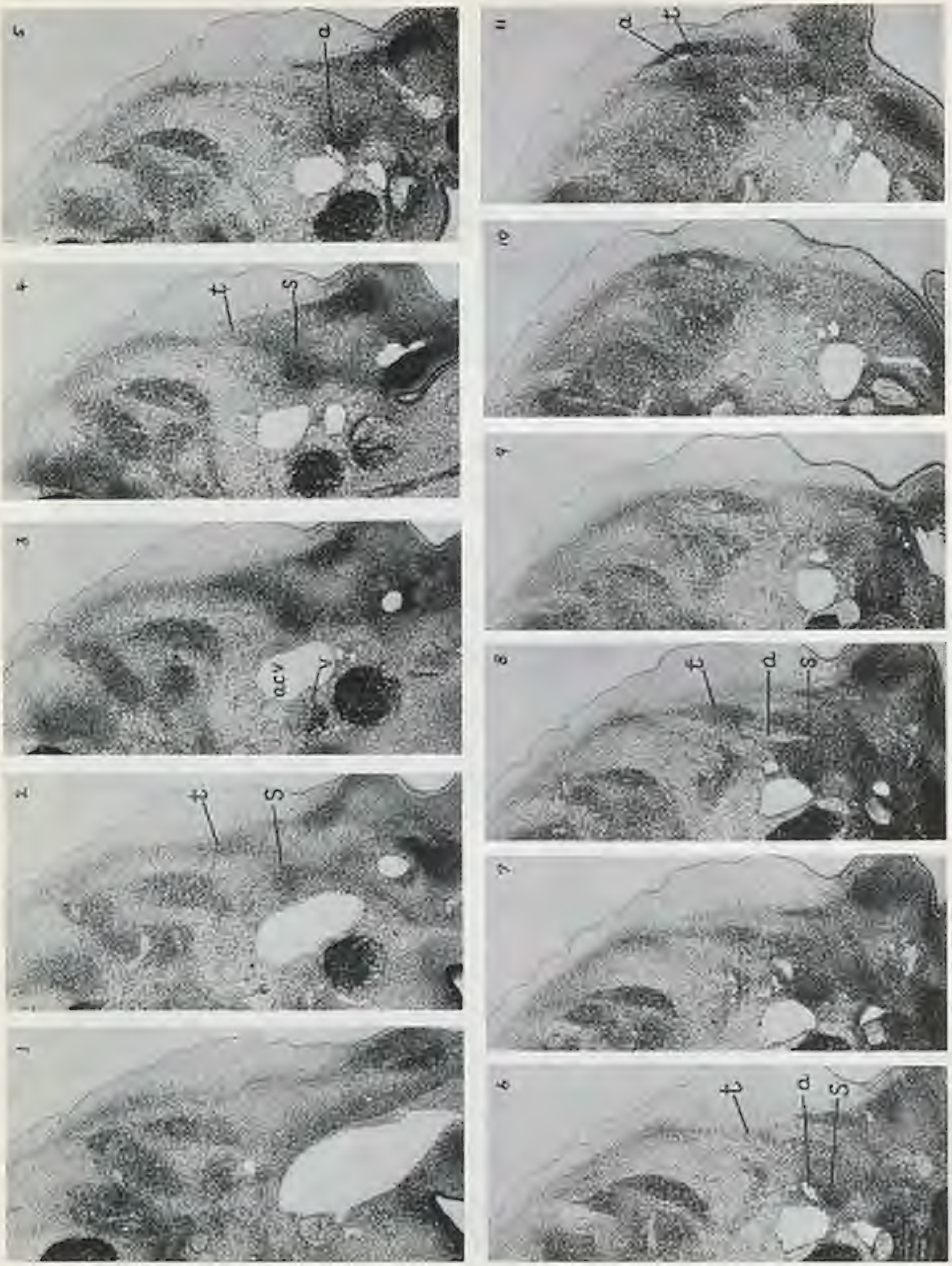

Embryo 6524, xviii, 11.76 mm. Sections cut at 10 µ. Serial numbers: figure 1, 18-2-4; figure 2, 19-2-4; figure 3, 19-3-5; figure 4, 20-2-4; figure 5, 21-1-5; figure 6, 21-2-5; figure 7, 21-3-5; figure 8, 22-1-5; figure 9, 23-3-5; figure 10, 24-3-5; figure 11, 25-3-1.

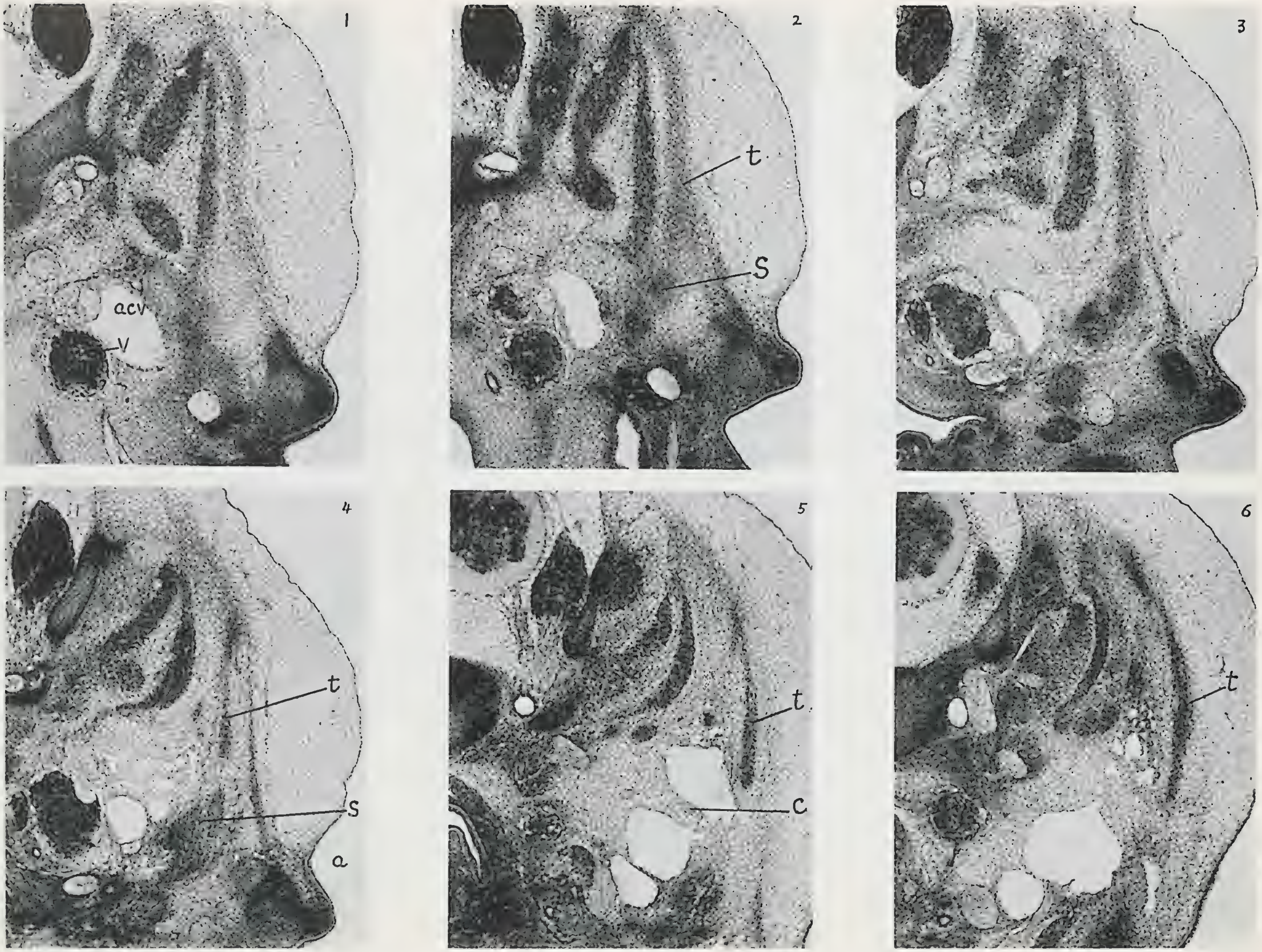

Embryo 4430, xviii, 13.95 mm. Sections cut at 15 µ. Serial numbers: figure 1, 12-1-6; figure 2, 12-3-1; figure 3, 13-1-2; figure 4, 13-2-6; figure 5, 14-2-4; figure 6, 15-2-6.